ANALYTICA CHIMICA ACTA

International monthly devoted to all branches of analytical chemistry
Revue mensuelle internationale consacrée à tous les domaines de la chimie analytique
Internationale Monatsschrift fur alle Gebiete der analytischen Chemie

ELSEVIER SCIENTIFIC PUBLISHING COMPANY
AMSTERDAM

Anal. Chim. Acta, Vol. 77, 1–358, July 1975
Published monthly

Complete in one issue

Publication Schedule for 1975

Vol. **74**, No. **1**	January 1975	
Vol. **74**, No. **2**	February 1975	**(completing Vol. 74)**
Vol. **75**, No. **1**	March 1975	
Vol. **75**, No. **2**	April 1975	**(completing Vol. 75)**
Vol. **76**, No. **1**	May 1975	
Vol. **76**, No. **2**	June 1975	**(completing Vol. 76)**
Vol. **77**	July 1975	**(complete in one issue)**
Vol. **78**, No. **1**	August 1975	
Vol. **78**, No. **2**	September 1975	**(completing Vol. 78)**
Vol. **79**	October 1975	**(complete in one issue)**
Vol. **80**, No. **1**	November 1975	
Vol. **80**, No. **2**	December 1975	**(completing Vol. 80)**

Subscription price for 1975 (covering Vols. 74–79): Dfl. 570.00 plus Dfl. 54.00 postage, US$ 265.53 inclusive of postage. Subscribers in the U.S.A. and Canada receive their copies by airmail. Additional charges for airmail to other countries are available on request. For advertising rates apply to the publishers.

Subscriptions should be sent to:
Elsevier Scientific Publishing Company, P.O. Box 211, Amsterdam, The Netherlands.

GENERAL INFORMATION

Languages

Papers will be published in English, French or German.

Detailed information

Authors should consult Vol. 73, p. 435 for detailed instructions. Reprints of this information are obtainable from Dr. MacDonald or from: Elsevier Editorial Services Ltd., Mayfield House, 256 Banbury Road, Oxford (Great Britain).

Submission of papers

Papers should be sent to:

PROF. PHILIP W. WEST,
Coates Chemical Laboratories,
College of Chemistry and Physics,
Louisiana State University,
Baton Rouge 3,
La. 70803 (U.S.A.)

or to:

DR. A. M. G. MACDONALD,
Department of Chemistry,
The University,
P.O. Box 363
Birmingham B15 2TT (Great Britain)

Reprints

Fifty reprints will be supplied free of charge. Additional reprints (minimum 100) can be ordered at quoted prices. They must be ordered on order forms which are sent together with the proofs.

PRINTED IN THE NETHERLANDS

ANALYTICA CHIMICA ACTA
Vol. 77 (1975)

ANALYTICA CHIMICA ACTA

International monthly devoted to all branches of analytical chemistry
Revue mensuelle internationale consacrée à tous les domaines de la chimie analytique
Internationale Monatsschrift für alle Gebiete der analytischen Chemie

ELSEVIER SCIENTIFIC PUBLISHING COMPANY
AMSTERDAM

Anal. Chim. Acta, Vol. 77 (1975)

PRINTED IN THE NETHERLANDS

Analytica Chimica Acta, 77 (1975) 1–8

THE POLAROGRAPHIC DETERMINATION OF TRACES OF TITANIUM-(IV) IN THE PRESENCE OF N-BENZOYL-N-PHENYLHYDROXYLAMINE

G. DONOSO N., I. CHADWICK W. and M. A. SANTA ANA V.
Department of Chemistry, Faculty of Sciences, University of Chile, Santiago (Chile)
(Received 4th November 1974)

N-Benzoyl-N-phenylhydroxylamine (BPHA) has been widely used as an analytical reagent but rarely in polarography. The low aqueous solubility of BPHA (0.0019 *M* at 25°C, ref. 1), and its precipitating action on many cations, require the use of non-aqueous solvents. Amperometric determinations of cerium-(IV), thorium and lanthanum with BPHA in ethanolic solutions have been described[2], as have an amperometric method for zirconium and a polarographic determination of tin and antimony[3]. Vernon and Hubbard[4] used a methanolic lithium chloride solution as supporting electrolyte for the polarography of metallic complexes extracted with chloroform, and obtained suitable analytical waves for Cu(II), Pb(II) and Fe(III). The polarographic behavior of several metal–BPHA complexes has been studied in various organic solvents; the chelates can be measured directly in the organic phase obtained by extraction[5].

In the present paper, the polarographic behavior of some cations in acidic water–ethanol solutions of BPHA is reported. In this medium, the formation of complexes such as the titanium(IV) BPHA complex[1–6,18] affects the polarographic behavior of some cations. The titanium wave is particularly interesting, because of its catalytic nature. As happens with other complexing and oxidizing agents[7–12], the titanium(III) formed at the dropping mercury electrode reduces BPHA and is oxidized back to titanium(IV). The resulting catalytic current depends on the rate of this subsequent oxidation. This current has been used in earlier work[7–12] for the polarographic determination of titanium or of the ligand (pyrogallol, pyrocatechol, sulfosalicylic acid, citric acid). In acidic solutions of BPHA, the titanium current allows the determination of titanium at concentrations as low as $5 \cdot 10^{-6}$ *M* in the presence of several metals.

EXPERIMENTAL

Apparatus

A Radiometer Polariter PO4 polarograph was used. An aqueous saturated calomel electrode was used as reference electrode. The dropping mercury electrode (DME) had the following characteristics: $t_1 = 2.7$ s; $m = 2.86$ mg s^{-1} at 49 cm.

The experiments were performed at 25 ± 0.2°C. Dissolved air was removed from the solution by passing oxygen-free nitrogen through the cell for 10 min.

Potentiometric measurements were done with a Radiometer pH meter type PHM-28; saturated calomel and platinum electrodes were used. A Spectronic 20 spectrophotometer was used.

Reagents

Titanium(IV) stock solution. This was prepared by fusing titanium dioxide (Merck, p.a.) with potassium hydrogen sulfate, and standardized by complexometric (EDTA) back-titration in the presence of hydrogen peroxide.

Ethanolic BPHA solution (0.2 M; Merck p.a.). Solutions were stable for about 15 days if kept in the dark. Acidic solutions in the presence of titanium(IV) gave currents which were constant for 1 h. The polarographic behavior of the reagent before and after recrystallization was identical, so that further purification was not necessary.

All other reagents were of p.a. grade.

RESULTS

Polarographic behavior of BPHA–cation systems

The polarographic behavior of some cations in acidic solutions of BPHA was examined. Table I shows the half-wave potentials in 0.1, 1 and 2 *M* sulfuric acid for (1+3) water–ethanol solvent.

BPHA shows no polarographic activity in the accessible potential range (+0.1 to −1 V SCE), even in saturated solution. The slow oxidation described in solutions of higher acidity (>1 *M*)[13,14] does not interfere.

TABLE I

HALF-WAVE POTENTIALS FOR SEVERAL CATIONS IN A (1+3) WATER–ETHANOL MIXTURE IN PRESENCE OF BPHA

($E_{\frac{1}{2}}$ values in V *vs.* SCE)

Cation	H_2SO_4		
	0.1 M	*1 M*	*2 M*
Cu(II)	+0.05	+0.02	+0.02
Cd(II)	−0.57	−0.57	−0.57
Sn(II)	−0.10	−0.08	−0.07
	−0.41	−0.41	−0.41
As(III)	−0.70	−0.63	−0.45
Sb(III)	−0.18	−0.17	−0.12
Bi(III)	−0.09	−0.06	−0.03
Ti(IV)	−0.42	−0.42	−0.42
	−0.70		
Sn(IV)	−0.16	−0.20	−0.20
	−0.48	−0.48	−0.48
V(V)	−0.41	−0.47	−0.50
U(VI)	−0.48	−0.47	−0.48
Mo(VI)	−0.04	−0.09	−0.02
W(VI)	−0.29	−0.26	−0.26

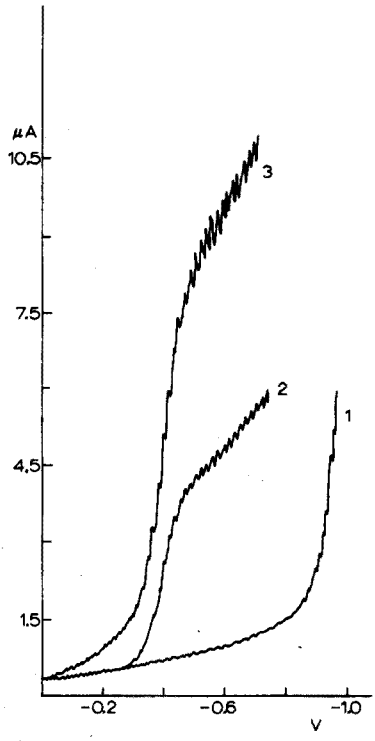

Fig. 1. Polarographic behavior of titanium(IV) in 2 *M* sulfuric acid with 0.05 *M* BPHA in (1+3) water–ethanol. (1) Supporting electrolyte; (2) supporting electrolyte $+2.5 \cdot 10^{-4}$ *M* Ti(IV); (3) supporting electrolyte $+5 \cdot 10^{-4}$ *M* Ti(IV).

Cu(II), Cd, As(III), Sb(III), Bi, Ti(IV), Sn(II), Sn(IV), V(V), Mo(VI), W(VI) and U(VI) show reduction waves in presence of the reagent, the better developed waves being those of Cu(II), Cd(II), Sb(III), Ti(IV) and U(VI). Titanium shows the highest limiting current (Fig. 1). This current is independent of mercury pressure, and its temperature coefficient is 6% in 2 *M* sulfuric acid and 0.05 *M* BPHA measured between 10°C and 46.5°C; this behavior indicates that the titanium current is kinetically controlled.

The molybdenum(VI) wave is well defined only below 10^{-6} *M* concentrations; at higher concentrations, a rounded maximum, which is insensitive to gelatine or Triton X-100, appears. The polarographic waves of tin(II) and tin(IV) are similar; tin(II) is oxidized by the excess of BPHA[3], and tin(IV) is then reduced at the electrode in two steps.

As expected, Ni, Zn, Pb, Fe(III), Ga(III) and Zr(IV) show no electrochemical activity, thus the determination of titanium in the presence of various other cations should be possible.

Effect of solvent

In aqueous solutions, precipitation of BPHA and its complexes causes irregular waves. In ethanol or water–ethanol mixtures the waves are well developed, the limiting current being larger in mixtures than in pure ethanol. The most

satisfactory titanium(IV) waves are obtained in a (1+3) water–ethanol mixture. This medium allows an excess of BPHA in solution, up to 0.1 *M*.

Effect of BPHA on the polarographic waves of titanium in acidic solutions

In aqueous sulfuric acid solutions, the polarographic behavior of titanium(IV) varies with acidity[15,16]; waves corresponding to reduction of TiO^{2+}, a $Ti(H_2O)(SO_4)_n^{+4-2n}$ complex, $Ti(OH)^{3+}$, or a $Ti(OH)(SO_4)_n^{+3-2n}$ complex appear depending on the conditions[15,16]. In (1+3) water–ethanol mixtures containing 2 *M* sulfuric acid, the waves are of the same nature as in aqueous media, but are better developed. The half-wave potentials of the irreversible $Ti(OH)^{3+}$ wave and the kinetic $Ti(OH)(SO_4)_n^{+3-2n}$ wave are shifted to more positive potentials: from −0.81 V and −0.37 V in aqueous solution to −0.43 V and −0.18 V *vs.* SCE, respectively. The total current increases linearly with increase in the titanium(IV) concentration, but not the fraction corresponding to the smaller kinetic wave. The effect of BPHA was examined in (1+3) water–ethanol mixtures containing 10^{-4} *M* titanium(IV) and 2 *M* sulfuric acid. With $5 \cdot 10^{-4}$ *M* BPHA, a new wave is superimposed on the kinetic titanium wave at −0.18 V (Fig. 2). With $5 \cdot 10^{-2}$ *M* BPHA, this wave shifts to more negative potentials and is superimposed on the $TiOH^{3+}$ wave at 0.43 V. The linear relationship of $E_{\frac{1}{4}}$ *vs.* log [BPHA] slows the formation of only one titanium(IV)–BPHA complex, but the limiting current of the new wave increases as the BPHA concentration increases, reaching a

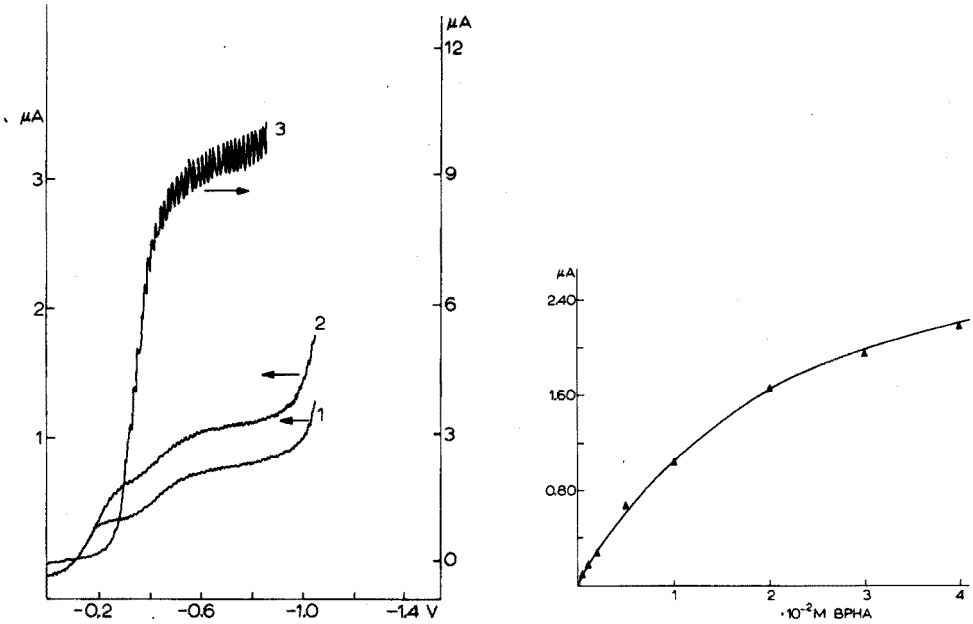

Fig. 2. Effect of BPHA concentration. (1) 2 *M* sulfuric acid, $5 \cdot 10^{-4}$ *M* Ti(IV) in (1+3) water–ethanol. (2) As (1) $+5 \cdot 10^{-4}$ *M* BPHA. (3) As (1) $+5 \cdot 10^{-2}$ *M* BPHA.

Fig. 3. Effect of BPHA concentration on the wave of 10^{-4} *M* titanium(IV) in 2 *M* sulfuric acid (1+3) water–ethanol medium.

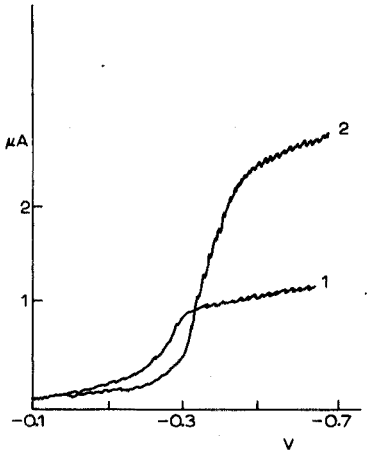

Fig. 4. Effect of BPHA in 2 *M* phosphoric acid (1+1) water–ethanol media containing $5 \cdot 10^{-4}$ *M* Ti(IV). (1) Without BPHA; (2) with 0.02 *M* BPHA.

maximum value (Fig. 3). In 0.05 *M* BPHA, the limiting current is 35 times the total current in the absence of BPHA.

In solutions which contain less than 2 *M* phosphoric acid, in the absence of BPHA, the reversible titanium(IV) wave[17] is completely deformed by the addition of much ethanol; above 2 *M* phosphoric acid, a well-developed wave ($E_{\frac{1}{4}} = -0.25$ V) is obtained in (1+1) water–ethanol (Fig. 4), but it is smaller than in aqueous solution. On addition of BPHA, the titanium wave increases and its half-wave potential shifts to −0.38 V in 0.05 *M* BPHA media. With less than 0.01 *M* BPHA present, a second, smaller and ill-defined wave appears at more negative potentials.

Effect of acidity

The effects of perchloric, sulfuric and phosphoric acids were observed in the presence of 0.05 *M* BPHA for 10^{-4} *M* titanium(IV). In perchloric acid, the waves are ill-defined. The effects of sulfuric and phosphoric acid are shown in Table II.

TABLE II

EFFECT OF ACIDITY ON THE TITANIUM WAVE IN (1+3) WATER–ETHANOL

Acidity	*Ti(IV)*		*Ti(IV)+0.05 M BPHA*	
	$E_{\frac{1}{4}}$	*Total current (μA)*	$E_{\frac{1}{4}}$	*Total current (μA)*
2 *M* H_2SO_4	−0.18, −0.43	0.08	−0.42	4.3
1 *M* H_2SO_4	−0.18, −0.43	0.08	−0.42	4.3
0.1 *M* H_2SO_4	−0.78	0.18	−0.42, −0.7	6.9
3 *M* H_3PO_4	−0.3	0.12	−0.38	1
2 *M* H_3PO_4	−0.3	0.12	−0.38	1

Although the limiting current is higher in 0.1 *M* sulfuric acid in the presence of BPHA, the simpler behavior in 1–2 *M* sulfuric acid is preferable for analytical purposes.

In (1+3) water–ethanol mixtures containing phosphoric acid, ill-developed waves are obtained; in (1+1) water–ethanol mixtures containing 2–3 *M* phosphoric acid, a well-developed wave appears at −0.38 V.

The above information indicates that the most suitable analytical conditions are: 2 *M* sulfuric acid, 0.05 *M* BPHA, and (1+3) water–ethanol mixtures. Under these conditions one kinetically controlled wave is obtained.

DISCUSSION

The titanium(IV) wave in the presence of BPHA is independent of the mercury pressure, has a high temperature coefficient, and increases with increase in the BPHA concentration. This polarographic behavior of titanium(IV) is similar to that observed in the presence of hydroxylamine, pyrogallol, citric acid, thiocyanate, etc., where catalytic effects have been described[7,12].

In the present case, it appears that the titanium(IV)–BPHA complex is first reduced, pushing the equilibrium $TiO^{2+} + HL \rightleftharpoons TiOL^{+} + H^{+}$ to the left; the "free" titanium(IV) then reacts with BPHA, and the titanium(III) produced in the reduction, is re-oxidized by BPHA, so that the titanium(IV) complex is regenerated. This oxidation was verified by potentiometric and amperometric titrations of titanium(III) with BPHA solutions, and *vice versa*, in 2 *M* sulfuric acid water–ethanol mixtures. The reduction of BPHA involved two electrons, and it was obvious from the course of the titrations that only titanium(IV) forms complexes with BPHA. The spectrophotometric continuous variations method proved that under the above conditions, only a 1:1 titanium(IV)–BPHA complex is formed, as has already been observed[6].

In the proposed method, BPHA acts both as the complexing agent for titanium(IV) and as the oxidant for titanium(III), whereas with other ligands[7–12], it is necessary to use a separate oxidizing agent for titanium(III).

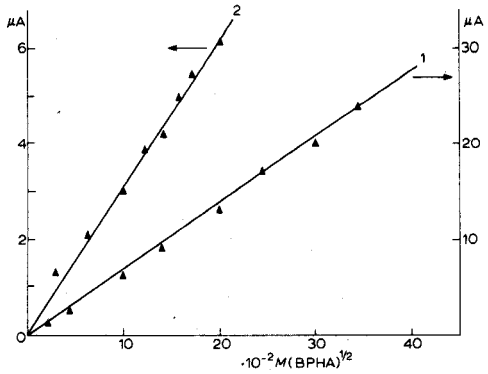

Fig. 5. Dependence of i_l/i_d on the square root of the BPHA concentration. (1) In 2 *M* sulfuric acid, (1+3) water–ethanol with 10^{-4} *M* Ti(IV). (2) In 2 *M* phosphoric acid, (1+1) water–ethanol with $5 \cdot 10^{-4}$ *M* Ti(IV).

Titanium(IV) measurements in the presence of increasing concentrations of BPHA make it possible to estimate the rate constant of the oxidation of titanium(III) with BPHA to $TiOL^+$, by the Koutecký method[19]. The plot of (i_l/i_d) *vs.* $[BPHA]^{\frac{1}{2}}$ is linear and passes through the origin (i_l is the limiting current obtained in 2 *M* sulfuric acid for 10^{-4} *M* titanium(IV) and increasing concentrations of BPHA, and i_d is the total current for titanium(IV) in the absence of BPHA. If the stoichiometric coefficient is accepted as 2, the ratio $i_l/i_d = 0.81\ (2kct)^{\frac{1}{2}}$ gives a value for k of $1.2 \cdot 10^3$ l mol^{-1} s^{-1} (Fig. 5).

The important point for analytical purposes is that the limiting current may be 35 times higher in the presence of BPHA than the diffusion current of titanium(IV) alone. Hydroxylamine increases the titanium(IV) wave by only 4-fold in oxalic acid medium[7].

In 2 *M* phosphoric acid solutions containing BPHA, the calculated rate constant is 290 mol^{-1} s^{-1} (Fig. 5). The rate constant k for the titanium(IV)–hydroxylamine reaction in 2 *M* phosphoric acid calculated by Saviant and Vianello[20] is 1.84 mol^{-1} s^{-1}.

ANALYTICAL APPLICATIONS OF THE TITANIUM WAVE

The results discussed above show that for the polarographic determination of low concentrations of titanium, the best supporting electrolyte consists of a (1+3) water–ethanol mixture containing 2 *M* sulfuric acid and 0.05 *M* BPHA. Under these conditions, the limiting current increases linearly with titanium(IV) concentration over the range 0–10^{-4} *M* (0–1·4 μA); it is possible to determine titanium(IV) in concentrations as low as $5 \cdot 10^{-6}$ *M*. As the titanium(IV) current in the absence of BPHA is very low compared to the catalytic current, the measurement of the limiting current is not affected. The current is constant for at least 1 h at constant temperature.

Interferences occur from Cd, Sn(II and IV), As(V), Mo(VI) and U(VI) (Table I). Although the $E_{\frac{1}{4}}$ value of the vanadium(V) wave is close to that of the titanium(IV) wave, no interference occurs at 10-fold levels of vanadium. The main interference is caused by molybdenum(VI); its maximum interferes with measurements even at $5 \cdot 10^{-6}$ *M* levels.

TABLE III

LIMITING RATIOS OF INTERFERING IONS FOR A MAXIMUM ERROR OF 5%

Ion	*Ion/Ti*
Mn(II), Zn(II), Al(III), or Fe(III)	100
Bi(III)	20
Pb(II), V(V), Cu(II), or Cr(VI)	10
Zr(IV)	5
U(V)	1
Sb(III), Mo, Cd	Interference

Other cations that form stable complexes with BPHA in this medium tend to decrease the limiting current of titanium(IV) only when they are present in large excess. Table III shows the limiting ratios of cation to titanium(IV) for a maximum error of $\pm 5\%$. The presence of strong oxidants, such as nitric acid, dichromate, permanganate and chlorate, does not increase the limiting current of titanium(IV), but the reduction current of 10^{-2} *M* dichromate affects the measurements.

The authors thank Dr. J. Kuta for valuable suggestions.

SUMMARY

The polarographic behavior of the titanium(IV)–N-benzoyl-N-phenylhydroxylamine (BPHA) system in acidic medium and in water–ethanol mixtures has been studied. In (1+3) water–ethanol containing 2 *M* sulfuric acid and 0.05 *M* BPHA, titanium(IV) gives a single kinetically controlled wave. Titanium(IV) can be determined at concentrations as low as $5 \cdot 10^{-6}$ *M*, in the presence of Fe(III), Cu(II), V(V), etc., but Cd(II), Sn(II and IV), As(V), U(VI) and Mo(VI) interfere.

REFERENCES

1 G. D. Lutwick and D. E. Ryan, *Can. J. Chem.*, 32 (1954) 949.
2 V. D. Vassilenko and G. S. Mazhavovskaya, *Ukr. Khim. Zh.*, 31 (*1*) (1965) 101.
3 A. D. Shendrikar, Ph.D. Thesis, Durham University, England, 1966.
4 F. Vernon and D. P. Hubbard, *Anal. Lett.*, 2 (*12*) (1969) 664.
5 I. V. Pyatnitskii and R. P. Ruzhanskaya, *Zh. Anal. Khim.*, 26 (1971) 1475.
6 J. E. Schwarberg and R. W. Moshier, *Anal. Chem.*, 34 (1962) 525.
7 A. Blazek and J. Koryta, *Collect. Czech. Chem. Commun.*, 18 (1953) 326.
8 J. Koryta, *Chem. Listy*, 48 (1954) 514.
9 V. E. Toropova, V. A. Vekslina and N. G. Chovnik, *Zh. Anal. Khim.*, 27 (1972) 346.
10 E. G. Chikryzova and Sya. Mashinskaya, *Zh. Anal. Khim.*, 26 (1971) 1105.
11 Ya. Y. Tur'yan and E. V. Saksin, *Zh. Anal. Khim.*, 25 (1970) 998.
12 E. V. Saksin and Ya. Y. Tur'yan, *Zh. Anal. Khim.*, 25 (1970) 2362.
13 U. Priyadarski and S. G. Tandon, *Anal. Chem.*, 33 (1961) 435.
14 E. M. Donaldson, *Talanta*, 17 (1970) 583.
15 J. Lingane and J. Kennedy, *Anal. Chim. Acta*, 15 (1956) 294.
16 G. M. Habashy, *Collect. Czech. Chem. Commun.*, 25 (1960) 3166; *Z. Anorg. Allg. Chem.*, 306 (1960) 302.
17 D. J. Kurbatov, *Izv. Sib. Otd. Akad. Nauk SSSR*, 10 (1958) 35.
18 Nec Che-Ming and Hang Shi-Chuan, *Acta Chim. Sinica*, 29 (1963) 403.
19 J. Koutecký, *Collect. Czech. Chem. Commun.*, 18 (1953) 331.
20 J. M. Saveant and E. Vianello, *Electrochim. Acta*, 10 (1965) 905.

Analytica Chimica Acta, 77 (1975) 9–17

SOME ALKYLPHOSPHORIC ACID ESTERS FOR USE IN COATED-WIRE CALCIUM ION-SELECTIVE ELECTRODES

PART II. SELECTIVITIES AND USE IN POTENTIOMETRIC TITRATIONS

R. W. CATTRALL and D. M. DREW*

Department of Inorganic and Analytical Chemistry, La Trobe University, Bundoora 3083, Victoria (Australia)

(Received 24th October 1974)

In Part I[1] the response characteristics of a series of coated-wire calcium-sensitive electrodes which were prepared from commercially available alkylphosphoric acids, were reported. In this paper, interference studies for these electrodes and the use of the electrodes as end-point sensors in potentiometric titrations are discussed.

The quantitative assessment of the selectivity of an electrode is difficult because there is no single, universally accepted method for carrying out the measurements, or for treating the results. Consequently, interference effects must be interpreted from selectivity ratios obtained by a variety of methods. The various methods for evaluating selectivities have been discussed by Moody and Thomas[2].

In this paper, the mixed solution technique[2,3] was applied, but for calculation of selectivity ratios, a modification of the equation used by Ross[4] was used.

THEORETICAL SECTION

The Eisenman equation[5] for determining the contribution made to the potential of a glass electrode by a monovalent interfering ion is well known:

$$E = E_0 + nRT/F \ln [a_m^{1/n} + (K_i a_i)^{1/n}] \quad (1)$$

where a_m and a_i are the ionic activities of the monovalent primary ion and interfering ion, respectively; K_i is a weighting factor which characterizes the selectivity; and n is an empirical constant which takes into account the "nonideal behaviour" of the exchanger. Eisenman used the separate solution technique in determining selectivities.

A second equation has been derived by Garrels *et al.*[6], and discussed in detail by Truesdell and Christ[7]. This accounts for the interference by any number of monovalent and divalent ions on a divalent ion electrode:

$$E = C_A + \frac{RT}{2F} \ln \left[\sum_{J=A}^{u} K_{AJ} \frac{[J^{Z+}]^{2/z}}{\lambda_{J_{2/z}X_2}} \right] \quad (2)$$

* Present address: Research Laboratory, Kodak (Australasia) Pty. Ltd., Coburg, Victoria 3058, Australia.

where J is any cation A to u of charge Z; C_A is a constant and λ is the rational activity coefficient of the ion attached to the ion-exchange site. In the derivation of eqn. (2), the following exchange equilibria were employed:

$$AX_{2(glass)} + 2\,J^{+}_{(aq)} \rightleftharpoons J_2X_{2(glass)} + A^{2+}_{(aq)} \quad (3)$$

$$AX_{2(glass)} + J^{2+}_{(aq)} \rightleftharpoons JX_{2(glass)} + A^{2+}_{(aq)} \quad (4)$$

Equation (3) appears unnecessarily idealistic in that two monovalent ions must occupy two exchange sites by the complete replacement of a divalent ion. A more realistic picture may involve a step-wise process where the initial step is the occupation of a single ion-exchange site by one monovalent ion, particularly in the case of chelating ion-exchangers.

Ross[4] employed another form of eqn. (2) to determine selectivity ratios by the mixed solution technique. Ross's equation is:

$$E_2 - E_1 = \frac{2.303\,RT}{nF}\log\left[1 + K_i\,\frac{a_i^{n/z}}{a_m}\right] \quad (5)$$

where E_2 is the potential of a mixed solution containing the primary ion and the interfering ion of activity a_m and a_i, respectively; E_1 is the potential of a solution containing only the primary ion of activity a_m; n and z are the charges on the primary ion and the interfering ion, respectively; and K_i is defined as the selectivity ratio.

Equation (5) is perhaps the most commonly used equation for determining single value selectivity ratios, and has been checked for many electrodes and many interfering ions at low levels of interference[8]. Bagg *et al.*[9], however, found that the results of selectivity determinations in mixed solutions of calcium chloride and alkali metal (and ammonium) chlorides or nitrates could not be satisfactorily fitted to eqn. (5) but produced good linear relationships when fitted to an alternative equation:

$$E_M = -\frac{RT}{F}\ln\left[1 + K_i\,\frac{a_i}{a_m^{\frac{1}{2}}}\right] \quad (6)$$

where E_M is the interference potential, defined as the difference between the observed biionic potential and the potential calculated assuming no interference; a_i and a_m have the same meanings as in eqn. (5).

In the present work, also, eqn. (5) sometimes produced selectivity ratios which were misleading in the analytical sense. The problem arises from the use of the power term n/z in the equation. For example, in the measurement of the interference of the sodium ion on one calcium-selective electrode, a potential difference $(E_2 - E_1)$ of 10 mV was obtained for solutions containing activities of the calcium ion and sodium ion of 10^{-4} M and 10^{-2} M, respectively. Calculation of the selectivity ratio by eqn. (5) gave a value of 1.15, which suggests that the electrode has a greater affinity for the interfering ion than for the primary ion. This is, of course, misleading, since the potential changed by only 10 mV for a 100-fold excess of the interfering ion, which itself suggests a quite small affinity of the electrode for the interfering ion.

This anomaly for mixtures of monovalent and divalent ions is even more pronounced for the case of mixtures of monovalent and trivalent ions. Harrell *et al.*[20]

investigated liquid membrane electrodes containing dinonylnaphthalene sulfonic acid for electrodes sensitive to trivalent ions and found that, for monovalent interfering ions, eqn. (5) gave values for the selectivity ratio of 100 to 1000 in cases where actual potential differences were only of the order of 2–3%. These results cast some doubts on the usefulness of eqn. (5) for determining selectivity ratios in cases where the primary ion and interfering ion differ in charge.

In general terms, the selectivity ratio of an interfering ion is a measure of the affinity of the exchange material for the interfering ion relative to the affinity for the primary ion. In many studies[2–4,9–19] the convention has been accepted that, for a primary ion and an interfering ion of the same charge, an electrode has equal affinity for both ions ($K_i = 1$) if the same measured potential is obtained for solutions of the primary ion and interfering ion which have the same activities. This is perfectly acceptable and straightforward. The situation is quite different, however, for the case of a primary ion and an interfering ion of different charges (because of the power term in eqn. (5)).

In view of these problems, the following general definition of equal affinity to describe all cases has been adopted in this paper: an electrode has an equal affinity for a primary ion and an interfering ion if the same measured potential is obtained for solutions of the primary ion and the interfering ion which have the same activities, regardless of the charges on the ions.

This definition gives rise to the following equation for the calculation of selectivity ratios:

$$E_2 - E_1 = \frac{2.303\,RT}{nF} \log\left[1 + K_i \frac{a_i}{a_m}\right] \tag{7}$$

It should be noted that the use of eqn. (7) gives a K_i value of 0.012 for the example discussed above for the interference of sodium on a calcium-selective electrode, which is a far more meaningful value for practical situations.

All K_i values reported in this paper have been calculated by eqn. (7).

EXPERIMENTAL

The preparation of the electrodes, the membrane compositions, and the sources and purities of all chemicals have been reported in Part I[1].

Determination of selectivity ratios

These were determined by measuring the cell potential for a pure calcium chloride solution (*e.g.* 10^{-3} *M*) followed by measurement of the cell potential for a solution containing a mixture of calcium chloride and the interfering salt (*e.g.* 10^{-3} *M* $CaCl_2 + 10^{-2}$ *M* MCl_n). The potential difference ($E_2 - E_1$) was corrected for variations in activity from ionic strength differences. The K_i values were then calculated from eqn. (7). Activities were calculated by the extended Debye–Hückel equation[21].

pH measurements

All pH measurements were made with a Radiometer pH meter model 28 in conjunction with a Titron combination glass/reference electrode. For studies of pH

effects, the pH of a 10^{-2} *M* calcium chloride solution was adjusted to about 1 with concentrated hydrochloric acid and the pH was then increased in increments of about 0.5 to a final value of 10.5–11 with aqueous ammonia or sodium hydroxide solution; the magnetic stirrer was stopped after each addition to allow the potential to stabilize.

Complexiметric titrations

In these studies, 10 cm^3 of a 10^{-2} *M* calcium chloride solution was adjusted to above pH 9.5 by addition of 1 cm^3 of an ammonia–ammonium chloride buffer or 2 *M* sodium hydroxide solution (depending on the sodium or ammonium ion interference), and titrated with a 10^{-2} *M* solution of the disodium salt of EDTA. Solutions were stirred except when potential readings were recorded.

RESULTS AND DISCUSSION

The selectivity ratios for nine interfering ions were studied for each of the electrodes described in Part I[1]. The results (Table I) indicate that very large changes in selectivity ratios are produced when the composition of the membrane is varied. This is not unexpected because Ross[8] demonstrated that, for the liquid-membrane calcium electrode, the selectivity ratios for alkaline earth ions were altered by changing the inert diluent. In general, Table I shows that sodium and potassium are the weakest interferents whereas the heavy metals lead and zinc frequently interfere very strongly.

Effect of plasticizer content

Decreasing the plasticizer (DEHEHP) content of the membrane from 65% to 55% (w/w) generally had the effect of reducing the interference of the strongly interfering ions (*e.g.* Zn^{2+}), but hardly altered the selectivity ratios for the weakly interfering ions (compare electrodes 14 and 15, and 27 and 28). The most dramatic effect was obtained by completely eliminating the plasticizer (DEHEHP) from the membrane. This increased the selectivity ratios for the weakly interfering ions and markedly decreased the interference caused by the strongly interfering ions (compare electrodes 4 and 16). In some cases (electrodes 2, 21, 24), the zinc interference was reduced to an insignificant amount.

Effect of reagent

The structure of the phosphoric acid ester used in the electrodes did not have a large effect on the selectivity ratios except perhaps for the commercial octylphenylphosphoric acid and the purified di-octylphenylphosphoric acid which produced electrodes with relatively low selectivity ratios for sodium, potassium, copper and lead (electrodes 7, 8, 23, 24 and 9, 25, 26).

Similarly, the form of the electroactive reagent had little effect, except in the case of zinc interference where very much lower selectivity ratios were observed when the normal calcium complex (CaX_2) was used instead of the calcium acid complex (CaH_2X_4) or the free acid ester (HX) (compare electrodes 14, 16 and 18, 20).

Effect of configuration

There was very little difference between the selectivity ratios obtained for

SELECTIVITY RATIOS (K_i) FOR THE CALCIUM-SELECTIVE ELECTRODES

Electrode number[a]	*Reagent*	*Composition*[a]	*Interfering ion*								
			Ba	*Mg*	*Ni*	*Sr*	*Na*	*K*	*Cu*	*Pb*	*Zn*
1	HDEHP	B	0.015	0.068	0.094	0.028	0.004	<0.001	0.440	4.06	38.8
2	HDEHP	E	0.403	0.197	0.650	0.399	0.010	0.045	2.11	2.69	<0.001
3[b]	HDEHP	A	0.009	0.050	0.028	0.024	0.003	0.023	4.95	46.2	69.6
4	HDOP	E	0.082	0.036	0.056	0.055	0.001	0.006	0.276	0.510	0.291
5[b]	HDOP	A	0.011	0.006	0.011	0.012	0.003	<0.001	1.50	5.29	15.9
6	IOPA	B	0.005	0.054	0.018	0.007	<0.001	<0.001	0.448	19.4	60.2
7	OPPA	B	0.038	0.052	0.012	0.025	<0.001	0.006	0.115	2.72	186.9
8[b]	OPPA	A	0.009	0.026	0.148	0.021	<0.001	<0.001	0.095	1.71	155.6
9	HDOPP	A	0.008	0.028	0.012	0.036	<0.001	0.061	0.170	1.65	168.6
10	H_2MOPP	I	0.004	0.022	0.012	0.028	0.003	<0.001	0.602	2.92	2.80
11	92-20-01	Orion liquid	0.002	0.010	0.009	0.015	0.003	<0.001	<0.001	2.06	0.248
12	HDEHP	D	0.012	0.032	0.017	0.050	<0.001	<0.001	1.35	22.2	196.5
13	HDEHP	F	0.436	0.189	0.524	0.492	0.028	0.189	2.11	3.35	0.271
14	HDOP	A	0.007	0.122	0.006	0.017	<0.001	<0.001	0.622	12.5	209.7
15	HDOP	B	0.004	0.118	0.005	0.008	<0.001	<0.001	0.498	3.81	54.5
16	HDOP	C	0.008	0.047	0.008	0.015	0.009	<0.001	2.27	4.10	12.8
17	HDOP	D	0.012	0.015	0.019	0.034	<0.001	<0.001	1.35	37.5	145.4
18	IOPA	A	0.018	0.005	0.003	0.011	<0.001	0.110	0.620	12.0	46.8
19	IOPA	G	0.004	0.002	0.008	0.020	<0.001	<0.001	0.776	36.1	131.5
20	IOPA	C	0.007	0.036	0.014	0.003	<0.001	<0.001	0.198	1.45	10.2
21	IOPA	F	0.276	0.140	0.314	0.512	0.037	0.138	2.31	0.755	<0.001
22[b,c]	IOPA	A	0.009	0.048	0.011	0.006	<0.001	<0.001	<0.001	<0.001	<0.001
23	OPPA	C	0.010	0.031	0.011	0.027	<0.001	<0.001	0.181	2.03	148.4
24	OPPA	F	0.417	0.133	0.858	0.672	0.022	<0.001	3.04	0.880	0.070
25	HDOPP	D	0.009	0.027	0.017	0.036	<0.001	<0.001	0.190	1.69	156.7
26	HDOPP	H	0.002	0.045	0.010	0.020	0.001	<0.001	0.040	0.680	969.9
27	H_2MOPP	A	0.002	0.018	0.011	0.022	0.011	<0.001	0.680	11.9	128.8
28	H_2MOPP	B	0.006	0.013	0.014	0.017	<0.001	0.005	0.254	3.37	18.9
29	H_2MOPP	J	0.022	0.016	0.008	0.009	0.002	0.038	90.2	0.050	0.110
30	H_2MOPP	K	0.582	0.454	0.262	0.496	0.087	0.185	2.83	0.200	0.420

[a] For the composition of the electrodes; see Part I[1].
[b] Moody configuration[16].
[c] This electrode was poisoned by soaking in a $CuCl_2$ solution, hence the K_i values are meaningless.

electrodes prepared by the technique of Moody *et al.*[16] and those obtained for coated wire electrodes, except for zinc, which tended to interfere more with the coated wire electrodes (compare electrodes 5 and 14).

The electrodes studied in this work and the commercial Orion liquid-membrane electrode (electrode 11) showed similar selectivity ratios for weakly interfering ions, but the selectivity ratios for copper, lead and, particularly, zinc were generally much lower for the Orion commercial electrode; however, when the secondary plasticizer (DEHEHP) was not added, selectivity was better than that of the Orion electrode, which suggests that DEHEHP complexes the heavy metals quite strongly.

These results show that it is possible to formulate calcium-sensitive polyvinyl chloride membranes for particular analytical applications, depending on which interfering ions are present in solution. For example, electrode 2 would be useful for determination of calcium in solutions containing quite high amounts of zinc, but would not be useful in solutions containing high amounts of copper, lead, nickel or alkaline earth metals. Electrode 7 would be useful in solutions containing copper, nickel and alkaline earth metals.

Hydrogen ion interference

Because of the acidic nature of the reagents used in this work, some degree of hydrogen ion interference was expected, but its extent would depend largely on the formation constant of the complex formed with calcium and on the acidity of the acid ester.

The hydrogen ion dependence (pH profile) of the Orion commercial liquid-membrane calcium electrode has been extensively studied[2,11,22]; the pH range where the potential is essentially constant is about 5–9.0. At about pH 4.5, there is a characteristic dip in the pH profile before the potential begins to increase owing to the large hydrogen ion interference at lower pH values. This effect has been discussed in detail by Růžička *et al.*[22], who related it to the extraction behaviour with organophosphate extractants, with which complexes of different stoichiometries can be extracted depending on the pH. The dip in the pH profile was observed in the present work for di-(2-ethylhexyl)-phosphoric acid at pH 4.5–5.0, which is the

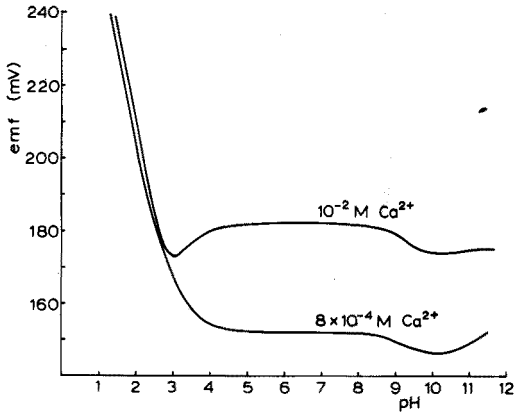

Fig. 1. pH profiles for electrode 7.

same region where the maximum occurs in the extraction of calcium by the reagent in benzene solution[23].

A representative pH profile is shown in Fig. 1 for electrode 7 for two calcium ion concentrations (10^{-2} *M* and $8 \cdot 10^{-4}$ *M*). The range of pH-independent behaviour is about 4–8.5; for the higher calcium ion concentration, the characteristic dip in the pH profile occurs at about pH 3.

TABLE II

REGIONS OF pH-INDEPENDENT BEHAVIOUR

Electrode no.	*Reagent*	*pH Region*	*Electrode no.*	*Reagent*	*pH Region*
1	HDEHP	5.0–8.0	16	HDOP	5.5–9.0
2	HDEHP	4.5–8.0	17	HDOP	5.0–9.0
3	HDEHP	6.0–9.0	18	IOPA	6.0–8.5
4	HDOP	5.0–7.5	19	IOPA	5.5–9.0
5[a]	HDOP	—	20	IOPA	5.5–7.5
6	IOPA	5.5–9.0	21	IOPA	5.5–8.5
7	OPPA	4.5–8.0	22[a]	IOPA	—
8	OPPA	4.0–8.5	23	OPPA	3.5–8.0
9	HDOPP	3.5–9.0	24	OPPA	6.5–9.0
10	H_2MOPP	4.0–8.5	25	HDOPP	4.0–8.0
11	92-20-01	5.0–9.0	26	HDOPP	4.5–7.5
12[a]	HDEHP	—	27	H_2MOPP	4.5–9.0
13	HDEHP	4.5–6.0	28	H_2MOPP	5.5–8.5
14	HDOP	6.5–10.0	29	H_2MOPP	5.5–8.0
15	HDOP	6.0–9.0	30[a]	H_2MOPP	—

[a] These electrodes gave no region of pH-independent behaviour.

The pH profiles for the electrodes are summarized in Table II in terms of the range of pH-independent behaviour. It can be seen that, except for electrodes 5, 12, 22 and 30, quite large ranges of pH-independent behaviour are obtained. It is interesting to note that the region of pH-independent behaviour for the electrodes containing the octylphenylphosphoric acids extends to a significantly lower value than for the other reagents. This suggests that the calcium complexes with the octylphenylphosphoric acids have considerably higher stability constants than the other complexes.

The decrease in potential in the pH region 8.5–9.0 (Fig. 1) is attributed to the hydrolysis of calcium. The increase in potential after pH 10 is due to ammonium ion interference; it was less serious when the pH was adjusted with sodium hydroxide, which reflects the much lower sodium ion interference observed for the electrodes.

Complexiметric titrations

The use of the calcium-sensitive electrodes for determining the end-point in the potentiometric titration of calcium with EDTA was investigated. The titration curve for electrode 7 is shown in Fig. 2; the potential drop was about 35 mV at the end-point (± 0.5 cm^3), hence electrode 7 was most suitable for use in a

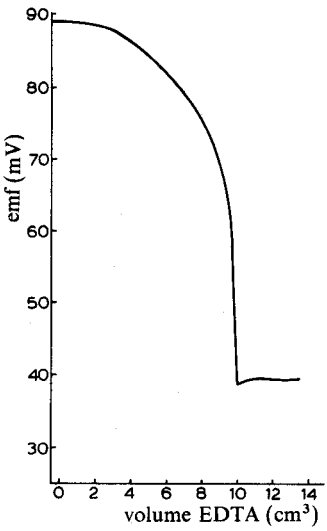

Fig. 2. Titration curve for 10^{-2} *M* $CaCl_2$ (electrode 7).

potentiometric titration under the conditions described. The only other electrodes which showed potential changes of 20 mV or greater at the end-points were 1, 7–11, 23 and 25–29. This group, which includes the Orion commercial liquid electrode, consists largely of electrodes prepared from octylphenylphosphoric acids.

All the results obtained in this work suggest that these reagents are the most satisfactory for use in the preparation of calcium-selective electrodes; similar observations have been made by Růžička *et al.*[22] for di-(n-octylphenyl)phosphoric acid in a calcium-sensitive electrode using a polyvinylchloride film and the Selectrode technique.

We are grateful to the Australian Research Grants Committee for financial support, and one of us (D.M.D.) wishes to thank Kodak (Australasia) Pty. Ltd. for generous leave of absence.

SUMMARY

The interferences of a range of ions (including the hydrogen ion) on the potential responses of a series of coated-wire calcium-selective electrodes are reported. The extent of the interferences is discussed as a function of the composition of the PVC membranes. The use of these electrodes as end-point sensors in potentiometric titrations of calcium with EDTA is also reported.

REFERENCES

1 R. W. Cattrall, D. M. Drew and I. C. Hamilton, *Anal. Chim. Acta*, 76 (1975) 269.
2 G. J. Moody and J. D. R. Thomas, *Selective Ion Sensitive Electrodes*, Merrow, Watford, 1970, Ch. 2.
3 G. J. Moody and J. D. R. Thomas, *Talanta*, 19 (1972) 623.
4 J. W. Ross, *Science*, 156 (1967) 1378.

5 G. Eisenman, D. O. Rudin and J. U. Casby, *Science*, 126 (1957) 831.
6 R. M. Garrels, M. Sato, M. E. Thompson and A. H. Truesdell, *Science*, 135 (1962) 1045.
7 A. H. Truesdell and C. L. Christ in G. Eisenman (Ed.), *Glass Electrodes for Hydrogen and Other Ions*, M. Dekker, New York, 1967, p. 295.
8 J. W. Ross in R. A. Durst (Ed.). *Ion Selective Electrodes*, National Bureau of Standards Special Publication No. 314, U.S. Gov. Print. Off., Washington, D.C., 1969, Ch. 2.
9 J. Bagg, O. Nicolson and R. Vinen, *J. Phys. Chem.*, 75 (1971) 2138.
10 J. Bagg and G. A. Rechnitz, *Anal. Chem.*, 45 (1973) 271, 1069.
11 J. Bagg and R. Vinen, *Anal. Chem.*, 44 (1972) 1773.
12 J. Bagg and W. P. Chaung, *Aust. J. Chem.*, 24 (1971) 1963.
13 E. Pungor and K. Toth, *Anal. Chim. Acta*, 47 (1969) 291; *Analyst (London)* 95 (1970) 625.
14 R. W. Cattrall and H. Freiser, *Anal. Chem.*, 43 (1971) 1905.
15 H. James, G. Carmack and H. Freiser, *Anal. Chem.*, 44 (1972) 853.
16 G. J. Moody, R. B. Oke and J. D. R. Thomas, *Analyst (London)*, 95 (1970) 910.
17 S. Back and J. Sandblom, *Anal. Chem.*, 45 (1973) 1680.
18 M. Whitfield and J. V. Leyendekkers, *Anal. Chim. Acta*, 46 (1969) 63.
19 K. Srinivasan and G. A. Rechnitz, *Anal. Chem.*, 41 (1969) 1203.
20 J. B. Harrell, A. D. Jones and G. R. Choppin, *Anal. Chem.*, 41 (1969) 1459.
21 R. G. Bates, B. R. Staples and R. A. Robinson, *Anal. Chem.*, 42 (1970) 867.
22 J. Růžička, E. H. Hansen and J. Chr. Tjell, *Anal. Chim. Acta*, 67 (1973) 155.
23 W. J. McDowell and C. F. Coleman, *J. Inorg. Nucl. Chem.*, 28 (1966) 1083.

Analytica Chimica Acta, 77 (1975) 19–27

AN INVESTIGATION OF POLYPHENYL-ONIUM BASES AND OTHER MATERIALS FOR PHOSPHATE ION-SELECTIVE ELECTRODES

M. NANJO, TIMOTHY J. ROHM* and GEORGE G. GUILBAULT

Department of Chemistry, University of New Orleans, Lakefront Campus, New Orleans, Louisiana 70122 (U.S.A.)

(Received 30th November 1974)

Electrodes are now available or can be constructed for a wide variety of anions, cations, dyes, surfactants, antibiotics, and vitamins. This increase in the production of ion-selective electrodes has accompanied a renewed interest in analytical potentiometry which has been largely the result of work by Eisenman and Pungor. The field is expanding rapidly and one of the objectives of on-going research is the development of an electrode that is sensitive and selective for phosphate ion. Since most analyses for phosphate involve the measurement of orthophosphate ion, an electrode that responds to this ion would be one of the most practical types and would find immediate application in the areas of environmental and clinical chemistry.

The earliest report of the development of an ion-selective electrode for phosphate was made by Pungor *et al.*[1]. Their electrode consisted of bismuth phosphate in a silicone rubber membrane. Rechnitz *et al.*[2] reported that this device had potential drifts of 1 mV per 10 min and did not show the required selectivity for phosphate.

The phosphate-complexing ability of the heteropoly compounds, 12-molybdophosphoric acid and 12-tungstophosphoric acid, was investigated for the construction of liquid ion-selective electrodes for phosphate by Guilbault and Brignac[3]. Their electrodes also did not possess the desired selectivity for phosphate ion.

Nagelberg *et al.*[4] prepared divalent phosphate electrodes from Aliquat 336 (methyltricaprylammonium chloride) and a primary amine (XLA3, Rohm and Haas). They stated that these electrodes showed linear response to monohydrogenorthophosphate even in the presence of 10 meq l^{-1} chloride[4]. The amines were used in the chloride form to prepare liquid ion-exchange electrodes.

Various inorganic phosphate salts impregnated in silicone rubber were used to prepare electrodes sensitive to phosphate ion by Guilbault and Brignac[5]. Although the electrodes showed Nernstian response to phosphate ion, they were not selective.

Shu and Guilbault[6] reported a phosphate-sensitive polymer of silver, thiourea and glutaraldehyde which is precipitated with dibasic phosphate (PCPX-1). They used this material with silver sulfide to prepare solid electrodes with selectivity

* Present address: The Procter and Gamble Company, Sharon Woods Technical Center, Cincinnati, Ohio 45241, U.S.A.

for monohydrogenphosphate over other anions such as sulfate, nitrate and acetate. However, the lifetime of the electrode was short (48 h). Pungor *et al.*[7] reported that silver ion reacts with thiourea to produce silver sulfide and silver cyanamide. This reaction is a probable cause of the loss of activity of the PCPX-1 electrode.

Quaternary compounds have been used successfully in the commercial (Orion) liquid ion-selective electrode for chloride ion. Coetzee and Freiser[8] prepared liquid ion-selective electrodes for several common inorganic anions as well as for organic anions from Aliquat 336S which had been converted to the proper quaternary ammonium salt by shaking with an aqueous solution of the salt of the anion under investigation. These authors did not report using the above procedures to prepare a phosphate electrode although phosphate was mentioned as a minor interference with a perchlorate electrode.

In the present study, results of tests of liquid-ion exchange electrodes prepared from quaternary ammonium, phosphonium and arsonium salts as well as organic tin salts are presented. Attempts to prepare electrodes from benzidine phosphate and hexamminocobalt(III) nitrate are also reported.

EXPERIMENTAL

All reagents used were of analytical-reagent grade and unless noted were used without further purification. Doubly distilled water was used to prepare all solutions.

Preparation of precipitate electrodes

Benzidine phosphate and sulfate were prepared by adding phosphoric acid and sulfuric acid respectively to an ethanolic solution of benzidine. The precipitates were washed several times with ethanol and water, and then dried at 100°C.

Hexamminocobalt(III) nitrate $[Co(NH_3)_6](NO_3)_3$ was prepared by a method listed in *Inorganic Syntheses*[9].

These salts were then mixed with silicone rubber (Dow Corning 3140 RTV) in a 1:1 weight ratio. The pastes obtained were pressed between glass plates which had been coated with paraffin. After drying (approximately 3 days were required), circles of 8-mm diameter were cut from the material and sealed to the end of glass tubes with silicone rubber adhesive. The tubes were then filled with a solution which was 0.05 *M* in monohydrogenphosphate and 0.05 *M* in chloride. A strip of silver foil wedged in the tube with a rubber stopper was used as the electrode lead.

Preparation of liquid ion exchange membrane electrodes

Electrode A. The outer chamber of a commercial (Orion-92) electrode was filled with Aliquat 336 solution (General Mills); and the inner chamber with 0.1 *M* $NaHPO_4$. A perchlorate-type porous membrane (Orion 92-81-04) was used in the electrode body. The same electrode body and the same porous membranes were used to prepare all of the following electrodes.

Electrode B. This was similar to electrode A except for a 0.1 *M* NaCl internal filling solution.

Electrode C. Tri-n-octylpropylammonium bromide dissolved in octanol (10%

by weight) was used as the external filling solution (the liquid ion exchanger), with 0.1 *M* $NaHPO_4$ internal filling solution.

Electrode D. The external filling solution was prepared by vigorously shaking a solution of 5 ml of tri-n-octylamine in 10 ml of octanol with a solution containing 2 ml of 85% phosphoric acid in 25 ml of water. The internal reference solution used was 0.1 *M* phosphoric acid in KCl–HCl buffer, pH 2.1.

Electrode E. Aliquat 336 was converted to the dihydrogenphosphate form by repeated shaking of a solution of 2 ml of the quaternary salt in 8 ml of octanol with 10 ml portions of 1.0 *M* NaH_2PO_4. This material was used as the external filling solution, and a solution that was 0.05 *M* in chloride and 0.05 *M* in dihydrogenphosphate was used as the internal reference solution.

Electrode F. This electrode had an external filling solution of triphenylethylphosphonium bromide (10% by weight in octanol) and an internal filling solution that was 0.05 *M* in chloride and 0.05 *M* in dihydrogenphosphate.

Electrode G. This device was the same as electrode F except that the quaternary salt was converted to the dihydrogenphosphate form by repeated shaking with a solution of 1.0 *M* NaH_2PO_4.

Electrode H. Triphenylbenzylphosphonium chloride was prepared by refluxing 26 g of triphenylphosphine and 8 ml of benzyl chloride in 100 ml of benzene for 4 h. After several washes with benzene, the salt was dried and a 10% (w/w) solution in octanol was prepared and converted to the dihydrogenphosphate form in the usual manner. This solution was used as the external filling solution with a 0.05 *M* chloride–0.05 *M* dihydrogenphosphate internal filling solution.

Electrode I. The external filling solution was prepared by repeated shaking of a 10% (w/w), solution of tetraphenylphosphonium bromide with 1.0 *M* dihydrogenphosphate. The internal filling solution was 0.05 *M* chloride–0.05 *M* dihydrogenphosphate.

Electrode J. Triphenyltin hydroxide was prepared from triphenyltin chloride (Eastman Kodak), and converted to the dihydrogenphosphate form by repeated shaking of a solution (10% w/w MIBK solution) with 50 ml of 0.25 *M* KH_2PO_4 at pH 4.0. This liquid ion exchanger–MIBK solution was used as the external filling solution and an internal reference solution was a 0.1 *M* KCl–KNO_3 mixture.

Electrode J'. Triphenyltin dihydrogenphosphate was diluted (1+9) with MIBK; the inner filling solution was the same as in electrode J.

Electrode K. The external filling solution was prepared by mixing the triphenyltin dihydrogenphosphate–MIBK solution and Millipore Filter (HAWPO-4700, Millipore Filter Co.). This mixing procedure gave a viscous liquid to prevent the loss of liquid through the membrane; the electrode showed more reproducible readings and longer lifetime than electrode J. In this case only, a Millipore membrane was used instead of the perchlorate type porous membrane. The internal filling solution was 0.05 *M* tris sulfate buffer, pH 8.2.

Electrode L. This electrode was prepared with a nitrobenzene solution of triphenyltin dihydrogenphosphate; this liquid ion exchanger was saturated with triphenyltin hydroxide powder. The internal reference filling solution was a 0.05 *M* tris sulfate buffer, pH 8.2.

Procedures

All solutions of anions were prepared by serial dilution of 1.0 *M* stock solutions, without the buffer, unless specified. The sodium or potassium salts of the anions were used to prepare the stock solution unless otherwise indicated.

All potential and pH measurements were made with an Orion Model 110 digital pH/mV meter. The reference electrode used was a S.C.E. to which was added a salt bridge at room temperature ($23 \pm 2°C$). The salt bridge consisted of a 1-mm thick disc of porous Vycor (Corning) *ca.* 8 mm in diameter sealed to the end of a glass tube with silicone rubber adhesive. The salt bridge was filled with 0.05 *M* KCl–0.05 *M* NaH_2PO_4.

RESULTS AND DISCUSSION

Precipitate electrodes

Benzidine phosphate, benzidine sulfate and hexamminocobalt(III) nitrate did not show response to solutions of orthophosphate (10^{-1}–10^{-4} *M*) which were adjusted to pH 2.1 and 7.1. These electrodes had a very high resistance and the measurements made with these devices were erratic and irreproducible.

Quaternary ammonium salt electrodes

The quaternary ammonium compounds, owing to their high molecular weight and water-insoluble characteristics, are useful in the separation of simple[10] or complex anions and have been used successfully in the commercial liquid ion-selective electrodes.

In this work, Aliquat 336, tri-n-octylpropylammonium bromide and tri-n-octylamine were examined for a phosphate-selective electrode. Electrodes A and B, prepared from Aliquat 336, showed only limited response when tested with

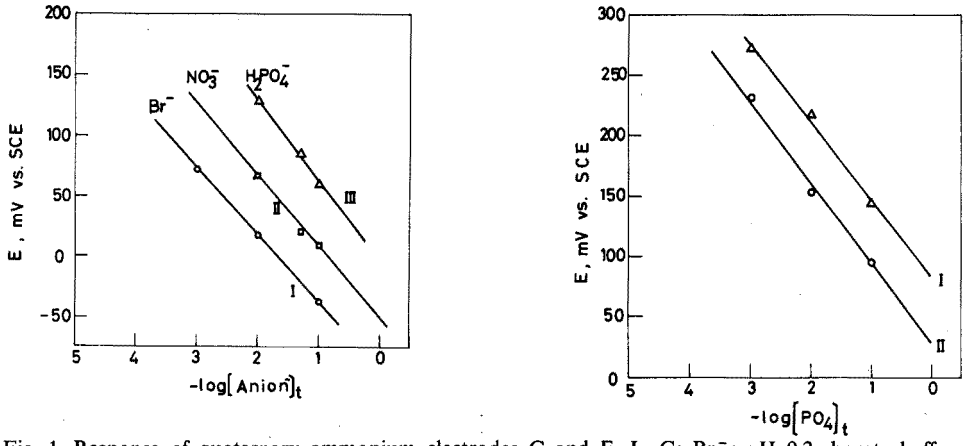

Fig. 1. Response of quaternary ammonium electrodes C and E. I=C: Br^-; pH 9.2; borate buffer; slope 54 mV/decade. II=E: NO_3^-; no buffer; slope 59 mV/decade. III=E: H_2PO_4; pH 5.0; no buffer; slope 70 mV/decade.

Fig. 2. Response of phosphonium electrodes F and I. I=F: pH 4.0; no buffer; slope 68 mV/decade. II=electrode I; pH 4.0; no buffer; slope 64 mV/decade.

solutions of orthophosphate (10^{-2}–10^{-4} *M*) which were buffered at pH 7.1 with tris sulfate buffer. Sulfuric acid was used as the mineral acid in the buffer in order to eliminate the interference by chloride reported by Nagelberg *et al.*[4]. Electrode C, prepared from trioctylpropylammonium bromide, showed only limited response when tested with orthophosphate solutions, but good response to bromide ion (Fig. 1, I). This electrode closely resembles the electrodes prepared by Coetzee and Freiser[8], and the response to bromide by this electrode parallels their results.

Electrode D exhibited little response when tested in solutions of orthophosphate which were adjusted to pH 7.1 with tris sulfate. The same electrode did respond to orthophosphate at pH 2.1 (HCl–KCl buffer), but the dynamic range was limited and repetitive measurements of the potential of the same solution differed by ± 3 mV even after prolonged soaking in 10^{-1} *M* phosphate solution.

Electrode E, prepared with Aliquat 336 that had been converted to the phosphate form, was sensitive to orthophosphate at pH 5.0 and to nitrate ion at pH 6.0, as can be seen in Fig. 1 (II and III). A comparison of the potentials obtained in solutions of phosphate and nitrate ion of the same concentration indicates that nitrate would be a serious interfering ion with this electrode. Solutions of orthophosphate (10^{-1}–10^{-3} *M*) which were 0.25 *M* in nitrate, had identical potentials when this electrode was tested in them.

In summary, the bulky quaternary ammonium salts do not show any selectivity for phosphate ion. Also, the potentials obtained from various anions could not be correlated with the solvent extraction parameter log *D*.

Quaternary phosphonium salt electrodes

Certain quaternary phosphonium compounds have found wide use in anion extraction, just like the ammonium salts. In this study, three phosphonium salts, tetraphenyl bromide, triphenylethyl bromide and triphenylbenzyl chloride, were tested for phosphate ion selectivity.

Electrode F, prepared from triphenylethyl bromide, showed only limited response to solutions of phosphate over the concentration range 10^{-1}–10^{-3} *M*, as shown in Fig. 2, I. However, conversion of the quaternary salt to the dihydrogenphosphate form (electrode G) made the electrode respond to solutions of dihydrogenphosphate. These results as well as those obtained in solutions containing other anions are given in Table I. Electrode G was used for several days during which the potential recorded for the 10^{-1} *M* dihydrogenphosphate

TABLE I

SELECTIVITY OF PHOSPHONIUM SALT TYPE ELECTRODES AT pH 4.0

Anions	*Potential observed for 0.1 M anion solution (mV)*		
	ϕ_4PBr	$\phi_3PCH_2\phi Cl$	$\phi_3PCH_2CH_3Br$
$H_2PO_4^-$	143	120	95
Cl^-	48	28	−20
SO_4^{2-}	124	130	114
NO_3^-	21	5	11
OAc^-	65	—	—

solution drifted, but the differences between the potentials measured in the various solutions remained constant. The lower potential measurements obtained in solutions of nitrate, chloride and hydrogenphthalate ions indicate poor selectivity of this electrode for phosphate ion.

Electrode H, prepared with triphenylbenzyl chloride as the liquid ion-exchanger, responded only slightly to changes in phosphate concentration. This electrode was not tested in solutions of other anions.

When tetraphenylphosphonium bromide was converted to the dihydrogenphosphate form and used as the liquid ion-exchanger in electrode I, the device responded to phosphate ion (Fig. 2, II) and to several other common anions as shown in Table I. Again, the lower potential readings of most of the anions tested *versus* those obtained in phosphate solution of the same concentration indicate serious interference by these anions.

The orders of selectivity obtained from electrodes F and I were as follows:

(a) electrode F: $Cl^- > NO_3^- > H_2PO_4^- > SO_4^{2-}$

(b) electrode I: $NO_3^- > Cl^- > OAc^- > SO_4^{2-} > H_2PO_4^-$

In an extraction study of the tetraphenylphosphonium cation in chloroform, the order of log D for extractions of various anions has been reported[10] as: $NO_3^- > Cl^- > H_2PO_4^- > SO_4^{2-}$, indicating considerable similarity between the response of the electrode and the extraction process. The substitution of a phenyl group on the normal alkyl chain did not improve the phosphate ion selectivity.

Although the quaternary phosphonium electrodes were not overly selective for phosphate ion (electrodes G and I), they did show better response and selectivity than the corresponding quaternary ammonium compounds. This trend is indicated by the extraction coefficients of phosphate ion by the various quaternaries that have been published[10].

Attempts to prepare electrodes from triphenylbenzylarsonium chloride, also failed to produce a phosphate-selective electrode.

Triphenyltin electrodes. Other polyphenyl-onium bases which are useful as liquid ion-exchangers, are the triphenyltin compounds. Indeed, the triphenyltin cation is known to be one of the better anion extraction reagents[10].

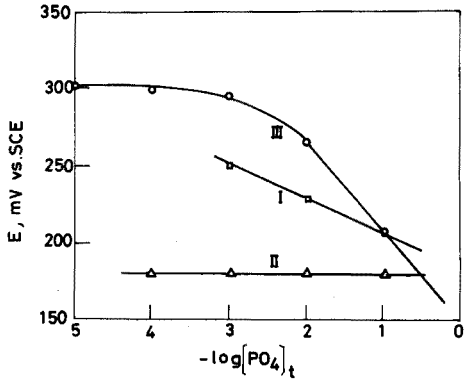

Fig. 3. Response of triphenyltin electrodes J and J'. I=J': pH 4.0 in 0.1 M acetate buffer; slope 46 mV/decade. II=J': pH 4.0 in 0.1 M KNO_3–0.1 M acetate buffer. III=J: pH 7.4 in 0.1 M Na_2SO_4; slope 60 mV/decade.

Schweitzer and McCarty[11] have reported the superior ability of the triphenyltin cation in MIBK solution to extract phosphate ion rather than other common anions at pH 4.0; the triphenyltin ion extracted phosphate ions ten times better than chloride or bromide ions at pH 4.0.

Figure 3, curve I, shows the response of electrode J', indicating a 46 mV/decade slope for dihydrogenphosphate at pH 4.0 in 0.1 *M* acetate buffer. However, the phosphate response measured in 0.1 *M* potassium nitrate at the same pH gave no potential change with change in phosphate concentration, as shown in Fig. 3, curve II. Electrode J, which has ten times more concentrated triphenyltin dihydrogenphosphate, also suffered from nitrate ion interference, but sulfate ion did not seriously interfere with the phosphate ion response, as shown in curve III.

Soaking of electrode J in a triphenyltin dihydrogenphosphate–MIBK solution was necessary to obtain a reproducible response. The selectivity of this electrode was poor in contrast with the reported data of an extraction study[11]. Another problem was the slow response of the electrode when the phosphate ion was changed from higher to lower concentration (about 20 min was necessary to obtain an equilibrium potential).

Electrode K was prepared to try to achieve an electrode with a rapid response time and which did not require extensive pre-soaking. Some improvement was obtained, but there was little selectivity for phosphate. Figure 4, curve I, is a typical calibration curve for phosphate ion obtained with electrode K at pH 4.0. A better selectivity for chloride ion was observed at every concentration measured. However, at pH 8.2, the response to phosphate ion became very small, 17 mV/decade, owing to the formation of HPO_4^{2-} species, and, as can be seen from Fig. 5, the phosphate and chloride ion response curves (I and II) crossed in the middle; a slightly better selectivity for phosphate over chloride was obtained at

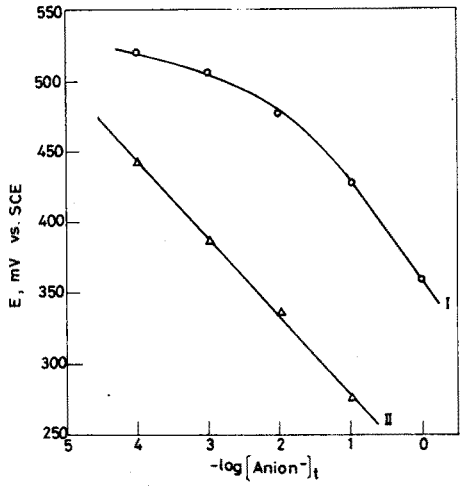

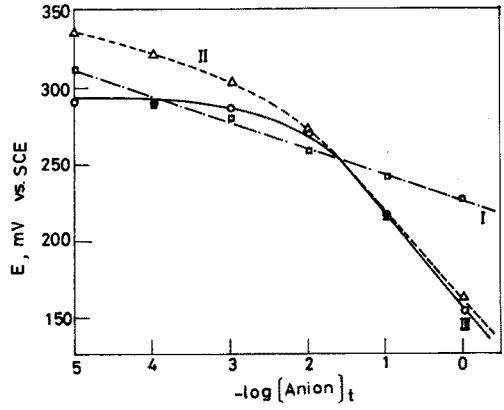

Fig. 4. Response of triphenyltin electrode K at pH 4.0. I = $H_2PO_4^-$: no buffer, pH adjusted by H_3PO_4 and NaOH; slope 71 mV/decade. II = Cl^-: no buffer, pH adjusted by HCl and NaOH: slope 54 mV/decade.

Fig. 5. Response of triphenyltin electrode K at pH 8.2. I = HPO_4^{2-}: no buffer; slope 17 mV/decade. II = Cl^-: 0.01 *M* phosphate buffer; slope 63 mV/decade. III = Cl^-: no buffer; slope 60 mV/decade.

concentrations below 10^{-2} *M*. Curve III was measured in chloride solution which contained 0.01 *M* phosphate. Below 10^{-2} *M* chloride, the potential was determined by the background phosphate ion, 0.01 *M*.

Several different solvents for the triphenyltin dihydrogenphosphate liquid ion-exchanger solution were tested to try to obtain phosphate selectivity: octanol, nitrobenzene, MIBK–octanol and MIBK–nitrobenzene mixtures were used. Electrode L, with nitrobenzene as solvent, gave the response curve shown in Fig. 6, which indicates poor phosphate selectivity, even at pH 4.0 where selectivity

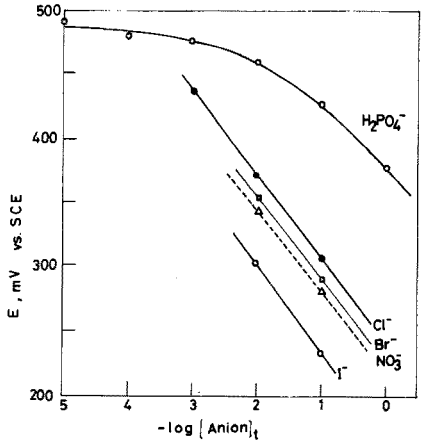

Fig. 6. Response of triphenyltin electrode L at pH 4.0. Slopes: Cl^-, 68 mV; Br^-, 63 mV; I^-, 7 mV; NO_3^-, 63 mV; $H_2PO_4^-$, 50 mV.

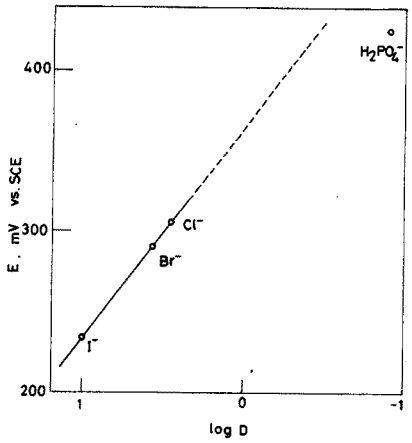

Fig. 7. Correlation curves of log *D* and electrode potentials measured by electrode L. Measuring solution: 0.1 *M*, pH 4.0. Log *D* taken from ref. (12).

for phosphate was obtained in the case of the extraction study[11]. The order of selectivity obtained was as follows:

$$I^- > NO_3^- > Br^- > Cl^- > H_2PO_4^- .$$

This order is closely related with the extraction study reported by Bock *et al.*[12]. Figure 7 shows the correlation between log *D* in nitrobenzene and the electrode potential obtained in 0.1 *M* solutions of each anion. As can be seen, monovalent anions, chloride, bromide and iodide fall on a straight line (slope 129 mV/decade), and monovalent phosphate ion ($H_2PO_4^-$ at pH 4.0) is located near that line. On the other hand, a divalent anion, sulfate, at pH 4.0, showed no correlation on that plot (log $D = ca. -3$, $E = +406$ mV).

CONCLUSION

Preparations of benzidine sulfate, benzidine phosphate and hexammino-cobalt(III) nitrate in silicone rubber proved unsatisfactory as electrode materials because of very high resistances.

Liquid ion-exchange electrodes prepared from quaternary ammonium salts exhibited only limited response to decade changes in the concentration of

orthophosphate. This type of electrode, however, showed Nernstian response to bromide in this study. Other authors have reported similar responses to halides by electrodes of these materials[8]. Electrodes prepared from quaternary phosphonium salts showed greater sensitivity to changes in phosphate concentration but lacked the selectivity necessary to make the devices practical for phosphate measurements.

Likewise, the triphenyltin electrode was found to lack phosphate selectivity. A linear relationship between log D and the selectivity of the anions measured by electrode K was obtained, which indicates that the most highly extractable anion also gives the better electrode response.

The financial assistance of the Environmental Protection Agency (Grant No. R-800359) is gratefully acknowledged.

SUMMARY

Precipitate-type electrodes (benzidine sulfate or phosphate and hexamminocobalt(III) nitrate in silicone rubber), and liquid ion-exchanger electrodes based on quaternary ammonium and phosphonium and triphenyltin salts were tested for the assay of phosphate ions. Good sensitivity was achieved with the phosphonium and triphenyltin salts, but both lacked sufficient selectivity for routine assays.

REFERENCES

1 E. Pungor, K. Toth and J. Havas, *Mikrochim. Acta*, 4 (1966) 689.
2 G. Rechnitz, Z. F. Lin and S. B. Zamochnick, *Anal. Lett.*, 1 (1967) 29.
3 G. G. Guilbault and P. J. Brignac, Jr., *Anal. Chim. Acta*, 56 (1971) 139.
4 I. Nagelberg, L. Braddock and G. Barbero, *Science*, 166 (1969) 1403.
5 G. G. Guilbault and P. J. Brignac, Jr., *Anal. Chem.*, 41 (1969) 1136.
6 F. R. Shu and G. G. Guilbault, *Anal. Lett.*, 5 (1972) 559.
7 M. Papay, K. Toth and E. Pungor, *Anal. Chim. Acta*, 56 (1971) 291.
8 C. J. Coetzee and H. Freiser, *Anal. Chem.*, 5 (1972) 559.
9 J. B. Work, *Inorganic Synthesis, Vol. II*, McGraw–Hill, New York, 1946, p. 221.
10 Y. Marcus and I. Kertes, *Ion Exchange and Solvent Extraction of Metallic Complexes*, Wiley–Interscience, New York, 1969, p. 796.
11 G. K. Schweitzer and S. W. McCarty, *J. Inorg. Nucl. Chem.*, 27 (1965) 191.
12 R. Bock, H. T. Niederauer and K. Rehrends, *Anal. Chem.*, 190 (1962) 33.

Analytica Chimica Acta, 77 (1975) 29–36

EFFECT OF SAMPLE PREPARATION ON BLOOD LEAD VALUES*

PAUL BAILY and TERENCE A. KILROE-SMITH

Department of Biochemistry, National Research Institute for Occupational Diseases, South African Medical Research Council, P.O. Box 4788, Johannesburg 2000 (South Africa)

(Received 10th December 1974)

The numerous methods suggested since 1968 for the preparation of samples for the determination of blood lead values bear testimony to the difficulties inherent in this particular determination. These difficulties have been increased greatly with the introduction of flameless atomic absorption techniques based on either the Massmann cuvette[1] or the carbon rod atomizer[2]. Since the graphite cuvette or the carbon rod techniques are more sensitive by several orders of magnitude than the conventional flame technique, further difficulties such as spectral and chemical interferences have been introduced.

Suggested preparative methods have ranged from low-temperature ashing techniques (such as that developed by Gleit[3], which is slow and may cause losses and contamination) to wet digestion of the sample with aqua regia (as carried out by Rose and Willden[4]). Despite the considerable purity of modern analytical reagents, the introduction of impurities from these reagents is still an ever-present problem.

Extracting elements into methyl isobutyl ketone with the chelating agent ammonium pyrrolidinedithiocarbamate (APDC) has long been practised. Malissa and Schoffman[5] showed that APDC reacts with over 30 metals. However, Manning and Fernandez[6] considered that the precision of atomic absorption with organic solvents was less than for aqueous solutions; there was about a relative standard deviation of 15%. The poorer precision was attributed to the soaking of the solution into the graphite tube. Several workers, *e.g.* Matousek and Stevens[7] and Rosen[8], used xylene to prevent the sample from soaking into the rod or cuvette; but Kubasik *et al.*[9] found that the application of 1–2 μl of xylene to the carbon rod before the blood sample was introduced did not prevent the sample from soaking into the rod.

The present work shows the results obtained by preparing, in 7 different ways, a sample of blood from a patient exposed to lead. For every preparation procedure, the final dilution of the blood was 10-fold. Most consistent and accurate results for lead in blood were obtained by a modification of the Einarsson and Lindstedt[10] non-extraction flame method. This modified technique has now been adapted to the Massmann cuvette[1], thus increasing the sensitivity of this deter-

* This paper was presented in part at the Fourth International Conference on Atomic Spectroscopy and the Twentieth Canadian Spectroscopy Symposium, Toronto, 1973.

mination by a factor of 1000. It is also shown that automatic background correction cannot be applied to curved calibration graphs.

EXPERIMENTAL

Instrumentation

A Beckman Model 444 double-beam atomic absorption spectrophotometer was equipped with a Varian-Techtron hollow-cathode lead lamp as light source operated at 10 mA. A fast-response Beckman 10-in. flatbed recorder provided permanent records of all traces. The response time for the 50-Hz model was less than 0.6 s for full-scale travel. Power was supplied to the Massmann-cuvette by a Beckman Model GRM1268 unit with variable time and temperature selectors for sequentially drying, charring and atomizing the samples. A fourth stage was also used after each analysis to "burn-out" the cuvette and ensure that it was free from any contaminating residues.

The graphite tubes (Ringsdorf-Werke, GMBH, Bonn-Bad Godesberg), 6.8 cm long and 1.0 cm in diameter, were larger than those normally used in the Perkin-Elmer instruments or the carbon rods in the Varian-Techtron instruments. This probably accounted for their longer life, as about 150 analyses were performed without any noticeable loss in performance. The cuvettes were purged with argon to prevent combustion of the tubes and to inhibit oxidation of the atomized lead. Hamilton precision syringes (25 μl) were used to introduce the solutions into the graphite tubes through a central hole in the tube wall.

Glassware and reagents

All glassware was carefully acid-washed overnight in 6 *M* nitric acid and then repeatedly rinsed with water double-distilled in glass. The 5-ml glass cups for holding the samples were then drained and oven-dried. All the reagents used, including those for precipitating the proteins in blood, were of analytical-reagent grade. The precipitating mixture as outlined by Einarsson and Lindstedt[10] was modified slightly by incorporating the diluent distilled water into the precipitating mixture. Thus the 5% (w/v) solution of trichloroacetic acid (3 volumes) and the 72% perchloric acid (1 volume), after mixing, was in turn mixed with glass double-distilled water in the ratio 3:1. This had the advantage of requiring only one addition of precipitation solution to the sample of blood to be analyzed.

Standard solutions of lead were prepared by diluting a stock solution, 1000 p.p.m. (w/v) lead in 0.1 *M* perchloric acid (Hopkins and Williams, Ltd., England) with 0.01 *M* hydrochloric acid. The working solutions (1 μg ml^{-1}, 2 μg ml^{-1} etc.) were prepared fresh daily and stored in polyethylene bottles.

Massmann-cuvette operating programme

The operating programme of the Massmann cuvette is shown in Table I. The times and temperatures shown were arrived at after several trial runs. During the ashing stage, any temperature above 500°C caused lower readings for lead in the bloods investigated. The elapsed time of 60 s for ashing allowed the recorder pen to return to the baseline, thus indicating that all material volatile at 500°C had been burnt off. Although the temperature recommended by the Beckman

TABLE I

MASSMANN-CUVETTE OPERATING PROGRAM

	Drying	*Ashing*	*Atomization*	*Burn-out*
Time (s)	30	60	10	5
Temp. (°C)	100	490	2600	3100

service bulletin for the atomization of lead is 2000°C, the maximum signal for lead in blood was obtained at a temperature, as read on the gauge, of 2600°C. An atomization time of 10 s was sufficient for maximum signal, and also allowed the recorder pen to return to baseline before burn-out. The signal from the burn-out showed that very little residue was left after atomization. The cuvette was nevertheless burnt out after each atomization to prevent any build-up of residue. The "burn-out" at 3100°C appeared to have no detrimental effect on the life of the cuvette.

Sample preparation

As an example of the investigations required to determine industrial metal toxicity, a sample of heparinized blood was taken from a patient who had been exposed to dust containing mainly lead oxides. Seven different extraction methods were used. All dilutions of reagents, such as Triton-X, and of the digests after reaction with "Unisol" were made up with glass double-distilled water. Unisol is a quaternary ammonium hydroxide. Details of the 7 methods of preparation are as follows:

(1) 0.5 ml of blood + 4.5 ml of double-distilled water;

(2) 0.5 ml of blood + 4.5 ml of 0.01 *M* hydrochloric acid;

(3) 0.5 ml of blood + 4.5 ml of 2% Triton-X;

(4) 0.5 ml of blood + 1.0 ml of Unisol; the mixture was allowed to stand overnight at room temperature until the solution was completely clear and then 3.5 ml of double-distilled water were added;

(5) procedure (4) with Unisol was repeated but after a clear solution had been obtained, 3.5 ml of 0.01 *M* hydrochloric acid was added:

(6) lead was extracted from the blood by a slightly modified Einarsson and Lindstedt[10] method: one volume of blood was extracted for 1 h at room temperature with one volume of the mixed perchloric acid–trichloroacetic acid preparation; after digestion the mixture was diluted with 8 volumes of 0.01 *M* hydrochloric acid, resulting in a final dilution of the blood to 10 volumes;

(7) digestion was carried out by the method of Mahin and Lofberg[11]: one volume of heparinized blood was placed in an acid-washed test tube fitted with a "Finn-Cap", an equal volume of 70% perchloric acid was added, the sample was mixed well on a vibration-mixer, and one volume of 30% hydrogen peroxide was added; the sample, after mixing again, was placed in a water bath at 70–80°C for 30–60 min with occasional agitation until the blood had completely dissolved; the mixture was then diluted with 7 volumes of double-distilled water to give a 10-fold final dilution of the blood.

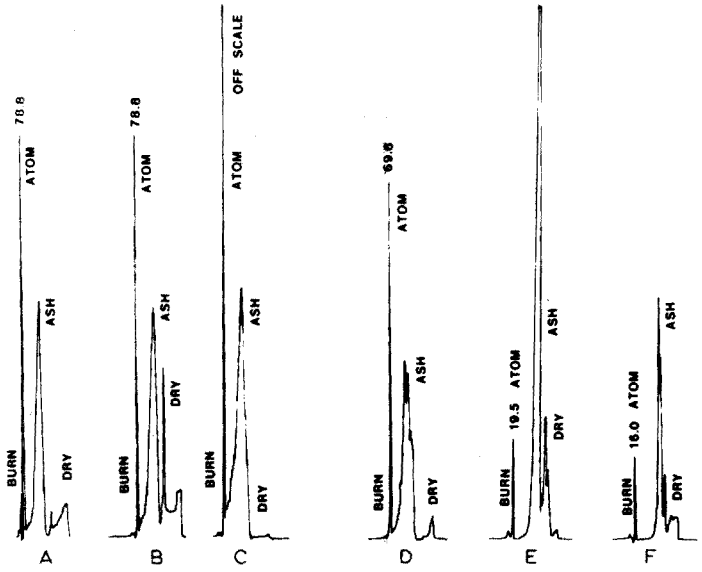

Fig. 1. Traces of signals showing drying, ashing, atomization and burn-out. A, Blood diluted (× 10) with water. B, Blood diluted (× 10) with 0.01 *M* HCl. C, Blood diluted (× 10) with 2% Triton-X. D, Digested with Unisol. E, Digested by the Mahin–Lofberg method. F, Digested by the Lindstedt method.

Method

For every determination, 20 μl of the prepared solution was injected from a 25-μl Hamilton syringe into the Massmann cuvette. In the Einarsson–Lindstedt preparation, the clear supernate was used after the blood proteins had been precipitated and centrifuged. The determinations were repeated at least 5 times at a wavelength of 283.3 nm for the atomic absorption peaks. Background correction for sample scattering and molecular absorption was carried out on separate aliquots at 287.5 nm for each sample. This gave the non-atomic absorption peaks. The flow rate of argon gas through the Massmann cuvette was of paramount importance, since the atomization peak-heights of lead depended on it; the best flow was determined experimentally as 1.0 kPa cm^{-2} (read on the pressure gauge; *ca.* 0.98 bar) to give a maximum atomization signal. No scale expansion was used in obtaining any of the atomization signals.

RESULTS

Typical traces obtained from the different methods of preparing the sample of blood are shown in Fig. 1. The various stages depicting drying, ashing, atomization and burn-out are illustrated and the relative heights of the lead peaks during the atomization stage are shown. The chart speed of 0.5 in. min^{-1} sufficed to allow a clear demarcation to be observed between the various stages. Table II illustrates the means of 5 readings obtained for both the percentage absorption at 283.3 nm and the non-absorption line at 287.5 nm. Standard deviations at 283.3 nm were calculated and the percentage contribution of the background at 287.5 nm is shown.

TABLE II

CONTRIBUTION OF BACKGROUND AT NON-ABSORBING 287.5 nm TO ABSORPTION AT 283.3 nm

Method[a]	*Mean % deflection at 283.3 nm*[b]	*Mean % deflection at 287.5 nm*[b]	*Nett deflection from lead*[c]	*% Contribution of background at 287.5 nm to % deflection at 283.3 nm*
1	78.6±5.7	62.1±8.0	16.5±13.7	79.0
2	81.9±7.2	62.7±3.6	19.2±10.8	76.6
3	Off-scale	92.5	—	—
4	75.8±7.0	55.5±8.9	20.3±15.9	73.2
5	78.4±9.0	67.5±6.1	10.9±15.1	86.1
6	15.0±0.7	5.1±0.3	9.9±1.0	34.0
7	18.8±0.8	6.4±1.3	12.4±2.1	34.0

[a] See Experimental.
[b] Mean of 5 readings ±standard deviation; 100% deflection = 1 absorbance unit.
[c] Difference of deflections at 283.3 nm and 287.5 nm ±sum of the two standard deviations.

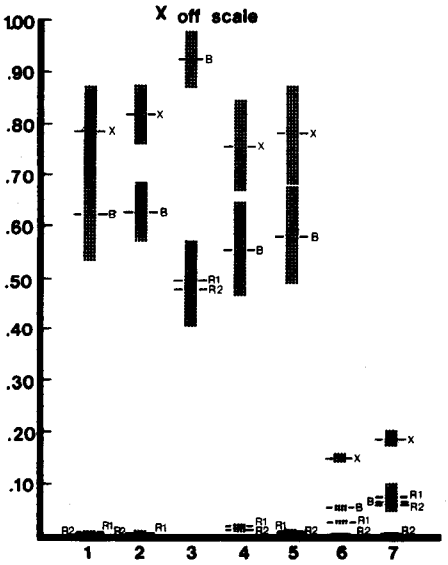

Fig. 2. Comparison of precision of different methods of sample preparation. The numbers on the horizontal axis refer to the methods described under Experimental. 95% Confidence limits were calculated on 5 readings. Lead in blood = (X − B) − (R1 − R2) where X = upper reading at 283 nm, B = lower reading at 287 nm, R1 = reagent blank at 283 nm, R2 = reagent blank at 287 nm.

DISCUSSION

Amongst the sources of error in the determination of lead in biological materials in the nanogram range, two of the most important are caused by loss of lead in the ashing stage and by contamination. The ashing temperature in lead determinations, especially in the presence of chloride, must not be in excess of

500°C since losses were found to occur, thus confirming the observations made by Christian[12]. When sufficient care was exercised in cleaning glassware (particularly the barrel and needle of the Hamilton syringe), contamination was obviated. Eppendorf or Oxford pipettes with plastic tips were not found to be suitable for injecting microlitre quantities of solution without loss into the 1.5-mm diameter hole of the Massmann cuvette. Possible contamination from any residues left in the cuvette after atomization was obviated by the "burn-out" stage which was part of the normal cycle of the operation. Although the Massmann cuvette was subjected repeatedly to the burn-out temperature of 3100°C, the cuvettes could be used for at least 150 determinations, whereas Amos *et al.*[2] noted that the carbon rod atomizer they used had a life span of between 20 and 40 determinations if subjected repeatedly to a temperature of 3000°C.

The decision to examine the various methods of sample preparation was prompted by the fact that the simplest method of sample preparation, namely that of dilution by water, gave a relative standard deviation of 7.2% for the atomic absorption lead peaks at 283.3 nm, while the non-atomic absorption peaks at 287.5 nm had a relative standard deviation of 12.9%. Furthermore, the contribution of the non-atomic absorption peaks by this method to the atomic absorption lead peaks was on the average 79% (Table II).

In Fig. 2, the 95% confidence intervals are shown for the different methods. There are large confidence intervals and high background absorbances in methods 1–5. Methods 6 and 7 have low background and small confidence intervals. The major portion of the background is not due to low-molecular-weight materials or to inorganic salts such as iron salts, sodium chloride or calcium phosphate; methods 6 and 7 should give high backgrounds if this were so. However, high-molecular-weight substances such as 2% Triton-X give large background values (method 3—blanks). This is not in agreement with the observations of Kubasik and Volosin[13] or Evenson and Pendergast[14], who found no background interference even with 5% Triton-X.

The discrepancy may be due to different types of apparatus. Indeed, it was found that different optimal conditions obtained for the Perkin-Elmer model 503 and for the Beckman 444; a Techtron apparatus was not available. In all the methods where proteins were not precipitated or digested, high background values were obtained. This indicates that high-molecular-weight substances are not completely ashed at 500°C in an argon atmosphere and tend to produce "smoke" because of further decomposition at the higher temperature used for atomization of the lead (2600°C), giving a non-specific light absorption. This background is very variable even in different aliquots of the same blood sample preparation. It is usually assumed that an automatic background corrector will correct for this. However, the variation in background absorption will only be unimportant if the working graph is linear. If a linear relationship holds between metal concentration and absorbance, *i.e.*, $C=KX$, then $(C_1-C_2)=K(X_1-X_2)$, where X_1 and X_2 are the absorbances at wavelengths λ_1 and λ_2, respectively, and C_1 and C_2 are the corresponding apparent metal concentrations. If a non-linear working curve obtains, the function of the independent variable for (C_1-C_2) is not the same as the original function of the independent variable. Hence one cannot use the same calibration curve if the background absorption is different and one is using the

automatic background corrector. However, if background correction is done by measuring non-specific absorbance at another wave-length, and a standard graph drawn for blood by the method of additions, this is generally a curved line. In this case, it is necessary to use the graph first to convert the absorbance readings at the two different wavelengths to apparent metal concentrations before subtraction. This is equivalent to moving the x-axis across to make the curve pass through the origin, instead of bringing the upper reading down by an amount equal to the blank. However, a difficulty arises in determining the absolute amount of lead in blood when curved calibration graphs are used, because of the uncertainty involved in extrapolating the graph to cut the x-axis. Is is therefore highly desirable that conditions be so arranged that a linear calibration curve is obtained if possible. This will greatly reduce the uncertainty in determining the intercept on the x-axis. (The conditions for linear graphs will be the subject of a subsequent paper.) However, in this work, as in most other published works[14–16], the calibration graphs for lead are not linear. Hence it is desirable to arrange that background interference should be as low as possible.

It is apparent that the choice, when the Beckman instrument is used, lies between the last 2 methods where only low background absorption is present. The percentage contributions of the background matrices in both the Einarsson–Lindstedt[10] and Mahin–Lofberg[11] methods are identical. The difference between the standard deviations of the nett deflection caused by lead for the two methods is relatively small compared to that for the other methods, so that there is little to choose between the methods from this point of view.

Because of the convenience of the Einarsson–Lindstedt method, which required no heat for digestion and which could be carried out in a single tube, and was therefore much faster than the Mahin–Lofberg method, this was the method finally adopted. A correction for lead in the reagents is unnecessary, as this amounts to a deflection equivalent to that caused by less than 1 μg of lead per 100 ml of blood, unless contamination of the reagents has occurred. The deflection shown in Fig. 2 is for undiluted reagent. However, it is essential to check the precipitating mixture for lead on each batch used, to see whether contamination has occurred.

SUMMARY

The determination of lead in blood by graphite-furnace atomic absorption spectrometry is markedly affected by the method of preparing the blood. Several different methods of preparation have been investigated for their sensitivity and reproducibility. The most reproducible, reliable and convenient method is a modification of the Einarsson and Lindstedt method based on treatment with perchloric and trichloroacetic acids.

REFERENCES

1 H. Massmann, *Spectrochim. Acta, Part B*, 23 (1968) 215.
2 M. D. Amos, P. A. Bennet, K. G. Brodie, P. W. Y. Lung and J. P. Matousek, *Anal. Chem.*, 43 (1971) 211.

3 C. E. Gleit, *Anal. Chem.*, 37 (1965) 314.
4 G. A. Rose and E. G. Willden, *Analyst (London)*, 98 (1973) 243.
5 H. Malissa and E. Schoffman, *Mikrochim. Acta*, 187 (1955) 74.
6 D. C. Manning and F. Fernandez, *At. Absorption Newslett.*, 9 (1970) 65.
7 J. P. Matousek and B. J. Stevens, *Clin. Chem.*, 17 (1971) 363.
8 J. F. Rosen, *J. Lab. Clin. Med.*, 80 (1972) 567.
9 N. P. Kubasik, M. T. Volosin and M. H. Murray, *Clin Chem.*, 18 (1972) 410.
10 Ö. Einarsson and G. Lindstedt, *Scand. J. Clin. Lab. Invest.*, 23 (1969) 367.
11 D. T. Mahin and R. T. Lofberg, *Anal. Biochem.*, 16 (1966) 500.
12 G. D. Christian, *Anal. Chem.*, 41 (1969) 24A.
13 N. P. Kubasik and M. T. Volosin, *Clin. Chem.*, 20 (1974) 300.
14 M. A. Evenson and D. D. Pendergast, *Clin. Chem.*, 20 (1974) 163.
15 E. Norval and L. R. P. Butler, *Anal. Chim. Acta*, 58 (1972) 47.
16 H. T. Delves, *Analyst (London)*, 95 (1970) 431.

Analytica Chimica Acta, 77 (1975) 37–42

ARSINE GENERATION AND DETERMINATION OF TRACE AMOUNTS OF ARSENIC BY ATOMIC ABSORPTION SPECTROMETRY

TOSHIHISA MARUTA and GIICHI SUDOH

Central Laboratory of Research and Development, Chichibu Cement Co., Ltd., Ohmiya, Chichibu-shi, Saitama-ken (Japan)

(Received 4th November 1974)

It is generally difficult to determine arsenic with high sensitivity by atomic absorption spectrometry, because the resonance line of arsenic is placed in the far ultraviolet region, where serious flame interferences occur. Ando *et al.*[1] have described the determination of 0.1–1 p.p.m. arsenic by means of a long-path Vycor cell and ring burner. Menis and Rains[2] have reported that an electrodeless discharge lamp as a light source is more effective than a hollow-cathode lamp. Kirkbright and Ranson[3] have described the determination of arsenic with conventional and nitrogen-shielded fuel-rich nitrous oxide–acetylene flames. For flameless atomic absorption spectrometry, Massmann[4] determined arsenic using an electrically heated graphite tube in an argon chamber, and Chu *et al.*[5] using an electrically heated absorption cell.

The determination of arsenic is based on reduction of arsenic to arsine, introduction of the generated arsine into a flame such as an argon–hydrogen flame, and atomization of arsine. As the reductant, zinc[6,7], sodium borohydride[8–10] and titanium trichloride and magnesium rod[11] have been used.

In this paper, a rapid, sensitive, accurate and precise method for the determination of arsenic is described, based on arsine generation and atomic absorption spectrometry with an argon–hydrogen flame. Various reductants for the generation of arsine from arsenic in aqueous solution have been examined, as well as the interferences of anions and cations on arsenic absorption.

EXPERIMENTAL

Apparatus

All measurements were done with a Nippon Jarrell-Ash Model AA-1E atomic absorption and flame emission spectrophotometer, equipped with a Nippon Jarrell-Ash Model ASD-1A arsenic measurement unit, a Rikadenki Kogyo Model B-140 recorder and a detector unit with a HTV R-106 photomultiplier. An arsenic hollow-cathode lamp (Westinghouse Electric Corp.,) was employed throughout. A 10-cm argon–hydrogen flame was used.

Reagents

Arsenic standard solution (1000 p.p.m.). Dissolve arsenic trioxide in dilute sodium hydroxide solution, and acidify slightly with hydrochloric acid. (For com-

parison, a standard solution was also prepared by dissolving potassium arsenite in metal-free water.) Prepare dilute solutions from the stock solutions as required.

All reagents used were of analytical-reagent grade. Deionized water was used throughout.

Procedures

Transfer the arsenic standard solution to a reaction flask. Add 6 *M* hydrochloric acid to make the final acidity about 1 *M*, 1 ml of aqueous 20% (w/v) potassium iodide solution, and 1 ml of 10% (w/v) tin(II) chloride solution in hydrochloric acid. Add water to give a final volume of sample solution of *ca.* 50 ml and mix well. Stand for 10 min. Add 0.8 g of zinc powder tablet, and immediately connect the reaction flask to the collection tank. React for 60 s by mixing the sample solution with a magnetic stirrer to ensure complete generation. Transfer the collected arsine to the flame with a stream of argon carrier gas. Atomize the sample and simultaneously record the absorption signal.

By the same procedure, measure the absorption at the analytical line of a reagent blank, and correct all the results for arsenic. Use the height of the absorption signal to determine the concentration of arsenic. Table I shows the working conditions.

TABLE I

WORKING CONDITIONS FOR ARSENIC

Wavelength (nm)	193.7
Slit width (μm)	100
Lamp current (mA)	15
Flow rate of argon (l min^{-1})	7.0
Flow rate of hydrogen (l min^{-1})	2.5
Flow rate of auxiliary argon (l min^{-1})	5.0

RESULTS

Effect of reductants for the generation of arsine

The effect of different reductants on the arsenic absorption was investigated to determine the optimal conditions; potassium iodide, tin(II) chloride and zinc powder tablet, titanium trichloride and magnesium powder, and sodium borohydride were examined. The highest absorption signal was obtained when potassium iodide, tin(II) chloride and zinc powder tablet was used. When a mixture of titanium trichloride and magnesium powder was used, the peak height of the arsenic signal was lower by 37% than that obtained with iodide, tin(II) and zinc. When sodium borohydride was used, the peak height was lower by 21% than that obtained with iodide, tin(II) and zinc. The procedure with other reductants instead of tin(II), added to potassium iodide and zinc powder, was therefore estimated. The results are shown in Fig. 1. It can be seen that all the reagents were effective but that tin(II) was the most efficient. The iodide–tin(II)–zinc mixture was therefore used for all further analyses.

Study of experimental conditions

Arsenic absorption was measured for sample solutions containing 0.5–4.0 *M*

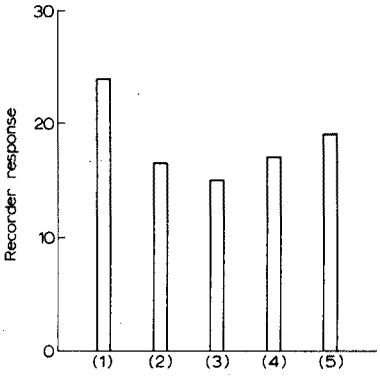

Fig. 1. Effect of reductants on absorption signal of arsenic. As, 0.8 μg. (1) 10% $SnCl_2 \cdot 2H_2O$, 1 ml. (2) 10% $NH_2OH \cdot HCl$, 2 ml. (3) 10% ascorbic acid, 2 ml. (4) 0.5% $(NH_2)_2 \cdot H_2SO_4$, 2 ml. (5) 10% $NaHSO_3$, 2 ml. In all cases, 1 ml of 20% KI and 1 piece of Zn powder tablet were added.

hydrochloric acid; no variation in absorption was observed over this range, and an acidity of 1.0 *M* was selected for further work.

Changes in the volume of sample solutions in the range 10–50 ml had no effect on absorption. A volume of 50 ml was chosen for convenience of stirring in the reaction flask.

The amounts of 20% (w/v) potassium iodide and 10% (w/v) tin(II) chloride solutions added were not critical in the range 0.5–3 ml, but at least 0.5 ml of each solution had to be used; 1-ml amounts were selected for further work. Arsenic absorption was constant in the range 0.8–2.4-g amounts of zinc powder tablet added. When the reaction time after the addition of 0.8 g (a piece) of zinc powder tablet was varied from 30 to 180 s, no change was found in the arsenic absorption signal. Therefore, a suitable reaction time was 60 s.

Effect of flow rate of carrier gas

The arsenic absorption signal (peak height) increased with increasing flow rate of argon up to 4 l min^{-1}, but then remained constant at flow rates up to 9 l min^{-1}. At flow rates below 4 l min^{-1}, broad low absorption signals were obtained, because of the slow introduction of arsine into the flame. For flow rates of 1–4 l min^{-1}, the peak areas obtained were constant; for flow rates of 4 l min^{-1} or above, the analytical precision was not affected whether the height or area of the absorption signal was measured. An argon flow rate of 5.0 l min^{-1} was selected and peak heights were measured.

Atomic population in flame

The absorption signal of arsenic was measured in various flame conditions and in various regions of the flame (Fig. 2). The signal decreased with increasing flow rates of hydrogen at 6 mm or 10 mm height above the burner top, but did not change at 21 mm, irrespective of the flow rate of hydrogen. Clearly, the degree of dissociation and atomization of arsine depended strongly on flame temperature in the relatively cool lower regions of the flame, but not in the hotter higher region. Signal-to-noise ratios tended to decrease with increasing hydrogen

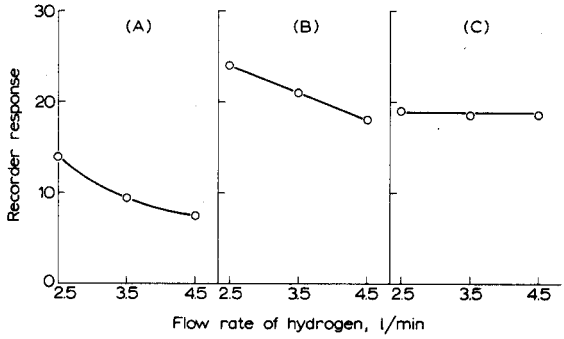

Fig. 2. Effect of flow rate of hydrogen on absorption signal of arsenic. (A) 6 mm above burner top; (B) 10 mm above burner top; (C) 21 mm above burner top. Flow rate of argon: 7.0 l min^{-1}.

flow rates, irrespective of measurement height. Optimal measurement conditions were as follows: 2.5 l min^{-1} for hydrogen, with measurements at 10 mm above the burner top.

The use of arsenic trioxide and potassium arsenite

Arsenic absorption signals were measured for sample solutions containing the same concentration of arsenic as arsenic trioxide or potassium arsenite. No differences were found, hence the reduction appears efficient, irrespective of the amount of oxygen in the sample.

Interferences of acids

Sample solutions of arsenic containing 0.05–1 *M* sulfuric, perchloric or phosphoric acid were prepared; each solution was also 1 *M* in hydrochloric acid. These mineral acids did not interfere. When conventional atomic absorption spectrometry with a nebulizer is used, high acid concentrations tend to depress the absorption signal because of changes in the rate of aspiration; such interferences are overcome in the proposed method. Nitric acid, however, caused a marked depressing effect on arsenic absorption (Table II); the strong oxidizing action of nitric acid seems to depress the generation of arsine. When nitric acid is used for the decomposition of samples, the solution should be boiled to remove all oxides of nitrogen.

Interferences of diverse metals

The interferences of 100-fold amounts (by weight) of 15 different metals were studied. No interference was observed for sodium, potassium, magnesium, calcium,

TABLE II

INTERFERENCE OF NITRIC ACID

HNO_3 (M)	0.05	0.1	0.5	1.0
% Change in signal[a]	−8	−24	−80	−100

[a] Average of five values.

manganese, cobalt, nickel, copper, aluminium, iron and vanadium. Ando *et al.*[1] reported that magnesium, calcium, manganese, cobalt, nickel and aluminum depressed the arsenic absorption signal in a nitrogen (entrained air)–hydrogen flame. The interferences obtained with the proposed method were widely different from these. Antimony, which generated stibine during the reduction, did not interfere, possibly because of the presence of iodide.

TABLE III

INTERFERENCES OF METALS

(0.8 μg As was used with a 100-fold (weight) amount of added metal)

Metal added	Se	Pb	Cr
% Change in signal[a]	−10	−13	−30

[a] Average of five values.

The metals which resulted in a change of absorption signal of more than 5% are listed in Table III. Chromium gave a marked depressing effect. Lead and chromium interfered not in the atomization process but in the reduction process. Selenium formed hydrogen selenide in the reduction and was thus introduced into the flame.

None of the metals investigated interfered at the 10-fold level.

Reproducibility and calibration curve

Sample solutions containing 0.8 μg of arsenic were repeatedly analyzed under the optimal conditions to estimate the reproducibility of the method. The relative standard deviation calculated from eight determinations was 2.3%.

The calibration curve relating the amount of arsenic and the absorption signal was linear up to 1.0 μg of arsenic.

Conclusion

Of the various reduction methods investigated for the generation of arsine from arsenic compounds, the procedure with potassium iodide, tin(II) chloride and zinc powder tablet was the best. Atomic absorption spectrometry with an argon–hydrogen flame was suitable for determinations of trace amounts of arsenic after arsine generation. The recovery rate of arsenic by the method was about 100%. The time required for analysis of one sample was only about 12 min.

The method is applicable to the determination of arsenic in various samples which can be decomposed with acids.

The authors wish to thank H. Mori, Chief Central Laboratory of Research and Development Chichibu Cement Co., Ltd., for his suggestions throughout this work.

SUMMARY

Arsenic can be determined by atomic absorption spectrometry after reduction

to arsine with potassium iodide, tin(II) chloride and zinc powder tablet; the arsine generated is carried into an argon–hydrogen flame by means of argon. Accuracy, precision and speed are satisfactory. Serious interferences arise only from nitric acid, lead, chromium and selenium.

REFERENCES

1 A. Ando, M. Suzuki, K. Fuwa and B. L. Vallee, *Anal. Chem.*, 41 (1969) 1974.
2 O. Menis and T. C. Rains, *Anal. Chem.*, 41 (1969) 952.
3 G. F. Kirkbright and L. Ranson, *Anal. Chem.*, 43 (1971) 1238.
4 H. Massmann, *Z. Anal. Chem.*, 225 (1967) 203.
5 R. C. Chu, G. P. Barron and P. A. W. Baumgarner, *Anal. Chem.*, 44 (1972) 1476.
6 W. Holak, *Anal. Chem.*, 41 (1969) 1712.
7 D. C. Manning, *At. Absorption Newslett.*, 10 (1971) 123.
8 K-T. Kan, *Anal. Lett.*, 6 (1973) 603.
9 F. J. Fernandez, *At. Absorption Newslett.*, 12 (1973) 93.
10 F. J. Schmidt and J. I. Royer, *Anal. Lett.*, 6 (1973) 17.
11 E. N. Pollock and S. J. West, *At. Absorption Newslett.*, 12 (1973) 6.

Analytica Chimica Acta, 77 (1975) 43–52

RAPID DETERMINATION OF LEAD IN STEEL BY FLAMELESS ATOMIC ABSORPTION SPECTROMETRY

WOLFGANG FRECH

Department of Analytical Chemistry, University of Umeå, 901 87 Umeå (Sweden)

(Received 20th December 1974)

Even small amounts of some metals like antimony, lead and bismuth affect the working properties of steels. In the case of lead, the analytical method should be capable of determining 0–50 μg Pb g^{-1}, and should also be fast enough to allow results to be reported during processing. Byrne *et al.*[1] presented a short review of the methods available for the determination of residual elements in rotor steel. Since then many authors have described improved methods in this field. Colorimetric[2] procedures provide almost sufficient sensitivity (1–500 p.p.m.) and accuracy, but require a time of about 2 h, which is too time-consuming for routine analysis. Anodic stripping voltammetry[3] permits the analysis of a sample within 1 h; the detection limit is about 1 p.p.m. lead in steel.

Atwell and Golden[4] reported a (relatively) rapid method for the determination of bismuth and lead in iron and nickel-base alloy chips by d.c.-emission spectrography. The detection limit for lead was 0.5 p.p.m., but standards must have the same matrix composition as the sample, so that different calibration curves must be prepared for various types of steel.

Promising experiments for the direct determination of minor constituents in metal discs have been described by Walsh[5]. In a sputtering chamber, the sample is placed as cathode on a vacuum seal opposite an anode, and by cathodic sputtering an atomic cloud of the sample is produced for atomic absorption measurements.

Thomerson and Price[6] used a direct method for the determination of lead and other elements in steel by flame atomic absorption spectrometry. For 2% solutions, a detection limit of 10 p.p.m. lead in steel was reported. For the direct determination of lead in copper by atomic absorption spectrometry. Gandrud and Marshall[7] reported a detection limit of 20 p.p.m. These direct methods are fast and simple but they are too insensitive for the determination of lead as a residual element. Furthermore, interference from the complex matrix was reported[8].

If the residual elements are extracted before being determined in the flame, detection limits can be improved. Burke[9] extracted Pb, Sb, Bi and Sn with TOPO (trioctylphosphineoxide) in MIBK. Hofton and Hubbard[10] extracted lead as tetraiodoplumbate into MIBK, whereas Bohnstedt[11] extracted lead and bismuth as their dithizonates. The extractions make these procedures tedious and slow.

Recently, procedures based on flameless atomic absorption spectrometry in a Massmann-type furnace have been described. Welcher *et al.*[12] determined Pb, Bi, Se, Tl and Te in high-temperature alloys. The samples were dissolved in a

mixture of nitric acid, hydrofluoric acid and water (1:1:1), evaporated and diluted with water. Non-specific absorption made it necessary to use an instrument with a background corrector; the detection limit was 0.1 p.p.m. lead. Shaw and Ottaway[13] dissolved the sample in nitric acid (cast iron and mild steels) or in perchloric acid (high-alloy steels). A sample could be analyzed within 15 min; the detection limit for lead was 0.4 p.p.m., but again background correction was necessary. It should be emphasized that for routine analysis the use of perchloric acid demands extensive precautionary measures[14].

In the method described here, low-alloy as well as high-alloy steels were rapidly dissolved in aqua regia. The same dissolution procedure can be applied for the determination of antimony[15] and bismuth[16], so that all three elements can be determined after a single dissolution step. An instrument without background correction can be used. Interferences from the major constituents of high-alloy steel are discussed.

EXPERIMENTAL

Spectrometer

The atomic absorption spectrometer has already been described[17]. It was provided with a hydrogen background corrector. Both the specific and the non-specific absorption were recorded simultaneously. For the procedure described here, peak height for non-specific absorption was less than 0.01 absorbance units, so that for routine analyses the background corrector is not essential. The furnace was of the Massmann type and could be flushed with an inert gas such as argon or nitrogen[18]. The temperature of the graphite tube was monitored by an infrared-sensitive diode and the graphite tube could be heated (very rapidly) with full power to a preset temperature and then operated isothermally[17]. The important difference between this equipment and commercial instruments such as Perkin-Elmer 303 with HGA 72 is that temperature-controlled operation is possible.

Procedure

Weigh a 0.5-g sample and dissolve it in about 3 ml of water, 5 ml of concentrated hydrochloric acid and 2.5 ml of concentrated nitric acid in a 50-ml Erlenmeyer flask, with gentle heating. Transfer the dissolved sample to a 100-ml measuring flask and dilute to the mark with water. After mixing, transfer 2 μl of this solution to the graphite tube with a Unimetrics micropipette. Dry the sample for 15 s at about 80°C, ash for 50 s at 625°C and measure at an atomization temperature of 1150°C using the line at 283.3 nm and a slit-width of 160 μm. Flush the furnace with nitrogen (0.6 l min^{-1}) except during atomization which is performed with no gas flow. After each cycle, heat the furnace to a high temperature (2800°C) in order to remove matrix elements which would otherwise accumulate in the graphite cuvette. The total time required for the procedure described is less than 15 min.

Prepare a 1000-p.p.m. standard by placing 1.5985 g of recrystallized lead nitrate[19] in a 1-l measuring flask and diluting it with 0.1 *M* nitric acid to the mark. Dilutions to the required concentrations were made daily by adding μl increments of the stock solution to 10- and 20-ml portions of test solution.

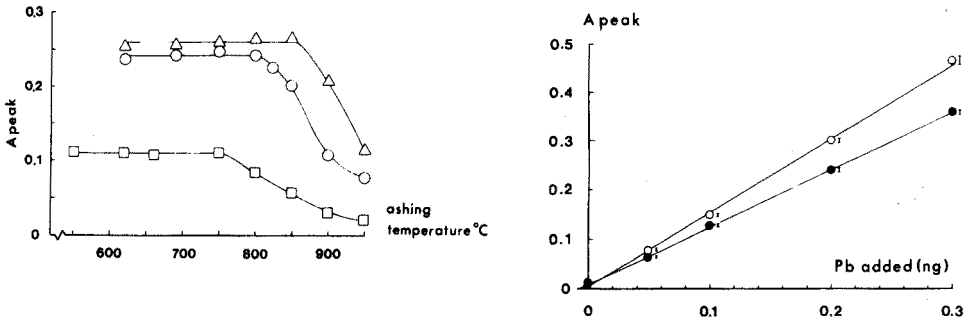

Fig. 1. Variation of absorbance peak with ashing temperature. (△) 0.2 ng Pb in 0.03 *M* HNO_3. (□) Dissolved austenitic stainless steel BCS 334. (○) 0.2 ng Pb added to dissolved mild steel JK 1C.

Fig. 2. Calibration curves obtained by standard additions to ultrapure steel JK 1C (●) and 0.1 *M* nitric acid (○).

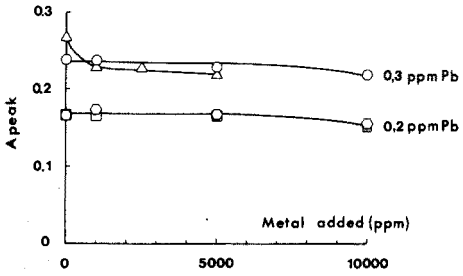

Fig. 3. Variation of absorbance peak for different amounts of Mo (△), Fe (○), Ni (⬭) and Cr (□).

RESULTS AND DISCUSSION

Samples containing lead in different matrices were analyzed after ashing for 50 s at various temperatures, which were adjusted with a temperature controller with i.r.-sensor[17]. The results are shown in Fig. 1; it can be seen that losses of lead start at different temperatures in different matrices. The nitric acid provided an oxidizing solution free from other metals; the mild steel was ultrapure with less than 1 p.p.m. lead; and the austenitic steel was certified to contain 26% Cr, 21% Ni and 11 p.p.m. Pb. The steel matrix reduced the sensitivity somewhat compared to nitric acid only. This was confirmed by comparing a calibration curve with standard additions to a JK 1C steel, as shown in Fig. 2, in which the bars drawn close to the circles give the standard deviations. Figure 3 shows the influence on sensitivity of a few other metals; it can be seen that iron, nickel and chromium all had the same effect, which makes it possible to use a single calibration curve, such as Fig. 2, for analysis of steels containing these three metals in various proportions. The decrease in the signal depended on the amount of matrix rather than on the element itself. The losses of lead during ashing, however, started at different temperatures in iron and in a mixture of iron, chromium and nickel (Fig. 1). Molybdenum interference was more pronounced (Fig. 3), which made it necessary to prepare standards with the same amount of

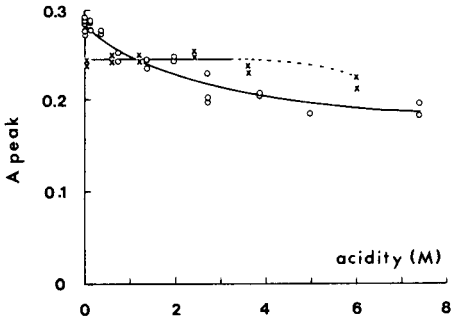

Fig. 4. Variation of absorbance peak for 0.2 ng of lead in hydrochloric (x) and nitric (o) acids at various acidities.

molybdenum as the sample. It was observed that burning-out of the graphite tube after atomization had to be carried out at a sufficiently high temperature, otherwise some molybdenum remained and caused a signal depression on the following sample.

For the determination of antimony in steel[15], some interferences from the matrix can be eliminated if a higher heating rate for the atomization is selected. In this work the influence of the heating rate was also investigated. Calibration curves for lead were obtained in an aqueous medium and in a steel matrix (JK 1C) at heating rates of 450, 675 and 950°C s^{-1}; in all cases about the same amount of interference from the steel matrix was observed. The sensitivity was almost independent of the atomization rate. At the lowest heating rate, reproducibility was best and therefore this heating rate was chosen.

Figure 4 shows that the concentration of nitric acid influences the peak height. It was observed that the signal depression was larger, the more the graphite tube had been used, and that it was somewhat different for various samples of graphite. Furthermore, the standard deviation was larger, the greater the acidity. The nitric acid normally vaporized in the drying step, and there should be no nitric acid present at the time of atomization as the furnace is flushed with argon both during drying and ashing. The effect is probably due to interaction between the graphite and the acid; this suggestion is supported by the observation that the structure of the graphite surface was also important. The concentration of nitric acid in the dissolved steel samples was normally about 0.3 *M*.

The amount of hydrochloric acid was not important below 3 *M*. The curves in Fig. 4 are displaced, as investigations were made on different occasions with adjustment of the working parameters in between. When the ashing temperature was below 500°C, the lead signal was lower than that on the plateau in Fig. 1. Shaw and Ottaway[13], who studied the determination of lead in steel by flameless atomic absorption reported strong interferences when the samples were dissolved in chloride media. Probably the lead was lost as species of lead chloride[13]. The chloride interferences were therefore studied in more detail on the instrument described above (with temperature-controlled heating) as well as on a Perkin-Elmer 300 with HGA 72 and on a Varian Techtron AA6 with CRA 63. All deter-

minations were made with background correction. On each instrument, comparisons were made between direct atomization after drying and atomization after drying and ashing. For each instrument the ashing conditions were determined from a series of ashings at various settings. At ashing temperatures above 750°C (see Fig. 1), losses of lead were noted and a lower temperature, about 600°C, was selected for the runs presented below. Table I shows the peak absorbances when solutions of BCS 330 steel (30 p.p.m. lead) were run. The steel samples (0.5 g) were dissolved in 7.5 ml of nitric acid or hydrochloric acid or in 5 ml hydrochloric acid and 2.5 ml nitric acid; the solutions were diluted to 100 ml. Table I shows that the ashing step did not affect the absorbance readings for the nitric acid solutions. The values obtained for samples dissolved in aqua regia should have been essentially the same as those obtained in nitric acid solutions, but if the ashing step was omitted significantly lower absorbances were obtained. If an ashing step was included the HGA 72 furnace gave the same reading as with nitric acid. The temperature-controlled furnace gave a somewhat higher reading; this is ascribed to the physical phenomenon of absorption into the graphite of the nitric acid solution. The readings on the Varian Techtron instrument were the same if the hydrogen and nitrogen flows were on, but if only nitrogen was used, lead was lost during ashing even when the temperature was considerably lower than 600°C. This shows that the interferences from chloride could be eliminated on all instruments if a suitable ashing step were included. Decreases in absorbance were noted for samples dissolved in hydrochloric acid but the effect was rather small in the temperature-controlled furnace when ashing was included.

Differences between the systems contribute to the noted divergence in peak absorbance. The Ringsdorff graphite in the temperature-controlled furnace has a larger surface area than the pyrolytically coated graphite used by Perkin-Elmer and Varian. The larger surface of uncoated graphite ensured better contact and more efficient reduction of lead to metal but the physical effects became stronger. Because maximum vapour concentration is affected by the permeability and by the lengths of the cuvettes, peak absorbance values depend on the construction. In the very short tube used by Varian, large losses were noted on ashing when the hydrogen flow was stopped. This indicates that the gas composition is important for the reduction of lead compounds. When the ashing step was omitted, lead compounds were still present when the atomization started. During the rapid heating of the graphite cuvette, decomposition of lead compounds occurred so that an absorption signal could be seen.

The results confirm the suggestions made by Shaw and Ottaway[13] that in these matrices lead can be lost as halides. However, these interferences can be eliminated by ashing in a reducing atmosphere. During this ashing step, lead halides are probably converted to lead metal. A more fundamental study of such reactions in a graphite tube has been started in this laboratory.

High- and low-alloy steel samples were analyzed on the temperature-controlled furnace (Tables II and III) and on the Perkin-Elmer and Varian instruments. On the commercial instruments almost the same procedure was employed. With the CRA 63 an accessory unit for temperature-controlled heating was also used[20]. For the Perkin-Elmer instrument, the lack of temperature-controlled heating made it necessary to select an atomization temperature of

TABLE I

ABSORBANCE PEAK VALUES IN DIFFERENT ACID MEDIA

(BCS 330; certificate value 30 p.p.m. Pb. Mean of 2–4 determinations. For the temperature-controlled heating and the Varian Techtron the same amount of dissolved sample as described in the procedure was used. With the HGA 72 the amount was increased by a factor of 1.25.)

	C tube length (mm)	*Nitric acid*		*Aqua regia*		*Hydrochloric acid*	
		Ashing	*No ashing*	*Ashing*	*No ashing*	*Ashing*	*No ashing*
Temp. controlled furnace Perkin-Elmer 300	100	0.220	0.218	0.259	0.208	0.244	0.164
with HGA 72	51	0.134	0.120	0.126	0.032	0.006	0.023
Varian Techtron AA6	9	0.180	0.180	0.020	0.120	0.002	0.002
with CRA 63	9[a]	0.153	0.153	0.156	0.093	0.06	0.015

[a] With H_2 flow.

2000°C in order to obtain rapid atomization of the sample, which means high sensitivity.

Good agreement with certified values and low standard deviations, 4% on the Perkin-Elmer and 3% on the Varian were achieved. The ashing procedure thus makes it possible to use aqua regia for dissolution, which is very important for rapid analysis of high alloy steel.

TABLE II

COMPARISON OF EXTRACTION METHODS WITH FLAMELESS ATOMIC ABSORPTION FOR THE DETERMINATION OF LEAD IN STEEL

(Values (p.p.m.) represent mean of three analyses.)

Designation	*Extraction with*		*Described procedure*	*Certificate value*
	TOPO in MIBK	*dithizone in $CHCl_3$*		
BCS 277				
Mild steel	71	65	75	—
BCS 334				
Austenitic stainless steel	—	—	11	11
BCS 335				
Austenitic stainless steel	—	14	15	15
Ni-base alloy	9	—	9	—

Analysis of steels

Several steel samples and nickel-base alloys were analyzed by the procedure described. Some of the samples had certificates of analysis; for others this work was part of an investigation leading to certification. For comparison, some uncertified samples were analyzed both by extraction with TOPO in MIBK[9] and by extraction with dithizone[11]. The results are shown in Table II. The extraction method with TOPO in MIBK[9] was also used by other laboratories. The proposed method was modified slightly: instead of organometallic standards, JK 1C samples with standard additions were run through the procedure. The interlaboratory comparison is shown in Table III; it can be seen that the method described here compares well with the other results. This also indicates that interference from elements not studied separately is probably small. The calibration curves obtained from the JK 1C sample with standard additions were linear up to 40 p.p.m. lead. Samples containing higher amounts of lead were diluted with dissolved JK 1C. The standard deviation of the absorption measurements increased as the amount of lead decreased. Figure 5 shows some traces from the recorder from JK 1C; the peaks are near the detection limit, which is estimated to be 0.3 p.p.m. lead in steel. The standard deviation for JK 1C was about 20% and 5% for JK 1C+20 p.p.m. lead.

The author is grateful to the steel works participating in the committee on determination of Sb, Pb and Bi in steels for financial support and for permission to publish the results of the interlaboratory comparison; also to Dr. S-E Lunner, Avesta Steel Factory, for providing the results on the Perkin-Elmer instrument, to Professor Gillis Johansson for help with the manuscript and to Dr. Gillis Lundgren for valuable discussions.

TABLE III

INTERLABORATORY COMPARISON OF RESULTS (p.p.m.) OBTAINED FOR DETERMINATION OF LEAD WITH TOPO/MIBK EXTRACTION AND COMPARISON WITH DESCRIBED PROCEDURE

(Most of the values represent the mean of 10 determinations.)

Designation	*Laboratory*[a]							*Described procedure*	*Certificate value*
	1	*2*[c]	*3*	*4*	*5*	*6*	*7*		
BCS 330 Mild steel	25	24	29	29	28	26	24	27	30
BCS 336 Austenitic stainless steel	7	6	8	8	7	6	9	7	7
JK 1C Ultrapure mild steel	<1	—	<1	<1	<1	<1	<0.7	0.3	<1
JK 2C Low alloy steel	4	4	4	4	4	4	3	4	4
JK 8C Austenitic stainless steel type 316	2	—	2	2	1	2	3	2	2
JK 16A Ferromolybdenum	8	7	9	9	11[b]	8	10	9	10
Tool steel	4	3	4	—	—	—	—	4	—
Tool steel	3	—	2	—	—	—	—	2	—
Tool steel	5	3	6	—	—	—	—	6	—
High speed steel type AISI M2	4	2	3	—	—	—	—	2	—

[a] (1) Fagersta AB, Fagersta, (2) ASEA, Västerås, (3) Domnarvet Steel Factory, (4) Nyby Steel Factory, (5) Ovako Oy, Imatra Steel Factory, (6) Avesta Steel Factory, (7) this laboratory.

[b] After iron has been separated.

[c] With a graphite furnace.

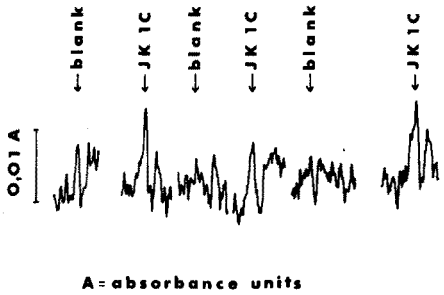

Fig. 5. Recorder traces for determination at the detection limits.

SUMMARY

A method for the determination of 1–100 p.p.m. of lead in high- and low-alloy steels by flameless atomic absorption is described. The sample was dissolved in aqua regia, and 2 μl of the diluted solution were pipetted into a Massmann-type furnace. Ashing of the sample at 625°C eliminated influences from hydrochloric acid. Fe, Cr and Ni gave similar negative interferences, which were compensated for by using low-alloy steel with standard additions. An interlaboratory comparison showed that this method gave the same result as extraction with TOPO in MIBK. The procedure could also be applied to commercial instruments. The time for a complete analysis including dissolution was 15 min.

REFERENCES

1 F. P. Byrne, R. J. Nadolin, J. Penkrot, J. S. Rudolph and C. R. Wolfe, *Amer. Soc. Test. Mater., Spec. Tech. Publ.*, 407 (1968) 237.
2 R. T. Postlethwaite, L. Kidman, B. Bagshawe, K. M. Bills, T. S. Harrison and J. A. Wattsmith, *J. Iron Steel Inst., London*, (1970) 500.
3 B. Metters and B. G. Cooksey, *Analyst (London)*, 99 (1974) 457.
4 M. G. Atwell and O. S. Golden, *Appl. Spectrosc.*, 27 (1973) 464.
5 A. Walsh, *Appl. Spectrosc.*, 27 (1973) 335.
6 D. R. Thomerson and W. J. Price, *Analyst (London)*, 96 (1971) 825.
7 B. Gandrud and J. C. Marshall, *Appl. Spectrosc.*, 24 (1970) 367.
8 C. Thulbourne and P. H. Scholes, *B.I.S.R.A. Committee Report, MG/D/511/68.*
9 K. E. Burke, *Analyst (London)*, 97 (1972) 19.
10 M. E. Hofton and D. P. Hubbard, *Anal. Chim. Acta*, 52 (1970) 425.
11 U. Bohnstedt, *DEW-Tech. Ber.*, 11 (1971) 101.
12 G. G. Welcher, O. H. Kriege and J. Y. Marks, *Anal. Chem.*, 46 (1974) 1227.
13 F. Shaw and J. M. Ottaway, *Analyst (London)*, 99 (1974) 184.
14 N. V. Steere, *Handbook of Laboratory Safety*, Chemical Rubber Company, Cleveland, 1967, p. 213.
15 W. Frech, *Talanta*, 21 (1974) 565.
16 W. Frech, submitted to *Z. Anal. Chem.*
17 G. Lundgren, L. Lundmark and G. Johansson, *Anal. Chem.*, 46 (1974) 1028.
18 G. Lundgren and G. Johansson, *Talanta*, 21 (1974) 257.
19 J. Vrestál, J. Havír, J. Brandstetr and S. Kotrlý, *Collect. Czech. Chem. Commun.*, 24 (1959) 361.
20 G. Lundgren and L. Lundmark, submitted to *Anal. Chem.*

Analytica Chimica Acta, 77 (1975) 53–63

MOLECULAR EMISSION CAVITY ANALYSIS—A NEW FLAME ANALYTICAL TECHNIQUE

PART V. THE DETERMINATION OF SOME SULPHUR ANIONS

R. BELCHER, S. L. BOGDANSKI, D. J. KNOWLES* and A. TOWNSHEND

Chemistry Department, Birmingham University, P.O. Box 363, Birmingham, B15 2TT (England)

(Received 23rd January 1975)

Sulphur-containing species give some of the most sensitive emission responses when subject to molecular emission cavity analysis (MECA). In a previous paper[1], it was shown that ng amounts of sulphuric or sulphurous acid could be determined by MECA, as well as equally small amounts of organosulphur compounds such as thiourea and dimethyl sulphoxide. The present paper describes the MECA behaviour of sulphate, sulphide, metabisulphite, thiosulphate, thiocyanate, sulphide and peroxodisulphate ions, on the basis of their S_2 emissions measured at 384 nm. Although metal ions depress most of the emissions, a simple method of eliminating this effect *in situ* is available. Most of the investigations were carried out on a newly designed, commercially available MECA spectrophotometer.

EXPERIMENTAL

Analytical-grade reagents were used where possible. Stock sulphite solutions (about 400 p.p.m. S) were stabilized with 2 ml of 0.05 *M* EDTA per 250 ml.

The instrument used was a prototype MECA spectrophotometer (Anacon Inc., Ashland, Mass., U.S.A.). It has a premixed nitrogen–hydrogen (air) flame, with a burner adjustable in a vertical and both horizontal directions. The cavity holder is inserted into a rotatable cylinder, with the cavity aperture upwards. The sample solution (in the present work 3 or 5 μl) is injected into the cavity in this position, after which the cylinder is rotated through 90° to position the cavity reproducibly in the flame (Fig. 1). The inclination of the cavity aperture to the flame gas flows[1] can be adjusted to the optimal value by an adjustment to the inclination of the block holding the cylinder. The emission from the cavity is passed via an 8.5-nm slit and a grating monochromator to a photomultiplier, the output of which is fed to an Oxford 3000 potentiometric recorder, (Oxford Electronic Instruments Ltd., Oxford, U.K.) which has a fast response time of 0.20 s for 90% f.s.d. Peak areas were measured by triangulation. The electronic integration and maximal peak hold facilities of the instrument were not used in the present work.

When all required emission responses from a given sample have been obtained, the cylinder is rotated through a further 90°, and the cavity holder, now very

* On sabbatical leave from the Preston Institute of Technology, Melbourne, Victoria, Australia.

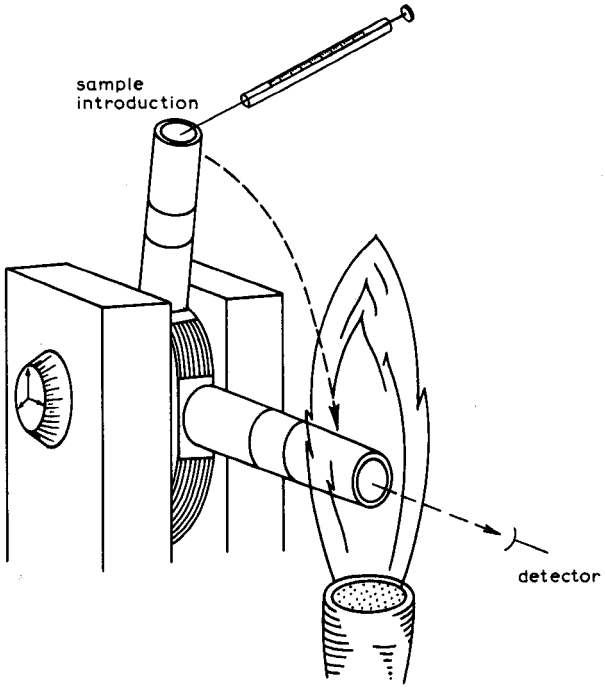

Fig. 1. Sample introduction to flame by cavity holding apparatus.

hot, drops into a drawer, where it is left to cool down before re-use. During this rotation, if another cavity is waiting in the sample injection position, that cavity is simultaneously moved into the flame. This enables very rapid analyses of successive samples to be made.

Alternatively, after emission from a cavity is complete, the cavity may be rotated back to the original injection position and cooled by an air blower before injection of the next sample. This procedure takes longer than the first method, but allows the same cavity to be used for all experiments, thus avoiding any possibility of variation arising from variable cavity characteristics (size, shape, etc.). This procedure was used in the present investigation.

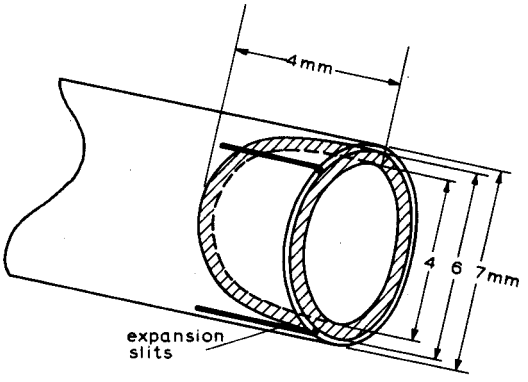

Fig. 2. Silica lined MECA cavity.

The cavity consists of a silica cup or liner inserted into an aperture at the end of a stainless steel rod (Fig. 2). They are constructed by drilling out the rod to accommodate the silica cup or liner (40 μl; 6 mm o.d.; 3 mm deep) and cutting four fine slits in the steel wall surrounding the cup to allow for expansion–contraction effects, which might otherwise crack the silica liner. The liner is made from a piece of clear silica tube. The end is sealed off and flattened in a flame and the sealed end is cut to the appropriate size with a diamond wheel. The silica-lined rod is fitted to an adaptor which allows it to be inserted into the rotatable cylinder for introduction to the flame.

In the flame, the cavity is pitched at an angle of 7° downward from the horizontal, as shown on the instrument scale, and is approximately 3 mm into the flame. The bottom edge of the cavity is 10 mm above the top of the burner. These positions were found to be the most sensitive for the cavity employed and the flame conditions set up. A nitrogen–diluted hydrogen flame is employed, the flow rates being 6.5 l min^{-1} and 4.5 l min^{-1} respectively. All emission intensities reported are peak areas.

RESULTS

Sulphate

The responses of sulphate as sulphuric acid and as the sodium, ammonium iron(II) and manganese(II) salts have already been studied. As described previously[1], the time from inserting the cavity into the flame to achieving maximal intensity (t_m) increases as the thermal stability of the compound increases, *i.e.*, $Na^+ > Fe^{2+} > Mn^{2+} > NH_4^+ > H^+$ (see Table I). Likewise, the emission intensity decreases as t_m

TABLE I

MECA CHARACTERISTICS OF SOME SULPHUR ANIONS

(Phosphoric acid is present unless otherwise stated.)

Compound	*Max. limit of linearity (μg S)*	*Slope of log–log plot*	t_m *(s)*	t_m *for simple aq. soln. (s)*
$FeSO_4$	1.2	1.7	8	40–60[c]
$MnSO_4$	1.2	1.8	8	40–60[c]
Na_2SO_4	1.0	1.6	8	40–60[c]
$(NH_4)_2SO_4$	≥1.3	1.7	8	11
H_2SO_4	1.2	1.8	8	9
$K_2S_2O_8$	1.2	1.6	8	11
Na_2SO_3	0.8	1.9	2.4	4.8
$Na_2S_2O_5$	0.6	2.0	1.7	3.5
$Na_2S_2O_3$	0.8[a]	1.7[a]	3.0[a]	4.0
KSCN	0.65	2.0	2.4	4.0
Na_2S	0.9[b]	1.4[b]	1.4[a]	3.5
	0.65[a]	2.2[a]		

[a] 1:1 $(NH_4)_2HPO_4$–$NH_4H_2PO_4$ buffer solution.
[b] Simple aqueous soln.
[c] Broad response.

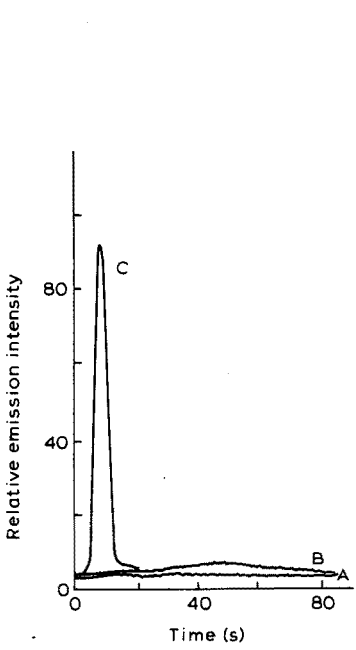

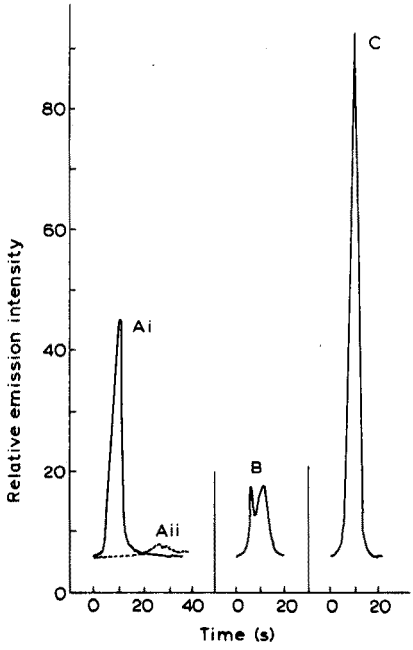

Fig. 3. Response from manganese sulphate: A, with perchloric acid; B, simple aqueous solution; C, with phosphoric acid.

Fig. 4. Response from ammonium sulphate: Ai, in aqueous solution; Aii, with NaCl; B, with perchloric acid; C, with phosphoric acid.

increases. Thus, in the diluted hydrogen diffusion flame, sulphuric acid gives a good emission response whereas the equivalent amounts of the more refractory compounds such as iron(II), manganese(II) and sodium sulphates give little or no response under these conditions. Figure 3, which shows the response of manganese(II) sulphate is typical. Ammonium sulphate gives about 50% of the response of the equivalent amount of sulphuric acid (Fig. 4), addition of sodium chloride to ammonium sulphate gives the same depressed response as sodium sulphate, thus indicating the trend for the sulphur to be vaporized as the least volatile compound thereby giving the least sensitive MECA response. Such depressive effects cause serious interference in the determination of sulphate ions by MECA, as they do in aspiration systems[2].

It was thought that such effects might be alleviated by adding an acid, the anion of which forms more thermally stable salts than sulphate with interfering cations, thus effectively releasing the sulphate as sulphuric acid. A series of acids was added to solutions of various sulphate salts, and the MECA response for sulphur was observed. No effect was observed with the addition of hydrochloric, hydrofluoric and nitric acids, while perchloric acid appeared to have a negative effect in most cases. The addition of perchloric acid decreases the already slight S_2 emission from iron(II), manganese(II) (Fig. 3), and ammonium sulphates (Fig. 4), and has no noticeable effect on the emission from sodium sulphate. The ammonium sulphate response is split to give two peaks (Fig. 4).

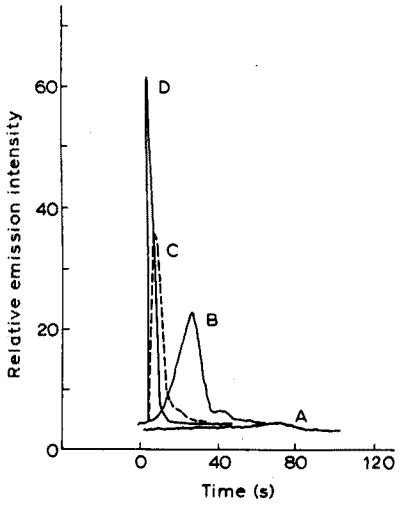

Fig. 5. Effect of phosphoric acid concentration on the response from 0.01 *M* iron(II) sulphate: A, 0.0 *M*; B, 0.01 *M*; C, 0.03 *M*; D, 0.07 *M*.

Phosphoric acid, which is the least volatile acid and forms the most refractory salts, has the desired effect.

The effect of increasing phosphoric acid concentrations on the emission of iron(II) sulphate is shown in Fig. 5. As the acid concentration increases, the emission peak with the t_m typical of iron(II) sulphate is gradually replaced by a more rapid, more intense response, with a t_m typical of sulphuric acid under the same conditions. Phosphoric acid concentrations greater than 0.07 *M* have no further effect on the emission from the amount of iron(II) sulphate used. In all subsequent experiments, the solutions studied were 0.10 *M* in phosphoric acid.

Phosphoric acid was found to have the same effect on iron(II), manganese, sodium and ammonium sulphates. All give intense peaks of $t_m = 8$ s (Figs. 3, 4), identical in t_m (Table I) and area (Table II) to sulphuric acid under the same conditions. In addition to removing the cationic interference, the phosphoric acid gives slightly sharper sulphuric acid peaks than when sulphuric acid alone is introduced into the cavity. The calibration graphs for sulphate, measured for the

TABLE II

MECA RESPONSES OF SULPHATE IN THE PRESENCE OF VARIOUS CATIONS IN 0.1 *M* PHOSPHORIC ACID

Compound	*S injected (ng)*	*Emission intensity*	*Intensity per ng S*
H_2SO_4	600	380	0.63 ± 0.04
$(NH_4)_2SO_4$	605	368	0.61
$FeSO_4$	595	377	0.63
$MnSO_4$	610	370	0.61
Na_2SO_4	600	375	0.62

various sulphates and as sulphuric acid in the presence of phosphoric acid, are identical. All give linear log (intensity) *versus* log (weight of sulphur) plots with slopes of 1.7 ± 0.1, up to 1 μg of sulphur, with the response bending towards the weight axis at higher amounts of sulphate. There is a slight difference in the weight of sulphur at which linearity decreases for the various sulphates (Table I). The limit of detection under these conditions is about 1 p.p.m. of S.

Sulphite, metabisulphite

As with sulphate, the presence of sodium ions decreases and delays the S_2 emission from sulphite compared with that from sulphurous acid (Fig. 6), but the effect is much less than the comparative effect on sulphate ions. Again, however, the addition of phosphoric acid markedly enhances, sharpens and speeds up the response. In the presence of phosphoric acid, S_2 emission from sulphite occurs very quickly, *i.e.* after very little heating in the flame (Table I). Since sodium sulphite is one of the most difficult sulphites to break down in the MECA cavity, there is no doubt that phosphoric acid will be equally effective in preventing other metal ion interferences in the determination of sulphite. The slope of the log–log calibration graph is slightly steeper (1.9) than that for sulphate, and the range of linearity is slightly smaller, with non-linearity becoming evident at about 0.8 μg of sulphur. Perchloric acid behaves similarly to phosphoric acid, but is less effective. The limit of detection is only *ca.* 10 p.p.m. under the conditions used, although the sensitivity is more than three times greater than that for sulphate (Table III). This happens because of the very rapid response from sulphite.

Potassium metabilsulphite behaves similarly to sodium sulphite, except that

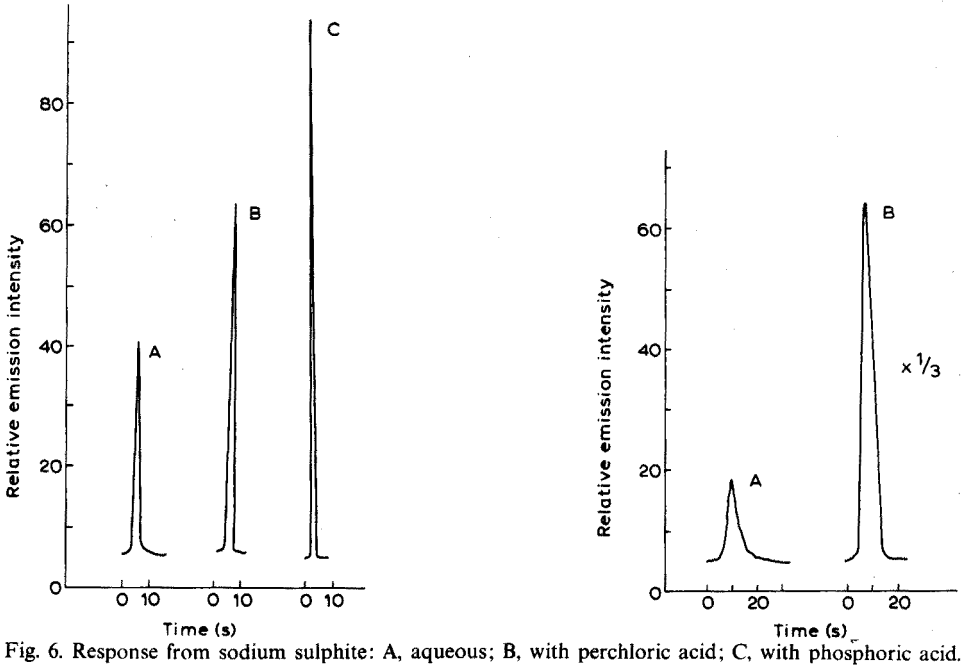

Fig. 6. Response from sodium sulphite: A, aqueous; B, with perchloric acid; C, with phosphoric acid.
Fig. 7. Response of potassium peroxodisulphate: A, aqueous solution; B, with phosphoric acid.

TABLE III

RELATIVE EMISSION INTENSITIES OF THE VARIOUS SULPHUR ANIONS

Compound	*S injected (ng)*	*Intensity per ng S*[a]
KSCN[b]	606	14
$Na_2S_2O_3$[c]	589	8.3
Na_2S[c]	605	5.8
$Na_2S_2O_5$[b]	591	3.6
Na_2SO_3[b]	590	3.4
H_2SO_4[b]	600	1.0
$K_2S_2O_8$[b]	594	1.0

[a] Relative to $H_2SO_4 = 1.0$.
[b] 0.1 *M* in phosphoric acid.
[c] 0.01 *M* in $H_2PO_4^- - HPO_4^{2-}$ buffer.

the responses of the former in the presence and absence of phosphoric acid, are slightly faster than those of sulphite under the same conditions (Table I).

Peroxodisulphate

Potassium peroxodisulphate alone gives a weak S_2 emission, which is little affected by the presence of perchloric acid, but is enhanced and speeded up by the addition of phosphoric acid (Fig. 7). In the presence of phosphoric acid, the response is very similar to that of sulphate ions (Table I).

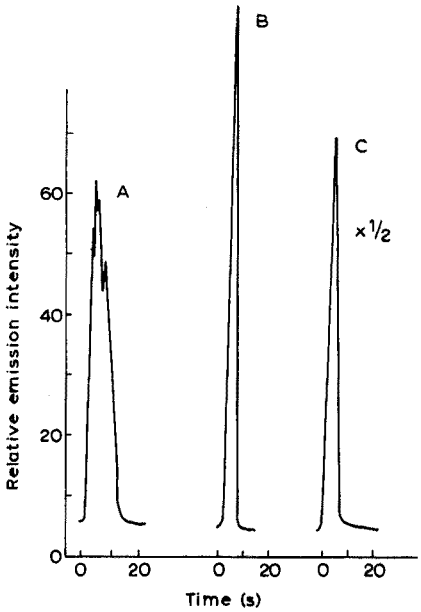

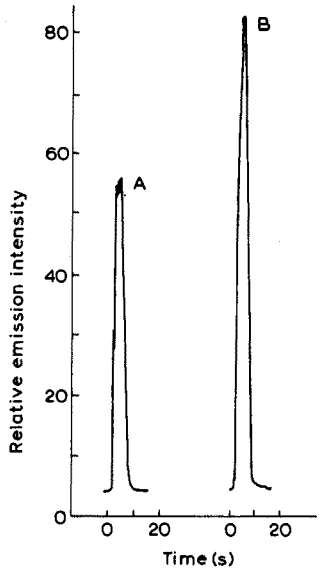

Fig. 8. Response from potassium thiocyanate: A, aqueous solution; B, with perchloric acid; C, with phosphoric acid.

Fig. 9. Response from sodium thiosulphate: A, aqueous solution; B, with ammonium phosphate buffer.

Thiocyanate, sulphide, thiosulphate

Potassium thiocyanate gives a broad, multipeaked response when present alone. Addition of perchloric acid produces a single, sharper, enhanced and more rapid peak, but again phosphoric acid is more effective in this respect (Fig. 8).

Sodium sulphide alone gives an extremely rapidly appearing, but broad emission peak ($t_m = 1.4$ s). Phosphoric acid addition is not of value in this instance, because of loss of hydrogen sulphide, which leads to irreproducible results. The use of a pH 7 ammonium phosphate buffer has little effect on the maximal emission intensity, but gives a much sharper peak.

Sodium thiosulphate gives a rapid multipeaked emission response when present alone. Perchloric or phosphoric acid addition is not feasible because of the decomposition of thiosulphate in acidic media. Addition of the pH 7 buffer somewhat increases the emission intensity (Fig. 9).

The maximal limit of linearity, and the slopes of the log–log calibration plots are included in Table I.

The relative sensitivities for the various sulphur anions are given in Table III.

DISCUSSION

The results described above show that MECA can be used to determine ng amounts of the sulphur anions studied. For sulphate and peroxodisulphate, the best medium found for production of S_2 emission was 0.10 *M* phosphoric acid. The addition of phosphoric acid has a remarkable effect on the S_2 response obtained by the MECA technique. This effect is applicable to the determination of inorganic sulphur compounds by MECA.

The presence of the phosphate anion is believed to have several functions. It is likely that phosphoric acid addition causes the formation of more refractory metal phosphates, so that sulphuric acid is released from the sample in the MECA cavity. This interpretation is indicated by the change in the time of the emission after introduction of the cavity to the flame (t_m). It is further indicated by the basic trend which exists with MECA for the least volatile compound to be formed.

The emissions from volatile ammonium sulphate and sulphuric acid are also enhanced by the addition of phosphoric acid. This occurs along with a slight decrease in the t_m values, which indicates that the thermal conductivity between the cavity wall and the sample deposited within the cavity may be improved by the presence of a liquid coating of the acid.

The phosphoric acid may also serve another role. Free radical studies often utilize a phosphoric acid coating to reduce the rate of hydrogen atom recombination, and such a function in the cavity would lead to an increased hydrogen atom concentration and thus to an enhanced production of S_2 molecules. Such mechanisms may also partly explain the enhancement of S_2 emision from the already rapid sulphite, metabisulphite and thiocyanate emissions.

Perchloric acid decreases the emission from the sulphates, but slightly enhances those from thiocyanate and sulphite. This behaviour may be reconciled by considering the vaporization of perchloric acid. After the perchloric acid has volatilized as $HClO_4$, it breaks down to liberate OH, ClO_3, ClO and O_2 species. The presence of such oxidizing species, *i.e.* oxygen in particular, in a H_2–N_2 flame

has been shown to decrease the S_2 emission. This negative effect can be observed with MECA only when oxygen is added directly to the sheltered region of the cavity space.

A study of perchloric acid alone in the cavity shows that a brief white emission, similar to that obtained when adding oxygen to the cavity, is obtained. This response could be measured by reading the increase of the OH emission at 306 nm, indicating that vaporization was initiated about 4 s after cavity introduction. Any metal perchlorate salts which would form would be expected to release the deleterious oxidizing vapour at a later time. Thus species giving emissions with $t_m \leqslant 4$ s would not interact significantly in the vapour phase with perchloric acid fragments, and there would be no reduction in emission. There would be the possibility of a slight enhancement because of the formation of the more volatile acid of the anion in question. Emission from species with $t_m > 3$ s, however, would be reduced in the presence of perchloric acid. These postulations were borne out in practice. Thiocyanate ($t_m = 3$ s) and sulphite ($t_m = 2.5$ s) are slightly enhanced, whereas sulphate ($t_m = 11$ s) is depressed.

Previous studies of the flame photometric determination of sulphur based on S_2 emission have indicated wide variations in responses for different sulphur compounds[1–4]. If the rate of production of S_2 emission is determined by the interaction of two sulphur-containing species, the slope of the linear portion of the log–log calibration plot will be 2. In practice, values between 1 and 2 have been found, depending on the compound and the experimental conditions[3–7]. In the above studies, the slope varies between 1.6–1.7 for emissions of $t_m = 8$ s (SO_4^{2-}, $S_2O_8^{2-}$) to 2.2 for emissions of $t_m = 1.4$ s (S^{2-}), intermediate values being found for intermediate t_m values. This variation may indicate changes in the mechanism of formation of excited S_2 molecules at different temperatures and reflect the instantaneous concentrations of sulphur in the cavity obtained from various sulphur compounds. The sensitivities generally follow the order found by Dagnall *et al.*[2] in an aspiration system.

The log–log calibration plots bend away from the intensity axis when large amounts of sulphur anions are present, almost certainly because of self-absorption. Greer and Bydalek[6] have devised an expression to correct for non-linearity arising from self-absorption in aspiration systems. No doubt a similar expression could be devised for correcting the MECA responses. It is interesting that the onset of non-linearity occurs at smaller amounts of sulphur, the shorter the t_m value. This probably arises because of the higher instantaneous relative concentration of S_2 molecules in the cavity produced by the species with shorter t_m values. The most sensitive responses come from anions in which a sulphur atom is not bound to oxygen (SCN^-, S^{2-}), that of thiocyanate being most sensitive. Sulphite and metabisulphite have an intermediate sensitivity, and give the same intensity as each other per sulphur atom; sulphate and peroxodisulphate also have the same intensity per sulphur atom as each other, and the same t_m values in the presence of phosphoric acid, indicating that peroxodisulphate is converted to sulphate, or to a common product with sulphate, in the cavity, before forming S_2 species. The sensitivity is less than that for the other anions studied.

As many of the sulphur anions have appreciably different t_m values, it should be possible to resolve the responses from mixtures of certain of the anions. For

example, in the presence of phosphoric acid, sulphite has a t_m of 2.4 s and the emission is essentially complete after 5.0 s. Sulphate ion has a t_m of 8 s, emission first occurring approximately 6 s after introduction into the flame. A preliminary study has shown that two well-defined responses are obtained with a sulphite–sulphate mixture. A more extensive study of this and other mixtures (for example, thiosulphate and sulphate) will be published in the near future.

Use of silica cavities

When stainless steel cavities are used for MECA, thermally stable materials, such as various sodium salts, remain in the cavity after the analysis is complete, because the maximal temperature achieved by the cavity is usally only *ca.* 1000°C. The gradual build-up of involatile species affects the reflective properties of the cavity, and gradually causes decreased emissions by retarding volatilization. It is, however, difficult to remove these materials from the cavity by washing as the material appears to impregnate the metal. The metal itself also changes in character after repeated heatings. It was noted that the front surface of the cavity becomes "porous"; that is, after injection of a sample, some of the solution "wets" the front of the cavity with a consequent change in the behaviour of the sample when placed in the flame. Several responses were observed presumably from volatilization of the solution from the front surface initially and then that contained in the cavity itself. A cavity in this condition must be discarded. The introduction of a silica thimble removes this effect, solutions being maintained in the cavity until placement in the flame. It was also found that one could clean the inside of the cavity, with distilled water in the case of aqueous solutions, and the cavity functioned satisfactorily for at least 200–300 measurements.

The first liners used were subject to fracture on cooling after four or five measurements, no doubt because of the different expansion rates of the silica and stainless steel. This problem was overcome by cutting four fine slots in the top of the steel tube. This procedure had the added advantage of allowing the steel tube to be widened or closed to compensate for variations in the outer diameter of the silica liner.

The silica cavities heat up more slowly than steel cavities of similar size. This slows down the emission response, which is an advantage when analysing anions of fast response or resolving mixtures.

D.J.K. thanks the Council of the Preston Institute of Technology for the generous leave provisions afforded him. The authors thank Anacon Inc., for the gift of a MECA spectrophotometer and recorder.

SUMMARY

An investigation of the MECA behaviour of sulphate, sulphite, metabisulphite, peroxodisulphate, thiocyanate, thiosulphate and sulphide ions, has shown that ng amounts of these anions may be determined in samples of a few μl. Metal ion interferences in the determination of sulphate and sulphite are removed by addition of phosphoric acid.

REFERENCES

1 R. Belcher, S. L. Bogdanski and A. Townshend, *Anal. Chim. Acta*, 67 (1973) 1.
2 R. M. Dagnall, K. C. Thompson and T. S. West, *Analyst (London)*, 92 (1967) 506.
3 A. Syty and J. A. Dean, *Appl. Opt.*, 7 (1968) 1331.
4 T. Sugiyama, Y. Suzuki and T. Takeuchi, *J. Chromatogr. Sci.*, 11 (1973) 639; *J. Chromatogr.*, 77 (1973) 309.
5 R. K. Stevens, J. D. Malik, A. E. O'Keefe and K. J. Krost, *Anal. Chem.*, 43 (1971) 827.
6 D. G. Greer and T. J. Bydalek, *Environ. Sci. Technol.*, 7 (1973) 153.
7 C. Veillon and J. Y. Park, *Anal. Chim. Acta*, 60 (1972) 293.

Analytica Chimica Acta, 77 (1975) 65–70

DETERMINATION OF SILVER IN BIOLOGICAL MATERIALS BY HIGH-FREQUENCY PLASMA-TORCH EMISSION SPECTROMETRY

RYOZO NAKASHIMA, SHOZO SASAKI and SHOZO SHIBATA
Government Industrial Research Institute, Nagoya, Hirate-machi Kita-ku, Nagoya (Japan)
(Received 13th January 1975)

High-frequency plasma torches have recently become more widely studied for excitation in emission spectrometry. They provide better reproducibility than conventional methods of excitation, and much higher temperatures than flames, and they can be applied to gaseous, liquid and solid samples.

In previous work from this Laboratory[1], a Hitachi UHF plasma Spectrascan was used for the determination of niobium, titanium and zirconium in steels. The method has the advantages outlined above, but when aqueous solutions are used, the moisture which is not trapped in the condenser at the front of the atomizer, can lower the efficiency of the plasma and thus the emission intensity.

Silver can be detected with very high sensitivity when a plasma torch is used, but even better sensitivity may be necessary when the amount of sample available is limited. A considerable improvement in sensitivity can be achieved if the silver spectral line is enhanced by the presence of bismuth, and if a second condenser is maintained at about -3–5°C at the front of the atomization chamber described previously[1]. Silver can be collected from biological samples by co-precipitation with bismuth iodide, before plasma-torch emission spectrometry. The combination of techniques allows the detection limit to be improved to 0.5 ng of silver for 0.2 ml of solutions of samples such as whole blood.

EXPERIMENTAL

Apparatus

A Hitachi UHF-Plasma Spectrascan Model 300, which has already been described[1], was used. In preliminary experiments, spectral intensities were measured by wavelength scanning during continuous introduction of the sample solution. The instrumental conditions were as follows: wavelength, 328.07 nm; plasma gas, 3.0 l Ar min^{-1}; sheath gas, 3.5 l Ar min^{-1}; cooling water, 5°C; heating chamber, 180 ± 10°C; entrance slit, 30 μm; exit slit, 50 μm; pneumatic nebulizer, 3.5 ml min^{-1} with water at 3.0 l min^{-1}; anode current, 300 mA; field current, 400 mA; photomultiplier, Hamamatsu TV, R106, at 600 V.

For actual analyses, the wavelength of the scanning monochromator was fixed at 328.06 nm and a definite aliquot of sample solution was introduced. When the second condenser was used, the field current was set at 270 mA, which was the maximum value possible for a stable plasma.

The nebulizer was provided with a two-way tap, so that either rinsing

water or sample solution from a 2-ml vessel could be introduced. An aliquot of solution was pipetted into the vessel, and the sample was introduced by quickly turning the tap. At the end of the sample introduction, the tap was turned as soon as possible, to minimize introduction of air, so that distilled water was introduced through the other arm of the tap. The sampling vessel was then rinsed with distilled water for the next sample.

Reagents

Standard silver solution (1000 p.p.m.). A standard silver nitrate solution in 0.1 *M* nitric acid (Wako Pure Chemical Industries) was suitably diluted with twice-distilled water.

Standard bismuth solution (5000 p.p.m.). Bismuth metal (>99.999%; Mitsubishi Metal Mining Co.) was dissolved in nitric acid and the solution was suitably diluted.

Other standard solutions (2000 p.p.m.) were prepared from iron, manganese or thallium wire (Johnson-Matthey), antimony and tin (>99.999%; Mitsubishi Metal Mining) and yttrium oxide (Shinetsu Chemicals). These metals and oxide were dissolved in as little hydrochloric or nitric acid (super-special-grade; Wako Chemicals) as possible, and the solutions were diluted suitably with twice-distilled water in volumetric flasks. All other reagents used were of high purity or superior to analytical-grade chemicals. Twice-distilled water was used throughout.

Procedure for biological materials

Pipette a 1–2-ml aliquot of sample, 0.5 ml of perchloric acid (70%) and 1.0 ml of concentrated nitric acid into a 10-ml beaker, and cover with a watch-glass. Heat gently on a hot plate; when decomposition is complete, continue heating until the perchloric acid has almost evaporated, but do not evaporate to dryness. Dissolve the residue in 2–3 ml of water, and transfer the solution quantitatively to a 15-ml centrifuge tube. Add 1.0 ml of 0.4 *M* sodium iodide and 1.0 ml of bismuth solution while stirring. After 10 min, centrifuge, decant the solution and rinse the precipitate several times with 2 ml of water. Pour 0.1–0.2 ml of concentrated nitric acid on the collected precipitate, and heat until violet fumes cease to appear. Transfer the solution to a 2-ml measuring cylinder (graduated at 0.05-ml intervals) and rinse the tube into the cylinder at least five times with the minimal volume of water. Then, read the volume exactly, and stopper and shake the cylinder. Analyze this solution by the standard addition method.

RESULTS AND DISCUSSION

Preliminary experiments

The resonance line of silver at 328.07 nm was compared with the 338.28-nm line for sensitivity; the former line had the better detection limit and was therefore used. The profile of the emission intensity over the width of the plasma (Fig. 1) showed that intensity was maximal at 3.5–4.0 mm from the plasma axis at a fixed height of 15–30 mm from the tip of the electrode.

The effect of inorganic acids on the emission intensity is shown in Fig. 2.

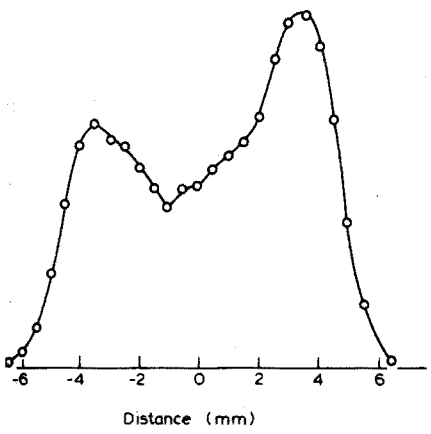

Fig. 1. The profile of the emission intensity at 328.07 nm over the plasma width for 0.1 p.p.m. silver.

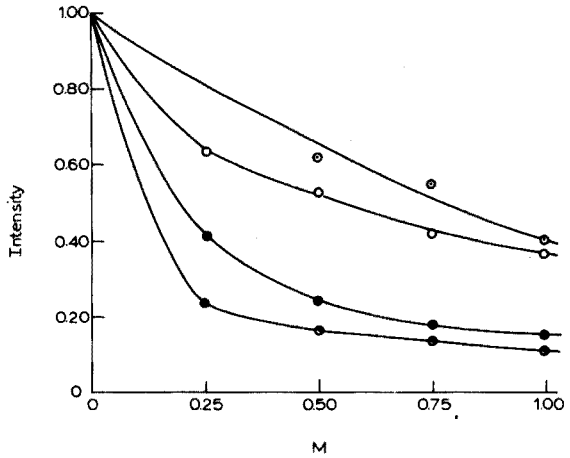

Fig. 2. Effects of acid concentrations on the silver line intensity: (⊙) HNO_3, (○) HCl, (●) $HClO_4$, (◑) H_2SO_4.

As the acidity increased, the intensity gradually decreased. Nitric acid had the smallest effect and was therefore used in subsequent work.

Effect of diverse metals

Whole blood usually contains about 3000 p.p.m. of sodium and 300 p.p.m. of iron. The effects of these metals on the emission intensity for silver must therefore be known, as must their effects when traces of silver are precipitated with a carrier metal[3–5] or an organic reagent[6,7] and the precipitate is dissolved before analysis with the plasma torch. Although it was not explicitly stated earlier[1,2], organic material tends to decrease intensities, probably because of scattering of radiation by carbonized particles in the outer region of the plasma torch; organic reagents were therefore not examined further.

The effects of diverse metals (1000 p.p.m.) on the emission intensity of 0.1 p.p.m. of silver were studied. Antimony, bismuth, iron, lead, tin and yttrium all enhanced the emission intensity, but the intensity profile was unchanged. With sodium, as the concentration increased, the intensity was enhanced gradually, and the position of maximum intensity shifted towards the plasma axis, coinciding with it at 200 p.p.m. of sodium; at higher concentrations, the intensity decreased gradually, but the intensity profile was unchanged. At sodium concentrations of 1000–3000 p.p.m., the intensity was less than one tenth that in the absence of sodium. Similar behavior was found with thallium. Manganese showed such a strong line at 328.08 nm that the silver line could not be measured. Iron showed a weak line at 328.03 nm, but the emission intensity for 250 p.p.m. of iron was only a few percent of that for 0.1 p.p.m. of silver. In the analytical method, the silver line could be recorded without interference from iron, except for increased background noise. These results indicate that iron, manganese and sodium must be eliminated from the final solution. Other elements with neighbouring lines, *i.e.* molybdenum, titanium, vanadium and zirconium, did not interfere at the 10-p.p.m. level.

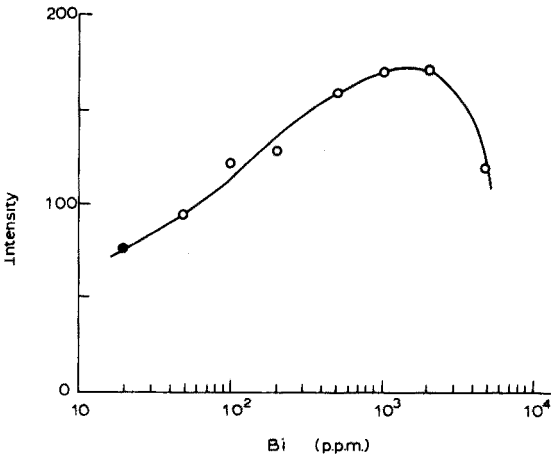

Fig. 3. Effect of concentration of bismuth on the emission intensity of 0.1 p.p.m. silver. (●) In the absence of bismuth.

TABLE I

PRECISION AND ACCURACY FOR SILVER DETERMINATIONS

Silver taken (ng)	*Average found (ng)*[a]	*s*	s_r (%)
2.0	15.5	2.77	18
4.0	29.0	2.45	8.4
10.0	84.0	6.06	7.2
20.0	168.0	5.66	6.7
40.0	386.0	13.9	7.2

[a] Average of 10 determinations.

Detection limit and precision

The detection limits defined as the concentration or the amount of metal needed to give a signal–noise ratio of 2, were examined. When the temperature of the condenser was set at 5°C, the detection limit was 0.005 p.p.m. but this was improved to 0.002 p.p.m. by addition of 1000 p.p.m. of bismuth to the sample solution. The relationship between the emission intensity and the added quantity of bismuth is shown in Fig. 3; the intensity increased with bismuth concentration up to 1000 p.p.m., but then decreased beyond 2000 p.p.m. The most enhanced value was nearly 2.5 times that in the absence of bismuth. When a second condenser (22 cm long, 5.5 cm diameter) designed so as to cool the inlet gas from inside and outside, was maintained at -3 to -5°C, the detection limit improved again to 0.001 p.p.m. or 0.5 ng (for discrete samples) in the presence of 1000 p.p.m. of bismuth.

Standard deviations were calculated from the peak areas of ten replicate measurements of 0.2-ml aliquots of silver solutions (Table I). The relative standard deviations were in the range 7–9%, except that the value was 18% for 2 ng of

silver. The calibration curves were linear and passed through the origin whether peak areas or heights were measured.

West *et al.*[8] reported an adsorption loss of silver on borosilicate glass surfaces at low concentrations. These authors mentioned that losses were avoided by addition of 0.1 *M* sodium thiosulphate, but this was precluded in the present method because of the sodium interference mentioned above. In order to check adsorption losses, the peak heights for 0.025-, 0.05- and 0.10-p.p.m. silver solutions containing 1 ml of concentrated nitric acid per 10 ml, which had been stored in pyrex glass vessels for a few days, were compared with the peak heights for freshly prepared solutions; no changes in the concentrations were found.

Analysis of biological materials

In the method finally developed, bismuth iodide acted as a carrier for silver ions, the bismuth also providing an enhancement effect, after removal of iodine.

Before the carrier precipitation, the pH of the sample solution was adjusted to 0.5–1.5 with 20% sodium hydroxide solution, if necessary. Since even analytical-grade sodium hydroxide may contain a significant amount of silver, only the minimal quantity should be used.

When a solution containing silver and hydrochloric acid was nebulized, an anomalous momentary noise appeared to obscure not only the silver peak but also the base line. This phenomenon may have been caused by large particles of silver chloride on the wall of the nebulizer, drifting occasionally into the torch flame. Hydrochloric acid was therefore avoided in the procedure.

TABLE II

RECOVERY OF SILVER BY CARRIER PRECIPITATION

Silver taken (μg)	*Silver found* (μg)[a]	*Recovery* (%)
1.00	1.10	110
0.50	0.485	97
0.20	0.185	94
0.10	0.089	90
0.050	0.050	99
0.025	0.027	110

[a] Average of 2 determinations.

Recoveries of silver by the carrier method were examined for standard solutions. Values of 90–110% were obtained in the range 0.03–1.00 μg of silver taken (Table II). The reagent blank was less than 0.01 μg, which has been deducted from the tabulated values. Recovery tests were also made with commercial condensed milk: 1.0 and 2.0-ml aliquots of the milk alone and with 0.20 μg of silver added were analyzed. The mean recoveries (3 analyses) were 94% and 89%, respectively, for the 1.0 and 2.0-ml aliquots. The amount of silver present in the milk itself was 0.01 (4) μg ml^{-1} (average of 6 determinations).

Blood samples. Whole blood samples were analyzed by the recommended method. After deduction of reagent blanks, the silver contents found were 0.02(0)

and 0.01(2) μg ml^{-1}, respectively (average of 3 determinations with ranges of 0.016–0.024 and 0.009–0.014).

SUMMARY

Nanogram amounts of silver in small samples of biological materials can be determined by high-frequency plasma-torch emission spectrometry. Samples are digested with perchloric and nitric acids, silver is collected with a bismuth iodide carrier, and the precipitate is decomposed with concentrated nitric acid before dilution. Bismuth shows an enhancing effect on the silver emission at 328.06 nm, and the sensitivity is further improved by elimination of moisture in the aerosol with a second condenser at -3 to -5°C. The detection limit is 0.5 ng per 0.2 ml of sample solution. Condensed milk and whole blood were analyzed satisfactorily.

REFERENCES

1 R. Nakashima, S. Sasaki and S. Shibata, *Anal. Chim. Acta*, 70 (1973) 265.
2 G. W. Dickinson and V. A. Fassel, *Anal. Chem.*, 41 (1969) 1021.
3 V. G. Tiptsova-Yakoleva and A. G. Drortsan, *Zh. Anal. Khim.*, 24 (1969) 114.
4 N. A. Rundney, L. I. Parlenko, G. I. Malofeeva and L. V. Simonova, *Zh. Anal. Khim.*, 24 (1969) 1223.
5 R. Ko and P. Anderson, *Anal. Chem.*, 41 (1969) 177.
6 M. C. Farquhar, J. A. Hill and M. M. English, *Anal. Chem.*, 38 (1966) 208.
7 K. Fukuda and A. Mizuike, *Anal. Chim. Acta*, 51 (1970) 77.
8 F. K. West, P. W. West and F. A. Iddings, *Anal. Chem.*, 38 (1966) 1566; *Anal. Chim. Acta*, 37 (1967) 112.

Analytical Chimica Acta, 77 (1975) 71–78

IMPROVEMENTS IN THE NON-FLAME ATOMIC FLUORESCENCE DETERMINATION OF MERCURY

J. E. HAWLEY and J. D. INGLE, Jr.*
Department of Chemistry, Oregon State University, Corvallis, OR 97331 (U.S.A.)
(Received 26th October 1974)

The non-flame atomic absorption technique is commonly used[1–4] for the determination of mercury because of its simplicity, relative freedom from interferences, and reported detection limits of about 1 part per billion (p.p.b.) to 0.02 p.p.b. In this technique, mercury is reduced in solution and the resulting elemental mercury is swept into an absorption cell for measurement. Recently, some researchers[5–9] have adapted the basic atomization technique to an atomic fluorescence (a.f.s.) measurement system. This paper describes the use of an efficient non-flame atomization system for a.a.s. measurements[10] in an improved non-flame a.f.s. system.

The a.a.s. technique is susceptible to spectral interferences in the form of absorption by organic contaminants or chlorine which are swept simultaneously into the absorption cell at the time of measurement, although background absorption correction techniques may be used to compensate for the interference. The proponents of the a.f.s. systems have pointed out that the non-flame a.f.s. system is relatively free from this spectral interference. Also, a.f.s. systems may possess a larger dynamic concentration range in terms of linearity, lower detection limits, and greater instrumental simplicity, since a system with a solar blind photomultiplier but no monochromator may be used[6,7,9]. The better detection limits for a.f.s. are not substantiated in the literature. Until recently, the best reported detection limits were 0.02 p.p.b. (ref. 1) or 0.2 ng (ref. 2) with a.a.s. and 0.06 p.p.b. (ref. 7) or 3 ng (ref. 9) with a.f.s.

Various non-flame a.f.s. systems have been reported. Some authors have used direct atomization from solution[7,8] while others have used a preamalgamation step[5,6,9] before final atomization into an absorption cell. Some workers[5,8] have eliminated the cell completely and vented the mercury vapor into the atmosphere where fluorescence excitation occurred.

A recent critical study[10] has suggested a few basic modifications to the normal apparatus for the non-flame atomic absorption determination of mercury which have resulted in significantly improved detection limits (1 part per trillion or 1 pg), smaller sample volumes (1 ml), and faster analysis times (about 30 per h). The improvements are due largely to the design of the reduction vessel which allows the mercury to be swept efficiently out of solution into a small volume of carrier gas. This provides a much more concentrated mercury plug than previous reduction vessels did. The reduction vessel is a modified sealing tube in which

* To whom correspondence should be addressed.

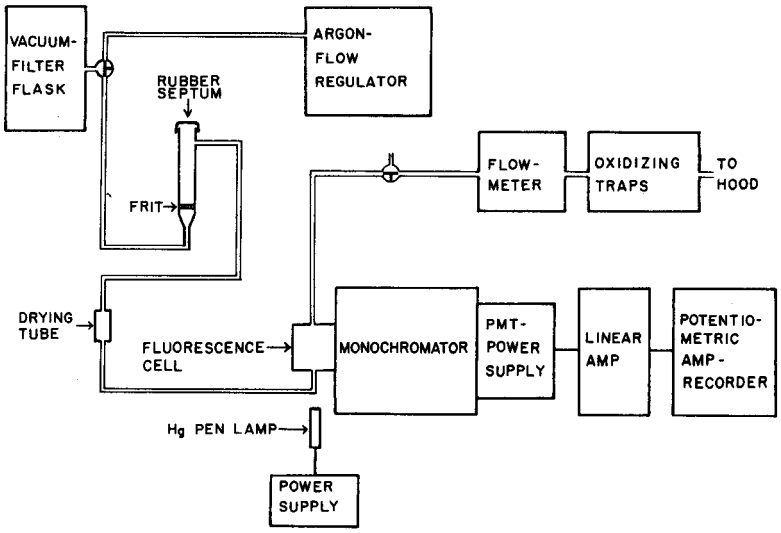

Fig. 1. Block diagram of system.

the carrier gas is bubbled through a frit and then through the sample solution on the other side. This vessel, coupled with the small sample volumes, small apparatus dead volume, and optimized absorption cell dimensions, results in a greater calibration sensitivity or larger peak absorbance per p.p.b. or per ng of mercury(II), and in higher precision at sub-p.p.b. mercury concentrations.

This improved generation system has been adapted to an a.f.s. system to yield a detection limit of 5 parts per trillion or 5 pg of mercury(II). A comparison of the a.a.s. and a.f.s. systems with the same atomization device has shown little difference except that the a.a.s. system provides a lower detection limit and the a.f.s. system has a greater dynamic concentration range for linearity.

EXPERIMENTAL

Solutions and glassware

Stock solutions of 1% (w/v) tin(II) chloride, 0.2% (w/v) potassium permanganate, and 100 p.p.m. mercury(II) were prepared from reagent grade chemicals and distilled water as previously described[10]. Mercury standards were prepared from the stock solution and contained 1% (v/v) concentrated nitric acid and 0.002% (w/v) potassium permanganate as a preservative[10]. All glassware was cleaned as previously described[10].

Instrumentation

The a.f.s. instrument (Fig. 1) contains the specific components shown in Table I. The lower half of the figure represents an atomic fluorescence spectrometer with the flame replaced by a fluorescence cell. The linear amplifier was constructed from an OA, a power supply, and appropriate connectors mounted in a metal box. Rotary switches allow selection of various feedback precision resistors and capacitors. The OA is used as a current-to-voltage converter with

TABLE I

COMPONENTS OF INSTRUMENTATION

Item	*Supplier and model*
1 Source and power supply:	
mercury pen lamp	Ultra-Violet Prod.—11SC-1C
a.c. power supply	Ultra-Violet Prod.—SCT-1
2 Monochromator	Heath—EU-700/E
3 Photomultiplier tubes, power supplies, and holders:	
PMT	RCA—1P28
power supply	Heath—EU-42A
holder	Heath—EU-701-93
4 Linear amplifier:	
operational amplifier	Function Modules—3801
power supply	Analog Devices—915
5 Potentiometric amplifier	Heath—EU-200-01
6 Strip chart recorder	Heath—EU-205-11
7 Flowmeter	Gilmont—F7260
8 Flow regulators	Matheson—1L
	Matheson—70
9 Quartz windows	ESCO Optics Prod.

10^4–10^8 Ω feedback resistors and a variable time constant. The mercury pen lamp powered by the a.c. power supply is oriented at 90° with respect to the cell–monochromator axis.

The upper part of Fig. 1 shows the atomization and flow system which is as previously described[10] except for two modifications: the long path length absorption cell has been replaced by a fluorescence cell, and argon is used in place of air for the carrier gas, since air quenches the fluorescence of mercury[5]. The fluorescence cell (Fig. 2) is made from transparent rectangular plexiglass blocks cemented together. For inlet and outlet ports, holes are drilled and glass tubing is connected to the top and bottom sections of the cell. Quartz windows are glued to the cell and the cell is mounted about 1.5 cm from the slit of the monochromator. Alignment of the pen lamp is made with X–Y translation stages.

During analysis, argon flows from the tank, through a T-bore stopcock, the reduction vessel, a drying tube, the fluorescence cell, another T-bore stopcock, a flowmeter, two mercury oxidizing traps (chromic acid and acidic permanganate solutions in filtering flasks), and finally into the hood. The T-bore stopcocks can can be turned 90° to allow the solution in the reduction vessel to be evacuated into the filter flask without drawing the oxidizing solutions in the traps back into the line.

General procedures

The final instrumental variable settings used for a.f.s. measurements are shown in Table II. After optimization of the cell position, the feedback resistor of the linear amplifier, the gain of the potentiometric amplifier, and the photomultiplier supply voltage are adjusted to yield a reasonable peak deflection for analysis. The actual analytical procedure is identical to that described previously[10].

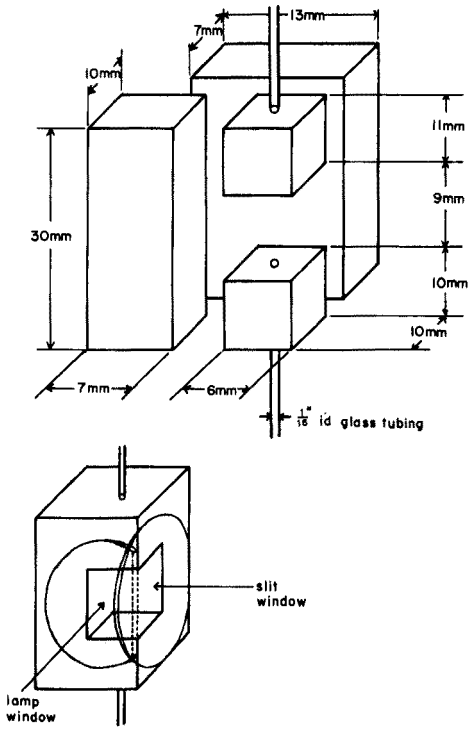

Fig. 2. Construction of fluorescence cell.

TABLE II

OPTIMAL SETTINGS FOR ANALYSIS

Flow rate	140 ml min^{-1}
Frit grade	Medium
Drying tube	5 cm long × 12 mm dia. $Mg(ClO_4)_2$
Gas carrier	Argon
Volume of reductant	0.1 ml
Volume of sample	1.0 ml
Slit width	2000 μm
Fluorescence cell	1 cm × 9 mm × 6 mm
Radiation source	Hg pen lamp (a.c.)
Lamp current	17 mA
RC time constant	1 s
Photomultiplier supply[a]	700—800 V
R_f[a]	10^6—10^8 Ω

[a] Adjusted as described in Procedure.

The reductant (0.1 ml) is injected with a 1-ml syringe into the reduction vessel after the carrier gas flow has been initiated through the frit. After the recorder pen has returned to the base-line, 1 ml of mercury(II) standard is injected with a 1-ml syringe into the reduction vessel. The fluorescence peak is similar in shape and half-width to the absorption peak reported previously[10]

To measure the peak fluorescence, a peak base-line is interpolated by drawing a line between the base-line before injection and after the peak has returned to the base-line. The difference between the fluorescence signal at the peak and the background signal of the interpolated base-line under the peak is taken as the peak fluorescence signal.

The sample is evacuated through the frit and a 1-ml blank is flushed through the frit to eliminate memory effects above 1 p.p.b. mercury(II) levels. The rubber septum and drying tubes are replaced after 20 injections and samples can be analyzed at a rate of about 30 per h.

Optimization

Since the basic atomization and flow system is identical to that used for the a.a.s. system, the previously determined[10] optimal magnitudes for experimental variables such as carrier gas flow rate, sample and reductant solution volumes, and design and size of the reduction vessel were used. These values produced the most concentrated mercury plug which should be optimal for either a.a.s. or a.f.s.

The following variables required optimization for a.f.s.: the volume of the fluorescence cell, the slit width, the alignments of the mercury pen lamp and of the fluorescence cell, the RC time constant, and the type of lamp and current conditions. The cell volume was a very critical variable for a.a.s. measurements and maximum absorbance was obtained only if the cell volume was below a critical value. The atomic fluorescence cell volume of 0.54 cm^3 was less than this critical value. The slit width, the alignments of the pen lamp and fluorescence cell, and the RC time constant were varied to yield the largest signal-to-noise ratio.

The d.c. background signal is due to reflection of the excitation radiation off the cell walls, and the alignment procedure maximizes the fluorescence-to-background ratio. The type of mercury lamp and lamp current were shown to be critical for a.a.s. measurements[10]. A mercury pen lamp was used instead of a mercury hollow cathode because of the much greater radiance of the pen lamp[7]. For a.a.s. measurements, d.c. operation of the pen lamp at low currents provided the highest calibration curve slope and the best linearity, probably because of emission line width effects. For a.f.s., d.c. operation at low currents provided no benefits and the simpler a.c. operation was used.

RESULTS

Table III shows calibration and precision data obtained from analysis of mercury(II) standards. The calibration curve is linear within 5% from 0 to 100 p.p.b. and the precision of analysis is 5% or better for concentrations above 0.05 p.p.b. The detection limit, defined as the concentration or mass which produces a fluorescence signal equal to twice the standard deviation for measurement of a blank, is equal to 0.005 p.p.b. or 5 pg.

To ascertain which factors affect the precision and detection limits, experimental and theoretical standard deviations were compared. The sources of noise in flame atomic spectrometry have been discussed[11]. The expressions presented here take into account the sources of noise that are significant for this particular

TABLE III

CALIBRATION AND PRECISION DATA

Concentration of standard (p.p.b.)	E_f[a] *(V)*	s[b] *(V)*	s/E_f
Blank	0	$4.0 \cdot 10^{-5}$	—
0.05	$9.3 \cdot 10^{-4}$	$4.6 \cdot 10^{-5}$	$5.0 \cdot 10^{-2}$
0.10	$1.90 \cdot 10^{-3}$	$5.5 \cdot 10^{-5}$	$2.9 \cdot 10^{-2}$
0.50	$9.20 \cdot 10^{-3}$	$2.3 \cdot 10^{-4}$	$2.5 \cdot 10^{-2}$
1.0	$1.87 \cdot 10^{-2}$	$4.5 \cdot 10^{-4}$	$2.4 \cdot 10^{-2}$
10	$1.82 \cdot 10^{-1}$	$5.7 \cdot 10^{-3}$	$3.1 \cdot 10^{-2}$
50	$8.90 \cdot 10^{-1}$	$2.6 \cdot 10^{-2}$	$2.9 \cdot 10^{-2}$
100	1.75	$6.4 \cdot 10^{-2}$	$3.7 \cdot 10^{-2}$
1000	10.3	$5.1 \cdot 10^{-1}$	$5.0 \cdot 10^{-2}$

[a] Peak fluorescence signal at output of linear amplifier.
[b] Standard deviation for measurement of E_f calculated from five measurements. For blanks which gave no peak, s was taken to be one-fifth of the background peak-to-peak noise.

non-flame system and are formulated in terms discussed in a recent paper[12]. Experimentally it was found that noise in the dark current or from the amplifiers or readout device was negligible. Hence the noise sources to be considered are analyte fluorescence shot and flicker noise and background shot and flicker noise. Flicker noise in both the background signal and analyte fluorescence signal is due to source flicker fluctuations. In addition, flicker noise in the fluorescence signal is due to fluctuations in the atomization process and imprecision in the injection of samples into the reduction vessel. The theoretical expression for the standard deviation for measurement of the fluorescence signal is given by

$$s = [mR_f K(E_b + E_f) + \xi_1^2(E_b^2 + E_f^2) + (\xi_f E_f)^2]^{\frac{1}{2}} \quad (1)$$

where

$m =$ current gain of photomultiplier, dimensionless;
$R_f =$ feedback resistance for current-to-voltage converter, Ω;
$K = 2e\Delta f(1+\alpha) = 4.08 \cdot 10^{-19}\ \Delta f$, A;
$e =$ charge of an electron, c;
$\Delta f =$ noise equivalent bandpass (equals $\frac{1}{4}R_f C_f$ for this system), s^{-1};
$\alpha =$ secondary emission factor (assumed to be 0.275), dimensionless;
$C_f =$ feedback capacitance, F;
$E_b =$ background signal, V;
$E_f =$ peak fluorescence signal, V;
$\xi_1 =$ source flicker factor or relative standard deviation in source radiance due to flicker noise, dimensionless;
$\xi_f =$ analyte fluorescence flicker factor or relative standard deviation in E_f from fluctuations in atomization efficiency and sample introduction imprecision, dimensionless.

It is assumed that the imprecision in determining the base-line is negligible compared to the imprecision in measuring the peak value. This is because the base line is determined by interpolation over a time much longer than the time

constant so that a good average can be obtained. If base-line noise were equally important, all background noise variances would be multiplied by a factor of 2.

Under the experimental conditions used to obtain the data in Table II, the experimental variables in eqn. (1) had the following values: $m=8.7\cdot10^{4}$, $R_f=10^{6}$ Ω, $K=1.02\cdot10^{-19}$ A, $E_b=0.030$ V, $\xi_1=7.7\cdot10^{-4}$, and $\xi_f=2.7\cdot10^{-2}$. Use of these values in eqn. (1) yields

$$s=[3.6\cdot10^{-8}(0.03+E_f)+5.9\cdot10^{-7}(0.03+E_f)^2+7.2\cdot10^{-4}E_f^2]^{\frac{1}{2}} \quad (2)$$

The photomultiplier gain was determined by taking the ratio of the photoanodic current from the photomultiplier to the photoanodic current from a vacuum phototube which had an identical photocathode and window (S-5, RCA 935). The source flicker factor was determined by equating the experimental noise in the background signal to eqn. (1) where $E_f=0$ and solving for s. The analyte fluorescence flicker factor is taken as the relative standard deviation in the fluorescence signal at higher concentrations where photocurrent shot and source flicker noise are negligible.

The above calculations and eqn. (2) show that, near the detection limit, the precision is limited by shot and source flicker noise in the background signal and that the magnitudes of these two noises are approximately equal. At concentrations of 0.05 p.p.b. and higher, the precision is limited by the reproducibility with which samples are introduced and atomized in the reduction vessel.

DISCUSSION

Use of an improved reduction aeration device with atomic fluorescence detection has resulted in an improved non-flame system for mercury determinations. For a.f.s., the concentration detection limit has been reduced from 0.06 p.p.b. (ref. 2) to 0.005 p.p.b. mercury(II) and the absolute detection limit has been reduced from 3 ng to 5 pg of mercury.

Comparison of the a.a.s. and a.f.s. systems with the new atomizer shows little difference except that the a.a.s. detection limit is about five times lower, that a.a.s. measurements are slightly more precise, and that a.f.s. has a slightly larger range of linearity. The dynamic range of a.a.s. measurements can be increased significantly by use of absorption cells of different path lengths. Both a.a.s. and a.f.s. were used for analysis of residual mercury levels in unpolluted water and background absorption was no problem. Clearly a.f.s. would be superior if significant absorption by other species occurred. The a.f.s. system is simpler instrumentally in that the pen lamp is a.c. powered and neither logarithmic ratio amplifiers nor double beam compensation is required. If the double-beam a.a.s. system previously described is run single beam, detection limits are worse than obtained with a.f.s.

It should be pointed out that the detection limit and precision at parts per trillion levels could be significantly improved. Near the detection limit, shot and flicker noise in the background signal are limiting. With the shutter closed to eliminate the background signal so that only dark current was present, s was measured to be $1\cdot10^{-6}$ V which gives a detection limit of 0.0001 p.p.b. This illustrates the potential of the technique if the background signal can be significantly

reduced without significantly changing the analyte fluorescence signal. The background reflection signal could be lowered by better design of the fluorescence cell or by its elimination[5,8]. Preliminary measurements have been made with mercury vented from the reduction vessel directly into the air in front of the monochromator entrance slit. This procedure reduced the background reflection signal by a factor of about 16 without significantly reducing the fluorescence signal. However, with the much smaller reflection signal, signals from scattering of the incident radiation by the mist that passes through the drying tube became obvious.

As for non-flame a.a.s. measurements, the problems of contamination and storage at sub- p.p.b. levels are significant and require more study. This, and various possibilities for improving the signal/noise ratio, *e.g.* by the use of the 184.9-nm mercury line to excite stepwise fluorescence at 253.7 nm (ref. 13), are now being investigated.

Acknowledgment is made to the donors of the Petroleum Research Fund, administered by the American Chemical Society, for partial support of this research. (After acceptance of this manuscript, another non-flame a.f.s. paper was published[14] in which detection limits better than 0.01 p.p.b. (or 0.5 ng Hg) were reported.)

SUMMARY

A new non-flame atomic fluorescence system with a detection limit of 5 parts per trillion (p.p.t.) or 5 pg of mercury(II) has been developed. The relative precision is 5% or better above 50 p.p.t. Hg(II), and the dynamic range in terms of linearity is from 0–100 p.p.b. Hg(II). The system is useful for analysis of residual mercury levels in water at a rate of about thirty samples per h.

REFERENCES

1 J. F. Kopp, M. C. Longbottom and L. B. Lobring, *J. Amer. Waterworks Ass.*, 64 (1972) 20.
2 J. H. Hwang, P. A. Ullucci and A. L. Malenfant, *Can. Spectosc.*, 16 (1971) 2.
3 T. C. Rains and O. Menis, *J. Ass. Offic. Anal. Chem.*, 55 (1972) 1339.
4 D. C. Manning, *At. Absorption Newslett.*, 9 (1970) 97.
5 K. C. Thompson and G. D. Reynolds, *Analyst (London)*, 96 (1971) 771.
6 F. L. Corcoran, Jr., *Amer. Lab.*, March (1974) 69.
7 V. I. Muscat and T. J. Vickers, *Anal. Chim. Acta*, 57 (1971) 23.
8 S. Shimomura and R. Hiroto, *Anal. Lett.*, 6 (1973) 613.
9 V. I. Muscat, T. J. Vickers and A. Andren, *Anal. Chem.*, 44 (1972) 218.
10 J. E. Hawley and J. D. Ingle, Jr., *Anal. Chem.*, 47 (1975) 719.
11 J. D. Winefordner, M. L. Parsons, J. M. Mansfield and W. J. McCarthy, *Anal. Chem.*, 39 (1974) 936.
12 J. D. Ingle, Jr., and S. R. Crouch, *Anal. Chem.*, 44 (1972) 785.
13 G. F. Kirkbright, T. S. West and P. J. Wilson, *Anal. Chim. Acta*, 66 (1973) 130.
14 S. W. Subber, S. D. Fihn and C. D. West, *Amer. Lab.*, November (1974) 38.

Analytica Chimica Acta, 77 (1975) 79–85

ELECTRONIC ABSORPTION AND FLUORESCENCE SPECTROPHOTOMETRY OF QUINACRINE

ANTHONY C. CAPOMACCHIA and STEPHEN G. SCHULMAN
College of Pharmacy, University of Florida, Gainesville, Florida 32610 (U.S.A.)
(Received 10th January 1975)

In the present study, the variations of the absorption and fluorescence spectra of the antimalarial drug quinacrine throughout the pH range and in concentrated sulfuric acid media have been investigated. The dealkylated precursor of quinacrine, 2-methoxy-6-chloro-9-aminoacridine, was also studied to evaluate the influences of the α-methyl-δ-diethylaminobutyl side-chain on the spectroscopic and prototropic properties of quinacrine.

EXPERIMENTAL

A pure sample of quinacrine hydrochloride was donated by Dr. S. Archer, Sterling-Winthrop Institute, Rensselaer, N.Y. The sulfate of 2-methoxy-6-chloro-9-aminoacridine was prepared[1] by dissolving quinacrine hydrochloride in 98% sulfuric acid. After standing at ambient temperature for 1 h, the yellow precipitate was filtered, washed with water until neutral to litmus, then dried under vacuum. Analytical reagent-grade sulfuric acid and sodium hydroxide were purchased from Mallinckrodt, St. Louis. Sulfuric acid solutions were prepared by dilution with distilled deionized water. The corrected Hammett acidity scale of Jorgenson and Hartter[2] was employed to calibrate the sulfuric acid solutions. Solutions for the pH region required were prepared by dilution of sulfuric acid or sodium hydroxide solution. Buffer salts were avoided because of their potential interference in fluorimetric titrimetry[3].

To prepare solutions for absorptiometric and fluorimetric pH titrations, a 100-μl aliquot of a $1 \cdot 10^{-3}$ *M* stock solution of quinacrine or of 2-methoxy-6-chloro-9-aminoacridine in ethanol was delivered to a 10.00-ml volumetric flask, filled to capacity with acid solution, and mixed by inversion. Each solution was prepared immediately before spectra were recorded in order to minimize errors through decomposition.

Fluorescence spectra were recorded with a Perkin-Elmer MPF-2A fluorescence spectrophotometer; the monochromators were calibrated against the xenon line emission spectrum and the output was corrected for wavelength-variable response of lamp, monochromators and phototube by means of a rhodamine-B quantum counter. Absorption spectra were recorded with a Beckman DB-GT spectrophotometer. Measurements of pH were made on an Orion model 801 digital pH meter with a Corning combination pH electrode.

RESULTS AND DISCUSSION

The ground state prototropic reactions of quinacrine in concentrated sulfuric acid and in water, and the corresponding equilibrium constants determined in these experiments, are depicted in Scheme 1.

Scheme 1

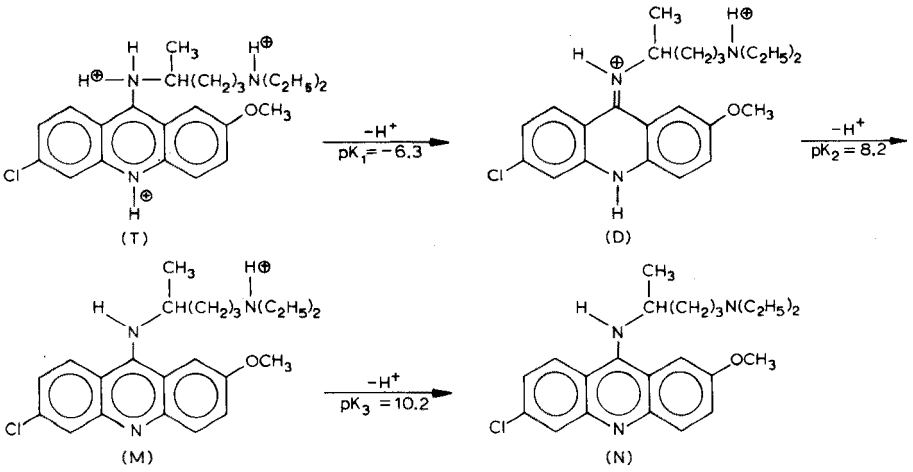

The triply (T), doubly (D), and singly (M) charged cations and neutral molecule (N) all demonstrate structureless fluorescence bands and long wavelength absorption bands with discernible vibrational structure. The spectral features of these species, given in Table I, correspond to the fluorescence band maxima,

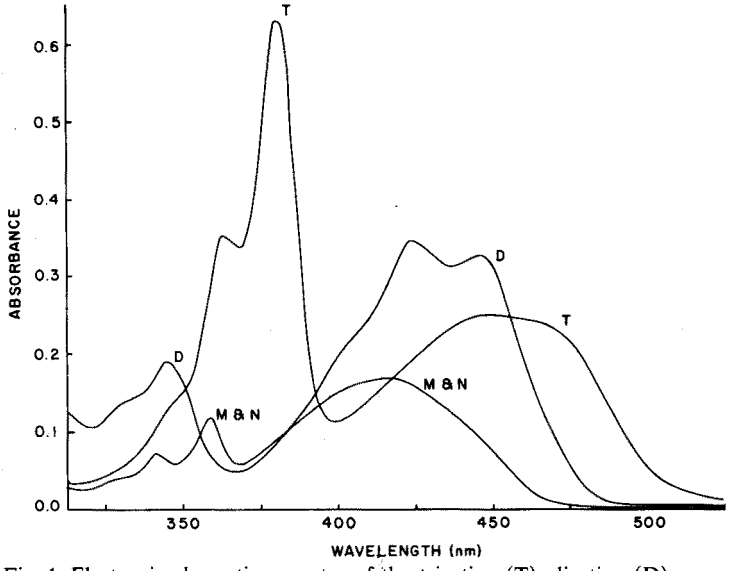

Fig. 1. Electronic absorption spectra of the trication (T), dication (D), monocation (M), and neutral molecule (N) derived from quinacrine.

the 0–0 and 0–1 vibronic features of the ^1L_a bands (the latter of which is also the band maximum for the ^1L_a transition) and the 0–0 features of the ^1L_b bands which coincide with the ^1L_b band maxima. The absorption spectra of these species are shown in Fig. 1. The values of pK_a for the equilibria between T and D ($pK_a = -6.3$) and between D and M ($pK_a = 8.2$; the value 7.7 was reported[4] previously) were determined spectrophotometrically. Since the conversion of M to N did not affect the absorption spectra sufficiently to be spectrophotometrically determinate, the value of pK_a was found potentiometrically to be 10.2.

TABLE I

ELECTRONIC ABSORPTION ($\lambda\,^1L_b$ AND $\lambda\,^1L_a$) AND FLUORESCENCE (λ_f) MAXIMA OF THE VARIOUS PROTOTROPIC SPECIES DERIVED FROM QUINACRINE AND 2-METHOXY-6-CHLORO-9-AMINOACRIDINE

	$\lambda\,^1L_b$ (nm)	$\lambda\,^1L_a$ (nm)	λ_f (nm)
Quinacrine			
Trication (T)	380 (0–0)	466 (0–0) 448 (max.)	522 (max.)
Dication (D)	344 (0–0)	448 (0–0) 427 (max.)	500 (max.)
Monocation (M)	362 (0–0)	437 (0–0) 418 (max.)	495 (max.)
Neutral molecule (N)	363 (0–0)	436 (0–0)	492 (max.)
Anion (A)	—[a]	416 (max.) —[a]	500 (max.)
2-Methoxy-6-chloro-9-aminoacridine			
Dication (D′)	378 (0–0)	458 (0–0) 435 (max.)	520 (max.)
Monocation (M′)	340 (0–0)	432 (0–0) 410 (max.)	478 (max.)
Neutral molecule (N′)	353 (0–0)	428 (0–0) 409 (max.)	475 (max.)
Anion (A′)	362 (0–0)	440 (0–0) 418 (max.)	498 (max.)

[a] Anion not formed in ground electronic state.

In all the reactions represented in Scheme 1, the fluorescence spectrum of each species changed within the same pH region as the absorption spectrum changed because of ionization. This suggests that excited state proton exchange does not occur in the reactions in Scheme 1.

Although changes in the absorption spectra were not observed above pH 12 the fluorescence of quinacrine red-shifted with increasing pH in the interval pH 11–15 with the mid-point at pH 12.7. A similar phenomenon observed in 9-aminoacridine was attributed[5] to proton abstraction in the fluorescent state from the amino group. Presumably, this also occurs in quinacrine, as represented in Scheme 2.

Scheme 2

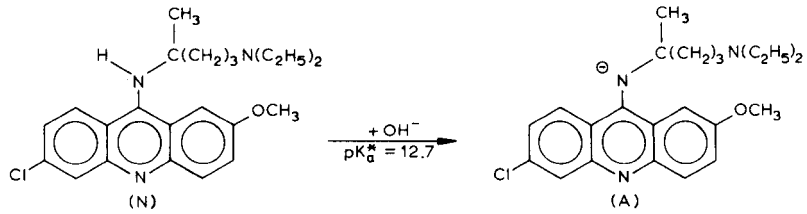

The inflection point in the titration curve of quinacrine fluorescence with increasing pH may be assigned to the dissociation constant for the excited state equilibrium represented in Scheme 2, and has the value 12.7. The corresponding dissociation cannot be observed in the absorption spectra because the anion (A) is too basic in the ground state to be generated at pH values less than 17.5 (the upper limit of pH studied here). That (A) can be generated in the excited state in the accessible pH range indicates that, in the excitation of (N), from the ground state to the excited state, the amino group of (N) loses electronic charge to the aromatic ring, rendering (N) a stronger acid (or (A) a weaker base).

The relative quantum yield of fluorescence of each species derived from quinacrine was estimated from the integrated area under the fluorescence peak divided by the molar absorptivity at the wavelength of excitation. Comparison of these yields permitted the identification of the most desirable species for fluorimetric analysis from the standpoint of sensitivity. The relative quantum yields of (T), (D), (M), (N) and (A), measured at Hammett acidity -10.0 and -0.7 and pH 9.2, 10.8 and 15.0 respectively, were in the ratio 3:2:1:1; the quantum yield of the neutral molecule fluorescence was 12 times greater than that of the excited anion. On the basis of sensitivity, therefore, (T) appears to be the most desirable species to determine fluorimetrically. However, the tendency for (T) to be dealkylated upon standing in concentrated sulfuric acid may create a problem if measurements cannot be made immediately, and the slight loss in sensitivity entailed in determining (D) fluorimetrically may be more than compensated by its long-term stability in dilute aqueous acid solutions.

2-Methoxy-6-chloro-9-aminoacridine has two basic nitrogen atoms, and exhibits the ground-state prototropic equilibria represented in Scheme 3.

Scheme 3

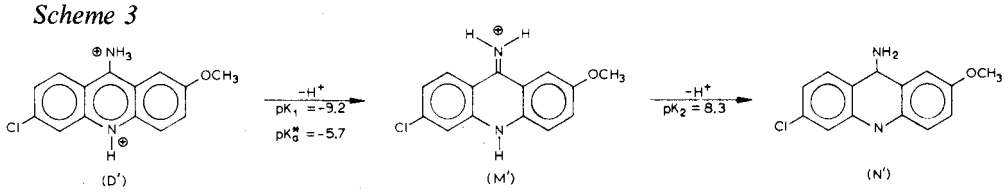

The trication (T) of quinacrine is chemically and spectroscopically comparable with the dication (D'), (D) is comparable with (M'), and (M) and (N) can both be compared with the neutral molecule (N') of the dealkylated quinacrine. All the corresponding species derived from quinacrine have spectra at slightly

longer wavelengths because of their alkyl side-chain. The electronic spectra of the species derived from 2-methoxy-6-chloro-9-aminoacridine are also presented in Table I and shown in Fig. 2. The ground (pK_a) and lowest excited singlet (pK_a^*) state dissociation constants for the equilibria between (D′) and (M′) were −9.2 and −5.7 respectively; for the equilibrium between (M′) and (N′), $pK_a = 8.3$ but pK_a^* was not apparent from the fluorescence spectra.

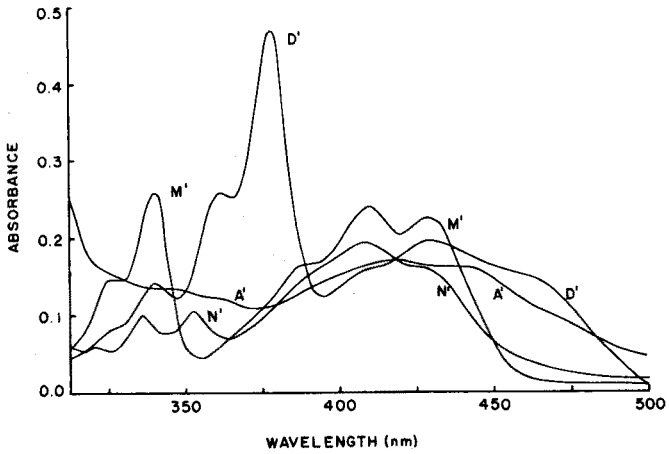

Fig. 2. Electronic absorption spectra of the dication (D′), monocation (M′), neutral molecule (N′) and anion (A′) derived from 2-methoxy-6-chloro-9-aminoacridine.

The representation of (D) in Scheme 1 and (M′) in Scheme 3 as protonated iminoacridans, rather than as protonated aminoacridines, is based on the extremely acidic ground-state pK_a and less acidic excited state pK_a^* for the equilibria between (D′) and (M′) in the ground and lowest excited singlet states, respectively and also on the shifting of the ^1L_a and ^1L_b absorption bands and the (T) and (D′) fluorescence bands to considerably shorter wavelengths upon dissociation to (D) and (M′), respectively. This shifting has been shown[5,6] for 9-aminoacridine to be associated with conversion from the ammoniumacridine (D′) to the iminoacridan structure (M′). This assignment is confirmed by the shifting of the ^1L_b band of (M′) to longer wavelengths on dissociation to (N′). That the ^1L_a absorption and fluorescence bands of (D) and (M′) shift to slightly shorter wavelengths on dissociation to (M) and (N′), respectively, does not parallel the corresponding process in 9-aminoacridine. The electronic spectra of the monocation of 9-iminoacridan shift to longer wavelengths on dissociation from the heterocyclic nitrogen atom because the aminoacridine structure in 9-aminoacridine is restored. In the molecules under consideration here, however, the substituents, especially the 6-chloro atom of the acridine ring, account for the anomalous spectral shift and also for the low pK_a values relative to the corresponding ionizations in 9-aminoacridine. The electron-withdrawing chlorine atom renders the heterocyclic and exocyclic nitrogen atoms in the ground states of (D′), (M′) and (N′) less basic than the corresponding species derived from 9-aminoacridine, and thereby decreases each corresponding pK_a value. In the longest wavelength ($^1L_a \leftarrow {}^1A$) absorption and fluorescence

($^1L_a \rightarrow {}^1A$) transitions the chlorine atom abstracts some of the electronic charge, which traverses the heterocyclic nitrogen–exocyclic nitrogen ($^1L_a \leftrightarrow {}^1A$) axis, thereby raising the energies of these transitions. The methoxy group, however, donates charge to the ring, partially offsetting the effect of the chlorine atom; in (M′) this effect is more pronounced because of the positive charge in the aromatic system. Hence the long-wavelength absorption and fluorescence bands of (N′) are relatively more raised in energy than those of (M′). In the monocation of 9-aminoacridine, the shifts to longer wavelengths (lower energies) on dissociation are small[5]. In 2-methoxy-6-chloro-9-aminoacridine, the effect of the chlorine atom on the lowest energy transitions of (N′) apparently causes a reversal of the spectral shift of (M′) upon dissociation.

All species derived from quinacrine absorb and fluoresce at longer wavelengths than the corresponding species derived from 2-methoxy-6-chloro-9-aminoacridine, as anticipated in the comparisons between (T) and (D′), and between (M) or (N) and (N′). The electron-donating inductive or hyperconjugative effect of the alkyl group stabilizes the excited states of the amine-like species relative to their ground states because, in these structures, the alkyl-substituted amino group loses electronic charge upon going from the ground to the ^1L_a or ^1L_b states. However, in the iminoacridan structures (D) and (M′), the presence of the alkyl group in (D) should destabilize at least the transitions involving the ^1L_a state (the ^1L_a absorption and fluorescence bands) because the ^1L_a state of the iminoacridan structure has more electronic-charge on the alkyl chain-bearing nitrogen atom in the ^1L_a state than in the ground state. Thus, the absorption and fluorescence spectra of (D) would be predicted to lie at higher energies than those of (M′). This is not the case; the bulky side-chain of (D) may interact with the 1 and 8 protons of the acridine ring to inhibit sterically the coplanarity of the alkylamino group with the ring. The steric inhibition of resonance may therefore force (D) to behave more as an aminoacridine than as an iminoacridan, as supported by the substantial lowering of the pK_a value of (T) relative to that of (D′). A decrease in acidity by three orders is well beyond the normal inductive effect of an alkyl substituent on an amino or ammonium group. Moreover, 2-methoxy-6-chloro-9-aminoacridine demonstrates excited-state equilibrium between (D) and (M′) ($pK_a^* = -5.7$) while quinacrine does not measurably demonstrate excited-state reactivity in the corresponding process between (T) and (D). This indicates that the alkyl side-chain of quinacrine is responsible, either by virtue of steric hindrance to excited-state protonation, or by shortening the lifetime of the lowest excited singlet state of (D) to the point where excited-state protonation cannot appreciably compete with deactivation of the excited state, or by some combination of both the steric and the non-radiative deactivational effects. In the absence of the alkyl group of quinacrine, the amino group of 2-methoxy-6-chloro-9-aminoacridine (N′) can be deprotonated in the ground state as well as in the lowest excited singlet state, to give (A′), as shown in Scheme 4. That (M) is more acidic in the excited state than in the ground state is consistent with the aminoacridine structure of (M′). The values of the dissociation constants in the ground (pK_a) and lowest electronically excited singlet (pK_a^*) states for the equilibrium between (M′) and (A′) are 15.2 and 12.5, respectively.

Scheme 4

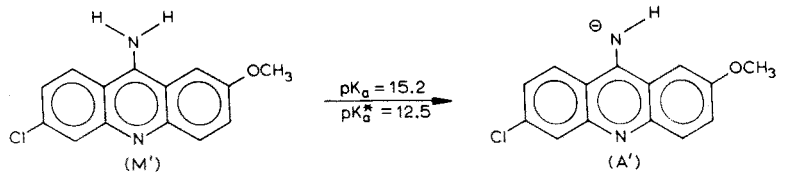

SUMMARY

The absorption and fluorescence spectra of quinacrine and its dealkylated derivative, 2-methoxy-6-chloro-9-aminoacridine, were studied as a function of pH and Hammett acidity. The relative stability and high quantum yield of the dication derived from quinacrine make it the most desirable species for fluorimetric determination. This species predominates in the region pH 8–H_0 – 6. The alkylamino side-chain of quinacrine appears to interfere with excited state protonation and dissociation of the dication. Moreover, in the dication, the steric interaction between the side-chain and the 9-amino group may prevent coplanarity between the 9-amino group and the acridine ring, thereby favoring the aminoacridine over the iminoacridan structure.

REFERENCES

1 O. Yu. Magidson and A. M. Grigorovskii, *Chem. Ber.*, 69 (1936) 396.
2 M. J. Jorgenson and D. R. Hartter, *J. Amer. Chem. Soc.*, 85 (1963) 878.
3 S. G. Schulman in E. L. Wehry (Ed.), *Acid–Base Chemistry of Excited Singlet States: Fundamentals and Analytical Implications, Modern Fluorescence Spectroscopy, Newer Techniques and Applications*, Plenum, New York, in press.
4 J. L. Irvin and E. M. Irvin, *J. Amer. Chem. Soc.*, 72 (1950) 2745.
5 A. C. Capomacchia, J. Casper and S. G. Schulman, *J. Pharm. Sci.*, 63 (1974) 1272.
6 A. C. Capomacchia and S. G. Schulman, *J. Pharm. Sci.*, in press.

Analytica Chimica Acta, 77 (1975) 87–96

INTERELEMENT EFFECTS IN X-RAY FLUORESCENCE SPECTROMETRY. ANALYSIS OF THE IRON–COPPER–SULFUR SYSTEM

B. W. BUDESINSKY

Phelps Dodge Corporation, Morenci, Arizona 85540 (U.S.A.)

(Received 25th October 1974)

The theory of x-ray fluorescence spectrometry developed by Gillam and Heal[1] has recently been reinvestigated and extended to tertiary fluorescence by Shiraiwa and Fujino[2,3]. There are many other papers dealing with the problem, but some of these contain errors either in the expression of the secondary fluorescence or in the designation of the angles of incident and emergent radiation.

Several attempts[3–5] have been made to use the theoretical relationship between fluorescence intensity and concentration of elements directly for quantitative analysis. However, this is not convenient, especially for analysis of multicomponent systems, because the mathematics is complicated. Another approach, *i.e.*, interpretation of the theoretical relationship by a simple empirical equation, seems to be more hopeful. It can be shown that the Lachance–Traill equation[6,7] and particularly the more recent Rasberry–Heinrich[8] and Claisse–Quintin[9,10] equations interpret the relationship quite well.

The effects of trace elements and structural effects[3,11] are the main reasons why the theory is insufficiently accurate, so that the introduction of empirical coefficients is necessary. Relatively, the best results (without empirical corrections) are obtained for alloys and fused borate pellets. The use of fused pellets is inconvenient for light elements (sodium, magnesium, aluminum) and for routine analysis (about one hundred samples per day), and the insolubility of some metal sulfides (such as copper (I), copper (II) and silver (I)) in alkaline borates presents a serious limitation[12]. Accordingly, the present measurements were made with powders.

EXPERIMENTAL

Apparatus

The instrument used was a Norelco Corporation (Mount Vernon, New York) machine with a generator, x-ray vacuum spectrometer (containing a chromium target tube) and data control and processor. The grinding and mixing of specimens was done by means of a "Wigl Bug" (Crescent Dental Co., Inc., Chicago, Illinois) with a tungsten carbide capsule of 6-ml effective volume.

Materials

Copper (I) and copper (II) sulfide, metallic copper and sublimed sulfur (all Ventren Corporation, Beverly, Mass.) were used for preparation of artificial mixtures.

The copper concentrates and reverberatory mattes were the usual daily samples. They were analysed by conventional methods: potentiometry with cerium (IV) for iron, electrolytic gravimetry for copper, and barium sulfate gravimetry for sulfur[13].

Measurements

Plastic cups of 26-mm diameter and 7-ml effective volume with a 1-mm hole in the bottom (for measurements in vacuum) were used. About 2 g of specimen (300 mesh) was placed into each cup, covered with Spex-Film (Spex Industries, Inc., Metuchen, New Jersey), inserted into the metallic holder, tapped gently on a bakelite plate and inserted into the spectrometer. The parameters of measurement for individual elements are listed in Table I.

TABLE I

INSTRUMENT SETTINGS FOR INDIVIDUAL ELEMENTS

Parameter	*Element*[a]		
	Fe	*Cu*	*S*
Pulse height analyser base line (V)	3.0	4.0	9.0
Pulse height analyser window (V)	30.0	21.0	19.0
Measurement time (s)	20	20	50
Spectrometer angle 2θ (°)	57.55	45.05	45.81
Crystal	LiF	LiF	PET[b]
Path medium	Air	Air	Vac[c]
Detector[d]	S	S	P
Detector voltage (kV)	0.8	0.8	1.5

[a] X-ray tube voltage of 45 kV, current of 18 mA, linear amplifier attenuation of 5, and coarse collimation were used throughout.
[b] Pentaerythritol.
[c] 200 μm (Hg) vacuum (10% methane and 90% argon).
[d] S = scintillation; P = proportional detector. All the measured intensities were corrected for the counting dead time (the dead time constant was $1.176 \cdot 10^{-6}$ for S and $1.680 \cdot 10^{-6}$ for P, both in s/count).

THEORY

Relationship of intensity and concentration

The relative fluorescence intensity, R_A, of an element A is given by the equation:

$$R_A = (I_A - I_{Ao})/(I_{1A} - I_{1Ao}) \quad (1)$$

where I_A, I_{1A} and I_{Ao}, I_{1Ao} are the fluorescence intensities of the element A and its background (subscript 0) is normal and 100% (subscript 1) specimens, respectively.

For a binary mixture of elements A and B, if the theoretical fluorescence intensities[1–3] are introduced into eqn. (1), then:

$$\frac{R_A}{c_A} = \frac{\sum_{\lambda_0}^{\lambda_{Ae}} \frac{\mu_{A\lambda} I_\lambda \Delta\lambda}{\mu_\lambda + \mu_a \sin\phi/\sin\psi} + \frac{1}{2} E_B c_B \mu_{Ab} \sum_{\lambda_0}^{\lambda_{Be}} \frac{L_\lambda \mu_{B\lambda} I_\lambda \Delta\lambda}{\mu_\lambda + \mu_a \sin\phi/\sin\psi}}{\sum_{\lambda_0}^{\lambda_{Ae}} \frac{\mu_{A\lambda} I_\lambda \Delta\lambda}{\mu_{A\lambda} + \mu_{Aa} \sin\phi/\sin\psi}} \tag{2}$$

where

$$L_\lambda = \frac{\sin\phi}{\mu_\lambda} \ln\left(1 + \frac{\mu_\lambda}{\mu_b \sin\phi}\right) + \frac{\sin\psi}{\mu_a} \ln\left(1 + \frac{\mu_a}{\mu_b \sin\psi}\right) \tag{3}$$

$$\mu_x = c_A/\mu_{Ax} + c_B/\mu_{Bx}; \qquad x = \lambda, a, b \tag{4}$$

$$E_B = \omega P_{iK}(S_K - 1)/S_K \tag{5}$$

c_A and c_B are the concentrations (as weight fractions, therefore $c_A = 1 - c_B$), μ_{Ax} and μ_{Bx} the mass absorption coefficients, a and b the characteristic lines of fluorescence radiation, and λ_{Ae} and λ_{Be} the absorption edge wavelengths of elements A and B, respectively; I_λ is the primary radiation intensity (from the x-ray tube) of the wavelength λ at the surface of the specimen; ϕ and ψ are the angles of the incident and emergent radiation beams with the surface of the specimen; ω is the fluorescence yield and S_K the absorption jump ratio, both for the K series of element B: P_{iK} is the fraction of the i-line emission ($i = \alpha, \beta, \ldots$) in the K series; λ_0 is the shortest wavelength of the primary radiation; the member with $\frac{1}{2}E_B$...vanishes for $\lambda_{Ae} < \lambda_{Be}$.

The summation form of eqn. (2) is more valid than the integral form, since the calculation is really performed with strips of $\Delta\lambda = 0.02$ Å. Direct integration is impossible. The tertiary fluorescence was neglected because of its low value[2,3]. The values of $I_\lambda \Delta\lambda$ for a chromium target x-ray tube were taken from Birk's book[14]. To assist in the calculation of eqn. (2), the spectrum of the tube was divided into four

TABLE II

SOME PARAMETERS FOR IRON, COPPER AND SULFUR[12,14,15a]

Element Y	*p*	*q*	*Interval λ*	μ_{Yx}	*x*	*ω*	S_K	P_{iK}	E_Y
Fe	99.7	2.81	0.1–1.74	74	1.936	0.32	8.66	0.886	0.251
				337	1.541				
				1059	5.372				
Cu	129.3	2.77	0.1–1.38	98	1.936	0.41	8.50	0.881	0.319
				51	1.541				
				1350	5.372				
S	34.8	2.58	0.1–5.02	156	1.936	0.09	11.60	0.958	0.078
				84	1.541				
				233	5.372				

[a] Parameters p and q refer to the empirical equation $\mu_{Y\lambda} = p\lambda^q$ for the given interval of wavelength λ, where the upper value corresponds to the edge λ_{Ye}. $\varphi = 67°$; $\psi = 35°$; x-ray tube voltage, 45 kV.

TABLE III

DEPENDENCE $c_A/R_A = f(c_B)$ FOR IRON, COPPER AND SULFUR

Eqn. (2)		c_A/R_A			*Eqn. (2)*		c_A/R_A		
c_B	c_A/R_A	*RH*[a]	*CQ*[b]	*LT*[c]	c_B	c_A/R_A	*RH*	*CQ*	*LT*
A = Fe		A_B = 0.1781	−0.1263	−0.2850	A = Cu		A_B = 2.9662	2.2848	1.9120
B = Cu		$\bar{A}_B$ = −0.6736	−0.3174	—	B = Fe		$\bar{A}_B$ = −1.5333	−0.7455	—
0.1	0.9827	0.9824	0.9842	0.9715	0.1	1.2242	1.2159	1.2210	1.1912
0.2	0.9611	0.9608	0.9620	0.9430	0.2	1.4272	1.4229	1.4271	1.3824
0.3	0.9345	0.9346	0.9335	0.9145	0.3	1.6143	1.6193	1.6183	1.5736
0.4	0.9022	0.9029	0.8987	0.8860	0.4	1.7876	1.8032	1.7946	1.7648
0.5	0.8633	0.8645	0.8575	0.8575	0.5	1.9483	1.9720	1.9560	1.9560
0.6	0.8167	0.8182	0.8100	0.8290	0.6	2.0966	2.1226	2.1025	2.1472
0.7	0.7608	0.7620	0.7561	0.8005	0.7	2.2328	2.2507	2.2341	2.3384
0.8	0.6937	0.6934	0.6958	0.7720	0.8	2.3570	2.3508	2.3507	2.5296
0.9	0.6122	0.6092	0.6292	0.7435	0.9	2.4689	2.4151	2.4525	2.7208
Average deviation[d] (±)		0.0010	0.0048	0.0370	Average deviation[d] (±)		0.0179	0.0058	0.0811
A = Fe		A_B = 0.3723	0.1366	0.0152	A = S		A_B = 3.1807	3.1803	3.1802
B = S		$\bar{A}_B$ = −0.5194	−0.2428	—	B = Fe		$\bar{A}_B$ = −0.0008	−0.0003	—
0.1	1.0099	1.0099	1.0112	1.0015	0.1	1.3180	1.3180	1.3180	1.3180
0.2	1.0164	1.0167	1.0176	1.0030	0.2	1.6361	1.6361	1.6360	1.6360
0.3	1.0195	1.0200	1.0191	1.0045	0.3	1.9541	1.9541	1.9541	1.9540
0.4	1.0187	1.0191	1.0158	1.0060	0.4	2.2721	2.2721	2.2721	2.2720
0.5	1.0134	1.0130	1.0076	1.0076	0.5	2.5901	2.5901	2.5901	2.5901
0.6	1.0023	1.0008	0.9946	1.0091	0.6	2.9081	2.9081	2.9081	2.9081
0.7	0.9835	0.9809	0.9766	0.0106	0.7	3.2261	3.2261	3.2261	3.2261
0.8	0.9534	0.9515	0.9539	1.0121	0.8	3.5440	3.5441	3.5440	3.5441
0.9	0.9055	0.9101	0.9263	1.0136	0.9	3.8620	3.8620	3.8620	3.8621
Average deviation[d] (±).		0.0014	0.0053	0.0284	Average deviation[d] (±)		0.0000	0.0000	0.0001

(continued)

TABLE III (*Continued*)

Eqn. (2)		c_A/R_A			*Eqn. (2)*		c_A/R_A		
c_B	c_A/R_A	*RH*[a]	*CQ*[b]	*LT*[c]	c_B	c_A/R_A	*RH*	*CQ*	*LT*
A = Cu		A_B = 0.0256	−0.1333	−0.2142	A = S		A_B = 4.1311	−4.1307	4.1305
B = S		$\bar{A}_B$ = −0.3488	−0.1618	—	B = Cu		$\bar{A}_B$ = −0.0009	−0.0005	—
0.1	0.9839	0.9842	0.9851	0.9786	0.1	1.4131	1.4131	1.4131	1.4130
0.2	0.9659	0.9664	0.9669	0.9572	0.2	1.8261	1.8261	1.8261	1.8261
0.3	0.9458	0.9461	0.9454	0.9358	0.3	2.2391	2.2392	2.2392	2.2391
0.4	0.9232	0.9230	0.9208	0.9144	0.4	2.6522	2.6522	2.6522	2.6522
0.5	0.8977	0.8965	0.8929	0.8929	0.5	3.0652	3.0653	3.0652	3.0652
0.6	0.8683	0.8659	0.8618	0.8715	0.6	3.4782	3.4783	3.4782	3.4783
0.7	0.8334	0.8301	0.8274	0.8501	0.7	3.8913	3.8913	3.8912	3.8913
0.8	0.7900	0.7879	0.7898	0.8273	0.8	4.3043	4.3043	4.3042	4.3044
0.9	0.7308	0.7376	0.7490	0.8073	0.9	4.7173	4.7173	4.7172	4.7174
Average deviation[d] (±)		0.0019	0.0045	0.0192	Average deviation[d] (±)		0.0000	0.0000	0.0000

[a] Rasberry–Heinrich equation.
[b] Claisse–Quintin equation.
[c] Lachance–Traill equation.
[d] General average deviation: 0.0037 (RH), 0. 0034 (CQ) and 0.0276 (LT).

intervals, which were described by empirical equations as follows:

$I_\lambda \Delta\lambda = 48.00\lambda^{1.49}$ for $0.29 \leqslant \lambda \leqslant 0.43$ Å;

$I_\lambda \Delta\lambda = 13.9$ for $0.45 \leqslant \lambda \leqslant 0.87$ Å,

$I_\lambda \Delta\lambda = 11.5\lambda^{-1.82}$ for $0.89 \leqslant \lambda \leqslant 2.05$ Å;

$I_\lambda \Delta\lambda = 119.8\lambda^{-3.53}$ for $2.09 \leqslant \lambda \leqslant 2.99$.

Other values for the calculation of eqn. (2) are collected in Table II.

The dependence $c_A/R_A = f(c_B)$ calculated from eqn. (2) is presented in Table III.

Empirical equations

From the large number of parabolic and hyperbolic equations investigated, the Rasberry–Heinrich equation[8]:

$$c_A/R_A = 1 + \sum_B^Z A_X c_X + \frac{1}{1+c_A} \sum_B^Z \bar{A}_X c_X \tag{6}$$

and the Claisse–Quintin equation[9,10]:

$$c_A/R_A = 1 + \sum_B^Z A_X c_X + \sum_B^Z \bar{A}_X c_X^2 \tag{7}$$

interpret the theoretical eqn. (2) in an optimum way, considering the complication of the equation and the extent of the deviations. The theoretical dependence $c_A/R_A = f(c_B)$ can be used for the calculation of the influence coefficients, A_x and $\bar{A}_x$, and then the value of c_A/R_A can be calculated by means of eqns. (6) and (7). The results of these calculations are collected in Table III. A similar treatment was also done with the Lachance–Traill equation[6,7]:

$$c_A/R_A = 1 + \sum_B^Z A_X c_X \tag{8}$$

because of its simplicity and the relative acceptability of the results.

Table III shows that the Rasberry–Heinrich and Claisse–Quintin equations give results with approximately the same average deviation. Enhancement effects ($c_A/R_A < 1$) are better interpreted by the former equation, which however, interprets a smaller absorption effect ($c_A/R_A < 2.5$) with a relatively great error. Rasberry and Heinrich did not find this case, because they investigated the nickel–chromium system in a narrow range of concentrations ($0.6 \leqslant c_{Ni} \leqslant 0.8$). In agreement with the findings of Tertian[16], the values of A_X in the Rasberry–Heinrich equation are not necessarily positive numbers only. For high absorption effects (average value $c_A/R_A > 2.5$), both eqns. (6) and (7) give practically identical results. In this case, the effect of enhancement is negligible, and the conditions are similar, as those described by Rasberry–Heinrich[8].

When the constants A_X and $\bar{A}_X$ are known, eqns. (6) and (7) can be used for evaluation of results in quantitative analysis. The iterative technique[17] is most convenient for that purpose. The mechanism of calculation with a computer is described in Fig. 1. The calculation is very simple and fast even for multielement systems (3–9 elements)*.

* Rasberry and Heinrich apparently described[8] the same technique but their results are better for concentrations >60% and worse for <60% than the present results. The differences are 0.01–0.96%. Calculations were done on a Monroe Corp. model 1860. Programs are available from the author on request.

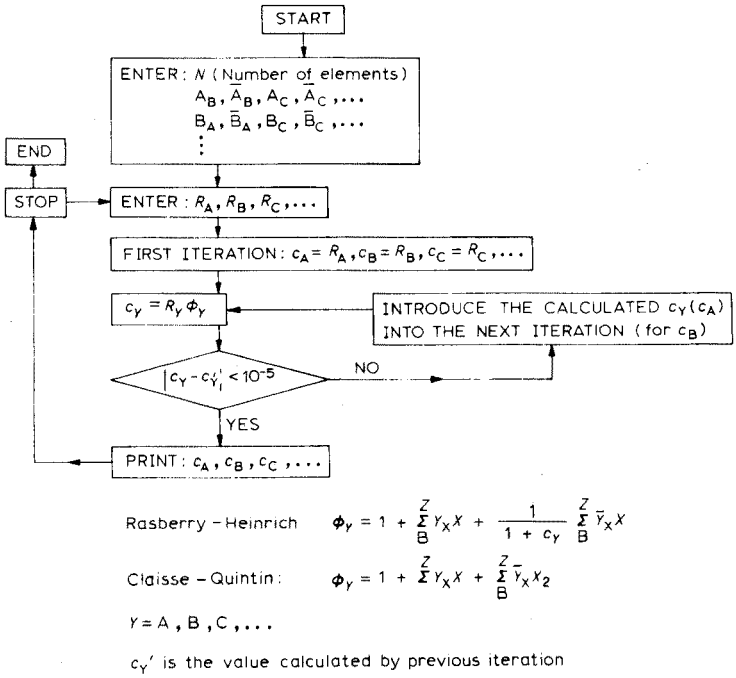

Fig. 1. Flow chart of the computer program.

Trace elements and structural correction

It is very difficult—and perhaps impossible—to develop a general theory for this correction. For samples of a relatively constant character, the correction can be linear

$$c_A^{corr} = k_1 c_A + k_2 \tag{9}$$

where c_A^{corr} and c_A are the corrected concentration and the concentration found by means of eqns. (6) and (7), respectively. The values of correction constants k_1 and k_2 can be estimated from a set of eqns. (9) (corresponding to the number of standards used), where c_A^{wet}(results of a wet method) is introduced instead of c_A^{corr}. The selected standards should cover the range of trace elements and structural modifications of practical samples as much as possible.

RESULTS AND DISCUSSION

The structural effect is demonstrated on mixtures of copper (I) and copper (II) sulfide with elemental sulfur and copper in Table IV. Sulfur enhances the fluorescence of copper, and copper absorbs the fluorescence of sulfur (see values of A_X and $\bar{A}_X$ in Table III). The copper (sulfur) fluorescence is greater (smaller) in copper (I) sulfide than in a percentually equivalent mixture of copper (II) sulfide and metallic copper, because the distance between copper and sulfur atoms is smaller in the former case. A similar situation occurs with copper (II) sulfide and an equivalent mixture of copper (I) sulfide and sulfur.

TABLE IV

STRUCTURAL EFFECT IN THE COPPER–SULFUR SYSTEM

Composition	*% Cu*	*% S*	R_{Cu}	R_S
Cu_2S	79.6	20.2	0.9011	0.0618
CuS[a]+S	79.6	20.2	0.8739	0.0946
CuS[a]	69.1	29.9	0.8582	0.0973
Cu_2S+S	69.1	29.9	0.8258	0.1346

[a] The CuS contained about 19.7% Cu_2S.

The results of analysis of reverberatory mattes and copper concentrates are presented in Table V. The latter case shows an example of trace element and structural effects on concentrates I and II of different origin. The constants k_1 and k_2 were determined by means of 8 standards. Table V shows that x-ray fluorescence spectrometry can furnish very accurate results provided that all necessary corrections are taken into account.

Undoubtedly the trace element and structural effects are a drawback of x-ray fluorescence spectrometry. However, it would be wrong to advocate on that basis the use of purely empirical methods[18,19]. The constants of such methods are interdependent and sensitive to many factors, including instrumental drift. For that reason, it is necessary to use a large number of standards for each measurement.

The empirical Rasberry–Heinrich and Claisse–Quintin equations represent the optimal interpretation of the theoretical intensity–concentration relationship, even though their results can differ by 0.01–1.00%. The iterative technique of calculation used can be another source of error of approximately the same extent. The question remains whether these equations are sufficiently accurate for description of a multicomponent system. A recent investigation with the Claisse–Quintin equation[10] answers that question positively.

The mass absorption coefficients were calculated for pure elements[12], hence their application in calculations cannot eliminate the structural effect. The determination of new coefficients for compounds with a specific structure could be one way of solving the problem of structural effect.

To check the instrumental drift, one standard in each set of measured specimens is quite sufficient.

SUMMARY

The Rasberry–Heinrich and Claisse–Quintin equations give a good interpretation of the theoretical intensity–concentration relationship in x-ray fluorescence spectrometry. The influence constants (A_X, $\bar{A}_X$) of these equations can be calculated. Trace element and structural effects require an empirical correction, which is important in iron–copper–sulfur systems (reverberatory mattes and copper concentrates). The empirical correction in combination with either of the above equations can furnish very good quantitative results from fluorescence intensity measurements.

TABLE V

ANALYSIS OF SOME COPPER INTERMEDIATES[a]

Specimen	R_{Fe}	R_{Cu}	R_S	% *Fe*			% *Cu*			% *S*		
				W	*RH*	*CQ*	*W*	*RH*	*Cl*	*W*	*RH*	*Cl*
Reverberatory matte												
5-268	0.4717	0.2710	0.1093	35.6	35.52	35.52	32.83	32.82	32.79	26.64	26.62	26.66
5-331	0.4394	0.3042	0.1059	32.0	32.11	32.12	37.17	37.33	37.29	26.42	26.35	26.43
5-336	0.4210	0.3131	0.1126	30.6	30.48	30.45	37.52	37.57	37.65	27.02	26.97	27.03
5-339	0.4295	0.3062	0.1042	31.4	31.29	31.34	37.23	37.13	37.26	26.16	26.04	26.19
5-344	0.4395	0.3094	0.1052	31.8	32.01	31.97	38.42	38.33	38.17	26.09	26.35	26.43
Average deviation (±)					0.13	0.12		0.08	0.11		0.10	0.03
k_1					0.899	0.953		1.175	1.133		0.274	0.245
k_2					−1.137	−4.146		−20.73	−20.16		14.09	15.26
Concentrate I												
2-18	0.3111	0.2809	0.1410	27.7	27.60	27.60	25.79	25.50	25.51	38.83	38.83	38.82
2-20	0.3226	0.2598	0.1445	28.2	28.42	28.42	23.23	23.58	23.57	38.62	38.88	38.88
2-22	0.3335	0.2303	0.1495	29.4	29.31	29.31	20.53	20.62	20.61	39.14	38.90	38.90
3-4	0.3376	0.2007	0.1498	30.2	29.87	29.87	17.82	17.46	17.46	38.59	38.59	38.58
3-5	0.3396	0.1976	0.1515	29.7	30.01	30.00	16.92	17.14	17.14	38.65	38.65	38.65
Average deviation (±)					0.21	0.21		0.26	0.26		0.10	0.11
k_1					0.590	0.616		0.783	0.776		0.158	0.162
k_2					12.11	10.34		−4.82	−6.60		31.18	30.60
Concentrate II												
7-1	0.3821	0.2403	0.1409	28.4	28.29	28.34	27.13	27.38	27.37	32.48	32.54	32.53
7-2	0.3724	0.2406	0.1414	27.9	27.82	27.80	27.33	27.10	27.13	32.32	32.44	32.45
7-3	0.3804	0.2368	0.1414	28.2	28.24	28.29	26.88	26.91	26.87	32.78	32.49	32.49
7-4	0.3825	0.2502	0.1459	28.0	28.20	28.17	28.50	28.45	28.49	32.84	33.08	33.09
7-5	0.3932	0.2559	0.1496	28.7	28.65	28.62	29.41	29.41	29.39	33.74	33.62	33.61
Average deviation (±)					0.10	0.10		0.11	0.10		0.17	0.17
k_1					0.525	0.649		0.778	0.877		0.216	0.224
k_2					10.74	5.740		−0.66	−6.19		21.76	20.87

[a] Most of the iron and copper was present as FeS and Cu_2S, respectively; W is the "wet" method. Concentrates I and II contained 6.0% SiO_2–2.2% Al_2O_3 and 4.6% SiO_2–1.8% Al_2O_3, respectively (average values).

REFERENCES

1 E. Gillam and H. T. Heal, *Brit. J. Appl. Phys.*, 3 (1952) 353.
2 T. Shiraiwa and N. Fujino, *Jap. J. Appl. Phys.*, 5 (1966) 886.
3 T. Shiraiwa and N. Fujino, *X-Ray Spectrometry*, 3 (1974) 64.
4 J. W. Criss and L. S. Birks, *Anal. Chem.*, 40 (1968) 1080.
5 D. A. Stephenson, *Anal. Chem.*, 43 (1971) 1761.
6 G. R. Lachance and R. J. Traill, *Can. Spectrosc.*, 11 (1966) 43.
7 R. J. Traill and G. R. Lachance, *Can. Spectrosc.*, 11 (1966) 66.
8 S. D. Rasberry and K. F. J. Heinrich, *Anal. Chem.*, 46 (1974) 81.
9 F. Claisse and M. Quintin, *Can. Spectrosc.*, 12 (1967) 129.
10 R. Rousseau and F. Claisse, *X-Ray Spectrometry*, 3 (1974) 129.
11 B. W. Budesinsky, *Talanta*, 1975.
12 H. A. Liebhafsky, H. G. Pfeiffer, E. H. Winslow and P. D. Zemany, *X-Ray Absorption and Emission in Analytical Chemistry*, Wiley, New York, 1960, pp. 207, 314.
13 I. M. Kolthoff, E. B. Sandell, E. J. Meehan and S. Bruckenstein, *Quantitative Chemical Analysis*, Macmillan, New York, 1969.
14 L. S. Birks, *X-Ray Spectrochemical Analysis*, Interscience, New York, 1969, pp. 125, 131.
15 S. I. Salem in R. C. Weast (Ed.), *Handbook of Chemistry and Physics*, Chemical Rubber Co., Cleveland, 53rd edn., 1972, p.E-183.
16 R. Tertian, *X-Ray Spectrometry*, 2 (1973) 95.
17 R. Mises and H. Pollaczek-Geiringer, *Z. Angew. Math. Mech.*, 11 (1929) 58, 152.
18 H. J. Lucas-Tooth and B. J. Price, *Metallurgia*, 64 (1961) 149.
19 H. J. Lucas-Tooth and C. Pyne, *Advan. X-Ray Anal.*, 7 (1964) 523.

Analytica Chimica Acta, 77 (1975) 97–106

DETERMINATION OF ^{17}O AND ^{18}O ISOTOPIC ABUNDANCES IN ^{238}Pu MATERIALS BY γ-RAY SPECTROMETRY

JOSEPH BUBERNAK and GEORGE M. MATLACK

University of California, Los Alamos Scientific Laboratory, Los Alamos, New Mexico 87544 (U.S.A.)

(Received November 1974)

Recent evaluation of several ^{238}Pu fuel-forms for biomedical applications has shown PuO_2 to have the best physical characteristics[1]. The plutonium isotopic abundances, in atom percent, in this material are ^{238}Pu—80%, ^{239}Pu—16%, ^{240}Pu—3%, and ^{241}Pu—1%. In order to lower the neutron emission rates to reasonable levels the ^{17}O and ^{18}O isotopic abundances must be reduced below their natural amounts (0.037% and 0.204%, respectively) since these isotopes undergo (α, n) reactions. The remaining isotope, ^{16}O, does not undergo an (α, n) reaction with the 5.5-MeV α-particles from ^{238}Pu decay, because the threshold energy is too high. When samples of PuO_2 are prepared with isotopic abundances as low as 0.005% ^{17}O and 0.001% ^{18}O, their neutron emission rates are only 5% greater than the 2450 n s^{-1} g^{-1} Pu arising from spontaneous fission in the chemically pure metal. As a comparison, PuO_2 made from natural oxygen has a neutron emission rate of 12,500 n s^{-1} g^{-1} Pu. The (α, n) reactions with ^{17}O and ^{18}O are accompanied by the emission of γ-rays, and measurements of the intensities of the γ-rays can serve as a means of nondestructively determining the oxygen isotope abundances. Such analyses are invaluable for assessing the cause of above-specification neutron emission rates from PuO_2 fuels.

Principle of the method

The reaction $^{17}O(\alpha, n)^{20}Ne$ produces only one γ-ray with an energy of 1634 keV, and the intensity of this γ-ray serves as a measure of the ^{17}O content; γ-rays at 1428 and 1436 keV emitted in ^{238}Pu decay are used as internal standards. These two γ-rays from ^{238}Pu have not previously been reported in the literature. Identification of these two γ-rays was based on the following facts: (1) they are emitted from various types of pure ^{238}Pu sources; (2) the intensity ratios of the γ-rays to each of three known ^{238}Pu γ-rays are constant in several ^{238}Pu metal and oxide samples; (3) the occurrence of at least one energy level at about 1430 keV has previously been observed in the ^{234}U nucleus, to which ^{238}Pu decays[2]. The absolute intensities of these two γ-rays at 1428 and 1436 keV are similar, about one photon per 10^{10} disintegrations of ^{238}Pu.

Figure 1 (a–d) shows a composite γ-ray spectrum of PuO_2 (natural oxygen) for the energy range 0–2800 keV; Fig. 1(c) shows the γ-rays involved in ^{17}O measurement. The principal difficulty in measuring these rays is their low intensities compared with the usually high Compton background in this region. The Compton

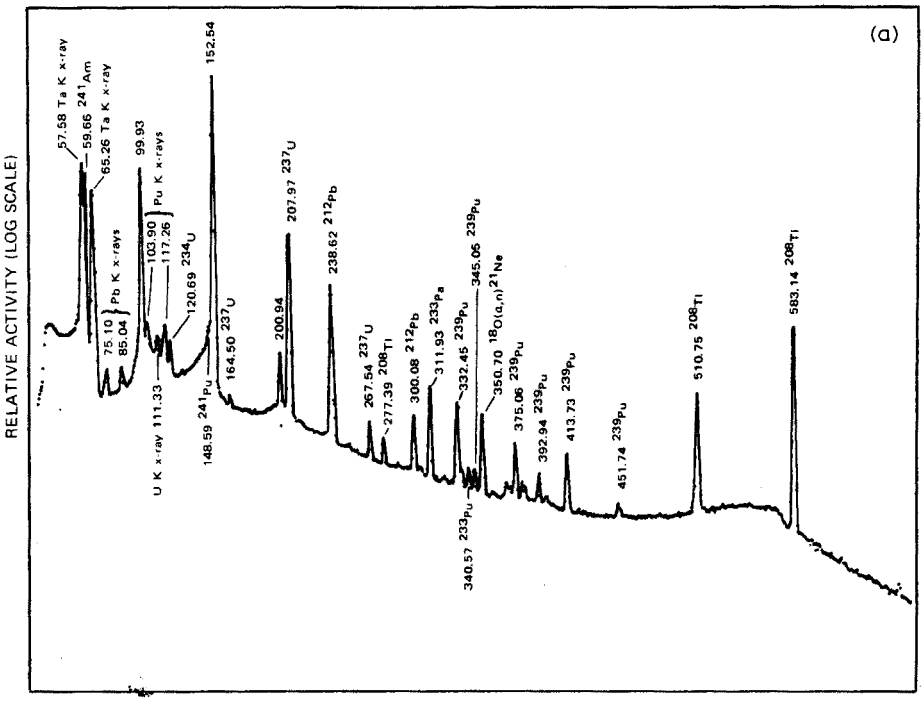
(a)
RELATIVE ACTIVITY (LOG SCALE)
57.58 Ta K x-ray
59.66 241Am
65.26 Ta K x-ray
75.10 Pb K x-rays
85.04
99.93
103.90 Pu K x-rays
117.26
120.69 234U
U K x-ray 111.33
148.59 241Pu
152.54
164.50 237U
200.94
207.97 237U
238.62 212Pb
267.54 237U
277.39 208Tl
300.08 212Pb
311.93 233Pa
332.45 239Pu
340.57 233Pu
345.06 239Pu
350.70 18O(α,n)21Ne
375.06 239Pu
392.94 239Pu
413.73 239Pu
451.74 239Pu
510.75 208Tl
583.14 208Tl
ENERGY, keV

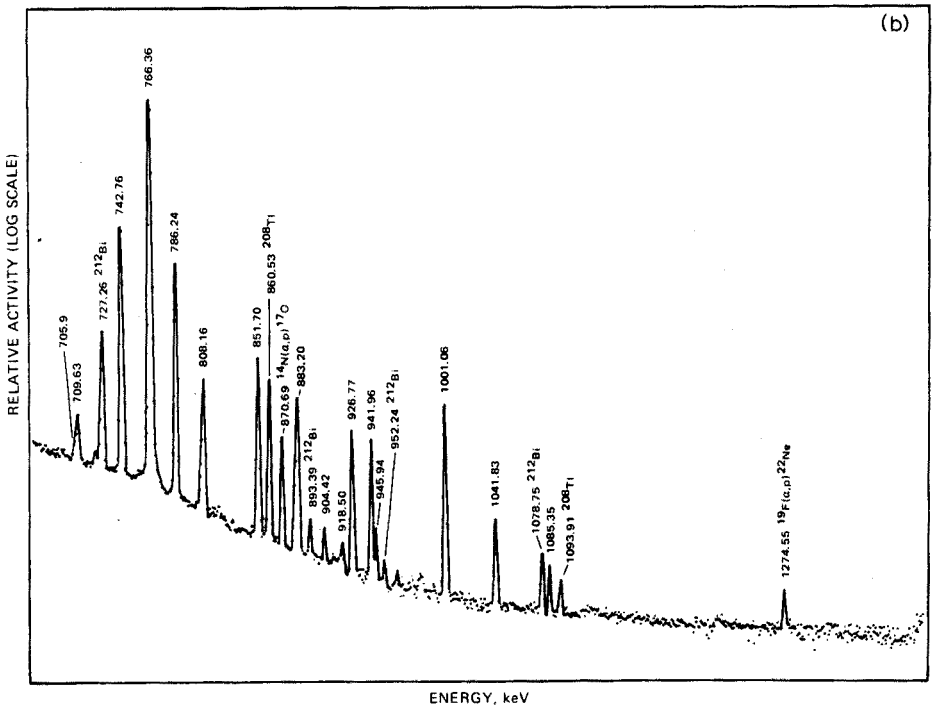
(b)
RELATIVE ACTIVITY (LOG SCALE)
705.9
709.63
727.26 212Bi
742.76
766.36
786.24
808.16
851.70
860.53 208Tl
870.69 14N(α,p)17O
883.20
893.39 212Bi
904.42
918.50
926.77
941.96
945.94
952.24 212Bi
1001.06
1041.83
1078.75 212Bi
1085.35
1093.91 208Tl
1274.55 19F(α,p)22Ne
ENERGY, keV

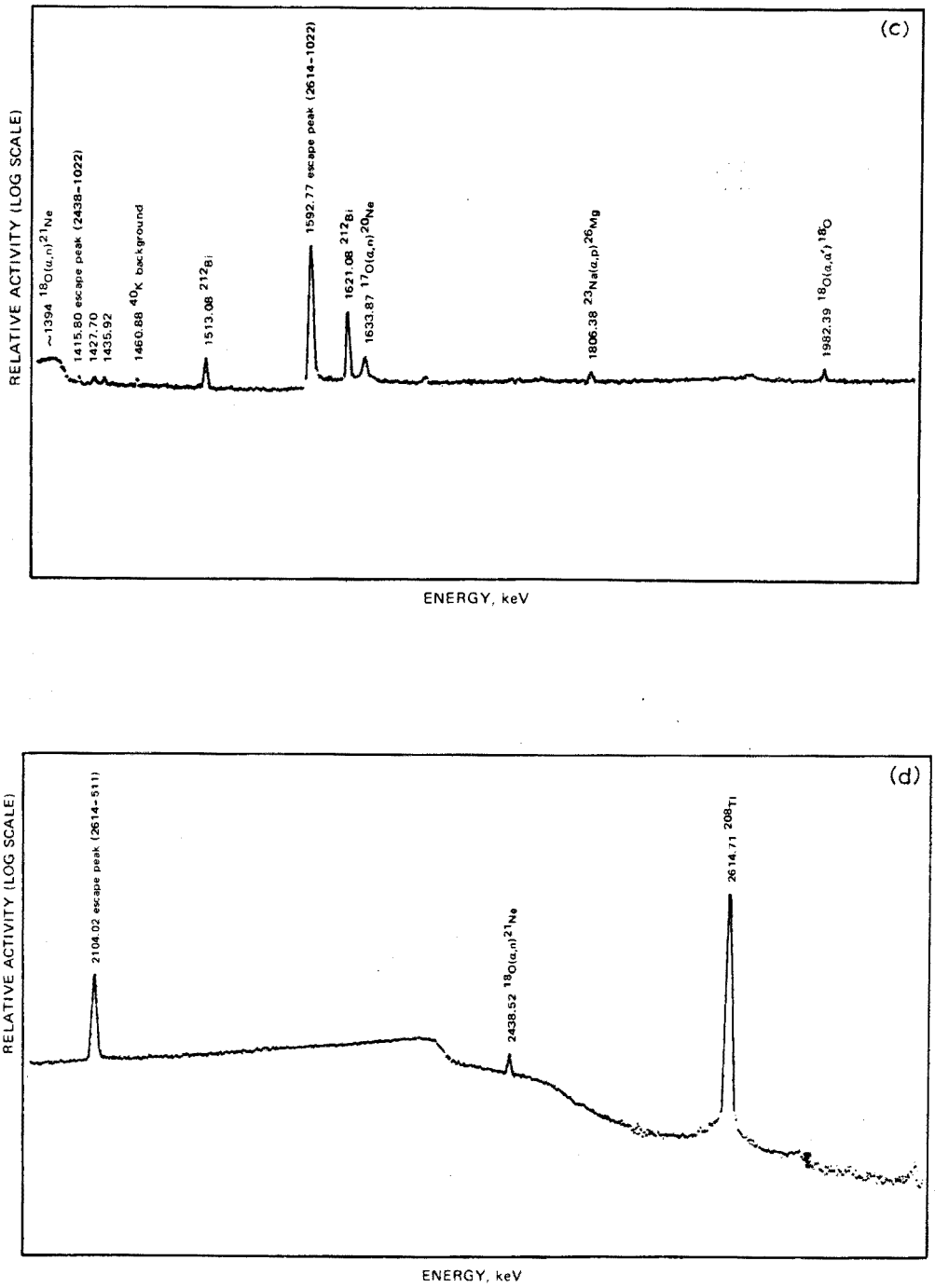

Fig. 1. γ-Ray spectrum of $^{238}PuO_2$ (natural oxygen). (a) 0–700 keV region. (b) 700–1400 keV region. (c) 1400–2100 keV region. (d) 2100–2800 keV region.

background is caused by γ-rays from decay of ^{236}Pu daughters, particularly the 2614-keV ray (Fig. 1(d)).

The reaction $^{18}O(\alpha, n)^{21}Ne$ produces γ-rays with energies of 351 keV (Fig. 1(a)), 2438 keV (Fig. 1(d)), and a 2690- and 2697-keV doublet (not shown). The most intense of these, 351 keV, is used as a measure of the ^{18}O content. The 345-keV γ-ray from ^{239}Pu decay was chosen as an internal standard as ^{238}Pu does not emit a suitable γ-ray in this energy region. This choice, however, requires a knowledge of the $^{238}Pu/^{239}Pu$ ratio. In the present work, a ratio of 80/16 was assumed for nominally 80% ^{238}Pu, and 90/9 was assumed for nominally 90% ^{238}Pu, experience having shown these ratios to vary by not more than 5%.

EXPERIMENTAL

Measurement technique

A γ-ray spectrometer system consisting of a Ge(Li) detector and pulse-height analyzer is recommended for the determination of ^{17}O and ^{18}O in $^{238}PuO_2$ fuels. The resolution of the system should be at least 2.1-keV full-width at half maximum at 1332 keV (^{60}Co). The analyzer should have 3000-channels capacity for simultaneous determination of both ^{17}O and ^{18}O, or 1000-channel capacity for individual determinations. The samples are welded in metal capsules in an inert atmosphere to avoid air contamination. If the metal capsule is stainless steel or a lighter material, a 0.75-mm thick tantalum or equivalent absorber is used to reduce the low-energy γ-flux seen by the detector. The amplifier gain is adjusted to allow accumulation in the energy range of at least 0–1650 keV with a conversion ratio of 0.7 keV per channel, although in the present work a range of 0–2800 keV was used. This larger range allowed other light element impurities to be detected through α-induced reactions.

^{18}O determination

Peak areas are determined for the 345- and 351-keV γ-rays from the sample and a background correction is applied from a separate measurement with the sample removed from the detector. This background, which is due to ^{226}Ra ($E = 351.9$ keV) in the building construction materials, was 85 counts per 10,000 s at the site used in this work. A calibration factor is calculated from average 351/345-keV peak-area ratios measured for several PuO_2 standards made with natural oxygen. The ^{18}O isotopic abundance of a sample is then calculated from its 351/345-keV peak-area ratio and the calibration factor. A blank correction is obtained from peak-area ratios of pure plutonium metal encapsulated in a manner similar to that of the standards and sample. A blank value equivalent to 0.0023%, which may have been due to traces of oxygen in the capsule, was found in the present work. If the sample contains different ^{238}Pu and ^{239}Pu contents from that of the standards, a correction is applied to the 351/345-keV ratio R:

$$\text{corr.}R = R \times \frac{\%\,\text{Pu-238(std.)} \times \%\,\text{Pu-239(sam.)}}{\%\,\text{Pu-238(sam.)} \times \%\,\text{Pu-239(std.)}}$$

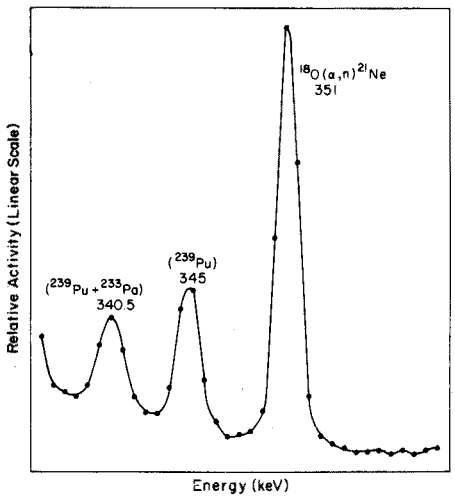

Fig. 2. Portion of $^{238}PuO_2$ (natural oxygen) spectrum used for ^{18}O determination.

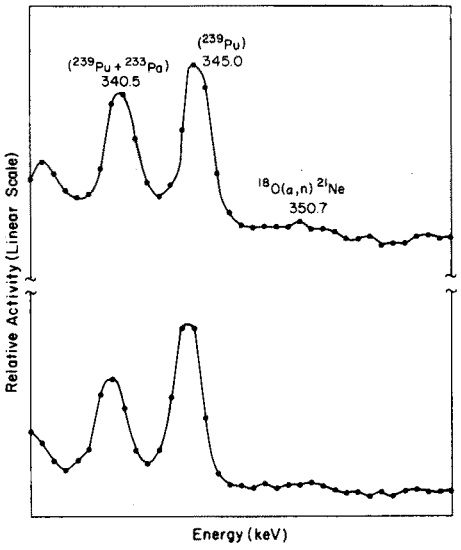

Fig. 3. Portion of ^{238}Pu $^{16}O_2$ (top) and ^{238}Pu metal (bottom) spectra used for ^{18}O determination.

^{17}O determination

Peak areas are determined for the 1428-, 1436-, and 1634-keV γ-rays from several natural-oxygen PuO_2 standards and from the sample. A calibration factor is calculated from the average 1634/(1428+1436)-keV peak-area ratios for the standards and the ^{17}O isotopic abundance of the sample is calculated from its 1634/(1428+1436)-keV peak-area ratio and the calibration factor. A blank correction is obtained from peak-area ratios of pure plutonium metal encapsulated in a manner similar to that of the standards and samples. The blank value obtained in the present work was equivalent to 0.0007% and may have been due to traces of oxygen in the container.

RESULTS AND DISCUSSION

γ-Ray peaks

An enlarged portion of the γ-ray spectrum of PuO_2 made from natural oxygen (Fig. 2) includes the peaks of interest for the determination of ^{18}O at 345 and 351 keV. Good resolution of these, as well as the 345-keV peak from the adjoining 340.5-keV peak, permits easy computation of peak areas. For PuO_2 highly enriched in the ^{16}O isotope, the 351-keV peak is difficult to distinguish from the high Compton background (Fig. 3) and the peak-area computation is less accurate. The spectrum for pure plutonium metal containing 80% ^{238}Pu (Fig. 3) shows evidence of a peak at 351 keV which is taken to represent the blank correction.

Another enlarged portion of the γ-ray spectrum of PuO_2 (natural oxygen)

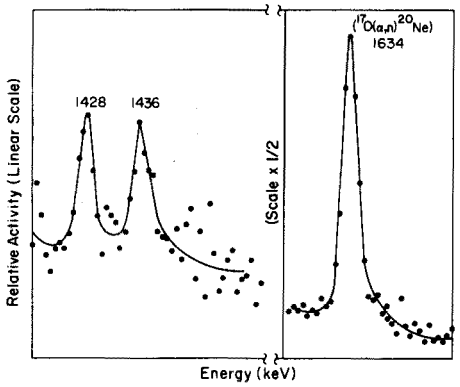

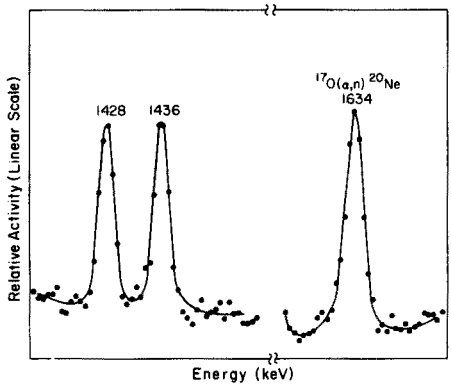

Fig. 4. Portion of $^{238}PuO_2$ (natural oxygen) spectrum used for ^{17}O determination, with high Compton background.

Fig. 5. Portion of ^{238}Pu $^{16}O_2$ spectrum used for ^{17}O determination, with low Compton background.

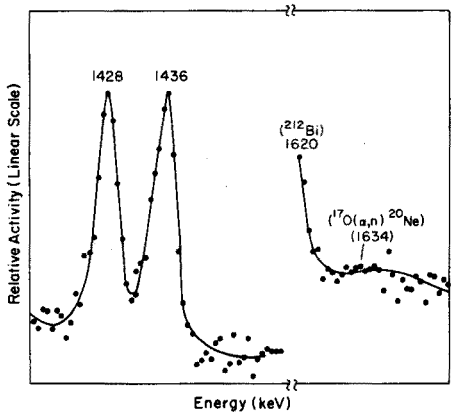

Fig. 6. Portion of ^{238}Pu metal spectrum used for ^{17}O determination.

(Fig. 4) includes the peaks of interest for the determination of ^{17}O at 1428, 1436, and 1634 keV. The first two peaks are partially hidden in the Compton continuum, making accurate computation of the peak areas difficult. This situation occurs for aged samples in which ^{236}Pu daughter growth is extensive. As a comparison, Fig. 5 shows that the peaks are more clearly defined in a sample of PuO_2 (^{16}O enriched) recently refined to remove ^{236}Pu daughters. The blank correction for ^{17}O is shown by a slight peak at 1634 keV in the spectrum of pure metal (Fig. 6).

Standards

Analyses for ^{18}O and ^{17}O are based solely on PuO_2 (natural oxygen) standards with assumed isotopic abundances[3] of 0.204% ^{18}O and 0.037% ^{17}O. Standards containing other accurately known amounts of these isotopes are not available. Attempts to evaluate the accuracy of these samples were made by

calculating neutron activities of samples, assuming that 2450 n s^{-1} g^{-1} of plutonium originate from spontaneous fission and that any additional neutron activity is from ^{18}O and $^{17}O(\alpha, n)$ reactions. Values of 5 and 0.5 n s^{-1} g^{-1} of plutonium were used for the contributions from 1 μg of ^{18}O and of ^{17}O per g of oxygen, respectively. Several comparisons of calculated with measured neutron activities showed differences ranging from -20% to $+8\%$. Negative differences could be due to the presence of unsuspected impurities that undergo (α, n) reactions, but the reason for large positive differences is unknown.

As more meaningful results might be obtained from the neutron activities of samples in which only the oxygen isotopic composition was changed, the neutron activities were determined for three sets of PuO_2 pellets originally containing less than 0.001% ^{18}O and 0.010%–0.016% ^{17}O. Each pellet was exposed three times to an atmosphere containing natural oxygen at 900–1000°C to effect exchange. After each treatment the samples were returned for measurements of ^{17}O and ^{18}O contents and neutron emission rates. The measured neutron activities (Table I) were then compared with those calculated, based on changes in ^{17}O and ^{18}O contents. Differences varied from -13% to $+6\%$.

TABLE I

COMPARISON OF MEASURED AND EXPECTED NEUTRON ACTIVITIES WITH INCREASING ^{17}O AND ^{18}O ABUNDANCE

Sample	^{17}O *(p.p.m.a.)*[a]	^{18}O *(p.p.m.a.)*[a]	*Measured* $n\ s^{-1}\ g^{-1}\ Pu$	*Expected* $n\ s^{-1}\ g^{-1}\ Pu$	*Difference (%)*
1	160	0	2679	—	—
	150	341	4054	4379	− 7.4
	150	389	4550	4619	− 1.5
	220	523	5504	5324	+ 3.4
2	120	0	2685	—	—
	180	353	4121	4480	− 8.0
	190	521	4645	5325	−13.0
	220	651	5583	5990	− 6.8
3	100	5	2685	—	—
	150	240	3946	3895	+ 1.3
	220	301	4451	4220	+ 5.5
	220	681	5320	6120	−13.0

[a] Atoms per 10^6 atoms of total oxygen.

Another two sets of PuO_2 pellets contained moderately enriched ^{16}O originally. One pellet in each set was analyzed for ^{17}O and ^{18}O, and its neutron emission rate measured (Table II). The other four pellets in a set were assumed to be identical with the first. Each of the four was exposed to an atmosphere containing highly enriched ^{16}O at different temperatures ranging from 1000°C (sample A) to 1650°C (sample D), thus causing the oxygen in each pellet to exchange with the oxygen in the furnace atmosphere to an extent dependent on the furnace temperature. Comparison of calculated and measured neutron activities varied from -6% to $+3\%$. The results given in Tables I and II indicate a

TABLE II

COMPARISON OF MEASURED AND EXPECTED NEUTRON ACTIVITIES WITH DECREASING ^{17}O AND ^{18}O ABUNDANCE

Sample	^{17}O *(p.p.m.a.)*	^{18}O *(p.p.m.a.)*	*Measured* $n\,s^{-1}\,g^{-1}\,Pu$	*Expected* $n\,s^{-1}\,g^{-1}\,Pu$	*Difference (%)*
1	320	927	7550	—	—
1-A	310	629	6130	6055	+1.2
1-B	250	709	6230	6454	−3.5
1-C	290	726	6660	6542	+1.8
1-D	250	598	5550	5870	−5.5
2	280	924	7250	—	—
2-A	280	679	6070	6025	+0.7
2-B	300	731	6440	6287	+2.4
2-C	280	687	6130	6065	+1.1
2-D	240	452	5030	4886	+2.9

satisfactory agreement of ^{17}O and ^{18}O measurements with neutron activity increase arising from (α, n) reactions on these isotopes.

Computer standards

A further evaluation of the oxygen isotope determinations was made with a set of "computer" standards. These were obtained from γ-ray spectra of PuO_2 made from natural oxygen and of plutonium metal, with the aid of a minicomputer. By successively adding data from individual channels of the metal spectrum to those of corresponding channels in the PuO_2 spectrum, simulated spectra were obtained representing ^{18}O and ^{17}O contents in successively halved amounts. A correction was necessary to account for the fact that an exactly equivalent amount of data was not accumulated in the two primary spectra, by normalizing the data for one of the peak areas. These computer-generated standards made possible the evaluation of methods for calculating peak areas and the establishment of limits for the procedure. Thus, one minicomputer program for calculating peak areas failed to yield a linear relationship of the 351 keV/345 keV peak ratio *vs.* ^{18}O content, until the program was modified. The same program was unsuitable for determinations below an ^{17}O abundance of 0.0050% because its peak-seeking function failed to locate the 1634-keV peak. Manual calculations for ^{18}O determination was found to be suitable, while a least-squares fit routine most accurately determined ^{17}O abundances. These latter results are shown in Figs. 7 and 8.

Precision

The precision for ^{18}O determinations is indicated in Table III for samples containing 20–50 p.p.m.a. (parts per million atomic) and also for the range above 50 p.p.m.a. ^{18}O. The average deviation for samples analyzed in duplicate is above 10% and erratic for the lower range, but smaller (*ca.* 4%) above 50 p.p.m.a. At the detection limit of 0.001% ^{18}O, the average deviation is estimated to be about 25%. The average deviation of ^{17}O determinations in the range 91–267 p.p.m.a. was 3%, with a much less significant range of error (0–9%). However, the samples

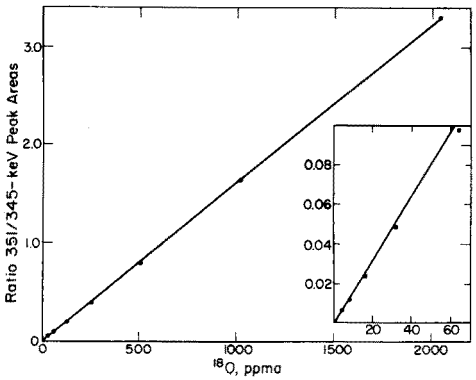

Fig. 7. Relation of 351/345 keV peak ratio to ^{18}O abundance found by manual calculations.

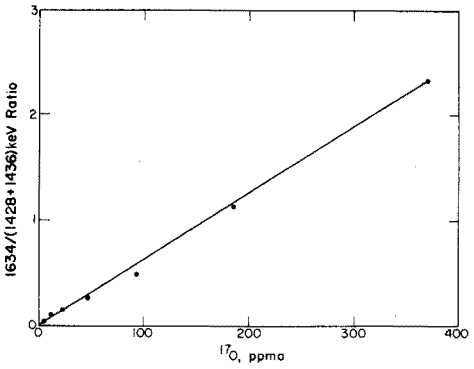

Fig. 8. Relation of 1634/(1418+1436)-keV peak ratio to ^{17}O abundance found by least-squares fit calculations.

TABLE III

PRECISION OF ^{18}O DETERMINATION

p.p.m.a. Found	*Av. Dev. (%)*	*p.p.m.a. Found*	*Av. Dev. (%)*
20	1	46	10
23	8	58	10
24	12	66	8
24	48	77	7
26	2	96	2
31	28	151	0
35	15	167	2
35	1	183	4
41	21	230	0
41	1	782	0
43	0		

in this list contained low amounts of ^{236}Pu daughter activities; samples with higher amounts of these activities would be expected to show poorer precision.

This work was done under the auspices of the U.S. Atomic Energy Commission.

SUMMARY

A procedure has been developed for nondestructive determinations of ^{17}O and ^{18}O isotopic abundances in $^{238}PuO_2$ fuels produced for biomedical application. Close control of these isotopes is important because they increase the neutron emission rate caused by (α, n) reactions. γ-Rays accompanying these reactions are measured by a lithium-drifted germanium [Ge(Li)] detector and related to their respective isotopic abundances. Each determination has a detection limit approxi-

mating the lowest contents encountered in PuO_2 samples of 0.005% ^{17}O and 0.001% ^{18}O. The average deviations for each determination are estimated to be about $\pm 25\%$ at their detection levels, and less than $\pm 10\%$ for abundances above 0.01%.

REFERENCES

1 L. Mullins, *USAEC report LA-4940*, 1972.
2 C. M. Lederer, J. M. Hollander and I. Perlman, *Table of isotopes*, Wiley, New York, 1968, p. 425.
3 H. Craig, *Geochim. Cosmochim. Acta*, 12 (1957) 133.

Analytica Chimica Acta, 77 (1975) 107–115

APPLICATIONS OF ELECTRON SPIN RESONANCE IN THE ANALYTICAL CHEMISTRY OF TRANSITION METAL IONS

PART I. FACTORS AFFECTING THE SIGNAL AMPLITUDE

W. G. BRYSON, (the late) D. P. HUBBARD, B. M. PEAKE and J. SIMPSON
Department of Chemistry, University of Otago, Box 56, Dunedin (New Zealand)
(Received 30th December 1974)

During the past few years electron spin resonance (e.s.r.) has found increased application in the study of transition metal ions and excellent review articles[1,2] are available. However, it is the analytical applications of the technique which have aroused our interest, in particular the potential use in the elucidation of the nature of metals ions in various environments. A study of the role of metals in, for example, biochemical processes or the marine environment, requires methods of analysis capable of discriminating not only the oxidation states of metals but also the various chemical forms of the metal. Much of the early work on the role of e.s.r. in analytical chemistry has been reviewed by Flockhart and Pink[3] and recently by Janzen[2]. Guilbault *et al.* have studied in some detail the e.s.r. of vanadium and copper(II)[4], manganese(II)[5,6], and chromium(III), vanadium(IV) and iron(III)[7]. In addition, a scheme of analysis involving solvent extraction and e.s.r. has been devised[8] for the separation and determination of each of the ions, Mn^{2+}, Cu^{2+}, VO^{2+}, Cr^{3+}, Fe^{3+} and Gd^{3+} simultaneously present in solution. Limits of detection and ranges of analytical utility for quantitative e.s.r. were included. Another scheme has been reported[9] involving the determination of several Group VIII metal ions.

One of the first analytical applications, involving the establishment of the different species present, was in the determination of vanadium[10] in a series of distillates, residues and full crudes in the range 0.1–200 p.p.m., where the vanadyl–etioporphyrin (I) complex was used as standard. In a recent publication[11], it has been proposed that several other vanadyl environments exist in petroleum in addition to the commonly recognised porphyrins. Angino *et al.*[12] have investigated the effects of dissolved nitrogen, oxygen and carbon dioxide at various pH levels on the e.s.r. of manganese in aqueous solution and their results suggested that $Mn(H_2O)_6^{2+}$ is the major species present over the pH range 2–6.3.

Variables such as power and modulation amplitude affect the e.s.r. signal. Since, in an analytical method, optimization of, for example, signal-to-noise ratios is a necessary step, it becomes important to understand the variation of signal with these experimental variables. Moyer and McCarthy[13] have evaluated the utility of e.s.r. for determinations of Gd^{3+}, Cr^{3+}, Fe^{3+}, Cu^{2+} and Mn^{2+} and attempted to remove the power dependence of the signal by a normalization procedure. In this paper an improved procedure, compared with that of Moyer and McCarthy, for power normalization is discussed. Results for Cu^{2+}, Mn^{2+} and VO^{2+}

are presented to show clearly the power dependence of the e.s.r. signal and also the need to maintain a constant modulation amplitude for optimal precision. Limits of detection and ranges of analytical utility are also included. It is intended that further investigations of the analytical applications of e.s.r. will be reported subsequently.

EXPERIMENTAL

Apparatus

A Varian E-4 spectrometer, with a modulation frequency of 100 kHz, was used for all e.s.r. measurements together with a standard quartz aqueous solution sample cell (Scanco S-812).

Reagents

Standard metal ion solutions were prepared by dissolving reagent grade chloride, sulphate or perchlorate salts in triply distilled water. All dilutions were made with triply distilled water which was deoxygenated *in vacuo* before use in order to minimize line broadening of the spectra by dissolved oxygen[14]. Copper(II) and vanadium(IV) solutions were measured at pH 3.0, whereas manganese solutions were measured at pH 5.0.

Procedure

General operation. The instrument was tuned by the method described by Guilbault and Lubrano[5]. This tuning procedure apparently allows measurements to be carried out with a precision of 0.4% and an accuracy of 2%. It was extremely important to align the aqueous sample cell correctly in the electric and magnetic fields if such precision was to be attained.

The modulation amplitude (M) was optimized for each particular metal ion. This involved finding the maximum value of M at which line broadening has not started to occur. M was then maintained at this value throughout the power variation studies.

The minimum time-constant which gave an acceptable noise level was used. A scan time was selected such that peak-to-peak scan time was $\geqslant 7\text{–}10 \times$ time-constant, so as to avoid distortion of absorption lines[7]. All studies were carried out at room temperature (21 ± 2°C).

Measurement of the e.s.r. signal. Manganese-55 (relative abundance, 100%) has a nuclear spin, I, of 5/2, hence manganese(II) gives an absorption curve containing 6 hyperfine components in dilute solution at room temperature. The fourth line from low field ($M_I = +\frac{1}{2}$) was used for peak-to-peak measurements as this line has been shown to be unbroadened by second order effects[15]. Vanadium-51 (natural abundance, 100%) has a nuclear spin, I, of 7/2; hence VO^{2+} gives an 8-line spectrum. The third line from low field ($M_I = -(3/2)$) was selected for peak-to-peak measurements. Copper-63 (natural abundance, 69.09%) and copper-65 (natural abundance, 30.91%) have a nuclear spin, I, of 3/2. However, only one line is observed in aqueous solution, partly because of broadening by tumbling[16,17].

RESULTS AND DISCUSSION

The area under the absorption curve is directly proportional to the number of unpaired spins in the sample[18]. In e.s.r. instruments the recorder signal appears as the first derivative of the absorption curve. The results presented in this paper rely on the principle that the peak-to-peak amplitude (A) of the first derivative curve is proportional to the area under the absorption curve and hence to the concentration of metal ion, provided that the line width and line shape and a number of instrumental variables remain constant.

There are several such variables which must be controlled and accurately known before a complete and thorough understanding of the analytical potential of the e.s.r. signal can be achieved. At constant incident microwave power (P), Guilbault and Lubrano[5] suggest an expression for the quantitative signal as the peak-to-peak amplitude (A) per unit receiver gain (G) per unit modulation amplitude (M). However, a constant modulation amplitude of 10 gauss was used throughout their work and consequently the direct proportionality of (A/G) to M was never established. Meisel and Guilbault[7] also used this expression for the signal, although a modulation amplitude of 10 gauss was generally utilized. Similarly, Moyer and McCarthy assumed direct proportionality between A and both G and M in their power variation studies on gadolinium(III). There seems no reason why the peak-to-peak amplitude should not be proportional to the receiver gain. However, its variation with modulation amplitude and power has never been studied.

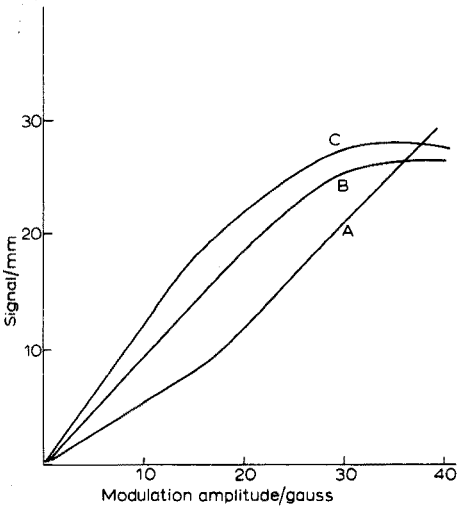

Fig. 1. Variation of Signal (A/G) with Modulation Amplitude (M). A, $5.0 \cdot 10^{-3}$ M $MnCl_2 \cdot 4\,H_2O$. B, $2.5 \cdot 10^{-2}$ M $CuCl_2 \cdot 2\,H_2O$. C, $5 \cdot 10^{-3}$ M $VOSO_4 \cdot 5\,H_2O$. Constant Power of 10 mW. The signal is the peak-to-peak amplitude in mm divided by the receiver gain *i.e.* A/G.

Variation of signal with modulation amplitude

Figure 1 shows the variation of signal (A/G) with M at constant P for the three ionic species. Note the linearity of all three plots up to a value of M of around 10 gauss. This is in reasonable agreement with the assumptions made in previous

work[5,7,13]. Theoretically as M approaches the line width (H_{pp}), the linear relationship between (A/G) and M ceases[19,20]. However, the area under the absorption curve is still proportional to M even at high values of M. The consequence of this is that (A/G) is less than expected because the line width has increased. In the case of manganese(II) a possible explanation for the shape of the curve is as follows. The hyperfine component ($M_I = +\frac{1}{2}$) used for measurement suffers from appreciable overlap from neighbouring hyperfine components at high modulation amplitudes. Consequently, the decrease in (A/G) caused by line broadening at high modulation amplitudes is more than compensated for by the increase in (A/G) from contributions by neighbouring lines. Hence (A/G) appears larger than expected as M increases. The single line of copper(II) behaves as expected as does the vanadyl(II) line ($M_I = -(3/2)$) since this line has negligible overlap with adjacent lines.

To preserve linearity of (A/G) *vs.* M, M should be maintained at much smaller values than the line width. However, it is recommended that one should operate at a constant value of M as high as possible before any measurable distortion in line shape. Occasionally, it may be necessary to alter M from its optimal value in order to extend the concentration range of analytical utility. Another reason for operating at a constant M is that the effect of M on (A/G) appears to be time-dependent (with our instrument at least) for $M > 10$ gauss. On adjusting M, 5–15 min elapsed, depending on M, before the detector current stabilized.

Variation of signal with power

Moyer and McCarthy[13] showed results which they interpreted as suggesting that the variation of signal (A/GM) with incident power (P) may be removed by dividing the signal by log P. However, their results could have been interpreted

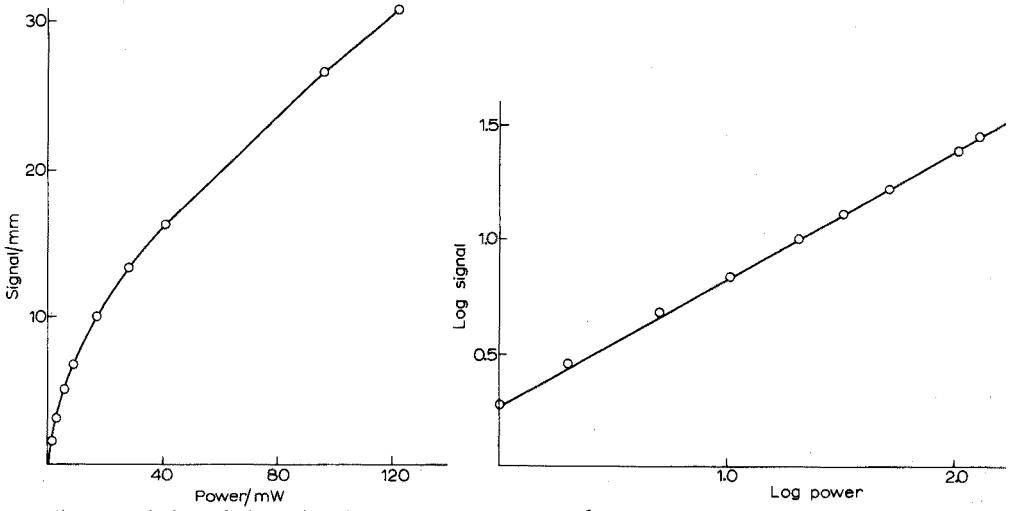

Fig. 2. Variation of Signal (A/G) with Power for $3.5 \cdot 10^{-3}$ M $MnCl_2 \cdot 4\,H_2O$. Modulation Amplitude, 10 gauss. Signal is defined as in Fig. 1.

Fig. 3. Variation of log A/G with log P. Same conditions as for Fig. 2.

differently, hence an independent study was undertaken. Figure 2 shows the variation of signal (A/G) with P, at constant M, for manganese(II) and Fig. 3 shows the corresponding plot of $\log(A/G)$ *vs.* $\log P$. The linearity apparent in the latter figure suggests that

$$\log(A/G) = k \log P + \log c \text{ or } A/G = cP^k$$

where c and k are constants.

In other words, to normalize the signal in terms of power, one needs to divide by P^k, where k is the gradient of the log plot as shown in Fig. 3. Table I shows

TABLE I

MEAN VALUES OF k

Species	*Mean k*	*No. of measurements*[a]
Mn^{2+}	0.55 ± 0.02	19
VO^{2+}	0.52 ± 0.01	9
Cu^{2+}	0.48 ± 0.02	23

[a] Each measurement of k was made at a different concentration within the linear range of concentration shown in Table III.

the mean values of k for Mn^{2+}, Vo^{2+} and Cu^{2+} in aqueous solution. The results were obtained by means of a computer program to fit $\log(A/G)$ to $\log P$ by linear least squares procedures*. Table II shows some typical results for manganese(II). Theory[20] predicts $k = 0.5$ and indeed Saraceno *et al.*[10], in their work on vanadium, assumed this relationship as early as 1961. Moyer[21] concluded that neither a $\log P$ nor $P^{0.5}$ normalization procedure exactly corrects for the power level variation. He introduced an α factor to explain the small difference in signal after power correction based on $\log P$ (α being an experimental constant which had to be determined for each metal ion–solvent system and power setting!). From Table II it should be obvious that (A/GMP^k) is a much better normalized signal than $(A/GM \log P)$ and slightly better than $(A/GMP^{0.5})$. The signals are presented in Table II in log form for convenience. Exactly the same trends were found in the cases of copper(II) and vanadium(IV). It appears that k will vary slightly from species to species depending on their power absorption characteristics. As with modulation amplitude, it is possible to use a constant power. However, provided that saturation does not occur, increasing power will increase the signal-to-noise ratio and therefore extend the range of analytical utility. Therefore it is indeed beneficial to have a means of normalizing the signal in terms of power.

Analytical curve and limits of detection

Table III shows the limits of detection, analytical ranges and precision of quantitative e.s.r. for the three species. The values quoted were measured at a modulation amplitude of 10 gauss and a power of 20 mW. With our instrument

* A listing and documentation of this program are available on request from the authors.

TABLE II

EFFECT OF POWER ON SIGNAL EXPRESSIONS

Concentration[a] *(mol dm^{-3})*	*Power (P) (mW)*	*Peak-to-peak amplitude (A) (mm)*	*Ga in (G)*	*Modulation amplitude (M) (gauss)*	*Log (A/GM)*	*Log [(A/GM log P)]*	*Log ($A/GMP^{0.5}$)*	*Log (A/GMP^{k})*[b]
$8.00 \cdot 10^{-2}$	10	127.9	$1.60 \cdot 10^{2}$	0.1	0.903	0.903	0.403	0.355
	20	142.2	$1.25 \cdot 10^{2}$	0.1	1.06	0.942	0.405	0.343
	50	121.8	$6.30 \cdot 10^{1}$	0.1	1.29	1.06	0.437	0.356
	100	145.8	$5.00 \cdot 10^{1}$	0.1	1.46	1.16	0.465	0.369
$8.00 \cdot 10^{-3}$	10	167.2	$1.60 \cdot 10^{1}$	10	0.019	0.019	−0.481	−0.529
	20	150.4	$1.00 \cdot 10^{1}$	10	0.177	0.063	−0.473	−0.535
	50	153.4	$6.30 \cdot 10^{0}$	10	0.386	0.156	−0.468	−0.544
	100	144.4	$4.00 \cdot 10^{0}$	10	0.558	0.256	−0.442	−0.538
$8.00 \cdot 10^{-4}$	10	140.2	$1.60 \cdot 10^{2}$	10	−1.06	−1.06	−1.56	−1.61
	20	159.8	$1.25 \cdot 10^{2}$	10	−0.893	−1.01	−1.54	−1.61
	50	174.8	$8.00 \cdot 10^{1}$	10	−0.661	−0.891	−1.51	−1.59
	100	209.0	$6.30 \cdot 10^{1}$	10	−0.479	−0.780	−1.48	−1.57
$8.00 \cdot 10^{-5}$	10	150.2	$1.60 \cdot 10^{3}$	10	−2.03	−2.03	−2.53	−2.58
	20	172.6	$1.25 \cdot 10^{3}$	10	−1.86	−1.97	−2.51	−2.57
	50	176.2	$8.00 \cdot 10^{2}$	10	−1.66	−1.89	−2.51	−2.59
	100	210.4	$6.30 \cdot 10^{2}$	10	−1.48	−1.78	−2.48	−2.57

[a] $MnCl_2 \cdot 4\ H_2O$ was the sample material in this study.
[b] Mean value of k (19 determinations) $= 0.55 \pm 0.02$.

TABLE III

LIMITS OF DETECTION, ANALYTICAL RANGES AND PRECISION OF QUANTITATIVE E.S.R.

Species	*Detection limit*[a] *(mol dm^{-3})*	*Analytical range*[b] *(mol dm^{-3})*		*Precision*[c] *(%)*
		Upper limit	*Lower limit*	
Mn^{2+}	$9.00 \cdot 10^{-8}$	$1.0 \cdot 10^{-1}$	$5 \cdot 10^{-6}$	0.4
VO^{2+}	$1.95 \cdot 10^{-7}$	$2.0 \cdot 10^{-2}$	$5 \cdot 10^{-6}$	0.7
Cu^{2+}	$2.01 \cdot 10^{-7}$	$1.0 \cdot 10^{0}$	$1.0 \cdot 10^{-5}$	0.2

[a] Detection limit is defined as being equal to twice the standard deviation of a concentration near the expected limit (10 measurements). Data were obtained at a power of 20 mW and a modulation amplitude of 10 gauss with a time constant of 10 s.
[b] The analytical range is defined as the range of concentration over which the analytical curve is linear.
[c] The precision is defined as the relative standard deviation of the gradient of the analytical curve over the linear range.

at least, increasing power did not increase the background noise, hence lower limits of detection can be achieved. For example, for manganese(II) at a power of 100 mW and modulation amplitude of 10 gauss, a detection limit of $3.66 \cdot 10^{-8}$ *M* was achieved. Similarly, increasing the modulation amplitude could decrease the limit further.

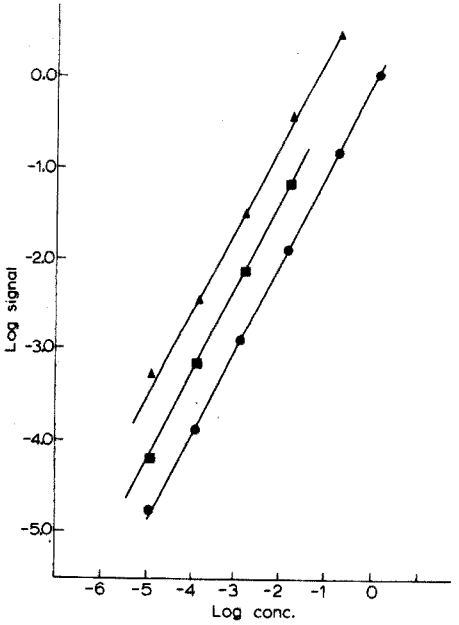

Fig. 4. Analytical curves for Mn^{2+}, VO^{2+} and Cu^{2+} in aqueous solution. Signal is defined as A/GMP^k, where k is as shown in Table I for the three species. (▲) $MnCl_2 \cdot 4\,H_2O$. (■) $VOSO_4 \cdot 5\,H_2O$. (●) $CuCl_2 \cdot 2\,H_2O$. Note that only a few points have been included in each case—the total number of concentrations within the linear range which was used to determine the analytical curve, is given in Table I.

The linear ranges of concentration of the three species are shown in Fig. 4 where the signal is defined as (A/GMP^k), with k being dependent on the species as described earlier. Since it is possible to take measurements from solutions of concentrations near the detection limit, e.s.r. is analytically useful at concentrations below the lower limit of the analytical range, and hence is useful over very wide ranges of sample concentration.

The precisions of measurement over the linear range were evaluated by fitting the best line to a large amount of data, *e.g.*, in the case of copper(II), 23 concentrations each with at least 5 different power settings were used. The precision observed, 0.2%, is quite good, and better than that of most analytical procedures.

CONCLUSIONS

Contrary to other findings[13,20], it is possible to vary power and normalize the signal for power by dividing the peak-to-peak amplitude by P^k, where k is a constant characteristic of a particular metal ion–solvent system. E.s.r. is a sensitive, precise and non-destructive technique which uses small sample sizes and has a wide concentration range of analytical utility. In future publications, the range of applications in analytical chemistry will be described.

We wish to thank the University of Otago for a Senior Demonstratorship to W.G.B. and the New Zealand Universities' Grants Committee for financial support.

SUMMARY

An evaluation of the effect of modulation amplitude (M) and microwave power (P) on the peak-to-peak amplitude (A) of the first derivative e.s.r. signal of each of Mn^{2+}, VO^{2+} and Cu^{2+} is described. It is shown that A is not directly proportional to M over all values of M and therefore for optimal precision of measurement, M should be kept constant. A varies with P^k, where k is a constant for a particular metal ion–solvent system. Limits of detection and concentration ranges of analytical utility are also reported.

REFERENCES

1 B. A. Goodman and J. B. Raynor, *Advances in Inorganic Chemistry and Radiochemistry, Vol. 13*, Academic Press, New York, 1970, 136.
2 E. G. Janzen, *Anal. Chem.*, 44 (1972) 113R; 46 (1974) 482R.
3 B. D. Flockhart and R. C. Pink, *Talanta*, 12 (1965) 529.
4 G. G. Guilbault and T. Meisel, *Anal. Chim. Acta*, 50 (1970) 151.
5 G. G. Guilbault and G. Lubrano, *Anal. Lett.*, 1 (1968) 725.
6 G. G. Guilbault and T. Meisel, *Anal. Chem.*, 41 (1969) 1100.
7 T. Meisel and G. G. Guilbault, *Anal. Chim. Acta*, 50 (1970) 143.
8 G. G. Guilbault and E. S. Moyer, *Anal. Chem.*, 42 (1970) 471.
9 W. J. Brinkman and H. Freiser, *Anal. Lett.*, 4 (1971) 513.
10 A. J. Saraceno, D. T. Fanale and N. D. Coggeshall, *Anal. Chem.*, 33 (1961) 500.
11 F. E. Dickson and L. Petrakis, *Anal. Chem.*, 46 (1974) 1129.

12 E. E. Angino, L. R. Hathaway and T. Worman, *Advan. Chem. Ser.*, 106 (1971) 299.
13 E. S. Moyer and W. J. McCarthy, *Anal. Chim. Acta*, 48 (1969) 79.
14 D. C. McCain and R. J. Myers, *J. Phys. Chem.*, 72 (1968) 4115.
15 R. G. Hayes and R. J. Myers, *J. Chem. Phys.*, 40 (1964) 877.
16 B. R. McGarvey, *J. Phys. Chem.*, 61 (1957) 1232.
17 W. B. Lewis, M. Alei and L. O. Morgan, *J. Chem. Phys.*, 44 (1966) 2409.
18 P. B. Ayscouth, *Electron Spin Resonance in Chemistry*, Methuen, London, 1967.
19 C. P. Poole Jr., *Electron Spin Resonance—A Comprehensive Treatise on Experimental Techniques*, Interscience, New York, 1967.
20 J. R. Bolton, D. C. Borg and H. M. Swartz (Eds.), *Biological Applications of Electron Spin Resonance*, Wiley–Interscience, New York, 1972.
21 E. Moyer, *Ph.D. Thesis, West Virginia University, 1970*, University Microfilms, Ann Arbor, Michigan.

Analytica Chimica Acta, 77 (1975) 117–123

DETERMINATION OF NICKEL IN STANDARD ROCKS AND GLASSES BY PHOTON ACTIVATION ANALYSIS WITH 30-MeV BREMSSTRAHLUNG

TOYOAKI KATO, EIICHI KITAZUME* and NOBUO SUZUKI

Department of Chemistry, Faculty of Science, Tohoku University, Sendai (Japan)

(Received 8th November 1974)

Nickel exhibits siderophilic properties in geochemistry. Many analytical methods have been employed so far to determine nickel abundances in rock materials and related matrices, but those are often subject to fairly high uncertainties or large spread in the observed results, as can be seen in the nickel data compiled by Fleischer[1] and Flanagan[2] on the U.S. Geological Survey standard silicate rocks. Activation analysis with thermal neutrons has frequently been used[3–6], even though this technique is not extremely sensitive for nickel. The method usually involves handling to isolate 2.58-h ^{65}Ni from a sample of high radioactivities from the elements with high thermal neutron capture cross-sections such as sodium, manganese and cobalt, although the intact measurement of ^{65}Ni has also been performed by strictly instrumental means[7]. The ^{58}Ni(n, p)^{58}Co reaction has also been useful[8,9], but by this method the precision and sensitivity are limited by the cobalt-to-nickel ratio in the sample to be analyzed. Steinnes[10] and Brunfelt *et al.*[11] have described the improvement of this method by introducing an epi-cadmium irradiation technique. Swindle and Schweikert[12] developed procedures based on charged particle activation and post-irradiation chemical separation. They found that the most favorable process for nickel determination was the ^{58}Ni(p, pn)^{57}Ni reaction by irradiation with 30-MeV protons. This method is sensitive for nickel down to p.p.b. levels but it appears to be likely to involve serious errors unless special attention is paid to monitoring beam intensities.

An alternative nuclear method which can meet various requirements for the present purpose is photon activation analysis. ^{57}Ni can be produced by the ^{58}Ni(γ, n)^{57}Ni reaction with excellent yield and selectivity by irradiating samples with bremsstrahlung photons with a maximal energy around 30 MeV[13]. Schmitt *et al.*[14] recommended in their purely instrumental version the use of the 1919-keV peak of ^{57}Ni in the determination of nickel in rocks. In previous work[15], however, the non-destructive method was found to be successful only for rocks with nickel exceeding 0.2% (dunite and peridotite), and it was generally accompanied by fairly large errors, especially with rocks of low nickel contents because of low signal-to-noise ratios. The use of the 1378-keV peak of ^{57}Ni was also unsatisfactory because of the nearby peak of ^{24}Na at 1369 keV.

The present work was aimed at establishing a more reliable method for nickel in silicate matrices by combining a simple chemical separation with high-

* Present address: Central Institute, Hitachi Manufacturing Co. Ltd., Kokubunji, Tokyo, Japan.

resolution γ-ray spectrometry. Ten standard silicate rocks and two kinds of elementally doped glasses (NBS Standard Reference Materials) were analyzed for nickel to check the accuracy and precision of the method through comparison of the results with data obtained by other analytical methods.

EXPERIMENTAL

Samples and irradiation

Twelve round-robin silicate samples were analyzed for nickel. The eight standard rocks were supplied by the U.S. Geological Survey: G-1, W-1, G-2, GSP-1, AGV-1, BCR-1, PCC-1 and DTS-1 rocks. The two Japanese rocks, granite JG-1 and basalt JB-1, were obtained from the Geological Survey of Japan. All rock samples were in a finely powdered form.

An amount of rock powder weighing 400 mg was wrapped in thin aluminum foil and formed into a disk with a diameter of 9 mm and a thickness of about 4 mm. Two kinds of glass samples (NBS SRM 614 and SRM 616) doped with 61 elements were also used; these were 3-mm thick wafers with a diameter of 13 mm.

Comparative standards were prepared by pipetting 0.1-ml aliquots of a standard solution of nickel (100 μg Ni) onto thin sheets of glass fiber with a diameter of 9 mm for rocks and of 13 mm for glasses, respectively. After drying, each sheet was wrapped in thin aluminum foil. The standards were placed face to face on the front and back of the sample and this unit was encapsulated into a silica tube for simultaneous irradiation. The tube was placed in a water-cooled sample holder for bremsstrahlung irradiation with a linear electron accelerator (Tohoku University) and was aligned along the beam axis with the front face of the tube immediately behind the photon-producing converter. The accelerator was operated at 30 MeV, and the electron beam, the peak current being 100 mA, produced bremsstrahlung in a platinum converter with a thickness of 2 mm. In a typical irradiation, the average beam current was 70 μA and a dose rate at the sample position was $6 \cdot 10^6$ R min^{-1}. The full-width at half-maximum of the bremsstrahlung intensity at 30 MeV was about 12 mm at 10 mm downstream from the converter. The vertical spread of flux did not have a pronounced effect on the results, if the samples were limited to dimensions of the above size, and the flux gradient along the length of the sample was 10% or less.

All irradiations lasted 2 h.

Radiochemical procedure

After irradiation, all the rock samples, except PCC-1 and DTS-1, were individually subjected to the simple chemical procedure outlined below.

The sample was transferred to a platinum crucible along with a 10-mg amount of nickel carrier and fused with 4 g of sodium carbonate. The fusion cake was dissolved in concentrated hydrochloric acid and transferred to a beaker with distilled water. The hydroxides were precipitated from this solution by addition of aqueous ammonia, and filtered. To recover the nickel included in the precipitate, it was dissolved in hydrochloric acid and again precipitated with aqueous ammonia. The filtrates were combined, and nickel dimethylglyoximate

Ni-DMG) was precipitated from the hot solution by adding 5 ml of ethanolic 5% DMG solution, and filtered. The Ni-DMG was dissolved with a small amount of 4 *M* nitric acid, and diluted with distilled water. To this was added an amount of an aqueous solution of copper nitrate (5 mg Cu), and copper sulfide scavenging was done by passing gaseous hydrogen sulfide; the mixture was then filtered. The Ni-DMG was again precipitated from the filtrate with additional DMG solution, filtered on a filter paper, and dried for at least 4 h at 90°C. A weighed amount of the final Ni-DMG was wrapped in a small piece of aluminum foil and formed into a disk with a diameter of 9 mm for γ-counting.

The irradiated glass wafer was rinsed in ethanol and in (1+1) nitric acid to remove surface contamination, and then treated with 5 ml of a (1+1) mixture of hydrofluoric acid and perchloric acid in a platinum dish along with nickel carrier (10 mg). The mixture was heated until gas evolution ceased. With more hydrofluoric acid, the procedure was continued until all the glass had dissolved. The mixture was brought to fumes of perchloric acid and evaporated nearly to dryness. The residue was diluted with distilled water, and the Ni-DMG was precipitated from this solution and then subjected to the procedure outlined above for nickel in rocks.

The chemical yield for nickel ranged within 50–70%.

The comparative standard was also dissolved with a small amount of a (1+1) mixture of hydrofluoric acid and perchloric acid by heating, evaporated to nearly dryness, and diluted with distilled water. To this was added aqueous ammonia, and the nickel was precipitated as Ni-DMG, which was filtered, washed, dried, weighed and made into a disk for γ-counting.

All separations were performed within 3 h after irradiation.

Counting and evaluation

γ-Counting was done with a lithium-drifted germanium detector with a sensitive volume of 33 cm^3 (Ortec Model 8101-0525) and its associated electronics coupled to a 4096-channel pulse-height analyzer (Toshiba Electric Co. Ltd., Japan). The system resolution was 2.4 keV (f.w.h.m.) for the 1332-keV γ-line of ^{60}Co. The Ni-DMG from the sample or the standard was mounted on the detector at a fixed position, and counting was made for periods of 1024 s–10 h, depending on the activity strengths of the sample to be measured.

Measurements were based on the full-energy areas under the 1378-keV peak, except for PCC-1 and DTS-1 in which the areas under the 1919-keV peak were used. The decay-corrected peak areas were then used to determine nickel abundances in the samples compared with the standards. A mean specific activity in terms of the peak areas from standards on both sides was used for calculation.

Duplicate analyses were performed on each sample material.

RESULTS AND DISCUSSION

A typical γ-ray spectrum of the Ni-DMG separated from a rock sample (AGV-1) is given in Fig. 1 together with that from the comparative standard. The principal γ-rays observed are those of ^{57}Ni except for peaks occurring in the natural background. Several unidentified minor peaks were also observed, but the

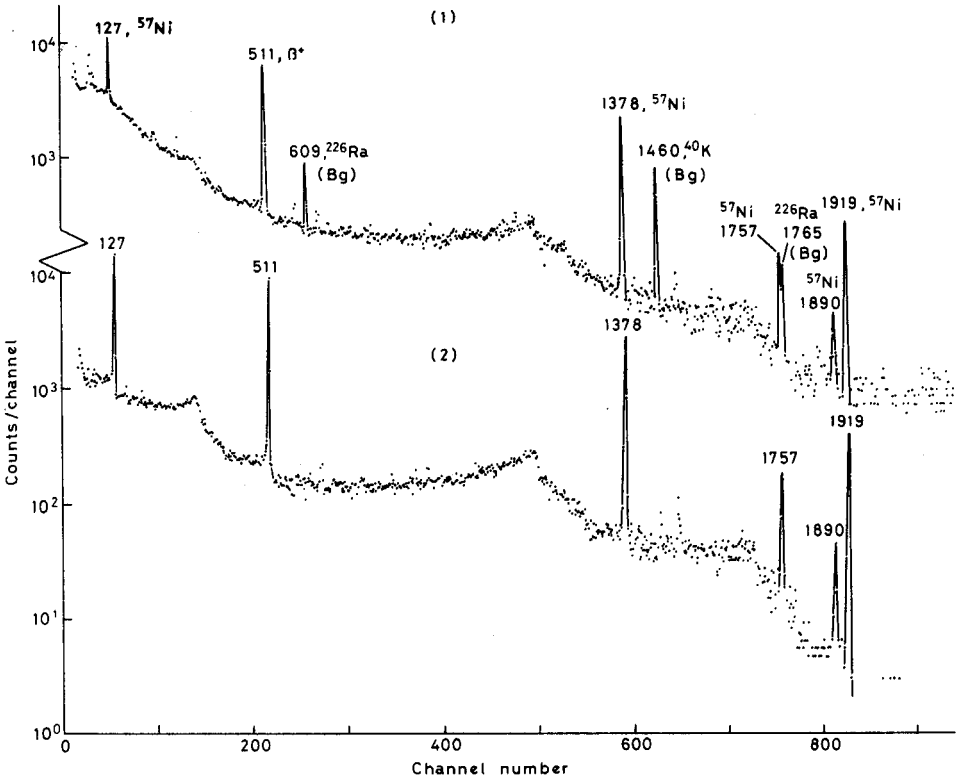

Fig. 1. Gamma-ray spectra of nickel dimethylglyoximate from (1) GSP-1 (d.t. 3h; c.t. 4.5 h) and (2) comparative standard (d.t. 8 h; c.t. 1024 s). D.t. and c.t. designate the time intervals between irradiation and counting, and the counting period, respectively. Bg indicates peaks occurring in background. Values on each peak are energies in keV.

decay curves followed on the 1378- and 1919-keV peaks showed a half-life of 36 h, corresponding to the literature value[16] of ^{57}Ni.

The results for nickel abundances obtained on the twelve silicate samples are listed in Table I, together with earlier literature data. It can be seen that the results from duplicate samples are quite compatible with a maximum deviation from the mean for these duplicate analyses of only $\pm 5\%$. In comparing the present results with previously published data, the data for the G-1 rock appears to be rather high; the nickel data listed in the Fleischer's compilation[1], mostly determined by means of optical spectrography and x-ray fluorescence, show unsatisfactory agreement for this rock. The data for the GSP-1 and AGV-1 are also high. These data suggest the possibility of inhomogeneity of the samples themselves or considerable variations of the concentrations of at least certain trace elements from one sample bottle to another. Wide variations in the abundances with respect to some trace elements have been observed for several of the USGS rocks, for instances, gold and iridium[17], antimony[18] in the new series of the USGS rocks, and antimony in G-1 and AGV-1[19]. The nickel data for the JG-1 rock found in the literature[20] also appear to show disagreement.

TABLE I

NICKEL ABUNDANCES IN STANDARD ROCKS AND GLASSES

(All results are given in p.p.m.)

Sample	*This work*[a]	*Previous work*	*Reference*[b]
G-1	8.7±0.1	1–14	Fleischer[1]; range
	8.6±0.1	(1–2)	(Recommended value)
W-1	87±1	60–82	Fleischer[1]; range
	94±1	(78)	(Recommended value)
		73±4	Schmitt *et al.*[14]; i.p.a.a.
		75.7±1.4	Steinnes[10]; e.n.a.a.
G-2	6.5±0.2	2–14	Flanagan[2]; range
(78/2)[c]	6.9±0.1	(6.4)	(Average value)
		3±1	Schmitt *et al.*[14]; i.p.a.a.
		7.5	Morrison *et al.*[7]; i.n.a.a.
		2.3±0.2	Steinnes[10]; e.n.a.a.
GSP-1	20.6±0.3	3–25	Flanagan[2]; range
(30/3)[c]	17.0±0.4	(10.7)	(Average value)
		9±1	Schmitt *et al.*[14]; i.p.a.a.
		7.0±0.7	Steinnes[10]; e.n.a.a.
AGV-1	26.8±0.4	11–27	Flanagan[2]; range
(54/7)[c]	28.6±0.5	(17.8)	(Average value)
		24±3	Schmitt *et al.*[14]; i.p.a.a.
		34	Morrison *et al.*[7]; i.n.a.a.
		13.0±0.6	Steinnes[10]; e.n.a.a.
BCR-1	18.9±0.6	8–30	Flanagan[2]; range
(2/12)[c]	16.9±0.6	(15)	(Average value)
		10±3	Schmitt *et al.*[14]; i.p.a.a.
		37, 40	Morrison *et al.*[7]; i.n.a.a.
		12.4±3.2	Allen *et al.*[6]; r.n.a.a.
		10.0±0.3	Steinnes[10]; e.n.a.a.
PCC-1	2360±120	1750–3400	Flanagan[2]; range
(79/6)[c]	2510±120	(2430)	(Average value)
		2460±80	Schmitt *et al.*[14]; i.p.a.a.
		2430±60	Steinnes[10]; e.n.a.a.
DTS-1	2360±80	1770–3300	Flanagan[2]; range
(41/31)[c]	2640±80	(2330)	(Average value)
		2140±80	Schmitt *et al.*[14]; i.p.a.a.
		2400±40	Steinnes[10]; e.n.a.a.
JG-1	11.2±0.5	6.1–14	Ando *et al.*[20]; range
	11.8±0.5		
JB-1	156±3	132–148	Ando *et al.*[20]; range
	176±4	(139)	(Average)
NBS Glass	0.99±0.04	0.95	NBS uncertified value[21]
SRM-614	1.00±0.04	1.0±0.2	Swindle and Schweikert[12]; c.p.a.a.
NBS Glass	0.22±0.02	0.27±0.05	Swindle and Schweikert[12]; c.p.a.a.
SRM-616	0.22±0.02		

[a] Results of duplicate analyses. Error limits are standard deviations based on counting statistics.

[b] I.p.a.a.: instrumental photon activation analysis. I.n.a.a.: instrumental neutron activation analysis. R.n.a.a.: radiochemical neutron activation analysis. E.n.a.a.: epithermal neutron activation analysis. C.p.a.a.: charged particle activation analysis.

[c] Split/position identification for new USGS rock standards.

The nickel abundance in the NBS SRM-614 glass is in good agreement with previous data[12,21]. For the SRM-616 glass, however, the nickel content was determined to be (0.22 ± 0.02) p.p.m. This value is about one order of magnitude higher than that of the nominal concentration level of 0.02 p.p.m.[21], but is fairly similar to the value reported by Swindle and Schweikert[12].

The sensitivity of this method was estimated on the basis of the experimental data. If the detection limit is assumed to be the amount of nickel needed to give a photopeak activity of 100 counts at 1378-keV for a counting period of 18 h (half the half-life of ^{57}Ni), it can be set at 50 ng of nickel. The possible interfering reactions yielding ^{57}Ni are the ^{63}Cu(γ, p5n)^{57}Ni and ^{64}Zn(γ, 2p5n)^{57}Ni reactions. However, interfering contributions are energetically forbidden in the energy region of 30-MeV bremsstrahlung, since their Q-values are -57.12 MeV and -64.82 MeV, respectively.

The determination of nickel utilizing the ^{58}Ni(γ, n)^{57}Ni reaction can thus be carried out interference-free by this method, and can be applied to a variety of materials of geochemical origins.

The authors express their appreciation to members of the linac and radioisotope groups at the Institute of Nuclear Science, Tohoku University, for their cooperation with the irradiations. The USGS standard rocks were kindly provided by Dr. F. J. Flanagan of the U.S. Geological Survey. We also thank Dr. Atsushi Ando of the Geological Survey of Japan for the JG-1 and JB-1 rocks.

SUMMARY

The determination of nickel in various silicate rocks and glasses by photon activation analysis with a linear electron accelerator is described. Simultaneous irradiation of the sample and comparative standards produces the ^{58}Ni(γ, n)^{57}Ni reaction, and a post-irradiation chemical separation is used in conjunction with Ge(Li) γ-spectrometry. Nickel abundances for ten standard silicate rocks and two elementally doped glasses are presented and compared with the data previously published. The method is quite simple and gives good reproducible results for nickel down to sub-p.p.m. levels.

REFERENCES

1 M. Fleischer, *Geochim. Cosmochim. Acta*, 33 (1969) 65.
2 F. J. Flanagan, *Geochim. Cosmochim. Acta*, 33 (1969) 81.
3 E. Goldberg, A. Uchiyama and H. Brown, *Geochim. Cosmochim. Acta*, 2 (1951) 1.
4 A. A. Smales, D. Mapper and A. J. Wood, *Analyst (London)*, 82 (1957) 75.
5 W. D. Ehmann, *Geochim. Cosmochim. Acta*, 19 (1960) 149.
6 R. O. Allen, L. A. Haskin, M. R. Anderson and O. Müller, *J. Radioanal. Chem.*, 6 (1970) 115.
7 G. H. Morrison, J. T. Gerard, A. Travesi, R. L. Currie, S. F. Peterson and N. M. Potter, *Anal. Chem.*, 41 (1969) 1633.
8 K. K. Turekian and D. P. Kharkar in A. A. Levinson (Ed.), *Proc. Apollo' 11 Lunar Science Conf., Vol. 2*, Pergamon, New York, 1970, p. 1659.
9 H. Wänke, R. Rieder, H. Baddenhausen, B. Spettel, F. Tesche, M. Quijiano-Rico and A. Balacescu in A. A. Levinson (Ed.), *Proc. Apollo 11 Lunar Science Conf., Vol. 2*, Pergamon, New York, 1970, p. 1719.

10 E. Steinnes, *Anal. Chim. Acta*, 68 (1974) 25.
11 A. O. Brunfelt, K. S. Heier, B. Nilssen, B. Sundvoll and E. Steinnes in D. Heymann (Ed.), *Proc. Third Lunar Science Conf., Vol. 2*, M.I.T. Press, Cambridge, Mass., 1972, p. 1133.
12 D. L. Swindle and E. A. Schweikert, *Anal. Chem.*, 45 (1973) 2111.
13 T. Kato, *J. Radioanal. Chem.*, 16 (1973) 307.
14 R. A. Schmitt, T. A. Linn, Jr. and H. Wakita, *Radiochim. Acta*, 13 (1970) 200.
15 N. Sato, T. Kato and N. Suzuki, *Radiochim. Acta*, 19 (1974).
16 C. M. Lederer, J. M. Hollander and I. Perlman, *Table of Isotopes*, Wiley, New York, 6th edn., 1967.
17 P. A. Baedecker, *USAEC Report, ORO-2670-17.*
18 J. T. Tanner and W. D. Ehmann, *Geochim. Cosmochim. Acta*, 31 (1967) 2007.
19 S. M. Lombard, K. W. Marlow and J. T. Tanner, *Anal. Chim. Acta*, 55 (1971) 13.
20 A. Ando, H. Kurasawa, T. Ohmori and E. Takeda, *Geochem. J.*, 5 (1971) 151.
21 *Provisional certificate of analysis, SRM 610-616 Doped glasses*, National Bureau of Standards, Washington, D.C., 1970.

Analytica Chimica Acta, 77 (1975) 125–131

PERIODATE OXIDATION ANALYSIS OF CARBOHYDRATES

PART IV. SIMULTANEOUS DETERMINATION OF ALDEHYDES IN DIALDEHYDE FRAGMENTS AS 2,4-DINITROPHENYLHYDRAZONES BY THIN-LAYER OR LIQUID CHROMATOGRAPHY

SUSUMU HONDA, KAZUAKI KAKEHI and KIYOSHI TAKIURA
Faculty of Pharmaceutical Sciences, Osaka University, Toneyama, Toyonaka, Osaka-fu (Japan)
(Received 12th December 1974)

Periodate oxidation of carbohydrates produces a variety of aldehydes along with carboxylic acids, and the determination of such aldehydes can give valuable structural information. Among these aldehydes, formaldehyde and acetaldehyde, which exist in unconjugated forms, may be determined by established methods[1,2], whereas glyoxal and several kinds of hydroxyaldehydes must be liberated from the oxidation products before their determination, since such aldehydes are connected through hemiacetal linkages in these products. The liberation process requires such drastic conditions that the products are partially decomposed, hence the determination of these aldehydes is difficult.

Fortunately, this undesirable decomposition can be eliminated by modifying the Barry degradation[3] with 2,4-dinitrophenylhydrazine hydrochloride. In a previous paper of this series[4], a spectrophotometric method was reported for the selective determination of glyoxal in the dialdehyde fragments formed from glycosides by periodate oxidation. In a continuation of this work, a simple method for the simultaneous determination of glyoxal and hydroxyaldehydes has been developed; thin-layer chromatographic (t.l.c.) separation of their 2,4-dinitrophenylhydrazones is followed by spectrophotometric measurement. On the basis of this t.l.c. study, a convenient method of fragment analysis by liquid chromatography (l.c.) on a small open column has also been developed.

EXPERIMENTAL

Materials

A reagent-grade sample of 2,4-dinitrophenylhydrazine hydrochloride (Tokyo Kasei Kogyo Co., Ltd) was used without further purification. All samples of aldehydes were also of reagent grade. All solvents were dehydrated by conventional methods before purification by distillation.

An authentic specimen of the bis-hydrazone of glyoxal was prepared as reported previously[4]. The hydrazones of D-glyceraldehyde, D-erythrose, D-arabinose and D-glucose were synthesized by refluxing the aldehydes with twice the equivalent amounts of 2,4-dinitrophenylhydrazine in ethanol. The hydrazones were recrystallized from ethanol. The melting points and the analytical data for the purified hydrazones were as follows.

D-glyceraldehyde 2,4-dinitrophenylhydrazone: m.p. 174–175°C; $C_9H_{10}N_4O_6$ requires 40.0% C, 3.7% H, 20.7% N; found, 39.8% C, 3.7% H, 20.6% N.

D-Erythrose 2,4-dinitrophenylhydrazone: m.p. 163–165°C; $C_{10}H_{12}N_4O_7$ requires 40.0% C, 4.0% H, 18.7% N; found, 39.5% C, 3.8% H, 18.2% N.

D-Arabinose 2,4-dinitrophenylhydrazone: m.p. 183°C; $C_{11}H_{14}N_4O_8$ requires 40.0% C, 4.3% H, 17.0% N; found, 39.9% C, 4.5% H, 16.8% N.

D-Glucose 2,4-dinitrophenylhydrazone: m.p. 123–125°C; $C_{12}H_{16}N_4O_9 \cdot H_2O$ requires 38.1% C, 4.8% H, 14.8% N; found, 38.8% C, 4.8% H, 14.9% N.

The dialdehydes I and II were prepared from methyl α- and β-D-glucopyranoside, respectively, by oxidation with periodic acid, followed by purification of the products on a column of silica gel with a 10:1 chloroform–methanol eluant. The yields of the syrupy products of I and II were 74% and 68%, respectively. The analytical results were: 40.0% C, 6.7% H for I, and 39.9% C, 7.0% H for II; $C_6H_{10}O_5 \cdot H_2O$ requires 40.0% C, 6.7% H. The preparation of the dialdehydes, III and IV was reported previously[4].

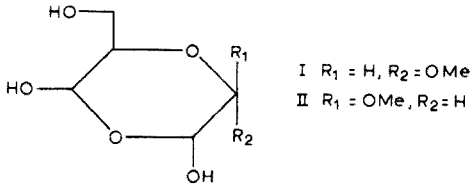

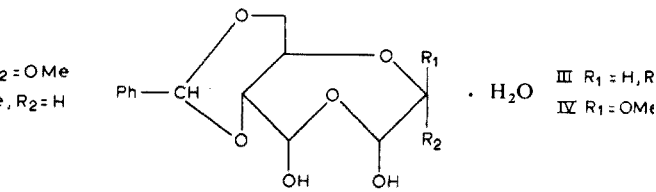

The alkali solution for developing the color of the glyoxal fraction was prepared by dissolving potassium hydroxide (12 g) in aqueous 80% ethanol (100 ml).

Apparatus

A Shimazu UV-200 spectrophotometer was used with 1-cm glass cells. Glass plates (10 × 20 cm) pre-coated with silica gel were used (Merck Silica Gel Plate No. 5721/0025).

T.l.c. of hydrazones

Heat the plates, before use, at 120°C for 10 min and cool to room temperature in a desiccator containing anhydrous silica gel. Apply samples of hydrazones (50 μg), dissolved in 1,2-dimethoxyethane (0.1 ml), in narrow bands and develop with 10:1 chloroform–methanol. Remove the solvent under a hood, and redevelop with 5:1 chloroform–methanol until the solvent front reaches the zone of the hydrazone of glycolaldehyde. Strip off the individual zones and extract with ethanol (5 ml). Read the absorbances at the absorption maxima, except for the bis-hydrazone of glyoxal. For this fraction, evaporate to dryness, and dissolve the residue in aqueous 20% dimethylsulfoxide (6.00 ml). Add the alkali solution (1.00 ml) to this solution, and read the absorbance at 576 nm. Calculate the amounts of hydrazones from their molar absorptivities.

Periodate oxidation of glycosides

To a 10^{-2} *M* solution (5.00 ml) of a glycoside sample add 10^{-1} *M* sodium

metaperiodate (5.00 ml), and maintain the solution for the required time at 25°C in a thermostated water bath, shielded from light. Remove a 3.00-ml aliquot, deionize by passing through a column of a mixture of Amberlite IR-120 (H^+ form, 1 ml) and Amberlite IRA-410 (HCO_3^{2-} form, 1 ml), and evaporate to dryness. Redissolve the residual syrup in water, and adjust the volume to 10.0 ml. Evaporate a 0.50-ml aliquot of this solution to dryness, and subject the residual syrup to fragment analysis by the standard procedure described below.

Standard l.c. procedure for the simultaneous determination of glyoxal and hydroxyaldehydes in products of periodate oxidation

Dissolve in 1,2-dimethoxyethane (0.1 ml) the syrup which was obtained from the carbohydrate sample (50–250 μg) by oxidation, followed by deionization and evaporation. To this solution add 2,4-dinitrophenylhydrazine hydrochloride (1.2 mg), and keep the resultant solution at 25°C for 3 h. Evaporate the reaction solution to dryness, and dissolve the residue in chloroform (0.5 ml). Introduce the chloroform solution to a column (1.0 cm i.d., 10 cm long) of silica gel (Mallinckrodt Chemical Works; 5.0 g, activated by heating at 120°C for 10 min, followed by storage in a desiccator containing anhydrous silica gel) impregnated with chloroform, and elute the column with the following solvent systems in this order; chloroform (60 ml), 20:1 chloroform–methanol (40 ml), 10:1 chloroform–methanol (80 ml). Collect the fractions as follows: the excess of 2,4-dinitrophenylhydrazine hydrochloride, 16–21 ml; glyoxal bis-2,4-dinitrophenylhydrazone, 27–35 ml; glycolaldehyde 2,4-dinitrophenylhydrazone, 37–47 ml; triose 2,4-dinitrophenylhydrazone, 74–91 ml; pentose 2,4-dinitrophenylhydrazone, 108–123 ml; hexose 2,4-dinitrophenylhydrazone, 143–162 ml. Dilute each fraction with methanol to 25.0 ml, and read the absorbances at the absorption maxima, except for the glyoxal fraction. Evaporate a 3.00-ml aliquot of the solution from the glyoxal fraction to dryness, and dissolve the residue in aqueous 20% dimethylsulfoxide solution (6.00 ml). Add the alkali solution (1.00 ml) to this solution, and read the absorbance at 576 nm. Calculate the amount of each aldehyde from the molar absorptivity of its hydrazone.

RESULTS AND DISCUSSION

1,2-Dimethoxyethane was employed as the reaction solvent for the formation of the hydrazones from the aldehydes, instead of dimethylsulfoxide which had been used in the selective determination of glyoxal[4], because the latter caused heavy tailing of t.l.c. spots. On standing for 3 h in the solution of the hydrazine hydrochloride, the aldehydes in the conjugates were converted quantitatively and directly to the corresponding hydrazones; no intermediate procedure to liberate the aldehydes by acid hydrolysis was needed. Since the dissociation of the conjugates to their component aldehydes is an equilibrium process, the removal of the aldehydes by conversion to their hydrazones probably facilitates the dissociation process. Under the conditions used, osazone formation was not observed, hydrazones being the only products in all cases.

T.l.c. studies were performed under various conditions with standardized pre-coated silica gel plates. Artificial mixtures of 2,4-dinitrophenylhydrazones of the aldehydes possibly formed from glycosides including oligo- and poly-saccharides,

were well separated by double development with 10:1, followed by 5:1 chloroform–methanol. The only exception was that the zone of the bis-hydrazone of glyoxal the fastest moving derivative, was superimposed on that of the hydrazine reagent Zones were extracted with ethanol, and individual hydrazones were determined from their absorbances at the absorption maxima, except for the bis-hydrazone o glyoxal. This particular hydrazone was converted to its ionized form by addin alkali. The absorption maximum was shifted bathochromically, so that this hydrazon could be determined without interference from the contaminating hydrazine reagent. Table I summarizes the mobilities and the optical data of these hydrazones, and give the recoveries of individual hydrazones from their equimolar mixtures; good re coveries with high reproducibilities were obtained.

TABLE I

T.L.C. SEPARATION OF EQUIMOLAR MIXTURES OF 2,4-DINITROPHENYLHYDRAZONE

Aldehyde	R_F *values*		λ_{max} *(nm)*	ε_{max} *(·10³)*	*Av. recovery*[c] *(%)*	*s*
	Solvent A[a]	*Solvent B*[b]				
Glyoxal	0.69	0.80	438 (576)[d]	40.2 (65.5)[d]	99.6	0.97
Glycolaldehyde	0.54	0.72	355	19.5	99.9	0.55
D-Glyceraldehyde	0.34	0.56	353	19.3	101	0.63
D-Erythrose	0.20	0.42	354	18.9	98.5	0.41
D-Arabinose	0.11	0.30	353	20.0	98.7	0.62
D-Glucose	0.04	0.16	345	16.2	101	0.71

[a] Solvent A, 10:1 chloroform–methanol.
[b] Solvent B, 5:1 chloroform–methanol.
[c] 5 Determinations were done for each aldehyde.
[d] After addition of alkali solution.

TABLE II
T.L.C. AND L.C. DETERMINATION OF COMPONENT ALDEHYDES IN MODEL DIALDEHYDE COMPOUNDS

(5 determinations were done for each dialdehyde sample.)

Dialdehyde	*Component aldehyde*	*Amounts of dialdehyde added (μ mole)*	*Amount of aldehyde (μmole)*			*Standard deviation (·10⁻²)*	
			Theor.	*Found t.l.c.*	*Found l.c.*	*T.l.c.*	*L.c.*
I	Glyoxal	0.55	0.55	0.55	0.56	0.79	0.82
	D-glyceraldehyde	0.55	0.55	0.55	0.56	0.32	0.55
II	Glyoxal	0.55	0.55	0.55	0.56	0.71	0.13
	D-glyceraldehyde	0.55	0.55	0.55	0.56	0.39	0.10
III	Glyoxal	0.79	0.79	0.79	0.78	1.1	0.78
	D-erythrose	0.79	0.79	0.79	0.77	1.4	0.35
IV	Glyoxal	0.79	0.79	0.77	0.76	0.73	1.3
	D-erythrose	0.79	0.79	0.77	0.77	1.2	2.3

TABLE III

L.C. DETERMINATION OF ALDEHYDES FORMED FROM SELECTED GLYCOSIDES

Glycoside	*Aldehyde formed*	*Amount formed (mole/mole of glycoside)*[a]		*Molar proportion formed*[a]		*Periodate consumption (mole/mole of glycoside)*		
		Found		*Found*		*Theor.*	*Found*	
		3 h	*24 h*	*3 h*	*24 h*		*3 h*	*24 h*
Methyl α-D-glucopyranoside	Glyoxal	0.98	0.95	1	1	2	2.03	2.16
	D-glyceraldehyde	0.97	0.93	0.99	0.98			
Methyl β-D-glucopyranoside	Glyoxal	0.98	0.97	1	1	2	1.95	2.12
	D-glyceraldehyde	0.96	0.96	0.98	0.99			
Methyl 4,6-O-benzylidene-α-D-glucopyranoside	Glyoxal	0.31	1.01	1	1	1	0.32	1.03
	D-erythrose	0.29	0.99	0.94	0.98			
Methyl 4,6-O-benzylidene-β-D-glucopyranoside	Glyoxal	0.30	0.99	1	1	1	0.30	0.99
	D-erythrose	0.30	0.97	1.00	0.98			

[a] The theoretical value is 1 in all cases.

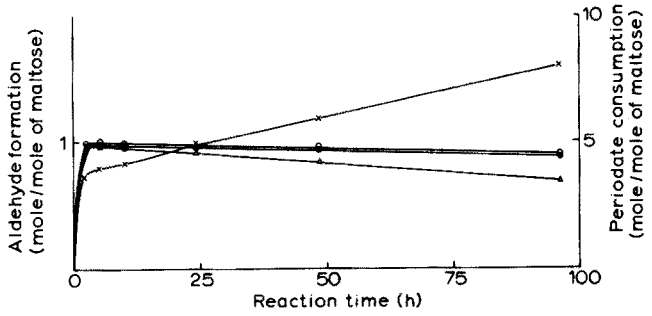

Fig. 1. Periodate oxidation of maltose. Concentration of maltose, $5 \cdot 10^{-3}$ *M*; initial concentration of sodium metaperiodate, $5 \cdot 10^{-2}$ *M*; reaction temperature, 25°C. (×) Periodate consumption. (○) Glyoxal formation. (●) D-Glyceraldehyde formation. (△) D-Erythrose formation.

The aldehydes in the model dialdehyde compounds I–IV were determined by the proposed method; the results are given in Table II. The dialdehydes I and II which were prepared from anomeric methyl D-glucopyranosides by periodate oxidation, should form glyoxal and D-glyceraldehyde in equimolar proportions. Table II indicates that the amounts of both aldehydes found were in good agreement with the theoretical values. Similarly, glyoxal and D-erythrose which were formed from dialdehydes III and IV, prepared from the 4,6-O-benzylidene derivatives of anomeric methyl D-glucopyranosides, were accurately determined without interference from benzaldehyde. Separation of hydrazones was also performed by column chromatography, since this simplifies the determination by eliminating the extraction procedure in the t.l.c. method.

On the basis of the above results, the aldehydes formed from selected glycosides were determined by the open column method, and the results were correlated to their periodate consumption. As can be seen from Table III, the periodate consumption of methyl α-D-glucopyranoside reached the theoretical value of 2 moles per mole of the glycoside after 3 h. Thereafter it increased gradually to give a value of 2.16 after 24 h, because of slight over-oxidation. The course of oxidation of the β-anomer of this glycoside was similar to that of the α-anomer, but slightly slower. The amounts of glyoxal and D-glyceraldehyde formed were consistent with the periodate consumption, taking into account the slight degradation caused by over-oxidation. For the 4,6-O-benzylidine derivatives of the foregoing glycosides, the reaction was much slower than that of the parent glycosides, but the amounts of aldehydes (glyoxal and D-erythrose) accorded well with the periodate consumption. It should be noted that the molar proportions of these aldehydes were approximately 1:1 without regard to the species and the reaction times.

Figure 1 shows the course of the oxidation of maltose. This 1,4-linked glucobiose should produce glyoxal and D-glyceraldehyde from its non-reducing moiety, all in equimolar proportions. Up to 5 h, the molar proportion of these aldehydes remained at this theoretical value, but the amount of D-erythrose decreased thereafter to reach 68% of the theoretical amount after 96 h, presumably because of the hydrolysis of the formyl ester, followed by over-oxidation of the resultant D-erythrose derivative. The amounts of glyoxal and D-glyceraldehyde

also decreased, but the decrease was slower, and the proportion remained approximately 1:1. The amount of periodate consumed within 24 h supported this reasoning about over-oxidation. However, the rise in the periodate consumption curve after this reaction time exceeded that expected from the drop of the curves for aldehyde formation. Unexpected non-Malaprade oxidation should be taken into account when such reactions proceed for many hours.

Thus, the simultaneous determination of glyoxal and hydroxyaldehydes in dialdehyde fragments provides more reliable information concerning the linkages of carbohydrates, as well as the mode and the degree of over-oxidation, than that obtained from the classical method based on the periodate consumption alone. It is worthy of special mention that the absolute amounts of samples need not be known, since this analysis is based on comparison of the amounts of aldehydes formed. Although there is some similar work on the simultaneous determination of oxidation fragments by gas chromatography, which is based on the Smith degradation of carbohydrates, followed by oximation and trimethylsilylation of products, the present method is preferable to this gas chromatographic analysis, because of its simplicity and accuracy.

SUMMARY

A method for the simultaneous determination of aldehydes in dialdehyde fragments, obtained from carbohydrate samples by periodate oxidation, is proposed. Reaction mixtures obtained from the periodate oxidation of carbohydrate samples are deionized by resins, and evaporated to dryness. The syrupy residues are treated with 2,4-dinitrophenylhydrazine hydrochloride in 1,2-dimethoxyethane at 25°C for 3 h. The resultant mixtures of hydrazones are separated by t.l.c. or l.c., and individual hydrazones are determined by spectrophotometric measurement. Reliable analyses of carbohydrate linkages are possible with 50–250-μg samples.

REFERENCES

1 M. Lambert and A. C. Neish, *Can. J. Res.*, 28B (1950) 83.
2 D. Aminoff and W. T. J. Morgan, *Biochem. J.*, 48 (1951) 74.
3 V. C. Barry, *Nature (London)*, 152 (1943) 537; V. C. Barry and P. W. D. Mitchell, *J. Chem. Soc. London*, (1954) 4020.
4 S. Honda, K. Kakehi, H. Yuki and K. Takiura, *Anal. Chim. Acta*, 1975.

Analytica Chimica Acta, 77 (1975) 133–143

SELECTIVE SEPARATIONS BY REACTIVE ION EXCHANGE

PART II. PRECONCENTRATION AND DETERMINATION OF COMPLEX IRON CYANIDES IN WATERS

GEORGE O. RAMSEYER and GILBERT E. JANAUER

Department of Chemistry, State University of New York at Binghamton, N.Y. 13901 (U.S.A.)

(Received 20th December 1974)

Complex iron cyanides, $Fe(CN)_6^{3-}$ and $Fe(CN)_6^{4-}$, are listed as inorganic pollutants in fresh water by the Environmental Protection Agency[1]. When irradiated by ultraviolet energy[2–5], these complexes dissociate, and the cyanide radical is released.

Burdick and Lipschuetz[6], Doudoroff *et al.*[7], and Broderius[8] have shown that a few p.p.m. of complex cyanides are toxic to various species of fish. New York State has established 400 p.p.b. as the total amount of hexacyanoferrate(II) and (III) permissible in fresh water, and Terhaar *et al.*[9] have confirmed this as a realistic standard.

The methods applicable for determining hexacyanoferrate(II) and (III) fall into two groups, those which determine "total cyanide" and those which determine the complex cyanide ions. The method advocated in Standard Methods[10] for "total cyanide" analysis does not include all of the cyanide complexed to iron[11]. Modifications made by Elly[11] and advocated by the E.P.A.[12] have increased the percentage of cyanide determined from various complex cyanides, although percent recoveries vary with the initial concentration of complex cyanides. Goulden *et al*[13] have used u.v. irradiation to dissociate complex cyanides and determine "total cyanide", but thiocyanate interferes. Casapieri *et al.*[14] have employed an auto-analyzer to determine total cyanide, although recoveries from complex iron cyanides were only about 5%. Goulden *et al.*[13] have also used u.v. irradiation in a total cyanide-determining automatic system, while Royer *et al.*[15] have developed an automatic colorimetric method, both of which achieve nearly 100% yields in complex iron cyanide determinations. While these methods do meet the criteria for total cyanide, they do not really meet the requirements of the New York State law, which requires specifically the total amount of hexacyanoferrate(II) and (III), because "simple cyanide" and cyanide from complexes with metals such as cobalt and nickel will interfere.

Methods suitable for iron cyanide determinations fall into three categories, those that determine hexacyanoferrate(II)[16–23], hexacyanoferrate(III)[24–29], and both[30–34]. Roberts and Wilson[21] have reported the spectrophotometric determination of hexacyanoferrate(II) at p.p.b. concentrations in a sodium chloride matrix. This method presumably gives the total amount of hexacyanoferrate(II) and (III),

although no data are reported for hexacyanoferrate(III). These authors use a precipitation–filtration method to preconcentrate the hexacyanoferrate(II) as Prussian blue. Similarly, Galik and Vopravilova[23] have extracted Prussian blue into chloroform. Because oxidizing and reducing agents can change the ratio of iron(II) to iron(III) ions reacting to form Prussian blue, the extent of formation may change, and less than quantitative yields may be obtained. Other suitable methods determine hexacyanoferrate(II) and/or hexacyanoferrate(III) at p.p.m. or p.p.t. levels, but not at p.p.b. levels.

Evaporation, extraction, precipitation, and ion exchange can be used to preconcentrate p.p.b. amounts of hexacyanoferrate(II) and (III). However, evaporation can lead to partial dissociation of the iron complexes, and extraction[23] suffers from many interferences. Organic anion exchangers have very high affinities for hexacyanoferrate(II) and (III), so that the elution of these complexes in a small volume of solution requires drastic measures. Burstall *et al.*[35] used various solvents and eluents in an attempt to elute iron cyanide, but found only sodium cyanide useful for quantitative elution. The use of 2 *M* sodium cyanide for elution as suggested by these authors creates two problems: first, eluting (according to their procedure) with 100 ml would require an initial sample volume of 10 l to be passed through a column in order to attain a preconcentration factor of 100; and secondly, 56,000 l of dilution water would be needed to reduce the ensuing concentration of cyanide in the effluent down to 100 p.p.b. for lawful fresh water disposal.

The use of precipitation as a means of preconcentration of hexacyanoferrate(II) has been shown to be effective[21], but involves a tedious filtration step at p.p.b. levels. Miller[16] has demonstrated that chemical reactions on a cation exchanger in the copper(II) or iron(III) form may be used to determine hexacyanoferrate(II) colorimetrically, but at concentration levels much higher than those encountered in the monitoring of fresh waters. Reactive ion exchange has been suggested as a general approach for trace preconcentration by Janauer *et al.*[36]. This paper describes the selective column precipitation/preconcentration of p.p.b. concentrations of these iron cyanides, and their separation from other contaminant species by reactive elution followed by a simple determination based on atomic absorption spectrometry.

EXPERIMENTAL

Equipment

A Beckman Expandomatic SS-2 pH Meter was used for all pH measurements. A regular Perkin-Elmer 303 atomic absorption spectrophotometer with a three-slot burner head was used for iron determinations. Sample absorbances were recorded with a Honeywell Electronix-194 Recorder.

Reagents, solutions, and glassware

The air-dried cation exchange resin AG50W-X4, 100–200 mesh, hydrogen form (Bio-Rad Laboratories) was used for most of the preconcentrations, although experiments were also carried out with X1, X8 and X12 resins of the same mesh size. Potassium hexacyanoferrate(II), potassium hexacyanoferrate(III), and all other reagents were prepared within one hour of use. The chloride salts of Ca(II), Mg(II), Zn(II), Mn(II), Ni(II), Co(II), Cd(II), Cr(III), Ba(II), and uranyl nitrate were used for bulk equilibrium experiments.

All dilutions, rinsing and other treatments were made with doubly distilled water, which was distilled the second time from an all-Pyrex still. All glassware was rinsed with 1 *M* nitric acid, five times with tap water, and then three times with doubly distilled water. Columns used in this work have been described earlier[37].

Procedures

Bulk equilibrations. Weighed quantities of air-dried cation-exchange resin (0.500 g of AG50W-X4(H^+)) were placed in 250-ml Erlenmeyer flasks and preswollen in 25 ml of water for 48 h. Then, 25 ml of a solution containing a three-fold amount (with respect to the resin capacity in meq) of the cations Ca(II), Mg(II), Mn(II), Ni(II), Zn(II), Co(II), Cd(II), Cr(III), Ba(II), and UO_2^{2+} were added to the Erlenmeyer flasks containing resin, in duplicate pairs. The pH of the solutions was adjusted to 4 with nitric acid and the flasks were shaken for 12 h. The ion-exchange resins were separated from the solutions on a medium-porosity glass fritted filter, washed three times with water to remove excess of unexchanged cations and returned to clean flasks with 100 ml of a solution containing 2 p.p.m. hexacyanoferrate(II) or (III). The flasks were again shaken for 12 h and then the concentration of hexacyanoferrate(II) or (III) left in the solution was determined by measuring the atomic absorption *versus* a blank prepared with the same resin in the hydrogen form. In cases where the results were of interest, the experiment was repeated, and the equilibration was carried out by shaking for 72 h before determinations.

Column preconcentrations. AG50W (H^+) resins of the desired cross-linkage (X1, X4, X8, or X12) were preswollen in water for 48 h. Resin slurries were poured into 0.7-cm diameter columns to make beds of 3.0-cm height, and a three-fold amount of copper(II) sulfate (with respect to total bed exchange capacity) was percolated through. The resin beds in the copper(II) form were washed with 100 ml of water. The appropriate "sample" solution (990 ml or 90 ml) was stirred with a magnetic stirrer and 10 ml of a hexacyanoferrate(II) and/or (III) solution were added. (When thiosulfate was used, 5 ml of hexacyanoferrate(II) and/or hexacyanoferrate(III) solution, plus 5 ml of $2 \cdot 10^{-3}$ *M* thiosulfate were added.) The pH was adjusted with a few drops of 1 *M* nitric acid, and the solution was poured into a 1-l separatory funnel. Suction was applied to the inverted separatory funnel in order to remove any dissolved gas. The funnel was wrapped in tin foil and placed in position for preconcentration[37]. Preconcentration was performed by passing through the column, at a flow rate of about 2 ml min^{-1}, the water "sample", usually between 100 and 2000 ml. After preconcentration (by *in situ* precipitation), the resin bed was washed with 10 ml of 1.5 *M* hydrochloric acid and the complex cyanide was eluted with 5 ml of aqueous 7.4 *M* ammonia into a 10-ml volumetric flask in the reversed flow direction, as described by Pankow and Janauer[37]. Copper, which had first been complexed with hexacyanoferrate(II) or (III) on the column, had by now been converted to the copper–ammine complex $Cu(NH_3)_4^{2+}$ during elution of the iron cyanide. Complete elution was effected with 5 ml of 1.5 *M* hydrochloric acid.

Determination of iron. Usually, 3-ml aliquots from the preconcentrate were pipetted into three 10-ml volumetric flasks. Then 3 ml of solution containing 0, 50, and 100% of the expected sample analyte concentration hexacyanoferrate(II) or (III) were added. A.a.s. signal recordings were measured and plotted for the purpose

of extrapolation. The iron content of hexacyanoferrate(II) or (III) solutions was determined with an oxidizing air–acetylene flame at 248.3 nm. Copper was determined by atomic absorption with an oxidizing air–acetylene flame at 324.7 nm (standard addition).

Suggested working procedure for 400 p.p.b. determinations. Dowex 50W-X4, 100–200 mesh (0.500 g slurried with water) is poured into columns having fritted discs at one end[37], and 50 ml of 0.1 *M* copper(II) sulfate solution are percolated through, followed by 100 ml of water. A plug of Pyrex wool filtering fibre is inserted on top of the bed in the column.

To 500 ml of sample are added 5 ml of freshly prepared 10^{-3} *M* thiosulfate, and the pH is adjusted to about 6.5 with 1 *M* nitric acid. The sample is poured into a separatory funnel, and preconcentration is carried out as described above. The precipitate forms just above the glass frit when ascending flow is used during "sorption". Elutions and analyses are performed as mentioned above.

RESULTS

Table I shows the results of bulk equilibrium experiments used to determine which cations (sorbed) on the typical sulfonate resin would react with measurable quantities of hexacyanoferrate(II) or (III) from solution in a period of 12 h or 72 h.

TABLE I

BULK EQUILIBRIUM CONCENTRATIONS OF $Fe(CN)_6^{3-}$ AND $Fe(CN)_6^{4-}$ FOUND IN SOLUTION FROM ORIGINAL 2 p.p.m. SOLUTIONS

(Average of three trials each.)

Cation	*Hexacyanoferrate(II) (p.p.m)*		*Hexacyanoferrate(III) (p.p.m.)*	
	12 h	*72 h*	*12 h*	*72 h*
Mg^{2+}	2.0	1.9	2.0	2.0
Ca^{2+}	2.0	1.9	2.0	2.0
Ba^{2+}	2.0		2.0	
Cr^{3+}	2.0		2.0	
Mn^{2+}	1.9		2.0	
Co^{2+}	1.7		1.9	
Ni^{2+}	1.7		2.0	
Cu^{2+}	1.1	0.7	1.8	0.5
Zn^{2+}	1.1	1.1	2.0	2.0
Cd^{2-}	2.0		2.0	
UO_2^{2+}	2.0		2.0	
H^+	2.0	2.0	2.0	2.0

Table II lists typical absorbances obtained (atomic absorption) for p.p.m. concentrations of hexacyanoferrate(II) and (III) in aqueous 3.7 *M* ammonia. Absorbances *versus* concentration of aqueous ammonia for 10 p.p.m. hexacyanoferrate(II) are given in Table III.

A series of experiments showed that in doubly distilled water at pH values

TABLE II

ABSORBANCE AGAINST CONCENTRATION OF $Fe(CN)_6^{3-}$ AND $Fe(CN)_6^{4-}$ IN AQUEOUS 3.7 *M* AMMONIA BY A.A.S.

Concentration (p.p.m.) of $Fe(CN)_6$	*Absorbance*	
	$Fe(CN)_6^{3-}$	$Fe(CN)_6^{4-}$
0	0	0
5	0.0168	0.0205
10	0.0329	0.0391
20	0.0711	0.0891
30	0.1085	0.1169
40	0.1439	0.1524
50	0.1746	0.1884

TABLE III

ABSORBANCE OF IRON IN $Fe(CN)_6^{4-}$ AGAINST THE CONCENTRATION OF AQUEOUS AMMONIA BY A.A.S.

$[NH_3]$ *(M)*	*Absorbance*	$[NH_3]$ *(M)*	*Absorbance*
0	0.0747	4.4	0.0757
1.5	0.0761	5.9	0.0751
2.4	0.0763	7.4	0.0752
3.0	0.0769	10.7	0.0736
3.8	0.0777		

3.0–9.0, 90% or more of the hexacyanoferrate(II) and (III) could be preconcentrated and determined. In another series of experiments with AG50W-X1, -X4, -X8, and -X12 of 100–200 mesh, similar results were obtained for all resins except for AG50W-X1. In the latter case, the flow rate was exceedingly slow, and the experiment was discontinued. Since preliminary work had been done with AG50W-X4, and the -X8, and -X12 resins offered no apparent advantage over the -X4 resin, the -X4 resin was used in all subsequent work.

Results given in Table IV were obtained in a number of preconcentrations for hexacyanoferrate(II) and/or (III) in doubly distilled water, in Binghamton Tap Water (BTW), in Susquehanna River Water (SRW), Endicott, N.Y., and in a synthetic Hard River Water (HRW) matrix (Table V). The ratio of analytically determined concentrations of hexacyanoferrate(II) and (III) in doubly distilled water as a function of the concentration of eluted copper (after conversion into copper–ammine complex during ammoniacal elution of cyanides) is given in Table VI.

DISCUSSION

The formation of slightly soluble precipitates in conjunction with ion exchangers has previously been exploited. Brochmann-Hanssen[38] was the first to use ion exchangers to dissolve slightly soluble salts, adsorbing the cations of the salt

TABLE IV

COLUMN PRECONCENTRATIONS AND DETERMINATIONS OF $Fe(CN)_6^{3-}$ AND/OR $Fe(CN)_6^{4-}$ IN VARIOUS WATER MATRICES

Sample[a]					*Precon-centration factor*	*Found (p.p.b.)*	*No. of trials*	*s (p.p.b.)*	s_r (%)	CL_{90} (%)	CL_{95} (%)
	$Fe(CN)_6^{4-}$ added (p.p.b.)	*$Fe(CN)_6^{3-}$ added (p.p.b.)*	*Vol. (ml)*	*Matrix*[b]							
1	100	—	1000	DDW	100	93	3	2.6	2.8	4.8	7.0
2	40	—	1000	BTW	100	36	4	1.3	3.6	4.3	5.7
3	100	—	1000	BTW	100	99	6	3.9	3.9	3.2	4.0
4	—	100	1000	DDW	100	89	3	2.5	2.9	4.8	7.2
5	—	100	1000	BTW	100	93	3	1.7	1.9	3.2	4.7
6	—	100	1000	DDW	100	91	3	1.0	1.1	1.9	2.8
7	—	100	1000	BTW	100	101	3	2.6	2.6	4.5	6.5
8	5	5	1000	BTW	100	9	4	1.3	14.4	17.3	23
9	50	50	1000	BTW	100	99	3	1.3	1.3	2.2	3.3
10	500	500	1000	BTW	100	1060	3	22	2.2	3.7	5.5
11	50	50	100	HRW	10	90	3	7.0	7.8	13.3	19.5
12	500	500	100	HRW	10	930	3	20	2.2	3.6	5.5
13	10	—	1000	SRW	100	17	5	2.8	16.4	15.6	20.3
14	100	—	1000	SRW	100	93	5	9.1	9.8	9.3	12.1
15	1000	—	1000	SRW	40	1030	5	45	4.4	4.2	5.5

[a] Samples 6–12 were 10^{-5} *M* in $S_2O_3^{2-}$.

[b] DDW = doubly distilled water. For other abbreviations, see Table V.

TABLE V

IONIC COMPOSITION OF WATER MATRICES USED

	Binghamton Tap Water (BTW)	*Susquehanna River Water (SRW)*	*Synthetic Hard River Water (HRW)*
Ca^{2+}	18 p.p.m.	24 p.p.m.	200 p.p.m.
Mg^{2+}	2 p.p.m.	4 p.p.m.	50 p.p.m.
Na^{+}	6 p.p.m.	—	100 p.p.m.
Ni^{2+}	41 p.p.m.	—	—
Cu^{2+}	19 p.p.b.	19 p.p.b.	—
Zn^{2+}	24 p.p.b.	15 p.p.b.	—
Fe^{3+}	—	50 p.p.b.	1 p.p.m.

LE VI

IO OF MOLES OF COPPER AMMINE COMPLEX TO MOLES OF ELUTED $Fe(CN)_6^{4-}$ AND $CN)_6^{3-}$

ained in representative experiments)

$CN)_6^{4-}]$	$[Cu^{2+}]$	$[Cu^{2+}]/[Fe(CN)_6^{4-}]$	$[Fe(CN)_6^{3-}]$	$[Cu^{2+}]$	$[Cu^{2+}]/[Fe(CN)_6^{3-}]$
$\cdot 10^{-5}$	$2.07 \cdot 10^{-5}$	1.88	$1.11 \cdot 10^{-5}$	$1.58 \cdot 10^{-5}$	1.42
$\cdot 10^{-5}$	$2.08 \cdot 10^{-5}$	1.89	$1.05 \cdot 10^{-5}$	$1.46 \cdot 10^{-5}$	1.39
$\cdot 10^{-5}$	$2.06 \cdot 10^{-5}$	1.86	$1.07 \cdot 10^{-5}$	$1.46 \cdot 10^{-5}$	1.36

on a cation-exchange resin, and thus pushing the dissociation equilibrium of the salt towards dissociation. Rich[39] extended this principle to other slightly soluble precipitates, and Segall and Schmuckler[40] studied the dissolution of sparingly soluble salts by ion exchange. Bunzl[41] has investigated quantitatively and in rigorous detail the kinetics and equilibrium of this type of reaction. Yamatera[42] used the perchlorate ion to promote the elution of cesium ion from a cation-exchange column (cesium perchlorate is a sparingly soluble salt). Lee and Lee[43] extended this principle to the elution of a series of salicylic acid derivatives. Morrison *et al.*[44,45] used the formation of precipitates to elute nonselectively a number of matrix cations after total sorption on a cation-exchange column. Miller[16] studied ionic reactions of various metal species with ion-exchange resins and suggested these for applications in various colorimetric determinations. Among the reactions listed by Miller was the formation of copper hexacyanoferrate(II), which suggested the possibility for a new preconcentration and analytical method to solve the problem of monitoring complex cyanides in natural waters.

The results of the equilibrium bulk experiments (Table I) indicated that a standard resin in the copper(II) form would produce the most favorable preconcentration of the complex iron cyanides from the water matrix. A one-step bulk ion-exchange process is similar to a one-step extraction, while a column ion-exchange process is similar to a multi-step extraction. The combination of selective precipitation with ion exchange proved successful in the quantitative preconcentration of the complex cyanides at the p.p.b. level.

Since the concentration of ammonia affects the a.a.s. signal recorded for iron (present as hexacyanoferrate(II) (see Table III), the concentration of aqueous ammonia must be the same for standard solutions and samples being determined. Ammonia forms the copper–ammine complex, and the concentration of ammonia in the eluate is, therefore, a function of the amount of hexacyanoferrate(II) and/or (III) preconcentrated. Also, any H^+-form resin present is converted to the ammonium form, so that the ammonia concentration in the preconcentrate is reduced by the amount which has reacted with H^+-form resin in the column. For these reasons, and because of the potential coprecipitation of species which might interfere with the a.a.s. determination, the use of standard additions is preferable to the use of a single calibration curve. When a Beer's law calibration curve was constructed for both hexacyanoferrate(II) and (III) in 3.7 *M* ammonia, it was almost linear up to 25 p.p.m. for each of the two species. However, the hexacyanoferrate(III) absorbance was about 10% less than that of hexacyanoferrate(II) (Table II). Because iron as hexacyanoferrate(II) has a higher apparent molar absorptivity than iron as hexacyanoferrate(III), the latter was always reduced. This can be done either before or after preconcentration. Preliminary experiments with several reducing agents showed that both ascorbic acid and thiosulphate gave fast, quantitative reduction. Thiosulphate was chosen for further work.

The yields of preconcentrated hexacyanoferrate(II) and/or (III) were little affected by pH—the pH range 3–9 was satisfactory in distilled water and 6–7 was satisfactory in river water—and were generally in the range of 90–105%. Results of less than 100% might be caused by the loss of small amounts of copper hexacyanoferrate(II) (or copper hexacyanoferrate(III)) present at the outer surfaces of the precipitate, and which may be lost (by peptization or mechanical washing out) when the resin bed swells on addition of 1.5 *M* hydrochloric acid (conversion of $\overline{Cu^{2+}} \rightarrow \overline{H^+}$). Samples which were preconcentrated from a distilled water matrix have generally shown a slightly lower yield than those from various river water matrices.

Another factor which may cause lower than 100% yields may be inherent in the method in which the respective precipitates are formed. Beasley *et al.*[46] have described the composition of freshly precipitated copper(II) hexacyanoferrate(II) gel, and have noted that the particle size of this gel increases from an initial size of about 10 Å to macro crystallites in about 10 min. Thus, minute quantities of the precipitate may be washed from the column initially before crystallization equilibrium has been reached.

In a river water matrix, calcium(II) and magnesium(II) displace some copper(II) from the ion-exchange resin bed. If the only cation present in the river water were calcium(II), 1 l of water 49 p.p.m. in calcium(II) could theoretically just displace all of the copper(II) from the column. To prevent the complete displacement of copper from the bed by these divalent cations in sample solutions containing higher concentrations of divalent cations, either the standard resin bed could be enlarged, or samples of less than 1 l of water could be used. Since a major potential application of this work is at and around the 400 p.p.b. maximum permissible level of hexacyanoferrate(II) and (III) in fresh waters of New York State, preconcentration factors of only 10 are needed for conventional atomic absorption determinations, and it is possible to reduce the sample volume to 100 ml. However. increased

reliability can be obtained by using a larger sample, and 500 ml of sample is recommended. Thus, if the calcium(II) concentration is $\geqq 100$ p.p.m., it is recommended that a larger resin bed be used.

The overall reaction sequences indicated below account for the observed preconcentration and separation of hexacyanoferrate(II) and (III).

(A) $2\,\overline{H}^+ + Cu^{2+} \rightarrow \overline{Cu}^{2+} + 2\,H^+$

(B) $2\,\overline{Cu}^{2+} + Fe(CN)_6^{4-} \rightarrow Cu_2[Fe(CN)_6]\downarrow$ or $3\,Cu^{2+} + 2[Fe(CN)_6^{3-}] \rightarrow Cu_3[Fe(CN)_6]_2\downarrow$

(C) $\overline{Cu}^{2+}(\text{excess}) + 4\,HCl \rightarrow CuCl_4^{2-} + 2\,\overline{H}^+ + 2\,H^+$

(D) $Cu_2[Fe(CN)_6]\downarrow + 12\,NH_3 + 8\,\overline{H}^+ \rightarrow 2[\overline{Cu(NH_3)_4^{2+}}] + Fe(CN)_6^{4-} + 4\,\overline{NH}_4^+ + 4\,H^+$ or $\overline{Cu_3[Fe(CN)_6]_2}\downarrow + 18\,NH_3 + 12\,\overline{H}^+ \rightarrow 3[\overline{Cu(NH_3)_4^{2+}}] + 2\,Fe(CN)_6^{3-} + 6\,NH_4^+ + 6\,\overline{H}^+$

(E) $\overline{Cu(NH_3)_4^{2+}} + 4\,HCl \rightarrow CuCl_4^{2-} + 2\,\overline{NH}_4^+ + 2\,NH_4^+$

Hexacyanoferrate(II) is precipitated by copper(II), producing a reddish brown precipitate, while hexacyanoferrate(III) produces a yellowish-green precipitate, both of which appear to be similar to the corresponding precipitates formed in solution. Neither precipitate caused clogging of the column, and flow rates remained nearly constant throughout preconcentration procedures.

Excess of copper is eluted by the formation of chlorocuprate anions, mainly $CuCl_4^{2-}$, with hydrochloric acid. Aqueous ammonia redissolves the copper hexacyanoferrate(II) (or III) precipitate with the formation of the copper–ammine complex, which is retained by the resin as a counter-ion while the hexacyanoferrate(II) (or III) is eluted. It is important for the practical applicability of the procedure that contaminant iron species, which may even be present as colloids (retained by the matrix of the exchanger), will be eluted from the column with hydrochloric acid, as will iron(III) or iron(II) species which may be adsorbed on the resin. Thus, hexacyanoferrate(II) is separated from any other iron species, and atomic absorption spectrometry will detect solely iron from the cyanide complexes.

Ratios of copper to eluted hexacyanoferrate(II) or hexacyanoferrate(III) were found to be less than the theoretical ratio of 2:1 or 3:2 (suggested by the reaction sequences). The smaller ratios found experimentally may be caused by partial inclusion of potassium(I) into the crystals, as described for hexacyanoferrate(II) by Bellomo[47] in the formation of $K_2Cu_3[Fe(CN)_6]_2$, and by Bellomo *et al.*[48] for hexacyanoferrate(III) in the formation of $KCu_{10}[Fe(CN)_6]_7$.

In common ion-exchange column procedures, the resin is washed with solvent between different elution steps. However, this produced alternating swelling and shrinkage of the resin bed, with the undesirable result that some of the copper hexacyanoferrate(II) precipitate was mechanically washed down and out of the resin column. Phenomena which are characteristic of normal precipitation processes (in the absence of resin) are super-saturation and peptization. It was found that at *high* flow rates, the first few ml of solution containing $\geqslant 5$ p.p.m. of iron cyanide (s) can pass through the $\overline{Cu}^{2+}$ resin bed unreacted. This suggests that initial nucleation or growth may be slow, or that small aggregates are peptized. However, in the practical case, *i.e.* at the p.p.b. level of complex cyanides with reasonable flow rates, this effect is not significant.

Because of its high affinity for the copper(II) ion compared to other divalent ions, the use of Chelex-100 for preconcentrating hexacyanoferrate(II) and (III) as

copper(II) complexes appeared to offer a possibility of overcoming the disadvantages of the elution of copper(II) from the regular sulfonated resin by contaminant cations. Initial column experiments with Chelex-100 confirmed that this was indeed the case, and hexacyanoferrate(II) and (III) were successfully preconcentrated as their respective copper(II) precipitates. However, satisfactory elution was not achieved because of too high a degree of swelling of the resin bed during attempted elutions with 1.5 *M* hydrochloric acid; 10 ml of this solution required nearly 24 h to pass through the resin bed, making the method impractical. It is possible that in a bulk equilibrium sorption procedure with certain modifications, this resin, in the copper-(II) form, could provide an effective means of removing low p.p.m. concentrations of hexacyanoferrate(II) and/or (III) from photographic processing and electroplating wastes.

CONCLUSIONS

The new application of reactive ion exchange described permits preconcentration of p.p.b. levels of hexacyanoferrate(II) and (III) from aqueous solutions with high efficiency and minimal cost and effort. The methodological problem posed by the New York State law requiring that these species be monitored at concentration levels around (and preferably much below) 400 p.p.b. in fresh waters has been solved.

The potential uses of the general technique in trace analysis for the efficient preconcentration of other toxic, valuable, or interesting species along with separations from interferences for superior analytical determinations seems limited only by the ability to find practical combinations or sequences of ion exchange and chemical reactions.

SUMMARY

Reactive ion exchange has been applied to the determination of p.p.b. concentrations of hexacyanoferrate(II) and hexacyanoferrate(III) in various water matrices. The *in situ* precipitation of copper hexacyanoferrate(II) or hexacyanoferrate(III) preconcentrates the complex cyanides on shallow beds of sulfonated cation-exchange resin in the copper(II) form. Hydrochloric acid reactively elutes other cations including concomitant iron species from the resin bed and, finally, aqueous ammonia reactively releases and elutes the hexacyanoferrate(II) (or III) species through the formation of the copper–ammine complex. Preconcentration factors of 100 or more are possible when 1-l samples are used. Final determination of the complex cyanides is performed by atomic absorption spectrometry (for iron).

REFERENCES

1 *Water Quality Criteria Data Book, Vol. 2*, Environmental Pollution Agency, Washington, D.C., 1971, p. 13.
2 R. P. Mitra, D. V. S. Jain, A. K. Bannerjee and K. V. Raghavachari, *Nature (London)*, 200 (1963) 163.
3 F. S. Dainton and P. L. Airey, *Nature (London)*, 207 (1965) 1190.
4 S. Ohno and G. Tsuchihashi, *Bull. Chem. Soc. Jap.*, 38 (1965) 1052.

5 L. Moggi, F. Bolletta, V. Balzani and F. Scandola, *J. Inorg. Nucl. Chem.*, 28 (1966) 2589.
6 G. E. Burdick and M. Lipschuetz, *Trans. Amer. Fish. Soc.*, 78 (1950) 192.
7 P. Duodoroff, G. Leduc and C. R. Schneider, *Trans. Amer. Fish. Soc.*, 95 (1966) 6.
8 S. Broderius, Dissertation, Oregon State University, 1973.
9 C. J. Terhaar, W. S. Ewell, S. P. Dziuba and D. W. Fassett, *Photogr. Sci. Eng.*, 16 (1972) 370.
10 *Standard Methods for the Examination of Water and Wastewater*, American Public Health Association, New York, 13th edn., 1971, pp. 397–406.
11 C. T. Elly, *J. Water Pollut. Contr. Fed.*, 40 (1968) 848.
12 *Methods for Chemical Analysis of Water and Wastes*, Environmental Protection Agency, Washington, D.C., 1971, pp. 41–52.
13 P. D. Goulden, B. K. Afghan and P. Brooksbank, *Anal. Chem.*, 44 (1972) 1845.
14 P. Casapieri, R. Scott and E. A. Simpson, *Anal. Chim. Acta*, 49 (1970) 188.
15 J. L. Royer, J. E. Twichell and S. M. Muir, *Anal. Lett.*, 6 (1973) 619.
16 W. E. Miller, *Anal. Chem.*, 29 (1957) 1891.
17 J. R. Marier and D. S. Clark, *Analyst (London)*, 85 (1960) 574.
18 W. U. Malik and M. Ajmal, *Anal. Chem.*, 34 (1962) 207.
19 M. R. F. Ashworth, H. Gottell and J. Schneider, *Anal. Chim. Acta*, 31 (1964) 17.
20 P. S. Dubey and K. N. Tandon, *Talanta*, 13 (1966) 765.
21 R. F. Roberts and R. H. Wilson, *Analyst (London)*, 93 (1968) 237.
22 D. K. Kidby, *Anal. Biochem.*, 28 (1969) 230.
23 A. Galik and J. Vopravilova, *Talanta*, 21 (1974) 307.
24 F. Burriel-Marti, F. Lucena-Conde and S. Arribas-Jimeno, *Anal. Chim. Acta*, 10 (1954) 301.
25 F. Lucena-Conde and J. S. Bellido, *Talanta*, 1 (1958) 305.
26 H. D. Drew and J. M. Fitzgerald, *Anal. Chem.*, 38 (1966) 778.
27 S. M. A. Alich, D. T. Haworth and S. M. F. Johnson, *J. Inorg. Nucl. Chem.*, 29 (1967) 1637.
28 J. T. Stock and R. J. Merrer, *Analyst (London)*, 92 (1967) 98.
29 R. J. Merrer and J. T. Stock, *Anal. Chim. Acta*, 53 (1971) 233.
30 G. Farsang and L. Toncsangi, *J. Electroanal. Chem. Interfacial Electrochem.*, 13 (1967) 73.
31 P. Luis, C. N. Carducci and A. Sa, *Mikrochim. Acta*, (1969) 7.
32 D. M. Drew, *Anal. Chem.*, 45 (1973) 2423.
33 T. Todorova, T. Getcheva and B. Mandova, *Mikrochim. Acta*, (1974) 503.
34 S. K. Tobia, Y. A. Gawargious and M. F. El-Shahat, *Analyst (London)*, 99 (1974) 544.
35 F. H. Burstall, P. J. Forrest, N. F. Kember and R. A. Wells, *Ind. Eng. Chem.*, 45 (1953) 1649.
36 G. E. Janauer, G. O. Ramseyer and J. L. Wang, *Anal. Chim. Acta*, 73 (1974) 311.
37 J. Pankow and G. E. Janauer, *Anal. Chim. Acta*, 69 (1974) 97.
38 E. Brochmann-Hanssen, *J. Amer. Pharm. Ass.*, 43 (1954) 307.
39 R. Rich, *J. Chem. Educ.*, 40 (1963) 414.
40 E. Segall and G. Schmuckler, *Talanta*, 14 (1967) 1253.
41 K. Bunzl, *Z. Phys. Chem. Neue. Folge*, 75 (1971) 118.
42 H. Yamatera, *J. Inorg. Nucl. Chem.*, 7 (1958) 299.
43 K. S. Lee and D. W. Lee, *Anal. Chem.*, 46 (1974) 1903.
44 F. Tera, R. R. Ruch and G. H. Morrison, *Anal. Chem.*, 37 (1965) 358.
45 R. R. Ruch, F. Tera and G. H. Morrison, *Anal. Chem.*, 37 (1965) 1565.
46 M. L. Beasley and W. O. Milligan, *Trans. N.Y. Acad. Sci.*, 31 (1969) 261.
47 A. Bellomo, *Talanta*, 17 (1970) 1109.
48 A Bellomo, A. Casale and D. De Marco, *Talanta*, 20 (1973) 335.

Analytica Chimica Acta, 77 (1975) 145–152

CHELATING ION-EXCHANGERS CONTAINING N-SUBSTITUTED HYDROXYLAMINE FUNCTIONAL GROUPS

PART I. N-AROYLPHENYLHYDROXYLAMINES

F. VERNON and H. ECCLES

The Ramage Laboratories, Department of Chemistry and Applied Chemistry, University of Salford, Salford, M5 4WT, Lancs. (England)

(Received 21st November 1974)

N-Benzoyl-N-phenylhydroxylamine (BPHA) has found many applications in analysis since its preparation by Bamberger[1] and the first exploratory work by Shome[2]. An excellent account of the preparations and widespread analytical uses of BPHA and its analogues has been given recently by Majumdar[3].

Despite the obvious potential of a chelating ion-exchanger containing BPHA units as the functional groups, the preparation of such an exchange resin has not been described in the literature. Cornaz *et al.*[4,5] and Petrie *et al.*[6] have briefly described the preparation and chelating properties of ion-exchangers containing the hydroxamic acid unit and noted the high selectivity for iron(III).

The difficulties in preparing a BPHA polymer are considerable; two approaches are described here and the chelating properties of the resulting polymers are discussed. The original approach was to take the method of synthesis described by Bamberger[1] and Shome[2], namely the reaction of benzoyl chloride with phenylhydroxylamine and apply it to two difunctional species, phenylenedihydroxylamine and terephthaloyl chloride. This reaction resulted in a linear BPHA polymer which was soluble in alkaline solution. The second synthetic method involved the production of a *p*-(bromomethyl)benzoylphenylhydroxylamine and its interaction with poly(ethyleneimine). The chelating properties of these polymers with iron, cobalt, copper, vanadium and uranium and the effect on the resin capacity of a competing ligand in solution are described in this paper.

EXPERIMENTAL

Preparation of polymer 1

m-Dinitrobenzene was crystallized from ethanol and recrystallized from aqueous acetone; 0.15 mole was dissolved in 200 ml of ether and added to 300 ml of 10% (w/v) ammonium chloride solution. With cooling in ice and continuous stirring, 0.67 mole of Analar zinc dust was added slowly, the temperature being maintained below 20 °C. The mixture was stirred for a further 30 min after the addition of zinc was completed, the zinc oxide was then removed by filtration, and the aqueous and ether layers were separated. Sodium hydrogencarbonate (0.35 mole) was added to the aqueous layer in preparation for the addition of the

acid chloride. Terephthaloyl chloride was prepared by the method of Rose[7] from terephthalic acid and phosphorus pentachloride; the product was crystallized from petroleum ether.

Dioxane (300 ml) was added to the above aqueous solution of *m*-phenylenedihydroxylamine and sodium hydrogencarbonate, and 0.15 mole of terephthaloyl chloride in dioxane was added dropwise to the hydroxylamine solution with vigorous stirring. A brown solid deposited on standing; this was filtered, washed with water, and then stirred with dilute sodium hydrogencarbonate solution overnight (the hydrogencarbonate solution acquired a yellow coloration during this period). The brown polymer was filtered, and washed with water, 1 *M* sulphuric acid, and finally with water until sulphate-free. A small sample of the polymer was dissolved in 0.88 ammonia liquor, reprecipitated by 2 *M* sulphuric acid, filtered, washed and dried in vacuum over phosphorus pentoxide. Elemental analysis gave: 59.0% C, 3.8% H, 10.67% N; expected: 62.2%C, 3.7%H, 10.37% N).

The polymer was insoluble in benzene, chloroform, carbon tetrachloride, acetone and ethanol but was completely soluble in dimethylformamide. Solubilities in aqueous acids and bases were determined; the polymer was completely soluble above pH 9 and appreciably soluble in sulphuric acid solutions greater than 5 *M*. The solubility in 10 *M* sulphuric acid was 50% based on polymer dry weight.

Preparation of polymer 2

For the preparation of *p*-(bromomethyl)benzoyl chloride, 0.05 mole of *p*-toluic acid was dissolved in 300 ml of carbon tetrachloride. The solution was refluxed and irradiated with ultraviolet light whilst a solution of 0.05 mole of bromine in 50 ml of carbon tetrachloride was added over 1 h. After a further 30 min of reflux, the solution was allowed to cool, so that *p*-(bromomethyl)benzoic acid crystallized out. The product was recrystallized from acetone; 0.10 mole of the acid was refluxed with thionyl chloride for 6 h. Excess of thionyl chloride was removed by vacuum distillation and the product was crystallized from petroleum ether.

For the preparation of *p*-(bromomethyl)benzoylphenylhydroxylamine, 0.35 mole of the acid chloride was dissolved in 30 ml of dioxane and added dropwise to a stirred suspension of phenylhydroxylamine (0.35 mole) and sodium hydrogencarbonate (0.35 mole) in 100 ml of dioxane over a period of 40 min. The solution was diluted with 300 ml of ice–water, and the product precipitated as a yellow solid which was crystallized from aqueous ethanol (m.p. 140 °C). Elemental analysis gave 55.1% C, 4.0% H, 4.6% N, 25.8% Br; expected: 54.5% C, 3.9% H, 4.6% N, 26.1% Br).

The substituted BPHA product (0.04 mole), 0.02 mole of ethylene dibromide and 0.01 mole of 1,4-di(bromomethyl)benzene were mixed with 0.1 mole of polyethyleneimine and 3 ml of methanol to give a homogeneous mixture which was heated in a sealed container for 24 h at 90°C. The black, rubbery product was soaked in ethanol overnight, filtered and dried to a brittle, dark green polymer. The polymer was washed with 1 *M* sodium hydroxide, water, 1 *M* hydrochloric acid and water, after which the washing procedure, commencing with ethanol, was repeated to ensure complete removal of unreacted materials. The material was stored moist in the chloride form.

For the preparation of a polyethyleneimine blank, the above procedure was

repeated, with 0.04 mole of benzyl bromide replacing the chelating ligand. The yellow polymer produced was subjected to the same washing procedure as the chelating resin.

Water regain

Samples of the resins were allowed to stand in deionized water for 48 h. The resins were then filtered by suction and pressed between filter papers to remove surface moisture. Weighed amounts of the swollen resins were dried at 100 °C for 48 h to determine water regain values.

Resin capacity

In order to compare resin capacities rigorously at varying pH values, the following conditions were standardized.

Exactly 0.5 g of moist polymer sample was pre-equilibrated with 50 ml of 1 *M* sodium sulphate solution, the pH of which was adjusted to the required value with sulphuric acid or sodium hydroxide. The polymer was allowed to equilibrate with periodic adjustments of pH until a constant value over a 6-h period was obtained; the sodium sulphate solution was then removed by filtration.

The total ionic strength of the equilibrating metal ion solution was adjusted to within the range 3.0–3.2 with 2 *M* sodium sulphate solution; the final volume of this solution was always 100 ml. The metal ion solution (10 ml of 0.2 *M*) was added to 43 ml of 2 *M* sodium sulphate and 40 ml of 1 *M* sodium acetate, the pH being adjusted to the required value by addition of sulphuric acid or sodium hydroxide. The solution, diluted to 100 ml, was added to the pre-equilibrated polymer and allowed to equilibrate for 2 days with agitation. After this period, the pH was checked for constancy, and the polymer was filtered off and washed sulphate-free with the appropriate acetate buffer. The metal ion was then eluted by 50 ml of 2 *M* sulphuric acid for cobalt, copper, iron(III), iron(II) and uranyl ions, and by 4 *M* sulphuric acid for vanadium.

To study the effect of a competing ligand in solution, the above procedure was repeated with a 1:1 ratio of metal ion to citric acid. An equivalent quantity of acetate solution was omitted and the volume of 2 *M* sodium sulphate used was increased to maintain the total ionic strength at 3.0–3.2.

Concentrations of eluted metal ions were determined colorimetrically, cobalt with thiocyanate in acetone medium[8], copper with sodium diethyldithiocarbamate[9], iron with thioglycollic acid[9], uranium with 8-hydroxyquinoline[9] and vanadium with BPHA[10].

Associated co-ion

If the metals form 1:1 complexes with the ion exchanger, as would be expected from steric considerations, the ratio of metal ion to co-ion on the resin should establish this and prove that the resin capacity is independent of metal ion valency, as has been shown by Loewenschuss and Schmuckler[11] for Dowex A1. Consequently, equilibrations and elutions in the manner described were carried out on copper(II), iron(III) and vanadium(V) solutions. Equilibrations involving metal sulphates and a sodium sulphate backing electrolyte were succeeded, after washing, by elution of metal with 4 *M* hydrochloric acid and determination of metal and

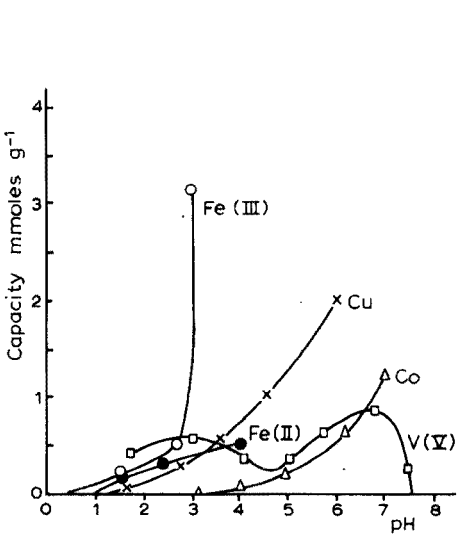

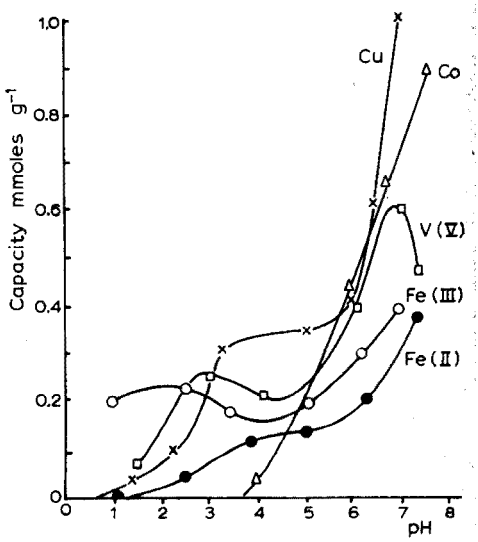

Fig. 1. Capacity *versus* pH curves for cations on a linear oxime–carbonyl polymer from acetate buffers. (○) Fe(III), (×) Cu, (△) Co, (□) V(V), (●) Fe(II).

Fig. 2. Capacity *versus* pH curves for cations on a linear oxime–carbonyl polymer in the presence of citrate. (×) Cu, (△) Co, (□) V(V), (○) Fe(III), (●) Fe(II).

sulphate ions in the eluate. For equilibrations involving metal chloride solutions, a backing electrolyte of sodium chloride was used and, after washing, elution was carried out with 4 *M* sulphuric acid, the metal and chloride concentrations in the eluate being determined.

RESULTS AND DISCUSSION

Behaviour of polymer 1

The water regain of this material was 1.9 g g^{-1}. Elemental analysis gave quite good agreement with the theoretical values. There may be peptide linkages resulting from some amino groups being produced at the reduction stage, but nitro groups cannot be present in the polymer, except as end-groups, as a residual nitro group would yield a molecule incapable of polymerization. As no free acid groups, derived from hydrolysis of terminal acid chloride groups were detected, it may be concluded that any affinity shown by the polymer for metal ions arises solely from the oxime–carbonyl grouping. For the formation of 1:1 metal chelates, the theoretical capacity will be 7.4 mmole g^{-1}. From Fig. 1, it can be seen that this value is not realized, the highest resin capacity measured being 3.2 mmole g^{-1} for iron(III) at pH 3.0. Being a linear polymer containing an ionizable group, the material is soluble in alkaline solutions and its working range as an ion exchanger has an upper limit of pH 8. As the polymer is insoluble in sulphuric acid at concentrations less than 5 *M*, elution of metal ions presents no difficulty. Random samples of resin, after elution of metal ion, were destroyed by wet oxidation with sulphuric–nitric acids and the metal content of the solutions determined. The

results proved that initial elution of metal ion was more than 98% efficient in each case.

The selectivity of the polymer for copper over cobalt at pH 4.5 is of interest. At this pH, the total capacity for copper is 1.0 mmole g^{-1}, whilst that for cobalt is negligible; a cobalt–copper separation would therefore appear to be possible. This copper selectivity is also apparent when citric acid is present as a competing ligand in solution (Fig. 2). The magnitude of the copper–cobalt difference is, however, much smaller, as the reduced copper capacity is due to the stability of the copper–citrate complex. A feature of Fig. 2 is the plateau for the range pH 3–6 which is characteristic of those metal ions forming stable citrate complexes.

The remarkable difference in capacity for iron(III) and iron(II) is the main feature of Fig. 1. In establishing the capacities for iron(II), a small quantity of sodium sulphite was added at the equilibration stage to ensure the presence of iron(II), and elution and determination of the metal were carried out in a nitrogen atmosphere. The curves indicate that an ion-exchange separation of iron(III) and iron(II) should be possible with an oxime–carbonyl polymer. The selectivity for iron(III) disappears when citrate is present, the total capacity being reduced from 3.2 to 0.2 mmole g^{-1}. The capacity *versus* pH curve closely resembles the curve obtained by Chwastowska and Minczewski[12] for the extraction of iron(III) with BPHA; these workers suggested the formation of a 1:1 complex at pH 2 and a 1:3 complex in the pH range 5–7. Although from steric considerations, a 1:3 complex is unlikely in the polymeric system investigated here, evidence for it was provided by the co-ion determinations carried out, as neither chloride nor sulphate were detected in the iron(III) eluates from the exchanger.

The vanadium–resin system is almost identical with the extraction of the vanadium–BPHA complex. Figure 1 indicates that two species are present, at pH 3 and at pH 6.8; the latter pH value is identical with the optimal pH for extraction with BPHA[13]. These maximal pH values for vanadium are not altered by the presence of citric acid; the capacity at pH 3 is decreased from 0.55 to 0.27 mmole g^{-1}, whilst the capacity at pH 6.8 is unaffected by the presence of the competing ligand. As with iron(III), no co-ion was detected for the vanadium system at pH 3. The closely related behaviour of the polymer and BPHA with vanadium was also observed in capacity determinations from sulphuric acid solutions. As the molarity of the acid increased, the vanadium capacity fell to a minimum from 1.8 *M* acid, rose to a maximum of 0.05 mmole g^{-1} from 2.5 *M* then fell to zero by 3 *M*.

The lowest measured capacities of the polymer were for uranyl ions. The maximum pH used for acetate system equilibrations was pH 4 where the uranyl capacity was 0.25 mmole g^{-1}; probably the uranyl–citrate system has a stability similar to or greater than that of the uranyl–resinate system. In the citrate system, the maximal capacity for uranyl ions, 0.1 mmole g^{-1}, was observed at pH 3.8. This is in agreement with Shendrikar[13] who reported the optimal pH for extraction of uranyl ion into BPHA in chloroform as pH 3.5. The resin capacity fell to a minimum at pH 5, and then rose to a value of 0.3 mmole g^{-1} at pH 7.5, the highest pH value at which measurements were made.

Behaviour of polymer 2

The water regain of the chelating resin was 1.2 g g^{-1} and that of the

polyethyleneimine blank 2.6 g g^{-1}. Polyethyleneimine was selected as a polymeric frame on which the chelating ligand was to be attached because of the low molecular weight per monomeric unit and its ready interaction with molecules possessing an active halogen. The *p*-(bromomethyl)benzoylphenylhydroxylamine was examined for its chelating properties. A solution in chloroform was used for the solvent extraction of vanadium, iron(III) and copper ions; the properties were found to closely resemble those of BPHA. For each ten nitrogen atoms of the linear polyethyleneimine, four were used as anchor points for the chelating ligand or, in the case of the blank, for benzyl groups; four were utilized in the cross-linking process with ethylene dibromide, and the remaining two also for cross-linking by 1,4-di(bromomethyl)benzene. Previous work on the ion-exchange of cross-linked polyethyleneimines[14] had shown that ethylene dibromide alone gave cross-linked polymers which were rubbery and had very high water regains, hence part of the ethylene dibromide was replaced by 1,4-di(bromomethyl)benzene in order to stiffen the polymer and reduce water regain.

Whilst metal ion capacities on this chelating exchanger were far higher than the values obtained for polymer 1, a comparison of capacities of the chelating resin and the blank were disappointing. The theoretical total capacity of the chelate resin should be 2.7 mmole g^{-1} if 1:1 complexes are formed, whilst the blank should of course be zero. Equilibrations with iron(III), copper(II), vanadium-(V) and uranyl ions were carried out in the presence of citrate, and the results shown in Table I should therefore be compared with those in Fig. 2 for the first polymeric BPHA exchanger.

TABLE I

MAXIMAL CAPACITIES AND pH VALUES OF THE POLYETHYLENEIMINE CHELATING EXCHANGER AND BLANK RESINS

	Maximal capacities (mmole g^{-1})		*pH*
	Chelating polymer	*Blank*	
Cu(II)	2.0	2.2	6.0
V(V)	4.8	5.2	3.0
	7.5	6.5	6.0
Fe(III)	1.7	2.6	3.0
UO_2(II)	1.2	1.5	2.0
	0.6	1.4	7.0

Whilst the theoretical capacity is considerably exceeded for vanadium, it is obvious from the capacity values obtained for the blank that ions are held on the lattice by lone-pair donation from the nitrogen of the tertiary amino groups. The capacity *versus* pH contours for the chelating exchanger had pH maxima at 3.0 and 6.0 for vanadium, the contour being similar to that for polymer 1 in Fig. 2. The contour for iron(III) was also similar to that shown in Fig. 2 with maxima at pH 2.8 and pH 6.5. As these values are in agreement with solvent extraction studies carried out on BPHA, it seems almost certain that the oxime–carbonyl groups are chelating with iron(III) and vanadium ions. The capacity for copper ions was quite different

from that of polymer 1, however; no plateau occurred between pH 3 and pH 5, the capacity of the chelating resin increasing steeply to a maximum at pH 6 in a similar manner to the blank.

The uranyl capacities for this chelating resin and blank were also higher than the values obtained for polymer 1. In the presence of citrate, maximal pH values for uranyl on polymer 1 were 3.8 and 7.5, whilst the corresponding maxima for polymer 2 were 2.0 and 7.0. However, as the blank resin showed an identical contour with increased capacity, no firm conclusions on the mechanism of uranyl ion retention may be drawn.

Conclusions

The linear oxime–carbonyl exchanger, polymer 1, behaved in accordance with the known properties of BPHA when used in solvent extraction. Results suggest that the exchanger may be used to separate copper and cobalt, and, of much greater importance, to separate vanadium from iron with 2.5 *M* acid as the eluant. The separation of iron(III) from iron(II) at pH 3 also seems feasible. This is the first chelating exchanger for which the latter two separations are practicable. The linear nature of this polymer, with its solubility above pH 8, is a drawback. The possibility of producing a cross-linked polymer by replacing a part of the tetraphthaloyl chloride by trimesoyl chloride is currently being investigated.

The location of the oxime–carbonyl group on cross-linked polyethyleneimine appeared to be successful. However, as lone-pair donation from polymer backbone nitrogen atoms caused the retention of metal ions in a blank resin, the extent to which the oxime–carbonyl functioned as a chelating group could not be determined. In fact, the introduction of a high-molecular-weight chelating ligand resulted in a diminution of capacity over that of a blank into which a benzyl group was introduced.

Cross-linked polyethyleneimines have been investigated for chelating capacity previously but not for vanadium or uranyl ions. In view of the high capacities of the polyethyleneimine blank reported here, the polymer may repay further investigation. The absence of chloride or sulphate co-ions when polymer 1 was equilibrated with various metal ions indicates the possibility that 1:1 complex formation, favoured on steric considerations, may not be a limiting factor. The possibility of 1:2 and 1:3 metal–chelate ratios is suggested for the metal–resin interaction in a manner similar to that of the metal–monomer when solvent extraction of the metal ion with a ligand in solution is carried out.

SUMMARY

Chelating ion exchangers containing N-carbonylphenylhydroxylamine functional groups have been synthesized and their exchange behaviour with copper, cobalt, iron, vanadium and uranium investigated. Of the two polymers described, a linear oxime–carbonyl polymer exhibited chelating capacity as a function of pH analogous to the chelates formed by BPHA. An oxime–carbonyl polymer based on polyethyleneimine had high capacities for the metal ions studied, but the principal mode of reaction was by electron donation from nitrogen atoms. The absence of co-ion in metal ion capacity studies indicates the possibility of formation of 1:2 and

1:3 metal complexes with the resin. Separations of iron(II)–iron(III) and vanadium–iron appear possible.

REFERENCES

1 E. Bamberger, *Ber. Bunsenges. Phys. Chem.*, 52 (1919) 1116.
2 S. C. Shome, *Analyst (London)*, 75 (1950) 27.
3 A. K. Majumdar, *N-Benzoyl-N-phenylhydroxylamine and its analogues*, Pergamon Press, Oxford, 1972, p. 39.
4 J. P. Cornaz and H. Deuel, *Experimentia*, 10 (1954) 137.
5 J. P. Cornaz, K. Hutschneker and H. Deuel, *Helv. Chim. Acta*, 40 (1957) 2015.
6 G. Petrie, D. Locke and C. E. Meloan, *Anal. Chem.*, 37 (1965) 919.
7 N. C. Rose, *J. Chem. Educ.*, 44 (1967) 283.
8 M. Pinta, *Detection and Determination of Trace Elements*, I.P.S.T., Jerusalem, 1966.
9 A. I. Vogel, *A Text-book of Quantitative Inorganic Analysis*, Longmans, London, 3rd. edn., 1962.
10 D. E. Ryan, *Analyst (London)*, 85 (1960) 569.
11 H. Loewenschuss and G. Schmuckler, *Talanta*, 11 (1964) 1399.
12 J. Chwastowska and J. Minczewski, *Chem. Anal. (Warsaw)*, 8 (1963) 157.
13 A. D. Shendrikar, *Talanta*, 16 (1969) 51.
14 P. G. Walker, Dissertation, University of Salford, 1973.

Analytica Chimica Acta, 77 (1975) 153–161

AN INTEGRATION METHOD OF ENZYME ANALYSIS*

LAWRENCE C. THOMAS and GARY D. CHRISTIAN
Department of Chemistry, University of Washington, Seattle, Washington 98195 (U.S.A.)
(Received 6th September 1974)

Integration techniques have been described for reaction-rate methods of analyses[1–3]. These methods measure the rate of change of a linear transducer signal, using a time-averaged two-point differential-rate technique. The scheme is to integrate a concentration-dependent signal over two different time intervals, and relate the difference between those integrals to a rate of reaction. Either two sequential integrals are subtracted[1–3] or the integration intervals are separated by an "idle interval"[3]. Increased precision is gained by integration of noisy signals over time intervals much longer than the period of the noise fluctuations.

Signal-averaging techniques can be applied to increase the accuracy, precision, and sensitivity of enzyme analyses. One approach is to develop a method of analysis in which transducer signals caused by substrates or products are integrated over a period of time and related to catalytic ability or initial substrate concentrations. In this paper, equations that relate the integrals to substrate or enzyme concentration are described, and experimental examples are given.

TABLE I

SYMBOLS USED

$[E]_0$, $[S]_0$, $[P]_0$	Initial concentrations of enzyme, substrate, and product.
$[E]_t$, $[S]_t$, $[P]_t$, $[X]_t$	Time-dependent concentrations of enzyme, substrate, product and general species X.
t_f	Time at end of integration period.
n	Number of intervals used for approximation of integral by method of rectangles.
ΔT	Time duration of integration period.
Δt	Time increment used in iterative method of rectangles.
i	Integration interval designator.
$[S]_i$	Concentration of substrate at the beginning of the ith iteration interval.
a_j	Coefficients incorporationg the constant terms in expanded eqn. (15).
$[NAD^+]_t$, $[NADH]_t$	Time-dependent concentrations of the oxidized and reduced forms of nicotinamide adenine dinucleotide.
$\Delta\tau$	Delay time in fixed-time differential rate method.
$\Delta[P]$	Fixed concentration change in variable-time differential rate method.

* Presented in part at the 29th Annual Northwest Regional Meeting of the American Chemical Society, Cheney, Washington, June 13–14, 1974.

THEORY

(The symbols used below are defined in Table I).

First-order and second-order reactions may be kinetically modeled by use of the simplest reversible enzymatic mechanism,

$$E+S \underset{k_{-1}}{\overset{k_1}{\rightleftharpoons}} ES \underset{k_{-2}}{\overset{k_2}{\rightleftharpoons}} E+P \tag{1}$$

for which one may develop a set of rate equations:

$$\frac{d[P]_t}{dt} \simeq k_2[E]_0 \text{ if } K_m \ll [S]_t \tag{2}$$

$$\frac{d[P]_t}{dt} \simeq \frac{k_2[E]_0}{2} \text{ if } K_m \sim [S]_t \tag{3}$$

and

$$\frac{d[P]_t}{dt} \simeq \frac{k_2[E]_0[S]_t}{K_m} \text{ if } K_m \gg [S]_t \tag{4}$$

where

$$K_m = \frac{k_{-1}+k_2}{k_1}, \quad \frac{d[ES]_t}{dt} = 0, \quad [E]_0 = [E]_t + [ES]_t$$

$$[S]_t = [S]_0 - [P]_t + [P]_0 - [ES]_t, \quad k_{-1}k_{-2}[P]_t \ll k_1k_2[S]_t$$

and

$k_{-2}[P]_t \ll k_{-1}+k_2+k_1[S]_t$ (refs. 4, 5).

For the case $K_m \ll [S]_t$, a pseudo first-order reaction results:

$$[P]_t = [P]_0 + \int_0^t \frac{d[P]_t}{dt}dt \simeq [P]_0 + \int_0^t k_2[E]_0 dt \tag{5}$$

and

$$\int_0^t ([P]_t - [P]_0)dt = \int_0^t \int_0^t k_2[E]_0 dt^2 = \int_0^t ([S]_0 - [S]_t)dt \tag{6}$$

if $[ES]_t$ is negligible. Thus, for a fixed-time interval, t_f,

$$\int_0^{t_f} [P]_t dt - \int_0^{t_f} [P]_0 dt = [E]_0 \cdot \text{constant} \tag{7}$$

The $K_m \sim [S]_t$ case yields a similar relationship between this difference integral and the enzyme concentration.

For the $K_m \gg [S]_t$ case, the reaction is second-order and

$$[P]_t - [P]_0 = \int_0^t \frac{k_2[E]_0[S]_t}{K_m} dt = [S]_0 - [S]_t \tag{8}$$

if $[ES]_t$ is neglected. $[S]_t$ is generally a complicated time-dependent function, so an approximation by an iterative method of rectangles is made. By defining $\Delta T/n = (t_f - 0)/n = \Delta t$, then $[S]_t$ at the end of the $(i+1)$ iteration interval is approximated by

$$[S]_{i+1} \simeq [S]_i + \int_{i\Delta t}^{(i+1)\Delta t} \frac{k_2[E]_0[S]_i}{K_m}\,dt \tag{9}$$

$$\simeq [S]_i\left(1 - \frac{\Delta t\, k_2[E]_0}{K_m}\right) \tag{10}$$

$$\simeq [S]_0\left(1 - \frac{\Delta t\, k_2[E]_0}{K_m}\right)^{i+1}. \tag{11}$$

Since

$$\int_0^{t_f} [P]_t dt - \int_0^{t_f} [P]_0 dt = \int_0^{t_f} ([S]_0 - [S]_t) dt \tag{12}$$

then

$$\int_0^{t_f} ([P]_t - [P]_0) dt \simeq \sum_{i=0}^{n-1} ([S]_0 - [S]_i)\Delta t \tag{13}$$

$$\simeq \sum_{i=0}^{n-1}\left[[S]_0 - [S]_0\left(1 - \frac{\Delta t\, k_2[E]_0}{K_m}\right)^{i+1}\right]\Delta t \tag{14}$$

$$\simeq [S]_0 \sum_{i=0}^{n-1}\left[1 - \left(1 - \frac{t_f k_2[E]_0}{nK_m}\right)^{i+1}\right]\frac{t_f}{n}. \tag{15}$$

Or,

$$\int_0^{t_f} ([P]_t - [P]_0) dt \sim [S]_0 \cdot \text{constant if } [E]_0 \text{ is fixed} \tag{16}$$

and

$$\int_0^{t_f} ([P]_t - [P]_0) dt \simeq \sum_{j=1}^{n} a_j [E]_0^j \text{ if } [S]_0 \text{ is fixed.} \tag{17}$$

The difference, then, between the integral of the initial substrate or product concentration over a time interval, ΔT, and the integral of the time-dependent substrate or product concentration over the same time interval is related to the enzyme or substrate concentration by eqns. (7), (16) and (17). The arguments above are subject to the assumptions depicted in the development of eqns. (2), (3) and (4)[4,5] and apply to first- and second-order reactions as modeled by those equations.

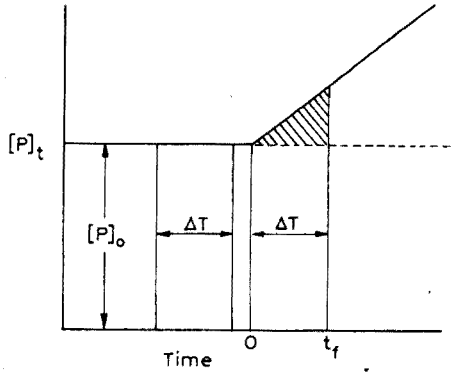

Fig. 1. Illustration of difference integral method to a first-order reaction far from equilibrium.

Figure 1 illustrates the application of this technique to a reaction which is first-order with respect to enzyme concentration and far from equilibrium. It should be noted that $\int_0^{t_f}[P]_0 dt$ may be substracted from $\int_0^{t_f}[P]_t dt$ by mathematical rather than experimental integration over the time period ΔT, if $[P]_0$ is well known.

For the enzymatic case, $K_m \ll [S]_t$, if $[E]_0$ is fixed, a zero-order reaction results such that $d[P]_t/dt$ is a constant. This trivial case leads to a fixed-time difference integral which is invariant, that is, $\int_0^{t_f}([P]_t - [P]_0)dt = \text{constant}$ for fixed $[E]_0$ and t_f.

For an irreversible pseudo first-order case such as $d[P]_t/dt = k[S]_t$, where k is the rate constant of the reaction $S \rightarrow P$, then

$$\int_0^{t_f}([P]_t - [P]_0 dt = \int_0^{t_f}([S]_0 - [S]_0 e^{-kt})dt$$
$$= [S]_0 \cdot \text{constant for fixed } t_f. \tag{18}$$

Less simple enzymatic mechanisms and rate equations are applicable to this integration method. The Dalziel form[6]

$$\frac{d[X]_t}{dt} = \frac{[E]_0}{\phi_0 + \frac{\phi_1}{C_1} + \frac{\phi_2}{C_2} + \frac{\phi_3}{C_1 C_2}} \tag{19}$$

although complicated in general by time-dependent concentration terms, is conducive to approximation of integrals over time when all terms may be calculated or defined over the entire time interval. Other forms are similarly compatible with the iterative integration format[7–11].

There should be some distinct advantages inherent in this integration technique. First, noise fluctuations may be averaged over a long time interval. This implies a decreased noise contribution in the measurements. Second, complicated reactions may be characterized. For example, a set of time *vs.* concentration curves such as those described by Fig. 2 may be distinguished by this method, whereas two-point rate methods with delay times greater than $\Delta\tau$ would yield identical results, even though the rates of reaction approaching equilibrium are markedly different. Similarly, reactions such as those illustrated in Fig. 3 may be characterized by this method, but would yield ambiguous results in two-point rate determinations over intervals $\Delta\tau$ or in variable-time determinations over fixed changes $\Delta[P]$.

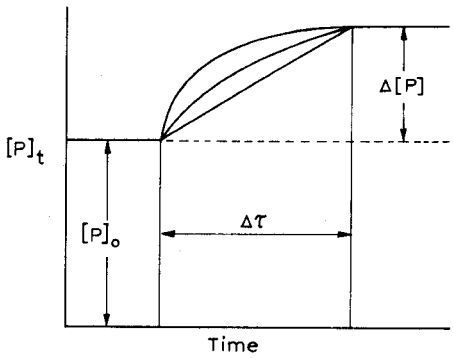

Fig. 2. Illustration of differential rate methods when equilibrium is achieved within delay interval, $\Delta\tau$.

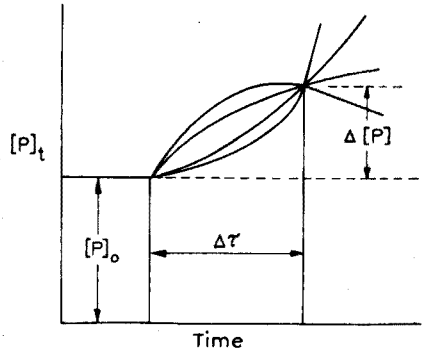

Fig. 3. Illustration of differential rate methods when complicated kinetics are shown within delay interval, $\Delta\tau$.

EXPERIMENTAL

Reagents

Glucose oxidase (GOP 3AA, 110 I.U. mg^{-1}; Worthington Biochemical Corporation) was used. All other chemicals were reagent-grade quality and deionized–distilled water was used for preparation of all solutions.

Apparatus

A Beckman Glucose Analyzer interfaced to a conventional strip-chart recorder was used to follow the oxygen tension and rate of change of oxygen tension as measured with a Clark electrode; the sample cell of the Analyzer was used to hold and stir the various solutions.

Procedure

Time-integral curves for lactate dehydrogenase reactions were generated from data of other workers[11]. A computer program was written to generate and plot fixed-time integrals of differences between initial and time dependent concentrations, consistent with the assumptions intrinsic in the rate equations used[11]. The program computed reaction rates according to the equation

$$\frac{d[P]}{dt} = \frac{[E]_0(V_{ab}/K_{ab}[A][B] - V_{pq}/K_{pq}[P][Q])}{1 + \frac{[A]}{K_a} + \frac{[B]}{K_b} + \frac{[P]}{K_p} + \frac{[Q]}{K_q} + \frac{[A][B]}{K_{ab}} + \frac{[P][Q]}{K_{pq}} + \frac{[A][P]}{K_{ap}} + \frac{[B][Q]}{K_{pq}}} \quad (20)$$

where all K and V values are kinetic parameters and the values [A], [B], [P], and [Q] are time-dependent concentrations for the reaction $A+B+E \rightleftharpoons \ldots \rightleftharpoons \ldots \rightleftharpoons P+Q+E$. The concentration changes and the integral of differences between initial and time-dependent concentrations over small intervals were calculated and accumulated over the entire integration time. The total approximated integral, estimated by this iterative method of rectangles, was then plotted as a function of the enzyme concentration, $[E]_0$.

First-order integration analyses were demonstrated by assays of glucose oxidase in aqueous solution. A standard solution of 0.01 M glucose in 0.1 M disodium

hydrogenphosphate, pH 5.5, was prepared. The solution was allowed to stand for 3 h to achieve mutarotation[12]. Solutions of glucose oxidase (110 I.U. mg^{-1}) were prepared in 0.1 *M* disodium hydrogenphosphate adjusted to pH 7.3. A 1 mg ml^{-1} solution of glucose oxidase was diluted sequentially by factors of 0.6 to a range of 1.1–0.011 I.U./10 μl. Aliquots (10 μl) of the various glucose oxidase solutions were added to 1.00 ml of the standard glucose solution which was saturated to air oxygen tension, and the oxygen tension was recorded as a function of time on the strip-chart recorder. The difference in the areas between the oxygen tension–time curves in the presence and absence of glucose oxidase were determined by weighing the various sections of chart paper after cutting the curves with scissors. Difference integrals for 4-, 3-, 2-, and 1-min integrations were thus determined for the various activities of glucose oxidase.

In addition, degrees of oxygen incorporation during the reaction were estimated by recording the continuous derivative output of the Glucose Analyzer in the absence of reaction at various degrees of oxygen depletion. Partially deaerated standard glucose solutions were introduced into the sample cell and the rate of oxygen incorporation and the fraction of oxygen saturation of the solution were monitored via the derivative and direct outputs, respectively, of the instrument.

RESULTS AND DISCUSSION

The application of this integration method to nicotinamide-adenine dinucleotide (NAD) oxido-reductase reactions was of particular interest. Previously reported kinetic parameters have been related to theoretical rate equations for some of these dehydrogenases[11]. For a reaction

$$NAD^+ + S \rightleftharpoons P + NADH + H^+$$

under specified steady-state conditions and assuming no ternary complexes, the reaction rate may be expressed as a function of $[S]_t$, $[NAD^+]_t$, $[NADH]_t$, $[P]_t$, and pH (see eqn. 20). Kinetic parameters for this functional form have been tabulated for various dehydrogenases[11] and were used for computer generation of integral-concentration curves for a fixed time interval.

Figures 4 and 5 are typical plots of numerical integrations of the net changes in NADH concentration over a fixed time. Figure 4 is a typical plot in which the reaction is enzyme limited and far from equilibrium. Figure 5 shows the nature of the same type of curve when the enzyme concentration is high and the system approaches equilibrium. Both cases show the relationship between the fixed-time integral of concentration changes to be a characterizing parameter for enzyme concentrations.

Figure 6 shows a family of current-time curves for various glucose oxidase activities. At low activities, the rate of oxygen depletion is approximately linear with respect to time, characteristic of an enzyme-limited reaction. At high activities, the rate of oxygen depletion is non-linear with respect to time–approximately exponential, characteristic of a first-order reaction with respect to oxygen approaching equilibrium.

The effect of oxygen incorporation caused by stirring and diffusion affects these curves, especially at higher enzyme activities where the depletion of oxygen in

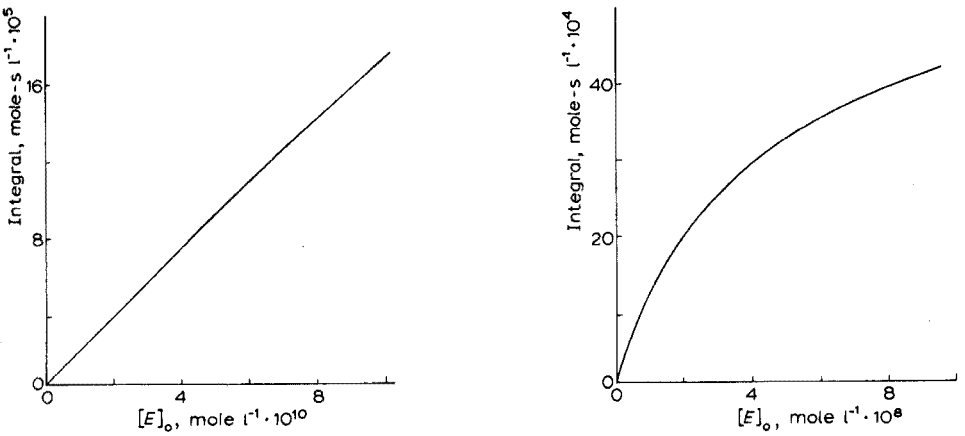

Fig. 4. Computer-generated difference integral *vs.* lactate dehydrogenase concentration curve when reaction is far from equilibrium; 3-min integration by 1-s increments. Initial concentrations of NAD, L-lactate, NADH, and pyruvate are $55 \cdot 10^{-6}$ *M*, 0.5 *M*, 0 *M*, and 0 *M*, respectively.

Fig. 5. Computer-generated difference integral *vs.* lactate dehydrogenase concentration curve when because the input resistance is very high and the input bias currents are very low,

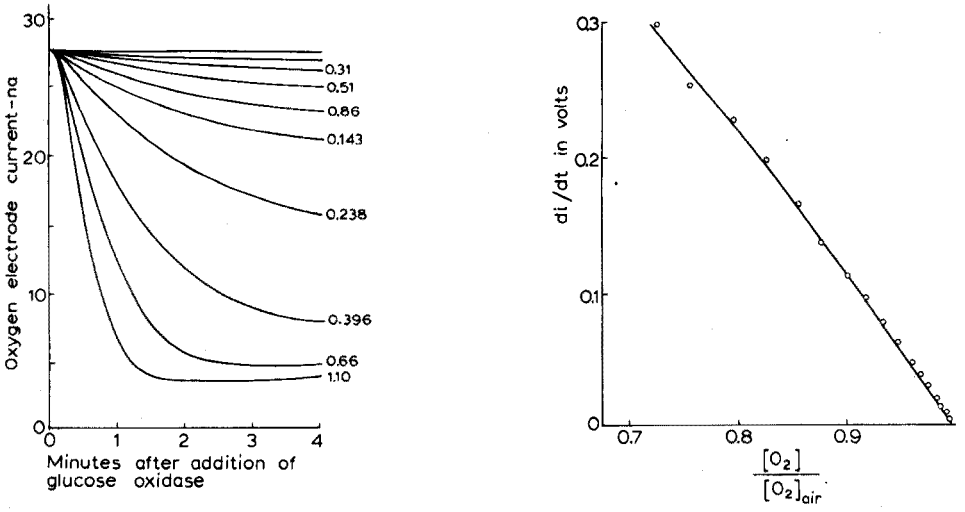

Fig. 6. Family of oxygen tension *vs.* time curves for various activities of glucose oxidase in 0.01 *M* glucose solution, pH 5.5, 0.1 *M* Na_2HPO_4. Numbers on curves represent glucose oxidase activity in I.U. ml^{-1}.

Fig. 7. Relative rate of oxygen incorporation into 1 ml of 0.01 *M* glucose solution, pH 5.5, 0.1 *M* Na_2HPO_4, as a function of degree of oxygen saturation in the sample cell.

solution is large and accumulations of peroxide inhibit the enzyme. Figure 7 illustrates the dependence of the rate of oxygen incorporation upon the degree of oxygen saturation of the standard glucose solution. The equation

$$\frac{d[O_2]}{dt} = k'[E]_0[O_2]_t - k'' \frac{[O_2]_t}{[O_2]_{saturation}} \tag{21}$$

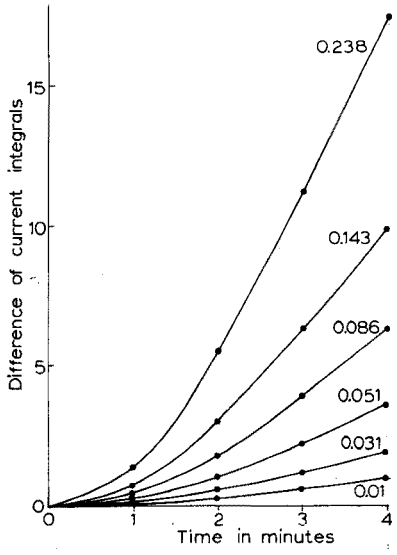

Fig. 8. Difference integral *vs.* time curves for various activities of glucose oxidase in 0.01 *M* glucose, pH 5.5, 0.1 *M* Na_2HPO_4. Numbers on curves represent glucose oxidase activities in I.U. ml^{-1}.

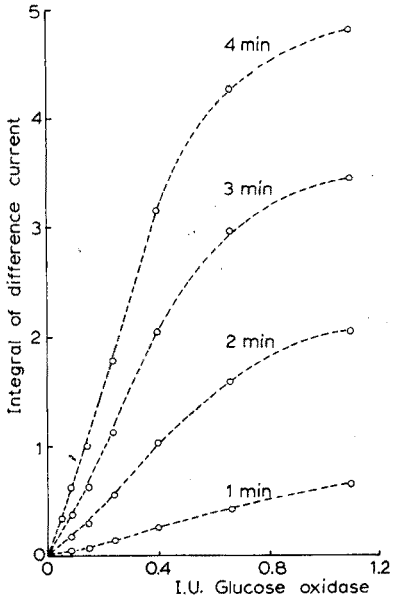

Fig. 9. Difference integral *vs.* glucose oxidase activity in 0.01 *M* glucose, pH 5.5, 0.1 *M* Na_2HPO_4. 1-, 2-, 3-, and 4-min integrations are shown.

approximates the slopes of the curves in Fig. 6, where k' is the rate constant of the enzymatic reaction and k'' is a rate constant for the oxygen incorporation; $k'' \ll k'$ in general, and the curves in Fig. 6 as described by eqn. (21) approximate a first-order reaction with respect to oxygen.

Figures 8 and 9 show the dependence of the difference integrals (between background air oxygen tension and the time-dependent enzymatically depleted oxygen tension) on time and glucose oxidase activity, respectively. At 1 min, the difference integral shows an enzyme concentration dependence characteristic of a first-order reaction with respect to $[E]_0$, consistent with an enzyme-limited reaction far from equilibrium with minor changes in oxygen concentration. The 2-, 3-, and 4-min curves show a non-linear relationship characteristic of first-order or second-order reactions approaching equilibrium. The time dependence for the various curves in Fig. 8 illustrates the non-linear increase of the difference integral with time, characteristic of non zero-order reactions which are not at equilibrium. The difference integral in all cases is distinctly related to the enzyme activity. Similar relationships should apply to variable-time integration methods over fixed concentration or transducer signal changes.

SUMMARY

The application of an integration method of kinetic analysis to first-order and second-order reactions is discussed with particular emphasis on enzyme analyses.

Transducer signals or concentrations of products or substrates are integrated for a fixed time and the net integral of the increased or decreased signal or concentration is related to the initial substrate or enzyme concentration. Equations are developed describing the dependence of the integrals on enzyme and substrate concentrations for first- and second-order reactions, and examples are presented illustrating different cases. The application of this method to complicated enzymatic systems is discussed.

REFERENCES

1 J. D. Ingle, Jr. and S. R. Crouch, *Anal. Chem.*, 42 (1970) 1055.
2 G. P. Hicks, A. A. Eggert and E. C. Toren, Jr., *Anal. Chem.*, 42 (1970) 729.
3 E. M. Cordos, S. R. Crouch and H. V. Malmstadt, *Anal. Chem.*, 40 (1968) 1812.
4 G. E. Briggs and J. B. S. Haldane, *Biochem. J.*, 19 (1925) 383.
5 I. Amdur and G. G. Hammes, *Chemical Kinetics: Principles and Selected Topics*, McGraw–Hill, New York, 1966.
6 K. Dalziel, *Acta Chem. Scand.*, 11 (1957) 1706.
7 L. Peller and R. A. Alberty, *J. Amer. Chem. Soc.*, 81 (1959) 5907.
8 R. A. Alberty, *J. Amer. Chem. Soc.*, 75 (1952) 1928; 80 (1958) 1777.
9 G. G. Hammes and P. Fasella, *J. Amer. Chem. Soc.*, 84 (1962) 4644.
10 C. Walter, *Steady State Applications in Enzyme Kinetics*, Ronald Press, New York, 1965.
11 V. Bloomfield, L. Peller and R. A. Alberty, *J. Amer. Chem. Soc.*, 84 (1962) 4367, 4375.
12 J. C. Sternberg and J. P. Frain, *24th National Meeting of Amer. Assoc. Clin. Chem., Cincinnatti, Ohio, August 1972.*

Analytica Chimica Acta, 77 (1975) 163–169

A VERSATILE AMPEROMETRIC INTEGRATOR

LAWRENCE C. THOMAS, GARY D. CHRISTIAN and J. D. S. DANIELSON
Department of Chemistry, University of Washington, Seattle, Washington 98195 (U.S.A.)
(Received 10th December 1974)

Integration techniques have been described for coulometry[1,2], chronocoulometry[3], subtractive sampled direct current polarography[2], anodic and cathodic stripping[4], solid electrode amperometry[5], kinetic analyses[6–8], and alternating current and rapid derivative polarography[9]. These techniques have resulted in excellent precision and sensitivity[2,4,6–9], predictive capabilities[1,2], and a rapid, inexpensive clinical analyzer[5]. The coupling of these techniques with digital control and data acquisition has increased the general capabilities of electrochemical methods and reduced the size, weight, and cost of the apparatus.

Our interest has been in applying amperometric measurements to enzyme analyses. Integration techniques are attractive because of their time averaging capabilities with possible increases in accuracy, precision, and sensitivity. Preliminary investigations indicated that integration of amperometric currents dependent on enzyme substrate or product concentrations over a period of time could be as accurate as, and more precise than, the common differential methods[7,8] used to measure enzyme reactions.

In order to apply amperometric integration techniques to a wide range of samples and electrodes, a need existed for an electrochemical integrator with a wide current range, bipolar adjustable potential control, three-electrode capability, continuous adjustable output proportioning, and timed logic functioning. In addition, high precision output, low leakage currents, and good linearity over a wide range of currents was needed. Although most of these capabilities have been developed separately, no previous instrument combines them all over the current range from a few nA to several mA[1–5]. Hence, to fulfil the above requirements, an integrator/potentiostat has been developed which monitors small changes in direct currents ranging from 10^{-9} to 10^{-2} A. Conventional analog techniques are used for the potentiostatic and integration units. Digital logic controls the timing and switching of the instrument. Integration output may be displayed on a digital panel meter.

EXPERIMENTAL

Instrumentation

A wide-range bipolar analog electrochemical potentiostat/integrator was developed. It consists of a potentiostat for applying potentials to voltammetric electrodes, and an integrator for integrating the resultant voltammetric current. A simplified schematic diagram of the instrument is shown in Fig. 1.

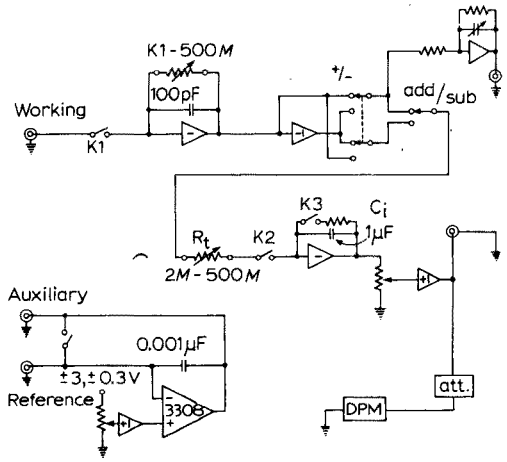

Fig. 1. Simplified schematic diagram of integrator/potentiostat.

The potentiostat is operable over continuous ranges of ± 3 V or ± 0.3 V, and operates in either a two- or three-electrode mode. The sensitivity of the amperometric circuitry spans 20 nA to 10 mA full-scale in a 1, 2, 5, 10, sequence, with a 0.01–10.0-s range in time constant (1, 3.3, 10 sequence) and $+10$ V full-scale analog output. This amperometric circuitry may be operated in a continuous mode or timed modes initiated by an operator start-pulse and interrupted by timed switching.

The integration is timed and controlled by logic circuitry with a selected 0, 0.1, 2, 4, 8, 16, or 32-s start-delay, and a subsequent selected 2^N, ($N=$ 0–9)-s integration time. This integration is performed by operational amplifier capacitor charging and the resultant potential across the capacitor is displayed, with variable proportioning, on a digital panel meter.

The potentiostat produces a voltage of specified known magnitude between the reference electrode and the working electrode. In either two- or three-electrode electrolysis, the working electrode of this system is maintained at ground potential.

A FET input Burr-Brown 3308 amplifier was chosen for the voltage follower because the input resistance is very high and the input bias currents are very low, measured to be *ca.* 2 pA. The maximum output of the 3308 amplifier is 5 mA. Current amplification (not indicated in Fig. 1) expands the current range to 10 mA. A saturation value of ± 10 V output for the 3308 amplifier limits the maximum potential of the auxiliary electrode.

The working electrode is connected to the summing junction of a conventional current-to-voltage transducing stage. The feedback resistance of the transducing stage is selected by a front panel current range control. This current-to-voltage transducing amplifier has a summing junction voltage that is very close to zero and an output impedance that is low. An analog output is taken as a $+10$ V full-scale potential proportional to the current drawn by the working electrode, independent of the sign of the integration. A pair of switches allows either an addition or a subtraction mode of the integration with either cell polarity.

The integrator is of conventional design, consisting of an inverting operational

amplifier with a very high input resistance and a very low input current. The feedback circuit is a high quality 1-μF polystyrene capacitor with low leakage and a minimally polarizable dielectric. In order to adjust the output of the integrator, a potentiometer is used to scale the output voltage of the integrator and this allows one to proportion current units into other units, such as concentration units.

K1 is an electromechanical relay with a leakage resistance greater than 10^{12} Ω. It may be closed manually or by the logic circuitry of the instrument. K2 is a pair of complementary insulated-gate field-effect transistors. This relay results in very low leakage currents. K3 is a manual switch which allows the discharge of the integration capacitor. A START switch is closed manually and begins the cycle of timed sequences and the timing functions of the apparatus. Manual depression of the START switch sets the output of all logic stages. A delay time between the start of a timing cycle and the beginning of the timed integration period may be used. Upon termination of the delay time, relay K2 is closed, and the integration time begins. When the designated integration time is achieved K2 is opened, terminating the timing cycle.

The control and switching leakage currents were measured to be less than $5 \cdot 10^{-5}$ times the full-scale current for all current ranges. This corresponds to less than 10^{-12} A in the 20-nA full-scale range. The low leakage current at all ranges adds to the sensitivity and accuracy of the instrument.

Reagents

Beckman Glucose Reagent and diluted Beckman Standard Glucose Solution were used for the enzymatic glucose determinations. Triple distilled mercury, and Calbiochem uric acid were used; other chemicals were of reagent grade. All dilutions were made with deionized–distilled water.

Procedure

Glucose was analyzed enzymatically by amperometric measurement of the decrease in oxygen pressure in the presence of glucose oxidase with a Clark electrode. A Beckman Glucose Analyzer was interfaced to the integrator analyzer for the enzymatic assays (Fig. 2). The resistor, R_i, is required to limit the current to 50 nA at 10-V full-scale output from the integrator. This allowed direct

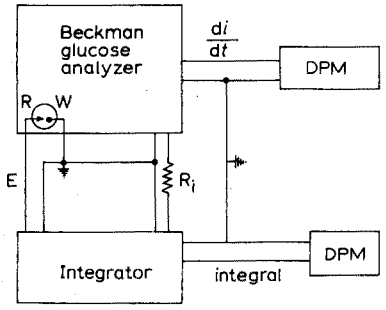

Fig. 2. Interfacing of integrator and Beckman Glucose Analyzer. E = Applied potential, R = reference electrode, W = working electrode, $R_i = 2 \cdot 10^8$ Ω current attenuation resistor, di/dt = derivative of amperometric current signal, integral = integral of amperometric current.

comparison of the integrator results with those of the glucose analyzer. An oxygen electrode potential of −0.55 V *vs.* Ag/AgCl was supplied by the integrator and its +10-V full-scale analog output for the 50-nA full-scale amperometric current was fed into the Glucose Analyzer derivative circuitry. Thus, both derivative (from the Glucose Analyzer) and integral (from the integrator) output were simultaneously obtained for each glucose analysis.

All samples were analyzed by the procedure recommended by Beckman Instruments, with the exception of the interfacing described above and a 16-s integration of current before addition of each sample. Each sample was added 2 s after beginning a 4-s delay time. A 16-s integration after the delay interval was electronically subtracted from the integral obtained before the sample addition.

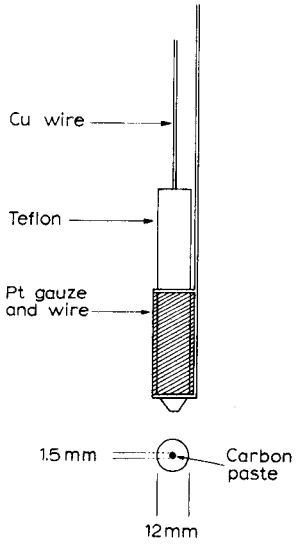

Fig. 3. Carbon paste working electrode and platinum auxiliary electrode configuration.

Uric acid was determined amperometrically at a carbon paste working electrode, with a platinum gauze counter electrode (Fig. 3) and a Coleman C-712 saturated calomel reference electrode. Solutions of uric acid in 0.1 *M* disodium hydrogenphosphate adjusted to pH 7.3 with sodium hydroxide were electrolyzed in quiet solution at +0.65 V *vs.* SCE. The operation was started with an open circuit. Closing of the amperometric circuit initiated an 8-s delay time, followed by an 8-s integration with a 2-μA full-scale current sensitivity.

Copper(II) was measured amperometrically at a dropping mercury electrode (DME) with a 6.49-s drop-time, at an applied potential of −0.04 V *versus* a Coleman C-712 SCE reference electrode. A 45-cm^2 mercury pool auxiliary electrode was used. The potentiostat of the integrator, in the three-electrode mode, was used with a manually started sequence of a 0.1-s delay followed by a 64-s integration of the DME current at constant applied potential. Solutions of copper sulfate in 0.1 *M* KNO_3 and 0.003% Triton X-100, were electrolyzed at a full-scale current range of 10 μA.

RESULTS AND DISCUSSION

Measurement of glucose

Forty-nine measurements of five different dilutions of 150 mg % glucose standard were made. Each measurement resulted in an integral as well as a derivative output. The read-out represented the difference between the two integrations of the background current level and the decreasing current caused by the enzyme reaction (Fig. 4). The principles of this method of enzyme analysis have been described elsewhere[10]. The difference output was normalized to a reading of 150 for the mean output of nine 150 mg % samples. A correlation coefficient of 0.998 between the derivative results and the integral results was obtained, and a least-squares line, $y=0.997x+2.34$, for the range 0–150 mg % was computed.

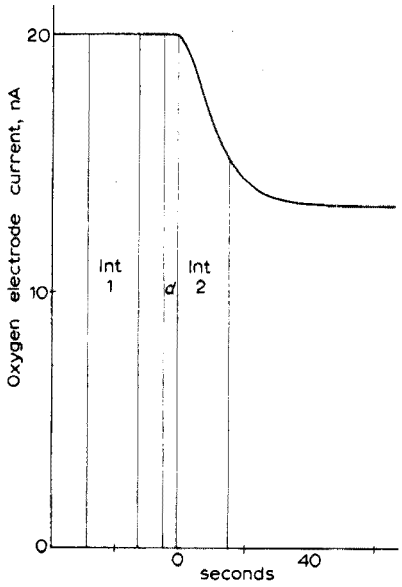

Fig. 4. Oxygen electrode current *vs.* time for glucose reaction. Int 1 = integration of current before sample addition, d = delay time, Int 2 = integration of current after sample addition.

The glucose results show a precision similar to that obtainable with the Glucose Analyzer under the conditions of the experiment. A net standard deviation of ± 2.9 mg % for ten 150-mg % samples for the integration method approximates the ± 1.9 mg % for ten 150-mg % samples for the accepted Beckman Glucose Analyzer derivative method. A precision of ± 2.5 mg % was achieved with the Glucose Analyzer when operated independently of the Integrator under the same conditions. The accuracy of the Glucose Analyzer is well documented[11] and this analysis illustrates the utility of the integrating instrument for measurements at the nA-level.

Measurement of uric acid

Uric acid at concentrations ranging from 0 to 11.7 mg/100 ml in phosphate

buffer pH 7.3, was electrolyzed. Each determination resulted in an integrated current output generated during the period 8 and 16 s after the beginning of the electrolysis. The net integral output (sample integration less the integral output for the 0 mg/100 ml solution) was normalized to a reading of 10.0 for the 10.0 mg/100 ml sample. The blank integral represented 2.3% of the 10.0 mg/100 ml and 10% of the 2.5 mg/100 ml integral outputs. A correlation of 1.00 and a least-squares line of $y=1.01x+0.015$ were computed between the concentrations and the adjusted integration data. The linearity of the change in uric acid electrolysis current with concentration also indicates good accuracy in measurements at solid electrodes. This is consistent with previous data[5].

Measurement of copper(II)

The DME measurement, at constant potential, of copper sulfate solutions was performed by integration of the current for 64 s. The sequence was manually started at the beginning of a drop life with the integration starting after a 0.1-s time delay. This amperometric integration over 9.86 drop lives was performed on solutions ranging from 0 to $1.23 \cdot 10^{-3}$ *M* copper; the concentration dependence of the integrated current was linear over this range. A relative standard deviation of $\pm 0.07\%$ was attained for 32 measurements on the $1.23 \cdot 10^{-3}$ *M* solution. This precision approximates the precision of the digital output device, *i.e.* ± 1.5 for full-scale reading of 1999, and approximates the increased polarographic precision of sampled direct-current methods[2]. The integration over several drop lives increases the polarographic precision and gives the capability for subtractive polarography.

The instrument has the capability of measuring relatively small differences in currents with good precision. The application of integral amperometry to enzyme assay shows great promise. Enzyme reactions can be monitored by measuring the formation of a product as well as by the reactant depletion method used here.

SUMMARY

A wide-range bipolar electrochemical integrator/potentiostat is described. The instrument uses digital logic for timing and switching of analog control and output functions. Digital output is included with variable proportioning for adjustment to concentration units. Currents ranging from a few nA to 10 mA may be monitored and integrated with high precision. The capabilities of the instrument are illustrated by integral monitoring of an enzyme reaction, integration of an organic electrolysis at a solid electrode for a fixed time, and integration of a dropping mercury electrode current over several drop lives.

REFERENCES

1 F. B. Stephens, F. Jakob, L. P. Rigdon and J. E. Harrar, *Anal. Chem.*, 42 (1970) 764.
2 R. G. Clem and W. W. Goldsworthy, *Anal. Chem.*, 43 (1971) 918.
3 G. Lauer and R. A. Osteryoung, *Anal. Chem.*, 38 (1966) 1137.
4 W. W. Goldsworthy and R. G. Clem, *Anal. Chem.*, 44 (1972) 1360.
5 G. Park, R. N. Adams and W. R. White, *Anal. Lett.*, 5 (1972) 887.
6 J. D. Ingle and S. R. Crouch, *Anal. Chem.*, 42 (1970) 1055.

7 G. P. Hicks, A. A. Eggert and E. C. Toren, *Anal. Chem.*, 42 (1970) 729.
8 E. M. Cordos, S. R. Crouch and H. V. Malmstadt, *Anal. Chem.*, 40 (1968) 1812.
9 H. L. Kies and M. Denos, *Anal. Chim. Acta*, 67 (1973) 246.
10 L. C. Thomas and G. D. Christian, *Anal. Chim. Acta*, in press.
11 J. C. Sternberg and J. P. Frain, *24th National Meeting of the Amer. Assoc. Clin. Chem., Cincinnati, Ohio, August 1972.*

Analytica Chimica Acta, 77 (1975) 171–182

NOUVELLE MÉTHODE DE DOSAGE AUTOMATIQUE DE SUBSTANCES OXYDANTES OU RÉDUCTRICES PAR POTENTIOMÉTRIE DIFFÉRENTIELLE

PARTIE III: APPLICATION À L'ANALYSE EN FLUX CONTINU (LACTOSE PAR CÉRIMÉTRIE)

J. BOSSET et B. BLANC

Station fédérale de recherches laitières, CH-3097 Liebefeld-Berne (Suisse)

E. PLATTNER

Institut de génie chimique de l'Ecole Polytechnique Fédérale de Lausanne, CH-1025-Lausanne (Suisse)

(Reçu le 15 novembre 1974)

Lors des deux études précédentes[1,2], les bases théoriques de cette méthode ont été établies, puis vérifiées par une série d'essais destinés à optimiser les principaux paramètres de la réaction, à savoir: (a) Le rapport des teneurs en oxydant et en réducteur (Q). Lorsque Q croît, la vitesse de réaction augmente, mais la sensibilité finale ($\Delta E_{\text{rédox}}{}^{i}_{j}$) de la méthode diminue. Il existe donc un optimum. (b) La température (T) de la réaction: aussi élevée que possible. (c) Le temps (t) de réaction: aussi grand que possible.

La différence de potentiel rédox $\Delta E_{\text{rédox}}{}^{i}_{j}$ mesurée, en mode discontinu, entre deux instants consécutifs i et j de la même réaction devient, en flux continu, la différence de potentiel rédox $\Delta E_{\text{rédox}}$ que l'on mesure—pour un même échantillon—entre deux points consécutifs de ce flux. Il n'est donc plus nécessaire de recourir à une électrode de référence du type Ag/AgCl: il suffit de deux électrodes de platine lisse, l'une servant de référence, l'autre à la mesure.

PARTIE EXPÉRIMENTALE

Diagramme des flux et appareillage

Sur le diagramme des flux (Fig. 1), on reconnaît les opérations suivantes: la thermostatisation (5), une première mesure du potentiel rédox du couple Ce(IV)/Ce(III) (7) et la segmentation (par bulles d'air) du réactif; puis l'injection (4), le mélange (5′) et la réaction d'oxydation (10) du lactose, suivie du débullage (2) et d'une mesure du nouveau potentiel rédox Ce(IV)/Ce(III) (7′) du flux. Le circuit est électriquement fermé par un pont électrolytique (1/9/9′) à diaphragme en verre fritté (8). Lors des essais de dosage du lactose dans le lait, un dialyseur a encore été monté en amont de la pompe pour éliminer les protéines qui interfèrent.

Le "manifold" proposé diffère des types habituels: il est presque entièrement situé dans un plan vertical (et non sur le plateau de la pompe) et immergé dans un bain-marie thermostatisé. La Fig. 2 montre dans le détail comment est réalisé cet assemblage, entièrement en verre, monté sur un léger chassis fait de cornières

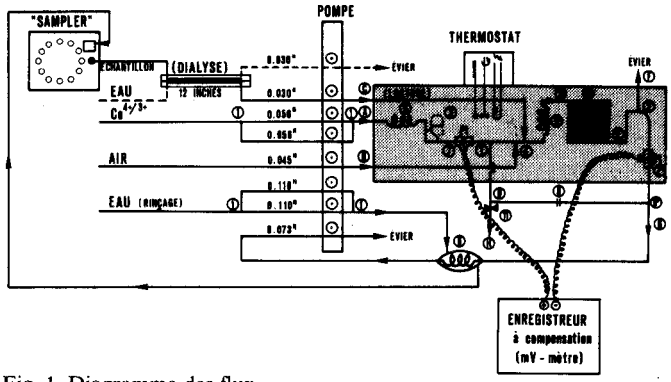

Fig. 1. Diagramme des flux.

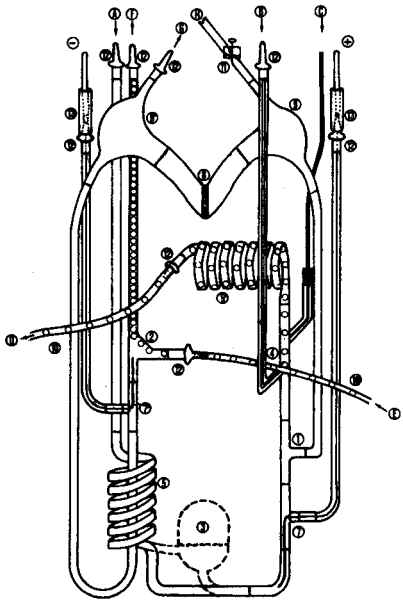

Fig. 2. Détail du 'manifold' (situé dans le thermostat). Les pièces dessinées avec une grosse section (8,9,9') ont un diamètre intérieur voisin de 14 mm.

d'aluminium. L'emplacement et la position de chaque élément sont déterminants pour un fonctionnement correct du système. L'ensemble doit être aussi compact que possible.

Les petits éléments de construction de ce 'manifold' (numérotés comme sur les Figs. 1 et 2) sont les suivants: (1) connection DO (116-0203-00) ou AO (116-0200-00); (2) débulleur Cl (116-0202-01) ou C2 (116-0202-02); (3) régulateur de débit PC 1 (116-0120) (*cf. La réalisation de l'analyseur*); (4) cactus HO (116-0207-00); (5/5') bobine de mélange, 14 spires, 2,4 mm i.d. ('single') (105-0086); (6) bobine de mélange, avec manteau de thermostatisation (114-0209-01); (7/7') électrodes de Pt fin, lisse (*cf. La réalisation de l'analyseur*); (8) diaphragme (fritte G7) soudé dans tube de verre en V; (9/9') connections de verre en forme de T; (10) spirale de

réaction de verre (1,6 mm i.d.; 12 m long); (11) petite pince de Mohr; (12) 'nipples' N5 (116-0002-01); (13) fiches bananes montées sur 'nipples' N5 enserrant les fils de Pt. Les éléments (1)–(6) et (10)–(13) sont de Technicon; (7)–(9) d'exécution spéciale (verrier).

Les tuyaux de pompe Technicon utilisés sont les suivants (débits mesurés avec la pompe utilisée sur le rapport 10): jaune/jaune (2×3.00 ml min^{-1}), en tygon, pour le réactif; noir/noir (0,80 ml min^{-1}), en tygon, pour l'échantillon; noir/noir (0,80 ml min^{-1}), en tygon, pour la dialyse; rouge/rouge (2,00 ml min^{-1}), en tygon, pour l'air; vert/vert (5,00 ml min^{-1}), en tygon, pour le "push-pull"; violet/blanc ($2 \times 9,75$ ml min^{-1}), en tygon, pour l'eau de rinçage.

Les lettres majuscules communes aux Figs. 1 et 2 repèrent les flux suivants: (A) entrée du réactif (Ce(IV)); (B) entrée de l'air pour la segmentation (bulles) (les essais ont démontré que l'on peut remplacer le flux d'azote utilisé antérieurement[2] par un flux d'air sans modifier les valeurs obtenues.); (C) entrée du réactant (lactose); (D) entrée dans la spirale de réaction; (E) sortie de la spirale de réaction; (F) sortie des bulles (après 'débullage'); (G) sortie de l'aliquot (mesuré); (H) sortie des bulles de la première partie du pont électrolytique (utilisée uniquement lors de la mise en marche).

L'appareillage utilisé, choisi en fonction des disponibilités du laboratoire, comporte les modules suivants: passeur d'échantillons 'sampler' SD3 modèle 1512 (Carlo Erba); dialyseur, 12 pouces, modèle 177-B010+177-B078 (Technicon ou Elkay); pompe péristaltique, modèle mp 25 GJ-4 (Ismatec, Zürich); bain-marie thermostatisé, modèle WB 20 D (Lauda) équipé d'un thermomètre à résistance de platine et des relais R 10, R 20 et R 30; enregistreur, modèle W+W 3012 (Kontron) ou 165 (Perkin-Elmer) qui sert en même temps de mV-mètre. (Si l'on ne dispose pas d'un enregistreur (à compensation) à impédance d'entrée suffisamment élevée pour mesurer $\Delta E_{\text{rédox}}$ (plusieurs MΩ V^{-1}), on peut monter un pH-, mV-mètre classique avant l'enregistreur.)

La mise en marche de cet analyseur se fait en deux temps. On ne peut en effet mesurer le $\Delta E_{\text{rédox}}$ entre les électrodes que si le pont électrolytique a préalablement été purgé. On ouvre la pince de Mohr (11) prévue à cet effet et fait circuler le réactif aussi bien dans A (comme en régime normal) que dans B (suppression momentanée des bulles). Les spirales de mélange (5') et de réaction (10) sont alors court-circuitées. Dès que la partie du pont électrolytique délimitée par les pièces (1), (8) et (11) est rincée et exempte de toute bulle, on peut refermer la pince de Mohr et injecter à nouveau de l'air dans B. Après quelques minutes, l'analyseur est prêt à fonctionner normalement, le flux circulant à nouveau dans les spirales (5') et (10). La ligne de base se stabilise alors à la valeur qui correspond à une concentration nulle en lactose.

Réactifs

Les produits utilisés sont les suivants: lactose monohydraté (lab, Merck); sulfate de cérium(IV) tétrahydraté (p.A., Merck); acide sulfurique (p.A., Merck) dilué à 0,5 *M*.

Réalisation de l'analyseur

Le modèle présenté par les Figs. 1 et 2 est l'aboutissement d'un long travail

de développement. Vu leur importance pratique, certaines des expériences faites avec les divers prototypes testés sont rapportées ci-dessous.

Thermostatisation du 'manifold'. Lors des premiers essais, le 'manifold' a été monté horizontalement sur le plateau de la pompe, les cellules de mesure se trouvant donc à la température ambiante. Il s'est alors avéré que le flux traversant de telles cellules était insuffisant pour compenser les variations habituelles de la température du laboratoire. Une thermostatisation par circulation d'eau dans le double manteau de chacune des électrodes se révèle efficace, mais accroît le volume mort de la veine liquide non segmentée au niveau de la seconde électrode. De plus, elle augmente l'encombrement général du "manifold", surtout si l'on désire encore préthermostatiser les flux qui entrent dans les cellules de mesure, d'où l'idée en définitive d'un montage vertical compact, entièrement immergé dans un seul bain-marie. Un tel système de thermostatisation conditionne le choix du matériau à utiliser pour manchonner les divers éléments. Mieux que le caoutchouc au silicone, le 'viton' ou 'l'acidflex' de Technicon donne entière satisfaction, tant du point de vue chimique que mécanique.

Géométrie des électrodes. La géométrie des électrodes joue un rôle considérable. Une électrode de platine ponctuelle en forme de tête d'épingle (Fig. 3, a), telle que l'utilisent Porter et Sawyer[3] ou Buckee[4] est favorable à l'écoulement du flux (peu d'obstruction), mais donne une mesure peu stable du potentiel à cause des variations périodiques de ce même flux. Une électrode filiforme, située dans l'axe de la cellule, en contact sur environ 2 cm avec la solution (Fig. 3, b), pare relativement bien à cet inconvénient en donnant une meilleure valeur moyenne pour l'échantillon (et non une valeur instantanée unique), mais augmente le risque surtout pour la seconde électrode, de retenir une éventuelle bulle par capillarité (le pont électrolytique ne fonctionne alors plus de manière satisfaisante). Dans l'idée de concilier les avantages des systèmes (a) et (c), un troisième type d'électrode a été testé, constitué d'un petit tube de platine lisse. La jonction électrique est réalisée par soudure d'un petit fil de cuivre sur le milieu du côté extérieur. Au moyen d'une couche suffisante de Coltogum (caoutchouc synthétique pâteux, qui durcit après séchage), on réalise l'isolation extérieure de chaque électrode (Fig. 3, c). La tenue de cet isolant est par contre moins bonne que celle du verre utilisé pour les cellules du type (a) et (b).

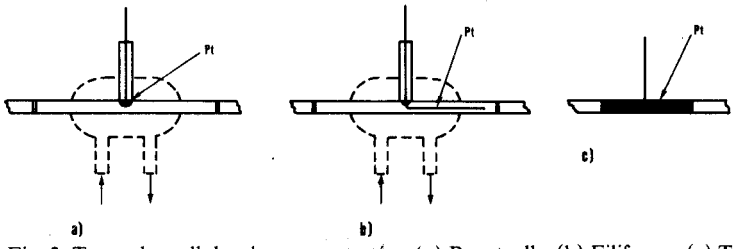

Fig. 3. Types des cellules de mesure testées. (a) Ponctuelle. (b) Filiforme. (c) Tubulaire.

Géométrie du pont électrolytique. La réalisation du pont électrolytique a longtemps été problématique. Dans les premiers prototypes, le pont était monté horizontalement reliant directement les deux électrodes. Sa position (horizontale) et son faible diamètre intérieur (le même que celui des autres tubulures de verre) rendaient

des plus difficiles le déblocage des bulles dues à un lent dégazage de l'électrolyte au voisinage du diaphragme. En combinant des formes en V et T (Fig. 2), on dispose d'un système autovideur, à condition de choisir un diamètre intérieur suffisamment gros (par exemple 14 mm). La fritte doit par contre avoir la porosité la plus faible possible (G7) pour limiter au maximum la perte de réactif (court-circuit pour la spirale de réaction).

Contrôle de la température. Le contrôle de la température du bain-marie (thermostat) doit être aussi précis que possible, cette grandeur intervenant de façon multiple lors du dosage, notamment sur le facteur de Nernst RT/F, le développement de la réaction rédox[2], et l'écoulement du flux (coefficients de dilatation des fluides, viscosité, tensions interfaciales, etc.). Un thermomètre à résistance de platine ($\pm 0.02°C$) est donc préférable à un thermomètre à contact de mercure ($\pm 0{,}1°C$).

Régulation du débit. Les essais entrepris indiquent que le volume d'air contenu dans l'analyseur doit être aussi faible que possible. De par son importante perte de charge dans le système, particulièrement dans la spirale de réaction, le flux qui traverse cette dernière a une certaine tendance à pulser. Lors des premiers essais, un 'régulateur de débit', (indiqué en traitillé par (3) sur les Figs. 1 et 2) a été monté sur le flux principal, en amont de la spirale de réaction. Or une longue série d'essais a montré que, contrairement à ce que laisse supposer sa dénomination, ce 'régulateur de débit' perturbe considérablement l'écoulement du flux; du fait même de la compressibilité de son volume d'air (*ca.* 8 ml), cette pièce amplifie en effet les à-coups observés. Elle a donc été supprimée. Dans le but de limiter au maximum le volume d'air, le tuyau d'amenée de l'air au cactus (4) (flux B) est un capillaire de téflon. Une diminution du flux d'air utilisé pour la segmentation n'est par contre pas à conseiller: de trop petites bulles ne suivent pas bien le flux liquide.

Limitation de la diffusion. Afin de diminuer au maximum la longueur des conduites (lactose et air) le cactus (4) est monté à l'envers. Ceci est possible si l'angle d'injection est égal à 90°. De plus le tuyau d'amenée du lactose au cactus (4) est un capillaire de téflon qui limite au maximum la diffusion entre échantillons consécutifs.

Choix de la spirale de réaction. Concernant la spirale de réaction, l'idée première a été de la réaliser au laboratoire même avec un tuyau de téflon souple. Cette solution présente de multiples avantages: choix de la géométrie de la spirale (longueur, diamètre du tube, hauteur), faible contamination, prix modique, stabilité chimique et mécanique. Les premiers essais ont démontré malheureusement qu'une telle spirale est inadéquate dans un tel cas. Le flux, une fois segmenté par les bulles a une très forte tendance à pulser. L'instabilité des mesures qui en résulte a fait finalement abandonner cette solution au profit de la classique spirale de verre. Un travail séparé[5] est spécialement consacré à l'étude de ce problème.

Conditions expérimentales

Vitesse de pompage. L'expérience montre qu'une vitesse de pompage élevée, c'est à dire un débit élevé, stabilise l'écoulement du flux (les premiers essais effectués avec la spirale de téflon le montrent particulièrement bien) et par conséquent les divers potentiels électrocinétiques* (ref. 6) qui en dépendent. Un débit élevé accroît

* On désignera par ce terme tous les potentiels électriques liés au déplacement des ions (diffusion, écoulement, double couche, etc.) qui s'ajoutent aux potentiels rédox proprement dits.

de plus la cadence d'analyse de l'appareil puisqu'on diminue les temps de rinçage de l'installation.

Inversément, une petite vitesse de pompage, c'est à dire un temps de séjour prolongé dans la spirale de réaction, augmente le nombre d'équivalents de réducteur fournis par une mole de lactose: la sensibilité de la méthode croît. A signal égal, on peut donc diminuer l'expansion d'échelle. Cette seconde condition est cependant moins impérative que la première, puisqu'une élévation de température permet de compenser largement la perte de sensibilité due à un pompage rapide: on a donc finalement opté pour l'emploi de la vitesse de pompage la plus élevée (rapport = 10) pour la suite des essais.

Température de réaction. Comme l'indique le paragraphe précédent, la température T joue un rôle considérable[2], plus important même que le temps de réaction, influençant de plusieurs manières le dosage (d'où la nécessité d'un contrôle précis de ce paramètre). Du point de vue réactionnel, il vaut la peine de travailler avec T aussi élevée que possible, comme l'indique le Tableau I. Pour cet essai, le réactif est une solution de sulfate cérique à 20 mM, en milieu sulfurique (0,5 M), le réactant, une solution de lactose à 5 g l^{-1} (sans dialyseur). Les tensions d'entrée sur l'enregistreur sont à chaque fois indiquées en mV (sensibilité). Inversément, l'élévation de la température exerce une influence défavorable sur la stabilité de l'écoulement du flux (pulsations) même si la spirale est en verre (le phenomène est encore plus marqué si la spirale est en téflon). La viscosité qui décroît lorsque T augmente, présente un moins bon coefficient d'amortissement aux à-coups de la pompe, auxquels s'ajoutent ceux dus au dégazage brutal du flux.

TABLEAU I

HAUTEUR DU PIC À L'ÉQUILIBRE ($\triangleq$ PLATEAU) EN FONCTION DE LA TEMPÉRATURE DE LA SPIRALE DE RÉACTION

Température (°C)	*Hauteur pic (cm)*	*Sensibilité (mV)*	*Température (°C)*	*Hauteur pic (cm)*	*Sensibilité (mV)*
45	11,8	50	70	20,9	100
50	16,5	50	75	11,9	200
55	22,1	50	80	13,8	200
60	14,2	100	85	15,7	200
65	17,1	100	90	18,0	200

L'expérience montre que le domaine de travail optimum se situe entre 70°C et 85°C. La température de 75°C a été retenue pour la plupart des essais, dont certains ont été répétés à des températures plus élevées ($\leqslant$ 90°C). [Le dégazage provient d'une part de la diminution de la solubilité de l'air dissous, d'autre part de la formation du CO_2 produit par oxydation du lactose[2]. C'est vraisemblablement la raison pour laquelle la stabilité du signal est nettement meilleure lorsque le réactif a reposé pendant quelques jours ou qu'il a été préchauffé (opération que l'on peut également faire en flux continu)].

RÉSULTATS ET DISCUSSION

Vérification de la (pseudo)linéarité

Sans dialyse. L'analyseur a été testé au moyen d'une série de solutions de lactose dont la concentration varie de 0,2 à 5 g l^{-1}. Ce domaine de concentration a été choisi en fonction des rendements que l'on peut atteindre par la dialyse d'un lait contenant environ 50 g l^{-1} de lactose. Le réactif est le même que celui mentionné au paragraphe précédent; la température de réaction est fixée à 75°C, puis à 80°C. La Fig. 4(a) donne la hauteur moyenne des pics obtenus sur l'enregistreur pour des temps d'aspiration de l'échantillon et de rinçage (t_a et t_r) de 30 s chacun (c'est à dire pour 60 analyses/h). On remarque que, dans un certain domaine de concentration, la hauteur du pic, donc $\Delta E_{\text{rédox}}$, est bien proportionnelle, à une constante additive près, au logarithme de la concentration en lactose ("pseudo-linéarité"), ce qui est en accord avec la théorie[1] et avec la vérification manuelle[2]. La forme générale est celle d'une branche d'hyperbole[1].

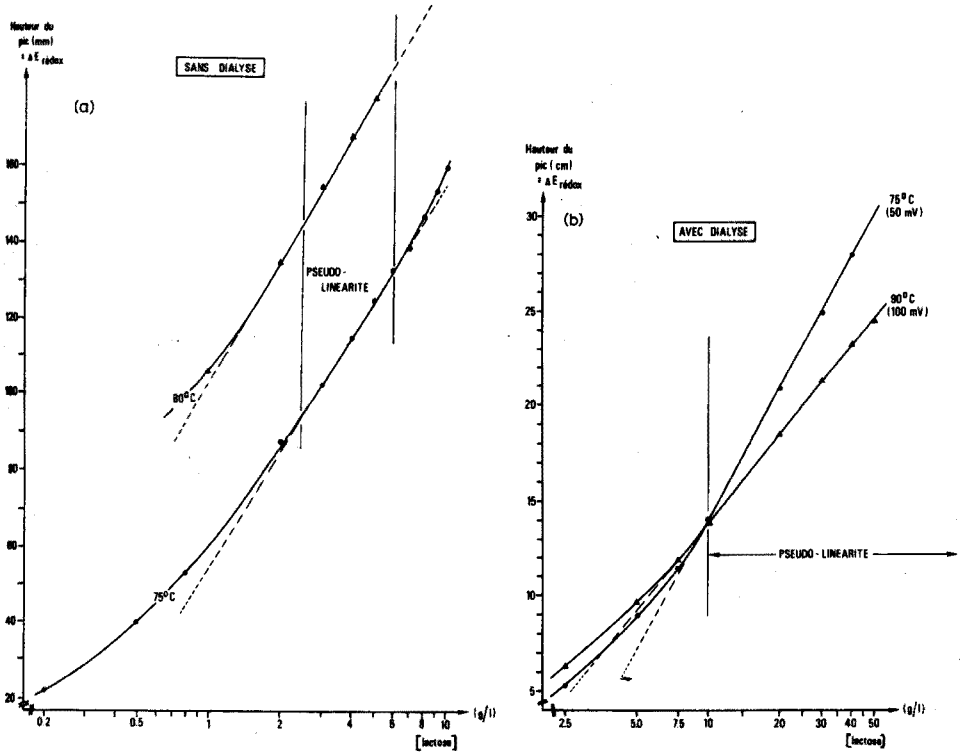

Fig. 4. Signal obtenu ($\triangleq \Delta E_{\text{rédox}}$) en fonction de la concentration du lactose engagé, sans dialyse (a) et avec dialyse (b).

Avec dialyse. L'essai est effectué à 75°C et à 90°C dans les mêmes conditions que précédemment. Cette fois, les solutions de lactose, dont la concentration varie de 2,5 à 50 g l^{-1}, sont dialysées (membrane Technicon type 157-0144) à température ambiante contre de l'eau contenant 0,1% de détergent (Teepol), qui stabilise

le flux à travers l'appareillage. La Fig. 4(b) montre la hauteur des pics obtenus en fonction de la concentration du lactose engagé, l'enregistreur étant directement relié aux 2 électrodes. On constate qu'en dessous de 30 g l^{-1} pour 75°C—respectivement de 20 g l^{-1} pour 90°C—les valeurs s'écartent notablement de la droite de régression, ce qui est en accord avec la théorie; le "seuil inférieur de linéarité"[2] n'est pas atteint: la concentration du lactose dans le dialysat est trop faible, le rendement de la dialyse étant de 2,5% seulement. En d'autres termes, on peut dire que la dialyse équivaut à une dilution de 1:40.

Reproductibilité

Sans dialyse. La reproductibilité des mesures électrochimiques classiques en flux continu, en particulier des mesures de potentiel rédox, dépend étroitement de la régularité du flux, en raison notamment des divers potentiels électrocinétiques[6] engendrés. C'est probablement l'un des principaux inconvénients de telles méthodes comparativement aux méthodes colorimétriques.

Un essai de reproductibilité à été effectué en répétant 62 fois consécutives le même dosage dans les conditions suivantes: [Ce(IV)] = 20 mM; [lactose] = 5 g l^{-1}; $T = 90°C$; $t_a = t_r = 30$ s ($\triangleq 60$ analyses/h); la spirale de réaction (encore en téflon) a 12 m de longueur et 1,8 mm de diamètre intérieur. Bien que de telles conditions soient assez sévères, on obtient encore une déviation standard $s = 0{,}370$ pour une hauteur moyenne de pics de 90,61 unités d'enregistreur (utilisé sur 200 mV), c'est à dire $s_r = 0{,}0040$. Le plateau correspondant à une aspiration continue est régulier.

Avec dialyse. Le même essai a été répété en dialysant un lait entier au lieu d'introduire directement du lactose dilué dans le conduit (C) (*cf.* Fig. 2). Vu l'élargissement des pics enregistrés par suite d'une contamination entre échantillons au niveau du dialyseur, $t_a = 1{,}5$ min et $t_r = 2{,}5$ min ($\triangleq 15$ analyses/h). L'essai donne $s = 0{,}739$ pour une hauteur moyenne de pics de 93,10 unités d'enregistreur (réglé cette fois sur 100 mV), ce qui correspond à $s_r = 0{,}0079$ (l'essai porte sur 33 déterminations consécutives). La reproductibilité est donc satisfaisante si l'on veille à stabiliser l'écoulement du flux (*cf.* les remarques correspondantes faites à propos de la réalisation de l'analyseur). On ne constate pas de dérive systématique de la ligne de base ou de la hauteur des pics, ce qui signifie que la résistance chimique et mécanique des tuyaux de pompe est suffisante, même vis-à-vis du réactif.

Sensibilité

Dans le domaine où la hauteur h du pic est proportionnelle, à une constante additive près, au logarithme de la concentration c du lactose, la sensibilité absolue de la méthode croît lorsque la pente dh/dc croît, c'est à dire lorsque c diminue. La sensibilité relative, qui est le critère le plus important pour une méthode d'analyse recourant à des solutions étalons, tient compte non seulement de la pente dh/dc, mais également de la valeur absolue de h. On peut la définir par la nouvelle fonction:

$$H_c = (dh_c/dc) \cdot h_c$$

fonction dont la dérivée première par rapport à c est une constante, donc indépendante de c. On en déduit que la sensibilité relative de la méthode, pour une température et un temps de réaction donnés, est toujours la même, quels que soient la concentration de l'échantillon et/ou le rendement de la dialyse. La méthode

proposée est donc particulièrement avantageuse si le composé à doser se trouve en faible quantité, puisque la limite de détection s'en trouve ainsi abaissé.

Un essai consistant à faire varier chaque fois de 1% la concentration en lactose d'une solution donnée (100% relatifs égalent ici 1,25 g l^{-1}*) a donné les résultats que présente le Tableau II. La sensibilité obtenue permet donc une mesure exacte à $\pm 1\%$ relatif.

TABLEAU II

SENSIBILITÉ DE LA MÉTHODE

Concentration du lactose		*h(mm) à 85°C*[a] *(sur 100 mV)*	*h(mm) à 75°C*[a] *(sur 50 mV)*
Relative (%)	*Absolue (g l^{-1})*		
96	1,200	175	224
97	1,213	176	225
98	1,225	177	226
99	1,238	178	228
100	1,250	178	228

[a] Hauteur *h* du plateau enregistré (sur 50 mV ou 100 mV), à $\pm 0{,}5$ mm près.

Spécificité

La méthode proposée n'est pas, en elle-même, spécifique au dosage d'un composé donné (au lactose par exemple) à l'exclusion de tout autre. Aussi tous les essais, à une exception près, ont-ils été effectués jusqu'ici avec des solutions ne contenant que du lactose (en montant parfois un dialyseur pour simuler une application au lait). Il était en effet préférable de développer et de mettre au point ce nouveau type d'analyseur en flux continu dans les conditions idéales qu'offre le dosage d'une substance pure.

Il est clair que, dans la pratique, de telles conditions de travail ne se rencontrent que rarement. Dans la plupart des cas, la matrice est complexe et interfère avec la réaction rédox désirée. Lors de l'étude de l'application manuelle de cette méthode au dosage cérimétrique du lactose du lait, il s'est avéré que les protéines lactiques donnent une très importante réaction rédox avec le cerium(IV). Il avait alors été proposé d'éliminer ces dernières par l'une des techniques classiques auxquelles on recourt en pareil cas: la dialyse ou la précipitation. Les essais de spécificité sont très simples: on fait passer successivement un échantillon de lait (contenant 50 g l^{-1} de lactose) et une solution ne contenant que du lactose (à 50 g l^{-1} également). Si la séparation (par dialyse ou par précipitation) est quantitative, on doit retrouver le même signal.

L'expérience montre malheureusement qu'il n'en va pas ainsi:

(a) Avec une dialyse (contre l'eau), on obtient des pics à l'équilibre de 230 mm de hauteur pour le lait, contre 176 mm seulement pour la solution ne contenant

* On tient compte du rendement de la dialyse qui est environ 2,5% (*cf. Vérification de la (pseudo)-linéarité–Avec dialyse*).

que du lactose (la température de réaction est de 75°C; l'enregistreur est utilisé sur 50 mV; les autres conditions expérimentales sont les mêmes que précédemment).

(b) Avec une précipitation par l'acide trichloracétique, on obtient des pics (équilibre également atteint) de 210 mm de hauteur pour le lait, contre 160 mm pour la solution équivalente de lactose (les conditions expérimentales sont les mêmes que pour (a), sauf pour l'enregistreur utilisé sur 200 mV, les solutions de lactose étant plus concentrées).

À concentration égale en lactose, on remarque donc que le signal obtenu avec le lait est nettement plus grand que celui obtenu avec la solution de lactose, quel que soit le mode d'élimination des protéines utilisé (a ou b). On en déduit que ces deux techniques ne peuvent hélas éliminer quantitativement les autres composants du lait qui réagissent aussi avec le cerium(IV). L'essai (b) a été répété à deux autres températures pour la réaction rédox, l'une inférieure (45°C) et l'autre supérieure (90°C), les solutions (lait et lactose pur) étant testées à deux concentrations différentes (45 et 50 g l^{-1}). Les résultats sont consignés dans le Tableau III. Cette dernière expérience confirme la conclusion précédente. On remarque en effet que la difference relative des signaux obtenus avec le lait et avec la solution de lactose décroît lorsque la température augmente. La raison en est vraisemblablement la suivante: le coefficient Ψ_1 (nombre d'équivalents de réducteur que fournissent pendant la réaction les substances rédox autres que le lactose) augmente moins que le coefficient Ψ_2 (nombre d'équivalents de réducteur que fournit le lactose pendant la réaction rédox) avec la température. C'est donc bien une preuve de la présence dans le lait (après déprotéinisation) de substances réductrices autres que le lactose, plus réactives même que ce dernier vis à vis du cerium(IV). C'est probablement la raison pour laquelle on ne trouve semble-t-il pas d'exemple dans la littérature de dosage cérimétrique des glucides dans des milieux biologiques; on recourt pratiquement toujours au $K_3[Fe(CN)_6]$ qui est un oxydant beaucoup plus faible ($E_0 = 1{,}44$ V à 25°C pour le couple Ce(IV)/Ce(III), contre $E_0 = 0{,}46$ V à 25°C et à pH = 12 pour le couple $[Fe(CN)_6]^{3-}/[Fe(CN)_6]^{4-}$) donc moins sensible, mais plus sélective.

TABLEAU III

SPÉCIFICITÉ APRÈS TRAITEMENT À L'ACIDE TRICHLORACÉTIQUE

Température réaction rédox (°C)	*Hauteur du pic (plateau) enregistrés (en mm)*[a]			
	Sol. lactose (45 g l^{-1})	*Sol. lactose (50 g l^{-1})*	*Lait (45 g l^{-1})*	*Lait (50 g l^{-1})*
45	53±1	61±1	232±1	249±1
75	308±2	320±2	390±2	420±2
90	550±5	610±5	690±5	770±5

[a] Les hauteurs indiquées pour les pics à 75° et 90°C ont été rapportées à 100 mV/250 mm.

Une étude de la concordance de cette méthode avec une méthode de référence (coefficient de corrélation) ne se justifie donc pas dans le cas d'une application au lait.

Conclusion

Le modèle théorique[1], déjà vérifié manuellement en discontinu[2], est également vérifié en flux continu. L'analyseur automatique proposé dans ce travail est utilisable en principe pour n'importe quel couple rédox (réversible ou non). Si le cerium(IV) est un oxydant insuffisamment sélectif pour doser le lactose dans le lait, à cause des réactions que produisent les autres composants de la matrice, le dosage rédox étudié est néanmoins intéressant en tant qu'exemple. Puisque la méthode générale proposée permet de travailler entre n'importe quelles étapes *i* et *j* de la réaction rédox, on pourrait éventuellement faire subir au lait un prétraitement (différentiel) pour oxyder au maximum les composants indésirables du lait tout en ménageant le lactose, mais un tel dosage perdrait alors beaucoup de son intérêt pour la pratique (il faudrait encore faire disparaître ce réactif intermédiaire). Mieux vaut recourir à un changement d'oxydant (par exemple $K_3[Fe(III)(CN)_6]$). L'application possible de cette même méthode pour le dosage des solides totaux non gras du lait entier[2] n'a pas encore été testée.

RÉSUMÉ

La première partie du présent travail a pour objet le développement d'un analyseur automatique conçu pour des mesures de systèmes rédox par potentiométrie différentielle en flux continu. Sur la base d'un diagramme des flux, diverses variantes sont étudiées pour la réalisation pratique de cet analyseur, en ce qui concerne notamment le choix des matériaux, la disposition des composants, la thermostatisation du "manifold", la géométrie des électrodes et du pont électrolytique. La seconde partie du travail est consacrée aux résultats obtenus lors de l'utilisation de cet analyseur pour le dosage cérimétrique d'un glucide (le lactose) dans des solutions pures d'abord, puis le lait (matrice complexe). Les essais effectués visent à déterminer l'influence des conditions expérimentales (température et temps de réaction), à vérifier la (pseudo)linéarité, puis la reproductibilité, la sensibilité et la spécificité de la méthode. Les résultats concordent parfaitement avec ceux obtenus manuellement en discontinu (*cf.* Partie II), ce qui vérifie donc à nouveau le modèle théorique général proposé (*cf.* Partie I). On constate néanmoins que le Ce(IV) est un oxydant trop puissant pour un dosage dans le lait. Si cet oxydant est intéressant parce qu'il augmente considérablement la sensibilité de la méthode (le $\Delta E_{\text{rédox}}$ associé est d'autant plus grand que la réaction rédox est importante), il est par contre insuffisamment spécifique: ni la dialyse, ni la précipitation dans l'acide trichloracétique ne parviennent à éliminer quantitativement toutes les substances qui peuvent réagir avec le Ce(IV), même à froid. L'emploi d'un oxydant plus ménageant doit être envisagé, tel le $K_3[Fe(III)(CN)_6]$ par exemple.

SUMMARY

The development of an automatic analyzer for the measurement of redox systems by differential potentiometry in continuous flow is described. Variations in several instrumental parameters were studied. The analyzer was applied to the determination of a carbohydrate (lactose) with cerium(IV) solution, first in distilled water and then in milk. The results obtained in examining the influence of different

experimental conditions, and the linearity, sensitivity and the specificity of the method, confirmed the previous results obtained manually. However, cerium(IV) proved to be too strong an oxidant for the measurement of lactose in milk. Cerium(IV) increased the sensitivity of the method, but was insufficiently selective; neither dialysis nor precipitation with trichloracetic acid eliminated quantitatively all interferences, even at low temperatures. Milder oxidants are necessary.

RÉFÉRENCES

1 J. O. Bosset, B. Blanc et E. Plattner, *Anal. Chim. Acta*, 67 (1973) 403.
2 J. O. Bosset, B. Blanc et E. Plattner, *Anal. Chim. Acta*, 68 (1973) 161.
3 D. G. Porter and R. Sawyer, *Analyst (London)*, 97 (1972) 569.
4 G. K. Buckee, *J. Inst. Brew, London*, 78 (1972) 222.
5 J. O. Bosset, B. Blanc et E. Plattner, *Anal. Chim. Acta*, 75 (1975) 474.
6 P. Van den Winlzel, J. Mertens and D. L. Massart, *Anal. Chem.*, 46 (1974) 1765.

Analytica Chimica Acta, 77 (1975) 183–190

EXTRACTION OF METALS BY NEUTRAL SULFUR-CONTAINING EXTRACTANTS

PART I. O-ISOPROPYL-N-ETHYLTHIOCARBAMATE

I. V. SERYAKOVA, G. A. VOROBIOVA, A. V. GLEMBOTSKY and YU. A. ZOLOTOV

V. I. Vernadsky Institute of Geochemistry and Analytical Chemistry, USSR Academy of Sciences, Moscow (U.S.S.R.)

(Received 7th January 1975)

Extraction of metals in the form of neutral coordinately solvated compounds by oxygen-containing extractants is a well known process. However, the selectivity of extraction by oxygen-containing extractants is, as a rule, not very high. The reason is that these extractants may extract metals not only in the form of coordinately solvated compounds, but also in the form of complex acids. The oxygen-containing extractants are relatively easily introduced into the coordination sphere of most metals and are also easily protonated, the latter being the condition for complex acid extraction.

The selectivity of neutral sulfur-containing extractants must be higher as they usually are protonated only with difficulty, especially compounds with the thiocarbonyl group[1]. Therefore solutions of such extractants in inert diluents should not extract metal-containing acids. Moreover, these extractants give coordinately solvated neutral complexes only with those elements which strongly bind sulfur—Ag, Au, Hg, Cu(I) and Pd. High selectivity with regard to such metals is displayed by dialkyl sulfides[2–4]; trialkylthiophosphates and trialkylphosphine sulfides[5,6], and alkylthiophosphoramides[7].

If the anion of the mineral acid and its concentration are changed, as well as the extractant (changing the donor–acceptor properties of sulfur), conditions for the separation of some chalcophilic metals from each other may be selected. It is of importance that the promising extractants are some sulfur-containing compounds which are used on a large scale for other purposes (additives to oils, flotation reagents, etc.). The possibility of selective extraction of silver with diphenylthiourea has already been described[8].

The present paper contains the results of a systematic investigation of the extraction of many elements by one of the effective flotation reagents and collectors, O-isopropyl-N-ethylthiocarbamate (IPETC; the technical name of the flotation reagent[9] is Z-200). Preliminary results of investigations have already been published[10,11].

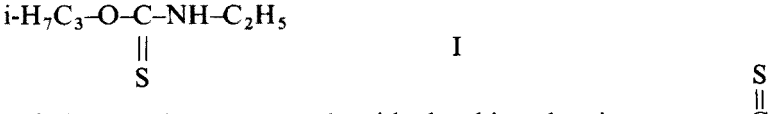

I

It is known that compounds with the thiocarbamino group, –C(=S)–NH, are

capable of tautomerization with the formation of the thiol form –C(SH)=N–. According to data from an i.r. spectroscopic investigation, dialkylthiocarbamates in the pure form and in solutions in a polar solvent, are present in the thione form; IPETC is in this form in acidic and neutral aqueous solutions. Only in alkaline solutions (>1% NaOH) is the reagent present in the thiol form according to u.v. spectrophotometric data[12].

EXPERIMENTAL

Reagents and chemicals

Pure IPETC is a clear slightly yellowish liquid. It was synthesized from potassium propylxanthate and ethylamine[13] and purified by distillation under vacuum (b.p. 97–98°C at 8 mm Hg). A 0.05 *M* solution of the reagent in chloroform was used. Chloroform was washed with water, distilled and stabilized with 1% of ethyl alcohol.

Acidified solutions of metal nitrates or sulfates were used; these were labeled with radioactive isotopes (^{64}Cu, ^{110}Ag, ^{198}Au, ^{65}Zn, ^{115m}Cd, ^{203}Hg, ^{72}Ga, ^{114m}In, ^{204}Tl, ^{207}Bi, ^{99}Mo, ^{185}W, ^{75}Se, ^{125m}Te, ^{59}Fe, ^{60}Co). The concentrations of the metals in solution before extraction were 10^{-5}–10^{-6} g-ion l^{-1}. Bismuth was used as a chloride solution containing 10^{-8} g-ion l^{-1}. Gold, as tetrachloroauric acid was converted to a sulfate solution by evaporation with a large excess of sulfuric acid. Copper(I) solution was obtained by treatment of aqueous copper(II) solution with ascorbic acid in the presence of chloride[14].

Mineral acids (HCl, HBr, HNO_3, H_2SO_4 and $HClO_4$) and KCl, KBr and KI (reagent grade) were used without additional purification. Hydroiodic acid was purified from iodine by extraction with a 15% (v/v) tributyl phosphate solution in benzene and then distilled; freshly prepared hydroiodic acid was used. Concentrations of acids were established by titration with alkali, and solutions of known acidity were prepared by appropriate dilution.

Procedure

A solution of metal salt (3 ml) containing a definite amount of mineral acid, or a mixture of sulfuric acid and potassium halide, was mechanically shaken for 5 min (or longer) at 20–22°C with an equal volume of a 0.05 *M* IPETC solution in chloroform. The phases were separated and the radioactivity of aliquot parts was measured on a scintillation γ-counter with a Na(Tl)I crystal or on a β-counter of the MST-17 type.

The extractions of Cu(I,II), Ag, Au(III), Zn, Cd, Hg(II), Ga, In, Tl(I,III), Bi,Mo(VI), W(VI), Se(IV,VI), Te(IV), Fe(III) and Co were investigated in the presence of Cl^-, Br^-, I^-, NO_3^-, ClO_4^- and SO_4^{2-} ions.

RESULTS AND DISCUSSION

Extraction from halide solutions

The extraction of elements from solutions containing 2.5 *M* sulfuric acid and potassium halide was first studied. Under these conditions, silver, mercury(II),

TABLE I

EXTRACTION OF METALS BY IPETC SOLUTION FROM 2.5 *M* SULFURIC ACID SOLUTION CONTAINING POTASSIUM HALIDE

Halide ion	*Amount added (g-ion l^{-1})*	*Distribution coefficients*						
		Cu(I)	*Cu(II)*	*Ag*	*Hg(II)*	*Au(III)*	*Tl(III)*	*SeIV,V*
Chloride	0.3	0.2	~0.01	$>10^2$	~50	—[a]	~0.1	~0.05
	1.2	1.2	~0.01	$>10^2$	~50	—[a]	~0.1	~0.05
	2.6	13	~0.01	$~10^2$	~50	—[a]	~0.1	~0.05
Bromide	0.3	1.5	0.05	$>10^2$	7	—[a]	10	12
	1.2	$>10^2$	1.5	3.0	0.8	$>10^2$	3.0	12
	3.3	$>10^2$	13	0.5	0.3	$>10^2$	1.2	15
Iodide	0.3	$>10^2$	—	0.1	0.03	$>10^2$	30	10
	1.2	$>10^2$	—	0.003	0.005	1.5	8.0	—[a]
	3.3	$>10^2$	—	0.003	0.003	13	1.5	—[a]

[a] Poor mass balance.

gold(III), copper(I,II), thallium(III), selenium(IV,VI) and, partly, tellurium and molybdenum were extracted. The values of the distribution coefficients of these elements (*D*) obtained in the presence of halide at concentrations of 0.3–3.3 (2.6) g-ion l^{-1} (the upper limit was determined by the potassium halide solubility) are listed in Table I. The other elements studied, *i.e.* zinc, cadmium, gallium, indium, bismuth, tungsten, iron and cobalt, were practically not extracted.

Silver, mercury, copper(II) and thallium(III) extractions were also studied from HCl, HBr and HI solutions of different concentrations (Figs. 1–3). From chloride solutions, only silver and mercury were effectively extracted over a wide range of chloride concentrations; copper was extracted only at high concentrations of hydrochloric acid (above 6 *M*). From bromide solutions, gold, copper, silver, mercury, thallium and selenium were readily extracted. Copper and gold extraction was effective at high concentrations of bromide. Thallium, silver and mercury, on the contrary, were better extracted from solutions which were less concentrated in bromide (up to 0.5–1 *M*).

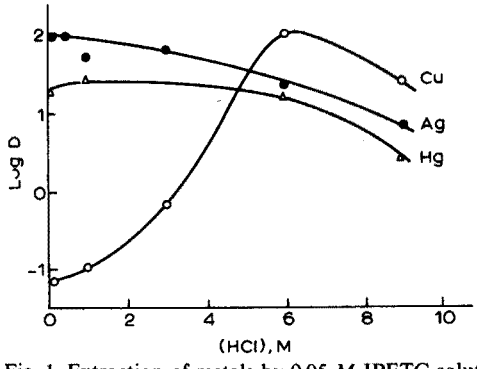

Fig. 1. Extraction of metals by 0.05 *M* IPETC solution in $CHCl_3$ depending on HCl concentration.

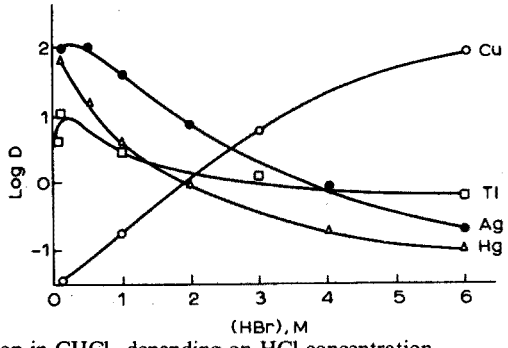

Fig. 2. Extraction of metals by 0.05 *M* IPETC solution in $CHCl_3$ depending on HBr concentration.

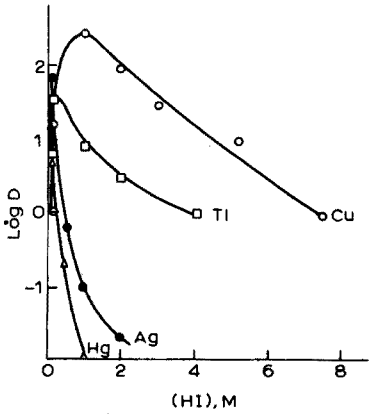

Fig. 3. Extraction of metals by 0.05 *M* IPETC solution in $CHCl_3$ depending on HI concentration.

From iodide solutions, gold and copper were extracted over a fairly wide range of iodide concentrations. Thallium was better extracted at low concentrations of iodides. Silver and mercury could only be extracted from solutions with iodide connected with IPETC oxidation and may be used for silver back-extraction.
detail. At least a 10-fold excess of iodide was necessary for complete thallium extraction from 2.5 *M* sulfuric acid. The upper limit of iodide concentration was slightly lowered with increase in the thallium concentration; thallium was completely extracted at the 10^{-4} g-ion l^{-1} level from up to 0.5–1 *M* iodide solutions, but at the $5 \cdot 10^{-3}$ g-ion l^{-1} level from up to 0.2–0.3 *M* potassium iodide solutions.

Extraction from solutions of oxygen-containing acids

Of all the elements studied, only silver and mercury could be extracted from perchloric, nitric and sulfuric acid solutions. Silver was quantitatively extracted over a wide concentration range of sulfuric and perchloric acids: up to 10 *M* sulfuric acid or 6 *M* perchloric acid. When nitrate solutions were used, extraction was complete only up to 5 *M* nitric acid; with further increases in the acid concentration, the distribution coefficients of silver decreased, which is apparently connected with IPETC oxidation and may be used for silver back-extraction

TABLE II

DISTRIBUTION COEFFICIENTS FOR SILVER AND MERCURY FROM SULFURIC ACID SOLUTIONS

(Values are given as log *D*)

Metal	*Metal concentration (g-ion l^{-1})*	*H_2SO_4 concentration (M)*				
		0.1	*0.5*	*2.5*	*5*	*10*
Silver	$2.5 \cdot 10^{-5}$	2.0	2.1	2.5	2.5	2.5
	$1.0 \cdot 10^{-3}$	>2	—	—	—	2.5
Mercury	$1.5 \cdot 10^{-5}$	−0.1	−0.1	−0.4	−0.52	−1.5

TABLE III

DISTRIBUTION COEFFICIENTS FOR SILVER AND MERCURY EXTRACTED FROM 10 *M* SULFURIC ACID BY 0.05 *M* IPETC SOLUTION

Hg:Ag ratio	*Concentration (g-ion l^{-1})*		*Distribution coefficient*	
	Hg	*Ag*	*Hg*	*Ag*
1:1.7	$1.5 \cdot 10^{-5}$	$2.5 \cdot 10^{-5}$	0.02	140
1:5	$1.0 \cdot 10^{-3}$	$5.0 \cdot 10^{-3}$	0.002	15
1:330	$1.5 \cdot 10^{-5}$	$5.0 \cdot 10^{-3}$	0.003	—
40:1	$1.0 \cdot 10^{-3}$	$2.5 \cdot 10^{-5}$	—	97

Mercury, like silver, was quantitatively extracted from perchloric and nitric acids, but differed in its behavior during extraction from sulfuric acid solutions. Table II shows the values for the distribution coefficients of silver and mercury (taken as their nitrate salts) depending on the concentration of sulfuric acid. Mercury extraction became poorer as the sulfuric acid concentration increased, so that from 10 *M* sulfuric acid only 1–2% of mercury was extracted.

Silver at concentrations of 10^{-5}–$5 \cdot 10^{-3}$ g-ion l^{-1} was quantitatively extracted from sulfuric acid solutions; the distribution coefficients for mercury increased with increase in its concentration for extraction from 2.5 *M* sulfuric acid:

[Hg], g-ion l^{-1}	$1.5 \cdot 10^{5}$	$1 \cdot 10^{-4}$	$1 \cdot 10^{-3}$	$1 \cdot 10^{-2}$
D	0.4	1.3	3.1	27

The difference in the behaviour of silver and mercury may be used for the separation of these metals. The values of the distribution coefficients of silver and mercury obtained with the metal ions present simultaneously are given in Table III.

Effect of acidity on extraction

The influence of acidity on extraction of copper(I and II) and thallium(III)

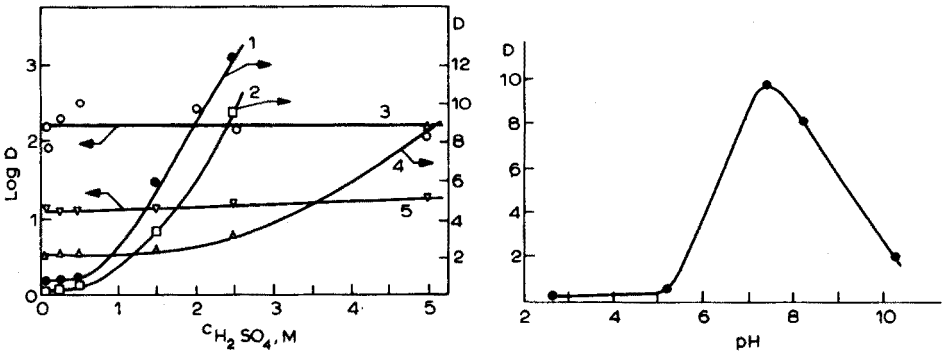

Fig. 4. Effect of acidity on copper(I and II) and thallium(III) extraction from bromide and iodide solutions by 0.05 *M* IPETC in $CHCl_3$. 1, Cu(II) in the presence of 2.7 *M* KBr; 2, Cu(I) in the presence of 1 *M* KBr; 3, Cu in the presence of 1 *M* KI; 4, Tl in the presence of 0.5 *M* KBr; 5, Tl in the presence of 0.5 *M* KI.

Fig. 5. Dependence of the distribution coefficient of copper(II) on pH.

from bromide and iodide solutions was studied (Fig. 4). The distribution coefficients of thallium and copper did not depend on the concentration of hydrogen ions during extraction from iodide solutions. When bromide solutions were used, thallium and especially copper extraction substantially increased with increase in the sulfuric acid concentration (beginning with 1.5–2.5 *M*). The copper yield was also substantial in extraction from neutral and slightly alkaline solutions (Fig. 5); under these conditions IPETC was present in the thiol form and extraction was probably accomplished by a cation-exchange mechanism.

Time of equilibrium

During the extraction of all elements studied, except for copper, the extraction equilibrium was established quite rapidly within 5 min. During extraction of copper, the time for equilibrium attainment depended on the nature of the inorganic ligand. In the presence of iodide, complete extraction was achieved within 3–5 min, while from chloride and bromide solutions, extraction was slower. A similar picture was also observed during extractions with diphenylthiourea[11]; in some cases a period of 60–80 min was necessary for attainment of equilibrium, possibly because copper was reduced by diphenylthiourea to copper(I)[15], the distribution coefficients of which are higher than for copper(II). However, the dependence of distribution coefficients on the time of shaking, when copper(I) is present in the initial solution, makes the extraction picture complicated.

Composition of compounds extracted

By means of radioactive isotopes of the elements under investigation, as well as bromide and iodide isotopes (^{82}Br and ^{131}I) taken in the form of ammonium bromide and sodium iodide, the metal–halide ratios in the complexes extracted were determined. Two series of experiments were conducted: in one series, extraction was carried out with the radioactive metal isotope and the stable halide isotope; in the other series, with all other conditions maintained strictly constant, the radioactive halide isotope and the stable metal isotope were used. During extraction in the presence of iodide, a correction was made for free iodine passing into the organic phase. The results obtained are listed in Table IV.

These data indicate that IPETC extracted metals in the form of mixed complexes, the composition of which involved halide neutralizing the metal charge and apparently the extractant in the molecular form. The amount of bromide in some silver extracts was less than required for stoichiometry, but this may be accounted for by the fact that nitrate is also a suitable co-ion (silver was also easily extracted from nitrate solutions containing no halide).

Gold was obviously extracted from iodide solutions in the monovalent state; the excess of iodide in the extract compared to stoichiometry can probably be explained by an error in the correction made for the extraction of elemental iodine isolated during the reaction.

The extraction of thallium, which is obviously extracted from iodide solutions in the trivalent state, is particularly worthy of note. This trivalent state is stabilized in the system because of the very firm bond with iodide ($\beta_{TlI_4} = 6.8 \cdot 10^{31}$)[16], and also because of an equilibrium shift towards the formation of a different ligand complex ($TlI_3 \cdot pS$]. The solvate number found from the relationship between log *D*

TABLE IV

RESULTS OF THE ANALYSIS OF EXTRACTS

(Extraction was carried out from 2.5 *M* H_2SO_4 in the presence of KX(X=Br,I).)

Metal (M)	*Metal concentration (g-ion l^{-1})*	*KX concentration (M)*	*X:M ratio*
Ag	$1 \cdot 10^{-3}$	0.01[a]	1.0
	$1 \cdot 10^{-4}$	0.01[a]	0.7
Cu	$5 \cdot 10^{-3}$	0.5[b]	1.0
Hg	$1 \cdot 10^{-4}$	0.001[a]	2.0; 2.5
Tl	$1 \cdot 10^{-4}$	0.005[a]	2.9
	$1 \cdot 10^{-4}$	0.005[b]	4.2
Au	$1 \cdot 10^{-4}$	0.001[b]	2.0; 1.3

[a] Potassium bromide.
[b] Potassium iodide.

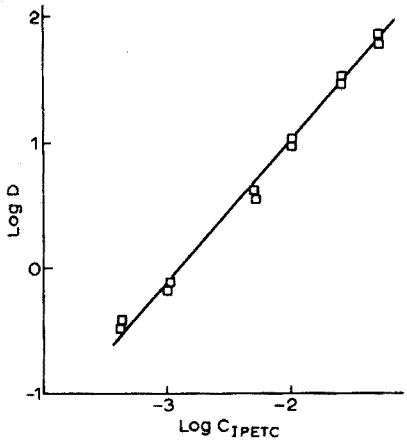

Fig. 6. Dependence of the distribution coefficient of thallium(III) on IPETC concentration. Extraction from 0.25 *M* H_2SO_4 in the presence of 0.1 *M* KI.

and log [IPETC] is equal to 1 (Fig. 6). The fact that, after back-extraction of elemental iodine by thiosulfate, all the thallium and a substantial part of the radioactive iodine remain in the organic phase indicates that thallium(III) iodide is extracted rather than thallium(I) iodide[17]. The excessive I:Tl ratio in the extract (Table IV) was probably obtained because the free iodine was not completely washed out of the extract. Of importance also is the fact that if thallium is initially present in the monovalent state, it cannot be extracted. Attempts to obtain unambiguous data during the determination of the Tl/I ratio by the slope method were unsuccessful, because in the region of very low iodide concentrations, the values of the distribution coefficients were not reproducible. This irreproducibility is probably connected with differences in the elemental iodine concentration in the system.

SUMMARY

The formation of neutral mixed complexes of the MX_mS_p type (where M is a metal ion with $m+$ charge, X the inorganic anion, and S the sulfur-containing extractant) allows a selective extraction of various elements. The extraction of many metals from mineral acid solutions or from halide–sulfuric acid mixtures by 0.05 *M* O-isopropyl-N-ethylthiocarbamate (IPETC) solution in chloroform has been studied. IPETC possesses very high selectivity for silver and mercury ions in extractions from HNO_3, H_2SO_4, $HClO_4$ and HCl solutions. In addition to silver and mercury, Cu, Au, Tl and Se are readily extracted from solutions containing bromide. From iodide solutions, copper, gold and thallium ions may be selectively extracted because silver and mercury cannot be extracted at concentrations of iodide above 0.1 *M*. IPETC extracts metals as mixed complexes, containing the halide and apparently the extractant in the molecular form.

REFERENCES

1 W. I. Congdon and J. T. Edward, *J. Amer. Chem. Soc.*, 94 (1972) 6096.
2 A. V. Nikolaev, V. G. Torgov, E. N. Gilbert, V. A. Mikhailov, V. A. Pronin, L. G. Stadnikova and I. L. Kotlyarevsky, *Izv. Sib. Otd. Akad. Nauk SSSR*, No. 14, *Ser. Khim. Nauk*, (1967) 129.
3 V. G. Torgov, V. N. Andrievsky, E. N. Gilbert and I. L. Kotlyarevsky, *Izv. Sib. Otd. Akad. Nauk SSSR*, No. 12, *Ser. Khim. Nauk*, 5 (1969) 148.
4 V. A. Mikhailov, V. G. Torgov and A. V. Nikolaev, *Izv. Sib. Otd. Akad. Nauk SSSR*, No. 7, *Ser. Khim. Nauk*, 3 (1973) 3.
5 T. H. Handley and J. A. Dean, *Anal. Chem.*, 32 (1960) 1878.
6 D. E. Elliot and C. V. Banks, *Anal. Chim. Acta*, 33 (1965) 237.
7 T. H. Handley, *Anal. Chem.*, 36 (1964) 2467.
8 I. V. Seryakova, G. A. Vorobiova and Yu. A. Zolotov, *Zh. Anal. Khim.*, 27 (1972) 1840.
9 A. V. Glembotsky, *Investigation of dialkylthiocarbamates reagent-collectors during flotation of copper–molybdenic sulfide ores*, Dissertation, Gintsvetmet, Moscow, 1968.
10 Yu. A. Zolotov, I. V. Seryakova and G. A. Vorobiova, *IV Conference on Extraction Chemistry, May 15–18 1973, Donetsk, Abstracts of papers*, Donetsk, 1973, p. 58.
11 Yu. A. Zolotov, I. V. Seryakova, G. A. Vorobiova and A. V. Glembotsky, *Dokl. Akad. Nauk SSSR*, 209 (1973) 909.
12 A. K. Livshits, A. V. Glembotsky and S. M. Gurvich, *Tsvet. Met.*, 2 (1968) 19.
13 C. N. V. Nambury, *J. Vikram. Univ.*, 2 (1958) 101; *Chem. Abstr.*, 54 (1960) 4382.
14 T. H. Handley and J. A. Dean, *Anal. Chem.*, 33 (1961) 1087.
15 V. M. Shulman, Z. A. Savelyeva, I. M. Cheremisina, Ya. V. Vasilyev and V. F. Anufrienko, *Izv. Sib. Otd. Akad. Nauk SSSR*, No. 2, *Ser. Khim. Nauk*, 1 (1972) 77.
16 F. A. Cotton and G. Wilkinson, *Advanced Inorganic Chemistry, Vol. 2*, Interscience, New York, 1972.
17 F. Ya. Kulba and V. E. Mironov, *Khimia thallia*, Goskhimizdat, Leningrad, 1963, p. 145.

Analytica Chimica Acta, 77 (1975) 191–198

FLUORIMETRIC ASSAY OF SERUM GLUTAMATE OXALOACETATE TRANSAMINASE, GLUTAMATE PYRUVATE TRANSAMINASE AND α-HYDROXYBUTYRATE DEHYDROGENASE BY SOLUTION AND SOLID SURFACE FLUORESCENT METHODS

B. RIETZ and G. G. GUILBAULT*

Chemistry Department A, Technical University of Denmark, 2800 Lyngby (Denmark)

(Received 25th November 1974)

The enzymes glutamate oxaloacetate, transaminase (GOT) and glutamate pyruvate transaminase (GPT) catalyze the transfer of an amino group to an α-keto group of α-ketoglutaric acid. α-Hydroxybutyrate dehydrogenase (α-HBD) catalyzes the reversible conversion of α-hydroxybutyrate to α-ketobutyrate:

$$\alpha\text{-Hydroxybutyrate} + \text{NAD} \underset{\text{pH 7.4}}{\overset{\text{pH 9}}{\rightleftharpoons}} \alpha\text{-ketobutyrate} + \text{NADH} \qquad (1)$$

All three enzymes are of clinical significance, elevated values in serum indicating myocardial, hepatic and jaundice diseases.

Many spectrophotometric methods exist for the assay of these enzymes[1–6], all based on a measurement of the decrease in absorbance of NADH ($\lambda_{max} = 340$ nm) in eqns. (1), (3) or (5):

$$\text{L-Aspartate} + \alpha\text{-ketoglutarate} \overset{\text{GOT}}{\rightleftharpoons} \text{oxaloacetate} + \text{L-glutarate} \qquad (2)$$

with coupled reaction:

$$\text{Oxaloacetate} + \text{NADH} + \text{H}^+ \xrightarrow{\text{pH7.4}} \text{malate} + \text{NAD} \qquad (3)$$

$$\text{L-Alanine} + \alpha\text{-ketoglutarate} \overset{\text{GPT}}{\rightleftharpoons} \text{pyruvate} + \text{L-glutarate} \qquad (4)$$

with coupled reaction:

$$\text{Pyruvate} + \text{NADH} + \text{H}^+ \xrightarrow{\text{pH7.4}} \text{L-lactate} + \text{NAD} \qquad (5)$$

Some fluorimetric methods for assay have been described[7–10], most of which are based on the use of NADH fluorescence and the Autoanalyzer. Many of these methods are time-consuming and require relatively large amounts of reagents and expensive equipment.

Recently, a new, more stable and less expensive reagent for the assay of these enzymes was described and evaluated: a reagent tablet (35–350 mg) stabilized by the addition of mannitol, sucrose and PEG-4000. A comparison of the use of this reagent tablet *versus* ordinary reagent kits in the accepted spectrophotometric

* Guest Professor of Analytical Chemistry on leave from the University of New Orleans, Louisiana.

assay used in most clinical laboratories[11] showed that the tablets are very useful for reliable, precise assays of these enzymes.

In this paper, the use of these excellent reagent tablets is described in fluorimetric methods for the assay of GOT, GPT and α-HBD, both in solution and via the reagentless solid-surface method developed by Guilbault *et al.* for the assay of cholinesterase[12], alkaline phosphatase[13], LDH[14], creatinephosphokinase[15], urea[16] and γ-L-glutamyl transpeptidase[17]. The resulting procedures have the characteristic advantages of the higher sensitivity of fluorimetric procedures, as well as simplicity, speed and precision.

EXPERIMENTAL

Reagents

Serum. Monitrol I and II (freeze-dried human serum of standard activity, Dade, Miami, Florida) were used for preparation of calibration plots. Final studies were performed with fresh blood serum samples from Rigshospitalet, Copenhagen.

For assay of GOT and GPT. Dade reagent tablets (experimental samples, 50 mg, Dade, Miami) contained all the reagents for GOT or GPT assay; mannitol and PEG-4000 are added to the tablets for stabilization and rapid solubilization in water.

For assay of α-HBD by reverse reaction (eqn. 1). Dade reagent tablets (experimental samples, 35 mg, Dade, Miami) contained all the reagents for the assay of α-HBD by the oxidation of NADH (reverse reaction, eqn. 1), including buffer, and sucrose and PEG-4000 for stability and rapid solubility in water.

For assay of α-HBD by forward reaction (eqn. 1). The reagents required were $5 \cdot 10^{-3}$ *M* β-nicotinamide adenine dinucleotide (NAD, Boehringer, Mannheim, Germany), $5 \cdot 10^{-3}$ *M* sodium-2-hydroxybutyrate (Fluka, Switzerland), 0.1 *M* glycine–hydrazine buffer pH 9.3 (Fluka), plus sucrose and mannitol (Analar, BDH, England) for stabilization.

Triply distilled water was used for preparing all solutions and dilutions.

Apparatus

All fluorimetric measurements were made on an Aminco filter fluorimeter with a Corning 7-60 primary filter ($\lambda = 365$ nm) for excitation and a Wratten combination 47B/48 secondary filter ($\lambda = 455$ nm) for emission. An RCA IP 28 photomultiplier was used as detector.

Semi-solid surface fluorescence measurements were made with the filter instrument set on its side (turned 90°) so that the pad and sample were placed in a horizontal position on the slide in the fluorimeter.

The fluorimeter was standardized daily with a 10^{-6} *M* solution of quinine sulfate in 0.05 *M* sulfuric acid.

Pipettes and micropipettes (10, 20, 30, 50, 100 μl, H.E. Pedersen, Copenhagen) were used to apply substrate, buffer and serum to the cuvettes (Pyrex) and onto the pads.

Procedures

Fluorimetric assay of GOT or GPT. Dissolve ten tablets for GOT or GPT

assay in 3.0 ml of distilled water. Place 0.5 ml of one of these solutions (solutions A and B) for each assay into the pyrex fluorimetric cell and add 2.5 ml of distilled water and 0.1 ml of Monitrol standard or serum to be assayed. Heat the resulting solution at 37°C for 3 min, and then record the change in fluorescence. Plot the fluorescence change per min (ΔF min^{-1}) *versus* the GOT or GPT concentration (I.U. l^{-1}) for a series of Monitrol standard serum samples. Obtain the GOT or GPT activity of the unknown serum from the calibration plot.

Fluorimetric assay of HBD. Dissolve five 35-mg tablets in 1.0 ml of distilled water. Place 0.5 ml of this solution (solution C) into the cuvette, add 2.5 ml of distilled water, heat at 37°C for 2.5 min, then add 0.1 ml of Monitrol standards or serum to be assayed, mix, and heat for an additional 0.5 min. Record the decrease in fluorescence with time, ΔF min^{-1}, and prepare a calibration plot using Monitrol standards. Calculate the activity of α-HBD present in serum from the calibration plot.

Semi-solid surface assay method for GOT, GPT and α-HBD. Prepare the silicone rubber pads for use as described by Lau and Guilbault[15]. Place 30 μl of solutions A, B or C (see above) onto each pad with the aid of a micropipette. Prepare a large number of pads simultaneously, enough for 30 days of α-HBD tests by the forward reaction (see below), or 3–4 days of GOT, GPT, and reverse reaction HBD tests (several hundred pads can be prepared for each test at one time). Place the pads in a vacuum desiccator (containing silica gel as desiccant) and lyophilize under vacuum for 1 h. The dried pads can be used immediately or can be stored in a closed brown bottle containing silica gel at −20 °C in the dark.

For assay, place a pad for either GOT, GPT or α-HBD on the slide in the center of the cell[15], add 50 μl of distilled water to reconstitute, and mix with a 1-μl pipette which has been sealed on the tip with a hot flame. After the well-mixed solution has been spread evenly over the whole pad, place the slide into the incident beam of the fluorimeter, and measure the background (this should be low and unchanging). Then add 10 μl of control serum or unknown serum to be assayed, mix, and record the change in fluorescence (for α-HBD immediately, and for GOT and GPT after a 3-min incubation). The measurement can be made at room temperature (21 °C in our case) or at 37 °C. Prepare calibration plots of ΔF min^{-1} *vs.* activity (I.U. l^{-1}), and calculate the activity present in the unknown serum from the calibration plot.

Semi-solid surface assay method for α-HBD (forward reaction)

Place 25 μl of NAD solution ($5 \cdot 10^{-3}$ *M*) and 25 μl of sodium-2-hydroxybutyrate ($5 \cdot 10^{-3}$ *M*) onto the pads, lyophilize and store as described above. Reconstitute the pads for use by adding 50 μl of glycine–hydrazine buffer (0.1 *M*, pH 9.3), and then add 10 μl of control serum or unknown to be assayed. Proceed as described above for α-HBD.

RESULTS AND DISCUSSION

Fluorimetric assay with Dade tablets

In a previous paper[11] the use of Dade reagent tablets was reported.

These tablets are a new concept in pre-packaged enzyme reagents in which all the necessary substrates, coenzymes and auxiliary enzymes for assay of GOT, GPT or α-HBD are placed together, with mannitol, sucrose and polyethylene glycol 4000 added, in the form of tablets of varying sizes: 35, 50 and 350 mg. The additives serve to both stabilize the tablet for long periods of time and to ensure that the tablet will dissolve instantly and homogeneously when placed in water. Excellent results were obtained in tests with these Dade pre-packaged reagents for the accepted spectrophotometric method used in most clinical laboratories.

The prepared tablets were therefore tested for use in sensitive fluorimetric methods, both in solution and on a reagentless semi-solid surface fluorescence technique[12–17], for the assay of these three enzymes.

Figure 1 shows a comparison of the results obtained fluorimetrically in solution with different Dade tablets and standards for assay of GOT. Plots A and B, obtained with Monitrol II and I as standards, show that a continuous linear range exists between 2.2 and 106 I.U. l^{-1}, when the 50-mg tablets are used. This is the lowest limit for reliable assay yet proposed. Slightly less sensitivity was obtained with the 35-mg tablets.

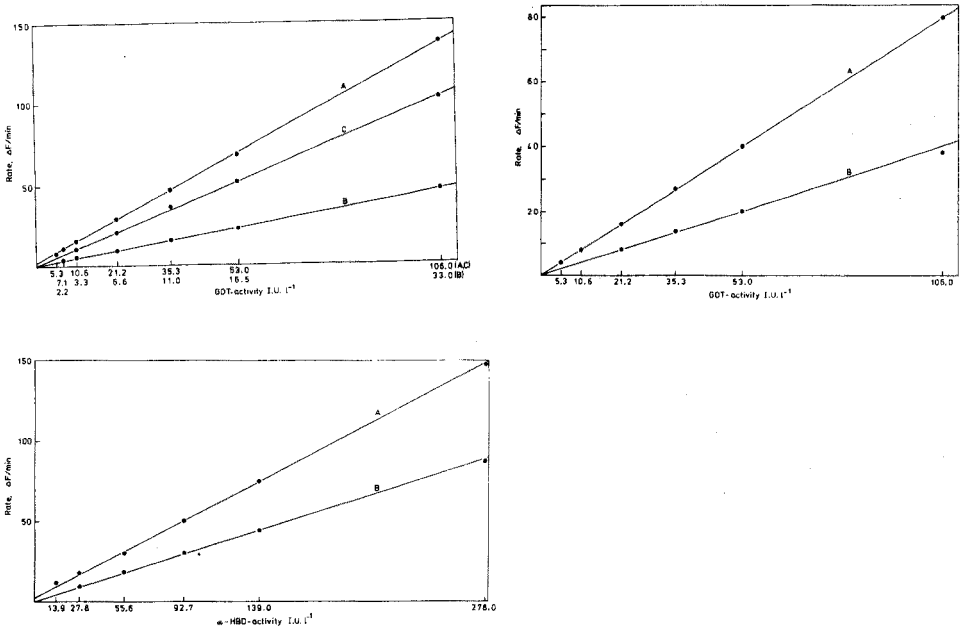

Fig. 1. Calibration plots for fluorimetric assay of GOT in solution. $T=37$ °C. (A) Monitrol II standards, 50-mg tablet; (B) monitrol I standards, 50-mg tablet; (C) monitrol II standards, 35 mg tablet.

Fig. 2. Calibration plots for solid surface assay of GOT. Monitrol II standards, 50-mg tablets; (A) 37°C; (B) 21°C.

Fig. 3. Calibration plots for fluorimetric assay of GPT. Monitrol II standards, 50-mg tablets. (A) 37°C; (B) 21°C.

Figure 2 shows the results obtained in the fluorimetric assay of GOT by the semi-solid surface method, at temperatures of 37°C (plot A) and 21°C (plot B). Since a lower limit of assay of GOT is possible at 37°C (5.3 I.U. l^{-1}) than at 21°C (21.2 I.U. l^{-1}), all further measurement were made at 37°C.

Figure 3 shows the calibration plots for assay of GPT with 50-mg tablets, Monitrol II as standard, and temperatures of 37°C (plot A, solution) and 21°C (plot B, pad); again, greater sensitivity is achieved at 37°C permitting a limit of detection of 5.3 I.U. l^{-1}.

Figure 4 shows a comparison of two types of tablets for the fluorimetric assay of α-HBD both in solution and on the pad, at the optimal temperature of 37°C. Monitrol II standards were used for preparation of the plots. The 35-mg tablets (plot A) showed a greater sensitivity than the 50-mg tablets (plot B) permitting the assay of as little as 13.9 I.U. of α-HBD per liter. Plots were linear up to 278 I.U. l^{-1}. All further measurements were made with the 35-mg tablets. In this case the decrease in fluorescence of NADH was measured (forward reaction, eqn. 1).

Figure 5 shows the calibration plot obtained in the assay of α-HBD by the reverse reaction of eqn. (1). *i.e.* the appearance of NADH fluorescence, rather than the disappearance of fluorescence in the above methods. A linear plot was obtained from 13.9 to 278 I.U. l^{-1} with Monitrol II as standard, at a temperature of 21°C. The results obtained with the NAD and hydroxybutyrate solutions in the reverse reaction were comparable to those obtained at 21°C with the forward reaction Dade tablets (Fig. 4, B). However, the pads for the former were much more stable than the latter, permitting storage for longer periods of time.

Blood sample analysis

Fresh blood sera were obtained from Rigshospitalet, Copenhagen, and were assayed by the two new fluorimetric methods proposed and also by a spectrophotometric method used in many hospitals (the method of Henry *et al.*[5], as modified by Rosalki and Wilkinson[6]). A comparison of the results obtained is shown in Tables I and II. The results from 6 blood samples for GOT showed that the fluorimetric and spectrophotometric methods agree quite well, the former

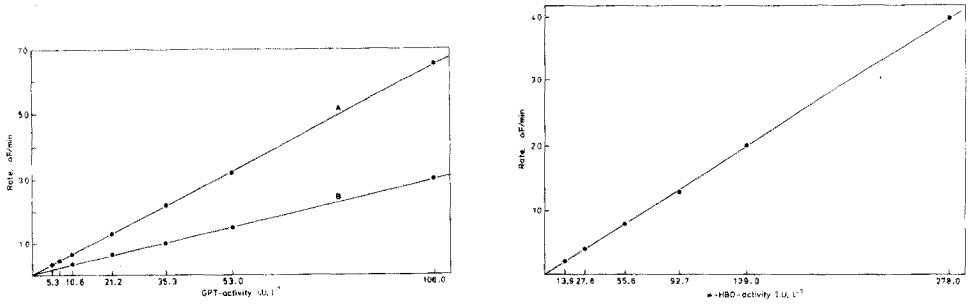

Fig. 4. Calibration plots for fluorimetric assay of α-HBD. $T = 37°C$, Monitrol II Standards. Reverse reaction (decrease of NADH). (A) 35-mg tablets; (B) 50-mg tablets.

Fig. 5. Fluorimetric assay of α-HBD by solid-surface method and forward reaction (NADH formation). $T = 21$ °C.

TABLE I

GOT-ASSAY IN BLOOD SAMPLES

Sample no.	Spectrophotometry[a]			Fluorimetry in solution[b]		
	I.U. l^{-1}	s^c	$s_r{}^c$(%)	I.U. l^{-1}	s	s_r (%)
1	25.0	1.4	5.6	25.2	1.2	4.6
2	150.0	14.1	9.4	154.0	0.6	0.4
3	22.5	1.1	4.7	24.0	1.0	4.5
4	20.0	1.1	5.3	21.5	0.6	2.9
7	30.0	2.1	7.1	30.0	1.7	6.0
8	70.0	3.5	5.1	75.5	1.0	1.5
	Average		6.2%			3.3%

[a] Results based on 2 measurements; method used, ref. (5).
[b] Results based on 3 measurements.
[c] Standard deviation and relative standard deviation.

TABLE II

α-HBD-ASSAY IN BLOOD SAMPLES

Sample no.	Spectrophotometry[a]			Fluorimetry in solution[b]			Fluorimetry (semi-solid state)[b,c]		
	I.U. l^{-1}	s	s_r (%)	I.U. l^{-1}	s	s_r (%)	I.U. l^{-1}	s	s_r (%)
6	138.0	8.5	6.2	139.0	0.6	0.8	140.0	2.3	5.0
7	150.0	8.5	5.7	156.0	2.6	3.1	151.0	1.5	3.1
8	130.0	7.1	5.5	136.0	1.7	2.3	143.0	1.6	3.5
9	140.0	6.4	4.6	143.0	2.9	3.7	146.0	1.0	2.1
10	155.0	8.5	5.5	158.0	3.1	3.6	148.0	2.5	5.3
	Average		5.5%			2.7%			3.8%

[a] Results based on 2 measurements; method used, ref. (6).
[b] Results based on 3 measurements.
[c] Reverse reaction

having a better precision ($s_r = 3.3\%$ compared to 6.2% for the spectrophotometric method).

The results for α-HBD assay show excellent agreement between the various methods (Table II). Again the fluorimetric methods possess better precision (2.7 and 3.8% compared to 5.5% for the spectrophotometric method). Generally, three or more analyses were run on each sample of Monitrol standard or blood serum.

Recovery of GOT and α-HBD added to blood serum

The addition of a GOT-standard (Monitrol II control serum) to a 31.5 I.U. l^{-1} blood serum sample up to a total activity of 84.5 I.U. l^{-1}, with Dade tablets for the assay, showed an average percentage recovery of 97.0–101.0% (assays performed fluorimetrically in solution).

The addition of an α-HBD-standard (Monitrol II) to a blood serum sample containing 143.0 I.U. l^{-1} of α-HBD up to a total activity of 282.0 I.U. l^{-1} showed

an average percentage recovery of 100.0–101.0% (assays performed fluorimetrically in solution, with tablets).

The addition of an α-HBD standard (Monitrol II) to a blood serum sample containing 148.0 I.U. l^{-1} of α-HBD up to a total activity of 287.0 I.U. l^{-1} showed an average percentage recovery of 97.0–101.0% (assays performed fluorimetrically on pad, with tablets).

This further illustrates the reliability of using Dade tablets and fluorimetric procedures for assays in actual blood sera.

Stability of pads and tablets

Substrate films on pads, made by lyophilizing solutions of Dade reagent tablets (containing stabilizers) are stable for only a few days (maximum a week) when stored in brown bottles (with desiccant) in darkness at −20°C. The pads produced from Dade tablets should be used as soon as possible after preparation.

The substrate films for the α-HBD forward reaction on the pad (reagents stabilized by addition of sucrose and mannitol) showed an excellent stability after 28 days of storage at −20°C in darkness in brown bottles with desiccant. Less than 10% deterioration was observed in 28 days. The greater stability of these forward reaction pads is probably because NAD is more stable on the pads than NADH used in the tablets.

A large batch of Dade tablets for the assay of GOT, GPT and α-HBD was stored at room temperature in brown bottles with desiccant (silica gel) for over 4 weeks. Periodic assays of these tablets were made by fluorimetric techniques. No deterioration of any of the tablets was noticed, and storage for longer periods seems feasible. Thus, unlike the reagent kits for enzyme assay which must be stored cold, under vacuum and in separate containers, large batches of tablets can be stored together at room temperature, if a disiccant is present. For this reason, and also since less reagent is needed per test with the tablets, a greater economy in cost per test is possible.

The extensive results shown above indicate that the reagent tablets work as well, or better, than the corresponding Dade reagents, and the fluorimetric methods proposed provide linear results over large ranges with good sensitivity, precision and accuracy. The pad method provides further simplicity to the assays with even more economy, freedom from reagent preparation, and availability for immediate testing.

A comparison shows that the results obtained by the fluorimetric methods are slightly higher than those obtained spectrophotometrically, but the agreement between these different methods is satisfactory. The fluorimetric methods have a better precision than the spectrophotometric methods and are more sensitive.

The financial assistance of the Danish Natural Science Research Council, Copenhagen, Denmark (No. 511-2873) in the form of a guest professorship for one of us (G.G.G.) and a fellowship for B.R. is gratefully acknowledged. The authors wish to thank Dade (Miami, Fla.) and Merz and Dade (Berne/Copenhagen) for donating the chemicals, control sera, and experimental reagent tablets evaluated; and Mr. J. Melchior Rasmussen of Rigshospitalet, Copenhagen, for providing the samples of blood serum.

SUMMARY

Fluorimetric methods have been developed for the determination of the activity of the enzymes GOT, GPT and α-HBD with Dade Reagent Tablets, both in solution and via a solid-surface method. In each case the rate of disppearance of NADH fluorescence at 455 nm ($\lambda_{ex}=365$ nm) was measured and equated to the concentration of these enzymes in control serum and blood serum. Pads were prepared for HBD assay with reagent films of the sodium salt of α-hydroxybutyrate and NAD; the fluorescence of the NADH produced on enzymic reaction was measured, and equated to α-HBD content of serum.

Linear responses were found in the ranges 2.2–106 I.U. GOT l^{-1}, 5–106 I.U. GPT l^{-1} and 14–278 I.U. α-HBD l^{-1}; agreement with standard accepted methods for the assay of these enzymes was excellent.

REFERENCES

1 A. Karmen, *J. Clin. Invest.*, 34 (1955) 131.
2 D. Steinberg, D. Baldwin and B. H. Ostrow, *J. Lab. Clin. Med.*, 48 (1956) 144.
3 F. Wroblewski and J. S. LaDue, *Proc. Soc. Exp. Biol. Med.*, 91 (1956) 569.
4 S. Reitman and S. Frankel, *Amer. J. Clin. Pathol.*, 28 (1957) 56.
5 R. J. Henry, N. Chiamori, O. J. Golub and S. Berkman, *Amer. J. Clin. Pathol.*, 34 (1960) 381.
6 S. B. Rosalki and J. H. Wilkinson, *Nature (London)* 188 (1960) 1110.
7 T. Laursen and G. Espersen, *Scand. J. Clin. Lab. Invest.*, 11 (1959) 61.
8 S. Passen and W. Gennaro, *Amer. J. Clin. Pathol.*, 46 (1) (1966) 69.
9 J. B. Levine and J. B. Hill, *2nd. Technicon Symp., New York 1965*, Mediad, Tarrytown, New York, 1966, p. 569.
10 J. C. Nixon and L. A. Cloutier, *Clin. Biochem.*, 2 (2) (1968) 115.
11 B. Rietz and G. G. Guilbault, *Clin. Chem. Acta*, in press.
12 G. G. Guilbault and R. L. Zimmerman, *Anal. Lett.*, 3 (1970) 133.
13 G. G. Guilbault and A. Vaughan, *Anal. Chim. Acta*, 55 (1971) 107.
14 R. L. Zimmermann and G. G. Guilbault, *Anal. Chim. Acta*, 58 (1972) 75.
15 H. K. Lau and G. G. Guilbault, *Clin. Chem.*, 19 (1973) 1045.
16 J. W. Kuan, H. K. Y. Lau and G. G. Guilbault, *Clin. Chem.*, 21 (1975) 67
17 B. Rietz and G. G. Guilbault, submitted to *Clin. Chem.*, June 1975.

Analytica Chimica Acta, 77 (1975) 199–203

SELECTIVE MICRO DETERMINATION OF UNCONJUGATED URONIC ACIDS BY FLUORESCENCE REACTIONS WITH ETHYLENEDIAMINE SULFATE

SUSUMU HONDA, KYOKO SUDO, KAZUAKI KAKEHI, HIDETAKA YUKI and KIYOSHI TAKIURA

Faculty of Pharmaceutical Sciences, Osaka University, Toneyama, Toyonaka, Osaka-fu (Japan)

(Received 16th August 1974)

Recently, it has been shown that reactions of reducing sugars with ethylenediamine sulfate in phosphate buffer produce a fluorescence having excitation and emission maxima at 400 and 465 nm, respectively; and these reactions were successfully applied to the micro determination of reducing sugars[1]. Further studies on the reactions of a variety of carbohydrates with this amine salt under various conditions showed that, when acetate buffer was used, another fluorescence having excitation and emission maxima at 328 and 406 nm, respectively, was formed specifically with uronic acids. This paper deals with a spectrofluorimetric method for the micro determination of uronic acids based on the latter reaction conditions. Under the neutral conditions employed, glycosidic linkages in aliphatic and aromatic uronides are not cleaved by hydrolysis. Therefore, unconjugated uronic acids can be determined accurately without interference from uronides.

Buffer and reagent

Among several kinds of buffer solutions having various pH values, acetate

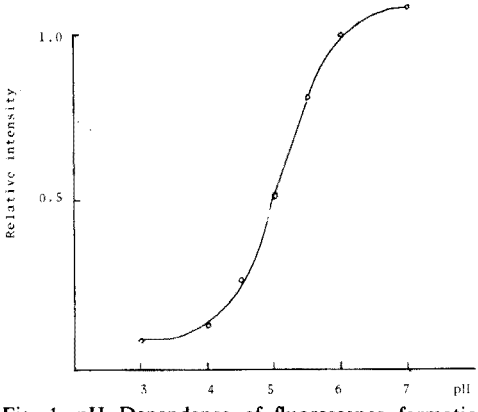

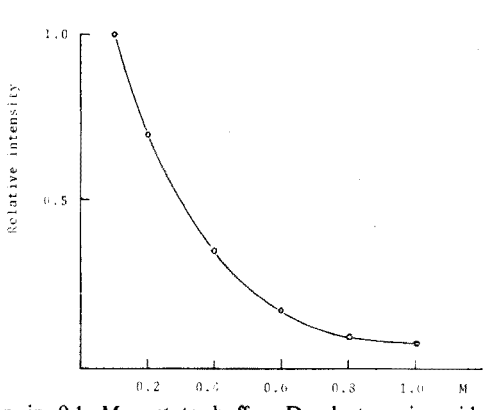

Fig. 1. pH Dependence of fluorescence formation in 0.1 *M* acetate buffer. D-galacturonic acid, $2.00 \cdot 10^{-4}$ *M*; reaction time, 3 h.

Fig. 2. Effect of buffer concentration. D-galacturonic acid, $2.00 \cdot 10^{-4}$ *M*; acetate buffer, pH 6.00; reaction time, 3 h.

buffer was found to give the most intense fluorescence at 328 (excitation)/405 nm (emission). In phosphate buffer another fluorescence was observed at 400/465 nm, as reported[1]. Figure 1 shows the pH dependence of fluorescence formation. The higher the pH of acetate buffer, the more intense the fluorescence. However, since very high pH values weaken the buffer effect, pH 6 was considered to be appropriate. Figure 2 shows the relationship between fluorescence intensity and the concentration of acetate buffer. The hyperbola indicates that fluorescence intensity decreased with increasing buffer concentrations. Therefore, a buffer concentration of 0.1 *M* was adopted in the standard procedure. Fluorescence formation was also dependent on the amount of the reagent if less than a 10-fold molar amount relative to uronic acids was present, but the use of larger excesses of the reagent gave a constant intensity of fluorescence. In the standard procedure the maximum concentration ($2 \cdot 10^{-2}$ *M*) of the reagent is used that allows a buffer effect.

Heating time

The fluorescence intensity increased gradually for 3 h. Thereafter it became almost constant. Accordingly, a heating time of 3 h was considered to be appropriate.

Fluorescence spectra and calibration

The fluorescence spectrum for D-galacturonic acid obtained by the standard procedure is depicted in Fig. 3. There are observed excitation and emission maxima at 328 and 405 nm, respectively. D-Glucuronic acid as well as its lactone gave similar spectra. Calibration curves for D-galacturonic acid and D-glucuronic acid are shown in Fig. 4. The lines form gently sloping sigmoid curves which show linearity for sample concentrations of $5.0 \cdot 10^{-6}$–$1.5 \cdot 10^{-5}$ *M* and $2.0 \cdot 10^{-5}$–$2.0 \cdot 10^{-4}$ *M* in both cases. The sensitivity of D-glucuronic acid was 82% lower than that of D-galacturonic acid. The low sensitivity is attributable to acid–lactone equilibration, since D-glucuronolactone gave the same intensity as D-glucuronic acid. D-Galacturonic acid does not equilibrate because it lacks the structural requirement for

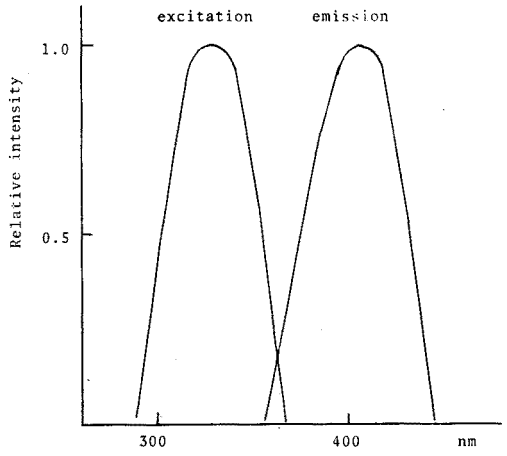

Fig. 3. Fluorescence spectrum. D-galacturonic acid, $2.00 \cdot 10^{-4}$ *M*; 0.1 *M* acetate buffer, pH 6.00; reaction time, 3 h.

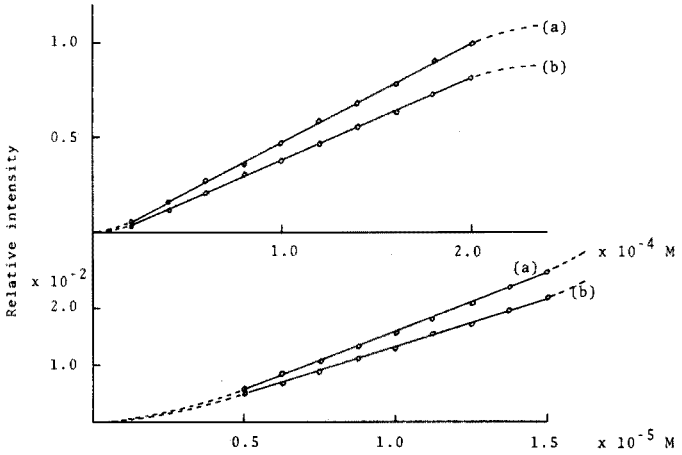

Fig. 4. Calibration curves of uronic acids obtained by the standard procedure. (a) D-galacturonic acid; (b) D-glucuronic acid or D-glucuronolactone.

TABLE I

REPRODUCIBILITY OF DETERMINATION

(5 determinations were done at each level.)

D-galacturonic acid added (μ mole)	*Av. D-galacturonic acid found (μ mole)*	*Standard deviation*
$3.00 \cdot 10^{-2}$	$2.99 \cdot 10^{-2}$	$0.11 \cdot 10^{-2}$
$2.00 \cdot 10^{-1}$	$2.00 \cdot 10^{-1}$	$0.08 \cdot 10^{-1}$
$4.00 \cdot 10^{-1}$	$4.00 \cdot 10^{-1}$	$0.15 \cdot 10^{-1}$

lactonization. Precision data for various concentrations of sample solutions are given in Table I. The results indicate that this method is accurate and reproducible.

EXPERIMENTAL

Material and apparatus

All reagents and samples of uronic acids were of reagent grade. Samples of uronides were kindly donated by Dr. K. Okui of Central Research Laboratories, Chugai Pharmaceuticals Co., Ltd. Fluorescence was measured with a Hitachi MPF-2A spectrofluorimeter in 1-cm quartz cells.

Standard procedure

To a buffered reagent solution (3.00 ml), prepared by mixing $2 \cdot 10^{-2}$ *M* ethylenediamine sulfate (1 volume) and 0.1 *M* acetate buffer (pH 6.00, 2 volumes), add a sample solution (2.00 ml) containing $1.0 \cdot 10^{-2}$–$3.0 \cdot 10^{-2}$ or $4.0 \cdot 10^{-2}$–$4.0 \cdot 10^{-1}$ μmole of a uronic acid. Heat the mixture for 3 h on a boiling water bath. Determine the concentration of uronic acid by reading the fluorescence intensity at 328 (excitation) and 405 nm (emission) within 24 h. Prepare a calibration curve

simultaneously. A reagent blank is made by replacing the sample solution with distilled water.

RESULTS AND DISCUSSION

Selectivity

Comparative studies under the standard reaction conditions indicated that these fluorescence reactions are highly selective for uronic acids. Various types of organic compounds examined, including alcohols, phenols, amines, nitro compounds, ketones, carboxylic acids, esters, amides, nitriles, and sulfonic acids gave no fluorescence with ethylenediamine sulfate. Some kinds of aromatic aldehydes, such as anisaldehyde and *o*-nitrobenzaldehyde, were the only exceptions. The relative fluorescence intensities at 328/405 nm, as referred to D-galacturonic acid, of all the carbohydrates ($1.0 \cdot 10^{-5}$ *M*) listed below did not exceed 0.01: aldoses (glycol aldehyde, DL-glyceraldehyde, D-erythrose, D-arabinose, D-ribose, D-xylose, D-galactose, D-glucose, D-mannose); ketoses (D-fructose, L-sorbose); 2-deoxy sugars (2-deoxy-D-ribose, 2-deoxy-D-glucose); methyl pentoses (L-fucose, L-rhamnose); alditols (erythritol, D-xylitol, D-galactitol, D-mannitol, D-sorbitol); amino sugars (D-galactosamine hydrochloride, D-glucosamine hydrochloride, N-acetyl-D-galactosamine, N-acetyl-D-glucosamine); aldonic acids (D-arabonic acid, D-gluconic acid); glycosides (methyl α- and β-D-glucopyranosides, phenyl α- and β-D-glycopyranosides); oligosaccharides (maltose, cellobiose, lactose, sucrose, raffinose); polysaccharides (dextran, glycogen, starch, chondroitin sulfates A and C). Determination of $1.0 \cdot 10^{-4}$ *M* D-glucuronic acid was not affected by 10-fold molar amounts of D-glucose, but the presence of a 100-fold molar amount D-glucose caused considerable depression of fluorescence intensity for unknown reasons.

Determination of D-glucuronic acid in the presence of glucuronides

It is noticeable that, unlike the colorimetric method[2–4] which use strongly acidic conditions, this fluorimetric method makes it possible to determine uronic acids without cleaving glycosidic linkages in aliphatic and aromatic uronides. Accordingly, unconjugated uronic acids can be determined without interference in the presence of large amounts of uronides. Uronides inspected include ethyl, n-

TABLE II

DETERMINATION OF *D*-GLUCURONIC ACID IN THE PRESENCE OF *D*-GLUCURONIDES

(In each case $2.00 \cdot 10^{-2}$ μmole *D*-glucuronic acid was used.)

Ethyl *D*-glucuronide added (μmole)	0.20	0.40	0.60	0.80	1.00	1.20	1.40	1.60	1.80	2.00
D-Glucuronic acid found ($\mu mole \cdot 10^{-2}$)	1.95	1.98	2.01	1.98	1.96	2.06	2.01	2.06	2.15	2.27
p-Tolyl *D*-glucuronide added (μmole)	0.20	0.40	0.60	0.80	1.00	1.20	1.40	1.60	1.80	2.00
D-Glucuronic acid found ($\mu mole \cdot 10^{-2}$)	1.94	1.96	1.98	1.97	1.98	2.05	2.07	2.06	2.18	2.25

propyl, isobutyl, phenyl, *p*-tolyl, and *p*-chlorophenyl glucuronides. Table II gives typical data obtained from ethyl and *p*-tolyl glucuronides. It is clear that $1.0 \cdot 10^{-5}$ *M* D-glucuronic acid can be determined accurately in the presence of at least 80-fold molar amounts of D-glucuronides.

The authors express their sincere gratitude to Dr. K. Okui for the gift of uronide samples. The authors are also grateful to Chugai Pharmaceuticals Co., Ltd. for financial support.

SUMMARY

A simple method for the spectrofluorimetric determination of uronic acids is proposed. The fluorescence at 328 (excitation) and 405 nm (emission) formed by heating sample solutions in acetate buffer containing large amounts of ethylenediamine sulfate, can be used to determine $1.0 \cdot 10^{-2}$–$3.0 \cdot 10^{-2}$ or $4.0 \cdot 10^{-2}$–$4.0 \cdot 10^{-1}$ μmole of unconjugated uronic acids accurately, without interference from other carbohydrate materials, especially uronides.

REFERENCES

1 S. Honda, K. Kakimoto, K. Kakehi and K. Takiura, *Anal. Chim. Acta*, 70 (1974) 133.
2 Z. Dische, *J. Biol. Chem.*, 167 (1947) 189; *J. Biol. Chem.*, 171 (1947) 725; *J. Biol. Chem.*, 183 (1950) 489.
3 H. Masamune and I. Aizawa, *Tohoku J. Exp. Med.*, 65 (1957) 359.
4 Z. Dische, *Arch. Biochem. Biophys.*, 16 (1948) 409.

Analytica Chimica Acta, 77 (1975) 205–221

SELECTIVE SPECTROPHOTOMETRIC DETERMINATION OF VANADIUM IN SILICATES WITH A NEW PYRIDYLAZOPHENOL IN THE PRESENCE OF HYDROGEN PEROXIDE

E. KISS

Research School of Earth Sciences, Australian National University, P.O. Box 4, Canberra, A.C.T., 2600 (Australia)

(Received 30th December 1974)

Vanadium is widely distributed in igneous and sedimentary rocks as well as in carbonaceous and bituminous shales of marine origin. Its accurate estimation is of geochemical interest because variations in its abundance ratio to some other trace elements may be used to characterize some important rock types.

This work describes the development of a spectrophotometric method, undertaken because none of the existing methods has proved entirely adequate for this element. In particular, although x-ray fluorescence spectrometry has advanced remarkably in recent years, especially in trace element analysis, it is unsuitable for vanadium because the Kα emission line is overlapped by the Kβ line of the much more abundant titanium. Emission spectrography is in general not capable of sufficient accuracy, and established spectrophotometric methods such as the hydrogen peroxide[1] and phosphotungstic acid procedures[2] possess grossly inadequate sensitivities (*e.g.*, $\varepsilon = 285$ l mole^{-1} cm^{-1} at 450 nm and $\varepsilon = 2550$ l mole^{-1} cm^{-1} at 375 nm, respectively). The two major classes of potentially promising reagents examined were (1) substituted hydroxamic acids (*i.e.* hydroxylamine derivatives) and (2) pyridylazophenols.

Jeffery and Kerr[3] achieved marked improvement in sensitivity and selectivity over established reagents[1,2] by using N-benzoyl-*o*-tolylhydroxylamine (BTH, $\varepsilon = 5{,}250$ l mole^{-1} cm^{-1} at 510 nm) for the selective extraction of the vanadate ion in silicates, titanium(IV) being masked by fluoride ions. However, a reasonably selective reagent for vanadium with an even greater molar absorptivity of the order of 10^4 or more is required. Hence, in addition to the hundreds of hydroxylamine derivatives prepared and examined elsewhere[4,5], forty new compounds were also prepared in this laboratory with a representative range of structural variation. Although none of these reagents has approached the required level of sensitivity, one structural modification has shown an encouraging combination of good sensitivity with selectivity for vanadium: PPPH (N-(5-phenyl-2,4-pentanedienoyl)-N-phenylhydroxylamine) which has previously been referred to[6] as N-phenyl-3-styrylacrylohydroxamic acid with $\varepsilon = 7{,}500$ l mole^{-1} cm^{-1} at 555 nm (this work: $\varepsilon = 7{,}900$ l mole^{-1} cm^{-1} at 570 nm). With fluoride ions present to mask titanium(IV), PPPH proved useful for the analysis of vanadium in silicates. Some cyclic hydroxamic acids may also have useful applications. For example, N-hydroxy-2-quinolone, which is easily prepared[7], was found to give a selective

vanadium reaction in the presence of fluoride although only with moderate sensitivity ($\varepsilon = 4{,}000$ l mole^{-1} cm^{-1} at 600 nm).

During the past twenty years or so, an ever-increasing number of heterocyclic azo compounds has been prepared and evaluated as potential metallochromic indicators and spectrophotometric reagents. The best known of these[8], 1-(2-pyridylazo)-2-naphthol (β-PAN) and 4-(2-pyridylazo)-resorcinol (PAR), have been widely used for a variety of analytical applications but the lack of selectivity was often a serious disadvantage. However, structurally analogous compounds with ligand components other than the hydroxyl group are notable exceptions[9,10]. The initial difficulties encountered in the synthesis of pyridylazo dyes have been largely eliminated. Anderson and Nickless[11] have prepared and studied a wide range of new dyes hitherto unavailable by conventional synthetic routes and have elucidated the role of *ortho*- and *para*-hydroxyl groups in PAR in relation to the stabilizing effect on the complexes and their characteristic visible spectra. Gusev and Shchurova[12] and Shibata *et al.*[13] recognised the important role of certain substituents (*e.g.*, $-NH_2$, $-N(CH_3)_2$ and $-N(C_2H_5)_2$, etc.) in the position *para* to the azo group which promote high molar absorptivity and stability in metal complexes. Of the eight compounds prepared by Gusev and Shchurova[12], Gusev and Shalamova[14] have investigated 2-(2-pyridylazo)-5-diethylaminophenol (PADAP) and its 5-bromo-2-pyridylazo- (5-Br-PADAP) and 3,5-dibromo-2-pyridylazo- (3,5-Br-PADAP) derivatives for the spectrophotometric determination of the vanadate ion. High molar absorptivity ($\varepsilon = 5.25 \cdot 10^4$, $4 \cdot 10^4$ and $5 \cdot 10^4$ l mole^{-1} cm^{-1} respectively) of the vanadium complexes of these reagents is a desirable advantage over hydroxamic acids, but once more several elements interfere. Bagdasarov *et al.*[15] have succeeded in utilizing PAR as a selective reagent for vanadium(V) by forming a 1:1:1 complex of V(V):PAR:H_2O_2 in normal sulphuric acid with the molar absorptivity of $1.65 \cdot 10^4$ l mole^{-1} cm^{-1} at 540 nm. In the presence of ammonium fluoride the reaction became specific to vanadium(V).

In attempts to explore the potentiality of other, more sensitive pyridylazo dyes in the ternary complex system, PADAP, 5-Br-PADAP and 3,5-Br-PADAP were chosen as representative compounds. However, analytically pure samples of these compounds could not be prepared; the samples lacked definite melting points and they were isolated as red oils which slowly changed to a tacky, wax-like material containing large amounts of dispersed crystals. In spite of this failure, the bromo derivatives of PADAP were successfully characterized as the dye components in the ternary complex system. When the diethylamino group was replaced by an amino group *para* to the azo group, *viz.*, 2-(2-pyridylazo)-5-aminophenol (PAAP) and its 5-bromo-2-pyridylazo- (5-Br-PAAP) and 3,5-dibromo-2-pyridylazo- derivatives (3,5-Br-PAAP), the products were isolated from the reaction medium as definite crystalline substances. The sensitivity of these reagents lies in an intermediate range between PAR and PADAP. In addition, two brominated derivatives of PAR (*e.g.*, 5-Br-PAR and 3,5-Br-PAR) were prepared for comparison purposes.

Also successful was the synthesis and isolation of another analogue of PADAP having a methyl group *para* to the nitrogen atom in the pyridine ring, 2-(3,5-dibromo-4-methyl-2-pyridylazo)-5-diethylaminophenol (3,5-Br-MEPADAP; I). In this paper, 3,5-Br-MEPADAP is shown to possess superior vanadium sensitivity

($\varepsilon = 5.43 \cdot 10^4$ l mole^{-1} cm^{-1} at 615 nm) in the ternary complex system and comparable selectivity with hydroxamic acids, and its use for the spectrophotometric determination of vanadium in silicates is described.

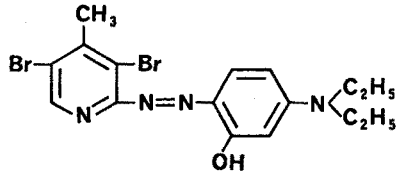

(1)

EXPERIMENTAL

Synthesis of reagent

The pyridylazo-diethylaminophenol, 3,5-Br-MEPADAP, was prepared by coupling *m*-diethylaminophenol with 3,5-dibromo-4-methyl-2-pyridyldiazotate in aqueous ethanol solution.

3,5-Dibromo-4-methyl-2-aminopyridine. 4-Methyl-2-aminopyridine (30 g) was dissolved in (1+3) sulphuric acid (100 ml) and the resulting warm solution was treated with bromine while stirring constantly. After the initially rapid halogen consumption had subsided, dropwise addition of bromine caused the separation of a heavy layer which was homogenized by heating. The dark orange solution was boiled slowly for 5–10 min, more bromine was added to the slightly cooled solution until re-heating failed to clear turbidity, and after cooling to room temperature, the crystalline slurry (presumably the sulphate salt of the product) was diluted to 500 ml and made strongly alkaline with potassium hydroxide. The precipitate was collected by filtration, washed several times with water until the filtrate was neutral, and then dissolved in boiling ethanol. The hot solution was treated with decolourizing charcoal and filtered, and the product was recrystallized from ethanol–water. After drying at 40 °C the derivative of off-white needles weighed 56.6 g (77% yield; m.p. 125–6 °C). Calculated for $C_6H_6N_2Br_2$: 27.1% C, 2.3% H, 10.5% N and 60.1% Br. Found: 27.2% C, 2.3% H, 10.1% N and 60.3% Br.

m-Diethylaminophenol sulphate. For purification, the free base (100 g) was suspended in warm water and enough sulphuric acid solution was added to effect dissolution. The boiling solution was treated with decolourizing charcoal and filtered by suction; this treatment was repeated. The light amber solution was evaporated under nitrogen to a thick syrupy consistency. On cooling to room temperature, the sulphate salt solution readily formed a transparent crust. Acetone was then added and crystallization was induced by stirring. The separated off-white/pinkish mass was suction-filtered, washed with acetone to remove the pink oxidation products and dried to yield 125 g of the phenol salt. Sulphate analysis gave a salt composition of 2 moles of the phenol to 1 mole of sulphuric acid.

Diazotization. Sodium amide (5 g) was dissolved in absolute ethanol (120 ml) and refluxed with 0.05 mole (13.3 g) of 3,5-dibromo-4-methyl-2-aminopyridine for 30 min. Freshly distilled tert-butyl nitrite (10 ml) was added dropwise through

the condenser to the slightly cooled reaction mixture, stirred and refluxed for 2 h. Periodic stirring was necessary as the heavy crystalline reaction product separated out. The sodium-3,5-dibromo-4-methyl-2-pyridyldiazotate was not isolated but used directly in the coupling reaction.

Coupling reaction. *m*-Diethylaminophenol sulphate (10 g; 0.025 mole) was dissolved in water (120 ml) and added to the cooled diazotate solution with constant stirring. A steady flow of carbon dioxide was introduced, the solution was held at 40–50 °C for 2 h, and then allowed to cool to room temperature, and the carbon dioxide flow was stopped. The heavy crystalline sediment formed from the intensely red solution, was collected by filtration and washed with water until the filtrate became colourless. The crude product was recrystallized from boiling pyridine (40 ml) by adding enough water to cause slight turbidity. The compound 3,5-Br-MEPADAP separated on cooling as blackish-red needles with a metallic lustre, and was collected by filtration, washed with water and dried at 80 °C overnight. The analytical sample was further dried *in vacuo* at 90 °C (15 mm Hg) for 16 h. Yield: 32.6% (7.2 g); m.p. 194–6 °C. Calculated for $C_{16}H_{18}N_4OBr_2$; 43.5% C, 4.1% H, 12.7% N and 36.1% Br. Found: 43.7% C, 4.2% H, 12.2% N and 36.1% Br.

All the other pyridylazo-phenols and pyridylazo-aminophenols were prepared by analogous methods.

When the sodium diazotate derivative of 3,5-dibromo-4-methyl-2-amino-pyridine was isolated by addition of anhydrous diethyl ether to the reaction mixture, a 40% yield of the dry salt was obtained. Prolonged refluxing failed to improve this yield, and an attempt was made to improve the conversion rate by using higher reaction temperatures. The sodium derivative of n-pentanol and an n-pentanol solution of sodium amide were used as representative reaction media. The amino-pyridine was added to these solutions together with the relatively involatile ester sec-octyl nitrite, and refluxed for 20 min. A significantly higher yield of the diazotate was obtained because of faster reaction conditions. Difficulties were encountered, however, in attempts to isolate the diazotate and the subsequent coupling reaction with the free phenol was carried out in the water-immiscible alcoholic solution. The resulting dye could not be separated in adequate purity. Further work on this approach may be of interest.

Reagents for spectrophotometric studies

Solutions ($2 \cdot 10^{-3}$ *M*) of 3,5-Br-MEPADAP and other pyridylazo-amino-phenols (*β*-PAN, PAR, 5-Br-PAR, 3,5-Br-PAR, PAAP, 5-Br-PAAP and 3,5-Br-PAAP) were prepared by dissolving the requisite amount of pure reagent in 100 ml of absolute ethanol. Solutions of the impure preparations PADAP, 5-Br-PADAP and 3,5-Br-PADAP were made in absolute ethanol to give a nominal concentration only (*ca.* $2 \cdot 10^{-3}$ *M*). When stored in amber bottles, these solutions were stable for several months.

Vanadium(V) solution was prepared by dissolving vanadium pentoxide ("Specpure") in the minimal amount of dilute ammonia solution, acidifying with sulphuric acid and diluting to volume in the presence of a trace of potassium permanganate. Vanadium(IV) solution was prepared by dissolving vanadium metal turnings (99.8%) in hot (1 + 1) sulphuric acid, allowing to stand in air for some time,

and diluting to volume. This solution was essentially the same as that obtained by hydroxylamine reduction of the vanadate.

Chromium(III) solution was prepared by dissolving chromium flake (99.999%) in hot (1+1) sulphuric acid and diluting. Chromium(VI) solution was prepared from potassium dichromate. Iron(III) solution was prepared by dissolving iron(III) oxide (99.999%) in 7 *M* hydrochloric acid, evaporating most of the acid, fuming with sulphuric acid, and diluting to volume. Titanium(IV) solution was prepared by fuming potassium titanyl oxalate repeatedly with (7+3) sulphuric acid until oxalate was completely removed, cooling and diluting; the solution was standardized by the hydrogen peroxide method. All other metal solutions were prepared from the best available grades of chemicals ranging from "Specpure" to analytical grade.

Chloroform was freed from ethanol by shaking with water, dried, distilled, and stored in a dark bottle.

Apparatus

Absorption spectra were recorded with a Unicam SP1800 recording spectrophotometer with 10-mm silica cells. Fixed wavelength measurements were made with a Pye-Unicam SP-500 S-2 spectrophotometer equipped with automatic sample changer and a recorder. pH Measurements were made with a Metrohm-Herisau Potentiograph and a Metrohm-Herisau Digital Piston burette was used for dispensing fixed volumes of chloroform.

SPECTROPHOTOMETRIC STUDIES

Colour reactions with metals

For the detailed studies only 3,5-Br-MEPADAP was examined; the structural similarity of other compounds made further work seem unwarranted. Like other pyridylazophenol dyes, 3,5-Br-MEPADAP forms coloured chelates with a wide range of metals. The test solutions containing the metal ions and the reagent were visually compared against the appropriate blank in three pH regions (*e.g.*, pH 1–3, pH 4–7 and pH 8–11) according to the observed chelate stability fields. Demasking with fluoride (where applicable) allowed confirmation of chelate formation with certain metal ions which produced extremely poor colour contrast, *e.g.*, Cr(III), Ta(V) and V(IV). Among the cations examined, only Bi(III), Co(III), Fe(II), Fe(III), In(III), Pd(II), Ta(V), Tl(I), Tl(III), Ti(IV), V(IV), V(V) and Zr(IV) formed stable chelates at pH 1–3; solutions containing Ta(V) and Zr(IV) required warming for chelation. In the pH range 4–7, Ag(I), Au(III) (red-brown opalescence), Cd(II), Co(II), Cr(III), Cu(I), Cu(II), Ga(III), Hg(II), Nb(V), Ni(II), Pb(II), Sb(III) (in ethanolic medium), Sn(II), Th(IV), U(VI) and Zn(II) produced more or less intense colouration. At pH 8–11, distinct colour changes occurred with Ba(II), Ca(II), Ce(III), La(III), Mg(II), Mn(II), Rb(I) ($\lambda_{max}=540$ nm in chloroform), Sr(II) and Y(III) ions. No reaction was observed at any pH range with Al(III), Be(II), Cr(VI), Cs(I), Li(I), K(I), Mo(VI), Na(I), Pt(IV) and W(VI). Some ions such as Bi(III), Co(III), Cu(I), Cu(II) and Pb(II), formed intensely coloured chelates within much wider pH limits (*i.e.*, pH 2–11). Palladium(II) formed stable chelates between pH 1–6. The presence of fluoride, EDTA, citrate, oxalate

and cyanide inhibited most colour reactions including that of vanadium(V), but niobium(V) reacted even in oxalic acid solutions.

In contrast to earlier reports, it was found that substituted hydroxylamines and cyclic hydroxamic acids formed coloured chelates of comparable intensity with either vanadium(IV) or vanadium(V). 3,5-Br-MEPADAP and other related dyes required vanadium(V) for sensitive reactions.

Colour reaction of 3,5-Br-MEPADAP with vanadium(V)

The chelate formation of vanadate with 3,5-Br-MEPADAP was examined quantitatively in the following media: (1) 80% acetic acid, (2) 10% acetic acid, (3) at pH 2 (acetate buffer) and (4) at pH 5 in 50% ethanol (hexamethylenetetramine buffer). The vanadium(V) chelates showed surprisingly poor stability in all these media; pronounced colour fading occurred after about 5 min. This behaviour contrasts sharply with the chelating ability of PADAP and its bromo derivatives which form stable chelates with vanadium(V) in weakly acidic media. When the colour intensities were measured immediately after mixing, the molar absorptivity of the vanadium(V)-3,5-Br-MEPADAP chelate showed wide variation according to conditions ($2.14–4.11 \cdot 10^4$ l mole^{-1} cm^{-1}) though the wavelength of maximal absorption (615 nm) was constant in all cases.

Reagent selectivity in the presence of hydrogen peroxide

Like other ions, vanadium(V) failed to form a coloured chelate in strong sulphuric acid medium. In the presence of hydrogen peroxide, vanadium(V) formed an intensely blue ternary complex with the reagent on heating. As no other metal ion formed a coloured chelate in the presence of fluoride, the colour reaction became specific for vanadate. However, because of the acidity and heating, large amounts of strong oxidants and reductants affected the reagent itself. Traces of permanganate added to maintain vanadium in the pentavalent state were unimportant because the ethanol of the reagent solution was preferentially oxidized.

Choice of mineral acid

Hydrochloric and other halo-acids are incompatible with the colour system because of the permanganate used for oxidation of vanadium. The formation of the ternary complex (from $1.2 \cdot 10^{-5}$ *M* vanadium) was examined in 0.5 *M* sulphuric, 1 *M* nitric and 0.5 *M* perchloric acids, the molar absorptivities being $5.49 \cdot 10^4$, $5.01 \cdot 10^4$ and $4.79 \cdot 10^4$ l mole^{-1} cm^{-1}, respectively, when absorbances were measured against reagent blanks at the absorption maximum, 615 nm. Perchloric acid caused rapid precipitation of the reagent, presumably as the perchlorate, which was redissolved by the chloroform extraction. Both sulphuric acid and nitric acid were suitable as acid media; for analytical applications sulphuric acid was chosen.

Extractability of the ternary complex

Initially, chloroform was used to extract the coloured species of vanadium formed with several pyridylazophenols in the presence of hydrogen peroxide in 0.5 *M* sulphuric acid. However, this extraction was not successful when the pyridylazo dye possessed a hydroxyl or amino group *para* to the azo group (PAR, 5-Br-PAR, 3,5-Br-PAR, PAAP and 5-Br-PAAP). In contrast, the ternary complexes

containing dyes with a diethylamino group *para* to the azo group (5-Br-PADAP, 3,5-Br-PADAP and 3,5-Br-MEPADAP) were easily and completely extracted into chloroform.

Detailed extraction studies were carried out only with the 3,5-Br-MEPADAP ternary complex. The most efficient solvents for both the free dye and the complex were chloroform, 1,2-dichloroethane, *sym*-tetrachloroethane and *sym*-tetrabromoethane; carbon tetrachloride and 1,2-dichlorobenzene were poor extractants for the complex. Extracts of the ternary complex and blank solutions in 1,2-dichloroethane showed an unusual tendency to undergo bathochromic shifts after short times. Nitrobenzene was a good solvent for both the free dye and the complex, but caused an extremely rapid rate of hypochromic shift. n-Pentanol, sec-octanol, 2-phenylethanol, benzyl acetate, diethyl phthalate and acetophenone were moderately effective solvents. Aromatic and aliphatic hydrocarbons were poor solvents. The behaviour of ethers (*e.g.*, diethyl ether and di-isopropyl ether) and decahydronaphthalene is interesting: the excess of free dye (orange colour) was selectively extracted by these solvents leaving the pure blue complex in the aqueous phase. However, the visually almost colourless aqueous blank obtained after extraction with decahydronaphthalene had identical absorbance to the blank which was extracted with chloroform; hence there was no advantage in separating the excess of reagent before the measurement.

Absorption spectra

The absorption characteristics of free 3,5-Br-MEPADAP and its ternary complex blank are shown in Fig. 1 together with those of the vanadium ternary complexes of 5-Br-PADAP, 3,5-Br-PADAP and 3,5-Br-MEPADAP. The striking bathochromic shift of free 3,5-Br-MEPADAP in 1,2-dichloroethane is shown by curves A and B. The dye absorbed maximally at 448 nm ($\varepsilon = 3.2 \cdot 10^4$ l mole^{-1} cm^{-1}) in chloroform, whereas in 1,2-dichloroethane, there was a plateau ($\varepsilon = 2.5 \cdot 10^4$ l mole^{-1} cm^{-1} at 500 nm) and a sharp peak at 564 nm ($\varepsilon = 3.5 \cdot 10^4$ l mole^{-1} cm^{-1}). The spectrum of 3,5-Br-MEPADAP in chloroform also changed profoundly when peroxide was present (curve C); the blank absorbance was maximal at 470 nm ($\varepsilon = 2.26 \cdot 10^4$ l mole^{-1} cm^{-1}), and negligible at the red end of the spectrum. The ternary vanadium complexes containing 3,5-Br-PADAP and 3,5-Br-MEPADAP showed characteristic secondary maxima: for 3,5-Br-PADAP, the maxima occurred at 484 nm and 618 nm and for 3,5-Br-MEPADAP, at 472 nm and 615 nm. There was no similar secondary peak for the 5-Br-PADAP ternary complex within the wavelength range examined.

Molar absorptivities and reagent sensitivities

The molar absorptivities and sensitivities of vanadium ternary complexes in 0.5 *M* sulphuric acid are shown in Table I.

Effects of some variables on chelation

The effects of acidity, reagent concentrations (*i.e.*, 3,5-Br-MEPADAP and hydrogen peroxide) and heating time were investigated; the results are summarized in Table II.

As expected, the colour system was sensitive to variations in acidity: there

was no complex formation in neutral or slightly acidic media as the unprotonated reagent precipitated. In 0.25 *M* sulphuric acid, some dye separated as a thin film on the liquid surface, and could not be washed off effectively with water. Significant bleaching of the dye occurred above 0.5 *M* acid. The optimal acidity for the ternary complex formation was *ca.* 0.5 *M* sulphuric acid.

Under the recommended conditions, 18.8 μg V in 20 ml of chloroform extract gives an absorbance of 1.00; according to the stoichiometry of the 1 : 1 : 1 complex formation, 163 μg of the reagent is required. It was found that 1 ml of $2 \cdot 10^{-3}$ *M*,

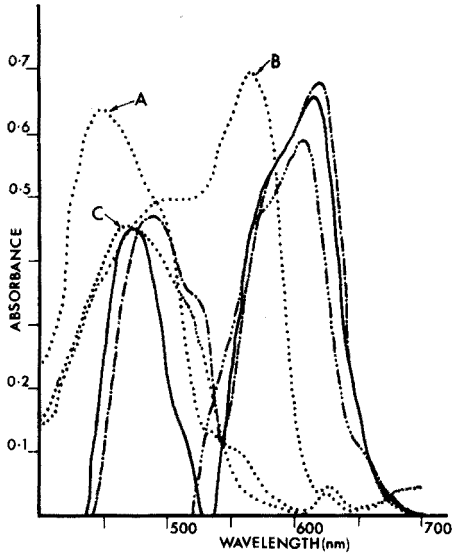

Fig. 1. Absorption spectra of vanadium–halopyridylazo-diethylaminophenol-hydrogen peroxide ternary complexes extracted in chloroform from 0.5 *M* sulphuric acid. Measured against corresponding reagent blanks in 10-mm cells. Vanadium concentration: $1.2 \cdot 10^{-5}$ *M*, reagent concentration: $2 \cdot 10^{-4}$ *M*. (——) 3,5-Br-MEPADAP; (–·–·–) 3,5-Br-PADAP; (–···–···–) 5-Br-PADAP. Curves A, B and C were measured against corresponding solvent: 3,5-Br-MEPADAP ($2 \cdot 10^{-5}$ *M*) absorption in chloroform (A); in 1,2-dichloroethane (B) and ternary complex blank spectrum (C) in chloroform.

3,5-Br-MEPADAP solution — a 5.4-fold molar excess — sufficed, but twice this amount was adopted in the analysis. Larger amounts of reagent (up to 22-fold) had no effect other than a slight increase in the blank absorbance at 615 nm, which required an increase in the slit adjustment.

Variation of hydrogen peroxide concentration in the range 2–10 ml of 3% solution per 50 ml of aqueous phase, had no effect on the recovery of vanadium. A volume of 3 ml was selected.

Colour formation took place readily in the cold, hence the reaction time for complete development was examined in aqueous medium at 25°C (Table II). The absorbance reached a maximum after 30 min of standing in the dark and remained constant for at least 4 h thereafter. Warming the solution on a boiling water bath increased the reaction rate greatly; heating times in the range 5–30 min did not affect the recoveries and a 5-min warming time was therefore selected.

TABLE I

MOLAR ABSORPTIVITY AND SENSITIVITY OF VANADIUM TERNARY COMPLEXES IN 0.5 *M* SULPHURIC ACID

Reagent	λ_{max} *(nm)*	$\varepsilon(\cdot 10^4$ *l mole*$^{-1}$ *cm*$^{-1})$	$\mu g\ V\ cm^{-2}$	*Medium (extractant)*
β-PAN	—[a]			
PAR	540	1.49[b]	0.0034	Aqueous
5-Br-PAR	550	1.85	0.0028	Aqueous
3,5-Br-PAR	560	1.50	0.0034	Aqueous
PAAP	560	2.79	0.0018	Aqueous
5-Br-PAAP	570	2.89	0.0018	Aqueous
PADAP	—[c]			
5-Br-PADAP	605	4.83	0.0011	Chloroform
3,5-Br-PADAP	484	3.90	0.0013	Chloroform
	618	5.60	0.0009	Chloroform
3,5-Br-MEPADAP	615	5.31 ± 0.05	0.0010	Aqueous
	615	5.68 ± 0.09	0.0009	1,2-Dichloroethane
	472	3.70	0.0014	Chloroform
	615	5.43 ± 0.04	0.0009	Chloroform
	628	5.22	0.001	*sym*-Tetrabromoethane
	~605	~6.10	~0.0008	Nitrobenzene[d]
	618	5.59	0.0009	1,2,3-Trichloropropane

[a] Absorbance is not appreciably different from that of reagent.
[b] Lit. value[15]: $1.65 \cdot 10^4$
[c] Reagent rapidly decolourized in contact with 0.5 *M* H_2SO_4.
[d] Rapid hypochromic shift.

TABLE II

EFFECT OF SOME VARIABLES ON CHELATION OF VANADIUM(V) WITH 3,5-Br-MEPADAP (12.25 μg V taken. Normal conditions: 0.5 *M* H_2SO_4. 2 ml of $2 \cdot 10^{-3}$ *M* reagent, 3 ml of 3% H_2O_2, heating time 5 min.)

Variable	*% Recovery*	*Variable*	*% Recovery*
Acidity (M)		*Reaction time (min) at 25°C (aqueous medium)*	
0.25	98.3	5	69.4
0.5	100.0	10	87.1
1.0	87.6	20	96.4
1.5	56.2	35	99.5
		40	100.0
Hydrogen peroxide (ml, 3%)		50	100.0
2.0	100.3	70	99.4
3.0	100.0	180	100.0
5.0	100.0		
10.0	100.2		
		Heating time (min)	
		2	94.2
		5	100.0
		10	100.0
		30	98.5
		60	93.0

Colour stability

The vanadium ternary complex (containing $1.2 \cdot 10^{-5}$ *M* V) formed with 3,5-Br-MEPADAP in 0.5 *M* sulphuric acid was stable for up to 4 h; after 20 h in the dark, an average of 3.3% colour fading occurred. Diffuse daylight accelerated the fading appreciably; a further 8.1% bleaching occurred in 24 h, and bleaching was complete after seven days.

Stability tests on the chloroform extracts, which were stored in PTFE bottles in the dark except during absorbance measurements, showed that the ternary complex was stable after 2, 4, 20, 27 h and up to 6 days. After 12 days there was 4.3% fading; intervening measurements showed a slight (0.6%) increase which could be attributed to colour concentration arising from the volatility of chloroform.

Interferences

In order to assess the approximate tolerance levels of a few important ions, fixed amounts of vanadium were determined in the presence of increasing amounts of chromium(III), chromium(VI), iron(III) and titanium(IV), by the recommended procedure. The results are given in Table III.

Chromium(III). Solutions having Cr(III)/V(V) ratios of 360–1,200 were analysed with only slight negative errors. Measurements of vanadium(V) in aqueous media containing large amounts of chromium(III) were subject to appreciable error, but the ternary complex was selectively extracted by chloroform, chromium(III) remaining in the aqueous phase.

Chromium(VI). Because of its strong oxidizing power in acidic media, chromate had a drastic effect on the vanadium complex. When solutions having Cr(VI)/V(V) ratios of 10–400 were analysed, a linear relationship was found between the chromate concentration and the extent of bleaching. When hydrogen peroxide was added, a strong "perchromic acid" colour was formed and remained in the aqueous phase after the extraction. Nevertheless, a 10-fold amount of Cr(VI) over V(V) was well tolerated. In another set of experiments, the importance of acidity in the interference was clearly illustrated. With all reactants added to the neutral solution, chromium(VI) preferentially oxidized the ethanol of the reagent solution. The acidity was finally adjusted to 0.5 *M* in sulphuric acid and the colour developed. By this approach, the tolerance for chromate was increased to 200-fold over vanadium. The aqueous phase after the extraction lacked the blue peroxidized chromate colour.

Iron(III). Solutions having Fe(III)/V(V) ratios of 400–4.000 were analysed under a variety of conditions; up to a 1,000-fold amount of iron(III) over vanadium was tolerated well. The addition of increasing amounts of ammonium fluoride reduced the negative error of the vanadium recovery. The addition of reagents to the neutral solution with subsequent acidification did not improve the yield when iron(III) was present, the vanadium recovery being very poor. When a large amount of iron(III) was present, the vanadium recovery did not improve when the acidified solution was heated with ammonium fluoride before colour development (Table III).

Titanium(IV). The tolerance levels were examined for Ti(IV)/V(V) ratios of 800–4,600. Titanium(IV) produced slight positive errors in the recovery of vanadium, but up to 3,000-fold amounts of titanium(IV) could be tolerated. The

(Fixed amount of vanadium: 12.25 μg)

Element added (mg)		*V found, (μg)*	*Error* μg	*Error* %
One-component systems				
Cr(III)	4.44	12.06[a]	−0.19	−1.5
	7.44	12.08[a]	−0.17	−1.4
	14.79	12.08[a]	−0.17	−1.4
Cr(VI)	0.121	11.98[a]	−0.27	−2.2
	0.242	11.85[a]	−0.40	−3.2
	0.603	11.64[a]	−0.61	−4.9
	1.21	11.48[a]	−0.77	−6.3
	2.41	10.80[a]	−1.45	−11.8
	4.82	10.12[a]	−2.13	−17.4
	1.21	12.35[b]	+0.10	+0.9
	2.41	12.49[b]	+0.26	+2.1
	4.82	12.82[b]	+0.57	+4.7
Fe(III)	4.80	12.05[c]	−0.20	−1.5
	9.60	11.96[c]	−0.29	−2.3
	12.00	11.93[c]	−0.32	−2.6
	24.00	11.76[c]	−0.49	−3.9
	48.00	11.87[c]	−0.38	−3.0
	12.00	11.86[a]	−0.39	−3.1
	24.00	11.86[a]	−0.39	−3.1
	48.00	11.67[a]	−0.58	−4.7
	42.90	11.78[d]	−0.47	−3.8
Ti(IV)	9.36	12.25[e]	0.0	±0
	37.44	12.30[e]	+0.05	+0.5
	46.80	12.79[e]	+0.54	+4.5
	56.16	12.81[e]	+0.56	+4.6

Element added (mg)		*V found, (μg)*	*Error* μg	*Error* %
Binary systems				
Fe(III)	21.45	12.09[e]	−0.16	−1.2
Ti(IV)	18.72			
Fe(III)	32.18	12.09[e]	−0.16	−1.2
Ti(IV)	18.72			
Four-component systems				
Cr(III)	1.11	12.25[f]	0.0	±0
Cr(VI)	0.07			
Fe(III)	1.80			
Ti(IV)	1.40			
Cr(III)	1.85	12.43[f]	+0.18	+1.5
Cr(VI)	0.12			
Fe(III)	3.00			
Ti(IV)	2.34			
Cr(III)	3.70	12.43[f]	+0.18	+1.5
Cr(VI)	0.24			
Fe(III)	6.00			
Ti(IV)	4.68			
Anionic interferences (5 g of neutral salt added)				
$(NH_4)_2SO_4$		12.19	−0.06	−0.5
$NaNO_3$		12.07	−0.18	−1.4
$(NH_4)_2HPO_4$		12.05	−0.20	−1.5
$NaClO_4$		11.91	−0.31	−2.7

[a] 5 ml 10% NH_4F added.
[b] Reagents added to neutral solution then acidified.
[c] 10 ml 10% NH_4F added.
[d] 10 ml 20% $NH_4F + H_2SO_4$ added; heated for 5 min before colour development.
[e] 10 ml 20% NH_4F added.
[f] 5 ml 20% NH_4F added.

error caused by larger amounts of titanium may be acceptable for certain applications. Solutions containing large amounts of titanium flocculated on addition of ammonium fluoride, but cleared on acidification.

Binary systems of Fe(III)–Ti(IV). Multi-component interference systems provide a more realistic approach for analysis of silicate compositions because the negative and positive errors observed with single interferences tend to cancel each other. This effect is clearly illustrated by the excellent recovery of vanadium from binary mixtures having Fe(III)–Ti(IV)/V(V) ratios of (1,800–1,500) and (2,600–1,500) (Table III).

Four-component systems. Three concentration levels of Cr(III)–Cr(VI)–Fe(III)–Ti(IV) mixtures with ratios to vanadium of 360, 600 and 1200, were also examined. The vanadium recoveries were excellent.

Anionic interferences. The effect of very large amounts (5 g) of neutral salts on the recovery of vanadium was investigated; Table III shows the excellent tolerance for sulphate, nitrate, phosphate and perchlorate. Chloride, bromide and iodide ions inhibited the ternary vanadium complex formation as follows: chloride caused total decolourization during heating; bromide decolourized the reagent on acidification in the cold and iodide caused immediate colour bleaching of permanganate.

The excellent sulphate tolerance of the reagent system justifies the use of potassium pyrosulphate fusion of those minerals which are not attacked satisfactorily by hydrofluoric acid. The tolerance for perchlorate shows that perchloric acid may be used instead of sulphuric acid to expel fluorides from hydrofluoric acid dissolution of silicates, if required.

Calibration curves

A standard stock solution of vanadium was prepared as described above and working solutions were prepared by dilution. The procedure used for calibration was identical to that for "Colour development" (below). Three calibration curves were made: (1) for aqueous medium, (2) for 1,2-dichloroethane extraction and (3) for chloroform extraction. Beer's law was obeyed closely within the concentration ranges tested. The calibration based on 1,2-dichloroethane extraction was subsequently rejected because a time-dependent colour instability was observed in the extracts which caused a large bathochromic shift in the blanks. The ranges and relative standard deviations for the calibrations at 615 nm in 10-mm flow-through cells were: (1) for aqueous medium, 11–48 μg V/50 ml (s_r=0.35%, 7 points); (2) for 1,2-dichloroethane extraction, 7–22 μg V/20 ml (s_r=0.41%, 7 points); (3) for chloroform extraction, 2–22 μg V/20 ml (s_r=0.25%, 12 points). All measurements were made against the corresponding reagent blank as reference.

Other solvents less volatile than chloroform could be used with advantage, *e.g.* bromoform, *sym*-tetrabromoethane or 1,2,3-trichloropropane. Because of the relatively low volatility of these solvents, further concentration of colour is possible to a convenient final volume of 10 ml. However, precautions should be exercised with these solvents because of their cumulative toxicity[16].

APPLICATION TO SILICATE ANALYSIS

The feasibility of employing PADAP (an impure preparation) for the

determination of vanadium in silicates was first examined. Because of its high molar absorptivity[14] with vanadium in weakly acidic solution ($5.25 \cdot 10^4$ l mole^{-1} cm^{-1}), PADAP offers obvious advantages at p.p.m. vanadium levels. The lack of adequate selectivity was a problem, but the procedure of Jeffery and Kerr[3] was successfully applied to the extraction of vanadium from silicate dissolutions by using N-benzoyl-*o*-tolylhydroxylamine as extractant in chloroform solution. After evaporation of solvent, the organic matter was destroyed by nitric acid/perchloric acid treatment and the inorganic residue containing all the vanadium was used to develop the V(V)–PADAP colour by the procedure of Gusev and Shalamova[14]. Although this approach to increased sensitivity was rather circuitous, the results (Table IV) were of acceptable precision and accuracy.

The ternary V(V)–3,5-Br-MEPADAP–H_2O_2 complex system offers high selectivity and sensitivity. Direct formation of vanadium complexes is possible in a wide range of silicate dissolutions. The amount of ammonium fluoride used for masking can be increased to suit individual sample requirements without affecting the vanadium recovery. A large excess of fluoride is necessary for most silicates because other non-interfering elements such as calcium, magnesium and aluminium form fluoro complexes in addition to iron and titanium; occasionally, the fluoride may cause the precipitation of some calcium fluoride from solutions of calcium-rich silicates, but vanadium retention by the precipitate was undetectable. The solvent extraction step is recommended not only for concentration of the coloured chelate, but because it eliminates any problems of opalescence or suspension (calcium fluoride) in the aqueous phase. Moreover, in contrast to aqueous media, chloroform extracts of the vanadium complex are remarkably stable. The measurement of vanadium absorbance in aqueous medium in the presence of large amounts of coloured ions (*e.g.* Cr(III)) is undesirable, because of significant change in hue. With a solvent extraction step, the coloured ions remain in the aqueous phase.

RECOMMENDED ANALYTICAL PROCEDURE

Sample dissolution

Samples can be prepared by one of the following methods.

(a) The silicate solutions prepared for the flame photometric determination of sodium by the internal standard method of Cooper[17] can be used. As the present x.r.f. instrumentation is unsuitable for the precise counting statistics necessary to determine sodium, this element is regularly determined by flame photometry. Approximately 80% of the rock solution is discarded after the sodium measurement; its utilisation for the determination of vanadium results in obvious time-saving. The only pre-requisite is to oxidize the decomposed sample with concentrated nitric acid during the final hydrofluoric acid evaporation. This approach is most suitable for basaltic rocks containing 100–500 p.p.m. vanadium.

(b) Better optimization of the expected vanadium concentration may be achieved, however, by direct processing of 0.25–1.0 g of rock sample and diluting to volume. An aliquot of this stock solution is taken for the vanadium measurement. Also, by weighing larger amounts of rock, sampling error is minimized.

(c) If limited amounts of silicate are available, direct spectrophotometry of 20–200-

mg samples may be carried out, the whole sample being processed. A typical dissolution procedure is as follows.

Depending on the expected vanadium concentration, weigh 0.25–1.0 g of silicate sample into a 100-ml platinum (or gold) evaporating dish, moisten with *ca.* 5 ml of water, add 5 ml of (1+1) sulphuric acid and 20 ml of concentrated hydrofluoric acid. Stir the contents with a PTFE rod and evaporate on a water bath to a small volume; add 5 ml of concentrated hydrofluoric acid and 3 ml of concentrated nitric acid, mix and evaporate again to incipient crystallisation. Transfer the dish to a hot plate set on low heat and gradually increase heating till copious fumes of sulphur trioxide are evolved. After cooling, dissolve salts by adding *ca.* 20 ml of water, stir and place on a water bath. (Calcium sulphate may precipitate at this stage, but will re-dissolve on further dilution). Dilute the cooled solution to 250 ml in a volumetric flask. If insoluble particles are present after the hydrofluoric acid treatment (*e.g.* chromite in ultra-basic rocks), filter the dissolved salts through a retentive filter paper into a 250-ml volumetric flask, wash a few times with hot water, and ash the residue in a platinum or a zirconium crucible. Fuse the refractory mineral residue with a suitable flux (if chromite is suspected, fuse with sodium peroxide in a zirconium crucible), neutralize the aqueous leach with sulphuric acid and add to the bulk of the solution in a 250-ml volumetric flask. Even minute amounts of insoluble residue should be recovered by fusion because significant proportions of the total vanadium content could be present in mineral residues such as chromite and titaniferous magnetite.

Magnetite and bauxite are best dissolved in hydrochloric acid and oxidized with bromine, and the chlorides are removed by heating with sulphuric acid to the fuming stage. Rutile, brookite and ilmenite may be brought in solution by fusion with potassium pyrosulphate. Vanadium can be determined also in chromite by the present analytical system. Sintering or brief melting is adequate to decompose chromite with sodium peroxide in a zirconium crucible. The aqueous leach should be neutralized with sulphuric acid and undesirably high levels of chromate may be reduced to chromium(III) by addition of ethanol, the excess being removed by boiling. Any vanadium(IV) is easily oxidized with permanganate in the cold. Chromium(III) is not oxidized significantly by this treatment.

Alternatively, if insufficient sample is available for the preparation of a 250-ml stock solution, which requires up to 1 g rock sample, the dissolution of 20–200 mg material may be effected by adding *pro rata* quantities of acids and the whole should be used for the subsequent measurement. In this case, the vanadium colour with the reagents may be developed directly in the platinum dish.

Colour development

Pipette aliquots containing up to 20 μg V (not exceeding 25 ml) into 100-ml beakers (graduated in 5-ml increments). Add 1 drop of 0.5% (w/v) potassium permanganate solution, to give a weak but stable pink colour and set aside for 5 min. Add 5–10 ml of 20% (w/v) ammonium fluoride solution, mix, add 5 ml of 5 *M* sulphuric acid, and dilute to *ca.* 40–43 ml. Pipette 2.00 ml of $2 \cdot 10^{-3}$ *M* 3,5-Br-MEPADAP solution, mix, add 3.0 ml of 3% hydrogen peroxide solution, and dilute to 50 ml. Prepare a reagent blank to be used as reference in the same manner. Heat the beakers on a rapidly boiling water bath for 5 min, cool

and wash the solution quantitatively into a 125-ml separatory funnel with 0.5 *M* sulphuric acid. Add exactly 20.00 ml of pure chloroform and extract the coloured compound by shaking for 50–60 s. (The chloroform extraction is highly efficient requiring only 30 s for completion; longer shaking time is allowed for sample variability.) In order to retain any water droplets, filter the organic phase through a fast filter paper into 15-ml sample bottles and seal the extracts promptly with polyethylene caps. Measure the absorbance at 615 nm in a 10-mm quartz flow-through cell against the reagent blank as reference. Calculate the vanadium content (in p.p.m.) by using the calibration data.

The results obtained on standard rocks and other materials are presented in Table IV.

CONCLUSIONS

The following conclusions may be drawn from the examination of these two major reagent systems for the spectrophotometric determination of vanadium in silicate rocks.

(a) Substituted hydroxamic acids form coloured chelates of medium sensitivity with either vanadium(IV) or vanadium(V) in strongly acidic (4–7 *M* HCl) medium. The only major interference—titanium(IV) —can be suppressed by fluoride ions. However, the somewhat large scatter in vanadium values of silicates (Table IV) shows that the titanium interference is incompletely suppressed by the small amount of fluoride added (2 ml of 4% NaF)[3]. The results suggest that other elements present in silicates in macro-amounts, especially aluminium, compete with titanium for fluoride ions. This problem may be illustrated by the performance of PPPH in extractive spectrophotometry: whereas the vanadium extracts obtained from pure solutions had a blue colour, those from silicates were greenish; when shaken with ammonium fluoride solution, the extracts became pure blue, indicating the removal of titanium. Absorbance measurement of the latter gave low values for vanadium, which was attributed to reagent consumption by the available free titanium ions. Further increase of fluoride concentration was impractical on account of marked corrosion of the glassware in the strongly acidic solution.

(b) The application of the 3,5-Br-MEPADAP–hydrogen peroxide system to the spectrophotometric determination of vanadium in silicates offers several major improvements over hydroxamic acids. The excellent sensitivity, high selectivity and solubility of the coloured species in several solvents make the ternary complex system ideally suited. Because of the lower acidity conditions, large amounts of fluoride can be added and any absorbance, formed in rock solutions, at 615 nm is due solely to vanadium. Moreover, the precision attainable by this method is significantly higher than that of the hydroxamic acid or emission spectrographic methods.

The analytical scheme may be readily applied to the determination of vanadium in bituminous and carbonaceous shales, heavy petroleum distillation residues and biological materials by preliminary mineralization with nitric–perchloric–sulphuric acids, followed by hydrofluoric acid evaporation if necessary. Prolonged heating of the digested sample at fuming temperatures will remove most of the perchloric acid. By a suitable pre-concentration procedure[18] vanadium

TABLE IV

DETERMINATION OF VANADIUM IN SILICATES

Sample	*V (p.p.m.)*	s_r	*No. of detns.*	*Other values*
Granite G-2	36.3	0.63	8	33 ± 2^a, 35[e], 34', 32 ± 2,5[h], 35.4[i]
Granodiorite GSP-1	52.8	0.46	8	52.9[a], 53[e], 49[f], 52.9[i], 43[h]
Granodiorite GSJ-JG-1	24.8	0.63	8	25[g], 21[g], 25[g]
Andesite AGV-1	123	0.21	8	110 ± 2^a, 112[b], 115[e], 125[f], 125[i], 104 ± 3^h
Basalt BCR-1	425	0.21	8	410 ± 2^a, 390 ± 12^b, 413 ± 5^c, 380[e], 410[f], 370 ± 36^h, 399[i]
Basalt BHVO-1	320	0.48	8	310 ± 17^j, 310[k]
Basalt GSJ-JB-1	198	0.28	12	200[g], 390[g], 240 ± 5^d
Peridotite PCC-1	34.7	0.34	8	30[e], 31[f], 30[i], 26 ± 2.7^h
Dunite DTS-1	14.0	0.98	8	10[e], 13[f], 10.3[i], 10.7 ± 0.9^h
Tonalite T-1	88	0.29	8	90[e], 81 ± 1.7^h, 96?[f]
Pyroxene-Ilmenite Xenolith, Monastery Mine, Sth. Africa	512	0.32	8	530[c]
Tertiary and quaternary volcanics, ex Java and Bali, Indonesia				
Basalt, TR 71-983 Un. 11	289 ± 0.5	—	2	250[b], 280[k]
Dacite, TR 71-989 Pp6	95.8 ± 1.3	—	2	101[b], 78[k]
Andesite, TR 71-1002 Sb-10	104.5 ± 0.0	—	2	120[b], 115[k]
Basaltic Andesite, 71-1028 Su 15	177.3 ± 0.0	—	2	202[b], 175[k]
Basalt, TR 72-955 Mh	279 ± 1.0	—	2	320[b], 285[k]
Basalt, TR 72-937 Mh	360 ± 1.2	—	2	390[b], 410[k]
Basalt, TR 72-970 BM-2	270 ± 0.9	—	2	287[b], 295[k]
Basalt, TR 72-976 BM-8	263 ± 1.8	—	2	290[b], 285[k]
Dacite, TR 72-991 Ba-1	6.3 ± 0.1	—	2	17[b], 10[k]
Andesite TR 72-985 Ag5	128 ± 0.8	—	2	140[b], 128[k]
Basalt TR 72-996 Pe-1	261 ± 0.6	—	2	284[b], 240[k]

[a] BTH extraction; PADAP spectrophotometry.
[b] PPPH extractive spectrophotometry.
[c] BTH extractive spectrophotometry.
[d] N-Furoyl-*o*-tolylhydroxylamine spectrophotometry.
[e] Preferred values for inter-laboratory standard rock samples (M. Kaye, Dept. of Geology, A.N.U.).
[f] S. Abbey, *Can. Geol. Surv. Pap. No. 72-30*, 1972.
[g] A. Ando *et al.*, *Geochem. J.*, 9 (1971) 151.
[h] P. G. Jeffery and G. O. Kerr, *Analyst (London)*, 92 (1967) 763.
[i] F. J. Flanagan, *Geochim. Cosmochim. Acta*, 37 (1973) 1189.

could probably be determined by the ternary complex formation at the p.p.b. level in natural and sea waters.

The author wishes to thank Mr. P. H. Beasley of the x.r.f. Analytical Section of this School for his practical help and supply of standard materials, and Dr. J. E. Fildes and her staff of the Micro-analytical Section for elemental analysis. He is also indebted to Dr. J. R. Richards of the Research School of Earth Sciences and Dr. E. H. Creaser, Genetics Section, Research School of Biological Sciences, for their assistance in various ways.

SUMMARY

The synthesis of a new heterocyclic azo compound, 2-(3,5-dibromo-4-methyl-2-pyridylazo)-5-diethylaminophenol (3,5-Br-MEPADAP) is described. The dye forms an intensely coloured ($\varepsilon = 4.11 \cdot 10^4$ l mole^{-1} cm^{-1} at 615 nm) unstable chelate with vanadium(V) in weakly acidic medium. However, vanadium(V) reacts with 3,5-Br-MEPADAP and hydrogen peroxide in 0.5 *M* sulphuric acid to form a stable 1:1:1 ternary complex which is extractable in several solvents. In the presence of fluoride, the reaction is highly selective for vanadium(V); only large amounts of halides, oxidizing and reducing agents interfere. The effective molar absorptivity is $5.43 \cdot 10^4$ l mole^{-1} cm^{-1} at 615 nm in chloroform. The reagent system was applied for the direct spectrophotometric determination of vanadium in a wide range of silicates; the average relative standard deviation was 0.45 %. The accuracy of the vanadium values obtained for ten international standard rocks compares well with the currently accepted most probable values.

REFERENCES

1 E. R. Wright and M. G. Mellon, *Ind. Eng. Chem., Anal. Ed.*, 9 (1937) 375.
2 A. P. Vinogradov, *C. R. Acad. Sci. U.R.S.S.*, 249 (1931A).
3 P. G. Jeffery and G. O. Kerr, *Analyst (London)*, 92 (1967) 763.
4 A. K. Majumdar, *N-Benzoylphenylhydroxylamine and its derivatives*, Pergamon Press, Oxford, 1972.
5 V. K. Gupta and S. G. Tandon, *Anal. Chim. Acta*, 66 (1973) 39.
6 D. C. Bhura and S. G. Tandon, *Anal. Chim. Acta*, 53 (1971) 379.
7 M. Hamana and M. Yamazaki, *Chem. Pharm. Bull.*, 10 (1962) 51.
8 A. E. Chichibabin, *J. Russ. Phys.-Chem. Soc.*, 50 (1920) 512.
9 S. Shibata, M. Furukawa, Y. Ishiguro and S. Sasaki, *Anal. Chim. Acta*, 55 (1971) 231.
10 E. Kiss, *Anal. Chim. Acta*, 66 (1973) 385.
11 R. G. Anderson and G. Nickless, *Analyst (London)*, 93 (1968) 13, 20; *Anal. Chim. Acta*, 39 (1967) 469.
12 S. I. Gusev and L. M. Shchurova, *Zh. Anal. Khim.*, 19 (1964) 799; 21 (1966) 1042.
13 S. Shibata, M. Furukawa and K. Toei, *Anal. Chim. Acta*, 66 (1973) 397.
14 S. I. Gusev and G. G. Shalamova, *Zh. Anal. Khim.*, 23 (1968) 686.
15 K. N. Bagdasarov, Kh. A. Akhmedova and O. A. Tataev, *Zavod. Lab.*, 35 (*1*) (1969) 12.
16 N. Irving Sax, *Dangerous properties of Industrial Materials*, Van Nostrand–Reinhold, 3rd edn., 1968.
17 J. A. Cooper, *Geochim. Cosmochim. Acta*, 27 (1963) 525; and personal communication.
18 K. M. Chan and J. P. Riley, *Anal. Chim. Acta*, 34 (1966) 337.

Analytica Chimica Acta, 77 (1975) 223–228

FLUORIDE IN SEA WATER: INTERCALIBRATION STUDY BASED ON ELECTROMETRIC AND SPECTROPHOTOMETRIC METHODS

THEODORE B. WARNER and MARK M. JONES
U.S. Naval Research Laboratory, Washington, D.C. 20375 (U.S.A.)
GERARD R. MILLER, JR.* and DANA R. KESTER
Graduate School of Oceanography, University of Rhode Island, Kingston, Rhode Island 02881 (U.S.A.)
(Received 20th November 1974)

INTRODUCTION

In the past ten years, estimates of the fluoride/chlorinity (F/Cl) ratio in sea water have ranged from 6.6 to $6.9 \cdot 10^{-5}$ (Table I). The colorimetric and electrometric methods used are so precise that these different average values, if accurate, would imply that fluoride is not conservative in "normal" sea water. Yet individual laboratories usually found that fluoride was conservative in their sample sets. (Those regions where anomalous increases of fluoride have been found at depth, are excluded here. They are distinguished by being very large increases, occurring only in near-bottom water at a few sites, with normal values found above in the water column.)

TABLE I

RECENT ESTIMATES OF FLUORIDE/CHLORINITY RATIO IN SEA WATER

Author(s)	*No. of samples*	*Location*	*F/Cl* $(gF^- \; kg^{-1}/^0/_{00} \; Cl) \cdot 10^5$
Greenhalgh and Riley[1] (1963)	~300	North Atlantic[a] South Atlantic[a] Pacific Indian	6.7±0.1
Riley (1965)[2]	—	North Atlantic[a]	6.7±0.1
Brewer *et al.* (1970)[3]	~200	North Atlantic	6.9
Kester (1971)[4]	104	North Atlantic	6.70±0.1
Bewers (1971)[5,6]	151	North Atlantic	6.82±0.1
	69	South Atlantic	6.59±0.1
	65	Pacific	6.66±0.1
Warner (1971)[7]	224	North Atlantic Pacific Caribbean Sea	6.71±0.03

[a] "Normal" waters (anomalous-increases of fluoride were found at depth).

* Present address: Black and Veatch, P.O. Box 8405, Kansas City, Missouri 64114.

This study was designed to answer several questions. First, do these different estimates imply true variability of F/Cl ratios with location, or do they represent random errors in the determination of a constant ratio? Secondly, if the latter is the case, how can the errors be reduced and what is the most probable value of the F/Cl ratio in sea water? These questions have been examined by comparing results obtained in different laboratories on the same sea water samples (Table I).

METHODS

One sample set was collected by the Naval Research Laboratory (Gibbs 570), one by the Bedford Institute of Oceanography (Hudson 71), and one by the University of Rhode Island (TR-102). Samples were labeled only with a code number. Each laboratory reported the measured fluoride content before receiving additional data such as salinity or sample location. Thus, results were obtained on completely blind samples when collection was done by others.

Sea water was stored in cleaned polyethylene bottles that had been pre-soaked with distilled or sea water for extended periods. URI determined fluoride by the spectrophotometric method of Greenhalgh and Riley[8]. NRL used a modified form of the known-addition electrode method of Warner[7,9] in which concentrations were computed by means of an exact expression given by Durst[10]. Previously reported results given in Table I were recomputed with this relation. Salinities were determined by inductive salinometer and titration to $\pm 0.01\%$.

TABLE II

VALUES OF FLUORIDE TO CHLORINITY RATIOS ($gF^- \; kg^{-1}/^0/_{00}$ Cl)·10^5 USED IN THE INTERCALIBRATION STUDY

Sample no.	*Depth (m)*	*Salinity (°/₀₀)*	*Replicate determinations of F/Cl°/₀₀ ratios*				
			NRL		*URI*		
			1	*2*	*1*	*2*	*3*
Gibbs 570 samples							
Station 1: 26 May 1970, 16°35.6'N, 75°58.4'W, sonic depth 1464 m							
43	45	35.90	6.69	6.75	6.60	6.69	6.70
44	970	34.84	6.79	6.84	6.77	6.63	6.81
45	1270	34.93	6.77	6.72	6.69	6.76	6.77
46	1470	34.95	6.77	6.71	6.68	6.74	6.75
Station 2: 30 May 1970, 8°14.3'N, 84°50.0'W, sonic depth 2250 m							
47	0	33.68	6.81	6.66	6.73	6.73	6.81
48	10	34.09	6.78	6.67	6.66	6.79	6.76
49	30	34.42	6.76	6.71	6.67	6.69	6.74
50	50	34.80	6.74	6.69	6.64	6.77	6.76
51	70	34.89	6.67	6.73	6.71	6.71	6.76
52	100	34.93	6.66	6.72	6.63	6.69	6.74
53	500	34.68	6.71	6.77	6.79	6.77	—

TABLE II (*continued*)

Sample no.	*Depth (m)*	*Salinity (‰)*	*Replicate determinations of F/Cl‰ ratios*				
			NRL		*URI*		
			1	*2*	*1*	*2*	*3*
Station 3: 4 June 1970, 16°20'N, 111°31'W, sonic depth 3750 m							
61	57	34.50	6.74	6.80	6.70	6.77	—
62	300	34.68	6.71	6.66	6.64	6.76	—
63	786	34.61	6.78	6.78	6.85	6.74	—
64	1179	34.65	6.77	6.72	6.78	6.78	6.72
65	1552	34.68	6.77	6.77	6.66	6.76	6.76
66	2117	34.71	6.76	6.76	6.67	6.72	6.74
67	2290	34.73	6.70	6.76	6.70	6.65	6.71
68	2465	34.74	6.76	6.65	6.78	6.77	—
69	2635	34.74	6.70	6.65	6.71	6.77	—
Station 4: 5 June 1970, 16°00'N, 120°29'W, sonic depth 3660 m							
74	30	34.56	6.73	6.69	6.60	6.65	—
81	100	34.19	6.66	6.81	6.68	6.68	—
82	500	34.66	6.66	6.66	6.65	6.64	6.68
Mean ±99% conf. limits			6.73±0.02		6.72±0.02		
Hudson 71 samples							
Station 2: 16 October 1971, 58°36.3'N, 52°32.8'W, sonic depth 3376 m							
1	0	34.21	6.78	—	6.69	6.67	—
2	300	34.83	6.74	—	6.75	6.68	—
3	600	34.90	—	—	6.68	6.68	—
4	900	34.93	—	—	6.72	6.64	—
5	1200	34.87	6.83	6.67	6.90	6.77	—
6	1500	34.93	—	—	6.68	6.67	—
7	1800	34.96	—	—	6.73	6.72	—
8	2100	34.98	6.76	—	6.70	6.70	—
9	2400	34.99	6.76	—	6.67	6.69	—
10	2700	34.96	6.71	—	6.76	6.74	—
11	3000	34.94	6.76	—	6.64	6.64	—
12	3300	34.95	6.71	6.71	6.67	6.66	—
Station 3: 17 October 1971, 56°42.4'N, 54°8.1'W, sonic depth 3215 m							
13	0	34.02	6.84	—	6.75	—	—
14	300	34.87	6.78	—	6.71	6.72	—
15	600	34.91	6.83	—	6.67	6.66	—
16	900	34.93	6.72	—	6.71	6.71	—
17	1200	34.94	—	—	6.66	6.64	—
18	1500	34.94	6.72	—	6.66	6.71	—
19	1800	34.97	6.76	—	6.60	6.64	—
20	2100	34.98	6.81	6.81	6.66	6.66	—
21	2400	34.97	6.71	6.81	6.62	6.64	—
22	2700	34.96	6.71	6.71	6.63	6.65	—
23	3000	34.93	—	—	6.59	6.65	—
Mean ±99% conf. limits			6.76±0.03		6.68±0.02		

RESULTS AND DISCUSSION

Results obtained independently in the two laboratories (a portion of which are shown in Table II) were examined to establish the precision of the methods, any significant differences in F/Cl ratios found in different samples measured in one laboratory, and any systematic errors between laboratories.

Precision of the analytical methods

The relative standard deviation for each method was 0.8% on a day-to-day basis; it was often less within a given day. This was based on replicate measurements in the same sample.

Variation of F/Cl ratios within laboratories

Analysis of variance showed that the variation between samples was not significantly different from the variation caused by the analytical method. Hence, fluoride was a conservative constituent of these sea water samples based on data from each laboratory.

Variation of F/Cl ratios between laboratories

Analysis of variance of various subsets of the data showed that the differences between laboratories were highly significant for the Hudson 71 samples, and not significant in the Gibbs 570 samples. One such analysis is shown in Table III. Here, F/Cl ratios differed by more than could be accounted for by chance; *i.e.*, systematic error existed between laboratories for this set of samples. This is also evident when comparing the mean values given in Table II.

TABLE III

INTERLABORATORY STUDY—ANALYSIS OF VARIANCE OF F/Cl BASED ON FIVE HUDSON 71 SAMPLES (NOS. 5, 12, 20, 21, 22)

Source of variation	*Degrees of freedom*	*Sums of squares*	*Mean squares*	*F*[a]
Laboratories	1	0.01922	0.01922	7.20 ($P<0.05$)
Samples	4	0.03657	0.00914	3.42
Lab. × samples	4	0.03433	0.00858	3.21
Analysis	10	0.02670	0.00267	—
Total	19	0.11682	—	—

[a] F = Ratio between corresponding mean square and analysis mean square.

Since different laboratories obtain significantly different means on the same set of samples, it is probable that the spread of the data in Table I is caused by similar interlaboratory errors rather than by real variations in the oceans. Every measurement must be considered to have two contributions to overall uncertainty, one from imprecision and one from possible systematic error. As Eisenhart[11] has discussed in detail, both must be assessed and reasonable limits given. The systematic error in this study was constant for analyses made at a given time,

TABLE IV

INTERLABORATORY RESULTS—MEAN F/Cl RATIOS ($gF^- \cdot kg^{-1}/^{o}/_{oo}$ Cl)$\cdot 10^5$

Measuring laboratory	*Cruise and collecting laboratory*		
	Gibbs 570 (NRL)	*TR-102 (URI)*	*Hudson 71 (BIO)*
Univ. of Rhode Island	6.72	6.68[a]	6.68
Naval Research Lab.	6.73	Acid[b]	6.76

[a] Set consisted of 23 samples collected between Iceland and Nova Scotia and measured in duplicate.
[b] Excluded from this study because water was acidified to pH 1 when stored, resulting in abnormally low values when later remeasured.

but could vary between sets measured at different times or in different laboratories. Probable systematic error can be estimated from the spread of such results.

Table IV gives the mean F/Cl ratios obtained by the two laboratories on different sets of samples. To obtain a best estimate of the true F/Cl ratio and the total uncertainty associated with this overall mean value, these five values are assumed to be normally distributed around the true value, owing to random interlaboratory errors. Their mean is $6.71 \cdot 10^{-5}$ mg F^- $kg^{-1}/^{o}/_{oo}$ Cl which represents the best estimate of the true value. The standard deviation of this mean is $0.015 \cdot 10^{-5}$, which with four degrees of freedom yields a 99% confidence limit of $\pm 0.07 \cdot 10^{-5}$. This value represents the total uncertainty of a mean value reported by a single laboratory on a set of fluoride samples; it includes a contribution from the analytical imprecision as well as an estimate of interlaboratory difference. This confidence limit provides a more realistic estimate of uncertainties for interlaboratory comparisons than the analytical imprecision of $\pm 0.02 \cdot 10^{-5}$. The difference between these two values of $\pm 0.05 \cdot 10^{-5}$ represents a systematic error which varies between laboratories and within a laboratory for different sample sets or periods of analysis. A similar treatment of the larger body of more divergent results in Table I gives a best estimate of $6.72 \cdot 10^{-5}$ which agrees well with the value based on Table IV. Systematic error can be eliminated in the future by calibrating each set of measurements against a reference sea water of known salinity whose F/Cl ratio is defined by convention. This will allow more sensitive tests as to whether two sets of samples have significantly different means.

The present results support the validity of unusually high fluoride concentrations reported in the past at a few restricted deep locations[1–4]. The spectrophotometric method used to measure those high values gave results consistent with electrometric measurements to within 1% during this study. The fluoride previously found in surface water at anomalous locations can serve as internal standards. Those ratios agreed closely with the most probable value found here.

We are indebted to J. M. Bewers and B. Sundby, who shared their Hudson 71 samples with us and contributed many helpful criticisms; to D. Bressan, J. M. Gieskes, E. D. Goldberg, and J. Greenslate for useful suggestions; and to Joris Gieskes, who provided a stimulating environment at the Scripps Institution of

Oceanography, La Jolla. This work was supported in part by the Office of Naval Research Contract No. N00014-68-A-0215-0003.

SUMMARY

Fluoride was shown to be a conservative constituent of sea water. Samples from the eastern tropical North Pacific, the Caribbean, the Labrador Basin, and the Reykjanes Ridge region indicated that the most probable F/Cl ratio in sea water is $6.71 \cdot 10^{-5}$ with an overall uncertainty of $\pm 0.07 \cdot 10^{-5}$ based on 99% confidence limits of $\pm 0.02 \cdot 10^{-5}$ and an allowance of $\pm 0.05 \cdot 10^{-5}$ for systematic error. Double-blind measurements from laboratories using electrometric and spectrophotometric methods agreed closely. Mean F/Cl ratios found were all within 0.7% of the most probable value.

REFERENCES

1 R. Greenhalgh and J. P. Riley, *Nature (London)*, 197 (1963) 371.
2 J. P. Riley, *Deep Sea Res.*, 12 (1965) 219.
3 P. G. Brewer, D. W. Spencer and P. E. Wilkniss, *Deep Sea Res.*, 17 (1970) 1.
4 D. R. Kester, *Deep Sea Res.*, 18 (1971) 1123.
5 J. M. Bewers, *Deep Sea Res.*, 18 (1971) 237.
6 J. M. Bewers, Unpublished MS, AOL 1971–4, Bedford Inst. Oceanog., Dartmouth, N.S., 1971.
7 T. B. Warner, *Deep Sea Res.*, 18 (1971) 1255.
8 R. Greenhalgh and J. P. Riley, *Anal. Chim. Acta*, 25 (1961) 179.
9 T. B. Warner, *Water Res.*, 5 (1971) 459.
10 R. A. Durst, *Mikrochim. Acta*, (1969) 611.
11 C. Eisenhart, *Science*, 160 (1968) 1201.

Analytica Chimica Acta, 77 (1975) 229–237

SPECTROPHOTOMETRIC STUDIES ON THE EQUILIBRIA OF VANADIUM(V)–4-(2-PYRIDYLAZO)-RESORCINOL–POLYAMINOPOLYCARBOXYLATE SYSTEMS

JUN-ICHI ITOH, TAKAO YOTSUYANAGI and KAZUO AOMURA

Laboratory of Analytical Chemistry, Faculty of Engineering, Hokkaido University, Sapporo 060 (Japan)

(Received 23rd October 1974)

The metallochromic indicator 4-(2-pyridylazo)-resorcinol (PAR; H_2R) has been used as a highly sensitive reagent for the colorimetric determination of many metal ions[1]. However, because of the poor selectivity of PAR, a preliminary separation of interfering ions is essential for practical analysis. Various selective masking methods have been studied; trace amounts of chromium(III)[2], palladium-(II)[3], iron(II)[4,5], cobalt(III)[4,6] and vanadium(V)[7,8] can be selectively determined with PAR if polyaminopolycarboxylates (*e.g.* EDTA, CDTA) are used as masking agents. The selective masking reactions with ethylenediaminetetraacetic acid (EDTA) and cyclohexanediaminetetraacetic acid (CDTA) were attributed to thermodynamic effects (for Pd(II), Fe(II), Co(III) and V(V)), and to kinetic effects (for Cr(III)). However, the equilibrium relationship among the PAR, CDTA and EDTA complexes of the vanadyl ion is unusual. EDTA breaks down the reddish purple PAR–VO_2^+ complexes but CDTA has little influence. CDTA has a special action towards the vanadyl ion, in that it does not form a stable complex, in contrast to other metal ions[9,10]. Thus, the stability order of the vanadyl complexes is established qualitatively as VO_2^+–EDTA > VO_2^+–PAR > VO_2^+–CDTA, however, an explanation of this order is impossible on the basis of the available constants: ($\log K_{VO_2EDTA} = 15.55$ (ref. 11) or 18.05 (ref. 12), $\log K_{VO_2CDTA} = 16.61$ (ref. 13) and $\log K_{VO_2PAR} = 16.49$ (ref. 14)). Therefore, it seemed worthwhile to reinvestigate the equilibria of these systems in order to understand the unusual selective masking behavior of CDTA for PAR–VO_2^+ complexes.

EXPERIMENTAL

Reagents and apparatus

PAR solution. A 0.005 *M* solution was prepared by dissolving 1.076 g of PAR (Dojindo Co. Ltd.) in 50 ml of 0.2 *M* sodium hydroxide solution and diluting to 1 l. The solution was standardized by spectrophotometric titration with standard nickel(II) solution.

Vanadium(V) solution. A 0.01 *M* solution was prepared by dissolving ammonium metavanadate and standardized by titration with EDTA.

The stock solutions of CDTA and EDTA were $5.00 \cdot 10^{-2}$ *M* and their concentrations were checked by titration with standard lead solution.

The pH was adjusted by means of dilute hydrochloric acid and potassium

hydroxide solutions. The ionic strength was adjusted to 0.1 with potassium chloride. All chemicals used were of analytical-reagent grade.

All photometric measurements were made with a Hitachi-124 Model Double-beam Recording Spectrophotometer equipped with 1-cm quartz cells. A Toa Dempa Model HM-5A pH-meter was used for pH measurements. The charges of VO_2^+–PAR complexes were examined by paper electrophoresis.

To determine the stability constants of VO_2^+–PAR complexes, methods based on the relationship, absorbance(A)=f(pH), were employed, on account of the high stability of the complexes studied. For estimation of the constants of the VO_2^+–CDTA and VO_2^+–EDTA complexes, ligand exchange equilibria were utilized.

$$\begin{matrix} VO_2^+\text{–CDTA} \\ \text{or} \\ VO_2^+\text{–EDTA} \end{matrix} + \text{PAR} \rightleftharpoons VO_2^+\text{–PAR} + \begin{matrix} \text{CDTA} \\ \text{or} \\ \text{EDTA} \end{matrix} \qquad (1)$$

All experiments were carried out for solutions with excess of ligands at 293 K (20°C). Thus, hydrolysis of vanadium(V), VO_2^+, was negligible.

RESULTS AND DISCUSSION

Formation of vanadium(V)–PAR complexes

Absorbance ($A_{comp.}$ see eqn. 7)–pH curves (Fig. 1) indicate that PAR reacts with the vanadyl ion to form two kinds of colored (reddish purple) complexes in acidic solution. The composition and the charge of the complexes were examined at pH 6 by Job's method and by electrophoresis, respectively. The results showed the presence of a 1:1 VO_2^+–PAR complex, VO_2R^-, which is in accordance with the formula proposed by Babko *et al.*[14].

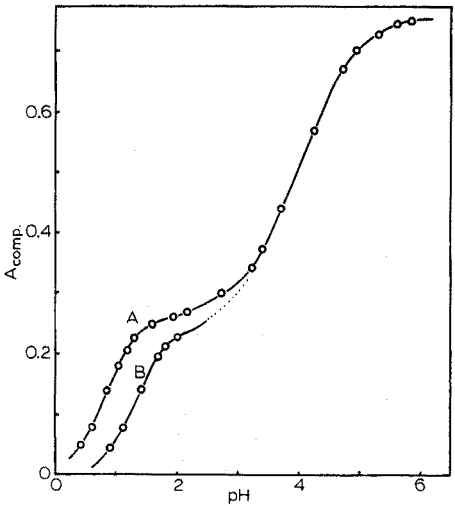

Fig. 1. Absorbance (A_{comp})–pH curves. 545 nm; 1-cm cells. (A) $C_V = 1.98 \cdot 10^{-5}$, $C_R = 2.04 \cdot 10^{-4}$. (B) $C_V = 1.98 \cdot 10^{-5}$, $C_R = 2.54 \cdot 10^{-5}$.

At pH values below 5, another complex is formed. Equilibrium measurements showed that this reaction involves the addition of one hydrogen ion:

$$VO_2HR \rightleftharpoons VO_2R^- + H^+ \tag{2}$$

with the acid dissociation constant

$$K^H_{VO_2HR} = \frac{[VO_2R^-]\cdot[H^+]}{[VO_2HR]} \tag{3}$$

Thus, the color change at pH values below 2 should be attributed to the formation of the complex VO_2–HR:

$$VO_2^+ + H_nR \rightleftharpoons VO_2HR + (n-1)\cdot H^+ \tag{4}$$

or

$$VO_2^+ + {}^*HR^- \rightleftharpoons VO_2HR \tag{5}$$

with the stability constant defined as

$${}^*K_{VO_2HR} = \frac{[VO_2HR]}{[VO_2^+]\cdot[{}^*HR^-]} \tag{6}$$

where $^*HR^-$ is a hypothetical ligand in which the 3-hydroxyl proton of resorcinol group is dissociated. In Fig. 1, the absorbance of the complexes, A_{comp}, is given by

$$A_{comp} = A - A_{PAR} = \varepsilon_1\cdot[VO_2HR] + \varepsilon_2\cdot[VO_2R^-] \tag{7}$$

where ε_1 and ε_2 are the molar absorptivities of VO_2HR and VO_2R^-, respectively; A_{PAR} is the absorbance of free PAR, C_R is the total concentration of PAR, and ε_R is the conditional absorptivity defined as

$$A_{PAR} = \sum_{n=0}^{3} \varepsilon_n^R\cdot[H_nR] = \varepsilon_R\cdot(C_R - \varepsilon_1\cdot[VO_2HR] - \varepsilon_2\cdot[VO_2R^-]) \tag{8}$$

where ε_n^R is the molar absorptivity of the PAR species, H_nR. The values of ε_R at various pH conditions were determined with pure PAR solutions. The values of ε_1 and ε_2 were found to be $1.25\cdot10^4$ and $3.80\cdot10^4$, respectively, from solutions with excess of metal ion at pH 1.5 and with excess of reagent at pH 6.

Thus, A_{comp} can be calculated from the following eqns. (9) and (10), since at pH values below 2 and above 2.5, the amounts of VO_2R^- ion and VO_2^+ ion can be effectively neglected, respectively, compared with the other vanadium(V) species in the solution.

$$A_{comp} = \varepsilon_1\cdot[VO_2HR] = \varepsilon_1\cdot\frac{(A - \varepsilon_R\cdot C_R)}{(\varepsilon_1 - \varepsilon_R)} \tag{9}$$

$$A_{comp} = \varepsilon_1\cdot[VO_2HR] + \varepsilon_2\cdot[VO_2R^-] = A - \varepsilon_R\cdot(C_R - C_V) \tag{10}$$

where C_V is the total concentration of vanadium(V) ion ($[VO_2^+]+[VO_2HR]+[VO_2R^-]$) and $C_R > C_V$.

The stability constant K_{VO_2HR} was calculated from eqn. (11):

$${}^*K_{VO_2HR} = \frac{f}{1-f}\cdot\frac{\alpha_{{}^*HR^-}}{(C_R - f\cdot C_V)} \tag{11}$$

where f is the molar fraction of VO_2^+ forming the complex, VO_2HR, $f=[VO_2HR]/C_V=A_{comp}/(\varepsilon_1 \cdot C_V)$ and α_{*HR^-} is defined as

$$\alpha_{*HR^-}=\frac{\sum_{n=0}^{3}[H_nR]}{[*HR^-]}=\frac{[H^+]^2}{k_{R1}\cdot k_{R2}}+\frac{[H^+]}{k_{R3}}+\frac{k_{R2}}{k_{R3}}+\frac{k_{R2}}{[H^+]} \tag{12}$$

where k_{R1}, k_{R2}, k_{R3} are the acid dissociation constants of PAR ($pk_{R1}=3.1$, $pk_{R2}=5.6$ and $pk_{R3}=11.9$)[15], respectively, and the dissociation constants of H_2R to form $*HR^-$, $*k_{R2}=[H^+]\cdot[*HR^-]/[H_2R]$, and that of $*HR^-$ to form R^{2-}, $*k_{R3}=[H^+]\cdot[R^{2-}]/[*HR^-]$, were taken as k_{R3} and k_{R2} of the PAR, respectively, according to the proposal of Corsini *et al.*[16]. The results of these calculations are shown in Table I.

TABLE I

CALCULATION OF STABILITY CONSTANT $*K_{VO_2HR}$ FROM EQUATION (11)

($\varepsilon_1=1.25\cdot10^4$)

$C_V=1.98\cdot10^{-5}$, $C_R=2.04\cdot10^{-4}$			$C_V=1.98\cdot10^{-5}$, $C_R=2.54\cdot10^{-5}$		
pH	A_{comp}	log $*K_{VO_2HR}$[a]	*pH*	A_{comp}	log $*K_{VO_2HR}$[a]
0.92	0.045	17.17	0.44	0.049	17.21
1.13	0.078	17.12	0.62	0.079	17.14
1.42	0.140	17.12	0.85	0.140	17.13
1.68	0.195	17.22	1.04	0.181	17.08
1.82	0.213	17.27	1.18	0.204	17.05
2.00	0.228	17.22	1.30	0.227	17.19

[a] log $*K_{VO_2HR}=17.16\pm0.05$ (average value of 12 experiments).

The acid dissociation constant $K^H_{VO_2HR}$ was calculated from

$$K^H_{VO_2HR}=\frac{1-f'}{f'}\cdot[H^+] \tag{13}$$

where $f'=[VO_2HR]/C_V=(\varepsilon_2\cdot C_V-A_{comp})/(\varepsilon_2-\varepsilon_1)\cdot C_V$. The results are shown in Table II.

TABLE II

CALCULATION OF ACID DISSOCIATION CONSTANT $K^H_{VO_2HR}$ FROM EQUATION (13)

($\varepsilon_1=1.25\cdot10^4$, $\varepsilon_2=3.80\cdot10^4$. $C_V=1.98\cdot10^{-5}$, $C_R=2.04\cdot10^{-4}$)

pH	A_{comp}	log $K^H_{VO_2HR}$[a]
3.24	0.342	3.87
3.40	0.374	3.87
3.72	0.439	3.93
4.25	0.569	4.00
4.72	0.670	4.00
4.95	0.703	3.97
5.31	0.727	4.01

[a] Av. 3.95 ± 0.05

The reasonable constancy of the values of K_{VO_2HR} and $K^H_{VO_2HR}$ in Tables I and II strongly supports the reaction scheme proposed in eqns. (2), (4) and (5). The average values are $\log K_{VO_2HR} = 17.16 \pm 0.05$ and $-\log K^H_{VO_2HR} = 3.95 \pm 0.05$, respectively. Thus the overall stability constant is:

$$K_{VO_2R} = \frac{[VO_2R^-]}{[VO_2^+]\cdot[R^{2-}]} = {}^*K_{VO_2HR}\cdot K^H_{VO_2HR}\cdot {}^*k^{-1}_{R3} = 10^{18.81} \quad (14)$$

Ligand exchange equilibria

In order to prove the unusual masking behavior of CDTA for the VO_2^+–PAR system, the following ligand exchange equilibria were directly studied by photometric means at pH 5.80 for $C_V = 1.0\cdot10^{-5}$ *M* and $C_R = 2.0\cdot10^{-5}$ *M*.

$$VO_2\text{–CDTA} + PAR \rightleftharpoons VO_2PAR + CDTA \quad (15)$$

The complex species participating in this reaction for the given conditions may be VO_2HCDTA^{2-}, VO_2CDTA^{3-}, VO_2HR and VO_2R^-. Therefore, the conditional ligand exchange constant K^{CDTA}_{ex} is defined as:

$$K^{CDTA}_{ex} = \frac{[VO_2\text{–PAR}]\cdot[CDTA]}{[VO_2\text{–CDTA}]\cdot[PAR]} \quad (16)$$

where $[VO_2\text{–PAR}] = [VO_2HR] + [VO_2R^-]$, $[VO_2\text{–CDTA}] = [VO_2HCDTA^{2-}] + [VO_2CDTA^{3-}]$, $[PAR] = \sum_{n=0}^{3} H_nR$ and $[CDTA] = \sum_{n=0}^{4} H_n\,CDTA$. The conditional constant K^{CDTA}_{ex} is correlated to the true ligand exchange constant $\mathbf{K}^{CDTA}_{ex}$ of the reaction

$$VO_2CDTA^{3-} + R^{2-} \rightleftharpoons VO_2R^- + CDTA^{4-} \quad (17)$$

$$\mathbf{K}^{CDTA}_{ex} = \frac{[VO_2R^-]\cdot[CDTA^{4-}]}{[VO_2CDTA^{3-}]\cdot[R^{2-}]} = K^{CDTA}_{ex}\cdot\frac{\alpha_{VO_2CDTA}\cdot\alpha_R}{\alpha_{VO_2R}\cdot\alpha_{CDTA}} \quad (18)$$

where α coefficients are defined as $\alpha_{VO_2R} = [VO_2\text{–PAR}]/[VO_2R^-] = 1 + [H^+]/K^H_{VO_2HR}$; $\alpha_{VO_2CDTA} = [VO_2\text{–CDTA}]/[VO_2CDTA^{3-}] = 1 + [H^+]/K^H_{VO_2HCDTA}$; $\alpha_{CDTA} = \sum_{n=0}^{4}[H_n\text{-CDTA}]/[CDTA^{4-}]$; and $\alpha_R = \sum_{n=0}^{3}[H_nR]/[R^{2-}]$. Judging from the value of the acid dissociation constant $K^H_{VO_2HR}$ ($10^{-3.95}$, Table II), the value of α_{VO_2R} is approximately one, *i.e.* $[VO_2\text{–PAR}] \simeq [VO_2R^-]$. Thus, $[VO_2R^{2-}]$ can be determined from eqns. (7) and (8) as

$$[VO_2R^-] = \frac{A - \varepsilon_R C_R}{\varepsilon_2 - \varepsilon_R} \quad (19)$$

where the value of $\varepsilon_R = 2.0\cdot10^2$ at pH 5.80. Equation (16) can be converted to:

$$\frac{[VO_2R^-]}{C_V - [VO_2R^-]} = K^{CDTA}_{ex}\cdot\left\{\frac{C_{CDTA} - C_V + [VO_2R^-]}{C_R - [VO_2R^-]}\right\} \quad (20)$$

Therefore, plots of $\log\{[VO_2R^-]/(C_V - [VO_2R^-])\}$ *vs.* $\log\{(C_{CDTA} - C_V + [VO_2R^-])/(C_R - [VO_2R^-])\}$ should be a straight line with a slope of 1. The plot for CDTA and that for EDTA, which was obtained by essentially the same treatment as for CDTA, are shown in Fig. 2. The values $\log K^{CDTA}_{ex} = 2.30$ and $\log K^{EDTA}_{ex} = 0.10$ were found at pH 5.80.

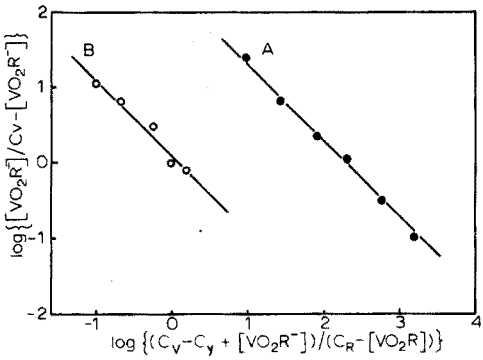

Fig. 2. Logarithmic plots of eqn. (20). $C_V = 1.0 \cdot 10^{-5}$, $C_R = 2.0 \cdot 10^{-5}$; C_Y (for CDTA and EDTA) were variable. (A) CDTA–VO_2–PAR, (B) EDTA–VO_2–PAR. (Solid lines A and B were obtained from eqn. (20) with $K_{ex}^{CDTA} = 10^{2.30}$ and $K_{ex}^{EDTA} = 10^{0.10}$, respectively.)

The ligand exchange constant IK_{ex} can be obtained by using the K_{ex} value and α coefficients (eqn. 18) evaluated from the acid dissociation constants of CDTA ($pK_1 = 2.43$, $pK_2 = 3.52$, $pK_3 = 6.12$, $pK_4 = 11.70$)[17], EDTA ($pK_1 = 1.99$, $pK_2 = 2.67$, $pK_3 = 6.16$, $pK_4 = 10.26$)[18], PAR[15], VO_2HR (see Table II), VO_2HCDTA^{2-} ($pK^H_{VO_2HCDTA} = -\log[H^+] \cdot [VO_2CDTA^{3-}]/[VO_2HCDTA^{2-}] = 4.00$)[13] and VO_2HEDTA^{2-} ($pK^H_{VO_2HEDTA} = 3.60$)[12]. The values were found to be $\log IK_{ex}^{CDTA} = 2.22$ and $\log IK_{ex}^{EDTA} = 1.43$.

The stability constants of the VO_2–CDTA and VO_2–EDTA complexes were obtained from the constants IK_{ex}^{CDTA}, IK_{ex}^{EDTA} and K_{VO_2R} (eqn. 15) as follows:

$$K_{VO_2CDTA} = \frac{[VO_2CDTA^{3-}]}{[VO_2^+] \cdot [CDTA^{4-}]} = \frac{K_{VO_2R}}{IK_{ex}^{CDTA}} = 10^{16.59} \tag{21}$$

$$K_{VO_2EDTA} = \frac{[VO_2EDTA^{3-}]}{[VO_2^+] \cdot [EDTA^{4-}]} = \frac{K_{VO_2R}}{IK_{ex}^{EDTA}} = 10^{17.38} \tag{22}$$

The value of K_{VO_2CDTA} in eqn. (21) is in fair agreement with that obtained in previous work (16.61) by analysis of absorbance–pH curves[13].

The equilibrium diagram for the VO_2–PAR–CDTA–EDTA system is shown in Fig. 3 with the constants obtained in this work.

Selective masking

The selective masking behavior of CDTA for the VO_2–PAR system can be understood on the basis of Fig. 3. In the case where large excesses of ligands are present ($C_Y \gg C_V$ and $C_R \gg C_V$), eqn. (20) can be simplified to:

$$\frac{[VO_2R^-]}{C_V} = \left\{1 + \frac{1}{K_{ex}} \cdot \frac{C_Y}{C_R}\right\}^{-1} \tag{23}$$

The values of $[VO_2R^-]/C_V$ (molar fraction of VO_2R^- complex) are shown in Fig. 4 as a function of $\log C_Y$ and $\log C_Y/C_R$ at pH 5.80. The curves A and B in Fig. 4 show that a 10-fold molar amount of CDTA decreases the value of $[VO_2R^-]/C_V$ by only about 5% with respect to its nominal value, but that 10-fold

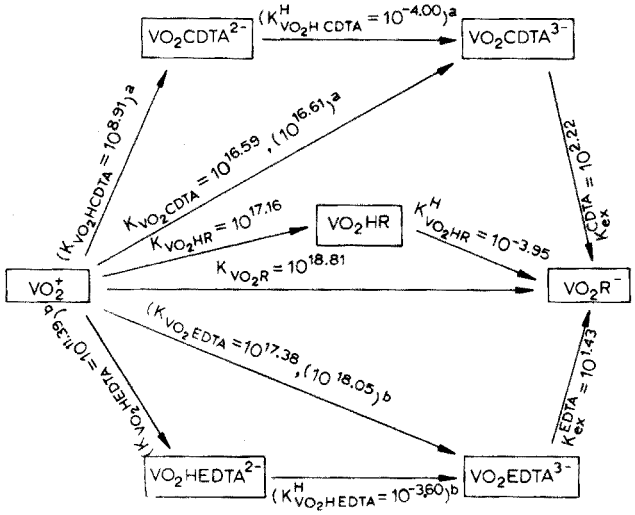

Fig. 3. Equilibrium diagram of VO_2^+–PAR–CDTA–EDTA system. (a) After Itoh *et al.*[13], and (b) after Ringbom *et al.*[12].

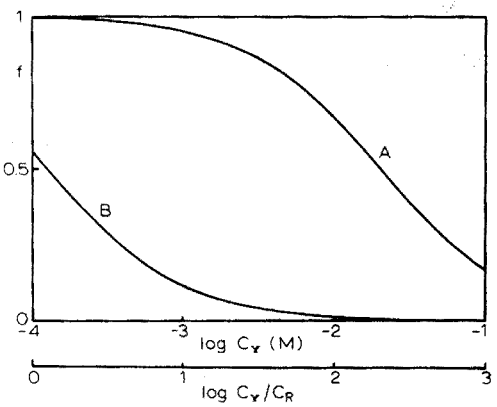

Fig. 4. Fraction of vanadium bound with R^-, $f=[VO_2R^-]/C_{VO_2}$. (A) In CDTA solution. (B) In EDTA solution. $C_R = 1.0 \cdot 10^{-4}$ M and pH 5.80.

and 100-fold molar amounts of EDTA decrease the value of $[VO_2R^-]/C_V$ by about 90% and 99%, respectively. Thus, by using a diagram such as Fig. 4, a highly sensitive and selective photometric method for vanadium(V) ion can be designed.

In order to know the relative positions of the equilibria for the VO_2^+–PAR, CDTA and EDTA complexes, log $^*K_{MHR}$ are plotted against log K_{MY} in Fig. 5. One can see that the positions of the VO_2^+, Pd^{2+}, UO_2^+ and Cu^{2+} ions are exceptional compared with most of the other metal ions, which have log $^*K_{MHR}$ values of less than 12. Thus the special masking behavior of CDTA in the VO_2–PAR system can be attributed not only to the unusual instability of the VO_2–CDTA complex, but also to the exceptionally high stability of the VO_2–PAR complex.

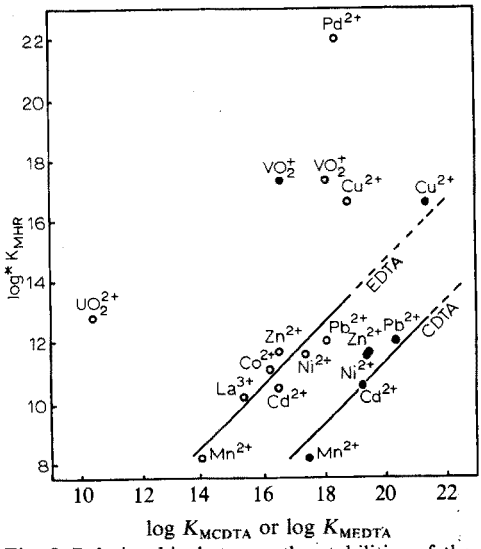

Fig. 5. Relationship between the stabilities of the PAR, CDTA and EDTA complexes of metal ions. (●) $^*K_{MHR}$ against K_{MCDTA}, (○) $^*K_{MHR}$ against K_{MEDTA}. (Pd^{2+}, estimated from Job's curves[19], and VO_2^+, this work. All other data were taken from Sillen and Martell[20].)

We thank Miss E. Nezu for some experimental assistance. This work was aided by a grant from the Ministry of Education, Japan, which is greatly appreciated.

SUMMARY

The complexation equilibria in the VO_2^+–PAR–polyaminopolycarboxylate-(EDTA and CDTA) systems were studied spectrophotometrically in order to establish the action of CDTA in the spectrophotometric determination of vanadium(V) with PAR. Analysis of absorbance–pH curve and ligand exchange equilibria yielded the following values of the constants; $K_{VO_2HR}=10^{17.16}$, $K^H_{VO_2HR}=10^{-3.95}$, $K_{VO_2R}=10^{18.81}$, $K_{VO_2EDTA}=10^{17.38}$ and $K_{VO_2CDTA}=10^{16.59}$ at 20°C and ionic strength 0.1 (KCl). Based on these constants, the selective masking behavior of CDTA for the VO_2^+–PAR system can be quantitatively explained.

REFERENCES

1 S. Shibata, in A. J. Barnard and H. Flaschka (Eds.), *Chelates in Analytical Chemistry, Vol. III*, M. Dekker, New York, 1972.
2 T. Yotsuyanagi, Y. Takeda, R. Yamashita and K. Aomura, *Anal. Chim. Acta*, 67 (1973) 297.
3 H. Hoshino, R. Yamashita, T. Yotsuyanagi and K. Aomura, *Nippon Kagaku Kaishi*, (1974) 495.
4 T. Yotsuyanagi, R. Yamashita and K. Aomura, *Anal. Chem.*, 44 (1972) 1091.
5 T. Yotsuyanagi, K. Goto and M. Nagayama, *Jap. Anal.*, 18 (1969) 184.
6 H. Ohkochi, *Jap. Anal.*, 21 (1972) 51.
7 O. Budevsky and L. Dzhonova, *Talanta*, 12 (1965) 291.
8 T. Yotsuyanagi, J. Itoh and K. Aomura, *Talanta*, 16 (1969) 1611.
9 O. Budevsky and R. Přibil, *Talanta*, 11 (1964) 1313.
10 W. J. Geary and C. N. Larsson, *S.A.C. Conference, 1965*, Heffer, Cambridge, 1965, p. 455.
11 L. Przyborowski, G. Schwarzenbach and Th. Zimmermann, *Helv. Chim. Acta*, 48 (1965) 1556.

12 A. Ringbom, S. Siitonen and B. Skrifvars, *Acta Chem. Scand.*, 11 (1957) 551.
13 J. Itoh, T. Yotsuyanagi and K. Aomura, *Anal. Chim. Acta*, 76 (1975) 471.
14 A. K. Babko, A. I. Volkova and T. E. Get'man, *Russ. J. Inorg. Chem.*, 11 (1966) 203.
15 L. Sommer and M. Hnilićková, *Anal. Chim. Acta*, 27 (1962) 241.
16 A. Corsini, I. M. Yih, Q. Fernando and H. Freiser, *Anal. Chem.*, 34 (1962) 1090.
17 G. Schwarzenbach and H. Ackermann, *Helv. Chim. Acta*, 32 (1949) 1682.
18 G. Schwarzenbach and H. Ackermann, *Helv. Chim. Acta*, 30 (1947) 1798.
19 R. Yamashita, Master Thesis, Hokkaido University, 1972.
20 L. G. Sillén and A. E. Martell, *Stability Constants of Metal–ion Complexes*, The Chemical Society, London, 1964; and its supplement, 1971.

Analytica Chimica Acta, 77 (1975) 239–244

SPECTROPHOTOMETRIC AND GRAVIMETRIC DETERMINATION OF SULFUR IN SEBACATE-BASE LUBRICANTS

GEORGE NORWITZ and HERMAN GORDON
Frankford Arsenal, Philadelphia, Pa. 19137 (U.S.A.)
(Received 27th November 1974)

There is little information in the literature on the determination of sulfur in sebacate-base lubricants. Sulfur in petroleum-base lubricants is usually determined by combustion in a bomb[1], or by high-temperature ignition[2] followed by precipitation as barium sulfate. These methods would seem applicable to sebacate-base lubricants but they are troublesome. The x-ray fluorescence method used for sulfur in petroleum-base lubricants offers difficulties when applied to sebacate-base lubricants because of interference from phosphorus[3].

In view of the need, the development of spectrophotometric and gravimetric methods for the determination of sulfur in sebacate-base lubricants was examined. The spectrophotometric method depends on the reduction of sulfate to hydrogen sulfide by treatment with a mixture of hydriodic, hypophosphorous, and hydrochloric acids, absorption of the hydrogen sulfide into ammonia solution, addition of a lead citrate reagent, and measurement of the brownish-yellow color of the lead sulfide sol. Such a technique has been used previously for the determination of sulfur in steels[4], nitrocellulose and propellants[5], and chromium plating baths[6]. In the gravimetric method, the sample is treated with nitric, hydrochloric, and perchloric acids, the solution is evaporated to fumes of perchloric acid, antimony and tin are volatilized by treatment with hydrobromic acid, and the sulfur is precipitated as barium sulfate.

EXPERIMENTAL

Spectrophotometric method

Apparatus. Prepare the apparatus as shown in Fig. 1. All the glass is Pyrex. The 50-ml round-bottom flask is held by a clamp about 1 f. above the bench. The inlet tube is connected to a tank of nitrogen by Tygon tubing; the nitrogen flow must be suitably controlled by a needle valve.

Standard sulfate solution (0.17 mg S ml^{-1}). Dissolve 0.9239 g of potassium sulfate (previously dried at 125°C) in water and dilute to 1 l in a volumetric flask.

Hydriodic–hypophosphorous–hydrochloric acid reagent. Transfer 200 ml of hydriodic acid (57%), 50 ml of hypophosphorous acid (50%), and 100 ml of hydrochloric acid (*d* 1.18) to a 500-ml ground-stoppered Erlenmeyer flask. Add several glass beads, boil for 5 min without a cover, remove from the hot plate, cover with a watch glass, allow to cool to room temperature, and insert the stopper.

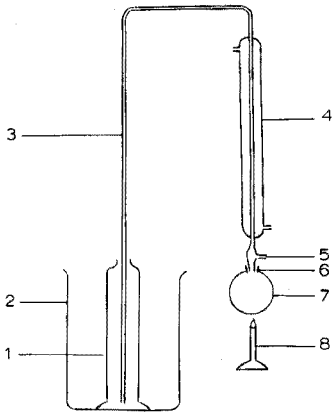

Fig. 1. Distillation apparatus. (1) 100-ml graduated cylinder, 25 cm high. (2) 1-l beaker. (3) Adapter tubing, 0.8 cm diameter (external); left arm, 60 cm long; horizontal (top) arm, 10 cm long. (4) Condenser; jacket, 25 cm long and 2 cm diameter (external). (5) Inlet tube for nitrogen, 10 cm long and 0.6 cm diameter (external). (6) 19/38 ground-glass joint. (7) 50-ml round-bottom flask. (8) Bunsen burner.

Lead citrate reagent. Dissolve 10 g of lead nitrate in 200 ml of water, add 40 g of citric acid monohydrate, and stir to dissolve. If salts settle out on standing overnight, use the supernatant liquid.

Preparation of calibration curve. Transfer 0.5, 1.0, 1.5, and 2.0 ml of the standard sulfate solution using a semimicro buret, to 50-ml round-bottom flasks (19/38 ground glass joints). Also carry a blank through the whole procedure. Attach an empty 50-ml round-bottom flask to the apparatus and insert the exit tube into a 100-ml graduated cylinder containing 90 ml of water. Connect to the nitrogen supply and regulate the flow to 65–85 bubbles per 15 s. Add 15 ml of ammonia solution (*d* 0.90) to each of five 100-ml graduated cylinders and dilute to about 90 ml with water. Place the graduated cylinders into broken ice contained in a tray. After a few min, place one of these graduated cylinders into the 1-l beaker and fill the beaker close to the top with broken ice. With the nitrogen flowing, attach the 50-ml round-bottom flask containing the sample to the adapter and insert the exit tube into the graduated cylinder in the beaker. Take care that the apparatus fits together properly and that the exit tube reaches the bottom of the cylinder. Lower the 50-ml round-bottom flask, add 20 ml of the hydriodic–hypophosphorous–hydrochloric acid reagent, and immediately reconnect the apparatus. Place a Bunsen burner with a flame about 2 in. high directly under the flask and heat for a total of 10 min (the solution should start to boil in about 3 min). At the end of the 10-min heating period, remove the cylinder, wash down the exit tube with water, add 6 ml of lead citrate solution, and dilute to the mark with water. Within 5 min, measure the absorbance at 400 nm against distilled water. Deduct the absorbance of the blank from the absorbance of the sample. Plot mg of sulfur against the corrected absorbance.

Procedure. Transfer a 0.2–0.3-g sample to a 50-ml round-bottom flask. Add 5 ml of nitric acid, 5 ml of hydrochloric acid, 3 ml of perchloric acid, and 3 ml of 25% (w/v) magnesium chloride solution. Carry along a blank. Place the

flask into a 150-ml beaker, place the beaker on a hot plate at its highest temperature, and heat until only dry salts remain. (If desired, the last 1–2 ml of perchloric acid can be driven off by heating directly over a small flame of a Bunsen burner). Allow to cool to room temperature and cool in ice. Proceed with the addition of the reagent, distillation, and development of the color as described for the preparation of the calibration curve.

Rinse the graduated cylinders with nitric acid (1+1) before using them for the next determination. Rinse the cells with concentrated nitric acid daily.

Gravimetric method

Transfer a 5-g sample to a 400-ml beaker and add 40 ml of nitric acid and 40 ml of hydrochloric acid. Carry along a blank. Cover with a watch glass and boil down to about 20 ml. Add 25 ml of perchloric acid, boil to fumes of perchloric acid, and fume for several min. Add nitric acid dropwise until the solution is colorless or only slightly yellow. If it is suspected that tin or antimony are present, add 10 ml of hydrobromic acid (48%), evaporate to fumes with the cover lid ajar, and continue fuming until the volume of perchloric acid is about 10 ml. Cool somewhat, wash down the watch glass and sides of the beaker with water, and evaporate to fumes again. Cool and dilute to about 200 ml with water. Heat to boiling, add 20 ml of 10% (w/v) barium chloride solution, and then boil for 2 min. Allow to stand overnight at room temperature. Filter through a tared sintered porcelain crucible of fine porosity, and transfer and wash with water. Dry the crucible at 150°C for 15 min, heat at 750°C for 30 min, cool in a desiccator, and weigh.

DISCUSSION AND RESULTS

The purpose of the magnesium salt in the spectrophotometric method is to prevent loss of sulfate (sulfuric acid) by volatilization. It is necessary to drive off practically all of the perchloric acid, otherwise low results are obtained for sulfur. The size of the sample must be relatively small, since the entire sample must be distilled; it is not possible to take an aliquot of a larger sample because of the precipitation of barium sulfate (resulting from the barium sulfonate present).

The type of apparatus used previously for the determination of sulfur in steels[4], nitrocellulose and propellants[5], and chromium-plating baths[6] did not give satisfactory results for sebacate-base lubricants. The reason for this was that incipient boiling required for this apparatus was inadequate to dissolve the barium sulfate. An improved apparatus with a reflux condenser was therefore developed that permitted vigorous boiling. A few min of boiling dissolved the small amount of barium sulfate in question. Vandael[7], who determined sulfate in barium sulfate titrimetrically after treatment with hydriodic and hypophosphorus acids, found that 1.5 h of boiling was required to dissolve 0.1 g of barium sulfate. When the improved apparatus was first fabricated, the adapter was so constructed that the inlet tube extended through the center of the adapter to the bottom of the reaction flask; unfortunately, the portion of the inlet tube inside the adapter broke repeatedly. Subsequently, excellent results were obtained with the simple adapter shown in Fig. 1, which is effective because the hydrogen sulfide is driven out of the flask

rapidly by the boiling and is swept rapidly through the condenser by the nitrogen.

The hydrogen sulfide is collected in a tall 100-ml graduated cylinder rather than as described previously[4–6]; the cylinder is more effective because of its greater height. For absorption, the recommended mixture is preferred to earlier ammoniacal absorbents[4–6], because, with the modified apparatus, less acid is driven over. Up to 5 ml of water can be tolerated in the distillation. Calibration curves should be prepared by treating portions of standard sulfate solution directly with the hydriodic–hypophosphorus–hydrochloric acid reagent, instead of evaporating to dryness as was done previously[4–6].

The effect of the amount of lead citrate reagent used for developing the color was investigated by distilling portions of potassium sulfate solution and adding different amounts of lead citrate reagent. The results showed that the color intensity was maximal with 5–10 ml of lead citrate reagent (although there was surprising intensity of color with 0.5 ml). The use of 6 ml of reagent is recommended.

With the improved method, the color follows Beer's law up to about 0.34 mg of sulfur (absorbance of 0.70). In the previous method, the color followed Beer's law up to about 0.25 mg of sulfur[5,6].

It can be concluded from previous work[4–6], that the following ions would not interfere with the method: alkali metals, alkaline earth metals, iron, chromium-(III), nickel, molybdenum, cobalt, manganese, zinc, cadmium, aluminum, magnesium, copper, bismuth, silver, mercury, lead, tin, germanium, antimony, selenium, chromium(VI), fluoride and fluorosilicate.

In the gravimetric method, it is not necessary to add the magnesium salt, because the solution is not evaporated to dryness. There is no danger of loss of sulfur by the hydrobromic acid treatment; the same results were obtained for samples not containing antimony and tin with or without the hydrobromic acid treatment.

The recommended range of the spectrophotometric method (for a 0.2–0.3-g sample) is 0.005–0.15% sulfur; the recommended range of the gravimetric method is 0.01–1% sulfur.

The results obtained for sulfur spectrophotometrically and gravimetrically in ten samples of sebacate-base MIL-L-46000B lubricant[8] are shown in Table I. It can be seen that the results agree well and that the precision of both methods is satisfactory.

MIL-L-46000B lubricant should have a barium dinonylnaphthalene sulfonate or barium petroleum sulfonate content of $1.5 \pm 0.3\%$ (ref. 8). Since the usual barium dinonylnaphthalene sulfonate or barium petroleum sulfonate used in this type of lubricant has a sulfur content of about 6%, the sulfur content of the lubricant should be about $0.09 \pm 0.02\%$. It can be seen from Table I that eight of the ten lubricants had approximately this amount of sulfur, while one sample had a very low sulfur content and one sample had a very high sulfur content.

The authors are indebted to Joseph F. Messina for furnishing the samples and giving advice. This work was conducted under an Army Materials Testing Technology Project (AMS Code 4931.OM.6350).

TABLE I

RESULTS FOR SULFUR IN SEBACATE-BASE LUBRICANTS

(Each result is the average of 2 or 3 determinations.)

Sample	*Sulfur (%)*		*Sample*	*Sulfur (%)*	
	Spectrophotometric	*Gravimetric*		*Spectrophotometric*	*Gravimetric*
1	0.10 ± 0.01	0.085 ± 0.005	6	0.05 ± 0.01	0.04
2	0.09 ± 0.01	0.085 ± 0.005	7	0.08	0.08
3	0.09 ± 0.01	0.08	8	0.08 ± 0.01	0.08
4		0.29 ± 0.02	9	0.08	0.08 ± 0.01
5	0.11 ± 0.01	0.095 ± 0.005	10	0.08 ± 0.01	0.085 ± 0.005

SUMMARY

Sulfur is determined in sebacate-base lubricants spectrophotometrically and gravimetrically. In the spectrophotometric method, a 0.2–0.3-g sample is treated with mixed acids, magnesium chloride is added, and the solution is evaporated to dryness. The sulfate is reduced to hydrogen sulfide by treatment with a mixture of hydriodic, hypophosphorous, and hydrochloric acids, and the hydrogen sulfide is distilled into ammonia solution. Lead citrate reagent is added and the brownish yellow color of lead sulfide sol is measured. An improved technique and apparatus for the distillation is described. In the gravimetric method, a 5-g sample is treated with mixed acids, antimony and tin are volatilized by treatment with hydrobromic acid, and sulfur is precipitated as barium sulfate. The recommended range of the spectrophotometric method is 0.005–0.15%, and that of the gravimetric method is 0.01–1% sulfur.

REFERENCES

1 *ASTM Designation D129-64, Sulfur in Petroleum Products by the Bomb Method*, American Society for Testing and Materials, Philadelphia, Pa., 1973.
2 *ASTM Designation D1552-64, Sulfur in Petroleum Products by High Temperature Method*, American Society for Testing and Materials, Philadelphia, Pa., 1973.
3 *ASTM Designation D2622-67, Sulfur in Petroleum Products (X-Ray Spectrographic Method)*, American Society for Testing and Materials, Philadelphia, Pa., 1973.
4 C. L. Luke, *Anal. Chem.*, 21 (1949) 1369.
5 G. Norwitz, *Analyst (London)*, 96 (1971) 494.
6 G. Norwitz, *Plating*, 59 (1972) 855.
7 C. Vandael, *Chim. Anal. (Paris)*, 44 (1962) 295.
8 *Military Specification, Lubricating Oil, Semi-Fluid (Automatic Weapons), MIL-L-46000B*, March, 1970.

Analytica Chimica Acta, 77 (1975) 245–254

A PERMEATION METHOD FOR THE DETERMINATION OF AVERAGE CONCENTRATIONS OF CARBON MONOXIDE IN THE ATMOSPHERE

DAVID R. BELL, KENNETH D. REISZNER and PHILIP W. WEST

Coates Chemical Laboratories, Environmental Sciences Institute, Louisiana State University, Baton Rouge, La. 70803 (U.S.A.)

(Received 20th January 1975)

Carbon monoxide is the most widely distributed air pollutant and appears to be principally a man-made pollutant. Because of the large variety of technological sources, significant differences in concentration from one location to another and the large variety in atmospheric conditions under which the measurements are taken, a great many methods for determining carbon monoxide have been developed. The methods range from fairly sophisticated instrumental techniques to less elaborate colorimetric techniques. The present method employs the silver sol colorimetric reagent[1] in a further extension of the permeation sampling concept previously used in the determination of sulfur dioxide[2]. The method is simple, inexpensive and reliable; no tedious sampling technique is required, and there are no electrical or mechanical connections to complex equipment.

In the permeation method a small quantity of the colorimetric reagent is placed in a glass tube enclosed on the bottom with a silicone rubber membrane and stoppered at the top. This permeation device is exposed to the ambient atmosphere. As air contacts the membrane, carbon monoxide in the air permeates through the membrane at a rate proportional to concentration and reacts with the reagent, producing a yellow silver sol. At the end of the exposure period the device is returned to the laboratory, and the intensity of the yellow color is used as a measure of the average carbon monoxide concentration in the air, as established from the predetermined permeation constant.

EXPERIMENTAL

Apparatus

A Beckman DB Spectrophotometer was used to measure all absorbance values.

Exposure chamber and permeation device

The exposure chamber and permeation device used in this study were identical to those used for sulfur dioxide (Fig. 1). The exposure chamber consisted of a glass tube (41-mm o.d., 75 mm long) through which the carbon monoxide–air mixtures were passed; side tubes were provided along one side for introducing one or more permeation devices. The permeation device consisted of a glass tube closed on one end with a silicone rubber membrane (1 mil); the membrane was sealed to the

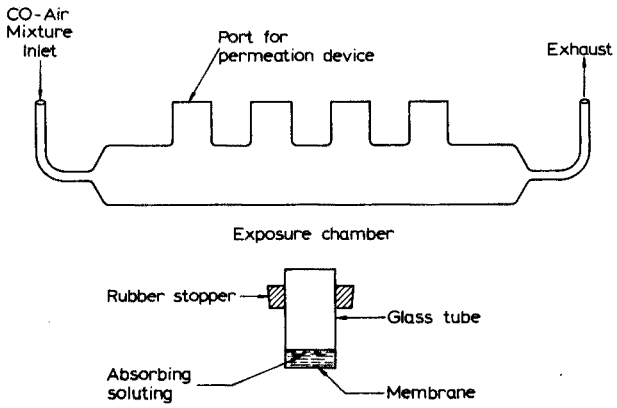

Fig. 1. Permeation device.

tube with silicone rubber cement. The device was inserted into a one-hole stopper and then inserted into the exposure chamber to make an air-tight seal. The chamber and devices then could be placed in a water bath for calibration of the devices at a specific temperature; or a series of exposure chambers, each exposed to different external conditions, could be connected together for rapid evaluation of one or more parameters.

Silver p-sulfamoylbenzoic acid reagent solution

To prepare the colorimetric reagent, 10 g of *p*-sulfamylbenzoic acid (Aldrich, *p*-carboxybenzenesulfonamide) and 2 g of sodium hydroxide were dissolved in 500 ml of deionized water using a magnetic stirrer. With continued good stirring, 500 ml of 0.1 *M* silver nitrate (Mallinckrodt) was added slowly; the resulting solution was cloudy white. This solution was stirred for 10 min to ensure complete reaction; 250 ml of 1 *M* sodium hydroxide was added, and the solution was stirred for an additional 10 min. The resulting solution was clear and colorless and was stored in a dark place for at least one week. Decolorizing charcoal was added, and the solution was filtered by suction through Celite 545 (Fisher). The reagent solution was stored in an amber bottle and kept in the dark. Solutions remained stable for up to six months and were discarded when blank values showed significant increases.

Procedures

Calibration of devices. To calibrate a permeation device, 10 ml of reagent solution was placed in the device in an exposure chamber, and the device was exposed to a known concentration of carbon monoxide for a specified period of time, typically 80 p.p.m. for 8 h. Preparation of carbon monoxide–air mixtures was accomplished by successive dilution of a pure carbon monoxide stream with streams of purified air or inert gases; rotameters were used to measure flow rates. Upon completion of the exposure the solution was stirred slightly (as any silver sol formed tends to collect at the bottom of the device), and the absorbance was measured against a reagent blank at 380 nm. The constant k (usually about 10^4 p.p.m. h) was calculated from:

$$k = Ct/A \tag{1}$$

where C is the concentration of carbon monoxide, t the time of exposure, and A the absorbance at 380 nm.

The constant k depends on the temperature of the measurement and the characteristics of the device; the value may be adjusted as appropriate to agree with the units of C and t. It should be noted that the constant k is not the same constant as that described previously[2], although there may be a definite relationship between them. The value must be determined experimentally for each device. Once the device has been calibrated, it may be used to determine carbon monoxide concentrations in the ambient atmosphere.

Analysis. The procedure for the determination of carbon monoxide with the silver *p*-sulfamoylbenzoic acid solution has been described by Ciuhandu[1]. In the present study 10 ml of the reagent were placed in a calibrated permeation device in a protective shelter[2] in the ambient atmosphere for a particular exposure period. Upon completion of the exposure the device was returned to the laboratory, and the absorbance was measured against a reagent blank at 380 nm. The concentration of carbon monoxide was determined from eqn. 1.

RESULTS AND DISCUSSION

Response time

The processes involved in the permeation of a gas through a solid do not occur instantaneously. There is a time delay between the moment that the gas is exposed to one surface of the membrane and the moment that a steady state is reached in the permeation process. In the development of a permeation method it is important to determine this time delay so that any experimental errors introduced in the measurement of a short-term exposure as a result of this delay may be predicted or eliminated. For carbon monoxide it was found that the permeation rate for the silicone membrane attained 100% of the steady state value within 10 min. All subsequent studies were conducted with exposure times of at least 2 h, and any error introduced in the measurements as a result of the response time delay was therefore considered to be negligible.

Temperature effect

As stated previously, the constant k in eqn. (1) is dependent on the temperature at which the measurement is made. In the previous study with sulfur dioxide the devices were calibrated at 25°C, and the accuracy of subsequent determinations made with those devices was dependent on the temperature dependence of permeability for the gas. For sulfur dioxide the temperature dependence of permeability was found to be very small, and the method developed for determining the gas was quite accurate over a fairly wide temperature range[2].

Unfortunately, the temperature dependence of permeability for carbon monoxide with this reagent is significantly higher than that for sulfur dioxide, as shown in Fig. 2, where each point represents an average of six determinations. The data indicate that there may be an error in the determination of carbon monoxide by this method of about 3.2% per °C, or about 2% per °F, for each degree of temperature difference between the temperature at which a measurement is taken and the temperature at which the device was calibrated.

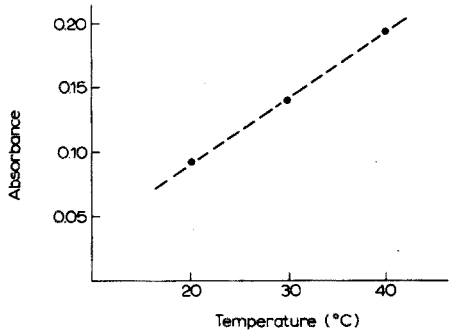

Fig. 2. Temperature dependence of permeability.

Response of measurement system

In order for eqn. (1) to be useful in an analytical method, the response of the system as measured by the product Ct must be uniform throughout the useful range of the method. The absorbance value obtained on exposure to 40 p.p.m. for 6 h should be the same as that obtained on exposure to 10 p.p.m. for 24 h, for example. Another way of stating this requirement is to state that the constant k must remain truly constant over the useful range of the method.

TABLE I

CONCENTRATION DEPENDENCE OF PERMEABILITY CONSTANT

CO concentration (p.p.m.)	*K ($\cdot 10^{-4}$ p.p.m. h)*
10	1.5
40	1.8
50	1.9
100	1.6
500	0.83

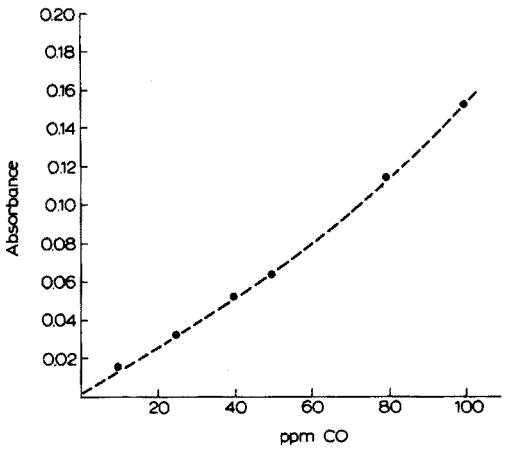

Fig. 3. Calibration curve.

Table I shows the average value of k determined for six permeation devices during calibrations at carbon monoxide concentrations from 10 to 500 p.p.m.; Fig. 3 is the calibration curve obtained. The value of k deviates by less than 12% at concentrations up to 100 p.p.m., and the response of the system is fairly linear up to a concentration of about 80 p.p.m. at which point the deviation from linearity reaches 10%. The useful range of the method is about 2–80 p.p.m. carbon monoxide for a 24-h exposure period.

Humidity effect on permeation

It has been shown[3] that in some cases permeability may be a humidity-dependent phenomenon. Fortunately in the present study the permeability of carbon monoxide through silicone rubber membranes was found to be independent of humidity. The average net absorbances of reagent solution in six devices exposed to 500 p.p.m. carbon monoxide for 2 h at 0% and 100% relative humidity were found to be identical.

Light effect

It has been reported[1] that exposure of the reagent to light will result in rapid deterioration. It was found during the present investigation that placement of exposed or unexposed reagent in direct sunlight results in complete loss of color in about 2 h. Indoor fluorescent lighting in the laboratory or sunlight penetrating translucent glass in the laboratory windows, however, produced no deterioration in either exposed or unexposed reagent for periods of up to 48 h. As a result of this observed deterioration in the presence of light, it was necessary to shield the device from light in the shelter used in field evaluations. As a precaution the reagent also was stored in amber bottles and kept in a dark place in the laboratory.

Stability of reagent

The present method was developed to determine average concentrations of carbon monoxide over periods of several hours. It was essential, therefore, that the response of the reagent be essentially uniform during the entire exposure period. Any silver sol formed early in the exposure period must be stable during the remainder of the exposure period, and the response of any unexposed reagent must be the same during the last portion of the exposure period as during the early portion.

To determine the stability of both exposed and unexposed reagent, carbon monoxide (500 p.p.m.) was bubbled through 50 ml of reagent at a flow rate of 600 ml min^{-1}, and samples of exposed and unexposed reagent were placed in constant temperature baths. The absorbance of each sample was measured at periodic intervals; the results are shown in Table II. Each absorbance value represents an average of at least three determinations.

The data indicate that the intensity of the color produced by the silver sol formed decreased with time; the net decrease averaged about 4% in 8 h and 12% in 24 h at 25°C, and the instability increased with temperature. The increase in blank value at higher temperatures probably was caused by a shift in the equilibrium between reagent components:

$$Ag^+ + OH^- + H_2NSO_2C_6H_4COO^- \rightleftarrows AgHNSO_2C_6H_4COO^- + H_2O$$

TABLE II

STABILITY OF EXPOSED AND UNEXPOSED REAGENT

Time	*Temp.* = 25°C		*Temp.* = 30°C		*Temp.* = 40°C	
	Blank	*Rgt.*	*Blank*	*Rgt.*	*Blank*	*Rgt.*
Initial	0.034	0.114	0.034	0.117	0.034	0.110
8 h	0.034	0.111	0.038	0.108	0.040	0.102
24 h	0.035	0.105	0.042	0.087	0.042	0.078

The blank value at higher temperatures tended to stabilize at an absorbance value of 0.045–0.060 after 48 h.

The decrease in absorbance value of the exposed reagent might be attributed in part to the adsorption of the silver on the surface of the permeation device; the adsorption of silver from solutions on the surface of laboratory glassware has been reported[4]. Attempts to stabilize the silver sol were unsuccessful. It has been reported[5] that polyvinylpyrrolidone can be used to stabilize colloidal silver, but use of the compound to stabilize this silver sol resulted in more rapid deterioration of the reagent. Variation in the relative concentrations of the components of the reagent produced no significant improvement in stability.

Interference studies

It has been reported[6] that hydrogen sulfide, acetylene and formaldehyde interfered in previous determinations of carbon monoxide with this colorimetric reagent. Since the permeabilities of these gases may be quite different, it was necessary to investigate any interference produced by the gases when the colorimetric reagent was used in a permeation method. Interference effects produced by sulfur dioxide, nitrogen dioxide, ammonia and chlorine also were investigated. In conducting the investigations, the concentration levels of possible interferent species were chosen in relation to appropriate Federal[7] or State[8] standards; the concentration of carbon monoxide chosen was 10 p.p.m., which corresponds to the typical background level of carbon monoxide found in the laboratory during this study and to the Federal ambient air quality standard for carbon monoxide of 9 p.p.m. (maximum 8-h concentration not to be exceeded more than once each year).

Two different techniques were used in the interference studies in order to produce the appropriate concentration of gas under study in the exposure chamber. The sulfur dioxide–air, nitrogen dioxide–air and hydrogen sulfide–air mixtures were prepared by using permeation tubes[9] placed in the air stream in an appropriate position in the dilution system. The acetylene–air, formaldehyde–air, ammonia–air and chlorine–air mixtures were prepared by using a motor-driven syringe to inject these vapors into the carbon monoxide–air stream between two exposure chambers. The syringe was filled with gaseous acetylene or solutions of formaldehyde (37%), ammonium hydroxide (58%) or saturated chlorine water, and the plunger speed was adjusted to give an appropriate concentration of the gas under study in the exposure chamber. The method of Lyles *et al.*[10] for determining formaldehyde was used to check the accuracy of this syringe technique.

TABLE III

INTERFERENCE STUDY

Species	*Concentration*	*Net abs.*	*Change*
CO	10 p.p.m. (12.5 mg m^{-3})	0.020	—
NO_2	180 p.p.b. (370 $\mu g\ m^{-3}$)	0.019[a]	−5
SO_2	120 p.p.b. (350 $\mu g\ m^{-3}$)	0.014[a]	−30
H_2S	70 p.p.b. (100 $\mu g\ m^{-3}$)	0.025[a]	+25
C_2H_2[b]	130 p.p.b. (150 $\mu g\ m^{-3}$)	0.021[a]	+5
CH_2O[b]	11 p.p.b. (15 $\mu g\ m^{-3}$)	0.027[a]	+33
NH_3[b]	33 p.p.b. (25 $\mu g\ m^{-3}$)	0.024[a]	+20
Cl_2[b]	1 p.p.m. (3.2 mg m^{-3})	0.020[a]	0

[a] Value is for 10 p.p.m. CO + interferent at indicated concentration.

[b] Data for this species were obtained using gas concentrations of 4 times the levels indicated. Data were collected during a 6-h exposure period.

The results of the interference studies are shown in Table III. Data reported for sulfur dioxide, nitrogen dioxide and hydrogen sulfide are based on 24-h exposures to 10 p.p.m. carbon monoxide and interferent species at the level indicated. It was impossible to maintain interferent levels of acetylene and formaldehyde for periods of more than 6 h by the motor-driven syringe apparatus; studies for these gases were conducted with 6-h exposures to 40 p.p.m. carbon monoxide and interferent species at four times the level indicated.

In addition to the interference effect observed, membranes exposed repeatedly to high concentrations of sulfur dioxide and hydrogen sulfide developed pinhole leaks. Black spots were observed at the leak sites. With the exception of those incidents, no other deterioration of membrane material was detected, and permeation devices were used repeatedly.

Numerous techniques for eliminating or reducing interferences were tried without success. It has been reported[11] that potential interferences for this reagent can be eliminated by passing the air sample through mercury(II) sulfate adsorbed on silica gel. The advantage of a permeation method over conventional bubbling techniques, however, is that the permeation method eliminates the need for a mechanical device for sampling (such as a pump). In order to maintain the independence from mechanical devices, investigations were undertaken to determine the feasibility of soaking a cloth or net in a solution of mercury(II) sulfate and attaching the cloth to the outside of the permeation device. Several types of cloth and netting were examined; covering the membrane with any type of material was found to restrict severely the flow of air across the membrane surface, and no detectable permeation of carbon monoxide occurred even at high concentrations (100 p.p.m.). No alternative was found to using a mechanical pump to pump the air through activated charcoal or mercury(II) sulfate to eliminate interferences.

Field evaluation

No development of a good analytical method is complete without at least some evaluation of the method in a real-world situation away from the "sterile

environment" of the laboratory. Normally in a field evaluation the proposed new method is compared to the reference method if a reference method has been established for the particular species being determined. The reference method for carbon monoxide is n.d.i.r. spectroscopy, but unfortunately an instrument was not available for comparison with this present method.

Of the experimental parameters investigated in the present study, the temperature dependence of the method and the interference effect of sulfur dioxide and formaldehyde would cause the most significant error in a determination. In the absence of a reference method it was decided to devise a system for field evaluation of the method which would provide some indication of the effect of the above parameters on an actual determination.

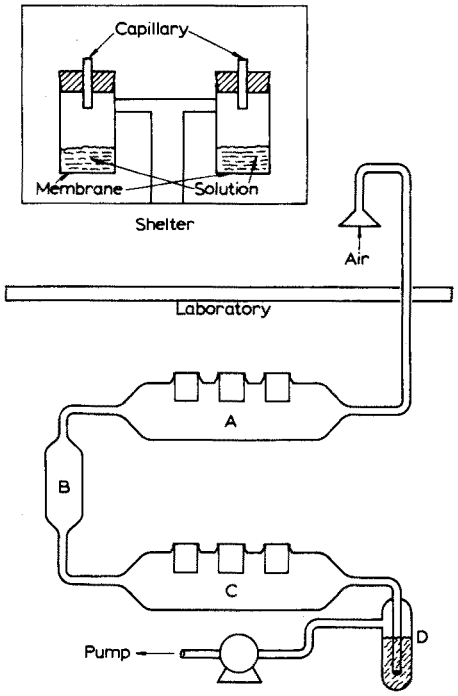

Fig. 4. Apparatus for field evaluation.

The apparatus for conducting the field evaluation is shown in Fig. 4. Two permeation devices covered with capillary and rubber stopper as shown were placed in the shelter in a parking lot outside the laboratory. Air was drawn at a flow rate of 600 ml min^{-1} from a point adjacent to the shelter through a Teflon line into the laboratory, where it passed through exposure chamber A, activated charcoal B, exposure chamber C and bubbler D. The parking lot is surrounded by buildings on four sides, thereby retarding air circulation, and cars and delivery trucks provided a continual source of carbon monoxide from about 7:30 a.m. to 10:30 p.m. The absorbance values from the devices placed in the shelter in the parking lot were compared with the absorbance values of the devices in exposure chamber A in the laboratory; the temperature in the laboratory was maintained at 25°C.

Any deviation between values could be attributed to temperature effects. Absorbance values from devices in exposure chamber A were compared with those in exposure chamber C. Any deviation between these values could be attributed to interference effects since potential interferent species were removed by the activated charcoal. The results of the study are shown in Table IV.

TABLE IV

FIELD EVALUATION

Date	*Temperature (°C)*			*Absorbance*		
	High	*Low*	*Lab.*	*Outside*	*Pos. A*	*Pos. C*
10/9/74	27	13	25	0.037	0.029	0.040
10/10/74	28	12	25	0.081[a]	0.032[a]	0.018[a]
10/14/74	29	17	25	0.027	0.033	0.033
10/16/74	21	6	25	0.015	0.029	0.027
10/17/74	24	10	25	0.027	0.032	0.029
10/18/74	29	12	25	0.043	0.038	0.029
10/19/74	28	11	25	0.029	0.014[a]	0.013[a]
10/20/74	24	11	25	0.012	0.029	0.022
Av.	26	12	25	0.027	0.032	0.030

[a] Data not considered in computing averages.

The data from the field studies show that with the exception of two dates, 10/10 and 10/19, the average error introduced by temperature differences is about 10%, and the average error introduced by interference species is about 7%. The data recorded at the exposure chambers in the laboratory on 10/19 are invalid because of a break discovered in the Teflon line. The membranes and solutions used in the shelter to collect data on 10/10 were turned dark brown in color, possibly indicating a very high concentration of interferent species in the air that particular day.

When the calibration chart of Fig. 3 and the data from exposure chamber C were used, the concentration of carbon monoxide in the parking lot ranged from 17 to 32 p.p.m. for a 24-h average. The lowest concentration was observed on a Sunday when traffic was lightest and the average concentration for the entire evaluation was about 25 p.p.m.

CONCLUSIONS

The method developed here is a simple inexpensive and reliable method for the determination of average concentrations of carbon monoxide in the ambient atmosphere. The technique requires no electrical or mechanical connections to complex equipment; no tedious sampling technique is required. The method has some limitations, however.

The method is not suitable for stack gas analysis where extreme temperature variations and high interferent concentrations may be present; nor is it suitable for process stream analysis where rapid measurement is required, and temperature

variations also may affect results. Because of the response time, exposure periods of less than 2 h are not recommended; and because of the instability of the silver sol, exposure periods should be limited to 8 h at high concentrations or 24 h at low concentrations (< 10 p.p.m.). Extreme temperatures also should be avoided.

The reagent is stable at ordinary room temperature for up to six months, and the absorbance value of the blank at 25°C is 0.034: this value varies by less than ± 0.001. A detection limit of 2 p.p.m. for a 24-h exposure can be stated, if the limit is taken as twice the standard deviation of the blank. The response of the reagent is linear up to a carbon monoxide concentration of 80 p.p.m. A thorough error analysis is inappropriate since varying field conditions, such as temperature, interferences and exposure time, will affect the amount of error introduced in the determination.

We wish to acknowledge support for this research from the National Science Foundation, RANN Grant GP-35114X and EPA Grant No. R 803193 01.

SUMMARY

A simple, inexpensive and reliable method for the determination of average concentrations of carbon monoxide in the atmosphere is described. Silver *p*-sulfamoylbenzoic acid is used as the colorimetric reagent in a specially designed permeation device. The calibration graphs are linear up to 80 p.p.m. carbon monoxide, and the limit of detection is 2 p.p.m. for a 24-h exposure. Tests under field conditions are discussed.

REFERENCES

1 G. Ciuhandu, *Acad. Rep. Populare Romine, Raza Cercetari Stiint. Timisoara, Studii Cercetari Stiint., Ser. I*, 2 (1955) 133.
2 K. D. Reiszner and P. W. West, *Environ. Sci. Technol.*, 7 (1973) 526.
3 J. Crank and G. S. Park, *Diffusion in Polymers*, Academic Press, London, 1968.
4 F. K. West, P. W. West and F. A. Iddings, *Anal. Chim. Acta*, 37 (1967) 112.
5 B. Jirgensons, *Makromol. Chem.*, 6 (1951) 30.
6 R. Bock and B. Bockholt, *Fresenius' Z. Anal. Chem.*, 260 (1972) 274.
7 *National Primary and Secondary Air Quality Standards, Fed. Reg.*, April 30, 1971.
8 K. D. Reiszner, Ph.D. Dissertation, Louisiana State University, 1972.
9 F. P. Scaringelli, E. A. O'Keefe, E. Rosenberg and J. P. Bell, *Anal. Chem.*, 42 (1970) 871.
10 G. R. Lyles, F. B. Dowling and V. J. Blanchard, *J. Air Pollut. Contr. Assoc.*, 15 (3) (1965) 106.
11 D. A. Levaggi and M. Feldstein, *Amer. Ind. Hyg. Assoc. J.*, 25 (1964) 64.

Analytica Chimica Acta, 77 (1975) 255–262

A SPECTROPHOTOMETRIC STUDY OF THE FORMATION OF THE PEROXOTITANIUM(IV) COMPLEX AND ITS APPLICATION TO THE DETERMINATION OF BERYLLIUM

CHIYO MATSUBARA and KIYOKO TAKAMURA

Tokyo College of Pharmacy, Uenosakuragi, Taito-ku, Tokyo 110 (Japan)

(Received 16th October 1974)

Ever since the yellowish orange coloration caused by the reaction of titanium(IV) and hydrogen peroxide in aqueous solution was noted in 1870, this reaction has served extensively as a very sensitive test in trace analysis for titanium(IV) or hydrogen peroxide[1]. The composition of the reaction product has also been of interest; the most reliable information is that the color is due to the complex formation between titanium(IV) and hydrogen peroxide in solution[2,3].

Recently, Fukamauchi[4] and Matsubara[5,6] examined the use of a Ti(IV)–H_2O_2–HF reagent for the colorimetric determination of some metal ions. The reagent is a mixture of sodium hexafluorotitanate(IV), sodium fluoride and hydrogen peroxide dissolved in aqueous hydrochloric solution. On addition of the reagent to a solution containing metal ions, titanium(IV) ions are liberated from the fluorotitanium(IV) complexes if the metal ions have a strong affinity with fluoride ions, and the yellowish orange color appears as a result of the reaction between the liberated titanium(IV) and hydrogen peroxide. The metal ions can thus be determined colorimetrically.

In order to utilize the Ti(IV)–H_2O_2–HF reagent properly for the determination of such metal ions, the entity showing the yellowish orange color should be established unequivocally. The present investigation was initiated for this reason, and the formation of a peroxotitanium(IV) complex was confirmed in strong acid solution containing titanium(IV) and hydrogen peroxide.

This paper is concerned with the formation of the peroxotitanium(IV) complex in systems such as Ti(IV)–H_2O_2, Ti(IV)–H_2O_2–HF and Ti(IV)–H_2O_2–HF–Be(II) followed by spectrophotometric measurements. The experimental results are then applied to the determination of beryllium in a Cu–Be alloy.

EXPERIMENTAL

Reagents

All the chemicals were reagent-grade and were used without further purification.

Standard titanium(IV) solutions (0.1000 *M*). A titanium(IV) chloride solution was prepared by dissolving 5.5 ml of titanium(IV) chloride in 500 ml of 4 *M* hydrochloric acid. A standard solution of titanium(IV) sulfate (0.0500 *M*) was prepared by dissolving 0.81 g of titanium(IV) oxide in 200 ml of 2 *M* sulfuric

acid; the titanium(IV) oxide was fused with potassium pyrosulfate before use. Both the solutions were standardized by titration with EDTA.

Standard hydrogen peroxide solution (0.1000 *M*). 2.6 ml of 30% hydrogen peroxide was diluted with water to 500 ml; the solution was standardized by titration with permanganate.

Standard beryllium(II) chloride solution. 4.65 g of beryllium metal (purity, *ca.* 99.5%) was dissolved in dilute hydrochloric acid, and the solution was diluted with water to 100 ml. The solution was standardized gravimetrically by homogeneous precipitation with ethylenediamine[7].

Ti(IV)–H_2O_2–HF reagent. 2.08 g of sodium hexafluorotitanate(IV), 1.68 g of sodium fluoride and 1.1 ml of 30% hydrogen peroxide were dissolved in 100 ml of 2 *M* hydrochloric acid.

0.4 M benzoylacetone–chloroform solution. 64.8 g of benzoylacetone was dissolved in chloroform to a final volume of 1 l.

Apparatus

Visible absorption spectra were recorded on a Hitachi double-beam spectrophotometer Model 323. Absorbances at a fixed wavelength (420 nm) were measured on a Hitachi spectrophotometer Model 139 in 10-mm quartz or resin cells.

Procedure for determination of beryllium in alloy

The Cu–Be alloy used (Hirano Co. Ltd.) was reported to contain 3.84% beryllium. The test solution was prepared as follows: a known amount of alloy (*ca.* 40 mg) was dissolved in dilute nitric acid, the solution was evaporated to dryness, and the residue was dissolved in dilute hydrochloric acid.

In the colorimetric determination of beryllium(II) with the Ti(IV)–H_2O_2–HF reagent, the presence of copper(II) and other metal components of the alloy may lead to serious errors, owing to the formation of some fluorocomplexes of these metals. To avoid such problems, beryllium(II) can be extracted from the test solution in the usual way. However, for application of the Ti(IV)–H_2O_2–HF reagent, back-extraction of beryllium(II) into an aqueous phase is essential because of the poor miscibility of the reagent with organic solvents. Such procedures lead to additional errors inherent in the stripping step.

The following method proved satisfactory for the present purpose. The absorbance at 420 nm was obtained with the test solution containing a given amount of Ti(IV)–H_2O_2–HF reagent. The effect of other metal components than beryllium(II) could be subtracted with the aid of the reference solution which was prepared by adding the same amount of Ti(IV)–H_2O_2–HF reagent to the residual aqueous solution after the removal of beryllium(II) by extraction; consequently, the content of beryllium(II) could be obtained.

As described previously[6], benzoylacetone in chloroform was chosen as a suitable extractant for beryllium(II) from the test solution. The extraction was carried out at pH 7–8, and EDTA was used as a masking agent for metal cations other than beryllium(II). The addition of EDTA scarcely affected the efficiency of the beryllium(II) extraction[6]. The content of beryllium in the alloy was determined by the standard addition method. In the absorption measurement, the transmittance ratio method[8] was preferred to the usual manner for a high accuracy.

RESULTS AND DISCUSSION

Formation of peroxotitanium(IV) complex

As a first step in examining the applicability of the Ti(IV)–H_2O_2–HF reagent for the colorimetric determination of metal ions such as beryllium(II), the equilibria involving titanium(IV), hydrogen peroxide, hydrofluoric acid and beryllium(II) in acidic solutions were studied. Titanium(IV) reacts with hydrogen peroxide in acidic solution to form a yellowish orange complex involving titanium-

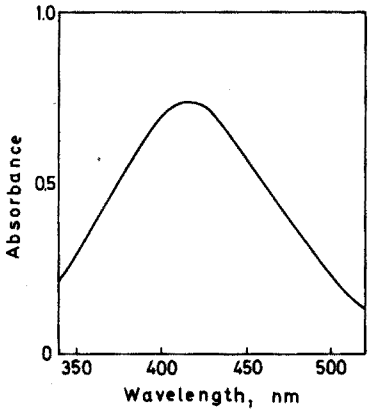

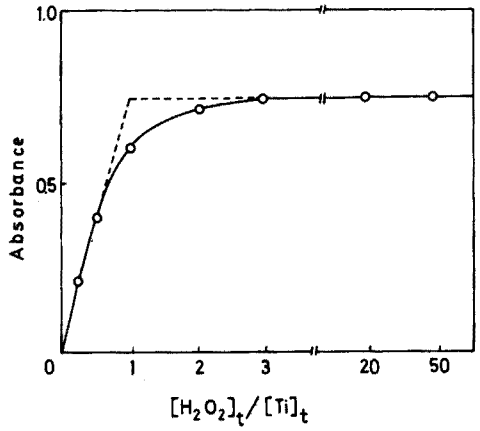

Fig. 1. Absorption spectrum of Ti(IV)–H_2O_2 system in 2 *M* hydrochloric acid. $[Ti]_t$, 1.00 m*M*; $[H_2O_2]_t$, 10.0 m*M* ([ ]$_t$ denotes the total concentration).

Fig. 2. Relationship between absorbance at 420 nm and $[H_2O_2]_t/[Ti]_t$ obtained in Ti(IV)–H_2O_2 system in 2 *M* hydrochloric acid. $[Ti]_t$, 1.00 m*M*.

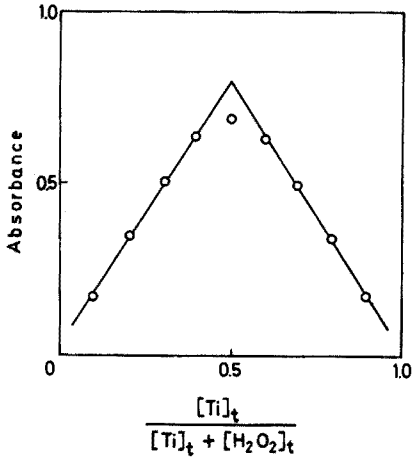

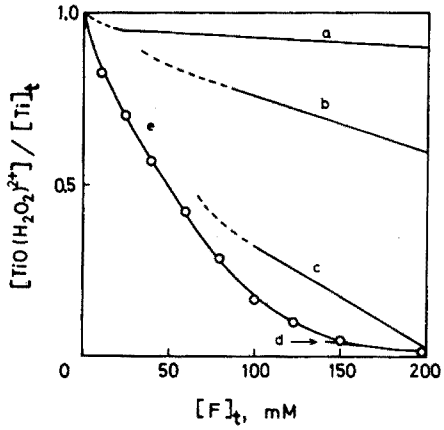

Fig. 3. Result obtained by continuous variations method applied to Ti(IV)–H_2O_2 system in 2 *M* hydrochloric acid. $[Ti]_t + [H_2O_2]_t = 2.5$ m*M*. Absorbance was measured at 420 nm.

Fig. 4. Formation of peroxotitanium(IV) complex in Ti(IV)–H_2O_2–HF system in 2 *M* hydrochloric acid. Curves a, b, c and d were obtained theoretically by eqns. (1)–(15) as $n = 1$, 2, 3 and 4, respectively. Curve e was obtained experimentally. $[Ti]_t$, 5.0 m*M*; $[H_2O_2]_t$, 5.0 m*M*.

(IV) and hydrogen peroxide. The formation of the complex was examined spectrophotometrically in the following three systems: Ti(IV)–H_2O_2, Ti(IV)–H_2O_2–HF and Ti(IV)–H_2O_2–HF–Be(II).

Ti(IV)–H_2O_2 system. The absorption spectrum of 1.000 m*M* titanium(IV) in 2 *M* hydrochloric acid containing an excess of hydrogen peroxide exhibits an absorption maximum at 420 nm (Fig. 1). The molar absorptivity is 690 ± 20. The molar ratio and continuous variations methods proved the existence of only a 1:1 peroxotitanium(IV) complex between titanium(IV) and hydrogen peroxide (Figs. 2 and 3).

These results are similar to the findings of Babko and Volkova[2] and Vasil'ev and Vorob'ev[3], who proved the existence of the 1:1 complex and proposed two alternative formulae: $Ti(H_2O_2)^{4+}$ and $TiO(H_2O_2)^{2+}$, respectively.

Since titanium(IV) is appreciably hydrolyzed in water and dissolved as TiO^{2+} even in strongly acidic solution[9], it seems reasonable to express the formation of the peroxotitanium(IV) complex under the present experimental conditions, as suggested by Vasil'ev and Vorob'ev[3]:

$$TiO^{2+} + H_2O_2 \rightleftharpoons TiO(H_2O_2)^{2+} \tag{1}$$

The equilibrium constant for this reaction is[3]:

$$K_1 = \frac{[TiO(H_2O_2)^{2+}]}{[TiO^{2+}][H_2O_2]} = 1.35 \cdot 10^4 \tag{2}$$

No evidence for the formation of other complexes, *e.g.* a 1:2 complex, is provided from Fig. 2, in which the absorbance at 420 nm remains constant irrespective of the hydrogen peroxide concentration, even when a large excess is present. This is in contrast to the reactions between zirconium(IV) or plutonium(IV) and hydrogen peroxide where 1:2 complexes were found[10,11].

The absorption spectrum obtained for the Ti(IV)–H_2O_2 system in 1 *M* sulfuric acid is essentially identical to that in Fig. 1. Both the spectra obtained in hydrochloric acid and in sulfuric acid solutions are virtually invariant irrespective of the acid concentration in the range of 0.1–6 *N*; thus the peroxotitanium(IV) complex is stable to high acidity.

The absorbance of the peroxotitanium(IV) complex at 420 nm was followed with lapse of time at various acid concentrations, at a constant temperature of 25°C; the results are given in Table I. The absorbance obtained in sulfuric acid solution is stable on prolonged standing; in hydrochloric acid solution, the absorbance becomes somewhat unstable with increasing acidity, possibly because of dissociation of peroxotitanium(IV) complex as a result of a slow reaction between chloride ions and hydrogen peroxide.

Ti(IV)–H_2O_2–HF system. The amounts of peroxotitanium(IV) complex formed in the system involving titanium(IV), hydrogen peroxide and hydrofluoric acid were obtained by measurement of the absorbance at 420 nm at varied hydrofluoric acid concentration; the total concentrations of titanium(IV) and hydrogen peroxide were kept constant. The result obtained with $[Ti]_t = [H_2O_2]_t = 5.00$ m*M* in 2 *M* hydrochloric acid is given as curve (e) in Fig. 4, in which the $[TiO(H_2O_2)^{2+}]/[Ti]_t$ ratio is plotted as a function of $[F]_t$, *i.e.*, the concentration

TABLE I

TIME DEPENDENCE OF ABSORBANCE (AT 420 nm) DUE TO PEROXOTITANIUM(IV) COMPLEX OBTAINED WITH VARIOUS CONCENTRATIONS OF HYDROCHLORIC ACID OR SULFURIC ACID

($[Ti]_t$, 1.00 mM; $[H_2O_2]_t$, 1.50 mM)

Acid	*[HCl] or [H_2SO_4] (N)*	*Absorbance*		
		0.1 h	*2 h*	*20 h*
HCl	0.1	0.652	0.656	0.650
	2.0	0.655	0.658	0.651
	4.0	0.651	0.657	0.650
	6.0	0.658	0.557	0.538
H_2SO_4	0.1	0.662	0.660	0.660
	2.0	0.678	0.678	0.678
	4.0	0.678	0.690	0.678
	6.0	0.678	0.699	0.678

of added hydrofluoric acid. The decrease in the amount of peroxotitanium(IV) complex with increase of $[F]_t$ is clearly seen.

Since titanium(IV) reacts with fluoride to form stable complexes such as $TiOF_n^{(n-2)-}$ ($n=1$–4), the observed relationship (Fig. 4) can be interpreted by considering the competitive formation of peroxo and fluoro complexes of titanium-(IV). Fluorotitanium(IV) complexes are formed in the following steps:

$$TiO^{2+} + F^- \rightleftharpoons TiOF^+, \quad k_1 = 4.50 \cdot 10^6 \tag{3}$$

$$TiOF^+ + F^- \rightleftharpoons TiOF_2, \quad k_2 = 1.22 \cdot 10^5 \tag{4}$$

$$TiOF_2 + F^- \rightleftharpoons TiOF_3^-, \quad k_3 = 3.76 \cdot 10^4 \tag{5}$$

$$TiOF_3 + F^- \rightleftharpoons TiOF_4^{2-}, \quad k_4 = 1.14 \cdot 10^4 \tag{6}$$

The successive stability constants (k_1, k_2, k_3 and k_4) are those reported by Nabivanets[12]. If the dissociation of hydrofluoric acid is considered:

$$HF \rightleftharpoons H^+ + F^-, \quad K_a = 8.7 \cdot 10^{-4} \tag{7}$$

where K_a is the dissociation constant of hydrofluoric acid[13], then the amounts of $TiOF_n^{(n-2)-}$ must be related to pH as well as the concentration of added hydrofluoric acid. The ligand substitution between the peroxo and fluoro complexes of titanium(IV) is given by:

$$TiOF^+ + H_2O_2 \rightleftharpoons TiO(H_2O_2)^{2+} + F^- \tag{8}$$

Provided that the reactions given by eqns. (1) and (3)–(8) can be related to an equilibrium in this system, (since the absorption spectrum obtained in this system is essentially identical to that in Fig. 1, the contribution of $TiOF_n(H_2O_2)^{(n-2)-}$ (*cf.* ref. 14) to this system can be neglected) the amount of peroxotitanium(IV) complex should decrease with increasing concentration of added hydrofluoric acid at a given pH.

The equilibrium constant for reaction (8) is

$$K_2 = \frac{[TiO(H_2O_2)^{2+}][F^-]}{[TiOF^+][H_2O_2]} = \frac{K_1}{k_1} = 3.0 \cdot 10^{-3} \tag{9}$$

The total concentrations of titanium(IV), hydrogen peroxide and fluoride are given by eqns. (10)–(12):

$$[Ti]_t = [TiO^{2+}] + [TiO(H_2O_2)^{2+}] + \sum_{n=1}^{4} [TiOF_n^{(n-2)-}], \tag{10}$$

$$[H_2O_2]_t = [H_2O_2] + [TiO(H_2O_2)^{2+}], \tag{11}$$

and

$$[F]_t = [HF] + [F^-] + \sum_{n=1}^{4} n[TiOF_n^{(n-2)-}]$$

$$= [F^-]\left\{1 + \frac{[H^+]}{K_a}\right\} + \sum_{n=1}^{4} n[TiOF_n^{(n-2)-}], \tag{12}$$

Then the following equations can be derived,

$$[F^-] = \frac{[F]_t - a}{1 + \dfrac{[H^+]}{K_a}} \tag{13}$$

$$[TiOF^+] = \frac{\{[Ti]_t - p - [TiO^{2+}]\}}{1+b} \tag{14}$$

where

$$a = \sum_{n=1}^{4} n[TiOF_n^{(n-2)-}]$$

$$p = [TiO(H_2O_2)^{2+}]$$

$$b = 0, (\text{at } n=1);\ k_2[F^-], (\text{at } n=2);$$
$$k_2[F^-] + k_2k_3[F^-]^2, (\text{at } n=3);$$
$$k_2[F^-] + k_2k_3[F^-]^2 + k_2k_3k_4[F^-]^3, (\text{at } n=4).$$

In eqn. (14), $[TiO^{2+}]$ is assumed to be approximately zero. When the above expressions are substituted in eqn. (9), then:

$$K_2 = \frac{p\{[F]_t - a\}\{1+b\}}{\{[Ti]_t - [TiO^{2+}] - p\}\{[H_2O_2]_t - p\}\left\{1 + \dfrac{[H^+]}{K_a}\right\}} \tag{15}$$

The relationship between $[TiO(H_2O_2)^{2+}]$ and $[F]_t$ can be derived rather simply from eqn. (15) if it is assumed that only one species of $TiOF_n^{(n-2)-}$ is formed in the system. For $[Ti]_t = [H_2O_2]_t = 5$ mM and $[H^+] = 1$ M*, eqn. (15) was calculated on the assumption that the value of a may be ignored. Such an assumption holds practically when $[F]_t$ is larger than $[Ti]_t$.

Curves a–d in Fig. 4 are the postulated relationship of $[TiO(H_2O_2)^{2+}]$/

* Under the present conditions, $[H^+]$ is estimated to be *ca.* 1 M, taking $\alpha = 0.5$ as the degree of dissociation of 2 M hydrochloric acid.

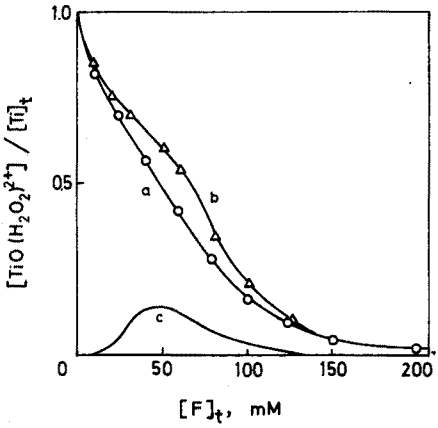

Fig. 5. Formation of peroxotitanium(IV) complex in Ti(IV)–H_2O_2–HF (curve a) and Ti(IV)–H_2O_2–HF–Be(II) (curve b) systems in 2 *M* hydrochloric acid at varied $[F]_t$. Curve c was obtained by subtracting curve a from curve b. $[Ti]_t$, 5.0 m*M*; $[H_2O_2]_t$, 10 m*M*; [Be], 0 (curve a) and 4.0 m*M* (curve b).

$[Ti]_t$ *vs.* $[F]_t$ provided that only one of the species of $TiOF_n^{(n-2)-}$ exists in solution. When curve e is compared with curves a–d in Fig. 4, the change in the predominant species of $TiOF_n^{(n-2)-}$ involved in the Ti(IV)–H_2O_2–HF system with the increasing $[F]_t$ is apparent. This indicates the validity of the assumption that reactions (1) and (3)–(8) are relevant to the equilibrium in this system.

Ti(IV)–H_2O_2–HF–Be(II) system. Addition of metal ions which have a marked tendency to form stable fluoro complexes, to the Ti(IV)–H_2O_2–HF system results in a partial dissociation of the fluorotitanium(IV) complexes, and consequently an increase in the amount of the peroxotitanium(IV) complex; this increase is related to the amount of the added metal ions as well as $[F]_t$.

In the case of beryllium(II), the formation of fluoro complexes is expressed as:

$$Be^{2+} + nF^- \rightleftharpoons BeF_n^{(n-2)-} \qquad (n = 1\text{–}4),$$

$$K_{BeF_4} = \frac{[BeF_4^{2-}]}{[Be^{2+}][F^-]^4} = 1 \cdot 10^{13}$$

is estimated as the overall stability constant from the data reported by Mesmer and Baes[15]. This large value indicates that the addition of beryllium(II) to the Ti(IV)–H_2O_2–HF system will produce a detectable amount of peroxotitanium-(IV) complex under appropriate conditions.

A change in the $[TiO(H_2O_2)^{2+}]/[Ti]_t$ ratio was also observed as a function of $[F]_t$ for a given beryllium(II) concentration (Fig. 5, curve b). On comparing curve b with curve a (without added beryllium(II)), the increase in the peroxotitanium(IV) complex is clearly seen. When the increase in the $[TiO(H_2O_2)^{2+}]/[Ti]_t$ ratio caused by added beryllium(II) is plotted against $[F]_t$ (see curve c), the maximum increase is obtained at $[F]_t = 50$ m*M*, *i.e.*, at the $[F]_t$ value which corresponds to ten times the amount of $[Ti]_t$.

Analytical application

The formation of the peroxotitanium(IV) complex in the Ti(IV)–H_2O_2–HF–

Be(II) system was followed as a function of the beryllium(II) concentration, with the concentrations of the other components constant. A linear relation exists between the absorbance at 420 nm and the concentration of added beryllium(II) over the range 0–4 m*M* beryllium(II) (absorbance 0–0.7). The absorbance remains unchanged for a prolonged time (up to 20 h). Thus beryllium(II) can be determined colorimetrically by means of the Ti(IV)–H_2O_2–HF reagent in 2 *M* hydrochloric acid solution. The results shown in Fig. 5 suggest that the best composition of the reagent is a mixture containing titanium(IV), hydrogen peroxide and hydrofluoric acid in the molar ratio of 1:1:10.

The use of the Ti(IV)–H_2O_2–HF reagent was examined for the determination of beryllium in a Cu–Be alloy by the procedure stated above. The actual content was 3.83% Be; the content found was 3.72 ± 0.12% Be (mean of 5 determinations).

The lower limit of detection of beryllium(II) was about 10 p.p.m. The reagent can probably also be used to determine other metals with a marked tendency to form stable fluoro complexes, such as aluminum and iron.

SUMMARY

The formation of peroxotitanium(IV) complexes has been studied spectrophotometrically in (a) Ti(IV)–H_2O_2, (b) Ti(IV)–H_2O_2–HF and (c) Ti(IV)–H_2O_2–HF–Be(II) systems containing 2 *M* hydrochloric acid. In system (a), only a 1:1 peroxotitanium(IV) complex is evident. In system (b), the competitive formation of the peroxotitanium(IV) complex and fluorotitanium(IV) complexes is discussed. In system (c), the formation of fluoroberyllium(II) complexes causes an increase in concentration of the peroxotitanium(IV) complex which is proportional to the concentration of added beryllium(II). The determination of beryllium in a Cu–Be alloy was successful with a Ti(IV)–H_2O_2–HF reagent.

REFERENCES

1 E. B. Sandell, *Colorimetric Determination of Traces of Metals*, Interscience, New York, 1950, p. 572.
2 A. K. Babko and A. I. Volkova, *Zh. Obshch. Khim.*, 21 (1951) 1949.
3 V. P. Vasil'ev and P. N. Vorob'ev, *Izv. Vyssh. Ucheb. Zaved., Khim. Khim. Tekhnol.*, 11 (1968) 971.
4 H. Fukamauchi, *Z. Anal. Chem.*, 229 (1967) 413.
5 H. Fukamauchi and C. Matsubara, *Jap. Anal.*, 20 (1971) 8.
6 C. Matsubara, *Jap. Anal.*, 23 (1974) 878.
7 W. G. Scribner, W. J. Treat and J. D. Weis, *Anal. Chem.*, 37 (1965) 1136.
8 J. D. Ingle, *Anal. Chem.*, 45 (1973) 861.
9 B. I. Nabivanets, *Zh. Neorg. Khim.*, 7 (1962) 417.
10 A. Ekstrom and A. McLaren, *J. Inorg. Nucl. Chem.*, 34 (1972) 1009.
11 G. V. Jere and G. D. Gupta, *J. Inorg. Nucl. Chem.*, 32 (1970) 537.
12 B. I. Nabivanets, *Ukr. Khim. Zh.*, 32 (1966) 886.
13 A. J. Ellis, *J. Chem. Soc., London*, (1963) 4300.
14 I. V. Pyatnitskii and D. V. Chung, *Zh. Anal. Khim.*, 25 (1970) 103.
15 R. E. Mesmer and C. F. Baes, *Inorg. Chem.*, 8 (1968) 618.

Analytica Chimica Acta, 77 (1975) 263–268

FORMATION OF MERCURY(II) ETHYLENEDIAMINEDIACETATE AND ITS MIXED-LIGAND COMPLEXES WITH ANIONS

T. NOMURA, T. KAWAI and K. IZUTSU

Department of Chemistry, Faculty of Science, Shinshu University, Asahi, Matsumoto, 390 (Japan)

(Received 8th January 1975)

The complexes of mercury(II) with ethylenediaminetetraacetate (EDTA) and its related compounds react with anions, such as cyanide, thiocyanate, iodide, and bromide to form mixed-ligand complexes[1,2]. Spectrophotometric and titrimetric methods have been developed for the determination of these anions by means of the different absorbances and stabilities of the mixed-ligand complexes.

Ethylenediaminediacetate(EDDA) reacts with chromium(II), cobalt(II), copper(II), cadmium(II), and lead(II) ions to form 1:1 and 2:1 complexes, the stability constants of which have been determined potentiometrically[3,4] and polarographically[5]. In the work described here, the complexation of mercury(II) by EDDA and the formation of the mixed-ligand complexes of Hg–EDDA with several anions were investigated by spectrophotometric methods. It was found that mercury(II) reacts with EDDA to form 1:1 and 1:2, complexes, and that Hg–EDDA reacts with anions(X), such as cyanide, thiocyanate, iodide, bromide, and chloride, to form 1:1:1 mixed-ligand complexes.

EXPERIMENTAL

Chemicals

All the chemicals were of analytical grade, used without further purification.

Mercury(II) perchlorate solution, $1 \cdot 10^{-3}$ M. A stock solution (0.01 *M*) was made by dissolving 5.26 g of mercury(II) perchlorate in 100 ml of $1 \cdot 10^{-2}$ *M* perchloric acid, diluting to 1 l with water, and standardizing with EDTA to a xylenol orange end-point. Working solutions were prepared by dilution with water.

EDDA solution, $1 \cdot 10^{-3}$ M. The solution was made by dissolving 176.2 mg of EDDA which had been dried for 2 h at *ca.* 80°C, and diluting to 1 l with water.

Standard anion solutions. Stock solutions were prepared by dissolving potassium salts, diluting to 1 l with water, and standardizing by the Volhard method. The cyanide solution was standardized immediately before use. Working solutions were prepared by dilution with water.

Buffer solutions. Buffer solutions of various pH values were prepared from the following solutions: pH < 5.3, 0.1 *M* perchloric acid; pH 5.3–8.3, 0.05 *M* potassium dihydrogenphosphate and 0.05 *M* disodium hydrogenphosphate; pH 8.4–11, 0.05 *M* potassium dihydrogenphosphate and 0.05 *M* borax, or 0.05 *M* sodium

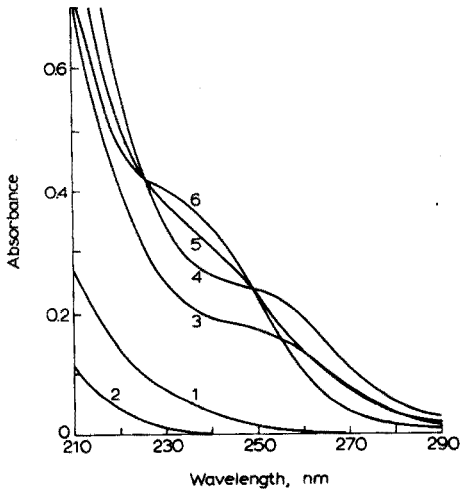

Fig. 1. Absorption spectra of the solutions of (1) $2 \cdot 10^{-4}$ *M* Hg(II), (2) $2 \cdot 10^{-4}$ *M* EDDA, and (3–6) $2 \cdot 10^{-4}$ *M* Hg(II)+$2 \cdot 10^{-4}$ *M* EDDA. pH: (1, 2) 5.40, (3) 2.53, (4) 3.94, (5) 5.40, and (6) 6.90–9.20. Reference: water.

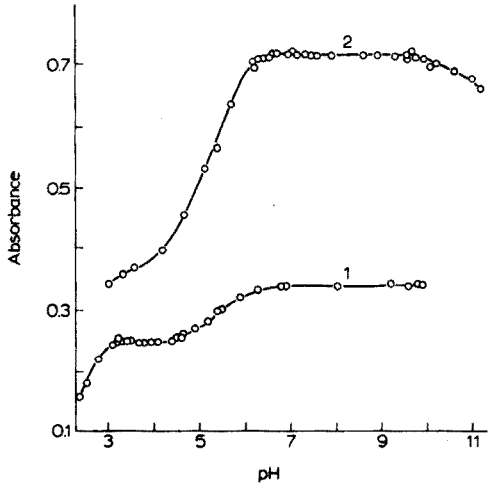

Fig. 2. Effect of pH on the absorbances of mercury(II) complexes. (1) $2 \cdot 10^{-4}$ *M* Hg(II)+$2 \cdot 10^{-4}$ *M* EDDA, 238 nm. (2) $2 \cdot 10^{-4}$ *M* Hg(II)+$4 \cdot 10^{-4}$ *M* EDDA, 232 nm.

carbonate and 0.05 *M* sodium hydrogencarbonate; pH > 11, 0.1 *M* sodium hydroxide.

Sodium perchlorate solution, 0.5 M. This was made by dissolving 20.0 g of sodium hydroxide in *ca.* 500 ml of water, neutralizing with 2 *M* perchloric acid, and diluting to 1 l with water. This solution was used to adjust the ionic strength to 0.10.

Apparatus

A Hitachi Perkin-Elmer Model 139 spectrophotometer, a Shimadzu Multipurpose Recording Spectrophotometer Model MPS-50L, with quartz 10.00-mm cells, and a Hitachi-Horiba M-4 pH meter were used.

RESULTS AND DISCUSSION

Complexes of mercury(II) with EDDA

Curves 1 and 2 in Fig. 1 show that mercury(II) and EDDA solutions gave only weak ultraviolet absorption. The solution containing mercury(II) and EDDA in the molar ratio of 1:1, however, gave a shoulder at 252 nm at pH 3.94 (Fig. 1, curve 4) and at 234 nm at pH 6.90 (Fig. 1, curve 5). The difference between these absorption curves and the appearance of isosbestic points (226 and 248 nm, curves 4–6, Fig. 1) indicate the formation of complexes between mercury(II) and EDDA. Similar results were also obtained from the spectra of solutions containing mercury(II) and EDDA in the molar ratio of 1:2.

The change with pH of the absorbance of solutions containing mercury(II) and EDDA in the molar ratios 1:1 and 1:2 is shown in Fig. 2. Two different complexes must be present, because two regions of constant absorbance occur at

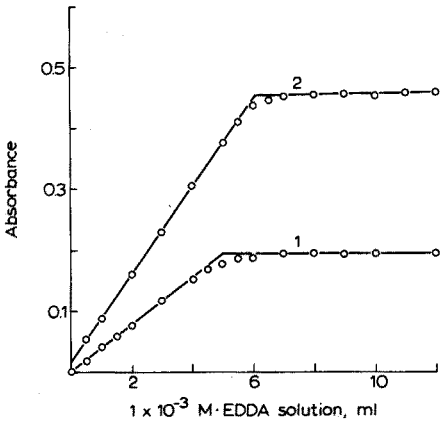

Fig. 3. Effect of the amount of EDDA on the absorbances of mercury(II) complexes. (1) 5 ml of $1 \cdot 10^{-3}$ *M* Hg(II), pH 3.70, 260 nm. (2) 3 ml of $1 \cdot 10^{-3}$ *M* Hg(II), pH 8.49, 232 nm.

pH 3.3–4.3 and pH 6.8–9.7. In the latter range, the absorbance of the 1:1 complex was *ca.* 50% of that of the 1:2 complex at the same wavelength, and both spectra have similar shapes. It appears, therefore, that the complex at pH 6.8–9.7 is $Hg(EDDA)_2$, and that the Hg–EDDA complex exists at pH 3.3–4.3.

The compositions of the complexes at pH 3.70 and 8.49 were investigated by the molar ratio method. The results are shown in Fig. 3. The molar ratio of mercury(II) to EDDA was 1:1 in the pH range 3.3–4.3, and 1:2 at pH 6.8–9.7. The same results were also obtained by the continuous variation method. The apparent stability constants for the formation of Hg–EDDA and $Hg(EDDA)_2$ were found by the molar ratio method to be $\log \beta_1' = 5.6 \pm 0.1$ (at pH 3.70) and $\log \beta_2' = 11.2 \pm 0.2$ (at pH 8.49), respectively, at an ionic strength of 0.10. The stability constants, corrected for the side-reaction coefficients[6,7] are 15.4 ± 0.1 and 24.2 ± 0.2, respectively. A hydroxo mixed-ligand complex was not taken into account in the calculation of the latter value.

Reactions of anions with the mercury(II)–EDDA complexes

The absorption spectra in Fig. 4 were obtained for solutions containing the Hg–EDDA complex and an anion in the molar ratio of 1:1. These spectra differ from those of the anions (X) and of the mercury(II) complexes (HgX_n^{2-n}). It appears, therefore, that the cyanide, thiocyanate, iodide, bromide, and chloride ions form mixed-ligand complexes with Hg–EDDA in the same way as mercury(II) complexes with EDTA and its related compounds[1].

The effect of pH on the formation of the mixed-ligand complexes was investigated by measuring the absorption spectra at various pH values. Figure 5 shows that the pH ranges for the formation of stable mixed-ligand complexes are pH 5.6–6.2 for the chloro mixed-ligand complex, *ca.* pH 7 for the bromo complex, pH 5.4–9.8 for the iodo complex, 4.0–6.5 for the thiocyanato complex, and 7.5–11 for the cyano complex. The spectra indicate that, below these pH ranges, the chloro and cyano complexes dissociate into the anions and the Hg–EDDA complex, while the other mixed-ligand complexes dissociate into HgX_n^{2-n} and EDDA. Above

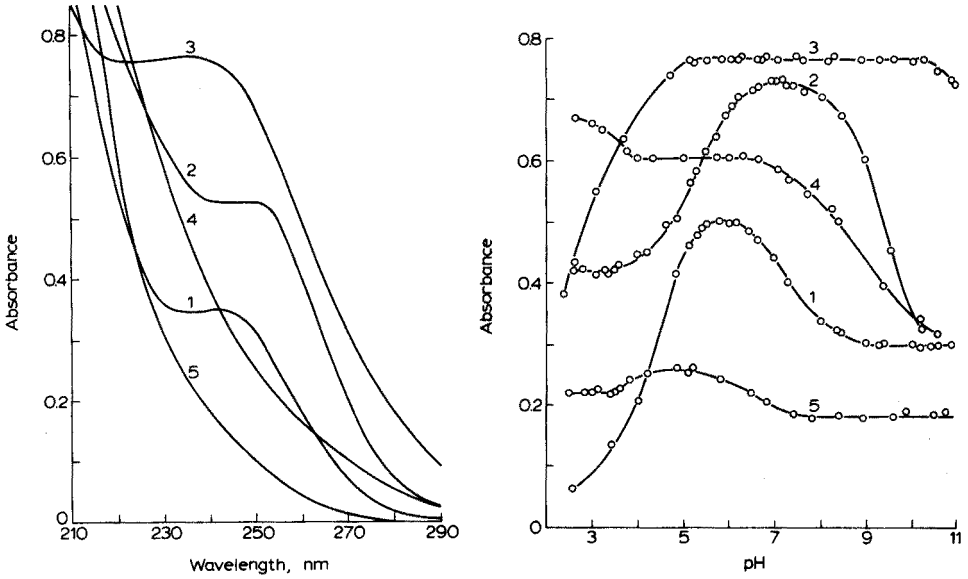

Fig. 4. Absorption spectra of mixed-ligand complexes. Concentration of Hg–EDDA: $2 \cdot 10^{-4}$ *M* for (1–3), but $8 \cdot 10^{-5}$ *M* for (4), and $4 \cdot 10^{-4}$ *M* for (5). (1) $4 \cdot 10^{-4}$ *M* Cl^-, pH 6.03. (2) $4 \cdot 10^{-4}$ *M* Br^-, pH 7.04. (3) $2 \cdot 10^{-4}$ *M* I^-, pH 7.65. (4) $8 \cdot 10^{-5}$ *M* SCN^-, pH 5.70. (5) $4 \cdot 10^{-4}$ *M* CN^-, pH 8.96.

Fig. 5. Effect of pH on the absorbances of the mixed-ligand complexes. Concentration of Hg–EDDA is $2 \cdot 10^{-4}$ *M* for (1–3), but $8 \cdot 10^{-5}$ *M* for (4) and $4 \cdot 10^{-4}$ *M* for (5). Hg:EDDA:X = 1:1:1 for (3–5), but 1:1:2 for (1, 2). (1) Cl^-, 244 nm, (2) Br^-, 249 nm, (3) I^-, 258 nm, (4) SCN^-, 230 nm, (5) CN^-, 240 nm.

these pH regions, however, the chloro, bromo, and thiocyanato mixed-ligand complexes dissociate into the complex ($Hg(EDDA)_2$) and the anions. The behavior of cyanide ions with Hg–EDDA in the pH range 3.5–7 is difficult to interpret.

Composition of the mixed-ligand complexes

The spectra of solutions of the mercury(II) complexes in the presence of anions were recorded at various pH values; the absorbances at the specified wavelength are shown in Fig. 6 against the amount of the anion. The addition of cyanide ion decreased the absorbance of the solution; the cyano mixed-ligand complex formed gives little ultraviolet absorption. Examination of the spectra showed that the abrupt decrease near the equivalent point in curve 5, and after the equivalent point in curve 3, resulted from the formation of the mercury(II) complex (HgX_n^{2-n}); the iodo and cyano mixed-ligand complexes dissociated to HgX_n^{2-n} and EDDA when excess of these anions were added to the solutions. The chloro, bromo, and thiocyanato mixed-ligand complexes, however, did not react thus. The curves in Fig. 7, obtained by increasing the amount of EDDA added to the Hg–X solution, show that although the chloro, bromo, and thiocyanato mixed-ligand complexes dissociated to $Hg(EDDA)_2$ and the respective anions in the presence of excess of EDDA, the cyano and iodo mixed-ligand complexes were stable. It cannot be assumed, however, from the absorption spectra that the

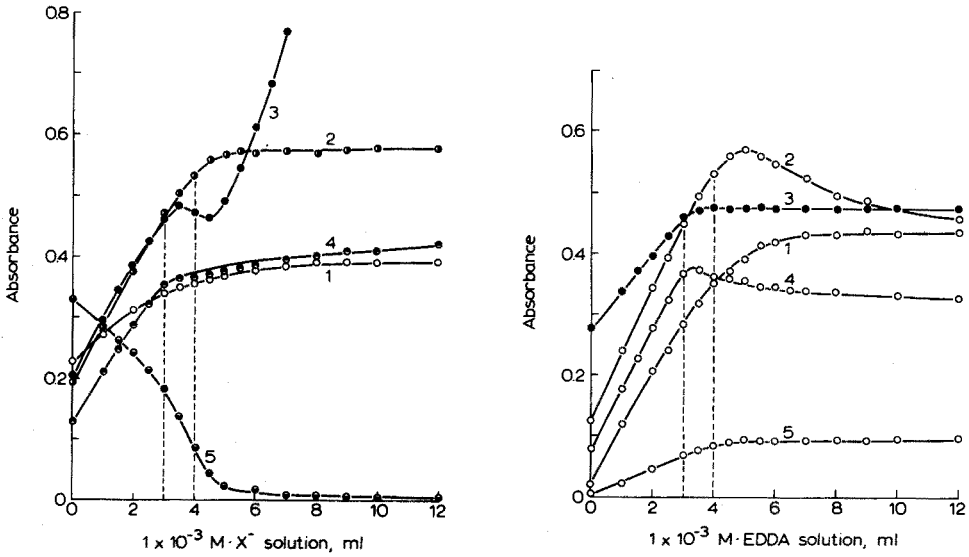

Fig. 6. Compositions of the mixed-ligand complexes (molar ratio method)—1. 4 ml of $1 \cdot 10^{-3}$ *M* Hg–EDDA for (1, 2 and 5), but 3 ml for (3, 4). (1) Cl^-: pH 5.68, 244 nm, (2) Br^-: pH 6.60, 249 nm, (3) I^-: pH 6.60, 240 nm, (4) SCN^-: pH 6.77, 250 nm, (5) CN^-: pH 8.68, 240 nm.

Fig. 7. Composition of the mixed-ligand complexes (molar ratio method)—2. 4 ml of ($1 \cdot 10^{-3}$ *M* Hg(II) + $1 \cdot 10^{-3}$ *M* X^-) for (1, 2 and 5), but 3 ml for (3, 4). (1) Cl^-: pH 6.03, 244 nm, (2) Br^-: pH 6.93, 249 nm, (3) I^-: pH 6.93, 240 nm, (4) SCN^-: pH 6.62, 250 nm, (5) CN^-: pH 8.68, 240 nm.

complex $Hg(EDDA)X_2$ is formed even in the presence of excess of anions. The molar ratio of anion to Hg–EDDA for all anions tested was 1:1 (molar ratio method).

The apparent stability constants of the mixed-ligand complexes

Consider a solution containing twice the molar amount of EDDA to that of mercury(II) and the anion. Equilibrium (1) is then expected:

$$Hg(EDDA)X + EDDA = Hg(EDDA)_2 + X \tag{1}$$

Under these conditions, if the concentrations and the apparent molar absorptivities of Hg(EDDA)X and $Hg(EDDA)_2$ are C_1, C_2 and ε_1, ε_2, respectively, and if the molar concentration of mercury(II) is C, and the absorbance of the solution is A_s, then eqns. (2) and (3) are obtained:

$$\left.\begin{aligned} C_1 + C_2 &= C \\ \varepsilon_1 C_1 + \varepsilon_2 C_2 &= A_s \end{aligned}\right\} \tag{2}$$

$$K'_x = \frac{[Hg(EDDA)X][EDDA]}{[Hg(EDDA)_2][X]} = \left(\frac{C_1}{C_2}\right)^2 \tag{3}$$

Since ε_1, ε_2, C, and A_s are measurable quantities, C_1 and C_2 can be determined from eqn. (2), and the apparent stability constant, K'_x, of eqn. (3) can be calculated. The apparent stability constant of the mercury(II) complex $Hg(EDDA)_2$, β'_2, is

TABLE 1

THE APPARENT STABILITY CONSTANTS OF THE MIXED-LIGAND COMPLEXES

Complex	*Wave-length (nm)*	*pH*	β'_2	*C* $(\cdot 10^{-4}$ *M)*	ε_1 $(\cdot 10^3)$	ε_2 $(\cdot 10^3)$	A_s	*Log* K_x
Hg(EDDA)Cl	238	6.03	10.4	1.60	2.31	3.42	0.485	9.9 ± 0.3
Hg(EDDA)Br	249	6.93	11.3	1.60	3.54	2.07	0.495	12.0 ± 0.3
Hg(EDDA)SCN	250	6.62	9.9	1.20	3.18	1.92	0.343	10.8 ± 0.3

known; the apparent stability constant of the mixed-ligand complex, K_x, can be calculated from eqn. (5):

$$\frac{[\mathrm{Hg(EDDA)_2}]}{[\mathrm{Hg}][\mathrm{EDDA}]^2} = \beta'_2 \tag{4}$$

$$K_x = \frac{[\mathrm{Hg(EDDA)X}]}{[\mathrm{Hg}][\mathrm{EDDA}][\mathrm{X}]} = \beta'_2 K'_x = \beta'_2 \left(\frac{C_1}{C_2}\right)^2 \tag{5}$$

The apparent stability constants found for the chloro, bromo, and thiocyanato mixed-ligand complexes are shown in Table I; values for the iodo and cyano mixed-ligand complexes could not be determined.

SUMMARY

The complexes of mercury(II) with EDDA and the formation of mixed-ligand complexes with some anions have been investigated spectrophotometrically. Mercury(II) reacts with EDDA to give 1:1 and 1:2 complexes, which have stability constants of 15.4 ± 0.1 and 24.2 ± 0.2 respectively, at ionic strength 0.1. These complexes react with anions (X), such as cyanide, thiocyanate, iodide, bromide and chloride, to form the mixed-ligand 1:1:1 complexes, Hg(EDDA)X. The apparent stability constants (log K_x) of the chloro, bromo, and thiocyanato mixed-ligand complexes are 9.9, 12.0, and 10.8, respectively.

REFERENCES

1 S. Komatsu and T. Nomura, *Nippon Kagaku Zasshi*, 87 (1966) 841, 845.
2 T. Nomura, *Nippon Kagaku Zasshi*, 88 (1967) 199, 635, 961.
3 S. Chaberek and A. E. Martell, *J. Amer. Chem. Soc.*, 74 (1952) 6228.
4 G. Schwarzenbach, G. Anderegg, W. Schneider and H. Senn, *Helv. Chim. Acta*, 38 (1955) 1147.
5 T. Nozaki and T. Hashimoto, *Nippon Kagaku Kaishi*, (1974) 1794.
6 S. Hietanen and L. G. Sillen, *Acta Chem. Scand.*, 6 (1952) 747.
7 L. C. Thompson, *J. Inorg. Nucl. Chem.*, 24 (1962) 1083.

Analytica Chimica Acta, 77 (1975) 269–273

SHORT COMMUNICATION

Periodate oxidation analysis of carbohydrates

Part II. P.m.r. determination of formic acid liberated by oxidation

SUSUMU HONDA, KAZUAKI KAKEHI and KIYOSHI TAKIURA
Faculty of Pharmaceutical Sciences, Osaka University, Toneyama, Toyonaka, Osaka-fu (Japan)
(Received 18th August 1974)

In the preceding Part[1] a spectrophotometric method was reported for the selective determination of glyoxal in dialdehyde fragments, formed from glycosides by periodate oxidation. In a continuation of these analytical studies of periodate oxidation fragments, the determination of formic acid was studied. This volatile acid is formed by oxidation of α-hydroxyaldehydes, vicinal trihydroxy compounds, and the corresponding amino derivatives. Sometimes it is also formed by oxidation which is not of the Malabrade type.

The amount of formic acid liberated has been usually determined by titration with dilute alkali and indicators such as methyl red[2] and bromocresol purple[3], but the use of this method is restricted to the cases where unbuffered systems are employed, and the possibility of the presence of other organic acids is excluded. The selective determination is based on the stoichiometric redox reaction between formic acid and mercury(II) chloride. The resultant mercury(I) chloride may be determined gravimetrically[4], iodimetrically[5], or colorimetrically[6]. Nevertheless, since some neutral fragments also reduce mercury(II) chloride, prior isolation of this acid by distillation is necessary to eliminate the interference from these reductants. This paper presents a simple direct method based on proton magnetic resonance spectroscopy, which makes it possible to determine selectively 10–100-μmole quantities of formic acid in oxidation mixtures.

Experimental

Instrumentation. P.m.r. spectra were obtained at 90 MHz in the frequency-sweep mode at 35°C with a Hitachi R-22 spectrometer, which was equipped with a thermostatically controlled permanent magnet and was locked with the external ^{19}F signal of trifluoroacetic acid. The sweep speed for signal observation was 1 Hz s^{-1}. Under these conditions the average signal/noise ratio for a 10^{-2} *M* D_2O solution of sodium 3-(trimethylsilyl)-1-propanesulfonate (TMS-PS-Na) was 75. Signals of formic acid and TMS-PS-Na (the internal standard) were integrated at a sweep speed of 8 Hz s^{-1}.

Standard procedure for the determination of formic acid in periodate oxidation mixtures. To a 0.2 *M* D_2O solution of sodium metaperiodate (0.50 ml) con-

taining TMS-PS-Na (5.0 μmole), add a carbohydrate sample which is expected to liberate *ca.* 45 μmole of formic acid by oxidation, and keep the resultant solution at 25°C on a thermostated water bath, shielding from the light. Observe the p.m.r. spectrum applying a H_1 field of 150 μgauss. The molar amount of formic acid is obtained as the product of the average value of the aldehydic–methyl proton-signal-response ratios and the molar amount of the internal standard used. At least five determinations should be done for each sample for averaging.

Results and discussion

The aldehydic proton in formic acid resonates at 8.23 p.p.m. as a singlet. In the spectra of periodate oxidation mixtures obtained from carbohydrate samples, this signal is well isolated from those of other fragments, as seen from a typical example of the oxidation mixture from methyl α-D-glucopyranoside (Fig. 1). As indicated in Fig. 2 the signal response of this aldehydic proton increased with increasing H_1 levels to reach a plateau at 80 μgauss, but irradiation with H_1 higher than 250 μ gauss caused a decrease in the response, owing to saturation of the nuclei. The curve for methyl protons in TMS-PS-Na (the internal standard) resembled that for the aldehydic proton except for the delay of arrival at plateau to 150 μgauss. Therefore, the H_1 level was controlled at 150 μgauss throughout this work.

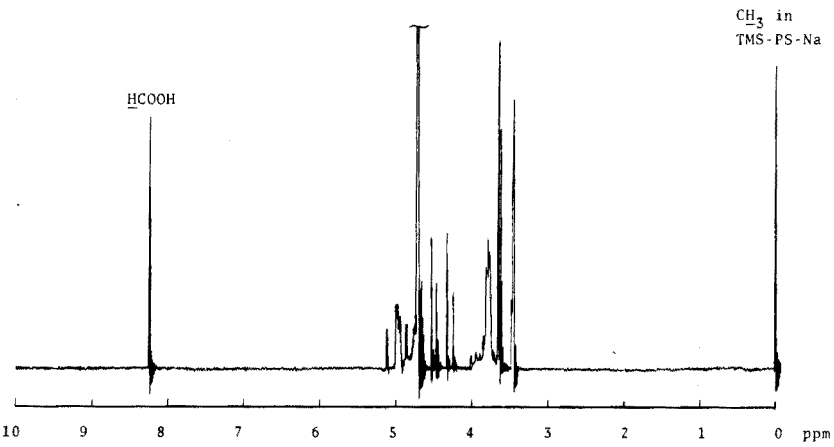

Fig. 1. 90-MHz p.m.r. spectrum of the periodate oxidation mixture obtained from methyl α-D-glucopyranoside in D_2O.

The abundance of both protons, aldehydic and methyl, was estimated by the signal integration method. When the integration was performed at the maximum sensitivity, the highest reproducibility was obtained for a sweep speed of 8 Hz s^{-1}. Under these conditions, the calibration curve was shown to be linear for 10–100 μmoles of formic acid; the relative signal response increased from about 0.22 to about 2.22. For this curve, formic acid was added directly to the periodate mixture. Table I indicates that this method is accurate and reproducible for various levels of sample amounts.

On the basis of the observations mentioned above, the standard procedure

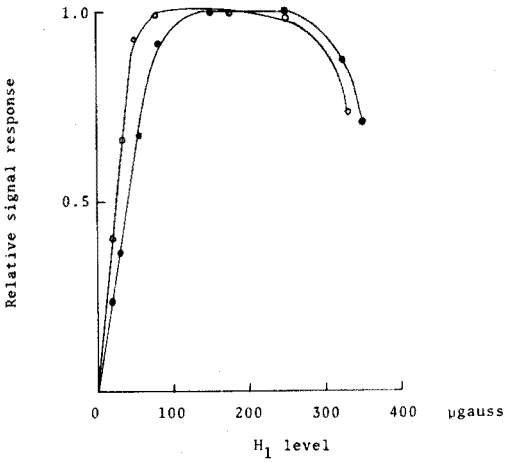

Fig. 2. Relationship between H_1 level and signal response, (○) HCOOH; (●) CH_3 in TMS-PS-Na. The concentration of both kinds of protons was $1.0 \cdot 10^{-1}$ *M*.

TABLE I

REPRODUCIBILITY OF THE P.M.R. DETERMINATION OF FORMIC ACID

(10 determinations were done for each level.)

Formic acid added (μmole)	*Ave. formic acid found (μmole)*	*Standard deviation*
10	9.9	0.41
50	50	1.6
100	99	2.3

was devised for the determination of formic acid liberated from carbohydrates by periodate oxidation. Table II summarizes the results obtained from the oxidation of selected carbohydrates. For alditols having different numbers of carbon atoms (erythritol, D-xylitol and D-mannitol), as well as glycosides (methyl α- and β-D-glucopyranosides), the amounts of formic acid as determined by this method were in good agreement with those determined by alkalimetry[2].

It is noticeable that the spectra of the oxidation mixtures obtained from D-arabinose and D-glucose gave a minor singlet at 8.17 p.p.m., ascribable to the formyl ester proton, along with the major singlet at 8.23 p.p.m. of the aforementioned aldehydic proton in free formic acid. Since the values obtained by alkalimetry lay between those of free and total formic acid as determined by the p.m.r. method, partial hydrolysis of resultant formyl esters should be involved during titration with alkali. Alkalimetry is, therefore, considered to be unsuitable for the determination of formic acid liberated from such aldoses, except when only the total formic acid is to be determined after the formyl esters have been hydrolyzed by *e.g.* heating.

Ketoses, aldonic acids, and uronic acids are groups of compounds the liberation of formic acid from which cannot be determined simply by alkalimetry,

TABLE II

LIBERATION OF FORMIC ACID FROM SELECTED CARBOHYDRATES BY PERIODATE OXIDATION

	Formic acid liberated (mole/mole)					
	P.m.r. method			*Alkalimetry*		
	1 h	*3 h*	*24 h*	*1 h*	*3 h*	*24 h*
Erythritol	2.0	2.0	2.0	1.98	2.01	2.00
D-Xylitol	2.9	3.0	2.9	2.97	3.00	2.99
D-Mannitol	4.0	4.0	4.0	3.98	4.01	4.00
Methyl α-D-glucopyranoside	0.73	0.90	0.94	0.74	0.88	0.93
Methyl β-D-glucopyranoside	0.73	0.88	0.93	0.73	0.86	0.92
DL-Glyceraldehyde	1.2	1.5	2.0	1.19	1.47	1.90
D-Arabinose	2.2[a]	2.3[a]	3.2[a]	2.90	3.03	3.58
	3.1[b]	3.3[b]	3.8[b]			
D-Glucose	2.6[a]	3.2[a]	4.1[a]	3.28	3.79	4.20
	3.6[b]	4.1[b]	4.6[b]			
D-Fructose	1.1	1.2	1.8	1.81	1.96	2.67
L-Sorbose	1.2	1.4	2.2	1.91	2.15	3.10
D-Gluconic acid δ-lactone	1.5	2.3	2.6	2.87	3.47	3.84
D-Galacturonic acid	4.1	4.1	4.2	5.62	5.64	5.47
D-Glucuronic acid	3.9	4.0	4.0	5.39	5.49	5.40

[a] Free formic acid.
[b] Total formic acid.

because glycolic or glyoxylic acid is expected to be formed along with formic acid in these cases. Indeed, the p.m.r. determination gave lower values of formic acid than alkalimetry. The differences between these values are considered to give the amounts of such carboxylic acids. From this consideration, the differences for both ketoses (D-fructose and L-sorbose), corresponding to the amounts of glycolic acid formed, were 0.7, 0.8, and 0.9 mole per mole of ketose after oxidation for 1 h, 3 h, and 24 h, respectively. However, D-gluconic acid δ-lactone and two uronic acids (D-glucuronic and D-galacturonic acids) gave differences higher than 1 mole for unknown reasons. The mechanism of the periodate oxidation of glyoxylic acid, presumed to be formed, should be clarified in future studies.

Conclusion

In the spectra of oxidation mixtures, aldehydic protons in free and esterified formic acid resonate as singlets at 8.23 and 8.17 p.p.m., respectively, isolated from other signals. From the response of these signals 10–100-μmole amounts of formic acid in both forms can be determined rapidly and simply.

REFERENCES

1 S. Honda, K. Kakehi, H. Yuki, and K. Takiura, *Anal. Chim. Acta*, submitted.

2 E. L. Hirst and J. K. N. Jones, *J. Chem. Soc., London*, 73 (1949) 1659.
3 M. Morrison, A. C. Kuyper and J. M. Orten, *J. Amer. Chem. Soc.*, 75 (1953) 1502.
4 J. R. Dyer, *Methods Biochem. Anal.*, 3 (1956) 111.
5 W. J. Hopton, *Anal. Chim. Acta*, 8 (1953) 429.
6 W. M. Grant, *Anal. Chem.*, 19 (1947) 206.

Analytica Chimica Acta, 77 (1975) 274–277

SHORT COMMUNICATION

Periodate oxidation analysis of carbohydrates

Part III. Potentiometric determination of periodate consumption by use of an iodide-selective electrode

SUSUMU HONDA, KYOKO SUDO, KAZUAKI KAKEHI and KIYOSHI TAKIURA
Faculty of Pharmaceutical Sciences, Osaka University, Toneyama, Toyonaka, Osaka-fu (Japan)
(Received 16th August 1974)

Primary information in periodate oxidation analysis of carbohydrates is obtained from knowledge of the periodate consumption. The quantities of periodate consumed by carbohydrate samples have been most frequently determined by titration of excess of periodate with arsenite[1,2] or iodimetrically[3]. A u.v. absorption spectrophotometric procedure[4] reduces the sample amounts to the 10^{-2}–10^{-1} μmole level, but determination of periodate is interfered with by photooxidation, during measurement, of liberated formic acid. A polarographic method[5] established in these laboratories is also suitable for micro determination of periodate consumed, but this technique has received scanty attention. This paper describes a potentiometric method by use of an iodide-selective electrode. In the proposed method, excess of periodate is reacted with excess of iodide, and the consumption of iodide by periodate is estimated potentiometrically. Rapid determination of periodate consumption for $1 \cdot 10^{-2}$–$5 \cdot 10^{-1}$-μmole quantities of carbohydrate samples is possible with a commercially available electrode.

Calibration of iodide electrode

As expected, there was a linear Nernstian relationship between the potentials and the logarithms of concentrations of iodide solutions. In 0.1 *M* acetate buffer (pH 6.0), linearity was observed for a concentration range of 10^{-6}–10^{-2} *M*.

Determination of periodate

A redox reaction occurs between periodate and iodide, as follows:

$$IO_4^- + 2\,I^- + H_2O = IO_3^- + I_2 + 2\,OH^-$$

Under conditions where this ionic reaction proceeds stoichiometrically, the amount of iodide consumed is equivalent to that of periodate present. Since iodide consumption is easily obtained by subtraction of the amount of the remaining iodide from that of the initial iodide, an indirect determination of periodate is possible. There is a problem of interference from the simultaneous liberation of iodine, which combines with the iodide ion to form the I_3^- ion. The complex

formation enhances the potentials of reaction solutions giving negative errors. However, since the complex formation is reversible, the removal of iodine from reaction media reduces the triiodide concentration, and the accuracy of determination is assured. Solvent extraction with various solvents indicated that carbon tetrachloride, carbon disulfide, and chloroform were effective. Extraction with ethyl acetate gave high apparent results for determination of 5.0 μmole of periodate, whereas ether caused slightly low results; when no extraction was used, the results for periodate were more than 10% low. Carbon tetrachloride was best suited for the purpose, because of the lowest volume change of the aqueous phase on extraction (carbon tetrachloride, 0.0%; carbon disulfide, +3.0%; chloroform, +1.2%; for 0.1 *M* acetate buffer, pH 4–6).

TABLE I

EFFECT OF pH AND CONCENTRATION ON THE DETERMINATION OF PERIODATE

Concentration of periodate added (M)	*Concentration of periodate found (M)*			
	pH 5	*pH 6*	*pH 7*	*pH 8*
$5.0 \cdot 10^{-3}$	$5.0 \cdot 10^{-3}$	$5.0 \cdot 10^{-3}$	$5.0 \cdot 10^{-3}$	$5.0 \cdot 10^{-3}$
$1.0 \cdot 10^{-3}$	$1.0 \cdot 10^{-3}$	$1.0 \cdot 10^{-3}$	$1.0 \cdot 10^{-3}$	$1.0 \cdot 10^{-3}$
$5.0 \cdot 10^{-4}$	$5.0 \cdot 10^{-4}$	$5.0 \cdot 10^{-4}$	$5.0 \cdot 10^{-4}$	$5.0 \cdot 10^{-4}$
$1.0 \cdot 10^{-4}$	$1.0 \cdot 10^{-4}$	$1.0 \cdot 10^{-4}$	$8.5 \cdot 10^{-5}$	$6.3 \cdot 10^{-5}$
$5.0 \cdot 10^{-5}$	$4.6 \cdot 10^{-5}$	$3.5 \cdot 10^{-5}$	$3.5 \cdot 10^{-5}$	$2.1 \cdot 10^{-5}$
$1.0 \cdot 10^{-5}$	$7.0 \cdot 10^{-6}$	$3.5 \cdot 10^{-6}$	$3.5 \cdot 10^{-6}$	$0.7 \cdot 10^{-6}$

Periodate of various concentrations was determined at various pH levels, and the results are summarized in Table I. Stoichiometry was observed for concentration higher than $1.0 \cdot 10^{-4}$ *M* at pH 5 and 6, whereas the lower limit of determinable concentration rose to $5.0 \cdot 10^{-4}$ *M* at pH 7 and 8 because of slower reaction speed. For pH values lower than 5, reaction speed was accelerated, but iodate resulting from periodate undergoes a similar redox reaction, giving positive errors. For these reasons, reaction media should be controlled at pH 5–6. Fortunately, this pH range accords with the optimal pH range of periodate oxidation that minimizes overoxidation of carbohydrates. The upper limit of concentration should be restricted to $5.0 \cdot 10^{-3}$ *M*, since at higher concentrations the amount of iodine liberated was too large to be removed simply by one solvent extraction, and negative errors arose.

Experimental

Material. All reagents and solvents were of reagent grade. Carbohydrate samples were of the highest grade commercially available.

Apparatus. The concentrations of iodide were determined by measuring the potentials of the solutions with a Toa Denpa I-125 electrode and a double-junction type HC-305 calomel electrode connected to a Toa Denpa HM-18A digital pH meter.

Determination of periodate. To a sample solution (5.0 ml) containing 0.5–2.5 μmole of periodate in 0.1 *M* acetate buffer (pH 5–6), add about a 10% excess of

$1.0 \cdot 10^{-3}$ *M* potassium iodide solution in the same buffer. After 5 min, shake the mixture with an equal volume of carbon tetrachloride for 5 min, and allow to stand. Measure the concentration of iodide remaining in the aqueous phase from the potential of this phase against the calibration curve, prepared from standard iodide solutions in the same buffer.

Since the molar amount of periodate present equals one-half of the molar amount of iodide consumed, the former was calculated as $\frac{1}{2}((10^{-3}-c)V_i - cV_s)\cdot 10^{-3}$ μmole, where c, V_i and V_s represent the iodide concentration of the aqueous phase (*M*), the volume of the iodide solution added (ml), and the volume of the sample solution (ml), respectively.

Periodate oxidation of carbohydrates. To a $5.0 \cdot 10^{-4}$ *M* solution (1.0 ml) of a carbohydrate sample, add a $5.0 \cdot 10^{-3}$ *M* sodium metaperiodate solution (1.0 ml) in 0.2 *M* acetate buffer (pH 6.0), and maintain the mixture at 25°C for 1 h on a thermostated water bath, shielding from the light. Add about a 10% excess of a $5.0 \cdot 10^{-3}$ *M* potassium iodide solution in 0.1 *M* acetate buffer (pH 6.0), and after 5 min measure the amount of the remaining periodate by the procedure described above.

Results and discussion

Reaction mixtures obtained from carbohydrates by periodate oxidation contain iodate and oxidation fragments, such as formaldehyde and formic acid, along with excess of periodate. Determination of $3.0 \cdot 10^{-3}$ *M* periodate in the presence of $3.0 \cdot 10^{-3}$ *M* iodate, $1.5 \cdot 10^{-2}$ *M* formaldehyde, and $1.5 \cdot 10^{-2}$ *M* formic

TABLE II

DETERMINATION OF PERIODATE CONSUMPTION FOR SELECTED CARBOHYDRATES

Carbohydrate	*Potentiometric method*	*U.v. method*[4]
D-Sorbitol	5.0	5.0
D-Glucose	4.8	4.9
D-Glucosamine hydrochloride	4.9	5.0
D-Glucuronic acid	5.1	5.0
D-Gluconic acid δ-lactone	4.7	4.8
Methyl α-D-glucopyranoside	0.76	0.76

TABLE III

DETERMINATION OF D-SORBITOL

(5 determinations were done at each level.)

D-Sorbitol added (μmole)	*Ave. D-sorbitol found (μmole)*	*Standard deviation*
$1.0 \cdot 10^{-1}$	$0.9 \cdot 10^{-1}$	0.13
$2.0 \cdot 10^{-1}$	$2.0 \cdot 10^{-1}$	0.21
$3.0 \cdot 10^{-1}$	$3.1 \cdot 10^{-1}$	0.29

acid, however, indicated that these compounds did not interfere with the determination significantly, the concentration of periodate found being $3.0 \cdot 10^{-3}$ *M*.

On the basis of the observations mentioned above, selected carbohydrates were oxidized with periodate, and its consumption was determined by this method. Table II shows that the periodate consumption obtained by this method is in good agreement with that determined by the u.v. absorption spectrophotometric method[4] for all carbohydrate samples examined. The smallest sample amount that can be analysed by this method was $5.0 \cdot 10^{-2}$ μmole when ordinary vessels such as 50-ml beakers were used for measurement. The use of hand-made solid paraffin microcells diminished the measurable volume to 1 ml, reducing the minimum sample amount to $1.0 \cdot 10^{-2}$ μmole.

Table III gives an example of the application of this method. Since 1 mole of D-sorbitol consumes 5.0 mole of periodate after oxidation for 1 h, and since this consumption is reproducible under control of reaction conditions, the amounts of D-sorbitol were determined from the amounts of periodate consumed.

Application of this method to the periodate oxidation analysis of carbohydrates makes it possible to estimate rapidly the periodate consumption for $1 \cdot 10^{-2}$–$5 \cdot 10^{-1}$ μmole quantities of carbohydrate samples.

REFERENCES

1 P. F. Fleury and J. Lange, *J. Pharm. Clin.*, 17 (1933) 107; 17 (1933) 196.
2 E. Müller and O. Friedberger, *Ber. Deut. Chem. Ges.*, 35 (1902) 2652.
3 L. Malaprade, *Compt. Rend.*, 186 (1928) 382; *Bull. Soc. Chim. France*, 43 (1928) 683.
4 J. S. Dixon and D. Lipkin, *Anal. Chem.*, 26 (1954) 1092.
5 K. Takiura and K. Koizumi, *Yakugaku Zasshi*, 78 (1958) 961.

Analytica Chimica Acta, 77 (1975) 278–282

SHORT COMMUNICATION

Application of a fluoride-selective electrode to the monitoring of fluoride in air

A. HRABÉCZY-PÁLL, K. TÓTH and E. PUNGOR
Institute for General and Analytical Chemistry, Technical University Budapest (Hungary)
F. VALLÓ
Aluminium Works, Ajka (Hungary)
(Received 30th December 1974)

Fluoride in air is harmful to plants, animals and human health, and its monitoring is therefore very important especially in areas near emission sources like alumina works, aluminium industry, enamel-ware works etc. Fluoride ion-selective electrodes seem to be a very useful tool in monitoring fluoride having the advantage of outstandingly high selectivity compared to other methods, *e.g.* spectrophotometry, combined with good sensitivity. This means that separation from interferences is usually unnecessary before the determination.

Very few papers have appeared so far on such applications of fluoride ion-selective electrodes. Elfers and Decker[1] determined very low levels (of the order of a few p.p.b.) of fluoride in air, by passing the air at a high rate for several hours through a filter paper impregnated with sodium formate. After the filter paper had been washed with sodium citrate buffer solution, the fluoride absorbed in the solution was measured with an ion-selective electrode. Buck and Reusmann[2] collected the fluoride content of air on a silver adsorbent and eluted it subsequently with a solution containing sodium citrate. The fluoride in the effluent was determined with a fluoride ion-selective electrode. Liberti and Mascini[3,4] have determined p.p.m. concentrations of fluoride in air after absorption in TISAB solution, by measurement with a fluoride ion selective electrode, and recommended the method for continuous monitoring. Oliver *et al.*[5] have constructed an apparatus for the continuous measurement of fluoride in air with a fluoride ion-selective electrode.

The aim of the work described here was to study the applicability of a fluoride ion-selective electrode for monitoring the fluoride content of air after absorption in a suitable solution. The conditions of the absorption and calibration of the system were investigated thoroughly.

Experimental

Equipment. Two types of absorbers were used. The first one was essentially like a gas washing bottle with the modification that a special plastic bubbler was used in place of the common glass frit (Fig. 1). The second absorber used was a recirculation absorber in which the absorbing liquid circulated continuously,

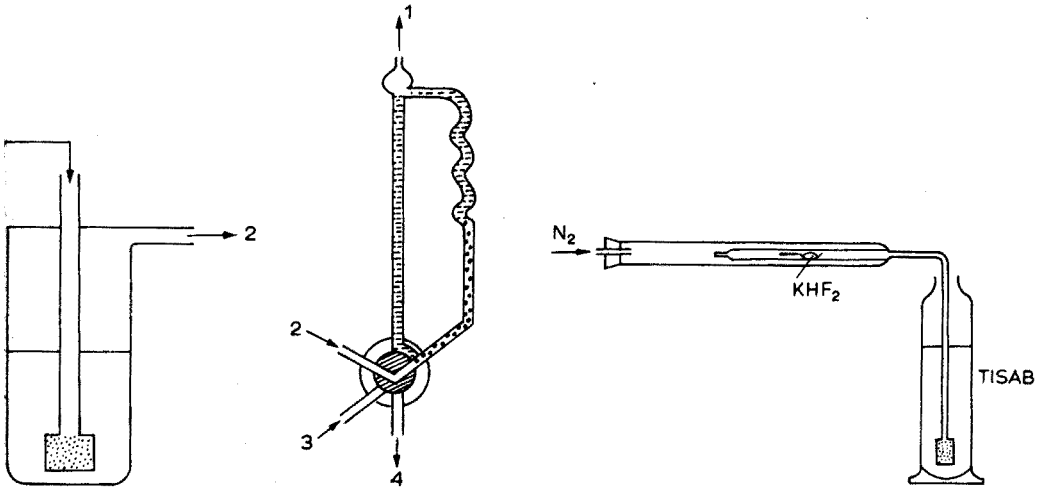

Fig. 1. Gas washing bottle absorber. (1) Gas inlet; (2) gas outlet.

Fig. 2. Recirculation absorber (1) Gas outlet; (2) gas inlet; (3) reagent filling; (4) to the measuring cell.

Fig. 3. The device used to produce hydrogen fluoride.

whereas the gas passed through in a single run. Here the circulation was maintained and the liquid was efficiently homogenized by the gas stream itself. A schematic diagram of this absorber is shown in Fig. 2.

The hydrogen fluoride standards were prepared from potassium hydrogen fluoride, as no standard gases are available. The system was calibrated and the absorption efficiency was checked with hydrogen fluoride liberated from potassium hydrogen fluoride by thermal decomposition, which was done in the apparatus shown in Fig. 3. Small amounts (a few mg) of potassium hydrogen fluoride were weighed (microbalance) into a platinum vessel which was placed into a platinum tube. The latter was drawn out at the end where the flushing gas, nitrogen, entered. This ensured a slight suction, thus preventing the hydrogen fluoride evolved from leaving the platinum tube in the reverse direction, against the gas stream. The platinum tube was placed within a wider silica tube which was connected with the absorber by silicone rubber tubing. The system was heated by an electric furnace at a temperature of about 600°C. The fluoride concentration of the absorbing solution was measured by direct potentiometry.

Gas flow rates were measured with a rotameter.

E.m.f. measurements were made with a precision pH meter type OP-205 (Radelkis, Budapest). A Radelkis fluoride ion-selective electrode was used as indicator electrode with a Radelkis saturated calomel reference electrode.

Calibration of the electrode and measurement of the fluoride concentration in the absorbing solution were done in flow-through cells which incorporated the indicator and reference electrodes separately (Fig. 4). The streaming of the solution was maintained by a Unipan (Poland) peristaltic miniflow pump type 304.

Reagents. The absorbing liquid was a TISAB solution diluted with an equal volume of distilled water.

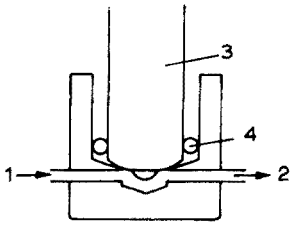

Fig. 4. Flow-through cell. (1) Sample inlet; (2) sample outlet; (3) ion-selective electrode (Radelkis); (4) O-ring.

TISAB solution. To 500 ml of distilled water were added 57 ml of glacial acetic acid, 58 g of sodium chloride and 0.36 g of sodium citrate. The solution was titrated with 5 *M* sodium hydroxide to a pH of 5–5.5, and diluted to 1 l with distilled water in a volumetric flask.

Standard fluoride solutions. Standard sodium fluoride solutions were prepared with distilled water. For calibration of the electrodes, standards were mixed with equal volumes of TISAB solution.

Results and discussion

The applicability of the two absorbers was studied. The type of absorber shown in Fig. 1 has the advantage of very simple construction. However, its drawback is that the pores of the bubbler retain a significant amount of fluoride; to obtain all the fluoride actually in the absorbing solution, the bubbler must be washed out very thoroughly and the solution mixed well. This makes the procedure lengthy and more difficult to automate. With this type of absorber, a liquid column about 20 cm high was sufficient to achieve practically complete absorption of hydrogen fluoride, since the gas was distributed as small bubbles with a diameter of 0.1–0.5 mm.

The operation of the absorber shown in Fig. 2 is based on the principle of the mammoth pump: the gas introduced at the bottom of one of two communicating vessels, lifts the liquid in this vessel over into the other side, so that the solution is continuously circulated. In this device the absorber was a plastic tube made into a spiral. As the bubbles had a diameter of about 4 mm, a tube length of 2 m was necessary to obtain practically complete absorption.

The hydrogen fluoride standards were prepared by thermal decomposition of potassium hydrogen fluoride, as shown in Fig. 3. By varying the gas flow rate and the amount of salt taken, the approximate concentration of hydrogen fluoride in the gas could be adjusted. Even when hydrogen fluoride was not evolved at a constant rate, the total amount evolved and to be absorbed could be determined from the weight of the salt taken. By assuming that the hydrogen fluoride was evolved at a constant rate, its approximate concentration in the gas could be calculated from the weight of the salt taken, the time of evolution and the flow rate of the diluent gas.

The completeness of the decomposition was checked by weighing the residue. With both absorbers, a second absorber was used (gas washing bottle)

TABLE I

ABSORPTION EFFICIENCY OF DIFFERENT ABSORBERS

No.	*HF taken (mg)*	*HF found (mg)*	*Error (%)*	*Gas flow rate ($l\ h^{-1}$)*
Gas washing bottle absorber				
1	1.27	1.26	−0.8	3
2	1.52	1.53	+0.7	6
3	1.52	1.46	−3.9	10
4	1.90	1.92	+1.1	20
5	4.06	3.92	−3.4	10
6	4.77	4.86	+1.9	6
7	5.01	4.63	−7.6	6
8	6.22	5.77	−7.2	3
9	7.17	6.67	−7.0	10
10	11.50	11.50	0	40
11	11.99	11.99	0	10
Recirculation absorber				
1	1.75	1.81	+3.4	10
2	2.23	2.23	0	12
3	2.25	2.09	−7.1	3.5
4	2.33	2.20	−5.6	2.5
5	2.94	2.71	−7.8	20
6	3.20	3.28	+2.5	14
7	3.90	3.88	−0.5	18
8	5.29	5.69	+7.6	5.5

to check whether or not the gas leaving the first absorber contained any hydrogen fluoride. Under the conditions indicated in Table I, no appreciable amount of hydrogen fluoride was found in the second absorber.

The gas washing bottle absorber operated well at flow rates from 3 to 40 $l\ h^{-1}$, and at approximate hydrogen fluoride concentrations in the gas from 0.2 to 4.2 mg l^{-1}. The recirculation type was satisfactory at flow rates from 2.5 to 20 $l\ h^{-1}$, at hydrogen fluoride concentrations between 0.15 and 1 mg l^{-1}.

Some results of the absorption efficiency studies made on the absorbers are shown in Table I.

Under the conditions used, the average relative errors of the measurements were −2.4 and −0.9%, and the relative standard deviations were 3.6 and 5.4% for the first and second types of absorber, respectively. It is quite understandable that negative errors occur more frequently because of adsorption of hydrogen fluoride on the plastic tubing in both types of absorber. These results show that the absorbing and the measuring device are suited to the determination of hydrogen fluoride in air.

On the basis of these experiments, the recirculation absorber can be considered more advantageous, since this involves no washing or additional homogenization of the liquid between gas absorption and concentration measurement with the fluoride-selective electrode. Therefore this absorber makes it easier to automate the whole process. In its present state, the apparatus can be used to measure the average hydrogen fluoride level in a gas over the period of time required to

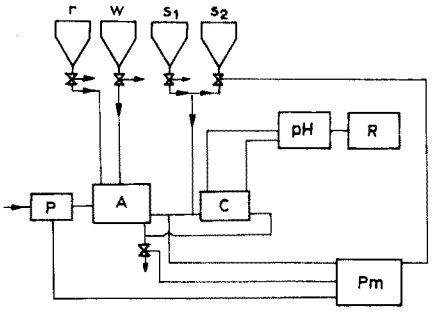

Fig. 5. Block diagram of the automated apparatus. (r) reagent, (w) wash liquid (water), (s_1), (s_2) standards, (P) pump, (A) absorber, (C) measuring cell, (pH) pH meter, (R) recorder, (Pm) programming unit.

ensure that the absorbing solution becomes at least 10^{-5} *M* in fluoride. Obviously, the absorber had to be washed free of fluoride after each run. The completeness of washing was checked with a fluoride-selective electrode.

On the basis of the results reported, a mechanized apparatus was constructed for the quasi-continuous determination of the fluoride content of air. This gives information about the integral of the concentration over a certain period of time. A block diagram of the apparatus is shown in Fig. 5.

REFERENCES

1 L. A. Elfers and C. E. Decker, *Anal. Chem.*, 40 (1968) 1658.
2 M. Buck and G. Reusmann, *Fluoride*, 4 (1971) 5.
3 A. Liberti and M. Mascini, *Anal. Chem.*, 41 (1969) 676; *Fluoride*, 4 (1971) 52; Proc. 2nd Int. Conf. of Air Pollution Prevention Associations, Washington, December, 1970, p. 519.
4 M. Mascini, *Inquinamento*, 13 (1971) 21.
5 R. T. Oliver, G. F. Lenz and W. P. Frederick, *Advances in Automated Analysis, Technicon Int. Congress, 1969, Vol. 2*, pp. 309–14.

Analytica Chimica Acta, 77 (1975) 283–287

SHORT COMMUNICATION

An assessment of the quinhydrone electrode for measurements in pickling baths

GILLIS JOHANSSON

Department of Analytical Chemistry, University of Umeå, S-901 87 Umeå (Sweden)

(Received 25th November 1974)

It has recently been suggested[1] that nitric acid in pickling baths can be determined with the quinhydrone electrode after dilution. A fresh pickling bath can contain 15–25% nitric acid and 3–5% hydrofluoric acid by weight. During use, large quantities of metals, mostly iron but also significant quantities of chromium and nickel, may accumulate. The use of a quinhydrone electrode in these baths is questionable as it is well known[2] that quinhydrone can be prepared from hydroquinone by oxidation with iron(III). There are, however, several examples of the usefulness of the electrode in systems in which an oxidation is thermodynamically possible[3]; owing to slow reactions, the ratio between quinone (Q) and hydroquinone (QH_2) remains essentially constant during measurements. The reactions of the quinhydrone electrode have therefore been studied in more detail.

The electrode potential may be written as

$$E = E_Q^\circ + \frac{RT}{F} \ln a_{H^+} + \frac{RT}{2F} \ln \frac{[Q]}{[QH_2]} + \frac{RT}{2F} \ln \frac{f_Q}{f_{QH_2}} \quad (1)$$

If $[Q] = [QH_2]$ = constant and the last term remains constant in eqn. (1), then the electrode will measure changes in the hydrogen ion concentration. In the presence of iron(III), oxidation may occur:

$$2\,Fe^{2+} + Q + 2\,H^+ \Leftrightarrow QH_2 + 2\,Fe^{3+} \quad (2)$$

The equilibrium constant of this reaction is:

$$K_e = (a_{QH_2} \cdot a_{Fe^{3+}}^2)/(a_{Fe^{2+}}^2 \cdot a_Q \cdot a_{H^+}^2) \quad (3)$$

The value of E and thus of K_e can be evaluated from the standard potentials of iron and quinhydrone. If it is assumed that eqn. (2) proceeds reversibly, and is the only source of iron(II), then if eqn. (3) is inserted into eqn. (1) the electrode potential in a solution containing iron is:

$$E = E_Q^\circ + \frac{RT}{F} \ln a_{H^+} + \frac{RT}{F} \ln \frac{[Fe^{3+}]}{[Fe^{2+}]} + \frac{RT}{F} \ln \frac{f_{Fe^{3+}}}{f_{Fe^{2+}}} \cdot \frac{1}{\sqrt{K_e}} \quad (4)$$

Equation (4) holds only for an unsaturated quinhydrone electrode.

The potential of a saturated electrode will also depend on the amount of quinhydrone present in solid form. As the amount of iron(III) increases it will

approach the quino–quinhydrone electrode. Because of the high concentration of quinone, the potential will be very sensitive to side reactions and will show large drifts even under carefully controlled conditions[2]. Equation (4) will also be valid for a redox electrode in solution without any quinhydrone, if K_e and E°_Q are replaced by E°_{Fe}.

Equation (4) shows that the electrode potential is a function of both the hydrogen activity and the Fe(III)/Fe(II) ratio. If $[Fe^{3+}] \gg [Q_2H_2]_a$, the original amount of quinhydrone, and if all iron(II) comes from reaction (2), then:

$$[Fe^{2+}] \simeq [Q_2H_2]_a = \text{constant} \tag{5}$$

Quinone has basic properties[4,5]:

$$Q + H^+ \rightarrow QH^+ \qquad K_b = 0.1 \pm 0.05 \tag{6}$$

and if eqn. (6) is taken into account and eqn. (5) is substituted into eqn. (4) the result will be:

$$E = E' + \frac{RT}{2F} \ln \frac{[H^+]^2}{(1+K_b[H^+])} + \frac{RT}{F} \ln \frac{[Fe^{3+}]}{[Q_2H_2]_a(1+K_b[H^+])} \tag{7}$$

where K_e, E°_Q and the activity coefficients have been compounded to a new constant E'.

Equation (7) indicates that the electrode should function as an iron(III)-selective electrode at a constant hydrogen ion concentration. This would, of course, be a most welcome property if it could be realized.

Experimental

A double liquid junction reference electrode, Orion 90-02, filled with 4 *M* KCl and one or two indicating electrodes were immersed in a titration vessel, Metrohm EA 880. The electrode potential was measured with an Orion 801 digital pH meter. An electrode switch was used to connect the respective electrodes to the pH meter. An Ingold glass electrode, a Permaplex membrane electrode as described earlier[6,7] and a platinum electrode (a foil 0.5 cm^2, in a glass stem) were used as indicating electrodes. Quinhydrone corresponding to 50 m*M* was added to the solution to give the saturated quinhydrone electrode. The unsaturated quinhydrone was made by adding solid quinhydrone in an amount corresponding to 4 m*M* solution.

Titrations were performed by adding 0.5 *M* iron(III) nitrate, dissolved in a solution of the same composition as that in the titration vessel.

Results

Figure 1 shows the responses of an unsaturated quinhydrone electrode, of a redox electrode and of a glass electrode towards additions of iron(III) to 1 *M* nitric acid. The measurements on the quinhydrone and the glass electrode were made on the same solution. A separate titration under identical conditions but excluding quinhydrone was made to obtain the redox electrode response. The potential of the glass electrode remained almost constant indicating a nearly constant pH. The potential changes of the quinhydrone as well as the redox electrode must therefore be caused by iron(III). This shows that reaction (2) readily takes place

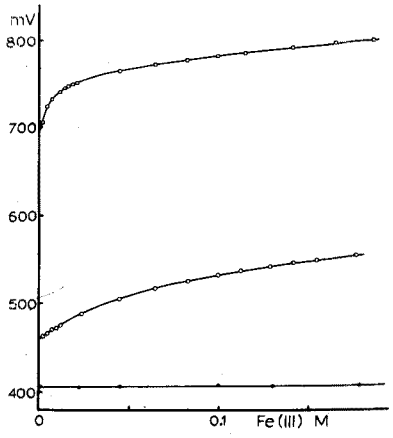

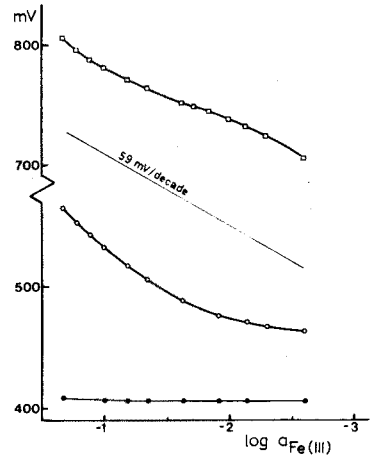

Fig. 1. Titration of 1 *M* HNO_3 with 0.5 *M* $Fe(NO_3)_3 + 1$ *M* HNO_3. Electrode potentials of the glass electrode (●), the unsaturated quinhydrone electrode (○) and a platinum redox electrode (□) are plotted *versus* the Fe(III) concentration in the titration vessel.

Fig. 2. Electrode potentials of the glass electrode (●), the unsaturated quinhydrone electrode (○) and a platinum redox electrode (□) plotted *versus* the logarithm of the Fe(III) concentration in 1 *M* HNO_3. The straight line represents 59 mV decade^{-1}.

in 1 *M* nitric acid. The potentials reached equilibrium values quickly and remained very stable.

Figure 2 shows a logarithmic plot of the responses of the quinhydrone and the redox electrodes. Ideal and reversible behaviour of the quinhydrone electrode according to eqn. (7) should have resulted in a line with a slope of 59 mV decade^{-1} at higher concentrations of iron(III). In fact, the slope is higher than that predicted, approaching 100 mV decade^{-1}. The redox electrode approaches a slope of 90 mV decade^{-1}. As the iron(III) concentration decreases, the slope levels off and approaches zero as predicted from eqns. (1) and (4). (Equation (8) is no longer valid).

These experiments were repeated in 3 *M* nitric acid; at some part of the titration the quinhydrone electrode changed quite rapidly from about 550 mV to about 880 mV. The iron(III) concentration at which this occurred was not reproducible. The change was completed in 3–6 min. Additions of iron(II) or quinhydrone had little effect on the potential once the change was complete. This transition is caused by nitric acid oxidation of either quinhydrone or iron(II). One of the products formed during the oxidation seems to catalyze the reaction so that the rate increases enormously.

Figure 3 shows the response of the quinhydrone electrode, the Permaplex electrode and a glass electrode to variations in acidity. The nitric acid oxidation of quinhydrone started even in the absence of iron. Almost identical potentials were obtained when the saturated quinhydrone electrode was used.

There still remained the possibility that the quinhydrone electrode might be useful if the solutions were diluted. Entwistle *et al.*[1] diluted their pickling baths 50 times. Figure 4 shows a comparison between a saturated quinhydrone electrode and a glass electrode in solutions having concentrations similar to those of diluted

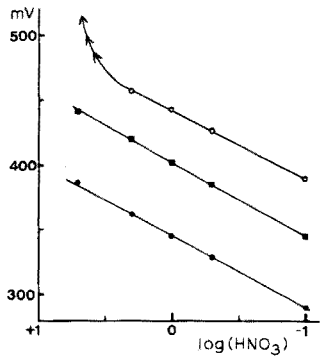

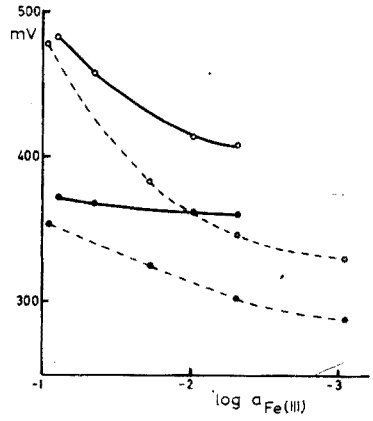

Fig. 3. Electrode potentials of the Permaplex electrode (■), the glass electrode (●) and the saturated quinhydrone electrode (○) plotted *versus* the logarithm of the nitric acid concentration. The Permaplex potential readings have been displaced by 300 mV.

Fig. 4. Titration of 0.1 *M* HNO_3+1 *M* KNO_3 (——), and 0.005 *M* HNO_3+1 *M* KNO_3 (---) with 2 *M* $Fe(NO_3)_3$. Glass electrode response (●), saturated quinhydrone electrode response (○) plotted *versus* the logarithm of the Fe(III) concentration.

pickling baths; the solutions were 1 *M* in KNO_3 to keep the ionic strength constant. Three concentrations of nitric acid were studied but only two are included in the Figure. The addition of iron(III) solutions resulted in a pH variation but the quinhydrone electrode potential increased much more than that of the glass electrode. This shows conclusively that the quinhydrone electrode even in dilute solutions gives a redox response as well as a pH response. Separate experiments showed that the unsaturated quinhydrone electrode behaved similarly, but that the potentials increased much more at high concentrations of iron(III). Both electrodes give very stable and reproducible readings.

Discussion

The experiments reported show that in solutions corresponding to pickling baths, the quinhydrone electrode responds to both hydrogen ion and iron(III). The response is far from ideal and further the quinhydrone may be oxidized by nitric acid. The electrode seems to be unsuitable for direct measurements in pickling baths. In pickling baths diluted with 1 *M* KNO_3, the quinhydrone electrode still responds to iron(III) and hydrogen ions. The potential in a solution containing iron(III) also depends on the amount of quinhydrone present.

Entwistle *et al.*[1] tested their electrodes in HNO_3–HF solutions and reported an error in the hydrofluoric acid concentration of 1%. A more rigorous testing in solutions containing iron(III) would probably have shown the mixed response of the quinhydrone electrode. Because of the complexes formed between fluoride and iron(III), the deviation from ideality of the quinhydrone electrode will be small in a fresh pickling bath. As the iron(III) concentration is increased with use, the electrode will give a markedly erroneous result.

As there are other electrodes[6,7] available for direct analysis of pickling

baths, there seems to be no reason for using the quinhydrone electrode for this application.

The author thanks Dr. T. Eriksson for making exploratory measurements, Mrs. K. Palmgren for performing the potentiometric measurements, and Dr. M. Sharp for linguistic revision.

REFERENCES

1 J. R. Entwistle, C. J. Weedon and T. J. Hayes, *Chem. Ind. (London)*, (1973) 433.
2 E. Biilman and H. Lund, *Ann. Chim. (Paris)*, 16 (1921) 321.
3 D. J. G. Ives and G. J. Janz, *Reference Electrodes*, Academic Press, New York, 1961.
4 G. Biederman, *Acta Chem. Scand.*, 10 (1956) 1340.
5 F. Granér, A. Olin and L. G. Sillén, *Acta Chem., Scand.*, 10 (1956) 476.
6 T. Eriksson and G. Johansson, *Anal. Chim. Acta*, 63 (1973) 445.
7 T. Eriksson and S-E. Lunner, *J. Iron Steel Inst., London*, (1973) 581.

Analytica Chimica Acta, 77 (1975) 288–292

SHORT COMMUNICATION

Determination of selenium in metallurgical samples by flameless atomic absorption spectrometry

KIYOHISA OHTA and MASAMI SUZUKI*

Department of Chemistry, Faculty of Engineering, Mie University, Kamihama-cho, Tsu-shi, Mie-ken 514 (Japan)

(Received 16th December 1974)

Flameless atomic absorption spectrometry is attractive for trace analysis because of its small sample requirement and high absolute sensitivity, and has been applied to the determination of selenium. Matoušek[1] reported that a 1000-fold amount of perchloric acid caused a 25% reduction of selenium absorption, quoting a detection limit of 72 pg with the flameless device. Baird *et al.*[2] described the determination of trace amounts of selenium in waste water with a carbon rod atomizer. Welcher *et al.*[3] evaluated the use of a graphite atomizer for determination of selenium in high-temperature alloys. Inhat and Westerby[4] studied the determination of selenium in biological samples with a carbon rod atomizer after separation from the interfering sample matrices by reduction–precipitation with ascorbic acid; they concluded that the range of perchloric acid concentration for optimal sensitivity of selenium was fairly broad (0.2–1.4 *M*) and that only a small drop in absorption occurred over the 4–10 *M* concentration range. In these cases, carbon or graphite was used as atomizer; information is sparse for metal atomizers.

This communication describes the flameless atomic absorption characteristics of selenium with a metal micro-tube atomizer[5] and its application to metallurgical samples.

Experimental

Apparatus. A Nippon Jarrell-Ash 0.5-m Ebert-type monochromator, fitted with R 106 photomultiplier (Hamamatsu TV Co.) and Hitachi 056-1001 recorder (0.4-s full scale deflection), was used for atomic absorption measurements. The slit width was 0.1 mm, corresponding to a bandpass of 0.02 nm. The light source was a selenium hollow-cathode lamp (Hamamatsu TV Co.), which was modulated electronically at 90 Hz. A deuterium lamp (Original Hanau D200F) was used for background correction. The amplifier for the detection system was that used for flame spectrometry.

* Author for correspondence.

The construction of the metal micro-tube atomizer has been described in detail elsewhere[5]. The micro-tube was machined from molybdenum sheet; its diameter was 0.5–2.5 mm and the overall length was 20 mm, with a 0.3-mm hole drilled at the mid-point in order to enable a sample solution to be introduced. The ends of the micro-tube were firmly bolted on the copper supports. The micro-tube atomizer was enclosed in a Pyrex chamber which had two silica end-windows to allow transmission of the light beam. The chamber was flushed with argon. The slit (a 0.5-mm diameter hole) was placed in front of the atomizer, so that only a narrow band of radiation was transmitted. The power for heating was supplied by a stepdown transformer. A Hokushin 202 optical pyrometer was used for measuring the working temperature. An electric shaking device (Iwaki KM type) was used for extraction. Samples were decomposed in a Uni-seal decomposition vessel.

Standard selenium solution. Dissolve 0.351 g of selenious acid in water and dilute to 250 ml.

All reagents were of analytical grade. Deionized–distilled water was used throughout.

Measurement technique. Place the sample solution (5 μl) in the micro-tube by means of a laboratory-made glass micro-pipet. Heat the micro-tube at low power (0.6 V, 11 A) to evaporate the solvent from the sample slowly without sputtering. Switch off the current and increase the voltage to that determined to be optimal for selenium. Then switch on the micro-tube current to atomize the sample, and measure the absorbance at the 196.0-nm resonance line.

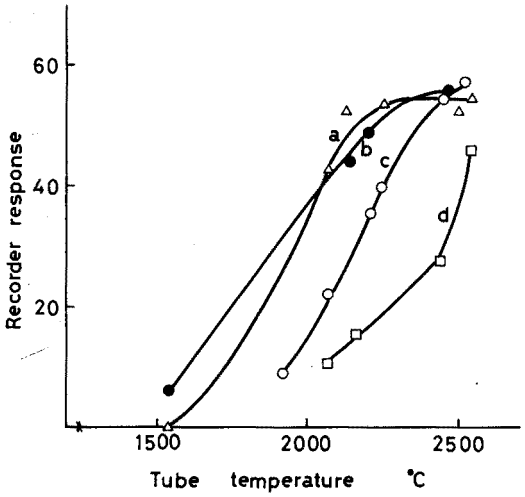

Fig. 1. Effect of tube dimension of atomizer on selenium absorption. (a) Mo tube (0.5-mm i.d., 20-mm long). (b) Mo tube (1.5-mm i.d., 20-mm long). (c) Mo tube (2.5-mm i.d., 20-mm long). (d) Ta tube (1.5-mm i.d., 20-mm long).

Effect of tube dimension and gas flow rate on selenium absorption

The micro-tube atomizer increases the analytical sensitivity[5]. The effect of micro-tube dimension on the sensitivity and reproducibility for selenium was determined. Figure 1 shows that similar absorption signals were obtained at

2500 °C irrespective of tube dimension, whereas the tube dimension had a marked effect at lower temperatures. The signals were more reproducible for the 1.5-mm diameter tube than for the 0.5- or 2.5-mm diameter tubes. Tantalum tubes gave lower signals than molybdenum tubes of the same dimension. Atomization of selenium was not attempted at temperatures above 2500 °C, because of the melting point of molybdenum.

Argon was used to provide an inert atmosphere in the Pyrex chamber; 1 volume of hydrogen was mixed with 23 volumes of argon to protect the atomizer from oxidation by traces of oxygen in the inert gas. The absorption signals were unchanged for argon flow rates of 0.5–3.0 l min^{-1}.

Sensitivity and reproducibility

Sensitivities under the optimal conditions are shown in Table I. Atomization from chelate and ion-association compounds was also examined; diaminobenzidine in toluene, dithiocarbamate in carbon tetrachloride and bromide in benzene were used, at the optimal extraction pH for each reagent as described in the literature being used.

TABLE I

ATOMIC ABSORPTION SENSITIVITIES AND REPRODUCIBILITY

Solution	*Sensitivity for 1% absorption* ($\cdot 10^{-11}$ g)	*Recorder response*	s_r (%)
Aqueous solution	3.8	48.4 ± 2.1	4.3
Aqueous solution (+10 μg Cu)	5.4	—	—
Aqueous solution (+1 μg Fe)	3.6	—	—
Diaminobenzidine complex in toluene	2.3	48.3 ± 1.7	3.6
Bromide in benzene	2.7	48.5 ± 2.5	5.2
Diethyldithiocarbamate complex in CCl_4	4.8	57.3 ± 5.2	9.0

The reproducibility was determined by repetitively measuring selenium under the optimal conditions, and calculating the standard deviation for each set of data; these results are also given in Table I. Absorption signals from dithiocarbamate solutions showed poorer reproducibility, the reason for which is not clear. It was shown that the signals at the absorbing line originated purely from atomic absorption by selenium.

Interference studies

Interferences in aqueous solution were examined for ions at 10-, 40- and 200-fold levels; all the chemicals were used as chloride except lead (nitrate), vanadium (vanadate) and molybdenum (molybdate). Background from matrices was corrected by measuring the absorption of a continuous source. Table II shows the effect of some selected elements on selenium absorption. At the 10-fold level, various ions caused enhancing effects, which may have been due to faster volatilization of selenium. As the concentration of interfering ion increased, absorption signals were reduced, probably because of physical occlusion of selenium ions. Some authors[6,7] have ascribed interferences to vapor-phase interactions, but

this was not confirmed for selenium.

TABLE II

EFFECTS OF DIVERSE ELEMENTS IN AQUEOUS SOLUTIONS[a]

Diverse ion	*10-Fold amount*	*40-Fold amount*	*200-Fold amount*
Mg(II)	−9	−23	0
Na(I)	0	−27	−12
Ca(II)	0	−26	−35
Fe(III)	+11	−21	−56
Cu(II)	0	−7	+19
Al(III)	0	−27	0
Pb(II)	+9	−47	−74
Co(II)	0	−34	−62
Zn(II)	0	−35	−17
Sn(II)	+12	−35	−43
Ni(II)	+21	−39	−55
Cr(III)	+12	+37	0
Te(IV)	+15	−10	+6
V(V)	0	−14	−66
Mo(VI)	+47	+19	+9
$HClO_4$			−14 (0.01 *M*)

[a] Percent change of absorption for 5 ng of selenium.

Determination of selenium in copper

Two methods were compared for the application of the method to the determination of selenium in copper.

Extraction method. Decompose the sample (0.1–0.5 g) with 3–5 ml of perchloric–nitric acid mixture (5+1) in a Uni-seal decomposition vessel by heating at 80 °C in an oven for 1 h. Transfer the contents to a beaker and rinse the vessel with 1 *M* nitric acid. Evaporate the solution to copious fumes of perchloric acid, and dissolve the residue in 5 ml of 6 *M* hydrochloric acid by warming. Dilute to volume with 6 *M* hydrochloric acid in a 50-ml volumetric flask. Transfer an aliquot (5 ml) of the solution to a centrifuge tube containing 2 ml of 0.25% (w/v) iron(III) chloride solution and add ammonia until the copper–ammine complex is formed. Centrifuge at 4000 r.p.m., and wash the precipitate with water. Dissolve the precipitate in 1 ml of 8 *M* nitric acid and neutralize the resultant solution with ammonia. Add 2 ml of 0.5 *M* EDTA solution, and adjust the pH to 2–2.5 with 2.5 *M* acetic acid. Add 2 ml of aqueous 0.5% (w/v) 3,3′-diaminobenzidine solution, leave for 40 min, adjust to pH 6–7 with ammonia and transfer to a separatory funnel. Extract selenium into 5 ml of toluene, and use 5 μl of the organic phase for measurement of selenium. Use the following sequence: 0.6 V–11 A for 10 s (drying); 1.8 V–25 A for 7 s (ashing); 5 V–50 A for 10 s (atomization). Prepare a calibration curve by extracting selenium as the diaminobenzidine complex.

Direct method. Dissolve the sample as described above and use the resultant solution for the determination of selenium. Prepare solutions for calibration from

pure copper and selenium standard solutions.

TABLE III

RESULTS FOR SELENIUM IN CRUDE COPPER

Sample	*DAB–toluene method*	*Direct method*	*Spectrophotometric method*
1[a]	$0.026_7 \pm 0.003_6$	$0.064_3 \pm 0.012_4$	0.025
2[b]	$0.015_0 \pm 0.000_8$	$0.030_9 \pm 0.000_5$	0.018
3[c]	$0.025_0 \pm 0.004_1$	$0.029_4 \pm 0.002_1$	0.029

[a] 0.024% Fe, 0.034% Pb, 0.005% Zn, 0.221% Ni, 0.0034% Te.
[b] 0.005% Fe, 0.075% Pb, 0.001% Zn, 0.135% Ni, 0.006% Te.
[c] 0.012% Fe, 0.305% Pb, 0.003% Zn, 0.170% Ni, 0.014% Te.

Table III shows the results obtained for selenium in crude copper by the two methods. The direct method showed higher values for selenium, probably because of the interfering effects of other elements in the copper; for sample 3, all the values were in reasonable agreement. As is apparent, the method based on extraction is adequate for accurate determinations in complex samples.

The authors wish to thank the Hamamatsu TV Co. for providing the selenium hollow-cathode lamp.

REFERENCES

1 J. P. Matoušek, *Amer. Lab.*, 3 (16) (1971) 45.
2 R. B. Baird, S. Pourian and S. M. Gabrielian, *Anal. Chem.*, 44 (1972) 1887.
3 G. G. Welcher, O. H. Kriege and J. Y. Marks, *Anal. Chem.*, 46 (1974) 1227.
4 M. Inhat and R. J. Westerby, *Anal. Lett.*, 7 (1974) 257.
5 K. Ohta and M. Suzuki, *Talanta*, 1975, in press.
6 G. F. Kirkbright, *Analyst (London)*, 96 (1971) 609.
7 G. L. Everett, T. S. West and R. W. Williams, *Anal. Chim. Acta*, 70 (1974) 291.

Analytica Chimica Acta, 77 (1975) 293–297

SHORT COMMUNICATION

A simple concentration procedure for trace metals for x-ray fluorescence and atomic absorption spectrometry

GÜNTER KNAPP
Institute for General Chemistry, Micro- and Radiochemistry, Institute of Technology, Graz (Austria)
BERNHARD SCHREIBER and ROLAND W. FREI
Analytical Research and Development, Pharmaceutical Department, Sandoz Limited, Basle (Switzerland)
(Received 11th December 1974)

Organic complexing reagents have been used successfully for concentration of trace elements and elimination of matrix problems; many concentration and separation problems can be solved by the proper choice of complexing ligands, pH and possibly ligand-exchange processes. Usually the complexes in the aqueous phase are isolated by extraction[1–3] or coprecipitation[4–8]. With the first approach, relatively large volumes of extract have to be handled and time-consuming evaporations are needed. The second approach requires the use of a carrier, which may introduce new matrix problems.

In this study, other concentration procedures which would not have these drawbacks were investigated. Ion-exchange procedures have been reported by Riley and Taylor[9] who used Chelex resin columns for preconcentrations from water before a.a.s. Reverse-phase techniques with organic solvents adsorbed on the surface of a small particle support seemed an interesting possibility; such processes correspond to repeated extraction and the complexing reagent can be added to either the aqueous or the organic phase. Support materials such as cellulose acetate[10], silica gel[11,12], kieselguhr[13,14], Teflon[15], polytrifluoromonochloroethylene[16], polyurethane foams[17] and silylated silica gels[18] have been used. If the concentrating procedure is to be used in conjunction with x-ray fluorescence, neutron activation or chromatographic techniques, it is desirable to choose chelating agents which react with many metals under the same conditions. In the present work sodium diethyldithiocarbamate (NaDDTC) was chosen. The support material was Chromosorb T (40–60 mesh) or Chromosorb W-DMCS (80–100 mesh).

Study of parameters

Carriers. Of the two carrier materials tested, the capacity of Chromosorb T was found insufficient, since only μg quantities of chelates were adsorbed. With Chromosorb W-DMCS columns mg quantities could be handled. The mechanical stability of columns filled with Chromosorb W was also vastly superior, so that the permeability remained good even after prolonged use.

Extraction agents. In liquid–liquid extractions, one prefers high distribution

coefficients in order to obtain good separations with as few extraction steps as possible. Reverse-phase techniques, however, simulate a multistep extraction and quantitative yields can therefore be expected even with relatively low distribution coefficients. The important characteristics of extraction agents in reverse-phase procedures include low water solubility of the organic phase and strong adsorptive forces between the organic phase and the surface of the carrier. Since the diffusion of the complexes into the organic layer is relatively rapid, high flow rates are possible[15].

The following solvents were studied with regard to their capacity and speed of separation: benzene, chlorobenzene, 1,2-dichlorobenzene, chloroform, carbon tetrachloride, tetrachloroethylene and trichloroethylene. Tetrachloroethylene and 1,2-dichlorobenzene gave the best results. It was shown that the dithiocarbamates can be directly adsorbed on activated charcoal[19] or a silanized surface[18], the capacity of such surfaces being higher than that of liquid extractants. Adsorption of the dithiocarbamates on silanized surfaces of kieselguhr was therefore chosen for further studies.

pH ranges. Recovery factors were studied for different concentrations of Zn, Cu, Ni, Pb, Hg, Co, Cd and Fe in sample solutions as a function of pH in the range 4–7. An acetate buffer was used for pH 4 and pH 5, a citrate buffer for pH 6 and a phosphate buffer for pH 7.

TABLE I

RECOVERY OF Zn, Cu, Ni, Pb, Hg, Co, Cd, Fe AT DIFFERENT pH VALUES

Element	*Recovery (%)*			
	pH 4	*pH 5*	*pH 6*	*pH 7*
Zn, Cu, Ni, Pb, Hg, Co	98–100	98–100	98–100	98–100
Cd	98–100	98–100	75–100	65–100
Fe	98–100	98–100	98–100	32–36

The results are summarized in Table I. Complete adsorption was observed between pH 4 and 7 for Zn, Cu, Ni, Pb, Hg and Co. Between pH 4 and 5 cadmium was adsorbed quantitatively, but at higher pH values the recovery decreased owing to foreign ion effects. The loss of iron at pH 7 must be attributed to hydrolysis.

Transfer of adsorbed metals to a suitable form for measurement. The dithiocarbamates adsorbed on the column can be eluted easily with suitable organic solvents, after the residual water on the column has been removed.

For atomic absorption spectrometry, methyl isobutylketone (MIBK) was added dropwise until the dead volume of the column (>1 ml) was filled. With addition of another 1 ml of MIBK, complete elution of the complexes was possible; this volume is suitable for evaluation by flameless a.a.s. in a graphite furnace. For aspiration into a flame, dilution to a suitable volume is needed.

For evaluation by x-ray fluorescence, the elements must be present in a thin

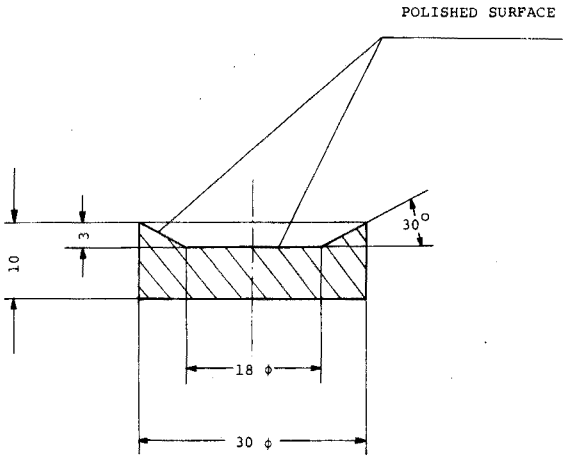

Fig. 1. Teflon cup used for evaporation of extracts. Dimensions in mm.

layer with homogeneous distribution. Several suggestions have been made to achieve this[1,2]. Stepwise application of the eluate on a filter paper is time-consuming and does not necessarily guarantee reproducible distribution. Direct evaporation of the eluate in the sample container also results in irregular deposits. The following procedure yielded reproducible samples: the carbamates were eluted with 2 ml of chloroform into a special Teflon container (see Fig. 1) with polished surfaces to avoid wetting. A disk of filter paper was placed on the bottom of the container before elution. The chloroform was then evaporated at room temperature within about 20 min, the residue remaining on the paper. The paper disk was glued to the plane surface of a Teflon disk for measurement.

Experimental

Reagents. Prepare the acetate buffer by adjusting 1 *M* sodium acetate solution to pH 5 with glacial acetic acid. Prepare an aqueous 2% (w/v) sodium diethyldithiocarbamate solution (Merck analytical grade) daily; filter before use. Chromosorb W-DMCS, 80–100 mesh (Merck) is used.

Instrumentation. A Perkin-Elmer Model 403 atomic absorption spectrophotometer with a graphite HGA 70 oven was used. For x-ray fluorescence work, a Siemens SRS 1 spectrometer equipped with a tabulator control for 36 lines, automatic sample changer for 10 samples, and chromium and molybdenum x-ray tubes, was used; parameters were adjusted according to the manufacturer's literature, and the counting time was 200 s per line.

Preparation of columns. Close the glass columns (8-mm diameter, 30-mm long) with a glass wool plug, fill with support to a height of 20 mm, and stopper at the upper end with glass wool. Pass ethanol through the column to displace air, and then displace all the ethanol with water; the column is then ready to use.

Concentrating step. Samples and ashing residues in aqueous solutions are used. Add buffer solution in a ratio of 1:5 and Na-DDTC solution in a ratio of 1:10. Adjust strongly acidic or basic solutions to pH 5 with sodium hydroxide or

acetic acid. Apply this solution to the column. For volumes above 100 ml, it is advisable to use a peristaltic pump at a maximum flow rate of 0.2 ml s^{-1}. Wash the column with 1 ml of distilled water and dry by air suction for 5 min. Elute the trace metals for a.a.s. or x.r.f. evaluation as described above.

Results and discussion

The method studied permits a rapid and simple concentration of metal carbamates on a silanized kieselguhr surface. Chromosorb W-DMCS used as described above proved most suitable. The advantages of this technique compared with conventional extraction and coprecipitation techniques are smaller elution volumes and the absence of carriers. In aqueous samples, a concentration of two orders of magnitude can be achieved rapidly; 100 ml of water can be pumped through the column in less than 10 min and the elution and drying step takes another 10–20 min. The method is suitable for a.a.s. or x.r.f. For the latter, a simple approach is described which permits transfer of the sample to a filter disk for evaluation. The measurement parameters and detection limits are given in Table II. The detection limits were determined by concentrating defined amounts of trace metals, so that errors introduced during the concentration were included. The columns can be re-used an indefinite number of times if they are carefully washed with ethanol after usage and then rinsed with distilled water.

TABLE II

DETECTION LIMITS AFTER CONCENTRATION FROM 100 ml OF WATER AND MEASUREMENT BY X-RAY FLUORESCENCE

Element	*Line*	*c.p.s. (blank)*	*c.p.s./μg (net)*	*Detection limit (μg)*
Zn	Kα	130	16.9	0.7
Cu	Kα	190	15.6	0.8
Ni	Kα	105	18.1	0.7
Pb	Lα	157	2.2	1.0
Hg	Lα	120	3.3	1.7
Co	Kα	80	20.6	0.4
Cd	Lα	2.3	0.5	0.08
Fe	Kα	140	21.9	0.6

The same concentrating procedure is also promising in connection with high-pressure liquid chromatography. In order to obtain a better chromophore for detection, dibenzyldithiocarbamates are used, the wavelength of maximal absorption being about 275 nm, with molar absorptivities of 40–50,000. Experiments in his area are under way.

Mr. H. D. Seltner is thanked for carrying out the x-ray fluorescence measurements.

REFERENCES

1 R. Püschel, *Mikrochim. Acta*, (1965) 770.
2 F. J. Marcie, *Environ. Sci. Technol.*, 1 (1967) 164.
3 A. W. Morris, *Anal. Chim. Acta*, 42 (1968) 397.
4 C. L. Luke, *Anal. Chim. Acta*, 41 (1968) 237.
5 R. Püschel, *Talanta*, 16 (1969) 351.
6 H. Hellmann and A. Griffatong, *Z. Anal. Chem.*, 257 (1971) 343.
7 H. Watanabe, S. Berman and D. S. Russell, *Talanta*, 19 (1972) 1363.
8 K. Hirokawa, *Z. Anal. Chem.*, 260 (1972) 4.
9 J. P. Riley and D. Taylor, *Anal. Chim. Acta*, 40 (1968) 479.
10 T. B. Pierce and P. F. Peck, *Analyst (London)*, 86 (1961) 580.
11 T. B. Pierce and P. F. Peck, *J. Chromatogr.*, 6 (1961) 248.
12 T. B. Pierce and P. F. Peck, *Anal. Chim. Acta*, 26 (1962) 557.
13 S. Siekierski and I. Fidelis, *J. Chromatogr.*, 4 (1960) 60.
14 K. Lorber, K. Müller and H. Spitzy, *Mikrochim. Acta*, in press.
15 J. S. Fritz and C. E. Hedrick, *Anal. Chem.*, 34 (1962) 1411.
16 R. Denig, N. Trautmann and G. Herrmann, *Z. Anal. Chem.*, 270 (1974) 6.
17 T. Braun and A. B. Farag, *Anal. Chim. Acta*, 71 (1974) 133.
18 D. E. Leyden, G. H. Luttrell and T. A. Patterson, *Anal. Lett.*, 8 (1975) 51.
19 E. Jackwerth, J. Lomar and G. Wittler, *Z. Anal. Chem.*, 270 (1974) 6.

Analytica Chimica Acta, 77 (1975) 298–304

SHORT COMMUNICATION

Infrarotspektroskopische Analyse von Thiuramdisulfidfungiziden Teil II. Gemischte Präparate von Thiuramdisulfid und Dithiocarbamaten*

WANDA SZTARK

Institut für Anorganische Chemie und Technologie der Technischen Hochschule Krakau, Kraków (Polen)

(Eingegangen den 4. September 1974)

Die Gruppe der Dithiocarbamat- und Thiuramdisulfid-Fungiziden (D-Fungizide und T-Fungizide) gehören zu den stärken angewandten Pflanzenschutzmitteln. Zur Ermittlung der D- und T-Rückstanden wurden zahlreichen Methoden veröffentlicht[1–26]. Viele von ihnen beruhen auf der Reaktion der Wirkstoffe mit Säuren wobei der Schwefelkohlenstoff abgespalten und in die Form von Kupferdithiocarbamat kolorimetrisch[1–7] oder direkt gaschromatographisch bestimmt wird[15–17]. Zur qualitativen Unterscheidung der D- und T-Fungiziden lässt sich sowohl die Papier[11,12] und Dünnschichtchromatographie[13,14] als auch die Atomspektroskopie[18] anwenden. Dagegen sind verhältnismässig wenig Methoden bekannt, die eine Differenzierung chemisch ähnlicher Verbindungen oder den Nachweis von Pflanzenschutzwirkstoffen in Gegenwart anderer gestatten. Zu den charakteristichsten Merkmalen einer Substanz zählt das Infrarotspektrum. IR-Spektroskopie als eine zerstörungsfreie Analysenmethode hat die grosse Bedeutung in der Rückstandanalyse. Es gibt Arbeiten, die sich mit der Identifizierung der Pflanzenschutzmitteln unter anderen Dithiocarbamaten befassen[19,20] und die IR-Banden für die quantitativen Analyse ausnützen[21–25].

Die vorliegende Arbeit ist eine Fortführung der Anwendung der IR-Spektrophotometrie zur Identifizierung und der Bestimmung der D- und T-Fungiziden[23–26].

Experimentelles

Chemikalien und Geräte. Thiuram (Tetramethylthiuramdisulfid, Thiram Vancide TM-95, Abk. TMTD) von der Firma Vanderbilt N.Y. Zineb (Zinkäthylenbisdithiocarbamat, Vancide Zineb-85) von der Firma Vanderbilt N.Y. Ziram (Zinkdimethyldithiocarbamat) von Schuchardt. Tuzet (Thiuram + Ziram + Tetramethyldithiocarbaminsäures Methylarsin + Füllstoffe) von der Firma Bayer- Austria. Thiodyl-Kartoffelbeize (Thiuram + Zineb + Schwefel + Füllstoffe) von der Firma Schering-Kwizda, Austria. Aceton p.a. Kaliumbromid zur Spektroskopie von Merck.

* Die Arbeit wurde im Institut für Analytische Chemie und Mikrochemie der Technischen Hochschule Wien ausgeführt.

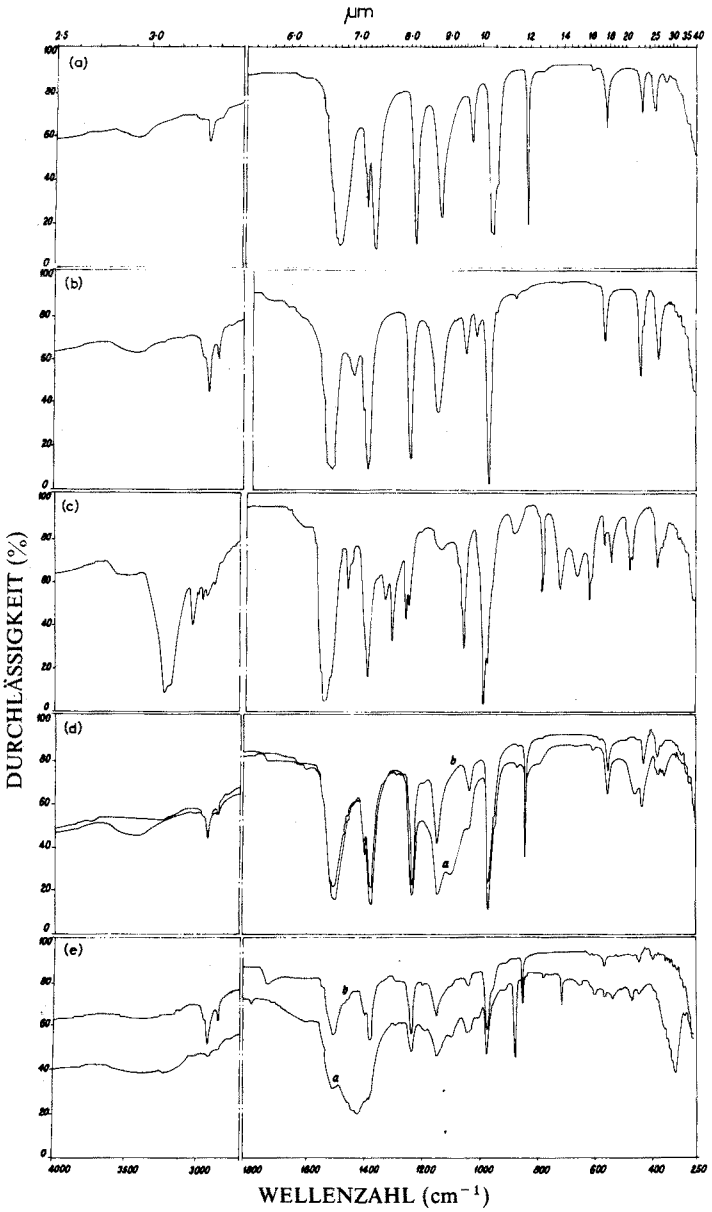

Abb. 1 (a) IR-Spektrum von Thiuramdisulfid (in KBr); Messbanden: 975 und 850 cm^{-1}. (b) IR-Spektrum von Ziram (in KBr); Messbande: 975 cm^{-1}. (c) IR-Spektrum von Zineb (in KBr); Messbande: 980 cm^{-1}. (d) IR-Spektren von "Tuzet"; (a) Handelspräparat, (b) Acetonextrakt. (e) IR-Spektren von "Thiodyl"; (1) Handelspräparat, (a) Acetonextrakt.

Die Übersichtsspektren der Wirkstoffe, Handelsprodukte und Acetonextrakte wurden mit dem Perkin–Elmer-Gitterspektrophotometer 457 (4000–250 cm^{-1}) aufgenommen (Abb. 1).

Probenvorbereitung. Zur Probenpräparation wurde die 13-mm KBr-Presslingsmethode herangezogen und die Acetonextraktion der Handelsprodukten nach der obengenannten Weise durchgeführt[26]. Die Auswertung der Intensitäten der analytischen Banden erfolgt nach dem Grundlinienverfahren.

Für die Überprüfung des Reinheitsgrades der Wirkstoffe wurden die Kohlenstoff- und Schwefel-Bestimmungen mit Hilfe der Wösthoff-Apparaten durchgeführt[27] (Tab. I). Im Rahmen der Reinheitsuntersuchungen der Wirkstoffe wurde die semiquantitative Emissionsspektralanalyse mit dem spektrographischen Analysator Modell ARL 26000-1 durchgeführt (Tab. II).

TABELLE I

ELEMENTARANALYSE DER WIRKSTOFFE

Name des Fungizides	% *C*			% *S*		
	Ber.	*Gef.*	*V (%)*	*Ber.*	*Gef.*	*V (%)*
Thiuram	29,97	29,21	1,75	53,34	53,38	0,50
Ziram	23,57	23,12	0,92	41,94	41,00	2,10
Zineb	17,42	16,43	1,99	46,51	44,36	1,44

TABELLE II

EMISSIONSSPEKTRALANALYSE DER WIRKSTOFFE

Elemente	*Probe*				
	Thiuram	*Ziram*	*Zineb*	*Thiodyl*	*Tuzet*
Zn	—	[a]	[a]	[a]	[a]
Na	—	[a]	[a]	[a]	[a]
As	—	—	—	0,200	[a]
Mn	0,01	0,05	0,08	0,04	0,002
Mg	—	0,06	0,06	0,60	0,06
Fe	—	0,001	0,006	0,06	0,02
Al	—	—	—	0,10	0,03
Cu	—	—	0,001	0,003	0,007
Ca	—	—	—	0,08	—
Mo	—	—	—	—	—
Pb	—	—	—	0,02	0,02

[a] Sehr viel.

Der Vergleich der I.R.-Spektren von Handelsprodukte und ihrer Acetonextrakte wurden in den Abb. 1d und 1e verglichen. Die Lage und die relativen Intensitäten der i.r.-Banden wurden auf einem Schema ausgearbeitet, das Auskunft über die Möglichkeit der Identifizierung der Wirkstoffe in Acetonextrakten der Handelsprodukte gibt (Abb. 2). Für den analytischen Zweck wurden zwei Messbanden (850 cm^{-1} und 975 cm^{-1}) für Tuzet und Thiodyl ausgewählt.

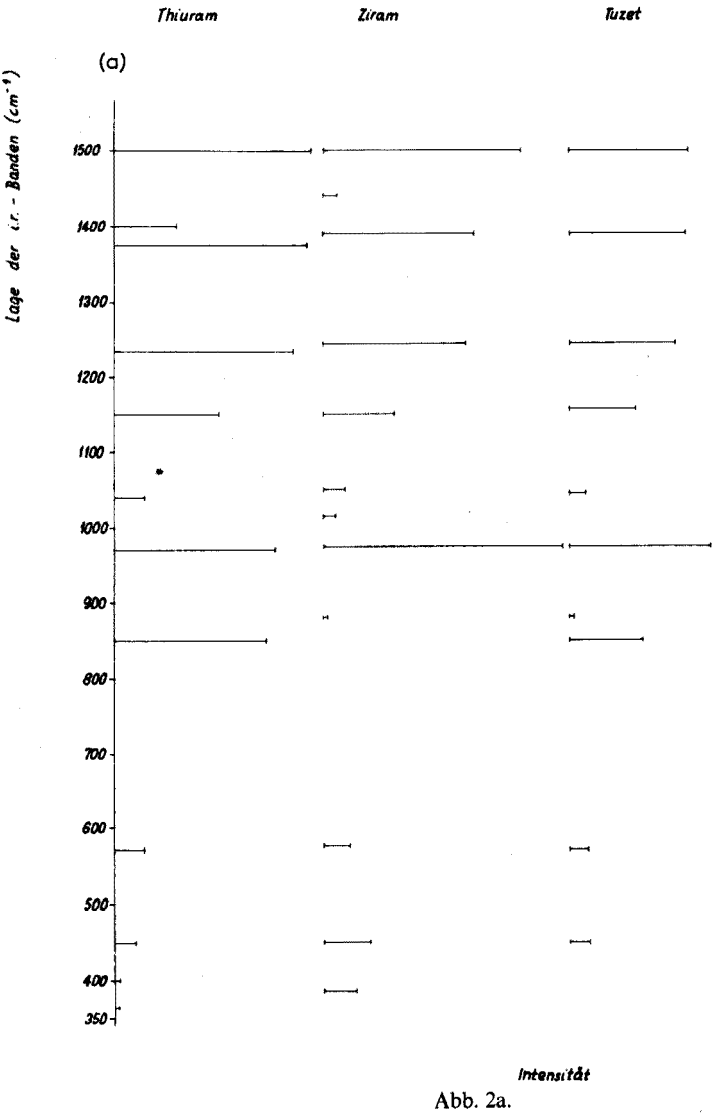

Abb. 2a.

Thiuramdisulfid zeigt bei der 850 cm^{-1} eine scharfe Absorptionsbande, ungestört von den Banden der Mischungspartner. Diesen Fall kann man als Absorptionsspektralanalyse am "Quasi-einstoffsystem" behandeln. Die Intensität der Bande bei 975 cm^{-1} wurde wie die Summe der Extinktionen der beiden Komponenten betrachtet. Weil für beide Komponente das Beerschen Gesetz erfüllt ist, kann man die Konzentration nach ein lineares Gleichungssystem rechnen (Tab. III, IV).

Für die Beurteilung der Richtigkeit der Ergebnisse wurden 10 Mischungen von Thiuram und Ziram nach dem obengenannten Verfahren analysiert und die gefundene Ergebnisse mit den bei der Analyse der einzelnen Wirkstoffen (Standardsubstanzen) erhaltenen Werten, verglichen (Tab. V). Die Unterschiede zwischen

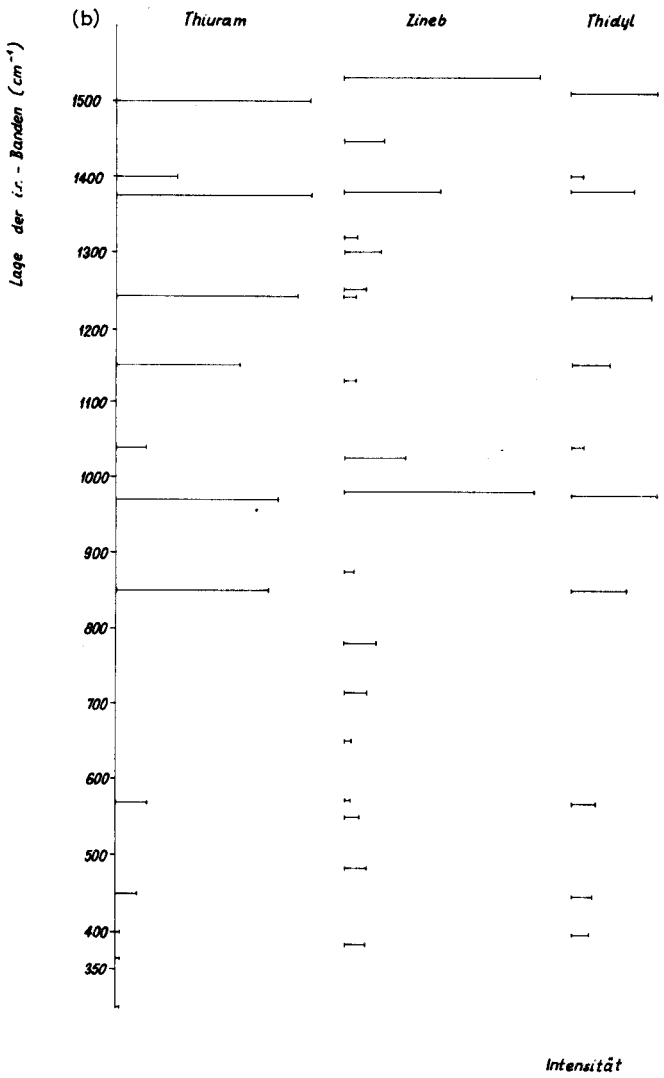

Abb. 2. Lage und Intensität der charakteristischen IR-Banden der Wirkstoffen und des Acetonextraktes von (a) Tuzet; (b) Thiodyl.

beiden Ergebnissen ($E_{ber.}$ und $E_{gef.}$) betragen im Fall der Analyse bei 850 cm^{-1} nur 2,3%, bei 975 cm^{-1} 4,6%.

Diskussion

Die IR-Spektralanalyse der gemischten Präparate des Thiurams und des acetonlösliches Zirams ermöglicht die quantitative Bestimmungen der beiden obengenannten Komponenten nebeneinander. Für dem Fall der Thiodylsanalyse kann man nur Thiuram quantitativ ermittelt. Schwer acetonlösliches Zineb bleibt wahrscheinlich im die Rückstand und es wurde lediglich (*ca.* 5%) die Intensität der Absorptionsbande an 975 cm^{-1} ermittelt.

TABELLE III

DIE ANGABEN DER REGRESSIVEN GERADEN ($y=a+bx$) DER WIRKSTOFFEN

(Substanzbedarf: 1,0–0,2 mg)

Wirkstoff	*Lage der Messbande* (cm^{-1})	*Koeffizient a*	*Koeffizient b*	*Korrelations-koeffizient r*
Thiuram	975	0,0333	0,8232	0,9796
	850	0,0276	0,7620	0,9958
Ziram	975	0,0265	1,3372	0,9878
Zineb	975	−0,0015	0,7311	0,9990

TABELLE IV

DIE ERGEBNISSE DER BESTIMMUNGEN VON WIRKSTOFFEN IN DEN UNTERSUCHTEN HANDELSPRODUKTEN AUF 1 mg EINWAAGE BEZOGEN

Name	*Mittlerer Wert der Extinktion*[a]		*Gehalt des Thiurams (mg)*	*Gehalt des Zirams (mg)*
	E_{975}	E_{850}		
Tuzet	0,755	0,355	0,442±0,015	0,264±0,006
	$s=0{,}0071$	$s=0{,}0055$		
	$v\%=0{,}94$	$v\%=1{,}54$		
Thiodyl	0,187	0,134	0,167±0,014	—
	$s=0{,}0026$	$s=0{,}0002$		
	$v\%=4{,}38$	$v\%=3{,}80$		

[a] s Standardabweichung des aritmetischen Mittels; $v\%$ Variationskoeffizient. Zuverlässigkeitsintervall des Mittelwertes wurde mit der Wahrscheinlichkeit $P=0{,}95/1-\mu=0{,}05$ (nach der Gleichung $x=\bar{x}-t(Pn)s$ berechnet. Anzahl der Bestimmungen $n=10$.

Die bearbeitete Methode eignet sich gut zur Bestimmung von Thiuramdisulfid und acetonlöslichen Dithiocarbamaten im p.p.m. Bereich, nach deren Extrahierten aus ihren Handelsprodukten.

Herrn o.Prof.Dipl.Ing.Dr.techn. Hanns Malissa möchte ich für die Ermöglichung der Ausführung meiner Forschungen und das grosse Interesse am Fortgang

TABELLE V

ANALYSE DER MISCHUNGEN VON THIURAM UND ZIRAM UND DER VERGLEICH MIT DEN WERTEN, ERHALTENEN BEI DER ANALYSE VON REINEN WIRKSTOFFEN

Anzahl der Bestimmungen	*Extinktionswerte*				*Differenz*	
	Bande 975 cm^{-1}		*Bande 850 cm^{-1}*		$\bar{D}$ (975 cm^{-1})	$\bar{D}$ (850 cm^{-1})
	$\bar{E}_{ber.}$	$\bar{E}_{gef.}$	$\bar{E}_{ber.}$	$\bar{E}_{gef.}$		
10	1,123	1,071	0,433	0,423	0,052	0,010

meiner Arbeit meinen aufrichtigen Dank ausdrücken. Herrn Dipl.Ing.Dr.techn. Robert Kellner bin ich für die praktische Unterstützung sehr verpflichtet. Den Firmen Vanderbilt N.Y., Bayer-Austria und Schering-Kwizda, Austria danke ich herzlich für die mir freundlicherweise übersandten Proben von Fungiziden.

LITERATUR

1 D. G. Clarke, H. Baum, E. L. Stanley und W. F. Hester, *Anal. Chem.*, 23 (1951) 1842.
2 H. L. Pease, *J. Ass. Offic. Agr. Chem.*, 40 (1957) 1113.
3 T. E. Cullen, *Anal. Chem.*, 36 (1964) 221.
4 R. F. Heuermann, *J. Ass. Offic. Agr. Chem.*, 40 (1957) 264.
5 G. E. Keppel, *J. Ass. Offic. Agr. Chem.*, 52 (1969) 162; 54 (1971) 528.
6 G. Belluci und C. Leoni, *Ind. Conserve*, 45 (1970) 220.
7 J. S. Padington, *J. Ass. Pub. Anal.*, 6 (1968) 25.
8 M. C. Kersen und P. Riepma, *Tijdschr. Plantenziekten*, 65 (1959) 27.
9 R. J. Romagnoli, J. D. Chazin und J. Messick, *Tappi*, 52 (1969) 51.
10 J. R. Rangaswamy, P. Poornina und S. K. Majumder, *J. Ass. Offic. Chem.*, 53 (1970) 1043; 54 (1971) 120.
11 W. P. McKinley und S. A. Magarvéy, *J. Ass. Offic. Agr. Chem.*, 43 (1960) 717.
12 J. W. H. Zijp, *Rec. Trav. Chim. Pays-Bas*, 75 (1956) 1083.
13 L. Fishbein und J. Fawkes, *J. Chromatogr.*, 19 (1965) 364.
14 K. Ballschmiter, *Z. Anal. Chem.*, 254 (1971) 348.
15 W. Zieliński Jr. und L. Fishbein, *J. Chromatogr.*, 23 (1966) 302.
16 H. A. McLeod und K. A. McCully, *J. Ass. Offic. Agr. Chem.*, 52 (1969) 1226.
17 C. Bighi, *J. Chromatogr.*, 14 (1964) 348.
18 B. J. Gudzinowicz und V. J. Luciano, *J. Ass. Offic. Agr. Chem.*, 49 (1966) 1.
19 W. Fischer und U. Uhlich, *Z. Anal. Chem.*, 172 (1960) 175.
20 W. W. Morris Jr. und E. O. Haenni, *J. Ass. Offic. Agr. Chem.*, 46 (1963) 964.
21 H. Susi und H. E. Rector, *Anal. Chem.*, 30 (1958) 1933.
22 D. Firestone und P. J. Vollmer, *J. Ass. Offic. Agr. Chem.*, 39 (1956) 866.
23 W. Sztark, H. Malissa und R. Kellner, *Anal. Chim. Acta*, 63 (1973) 285.
24 H. Malissa und R. Kellner, *Anal. Chim. Acta*, 63 (1973) 263.
25 W. Sztark, *Chem. Anal. (Warsaw)*, im Druck.
26 W. Sztark, *Anal. Chim. Acta*, 75 (1975) 315.
27 H. Malissa, *Mikrochim. Acta*, (1957) 553; (1960) 127.

Analytica Chimica Acta, 77 (1975) 305–308

SHORT COMMUNICATION

The determination of traces of chromium(VI) by solid-state reflectance

D. E. RYAN, J. HOLZBECHER and M. GRANDA

Trace Analysis Research Centre, Chemistry Department, Dalhousie University, Halifax, Nova Scotia, B3H 4J1 (Canada)

(Received 10th January 1975)

The toxicity of chromium(VI) has been recognised for years[1]. Chromium is used in many industrial processes and chromate is often present in cooling solutions to prevent corrosion. It can, therefore, enter potable water supplies through the discharge of industrial waters. Since chromium(VI) has carcinogenic properties, monitoring of its concentration in potable waters is of importance. Its level in U.S. drinking waters has been reported[2] to vary between 3 and 40 $\mu g\ l^{-1}$. Chromium(VI) effects as an environmental pollutant in natural waters, at sub-$\mu g\ ml^{-1}$ concentration levels, are also beginning to receive attention[3]. As a result, there is a need for analytical methods suitable for chromium(VI) determination at such low concentrations.

To determine traces of metal ions by solid-state reflectance, the coprecipitant ion must either form a light-absorbing species with the coprecipitating agent, or be colored itself and coprecipitated by a suitable carrier. In a recent communication[4], a method has been described for the determination of nickel by measurement of reflectance in the solid state after coprecipitation with a large excess of the organic chelating agent α-benzildioxime. The present method takes advantage of the coloration of lead sulphate by coprecipitated chromate.

Experimental

Apparatus, reagents, solutions. All reflectance measurements were made with a Zeiss Chromatogram Spectrophotometer. The sample cell was an aluminium sheet painted white with drilled holes (diam. 5 mm) which was covered with a thin glass plate. It was packed with a sample powder which was held in place by masking tape.

A 500 $\mu g\ ml^{-1}$ chromium(VI) stock solution was prepared with potassium dichromate (Shawinigan, Reagent grade) as a primary standard. The lead nitrate (Fisher, Certified A.C.S.) and sodium sulfate (Baker, Reagent grade) solutions were both 0.2 *M*.

Procedure: To 100 ml of a solution containing 0.1–10.0 μg of chromium(VI) add 1 ml of 0.2 *M* lead nitrate solution. Check the pH and, if necessary, adjust to *ca.* 5 with dilute nitric acid or sodium hydroxide. Precipitate by dropwise addition of 5 ml of 0.2 *M* sodium sulphate solution with rapid stirring. Allow to stand for 15 min; filter the precipitate through a filter crucible, wash with distilled water and dry *in*

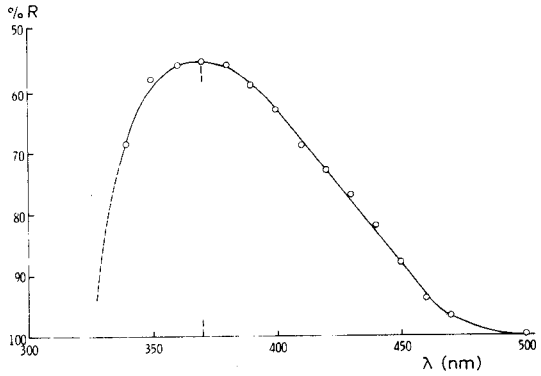

Fig. 1. Reflectance spectrum for 10 μg of chromium(VI) coprecipitated with 43 mg of lead sulfate; the curve is extrapolated below 340 nm.

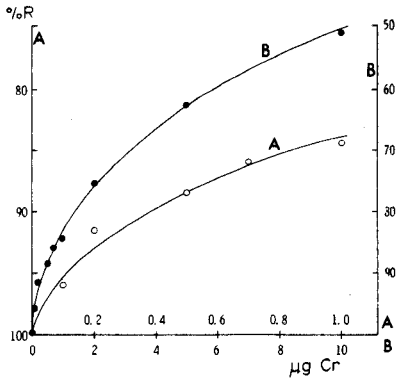

Fig. 2. Calibration curves for chromium(VI). (A) 0.1–1.0 μg; (B) 0.1–10.0 μg.

vacuo for 1 h (if < 100 μg of silver(I) are present, drying in the oven at 110°C is also possible). Pack the cell and measure the reflectance at a wavelength of 370 nm. Determine the amount of chromium(VI) from a calibration curve run concurrently.

Results and discussion

Figure 1 shows the reflectance spectrum of chromate coprecipitated with the lead sulfate. The absorption maximum of 370 nm was used for all the measurements.

Typical calibration curves are shown in Fig. 2; the reflectance (%R) of the blank was adjusted to read 100%. The relative standard deviation of eight determinations of 1 μg Cr/100 ml was *ca.* 10%; for five determinations of 10 μg Cr/100 ml the relative standard deviation was *ca.* 2%.

Factors affecting the method. The following reaction parameters were investigated for 1 μg of chromium(VI).

The method is independent of pH from 3.0 to 5.5. Upon adjustment to pH ca. 6, the solution turns turbid, owing to the precipitation of lead hydroxide. With decreasing pH, however, the amount of lead sulfate precipitated decreases so that below pH 3 there is hardly enough precipitate to fill a hole in the measuring cell. Therefore, a pH in the vicinity of 5 was chosen for the standard procedure.

For practical reasons (particle size, volume of precipitate, signal intensity of the sample *versus* the respective blank), sulfate is the precipitant added in excess. When a 10-fold excess of sulfate was added to the solution containing 10 μg of chromium(VI) and lead ions, the reflectance of the precipitate was 59%; for the same amount of sulfate initially present in solution with chromate, the addition of lead ions gave the same amount of precipitate but the reflectance was 70%. When lead(II) was present in a 10-fold excess, the reflectance was 76% with sulfate as the precipitant, but was 66% with lead(II) as the precipitating agent. It is evident that poorer sensitivity is obtained at a high relative supersaturation of lead sulfate. The signal is not influenced by an excess of sulfate from 5:1 to 15:1 but not enough precipitate is obtained for measurement with equivalent concentrations of sulfate and lead; a 5-fold excess of sulfate was used throughout the work.

The method is essentially independent of ageing of the precipitate up to at least 1 h. Similar results were also obtained for chromium coprecipitated from sample volumes of 50, 100, 250 and 500 ml.

No advantage results from precipitation at elevated temperatures and precipitation at room temperature is, therefore, recommended.

Interferences. At least 1,000-fold (weight) amounts of the following ions are without interference: Ba(II), Cd(II), Ca(II), Co(II), Cu(II), Mg(II), Mn(II), Hg(II), Ni(II), K(I), Ag(I), Sr(II), Zn(II), acetate, bromide, chloride, iodide, nitrate, perchlorate, phosphate, tartrate and thiocyanate. A 100-fold amount of Al(III), Cr(III) or EDTA, and a 10-fold amount of Fe(III), citrate or fluoride is also without interference. Iron(II) interferes strongly, presumably because of its oxidation–reduction reaction with chromate, and must be absent.

The large effect of some substances on the crystallization of lead sulfate has been reported by Hähnert and Kleber[5]. Aluminium(III) and iron(III) interference is probably due to positively charged hydroxy complexes of these metal ions which are coprecipitated with lead sulfate in slightly acidic medium; the lead sulfate particles have a negative charge because the excess of sulfate present is primarily adsorbed.

Applications

The applicability of the method to the determination of chromium in various complex matrices was studied.

Alloys. Attempts to determine chromium in a steel and a zinc-base alloy gave unsatisfactory results. Such results can be attributed to the coprecipitation of hydrolyzable higher valency metal ions as discussed above.

Synthetic blood. A 1-ml sample of synthetic blood (equal to 10 ml of blood) containing 19,900 μg Na, 16,900 μg K, 620 μg Ca, 410 μg Mg, 4,700 μg Fe(III), 130 μg Zn and 10 μg Cu was diluted to *ca.* 30 ml and iron(III) was separated by precipitation with ammonia. The solution was then diluted to 100 ml and the standard precipitation procedure was performed. For additions of 2.0 and 4.0 μg of chromium, 1.9 and 4.1 μg were found, respectively. Thus the method makes possible the determination of tenths of a p.p.m. of chromium in blood.

Leaves. Chromium was determined in a dry leaf sample after wet ashing. The 0.5-g sample was boiled with 10 ml of (1 + 1) nitric acid and three drops of 18 *M* sulfuric acid, evaporated to dryness, and baked for 5 min. After cooling to room temperature, 1 ml of 16 *M* nitric acid was added and the solution was evaporated and baked once again; this was repeated once more and then the last organic residue was destroyed by twice repeated evaporation with 2 ml of 16 *M* nitric acid and 1 ml of 70% perchloric acid. The white residue was then dissolved in about 20 ml of (1 + 10) nitric acid, the small amount of material undissolved was filtered off, the filtrate was diluted to *ca.* 50 ml and the chromium was oxidized to the hexavalent state with *ca.* 1 ml of saturated potassium persulfate in the presence of 0.3 ml of 0.1 *M* silver nitrate. The solution was boiled for 10 min, and the permanganate formed (pink coloration) was destroyed by addition of 1 ml of (1 + 1) hydrochloric acid and boiling for 5 min. The precipitate of silver chloride formed was filtered off and the filtrate made up to 100 ml. Aliquots of 10 ml were taken, and after dilution to 100 ml, the regular precipitation procedure was performed. The method of standard additions was applied; for additions of 1.0 and 3.0 μg of chromium, 0.7 and 3.0 μg

were found, respectively.

Thus the method is applicable to the analysis of chromium in organic matrices after digestion.

Tap water. The method should have particular merit in the analysis of very small amounts of chromate in large sample volumes where the full advantage of preconcentration by coprecipitation can be taken, *e.g.*, water pollution analysis. The procedure was, therefore, applied to the determination of chromium(VI) in tap water. After filtration, 100-ml aliquots of tap water were analyzed by the method of standard addition. The precipitates, however, exhibited a brownish tint because of the coprecipitation of impurities from tap water, resulting in a serious interference. Calcium oxalate precipitated from tap water was found to collect interfering impurities and at the same time was shown not to collect any significant amounts of chromium(VI). It was precipitated as described previously[6–8], so as to obtain the same weight of the precipitate as for lead sulfate. By measuring its reflectance, the results obtained for chromium were corrected for the background absorption, after taking into the account the different densities of calcium oxalate monohydrate and lead sulfate (volume of the precipitate rather than its weight is important in such corrections since it determines the concentration of chromium(VI) in the precipitate). For additions of 1.0 μg of chromium(VI), 1.1 μg was found; the tap water was found to contain 3 $\mu g\ l^{-1}$ which is in good agreement with the mean value (3.4 $\mu g\ l^{-1}$) for drinking waters in the United States.

Cooling solution. A calcium chloride cooling solution containing a relatively high amount of chromium(VI) was analyzed as an example of a practical sample known to contain some chromium, even though full advantage of the sensitivity of the method could not be taken. The cooling solution was filtered and diluted 500 times; 2-ml aliquots were taken and diluted to 100 ml, and the regular precipitation procedure was applied with the method of standard addition. For addition of 1.50 μg of chromium(VI), 1.45 μg was recovered and the cooling solution was found to contain 413 ± 13 p.p.m. of chromium(VI).

The results of the practical samples analysis show that the method should find many applications, especially when large sample volumes are available.

This work was supported by a grant from the National Research Council of Canada.

REFERENCES

1 M. B. Jacobs, *The Analytical Toxicology of Industrial Inorganic Poisons*, Interscience, New York, 1967, p. 396.
2 *Standard Methods for the Examination of Water and Wastewater*, American Public Health Association, Washington, D.C., 13th edn., 1971, p. 155.
3 J. F. Pankow and G. E. Janauer, *Anal. Chim. Acta*, 69 (1974) 97.
4 D. E. Ryan and J. Holzbecher, *Can. J. Chem.*, 53 (1975) 311.
5 M. Hähnert and W. Kleber, *Kolloid-Z. Z. Polym.*, 162 (1959) 36.
6 D. E. Ryan, R. J. Prime, J. Holzbecher and R. E. Young, *Anal. Lett.*, 6 (1973) 721.
7 D. E. Ryan, H. Rollier and J. Holzbecher, *Can. J. Chem.*, 52 (1974) 1942.
8 D. E. Ryan, J. Holzbecher and H. Rollier, *Anal. Chim. Acta*, 73 (1974) 49.

Analytica Chimica Acta, 77 (1975) 309–311

SHORT COMMUNICATION

Cis and *trans* fatty acids in cigarette smoke condensate

D. B. WALTERS, W. J. CHAMBERLAIN and O. T. CHORTYK

Richard B. Russell Agricultural Research Center, Agricultural Research Service, United States Department of Agriculture, Athens, Georgia 30604 (U.S.A.)

(Received 5th December 1974)

A rapid method for determining the *cis–trans* composition of unsaturated fatty acids of cigarette smoke with gas chromatography and the new stationary phase, Silar-10C (ref. 1) is described. Such lipid analyses have been performed by sophisticated techniques[2] or by gas chromatographic methods necessitating time-consuming formation of derivatives[3].

Various fatty acids have been found in cigarette smoke condensate ranging from the saturated C_2 to C_{26} compounds including odd and even numbered carbon lengths as well as branched-chain isomers[4–7]. Previous studies[8,9] have indicated the presence of several unsaturated fatty acids, most abundantly palmitoleic ($C_{16}^{1=}$), oleic ($C_{18}^{1=}$), linoleic ($C_{18}^{2=}$), and linolenic ($C_{18}^{3=}$), all of which have been reported as the *cis* isomer. No work has been done on the *trans* isomers present in smoke condensate.

The *cis–trans* composition of unsaturated fatty acid ester mixtures is of interest for several reasons: (a) nutritional studies indicate that the *trans* isomer may not be nutritionally equivalent to the naturally occurring *cis* isomer[10]; (b) animal studies indicate that blood-clotting time is altered when *trans* isomers are substituted for *cis* isomers[11]; (c) subtle molecular structural changes often account for major flavor changes[12]; and (d) the difference between the *cis* and *trans* acids could be a result of chemical changes which may produce important biological differences.

Experimental

A dual-column Varian Model 2800 gas chromatograph equipped with flame ionization detectors was used. Flow rates of 10, 30, and 300 ml min^{-1} were used for helium, hydrogen, and air, respectively. Stainless steel columns, 1/8 in. × 10 ft, packed with 10% Silar-10C on 100–120 mesh Gas-Chrom Q, were used isothermally at 170 °C, with injector and detector temperatures of 250 °C. A Varian Model 25A recorder was used at a chart speed of 0.25 in. min^{-1}. Peak areas were determined with a Varian Model 485 integrator. Percent compositions were normalized and reported relative to percent total volatiles. Individual peaks were identified by comparative retention times and co-chromatography with knowns. Retention time was measured relative to methyl palmitate.

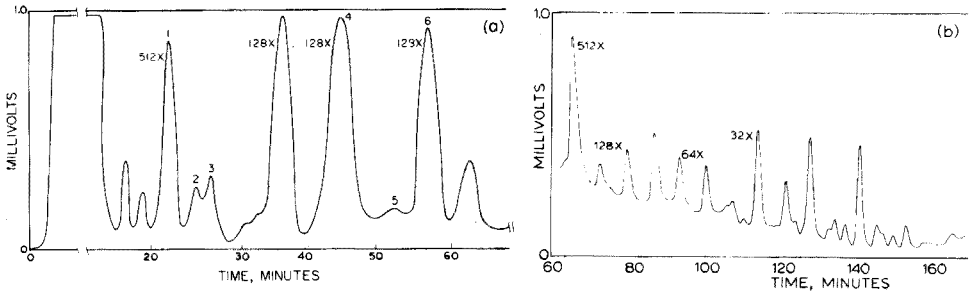

Fig. 1. Chromatogram of esterified cigarette smoke condensate fraction F-59. (a) 1 methyl palmitate; 2 methyl palmitoleate; 3 methyl palmitelaidate; 4 methyl oleate; 5 methyl linoleate; 6 methyl linolelaidate. (b) Continuation of Chromatogram at different attenuation.

Methyl ester standards (Applied Science Laboratories, Inc.) were certified 99^{+}% pure.

Cigarette smoke condensate (CSC), obtained from commercial cigarettes, was fractionated to yield a weak-acid fraction, F-8, in a manner previously described[13]. F-8 was further fractionated by partitioning it between equal volumes of petroleum ether and 90% methanol–water. The petroleum ether solution was then extracted with sodium hydrogen carbonate. The aqueous layer was adjusted to pH 1.0 with 6 *M* hydrochloric acid and extracted with diethyl ether to yield F-59, which represented about 0.5% of CSC.

A portion of F-59 was esterified with Methyl 8 (dimethylformamide dialkylacetal, Pierce Chemical Co.); 1 ml of Methyl 8 was used per 50 mg of F-59, as described elsewhere[14].

Results and discussion

Figure 1 shows the resulting chromatograms of esterified fraction F-59. The presence of the following unsaturated methyl esters was established by retention time and co-chromatography with knowns: palmitoleate, palmitelaidate, oleate, linoleate and linolelaidate. This study was primarily concerned with the detection and differentiation of the $C_{16}^{1=}$, $C_{18}^{1=}$, and $C_{18}^{2=}$ *cis* and *trans* isomers. Also, for the $C_{18}^{3=}$ compounds, the only standard available for comparison was the *cis* isomer (*cis, cis, cis*-9,12,15-octadecatrienate). This compound was detected only in trace amounts in smoke condensate.

Figure 1(a) shows baseline separation between methyl linoleate and methyl linolelaidate. Separation was poorer, but adequate for electronic integration, between methyl palmitoleate and palmitelaidate. Figure 1(b) shows the remaining portion of the chromatogram, at a different attenuation, beyond the area of interest.

Table I gives the experimental percent composition and the *cis* and *trans* isomers expressed as relative percent of total volatiles from fraction F-59. Relative retention time (*R*) was measured from the methyl palmitate peak. Similar amounts of palmitoleate (1.07%) and palmitelaidate (1.18%) were detected. However, a much smaller amount of linolelaidate (0.15%) compared to linoleate (13.77%) was found. Although 11.14% methyl oleate was detected, the level of methyl elaidate was either too low to be detected or its presence was masked by the oleate.

TABLE I

PERCENT COMPOSITION AND RELATIVE RETENTION TIMES (R) OF SOME ESTERIFIED UNSATURATED FATTY ACIDS FOUND IN F-59

Compound	*% of total volatiles of F-59*[a]	*R (min)*[b]
Palmitoleate, $C_{16}^{1=}$ (*cis*-9-hexadecenoate)	1.07	1.21
Palmitelaidate, $C_{16}^{1=}$ (*trans*-9-hexadecenoate)	1.18	1.33
Oleate, $C_{18}^{1=}$ *cis* (*cis*-9-octadecenoate)	11.14	2.11
Linoleate, $C_{18}^{2=}$ *cis* (*cis, cis*-9,12-octadecadienoate)	0.15	2.54
Linolelaidate, $C_{18}^{2=}$ *trans* (*trans, trans*-9,12-octadecadienoate)	13.77	2.78

[a] Values are an average of duplicate determinations.
[b] R—relative to methyl palmitate (peak 1 in Fig. 1).

Owing to yield variability in the fractionation–extraction procedures, no quantitation of acid contents in the condensate was attempted.

These findings illustrate the significance of the new g.c. support, Silar-10C, to the tobacco chemist and its use to other analytical organic chemists engaged in lipid research. Further work is in progress with this new support for identification of higher molecular weight fatty acids in cigarette smoke condensate.

The authors thank Mr. R. L. Atkins, Mr. Lamar Hendrix, and the Athens Area Technical School for their cooperation.

REFERENCES

1 *Gas-Chrom Newsletter*, 14 (1974) 1, Applied Science Laboratories, Inc., State College, Pa., U.S.A.
2 D. B. Walters and R. J. Horvat, *Anal. Chim. Acta*, 65 (1973) 198.
3 E. A. Emken, *Lipids*, 6 (1971) 686.
4 D. Hoffmann and H. Waziwodzki, *Beitr. Tabakforsch.*, 4 (1968) 167.
5 I. Mokhnachev, L. G. Serdyuk and M. Ivanov, *C. R. Bulgare. Sci.*, 20 (1967) 445.
6 B. L. van Duuren and A. I. Kosak, *J. Org. Chem.*, 23 (1958) 473.
7 M. Dymicky and R. L. Stedman, *Tobacco Sci.*, 12 (1969) 45.
8 R. L. Stedman, *Chem. Rev.*, 68 (1969) 153.
9 A. P. Swain and R. L. Stedman, *J. Ass. Offic. Agr. Chem.*, 45 (1961) 536.
10 P. G. Rand and F. W. Quackenbush, *J. Nutr.*, 87 (1965) 489.
11 G. Raccuglia and O. S. Privett, *Lipids*, 5 (1970) 85.
12 R. Teranishi, P. Issenberg, J. Hornstein and E. I. Wick, *Flavor Research, Principles and Techniques*, M. Dekker, New York, 1971, p. 282.
13 A. P. Swain, F. G. Bock, J. E. Cooper, W. J. Chamberlain, E. D. Strange, L. Lakritz and R. L. Stedman, *Beitr. Tabakforsch.*, 7 (1973) 1.
14 J. P. Thenot, E. C. Horning, M. Stafford and M. G. Horning, *Anal. Lett.*, 5 (1972) 217.

Analytica Chimica Acta, 77 (1975) 312–314

SHORT COMMUNICATION

Determination of uranium in sea water after anion-exchange separation

J. KORKISCH and I. STEFFAN
Institute for Analytical Chemistry, University of Vienna, Währingerstrasse 38 A-1090 Vienna (Austria)
(Received 16th December 1974)

In a previous paper[1] a method was described for the fluorimetric and spectrophotometric determination of uranium in natural non-saline waters after preliminary isolation of uranium by adsorption of its thiocyanate complex on the strongly basic anion-exchange resin Dowex 1. This technique proved to be most suitable for determinations of uranium in water samples collected in Austria and recent investigations have shown that it can also be used for the analysis of waters with high salt contents such as sea-water. The results of these experiments and determinations are outlined in the present communication.

Experimental

The preparation of the solutions and reagents, and the apparatus, were described earlier[1].

Procedure. The separation principle was the same as described previously[1], except that no ascorbic acid was added to the acidified sea-water sample containing 20 g of potassium thiocyanate per litre (to non-saline waters 10 g of KSCN were added[1]). For the determination of the separated uranium, the fluorimetric method was employed[1].

Results and discussion

The suitability of the anion-exchange technique in combination with the fluorimetric method for the determination of uranium in saline waters was tested by analysing artificial sea water (to which known amounts of uranium were added) and also samples from the Adriatic Sea and Pacific Ocean. The results of these investigations are shown in Tables I and II. Table I shows that quantitative recovery of uranium is obtained from solutions which contain 5–20 g of potassium thiocyanate per litre. At lower concentrations of thiocyanate, the uranium is much less strongly retained; this is in accordance with the values of the weight distribution coefficients of uranium, which in non-saline waters were found to be strongly dependent on the thiocyanate concentration[1]. The results of Table I also show that when a thiocyanate concentration of 20 g l^{-1} is used, it is possible to adsorb uranium quantitatively on the resin even if its concentration is as high as 100 $\mu g\ l^{-1}$.

TABLE I

RESULTS OF URANIUM DETERMINATIONS IN ARTIFICIAL SEA WATER[a]

KSCN (g l^{-1})	*Uranium (μg) added to 1 l of artificial seawater*	*Uranium in eluate (μg)*
0.0	5.0	0.10
0.5	5.0	2.30
1.0	5.0	4.76
5.0	5.0	5.17
10.0	5.0	5.16
20.0	5.0	5.15
30.0	5.0	5.10
20.0	0.0	0.01
20.0	1.0	0.99
20.0	2.5	2.47
20.0	5.0	4.82
20.0	10.0	10.04
20.0	20.0	19.72
20.0	50.0	49.90
20.0	100.0	100.50

[a] This artificial seawater was prepared by dissolving the following reagents in 20 l of distilled water: NaCl (560 g), KCl (16 g), $MgSO_4 \cdot 7\,H_2O$ (139.2 g), $MgCl_2 \cdot 6\,H_2O$ (20 g) and $CaCl_2 \cdot 2\,H_2O$ (26.5 g).

TABLE II

RESULTS OF URANIUM DETERMINATIONS IN SEAWATER SAMPLES

Sample	*Volume of sample used (l)*	*Uranium found (μg l^{-1})*
Adriatic Sea; sample taken	0.1	2.34
at shore near Lignano Pineta;	0.25	2.34
October 1974	0.5	2.34
	0.5	2.29[a]
	0.75	2.34
	1.0	2.25
	1.0	2.36[a]
	2.0	2.40
Pacific Ocean; sample taken	0.1	2.56
at shore near the Scripps	0.5	2.54
Institution of Oceanography	0.5	2.58[a]
La Jolla, Calif.; October 1974	1.0	2.62

[a] Results obtained after deduction of 1.0 μg of uranium which was added as a spike before the anion-exchange separation.

To investigate the effect of the volume of sea-water sample on the recovery and accuracy of the uranium determinations, varying volumes of sea water were analysed for the natural uranium contents. From the results listed in Table II, it can be seen that irrespective of the volume of sea water used, the uranium contents obtained show reasonably good agreement in all cases.

Since the samples analysed were collected very near the shore, their uranium

contents were found to be lower than the accepted average value for sea water of 3.1–3.4 μg uranium per l[2–6]. That sea-water samples which are taken near shores do actually contain less uranium was also demonstrated by Stewart and Bentley[7] who found 2.49 μg of uranium per l in samples of Pacific Ocean waters collected near the shore.

This research was sponsored by the Fonds zur Förderung der wissenschaftlichen Forschung, Vienna, Austria. Acknowledgement is also made to Prof. Dr. G. Arrhenius (Scripps Institution of Oceanography, University of California, La Jolla) and Mr. A. Sorio (Institute for Analytical Chemistry, University of Vienna) who supplied sample materials.

REFERENCES

1 J. Korkisch and L. Gödl, *Anal. Chim. Acta*, 71 (1974) 113.
2 H. V. Weiss, M. G. Lai and A. R. Gillespie, *Report USNRDL-TR-496*, December, 1960.
3 N. Ogata and N. Inoue, *Nippon Kaisui Gakkaishi*, 23 (1970) 148.
4 J. D. Wilson, R. K. Webster, G. W. C. Milner, G. A. Barnett and A. A. Smales, *Anal. Chim. Acta*, 23 (1960) 505.
5 G. W. C. Milner, J. D. Wilson, G. A. Barnett and A. A. Smales, *J. Electroanal. Chem.*, 2 (1961) 25.
6 T. Hashimoto, *Anal. Chim. Acta*, 56 (1971) 347.
7 D. C. Stewart and W. C. Bentley, *Science*, 120 (1954) 50.

Analytica Chimica Acta, 77 (1975) 315–316

SHORT COMMUNICATION

Rapid extraction–photometric determination of traces of iron(II) and iron(III) in water with 1,10-phenanthroline

HUBERT FADRUS and JOSEF MALÝ
Water Management Board, Vodohospodářská správa, Brno (Czechoslovakia)
(Received 1st November 1974)

The two valency forms of iron in a mixture are usually determined by procedures in which the total iron content is determined after conversion by oxidation or reduction to one of the two forms, which is then determined directly in an aliquot part[1]. The difference of the two determinations gives the content of the other valency form of iron. When the 1,10-phenanthroline method is applied for this purpose, the lowest concentrations of iron(II) cannot be determined precisely, because of the instability of iron(III) under the conditions used; the positive errors in the iron(II) determination and the unsatisfactory reproducibility of the results are caused by the effect of 1,10-phenanthroline on the Fe(II)/Fe(III) system.

These deficiencies can be overcome by adding the sodium salt of nitrilotriacetic acid (NTA), which permits the determination of iron(II) in the presence of iron(III)[2]. For favourable concentration ratios and with an extraction process[3], the two valency forms can be determined by a single procedure. First, iron(II) is extracted as the ion-association complex $(Fe\,phen_3)(ClO_4)_2$ from a glycocoll buffer, in which iron(III) is masked by NTA; then the aqueous solution is acidified so that the iron(III)–NTA complex decomposes, the iron(III) is reduced with ascorbic acid, and the iron(II) produced is determined after pH adjustment by further extraction.

Experimental

Reagent mixture. Prepare the following solutions: (a) 0.025 *M* 1,10-phenanthroline hydrochloride in distilled water; (b) 0.5 *M* glycocoll solution adjusted to pH 2.9 with 0.5 *M* hydrochloric acid; (c) 0.1 *M* nitrilotriacetic acid (sodium salt). Just before use, mix solutions a, b and c in the volume ratio 5:5:2.

Standard iron(II) solution (0.01 mg Fe ml^{-1}). Dissolve $(NH_4)_2Fe(SO_4)_2 \cdot 6\,H_2O$ (0.702 g) in distilled water containing 2 ml of concentrated sulphuric acid and dilute to 1 l. Standardize the solution by titration with permanganate.

Procedure

To 50 ml of neutral or slightly acidic sample, with a total iron content

of 0–25 μg in a 100-ml separating funnel, add 10 ml of the reagent mixture and 1 ml of 1 *M* sodium perchlorate. After 2 min add exactly 10.0 ml of nitrobenzene (spectrally pure) and extract the ion-association complex by intensive shaking for 1–2 min. Repeat the extraction with 10.0 ml of nitrobenzene and add 1–2 g of anhydrous sodium sulphate to the combined extracts. Measure the absorbance of the organic phase at 515 nm in 0.5- or 1-cm cells against a reagent blank. The iron concentration found corresponds to the iron(II) concentration in the original sample.

To the residual aqueous phase, add 5 ml of hydrochloric acid (1+1) and 1 ml of freshly prepared 0.25 *M* ascorbic acid. After 5 min, neutralize with an equivalent quantity of 2.5 *M* sodium hydroxide; the precise quantity must be determined in an aliquot sample (about 9.6 ml). Then continue the determination as described above. The iron content determined corresponds to the iron(III) concentration in the original sample.

Prepare calibration graphs in the range 0–0.5 mg Fe l^{-1} under the same working conditions with the standard iron(II) solution. This graph is the same for both of the described procedures.

TABLE I

ACCURACY AND PRECISION OF THE RESULTS

	Fe added (p.p.m.)	*e (%)*		*s*		*Fe found (p.p.m.)*	
		A	*B*	*A*	*B*	*A*	*B*
Fe(II)	0.246	0.019	7.72	0.0039	0.0047	0.247	0.265
Fe(III)	0.182	0.003	8.94	0.0039	0.0039	0.182	0.160

Results

None of the commonly occurring components of drinking, surface or ground water, in their usual concentrations, interferes with the determination. The accuracy and precision of the proposed method are indicated in Table I; accuracy is defined as the relative error (*e*) and precision as the standard deviation (*s*) of the results. Results are given for the recommended procedure (A) and for a comparison procedure (B), which was the same method except for the addition of NTA. In all cases, the extraction procedures were applied 20 min after the reagent addition, at which time the influence of NTA is conclusive.

REFERENCES

1 F. Vydra and M. Kopanica, *Chemist–Analyst*, 52 (1963) 88.
2 H. Fadrus and J. Maly, *Analyst (London)* June, 1975.
3 D. W. Margerum and C. V. Banks, *Anal. Chem.*, 26 (1954) 200.

Analytica Chimica Acta, 77 (1975) 317–319

SHORT COMMUNICATION

The flurimetric determination of dibucaine

JOEL D. MARTUCCI and STEPHEN G. SCHULMAN
College of Pharmacy, University of Florida, Gainesville, Florida 32610 (U.S.A.)
(Received 3rd January 1975)

Dibucaine (2-n-butoxy-N-(β-diethylaminoethyl)cinchoninamide) is about five times more potent than cocaine in producing local anesthesia but is also considerably more poisonous[1]. It is commonly employed either as the free base or as the hydrochloride in ophthalmic ointments to produce conjunctival anesthesia, or as the hydrochloride in dilute parenteral solutions to produce spinal or surface anesthesia. Because these dilute solutions (1:200–1:1500) are diluted even more by injection into the cerebrospinal fluid, fluorimetry may offer several advantages in the determination of dibucaine. Because the reagent contains several basic functional groups, it was desirable to study the pH dependence of its electronic spectra in order to determine the spectroscopic properties of its various prototopic forms and thus establish the optimal pH conditions for fluorimetric analysis.

Experimental

Dibucaine (free base; Pfaltz and Bauer, Inc., Flushing, N. Y.) was recrystallized twice from ethanol. Reagent-grade sulfuric acid, sodium hydroxide and chloroform (Mallinckrodt, St. Louis) and benzene-free ethanol were used. Sulfuric acid solutions, prepared by dilution with distilled–deionized water, were calibrated by means of the corrected Hammett acidity scale of Jorgenson and Hartter[2]. Solutions in the pH region 1–3 were prepared by dilution of sulfuric acid. Acetate, phosphate and borate buffers were employed to prepare solutions in the pH region 4–10. Dilute sodium hydroxide solutions were employed for solutions of pH 11–14. A 100-μl aliquot of a $1 \cdot 10^{-3}$ *M* stock solution of dibucaine in water was added to a 10.00 ml-volumetric flask filled to capacity with buffer or acid solution, and mixed by inversion to prepare each solution for spectroscopic measurement. For studies of non-aqueous solutions, the free base or monohydrochloride was dissolved directly in the appropriate solvent and diluted to $1 \cdot 10^{-5}$ *M*. Each solution was prepared immediately before spectra were recorded in order to minimize errors through decomposition.

Fluorescence and absorption spectra were recorded and pH measurements made as described previously[3].

Results and discussion

The long wavelength absorption and fluorescence maxima of dibucaine in

various solvents and at different aqueous pH values are presented in Table I. The pK_a values in aqueous media correspond Scheme 1 shown below.

TABLE I

LONG WAVELENGTH ELECTRONIC ABSORPTION (λ_a) AND FLUORESCENCE (λ_f) MAXIMA (IN nm) OF THE CHARGED CATIONS AND NEUTRAL SPECIES DERIVED FROM DIBUCAINE IN VARIOUS SOLVENTS

	λ_a	λ_f
Triply charged cation (T)		
H_2SO_4($H_0 = -7.9$)	325	508
Doubly charged cation (D)		
H_2SO_4 ($H_0 = -0.7$)	320	445
Singly charged cation (M)		
Water (pH = 6.2)	328	409
Ethanol	328	400
Chloroform	329	392
Neutral species		
Water (pH = 11.5)	328	403
Ethanol	327	390
Chloroform	328	388

Scheme 1

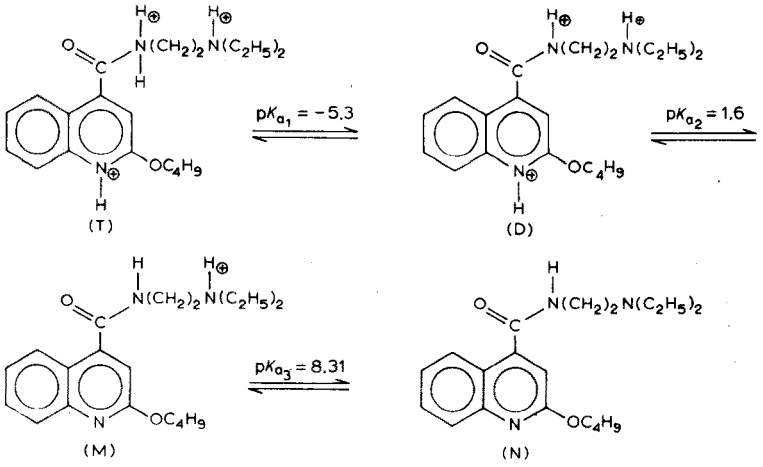

In Scheme 1, pK_{a_1} and pK_{a_2} were determined absorptiometrically. The absorption spectrum did not change sufficiently in the conversion of the singly charged (M) to the neutral species (N) to be of analytical value; consequently, pK_{a_3} was determined by potentiometric titration.

In the pH region near 8.3 (pK_{a_3}) the blue fluorescence of (N) shifts by 6 nm to longer wavelengths, with decreasing pH; the fluorescence is about nine times more intense at pH 6, where the monocation (M) predominates, than at pH 11, where the emission arises from (N). The occurrence of this fluorimetric titration at pH 8.3 ($pH = pK_{a_3}$) indicates that N is not converted to (M) in the

excited state; the relative intensities observed for each species are determined only by the relative fractions of the ground state species directly excited at each pH in the fluorimetric titration. In the region near $pH = pK_{a_3}$, the pseudo-first-order rate constants for protonation of (N) by the solvent, and for dissociation of (M) by the hydroxyl ion in the excited state, appear to be too slow for the acid–base reaction to occur.

In the region near pH 1.5, however, the blue fluorescence of (M) gives way to the blue-green fluorescence of (D) with decreasing pH and is diminished about five-fold in intensity. This fluorimetric titration has an inflection point at pH 2.1. Since the ground-state pK_a corresponding to protonation of (M) is 1.6, the heterocyclic nitrogen atom of dibucaine is apparently more basic in the lowest excited singlet state, the equilibrium constant for conversion of (M) to (D) being $pK^*_{a_2} = 2.1$.

Although the pK_a for the ground-state conversion of (D) to (T) is -5.3, the blue-green fluorescence of (D) is converted to the green fluorescence of (T) in a fluorimetric titration centered at $pK_{a_1} = 2.1$. The fluorescence of (T) is about five times less intense than that of (D). The inflection point in the fluorimetric titration at $H_0 - 2.1$ corresponds to the equilibrium constant $pK^*_{a_1}$; there is excellent agreement with the value of $pK^*_{a_1}$ calculated from the Förster cycle[4] when the ground-state pK_{a_1} of -5.3 and the shift of the fluorescence spectrum occurring on protonation of (D) are used.

The fluorescence intensities of (T), (D), (M) and (N) vary linearly with concentration below $1 \cdot 10^{-4}$ *M*. The limit of detection (that concentration which gives a fluorescence signal twice that of the background) of (M) is $6 \cdot 10^{-9}$ *M* at pH 4–6.5. The detection limits of (N) and (D) are about an order of magnitude higher, and that of (T) about two orders higher. Therefore, (M) is the most desirable species to determine fluorimetrically from the standpoint of analytical sensitivity, although the excited state protonation of (M) is a source of interference; if this did not occur, the useful analytical range for (M) would extend down to about pH 3.5.

In ethanol and chloroform the fluorescence spectra of the (N) and (M) shift to slightly shorter wavelengths, relative to the spectra in water. This reflects the diminished dielectric strengths and hydrogen-bond donor capacities of these solvents relative to water. The fluorescence intensities and detection-limits of (N) and (M) in organic solvents are almost identical to those of the respective species in water. It therefore appears that (M) gives the optimal analytical features and that the fluorimetric determination of dibucaine can be carried out equally well in aqueous media or in organic extracts.

REFERENCES

1 C. O. Wilson and O. Gisvold, *Textbook of Organic, Medicinal and Pharmaceutical Chemistry*, J. B. Lippincott, Philadelphia, 4th edn., 1962, p. 528.
2 M. J. Jorgenson and D. R. Hartter, *J. Amer. Chem. Soc.*, 85 (1963) 878.
3 A. C. Capomacchia and S. G. Schulman, *Anal. Chim. Acta*, 76 (1975) 000.
4 T. Förster, *Z. Elektrochem.*, 54 (1950) 42.

Analytica Chimica Acta, 77 (1975) 320–323

SHORT COMMUNICATION

Selective spectrophotometric determination of cobalt in silicates and meteorites

E. KISS

Research School of Earth Sciences, Australian National University, P.O. Box 4, Canberra, A.C.T., 2600 (Australia)

(Received 13th January 1975)

The heterocyclic azo dye 4-(2-pyridylazo)-1,3-diaminobenzene (PADAB) and several of its halogenated derivatives have recently been reported[1–3] to give extremely sensitive and selective reactions with cobalt(II) or cobalt(III). The cobalt reactions of 4-(3,5-dibromo-4-methyl-2-pyridylazo)-1,3-diaminobenzene have recently been studied in this laboratory. A further series of compounds structurally analogous to PADAB has also been prepared[4], and the most useful of these, 5-(3,5-dichloro-2-pyridylazo)-2,4-diaminotoluene has been used for the spectrophotometric determination of cobalt.

A characteristic of these compounds is their extreme sensitivity; the molar absorptivities of the cobalt complexes are $1.16 \cdot 10^5$ for 4-(5-bromo-2-pyridylazo)-1,3-diaminobenzene at 575 nm; $1.18 \cdot 10^5$ for 4-(3,5-dibromo-4-methyl-2-pyridylazo)-1,3-diaminobenzene at 590 nm; and $1.23 \cdot 10^5$ l mole^{-1} cm^{-1} for 4-(3,5-dibromo-2-pyridylazo)-1,3-diaminobenzene (3,5-Br-PADAB) at 590 nm. In earlier studies[3] the colour reactions of some of these reagents with metals, some interferences and the effects of experimental variables were assessed, and 5-Br-PADAB was used for the determination of cobalt in silicates and meteorites[3]. In the earlier method[3], the interference of macro amounts of iron (Fe/Co > 50) in silicates and meteorites was eliminated by a preliminary extraction of the chloroferrate ion from 7 *M* hydrochloric acid with methyl isobutyl ketone. The complete procedure was rather time-consuming because of the extraction step and subsequent removal of most of the acid. Moreover, the necessary preliminary adjustment to pH 2 occasionally produced an opalescence or precipitate of aluminium hydroxide, with which some cobalt was co-precipitated, and this cobalt was not always released by further treatment. Cobalt recoveries were unsatisfactory when direct colour development with 5-Br-PADAB was attempted in the presence of various masking agents.

In the present re-investigation, 4-(3,5-dibromo-2-pyridylazo)-1,3-diaminobenzene (3,5-Br-PADAB) was chosen because it has the highest sensitivity of its class. The possibility of solvent extraction of the coloured complex was first examined. The intensely coloured secondary complex of 3,5-Br-PADAB derived from the primary cobalt complex by acidification (2–5 *M* hydrochloric acid) could be extracted in the presence of perchlorate ions by several solvents such as benzyl alcohol, 2-phenylethanol, benzaldehyde, anisaldehyde and tri-n-butyl phosphate.

However, the colour stability was strongly dependent on the presence of free acid in these solvents, especially in aldehydes. The most efficient extractant was a 1:1 mixture of benzyl alcohol and 2-phenylethanol. The stability of the coloured extract was enhanced when the solution was diluted with absolute ethanol containing hydrogen chloride. However, a direct spectrophotometric determination of cobalt in the presence of fluoride proved more satisfactory and, when fluoride was added to the calibration solutions, a high degree of precision and accuracy was possible. The corrosive effect of fluoride on the glassware was practically undetectable in 2.4 *M* hydrochloric acid when ammonium fluoride was used, whereas appreciable etching occurred with potassium fluoride.

Experimental

3,5-Br-PADAB solution ($2 \cdot 10^{-3}$ M). Dissolve 74.4 mg of the pure reagent in absolute ethanol by warming, and dilute to 100 ml. The solution is stable over long periods if stored in an amber bottle.

Calibration curve. Dissolve cobalt sponge (99.998%) in hydrochloric acid and prepare a working solution (1.42 μg Co ml^{-1}) by suitable dilution. Proceed as described below for the colour development. Seven calibration points were measured within the range 4.25–25.5 μg Co/50 ml; the relative standard deviation was 0.19%. In the presence of large amounts of fluoride, the effective molar absorptivity was slightly suppressed, being $1.18 \cdot 10^5$ l $mole^{-1}$ cm^{-1} at 590 nm compared to $1.23 \cdot 10^5$ in fluoride-free solution. However, the reagent sensitivity (*i.e.* 0.00050 μg Co cm^{-2}) was not significantly affected by variations in fluoride concentration.

Sample dissolution. Weigh 0.5–1.0 g of finely ground silicate in a 100-ml platinum evaporating dish, moisten with *ca.* 5 ml of water, add 5 ml of (1+1) sulphuric acid and 15 ml of concentrated hydrofluoric acid, and evaporate on a water bath. Repeat the evaporation after adding 5 ml of concentrated hydrofluoric acid and 3 ml of concentrated nitric acid. Place the dish on a hot plate when most of the acid has evaporated, and heat gradually till copious fumes of sulphur trioxide are evolved. Dissolve the cooled salts in *ca.* 20 ml of water by warming and wash into a 250-ml volumetric flask. Any opalescence or precipitate of calcium sulphate will be slowly dissolved.

Drillings from iron meteorites should be prepared by a tungsten carbide tipped drill to minimize contamination. Weigh 30–50 mg of meteorite sample into a small beaker, dissolve the drillings in a mixture of concentrated hydrochloric and nitric acids and evaporate most of the acid on a water bath. Dilute to 250 ml in a volumetric flask and proceed as for silicates.

Colour development and measurement. Pipette suitable aliquots not exceeding 25 ml and containing less than 25 μg of cobalt into 50-ml volumetric flasks. Add 5 ml of aqueous 20% (w/v) ammonium fluoride solution, mix, and add by a pipette 2.00 ml of $2 \cdot 10^{-3}$ *M* 3.5-Br-PADAB solution followed by 5 ml of 4 *M* ammonium acetate solution. Mix, warm on a water bath for 10 min, cool, then add 10 ml of concentrated hydrochloric acid, and continue cooling to room temperature. After diluting to volume, measure the absorbance at 590 nm in a 10-mm flow-through cell against a reagent blank reference prepared in the same manner. Calculate the concentration of cobalt (p.p.m.) from the calibration data.

TABLE I

DIRECT SPECTROPHOTOMETRIC DETERMINATION OF COBALT

Sample	*Co (p.p.m.)*	s_r	*No. of detns.*	*Other values*
Andesite, AGV-1	16.4±0.2	—	3	15.7±0.4[a], 15[e]
Basalt, BCR-1	36.4±0.7	—	3	36.2±1.3[a], 37[e]
Dunite, DTS-1	143.0	0.14	7	143±2.8[a], 145[e]
Tonalite, T-1	11.6	0.78	6	14[e], 13?[f]
Basalt, TR 71-983 Un. 11	27.5±nil	—	2	32.7[a], 28[b]
Dacite, TR 71-989 Pp6	9.5±0.3	—	2	10.2[a], 11[b]
Andesite, TR 71-1002 Sb-10	13.2±0.1	—	2	16.6[a], 14.5[b]
Basaltic andesite 71-1028 Su15	18.7±nil	—	2	21.6[a], 18.5[b]
Basalt, TR 72-955 Mh	44.0±0.4	—	2	48.7[a], 44[b]
Basalt, TR 72-937 Mh	36.7±0.04	—	2	43[a], 38[b]
Basalt, TR 72-970 BM-2	54.8±nil	—	2	56[a], 58[b]
Basalt, TR 72-976 BM-8	53.6±0.05	—	2	54[a], 55[b]
Dacite, TR 72-991 Ba-1	3.9±0.35	—	2	4.7[a], 3.8[b]
Andesite TR 72-985 Ag5	13.4±0.2	—	2	15.7[a], 14.0[b]
Basalt TR 72-996 Pe-1	31.0±0.3	—	2	35.9[a], 32[b]
Mild Steel, BCS-272	2,450	0.14	4	2,455±3.7[a], 0.25%[c]
Low Alloy Steel, BCS-251	660	0.39	4	0.06%[c], 0.07%[c]
Box Hole Iron Meteorite	4,900	0.30	4	4,870±10[a], 0.48%[d]
Kyancutta Iron Meteorite	4,980	0.54	7	—
Pallasite, Glorieta Mtn.	5,640	0.07	4	—

[a] Spectrophotometry by 5-Br-PADAB, *Anal. Chim. Acta*, 66 (1973) 385.
[b] Emission spectrography, R.S.E.S., Australian National University by D. Whitford.
[c] British Chemical Standards Certificate value.
[d] C. F. Lewis and C. B. Moore, *Meteoritics*, 6 (1971) 195.
[e] M. Kaye, *Preferred values for inter-laboratory rock samples*, Department of Geology, Australian National Universit 1972 (pers. comm.).
[f] S. Abbey, *Can. Geol. Surv. Pap. No. 72-30*, 1972.

Results and discussion

The results obtained on some standard rocks and other materials as well as on meteoritic irons are presented in Table I.

Cobalt was initially determined on rocks decomposed by hydrofluoric and nitric acids (thus leaving all the cations as their fluorides) but without success; the low recoveries were attributed to the formation of complex fluorides in which cobalt was firmly held together with other transition elements.

The addition of ammonium fluoride to the aliquots of total rock dissolutions often caused the formation of some flocculent precipitate, which was an efficient adsorbent for 3,5-Br-PADAB; it was necessary to facilitate quantitative formation of the primary cobalt complex by heating. During the acidification, the fluoride precipitate re-dissolved for all types of rocks.

This analytical procedure offers simplicity and rapidity as well as maximal selectivity for the direct spectrophotometric determination of microgram quantities of cobalt. The average relative standard deviation was 0.34% for the silicates and meteorites tested.

REFERENCES

1 S. Shibata, M. Furukawa, Y. Ishiguro and S. Sasaki, *Anal. Chim. Acta*, 55 (1971) 231.
2 S. Shibata, *Bunseki Kagaku*, 21 (1972) 551.
3 E. Kiss, *Anal. Chim. Acta*, 66 (1973) 385.
4 S. Shibata, M. Furukawa and E. Kamata, *Anal. Chim. Acta*, 73 (1974) 107.

Analytica Chimica Acta, 77 (1975) 324–326

SHORT COMMUNICATION

Detection of various α-substituted nitriles and *gem* halonitroalkanes by chemiluminescence

HARVEY W. YUROW and SAMUEL SASS
Chemical Laboratory, Edgewood Arsenal, Aberdeen Proving Ground, Maryland 21010 (U.S.A.)
(Received 11th November 1974)

In a previous paper[1] the detection of various α-substituted ketones by chemiluminescence of 5-amino-2,3-dihydro-1,4-phthalazinedione (luminol) was reported. The reaction involved conversion of the ketone by hydrogen peroxide in basic solution to a hydroperoxide capable of oxidizing luminol to a chemiluminescent species. Hydroperoxide anion is an extremely powerful nucleophile which reacts readily with a variety of organic compounds[2]. Its enhanced reactivity has been ascribed to the "alpha effect", which is due to an unshared pair of electrons on an atom adjacent to the nucleophilic center[3].

Hydroperoxide is more reactive than hydroxide for carbon electrophiles in the order digonal > trigonal > tetrahedral. The trigonal compounds including 1,2-diketones were treated previously[1]. In the current work are reported the chemiluminescent reactions of nitriles (digonal carbon) and also of aliphatic halonitro compounds where attack may be on the oxygen rather than on the carbon.

Experimental

Reagents. The luminol (Aldrich) was 0.0025 *M* in 0.20 *M* sodium hydroxide solution. The hydrogen peroxide (Mallinckrodt, 30% reagent grade) was diluted (1+99) with 0.002 *M* tetrasodium ethylenediaminetetraacetate, stored in a dark bottle and prepared fresh daily. The organic compounds tested were commercial materials in the purest grades available. A number of the halonitro compounds are not commercially available but were readily synthesized. Chlorotrinitromethane was synthesized by reacting tetranitromethane with glycerol and aqueous potassium hydroxide to give the potassium salt of trinitromethane[4] which was halogenated with sodium hypochlorite[5]. The hypochlorite method was also used to prepare other halonitroalkanes. Dichlorodinitromethane was synthesized by distillation of 2,4,6-trichloroaniline and concentrated nitric acid[6].

Equipment. Relative light intensities were measured with the Aminco-Bowman spectrofluorimeter. The handle of the cell compartment cover-plate was removed to allow insertion of hypodermic syringe needles into a 1-ml microcell.

Procedure. A 0.2 ml aqueous sample (1.0 mg ml^{-1}) was introduced into the

TABLE I

CHEMILUMINESCENCE INDUCED IN LUMINOL BY VARIOUS NITRILES AND NITRO COMPOUNDS

Compound	*Intensity*	*Compound*	*Intensity*
Trichloroacetonitrile	260	Cyanogen bromide	2100
Chloroacetonitrile	80	Chlorotrinitromethane	60000
Iodoacetonitrile	50	Dichlorodinitromethane	8500
Methylthioacetonitrile	50	Trichloronitromethane	850
Dibromoacetonitrile	750	Tetranitromethane	4900
Acetone cyanohydrin	50	1,1-Dichloro-1-nitroethane	120
Malononitrile	3000	1,1-Dichloro-1-nitropropane	100
Dichloromalononitrile	450	2-Chloro-2-nitropropane	10
Ethoxymethylenemalono-nitrile	2900		

cell. The time-base mode was started at an emission wavelength of 410 nm and 0.2 ml each of luminol and peroxide were introduced simultaneously into the cell. The relative light intensities were measured and corrected for molecular weight differences among the various compounds. Results given in Table I are the mean of duplicate determinations.

Results and discussion

The results for the various compounds tested are given in Table I. Very weak chemiluminescence was given by: methoxyacetonitrile, acrylonitrile, hydracrylonitrile, 3-butenenitrile, 2-chloroacrylonitrile, and 1,2-dicyanocyclobutane.

In the Radziszewski reaction[7], a peroxyimidic acid is formed which reacts further with peroxide to give an amide, with k_1 usually being slower than k_2.

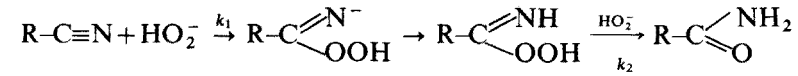

The enhanced reactivity of hydroperoxide anion with nitriles has been ascribed to hydrogen bonding in the transition state[7]; *i.e.*

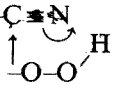

Relatively weak chemiluminescence was given by acrylonitrile and 3-butenenitrile even in the presence of phosphate and methanol, which are reported to stabilize the peroxyimidic acid appreciably, thus decreasing k_2 (ref. 8). Nitriles substituted by electron-withdrawing groups in the α-position would be expected to give relatively strong chemiluminescence. However, examination of the results shows no clearcut correlation between the value of the inductive effect for a given moiety and the relative intensity of the chemiluminescence for substituted acetonitriles.

The picture is somewhat clearer for the *gem*-halonitro compounds, for as the number of chloro groups increases and the number of nitro groups decreases, the chemiluminescence intensity decreases while its duration increases. Tetranitromethane reacts with hydroperoxide anion according to the following scheme[9]:

$$C(NO_2)_4 + HO_2^- \rightarrow [HO\cdots O\cdots O\text{–}N(\vdots O)\text{–}C(NO_2)_3^-] \rightarrow C(NO_2)_3^- + NO_2^- + H^+ + O_2$$

Similarly trinitromethyl compounds react to give dinitromethane[10]. The reaction of tetranitromethane is postulated to involve *p*-electron orbital overlap of the peroxy-anion oxygen with the nitro oxygen orbital and stabilization of the transition state by resonance[9]. With the halonitro compounds, an alternative mechanism may involve nucleophilic attack on the carbon atom because chloro is a better leaving group than nitro.

REFERENCES

1 H. W. Yurow and S. Sass, *Anal. Chim. Acta*, 68 (1974) 203.
2 J. G. Wallace, *Hydrogen Peroxide in Organic Chemistry*, DuPont, Wilmington, Del., 1962, pp. 31–47.
3 N. J. Fina and J. O. Edwards, *Int. J. Chem. Kinetics*, 5 (1973) 1.
4 A. K. Macbeth and W. B. Orr, *J. Chem. Soc., London*, (1932) 538.
5 R. Stroh, *Houben Weyl Methoden Der Organischen Chemie, Vol. 5*, Pt. 3, Thieme–Verlag, Stuttgart, 1962, p. 784.
6 S. M. Losanitsch, *Chem. Ber.*, 15 (1882) 471.
7 Z. Rappoport, *The Chemistry of the Cyano Group*, Interscience, London, 1970, p. 262.
8 Y. Ogata and Y. Sawaki, *Tetrahedron*, 20 (1964) 2065.
9 N. F. Sager and J. C. Hoffsommer, *J. Phys. Chem.*, 73 (1969) 4155.
10 D. J. Glover, *Tetrahedron Supp., 4*, 19 (1963) 219.

Analytica Chimica Acta, 77 (1975) 327–330

SHORT COMMUNICATION

Stepwise *versus* continuous addition of titrant for linear titration curves

W. E. VAN DER LINDEN

Laboratory for Analytical Chemistry, Nieuwe Achtergracht 166, Amsterdam (The Netherlands)

(Received 4th February 1975)

When titrations are based on linear indication methods, *e.g.* self-indicating photometric titrations, automatic titrators prove very satisfactory. With a homemade titration equipment developed in this Laboratory (Dr. H. Poppe), the titrant is delivered continuously from a piston-type burette; direct coupling of the speed of delivery from the burette and the chart speed is accomplished by two stepping motors and a synchronizing unit. Most titrations carried out with this equipment have yielded satisfactory results, but positive systematic errors may arise, especially in titrations at lower concentration levels. This can be misleading because, apart from this error, significant irregularities are not observed on the titration curves. The experimental curves appear to agree with the theoretically expected ones. If under exactly the same conditions these titrations are performed manually by stepwise addition of the titrant with waiting times after each addition, such that the total time necessary to reach the equivalence point is about the same for the automatically performed titrations, correct end-points are usually obtained. This phenomenon can be attributed either to the slowness of the titration reaction or to the fact that it takes some time to homogenize the solution. As mixing should not be less effective at lower than at higher concentrations, the slowness of the reaction is clearly the important factor.

In this communication the results obtained by stepwise and continuous addition of titrant are compared in terms of their dependence on the titration reaction rate.

Theory

The simple case of a bimolecular reaction:

$$M + L \underset{k_-}{\overset{k_+}{\rightleftharpoons}} ML; \quad K = \frac{k_+}{k_-}$$

can serve as an example. The following assumptions are made to facilitate solution of the rate equations: (a) mixing is instantaneous; (b) dilution is negligible; and (c) the influence of the back-reaction is neglected, *i.e.* k_- is small compared with k_+, so that the equilibrium constant K is much larger than unity.

The appropriate differential rate equations are:

$$\frac{d[M]}{dt} = \frac{d[L]}{dt} = -\frac{d[ML]}{dt} = -k_+[M][L] \qquad (1)$$

Stepwise addition of titrant. If M and L are mixed and their initial concentrations are $[M]_0$ and $[L]_0$ respectively, the concentration of ML will vary with time according to the equation:

$$\ln \frac{[ML]-[M]_0}{[ML]-[L]_0} = ([M]_0-[L]_0)k_+ t+\ln \frac{[M]_0}{[L]_0} \tag{2}$$

If $[M]_0 \simeq [L]_0$, this reduces to:

$$\frac{1}{[M]} - \frac{1}{[M]_0} = k_+ t \tag{3}$$

For the calculation of titration curves ([M] or [ML] *vs.* titration parameter *f*), eqns. (2) and (3) will be used in the following way. Let t^* be the time needed to reach the equivalence point. The amount of titrant added will be equally distributed over n additions. After each addition a waiting time t^*/n is observed. If C_M is the analytical concentration of M, the concentration of ML after the first addition is calculated from eqn. (2), taking $[L]_0 = C_M/n$, $[M]_0 = C_M$ and $t = t^*/n$. If [ML] is known, the values of [M] and [L] are calculated from the stoichiometric relations. The value of [M] thus obtained and the value of [L] increased by C_M/n after the new addition of titrant are the initial concentrations $[M]_0$ and $[L]_0$ in the calculation of [ML] after the second step, etc. At the nth addition, $[M] \simeq [L]$, and so eqn. (3) should be used.

Continuous addition of titrant. The derivation of the differential equation and its solution are given by Carr and Jordan[1] who express the speed of delivery (defined as the increase of the analytical concentration of L in the solution per unit time) by the symbol ρ. The total time necessary to deliver the amount of titrant $(C_L)_{ep}$ equivalent to C_M will be denoted again by t^*, thus:

$$(C_L)_{ep} = C_M = \rho t^* \rightarrow C_L = \rho t = C_M(t/t^*) = C_M f$$

At any moment during the titration the relationships:

$$[L] = C_L - [ML] = C_L - C_M + [M] = \rho t - C_M + [M]$$

are valid. According to eqn. (1):

$$\frac{d[M]}{dt} = -k_+[M][L] = -k_+[M](\rho t - C_M + [M]) \tag{4}$$

when the "reduced" concentration $m = [M]/C_M$ is introduced, eqn. (4) can be written as:

$$\frac{dm}{dt} = -k_+ m C_M (f-1+m) \tag{5}$$

or as:

$$\frac{dm}{df} = -k_+ m C_M t^* (f-1+m) = -\beta m(f-1+m) \tag{6}$$

in which $\beta = k_+ C_M t^*$.

The solution of this differential equation of the Bernoulli–Ricatti type is:

$$m = [M]/C_M = \frac{\exp \beta/2 \cdot \exp[-\beta/2(f-1)^2]}{1+(\pi\beta/2)^{\frac{1}{2}}[\mathrm{erf}\{(\beta/2)^{\frac{1}{2}}(f-1)+\mathrm{erf}(\beta/2)^{\frac{1}{2}}] \exp \beta/2} \tag{7}$$

Results and discussion

It can be seen from eqn. (2) that in stepwise additions the titration curve will also depend on the value of $k_+c_M t^* = \beta$. For different values of β, stepwise titration curves are calculated on the assumption that five additions of equal volume are required to reach the equivalence point. If the end-points determined from the resulting curves are compared with those obtained by continuous addition of titrant, the difference observed is remarkable, especially at somewhat higher values of β (Fig. 1). The stepwise titration method yields results which show positive systematic errors rapidly approaching zero, whereas with continuous delivery of titrant, the positive systematic error of several percent remains for much larger values of β. Care is required since the occurrence of these errors cannot be deduced from the curves themselves as no other significant deviations can be observed (Fig. 2).

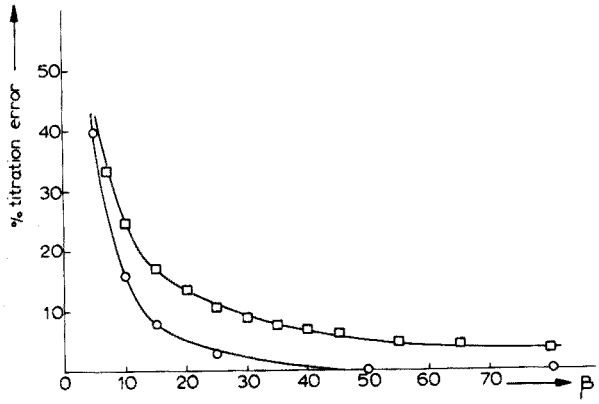

Fig. 1. Plot of the relative titration error for different values of $\beta = k_+C_M t^*$. (○) Stepwise addition of titrant. (□) Continuous addition of titrant.

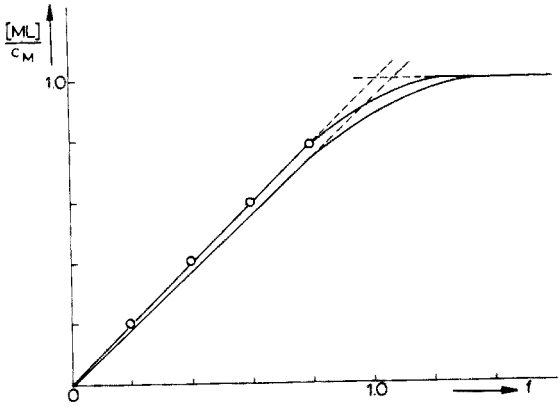

Fig. 2. Titration curve $[ML]/C_M$ *vs.* titration parameter f. $\beta \simeq 50$; (—) Continuous delivery of titrant. (○) stepwise addition of titrant. $n = 5$ where n = number of additions needed to reach the equivalence point).

It is recommended that every titration be tested for these possible errors before it is performed automatically. This is particularly important at lower concentration levels. An automatic titrator under development in this laboratory will take this factor into account. The titrant is added stepwise in equal volumes but after each addition the waiting period is extended until the derivative of the signal measured is smaller than a fixed value. Errors caused by the non-instantaneous mixing will thereby also be avoided.

REFERENCE

1 P. W. Carr and J. Jordan, *Anal. Chem.*, 45 (1973) 634.

Analytica Chimica Acta, 77 (1975) 331–336

SHORT COMMUNICATION

Bis(1,5-dimethyl-2-phenyl-3-pyrazolone) perchlorate and bis(1-butyl-2,6-dimethyl-4-pyridone) perchlorate as primary standards for non-aqueous titrations

ANIL K. MUKHERJI

Materials Analysis Area, Xerox Corporation, Webster, New York, 14580 (U.S.A.)

(Received 19th December 1974)

Busev *et al.*[1,2] have proposed bis(1,5-dimethyl-2-phenyl-3-pyrazolone) perchlorate (I), commonly known as antipyrene perchlorate, as a primary standard for acids and bases in non-aqueous solvents. Recently, bis(1-butyl-2,6-dimethyl-4-pyridone) perchlorate (II) has also been proposed[3]. Both compounds have excellent solubility characteristics in a variety of solvents, and have high molecular weights.

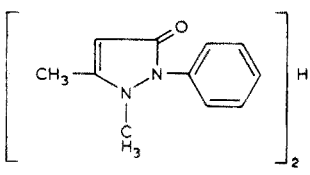

(I)

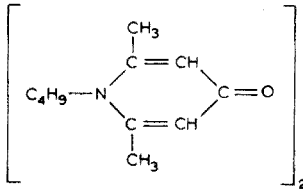

(II)

Investigations on the thermal stability of these compounds and on the precision possible in a variety of common solvents with both visual and potentiometric end-points, are described below.

Experimental

Thermogravimetric analysis. The weight loss experiments were carried out with the DuPont 990/950 TGA system. The heating rate was 20°C min^{-1}, and a nitrogen atmosphere was maintained at a flow rate of 170 ml min^{-1}.

Reagents. Bis(1,5-dimethyl-2-phenyl-3-pyrazolone) perchlorate (m.w. 476.92; 100.00 ± 0.18% pure; Eastman, EKX10891) and bis(1-butyl-2,6-dimethyl-4-pyridone) perchlorate monohydrate (m.w. 477.00; Eastman, EK11311) were used. A 0.1 *M* perchloric acid solution was prepared by diluting 8.5 ml of 70% perchloric acid in glacial acetic acid or in the solvent concerned. A 0.1 *M* hexadecyltrimethylammonium hydroxide (HDTMAH) solution in 9:1 benzene–methanol (Eastman, EKA10904) was diluted in an appropriate solvent.

Potassium hydrogenphthalate (Fisher certified reagent) and benzoic acid (N.B.S. standard) were used. All solvents were Baker analyzed-reagent grade, unless otherwise noted, and were used without further purification.

Procedures. For visual titrations, 15–20 mg of compound I or II were dissolved

in 30 ml of a solvent and titrated with a standard acid or base in presence of an appropriate indicator.

All potentiometric titrations were carried out similarly, with a Metrohm Potentiograph E436 and a combination glass electrode.

Results and discussion

Thermogravimetric analysis showed that compound I is stable up to 200°C, gradually loses weight up to 288°C (total loss 9.5%), and then detonates leaving a 2% residue. Compound II loses weight as soon as heating is commenced; at about 140°C the weight loss is stabilized at 3.63%, which corresponds to the loss of the one molecule of water (theor. 3.77%). It begins to lose weight again at 275°C and loses a total of 16% by 323°C, when it detonates leaving a residue of about 10%.

The compounds were also heated for a few hours at 110°C in an oven. About 0.5 g of the sample was put in a lidless weighing bottle; every hour, a few mg of the samples was removed, cooled in desiccator, dissolved in 30 ml of glacial acetic acid and titrated with a standard perchloric acid solution in glacial acetic acid, to a potentiometric end-point. Compound I showed a weight loss of about 0.1% in 1 h and this increased to about 1% after 6 h. No further weight loss was observed on heating overnight.

Compound II showed a weight loss of about 3% on heating for 1 h at 110°C. Alessi *et al.*[3] stated that compound II is a monohydrate under room conditions but drying under vacuum for 24 h effectively removes water of hydration. The present work showed that compound II is stable at room temperature for a long time and that heating must be avoided. No explosion hazard was experienced with either compound at 110°C. Both compounds showed excellent stability when their standard solutions in glacial acid were stored for six weeks.

Standardization of ca. 0.01 M perchloric acid. Titrations to visual end-points were carried out in glacial acetic acid, methyl ethyl ketone, dimethylformamide and denatured ethanol. In terms of precision and accuracy, titrations were best in glacial acetic acid with crystal violet as indicator (Table I). In methyl ethyl ketone and denatured ethanol, the molarities obtained with compounds I and II did not agree. In dimethylformamide, only compound II provided a sharp end-point with thymol blue indicator, but the precision was poor.

When potentiometric end-points were used, glacial acetic acid proved an excellent medium for standardizing perchloric acid against both the compounds, compound II being more satisfactory (Table II). With compound I up to 0.6% water, and with compound II up to 1.25% water, could be tolerated in the glacial acetic acid before the curves became distorted. Perchloric acid solutions (0.001 *M*) could easily be standardized with compound II. Neither of the compounds could be used in 1,4-dioxane. Titration of compound I was impossible even in dioxane–methanol mixtures, but compound II provided reasonable accuracy when titrated in 10–50% methanol in dioxane. Similarly in dimethylformamide and absolute ethanol, end-points were obtained only with compound II, but the precision and accuracy were very poor. Titrations in methyl ethyl ketone provided a sharp end-point with compound II and good precision for both I and II. No end-points were detected in dimethylsulfoxide or denatured ethanol.

Standardization of ca. 0.01 M hexadecyltrimethylammonium hydroxide

TABLE I

STANDARDIZATION OF PERCHLORIC ACID WITH VISUAL END-POINTS IN VARIOUS SOLVENTS

Compound	*M $HClO_4$*		*s_r (%)*	*Remarks*
	Found[a]	*Comparative method*[b]		
Glacial acetic acid				
I	0.0099[c]	0.0098	0.6	Sharp change
II	0.0098[c]	0.0098	0.7	Sharp change
I	0.0105[d]	0.0098	0.7	Blue–blue-green; not sharp
II	0.0100[c]	0.0098	0.7	Sharp change
Methyl ethyl ketone				
I	0.01512[e]	—	0.8	Orange–bright pink: sharp change
II	0.01231[e]	—	0.7	Dull orange–rose pink; not sharp
Dimethylformamide				
I	—[f]	—	—	Color changes on addition of a few drops of the titrant
II	0.01149[f]	—	13.7	Light green–tan; sharp change
Ethanol[g]				
I	0.00998[h]	—	0.8	Yellow-brown–orange; color change difficult to see
II	0.00908	—	1.1	Green–tan; transient change

[a] Average of five titrations
[b] Standardized against potassium hydrogenphthalate.
[c] 0.1% Crystal violet in glacial acetic acid.
[d] 0.1% Brilliant green in glacial acetic acid.
[e] Methyl red, saturated solution in glacial acetic acid.
[f] 0.2% Thymol blue in glacial acetic acid.
[g] Denatured ethanol (Fisher Scientific Co.) containing 1% each of ethyl acetate, methyl isobutyl ketone and aviation gasoline.
[h] 1 drop of 0.02% methyl orange + 5 drops of 0.5% thymolphthalein.

(HDTMAH). Results obtained for visual titrations in various solvents are presented in Table III. In chlorobenzene, the phenolphthalein end-point is sharp for both compounds I and II. In acetonitrile with thymol blue indicator, both can be titrated but the color change is not very sharp for compound II. In methanol and dioxan, only compound I can be used. For best results chlorobenzene is recommended with phenolphthalein indicator.

When potentiometric end-points are used, compounds I and II in methanol, 10% methanol–dioxane and chlorobenzene both provide reasonable accuracy and precision (Table IV). In dimethylsulfoxide only compound I provides acceptable accuracy. In denatured ethanol, the results obtained with compounds I and II agree within 1% of each other. In methyl ethyl ketone and dimethylformamide, the results obtained with compounds I and II do not agree with each other, and in the latter

TABLE II

STANDARDIZATION OF PERCHLORIC ACID WITH POTENTIOMETRIC END-POINTS

Compound	*Solvent*	*M $HClO_4$*		*s_r (%)*	*Remarks*
		Found[a]	*Comparative method*[b]		
I	Glacial acetic cid	0.0097	0.0096	0.7	Titration curve drawn out
II	Glacial acetic acid	0.0100	0.0096	0.6	Curves sharp; Δ mV at end-point larger than for I
II	10% Methanol in 1,4-dioxane	0.0126	0.0123	2.5	
II	25% Methanol in 1,4-dioxane	0.0124	0.0123	1.3	
II	50% Methanol in 1,4-dioxane	0.0123	0.0123	1.3	
I	Methylethyl ketone	0.01236	—	0.8	Skewed end-point
II	Methyl ethyl ketone	0.01246	—	0.3	Large mV change and sharp end-point

[a,b] See footnotes to Table I.

TABLE III

STANDARDIZATION OF HEXADECYLTRIMETHYLAMMONIUM HYDROXIDE WITH VISUAL END POINTS

Compound	*Solvent*	*M HDTMAH*		*s_r (%)*	*Remarks*
		Found[a]	*Comparative method*[b]		
I	Methanol	0.0164[c]	0.0101	2.1	Pink–yellow
II	Methanol	—[c]	—	—	Yellow–green; delayed colo change beyond the end-poi
I	Acetonitrile	0.0080[c]	0.0076	2.5	Yellow–blue; indistinct end-point
II	Acetonitrile	0.0073[c]	0.0076	4.9	
I	Chlorobenzene	0.0109[d]	0.0110	1.3	Colorless–pink; sharp end-point
II	Chlorobenzene	0.0102[d]	0.0110	1.1	Colorless–pink; sharp end-point
I	1,4-Dioxane	0.0126[c]	—	1.6	Colorless–yellow; sharp end-point
II	1,4-Dioxane	—[c]	—	—	Colorless–yellow on addition of first drop of the titrant

[a] Average of five titrations.
[b] Standardization against benzoic acid.
[c] 0.3% Thymol blue.
[d] Phenolphthalein, saturated solution.

BLE IV

ANDARDIZATION OF HEXADECYLTRIMETHYLAMMONIUM HYDROXIDE WITH POTENTIO-ETRIC END-POINTS

mpound	*Solvent*	*M HDTMAH*		s_r (%)	*Remarks*
		Found[a]	*Comparative method*[b]		
	Methanol	0.0133	0.0132	1.8	Large Δ mV
	Methanol	0.0128	0.0132	1.2	
	10% Methanol in 1,4-dioxane	0.0127	0.0124	1.3	
	10% Methanol in 1,4-dioxane	0.0123	0.0124	1.1	
	Dimethylsulfoxide	0.0123	0.0119	1.1	
	Dimethylsulfoxide	0.0109	0.0128	0.6	
	Chlorobenzene	0.0129	0.0123	0.8	Large Δ mV
	Chlorobenzene	0.0118	0.0123	1.4	
	Denatured ethanol[c]	0.01327	—	0.6	
	Denatured ethanol[c]	0.01315	—	1.0	
	Methyl ethyl ketone	0.01294	—	1.7	
	Methyl ethyl ketone	0.01113	—	1.0	
	Dimethyl formamide	0.02245	0.02423	1.0	
	Dimethyl formamide	0.02135	0.02423	3.0	

Average of five titrations.
Standardization against $HClO_4$.
See footnote [a] of Table I.

medium are lower than those found with standard perchloric acid. End-points were not obtained in 9:1 benzene–methanol or 1,4-dioxane. For best results, methanol, 10% methanol–dioxane and chlorobenzene are recommended.

Conclusions

Both compounds are satisfactory as primary standards under suitable experimental conditions. Both are monoacidic bases and can be titrated with perchloric acid solutions according to conventional stoichiometry; they are also monobasic acids and so can be titrated with hexadecyltrimethylammonium hydroxide solutions. Many of the differences observed in these titrations with the two compounds can be attributed to the fact that compound I is a weaker base but a stronger acid than compound II.

Thanks are due to Rosemary Hentschel for providing technical assistance.

REFERENCES

1 A. I. Busev, B. E. Zaitsen, V. K. Aksimov, Ya. Chelikhovskii and F. Kopetski, *Zh. Obshch. Khim.*, 38 (1968) 534.

2 A. I. Busev, V. K. Akimov and I. A. Emel'yanova, *Zh. Anal. Khim.*, 23 (1968) 616.
3 J. T. Allessi, D. G. Bush and J. A. VanAllan, *Anal. Chem.*, 46 (1974) 443.

Analytica Chimica Acta, 77 (1975) 337–339

SHORT COMMUNICATION

Effect of metal reducing agent on the titrimetric determination of tin in reference ore MP-1

H. F. STEGER

Mineral Sciences Division, Mines Branch, Department of Energy, Mines and Resources, Ottawa, Ontario K1A OG1 (Canada)

(Received 11th November 1974)

The Mines Branch has recently issued a zinc–tin–copper–lead ore, MP-1, as a certified reference material with recommended values for nine elements[1]. An assessment of the results for tin obtained in the inter-laboratory certification program for this material suggested that the values obtained by the titrimetric method vary with the nature of the metal used to reduce tin(IV) to tin(II)[2]. Because titrimetric analysis is a popular method for tin, it was thought worthwhile to evaluate this effect further.

Experimental

Samples of MP-1 were decomposed by fusion with a 1:1 mixture of sodium carbonate and sodium peroxide. Thereafter, various commonly accepted procedures were employed to make separations and to prepare the sample solutions for the reduction of tin by aluminum foil, iron granules, nickel powder or test-lead shot. The tin was then determined by titration with a potassium iodate solution which had been standardized for each metal reducing agent against solutions containing tin alone.

Results and discussion

The tin value for MP-1 was found to be 2.44, 2.42, 2.40 and 2.39% for aluminum, iron, nickel and lead reduction, respectively. The variation in these values was appreciably less than the value of 0.26% observed in the inter-laboratory certification program[1,2]. Nevertheless, a one-way analysis of variance[3] of the 49 results of the present investigation indicated a significant chemical difference in the titrimetric determination of tin in MP-1 with respect to the metal reducing agent.

Theoretically, the tin-equivalent value of the iodate titrant, TE_{Sn}, should be the same for all metal reducing agents. Table I illustrates that this is not so. This variation in TE_{Sn} which pertains to solutions containing tin alone, however, would be of no consequence if it were also valid for solutions derived from MP-1; that this is not so is also shown in Table I. TE_{MP}, the tin equivalent of the

iodate for solutions from MP-1, is given by $W\mu/V$, where W is the mean of the weights of eight samples of MP-1, V is the mean of the corresponding volumes of iodate, and μ is the true (unknown) tin content of MP-1. TE_{MP}/TE_{Sn} would be essentially constant if these quantities exhibited the same variation with metal reducing agent.

TABLE I

TIN EQUIVALENT OF IODATE TITRANT

Metal	*Tin equivalent (mg ml^{-1})*			
	TE_{Sn}	TE_{MP}	TE_{MP}/TE_{Sn}	TE_{MP}/TE_{cass}
Al	3.020	123.87 μ	41.02 μ	
Fe	2.976	122.35 μ	41.12 μ	41.02 μ
Ni	2.985	123.94 μ	41.53 μ	41.11 μ
Pb	3.030	126.66 μ	41.80 μ	41.08 μ

To investigate this effect further, 23 mg of cassiterite ore concentrate (NBS 137, 56.64% Sn) was added as an internal standard to one of a pair of samples of MP-1 each about 0.55 g with a weight difference of less than 0.2 mg. The tin equivalent of the iodate for solutions derived from the cassiterite and MP-1, TE_{cass}, was readily calculated from the difference in the volume of iodate. It was assumed, as seems reasonable, that the addition of the cassiterite to MP-1 did not significantly alter the action of the metal reducing agent; TE_{MP} and TE_{cass} should be the same. The value of TE_{MP}/TE_{cass} can be used as an estimation of the "goodness" of the corresponding value of TE_{MP}/TE_{Sn}. Table I clearly shows that the standardization of the iodate against solutions containing tin alone was satisfactory for aluminum and iron, but was not so for nickel and lead. The use of TE_{cass} for iron, nickel and lead to calculate the tin content of MP-1 gave 2.44, 2.43 and 2.43% respectively.

The reason why nickel and lead gave unsatisfactory results when the iodate was standardized against solutions containing tin only is not clear. The lower reduction potential of these metals relative to aluminum and iron suggests that the explanation may lie in differences in the ease of reduction of tin in the solutions containing tin alone and those derived from MP-1. In the latter, Fe(III), Cu(II), As(V), etc., were present and could form complex species with tin in which the tin was less easily reduced than in the strongly acidic standard solutions where only monomeric chloro–tin complexes existed.

The present investigation has demonstrated that some difficulty exists in the titrimetric determination of tin in MP-1. Furthermore, such difficulty may be expected with other tin-bearing ores and, in fact, has already been encountered in connection with the certification of KC-1, another reference material[4]. Therefore, to obtain optimal results in the titrimetric determination of tin in ores, the experimental method must be modified according to the metal used as the reducing agent.

REFERENCES

1 G. H. Faye, *Mines Branch, Tech. Bull. 155*, Department of Energy, Mines and Resources, Ottawa, Canada, 1972.
2 G. H. Faye, W. S. Bowman and R. Sutarno, *Anal. Chim. Acta*, 67 (1973) 202.
3 K. A. Brownlee, *Statistical Theory and Methodology in Sciences*, Wiley, New York, 1961.
4 G. H. Faye, *Mines Branch, Tech. Bull. 193*, Department of Energy, Mines and Resources, Ottawa, Canada, 1974.

Analytica Chimica Acta, 77 (1975) 340–343

SHORT COMMUNICATION

Indicator blanks for N-phenylanthranilic acid in redox titrations

A. A. OSAKWE, W. P. HAYES and D. THORBURN BURNS

Department of Chemistry, Loughborough University of Technology, Loughborough, Leicestershire (England)

(Received 12th November 1974)

Internal indicators are oxidized or reduced to produce the visual colour changes in redox titrations; the titrant so consumed is the indicator blank. Bishop[1] states that there are three components in overall titration errors: (i) the chemical error, *i.e.* the difference between the end-point and the equivalence point, (ii) the visual discrimination error, and (iii) the error from the consumption of titrant. The blanks discussed below are the sum of (ii) and (iii). The blanks still in use were determined 35–45 years ago[2], and the present work was undertaken to supply fresh data on N-phenylanthranilic acid (NPA).

The first detailed investigation of the indicator properties of NPA[3], was by Syrokomskii and Stiepin[4] who reported the oxidation potential to be 1.08 V, a value confirmed by Lederer and Ward[5]. However, Belcher *et al.*[6] found values of 0.89 V in 0.5 *M*, 0.87 V in 1 *M* and 0.88 V in 2 *M* sulphuric acid solutions, results confirmed by Rao and Dutt[7]. Avilov and Zolotar[8] also examined the dependence of the NPA redox potential on sulphuric acid concentration; specific values were not stated, but interpolation gives 0.95 V in 1 *M* sulphuric acid, which is lower than the original[4] but not in accord with other values[7]. Lower values are in line with the behaviour of NPA in chromium(VI)–iron(II) titrations. NPA has been advocated as an alternative to diphenylamine sulphonic acid in several titrations[4] but the colour change is said to be less satisfactory[9].

The oxidation of NPA was considered to be a two-stage reaction with a benzidine intermediate[10], but Bishop and Hartshorn[11] suggest that NPA and its derivatives are oxidized in single two-electron steps, without benzidine formation. NPA is oxidized to a bluish-red (524 nm, half-life 10 min) which then forms a green product (436 nm), the reactions being uncertain.

Experimental

N-Phenylanthranilic acid indicator (0.005 M). 0.2667 g was dissolved in 12 ml of 0.1 *M* sodium hydroxide solution and diluted to 250 ml with distilled water[12]; this was prepared every two weeks[13].

Cerium(IV), iron(II), chromium(VI) and hexacyanoferrate(II) solutions. These were prepared from analytical-reagent ammonium cerium(IV) sulphate, ammonium iron(II) sulphate hexahydrate, potassium dichromate and potassium hexacyanoferrate(II) trihydrate respectively[2]; the last was prepared daily.

Uranium(IV) solutions. Uranium(VI) acetate in 1 *M* sulphuric acid was passed through a Jones reductor, and the mixture of uranium(III) and (IV) was aerated to yield uranium(IV)[14].

Procedures. Titration blanks were determined by two methods: (a) by titrating 10- and 25-ml aliquots of sample solutions, each containing the same volume of indicator solution, and calculating the blank from simultaneous equations[2]; or (b) from the difference in titrant-volumes obtained between NPA and potentiometric end-points with 25-ml aliquots of sample solutions.

The following systems were examined: (i) iron(II) and chromium(VI); (ii) iron(II) and cerium(IV); (iii) hexacyanoferrate (II) and cerium(IV); and (iv) uranium(IV) and chromium(VI).

The visual end-point was taken as the first appearance of a pink colouration which persisted for about 45 s. Indicator blanks from the two methods agreed within ± 0.01 ml. The values given below are those determined by method (b) which is simpler in practice.

TABLE I

INDICATOR BLANKS FOR VARIOUS VOLUMES OF INDICATOR SOLUTION

(Titrant 0.02 *N* in each case; 25 ml of 0.02 *N* titrand diluted with 50 ml of sulphuric acid solution to the given acidity.)

Redox system	*Acidity (M)*	*Volume of indicator (ml)*	*Indicator blank (ml)*	
			Added at start	*Added just before end-point*
Fe(II)–Cr(VI)	0.5–1	0.2	0.03	0.03
		0.5	0.03	0.03
		1.0	0.06	0.04
Fe(II)–Ce(IV)	0.25–0.5	0.2	0.06	0.03
		0.5	0.07	0.04
		1.0	0.09	0.06
$Fe(CN)_6^{4-}$–Ce(IV)	0.5–1.25	0.2	0.18	0.10
		0.5	0.23	0.15
		1.0	0.33	0.23
U(IV)–Cr(VI)	1.25	0.5	0.20	—

TABLE II

INDICATOR BLANKS FOR THE Fe(II)–Cr(VI) TITRATION WITH VARIOUS TITRANT CONCENTRATIONS

Indicator Volume (ml)	*Blanks for titrant concentrations (N) of*		
	0.01	*0.02*	*0.10*
0.2	0.03	0.03	0.04
0.5	0.04	0.03	0.03
1.0	0.05	0.06	0.06

Results and Discussion

Indicator blanks for 0.02 *N* solutions at different acidities are given in Table I. Titrations were also made with 0.1 and 0.01 *N* concentrations of oxidant under the same conditions; the results (Table II) for the iron(II)–chromium(VI) system are typical. Clearly, the blanks are almost independent of titrant concentration, implying a reduction in relative error for dilute titrants; and they are not directly related to the volume of indicator taken, so that *pro rata* corrections cannot be made.

Indicator blanks increased when the indicator was added some time before commencement of titration. For the iron(II)–chromium(VI) titration in 1 *M* sulphuric acid with 0.5 ml of indicator solution, the indicator blank increased from 0.03 ml for standing times of 0–3 min, to 0.07 ml for 5 min, and to 0.15 ml for 15 min. When the indicator was added just before expected end-points, blanks were slightly reduced (0.01–0.01_5 ml) and colour changes were easier to observe; the data in Table II were obtained thus.

The effects of acidity were examined. Blanks slowly increased with increased acidity; the ranges for which no changes in blank were observed are noted in Table I. For the iron(II)–cerium(IV) titrations (0.05 ml of indicator) in 0.5, 1 and 2.5 *M* sulphuric acid, blanks were 0.03, 0.06 and 0.18 ml, respectively.

It is usual[1] to add phosphoric acid in the titration of iron(II) with chromium(VI). Stockdale[15] reported that for barium diphenylamine sulphonate, the presence of phosphoric acid made the colour change clearer but was not essential. Bishop and Crawford[12] stated that the normal blank for NPA (0.04 ml of 0.1 *N* dichromate) decreased slightly in the presence of phosphoric acid but the end-point was sluggish. Rao and Dutt[7] considered that phosphoric acid was not essential. In the present work, addition of 10 ml of 25% (v/v) phosphoric acid to each of the systems studied had no effect on the blank values, but end-points were easier to detect.

Variation in temperature of the titrated solutions had no effect in the range 20–50 °C; above 80 °C blanks were approximately doubled.

Conclusions

It is concluded that NPA can be used, though it is not recommended, for the titration of iron(II) with cerium(IV) or with chromium(VI), where low blanks obtain; it is less suitable for the uranium(IV)–chromium(VI) system, where blanks are high, though the colour change is good.

The indicator is unsatisfactory because of variable blank values. Blanks must be determined under the conditions in use, as they depend on acidity, temperature, volume of indicator solution added, time of addition, and/or the redox system in use.

The authors are grateful to Professor R. Belcher for drawing attention to the problem.

REFERENCES

1 E. Bishop, *Indicators*, Pergamon, Oxford, 1972.
2 R. Belcher and A. J. Nutten, *Quantitative Inorganic Analysis*, Butterworths, London, 2nd edn., 1960; 3rd edn., 1970.
3 A. Kirssanow and W. Tscherkassow, *Bull. Soc. Chim. Fr.*, 8 (1936) 817.
4 W. S. Syrokomskii and V. V. Stiepin, *Zavod. Lab.*, 5 (1936) 144.
5 M. Lederer and F. L. Ward, *Anal. Chim. Acta*, 6 (1952) 1.
6 R. Belcher, D. I. Rees and W. I. Stephen, *Chim. Anal., Paris*, 10 (1959) 397.
7 V. N. Rao and V. V. S. E. Dutt, *Z. Anal. Chem.*, 256 (1971) 358.
8 V. B. Avilov and R. N. Zolotar, *Zh. Anal. Khim.*, 25 (1970) 1418.
9 W. Furness, *Analyst (London)*, 75 (1950) 2.
10 I. M. Kolthoff and L. A. Sarver, *J. Amer. Chem. Soc.*, 52 (1930) 4179.
11 E. Bishop and L. G. Hartshorn, *Analyst (London)*, 96 (1971) 26.
12 E. Bishop and A. B. Crawford, *Analyst (London)*, 74 (1949) 365.
13 C. Woodward and H. N. Redman, *High-Precision Titrimetry*, Society for Analytical Chemistry, 1973.
14 V. P. Rao, B. V. S. R. Murty and G. G. Rao, *Z. Anal. Chem.*, 147 (1955) 99.
15 D. Stockdale, *Analyst (London)*, 75 (1950) 150.

Analytica Chimica Acta, 77 (1975) 344–347

SHORT COMMUNICATION

The thermal decomposition of the extracted complexes formed by uranyl chloride with long-chain aliphatic amines

TAICHI SATO

Department of Applied Chemistry, Faculty of Engineering, Shizuoka University, Hamamatsu (Japan)

(Received 31st December 1974)

The thermal decomposition of the sulphato and nitrato complexes of uranium(VI) with tri-n-dodecylamine and of the chloro complexes of copper(II) and zirconium(IV) with tri-n-octylamine has been investigated previously[1–3]. The present study extends the work to the chloro complexes of uranium(VI) with some long-chain aliphatic amines: tri-n-dodecylamine (TDA), tri-n-octylamine (TOA) and di-n-octylamine (DOA).

Experimental

Chemicals. The above three high-purity amines (Kao Soap Co., Ltd.) were used without further purification as solutions in benzene, which were not pre-equilibrated with hydrochloric acid solutions. Uranyl chloride hydrate was dissolved in hydrochloric acid solution of the required concentration. The other chemicals were of analytical-reagent grade.

Preparation of complexes. On the basis of the distribution results[4], 100 ml each of the 0.1 *M* amine solution in benzene and the aqueous solution of uranyl chloride (250 g l^{-1}) containing 0.1 *M* hydrochloric acid and 8 *M* lithium chloride were shaken for 15 min at 20°C. The mixture was centrifuged, and benzene was removed from the uranium-saturated organic phase under vacuum at 50°C. For chemical analysis, the complex obtained was dissolved in benzene, and the chloride and water in portions of the solution were determined by Volhard and Karl Fischer titrations, respectively. The benzene solution was then washed with 1 *M* nitric acid, and uranium in the acidic layer was titrated with EDTA to a xylenol orange end-point[5].

The thermogravimetric and differential thermal analyses (t.g.a. and d.t.a.), and the infrared and absorption spectral measurements were carried out as described previously[1,6,7].

Results and discussion

For the chloro complex of uranium(VI) with TDA, the t.g.a. and d.t.a. curves are shown in Fig. 1; the i.r. spectra of the complex and its products on heating at 200, 300 and 600°C are given in Fig. 2. Similar results were obtained for the complexes with DOA and TOA. In Fig. 1, the d.t.a. curve has endothermic

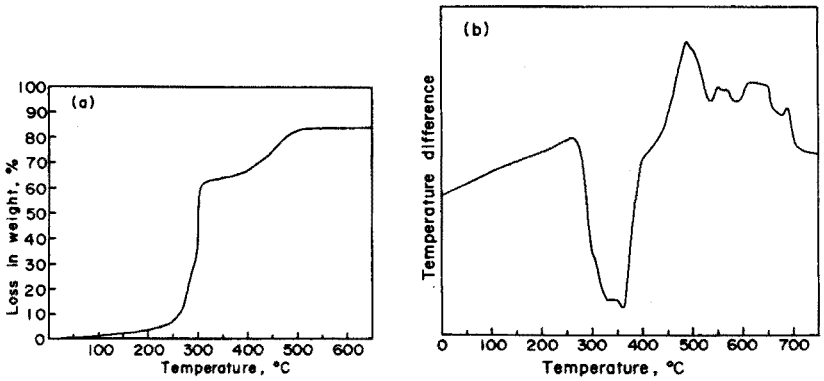

Fig. 1. T.g.a. (a) and d.t.a. (b) curves of the chloro complex of uranium(VI) with TDA. Heating rate, 5°C min^{-1}.

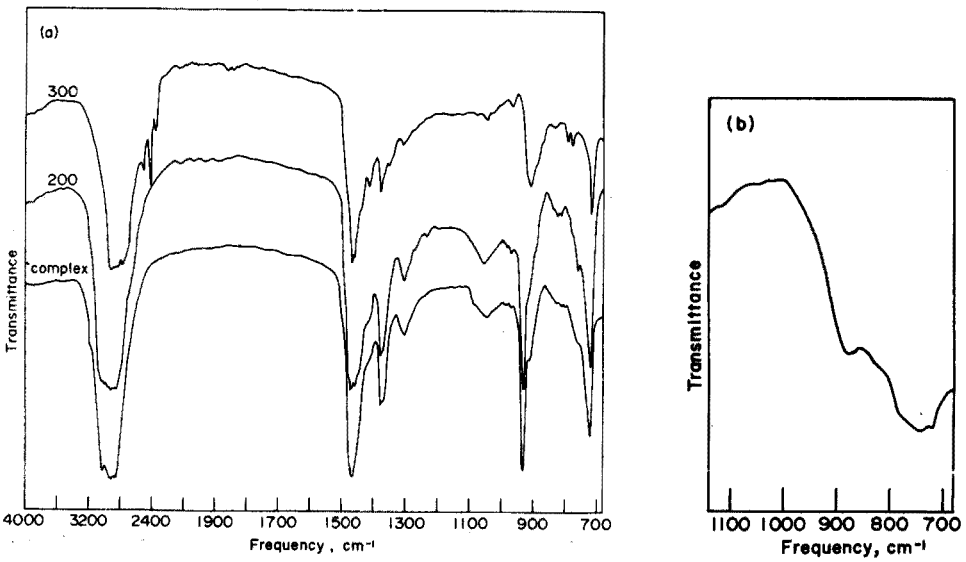

Fig. 2. Infrared spectra of materials derived from the chloro complex of uranium(VI) with TDA by heating to the stated temperatures. (a) Complex and products at 200 and 300°C. (b) Products at 600°C.

peaks at 300, 330, 360 and 400°C (broad) and an exothermic peak between 450 and 710°C with a maximum at 490°C, corresponding approximately to the changes in the t.g.a. curve.

The complex with TDA shows the following i.r. absorption bands (Fig. 2): the asymmetric stretching frequency of the uranyl group[8] at 930 and 910 cm^{-1}; the NH^+ stretching vibration at 3020 cm^{-1}; C–N asymmetric and symmetric stretching bands at 1050 and 760 cm^{-1}, respectively; C–H symmetrical and asymmetrical stretching vibrations at 2920 and 2860 cm^{-1}; the CH_3 degenerate (and CH_2 scissoring) and symmetrical bending modes at 1465 and 1375 cm^{-1}; CH_2 wagging and rocking frequencies at 1300 and 720 cm^{-1}, respectively. Figure

2 (a) shows that the i.r. spectrum is little affected when the complex is heated at 200°C. After heating at 300°C, the absorptions attributed to the presence of amine[9] remain, but the NH^+ stretching vibration at 3020 cm^{-1} shifts to 2410 cm^{-1}, and the asymmetric C–N stretching absorption becomes weaker. On further heating above 400°C, the absorptions caused by TDA disappear, and at 600°C (Fig. 2 (b)), the broad absorption band[10] of U_3O_8 appears at 750 cm^{-1}. The t.g.a. curve does not show a marked weight-loss on heating above 500°C.

The d.t.a. curve for TDA itself shows endothermic peaks at 275 and 380°C, which arise from the formation of hydrocarbon by cracking of the amine and then carbonization. The curve for TDA hydrochloride shows peaks at 285 and 335°C, which can be ascribed to thermal decomposition of the amine hydrochloride followed by carbonization. These results, in conjunction with the results of chloride determinations on the different residues, allow the d.t.a. curve for the uranyl–TDA complex to be interpreted as follows: at 300°C, some chloride is removed and the amine is coordinated immediately to the uranyl group by hydrogen bonding; at 330 and 360°C, more chloride is removed, the amine is thermally decomposed and the resulting hydrocarbon is carbonized; at about 400°C, the remaining chloride is removed; the exothermic peak with a maximum at 490°C indicates the combustion of carbon.

The TDA complex contained a 1:4:2 molar ratio for uranium:chloride:amine, indicating the composition $(R_3NH)_2UO_2Cl_4$. The complexes with DOA and TOA showed the same molar ratio. The i.r. spectra of the complexes showed no absorptions caused by OH groups, hence the complexes contain no coordinated water, and this was confirmed by Karl Fischer titration. The absorption results suggest that the complexes are hexa-coordinated species[11–13] analogous to the $UO_2Cl_4^{2-}$ type. The following structures, with a coordination number of six for uranium, are proposed for the complexes:

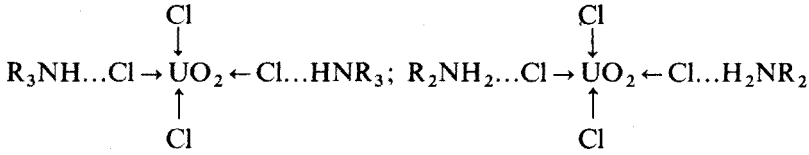

where R is $C_{12}H_{25}$ or C_8H_{17}.

The chloro complex of uranium(VI) with TDA is more stable thermally than the corresponding nitrato complex[2], but less so than the sulphato complex[1].

The author wishes to thank Mr. M. Nishizaki for assistance with experimental work, and also thanks the Kao Soap Co., Ltd. for samples of various amines.

REFERENCES

1 T. Sato, *J. Inorg. Nucl. Chem.*, 26 (1964) 2229; 27 (1965) 240.
2 T. Sato and K. Adachi, *J. Inorg. Nucl. Chem.*, 31 (1969) 1395.
3 T. Sato and H. Watanabe, *Anal. Chim. Acta*, 54 (1971) 439.
4 T. Sato, *J. Appl. Chem.*, 16 (1966) 143.
5 J. Kinnunen and B. Wennerstrand, *Chemist–Analyst*, 46 (1957) 92.

6 T. Sato, T. Yamashita and F. Ozawa, *Z. Anorg. Allg. Chem.*, 370 (1969) 202.
7 T. Sato, *Z. Anorg. Allg. Chem.*, 376 (1970) 205.
8 B. M. Gatehouse and A. E. Comyns, *J. Chem. Soc. London*, (1958) 3965; G. L. Caldow, A. B. Van Cleave and R. L. Eager, *Can. J. Chem.*, 38 (1960) 772.
9 J. R. Barcelo and J. Bellanato, *Spectrochim. Acta*, 8 (1956) 27.
10 H. R. Hoekstra and S. Siegel, *J. Inorg. Nucl. Chem.*, 18 (1961) 154.
11 E. Rabinowitch and R. L. Belford, *Spectroscopy and Photochemistry of Uranyl Compounds*, Pergamon, Oxford, 1964, p. 112.
12 W. E. Keder, *J. Inorg. Nucl. Chem.*, 24 (1962) 561.
13 T. Sato, *J. Inorg. Nucl. Chem.*, 34 (1972) 3835.

Analytica Chimica Acta, 77 (1975) 348–351

BOOK REVIEWS

Clinical Biochemistry–Principles and Methods, Edited by H. Ch. Curtius and Marc Roth, 2 vols, de Gruyter, Berlin, 1974. cxxxvii + 1677 pp, price DM 460.

This work comprises two volumes, weighs over 4 kg, runs to 1700 pages, and at the current rate of exchange costs £80. The book is edited by two eminent Swiss clinical chemists, who are joined by sixty-four other contributors from various parts of the world; they include physicians, statisticians, physicists and chemists.

The first volume deals mainly with the physical and chemical principles involved in the methods commonly employed in clinical chemistry laboratories. These include chromatography, electrophoresis, ultracentrifugation, dialysis, extraction by adsorption, photometry, atomic absorption, radio-immunoassay, mass spectrometry and ion-selective electrodes. There are also chapters on such general topics as collection of specimens, quantities and units, quality control and normal values, automation and computers.

At the end of the first volume and throughout the second volume, methods for the detection and determination of substances in biological fluids are described. They are grouped together under the headings of hormones, amines, bile acids, carbohydrates, vitamins, lipids, amino acids, enzymes, haemoglobin and porphyrins, organic acids, inorganic substances, proteins. Three chapters are devoted to kidney function tests, toxicology and acid-base balance.

The editing of this book was a monumental task which has been completed within a reasonable space of time; the references include many from the year 1973. With such length and so many contributors, it is inevitable that there should be both good and indifferent contributions; a mere listing of these would be uninteresting, but a few general comments are necessary.

The descriptions of the physical and chemical principles of many analytical techniques in the first volume are exceptionally well written and provide a unique collection. The one exception is that on "Automation and On-line computers" which is a personal and frequently biased account of an important subject. There is no description of the continuous-flow system, merely a condemnation of its commercial development. The general chapters in the first volume are too brief and as a result leave much unsaid or unclear.

The methods section, predominantly in Volume 2, is not nearly as satisfactory as Volume 1. The technical details of the methods are frequently inadequately described and if followed from this work poor results may be produced; particularly lacking are details on standardization of techniques and information on the stability of reagents. The description of the chemical principles used is well done and provides information frequently omitted in other text books on methods, though more chemical formulae would have been welcome.

In summary, this book would have been more satisfactory, as well as shorter and cheaper, if it had confined itself to a description of the chemical and physical principles of the methods in common use in clinical chemistry. The cost of this publication is five times that of Henry's "Clinical Chemistry. Principles and

Techniques", which attempts to cover the same ground. Parts of this work are superior to Henry's book, some are inferior. However, the net superiority is marginal and certainly well below that reflected in the ratio of the cost of the two publications.

T. P. Whitehead

H. P. Klug and L. E. Alexander, *x-Ray Diffraction Procedures for Polycrystalline and Amorphous Materials*, Wiley–Interscience, New York, 2nd edn., 1974, xxv + 966 pp., price £18.55.

This book, which appears twenty years after the original edition, gives a comprehensive survey of all aspects of x-ray powder diffraction. Theory is provided as well as practical details of all the techniques involved. This new edition is updated to include the many advances made during the past twenty years, the greatest expansion of material being in those sections concerned with the use of counter diffractometers and electronic computers.

The book is divided into twelve sections, starting from Elementary Crystallography and the Production and Properties of x-rays, and finishing with Stress Measurements in Metals and Radial-distribution Studies of Noncrystalline Materials. Each section is completed by lists of general and specific references, and there are ten appendices, providing tables of information necessary for most calculations, and such practical details as the layout for a diffraction laboratory, and the handling and processing of x-ray film.

The book will prove useful to anyone concerned with x-ray powder diffraction, at whatever level of sophistication.

A. J. Edwards (Birmingham)

R. T. Jacobsen, R. D. Stewart, R. D. McCarty and H. J. M. Hanley, *Thermophysical properties of nitrogen from the fusion line to 3500 R (1944 K) for pressures to 150000 psia*, SD Cat. No. C13.46:648, December 1973, 162 pp., $1.25.

Copies of these documents are available from the U.S. Government Printing Office, Washington, D.C. 20402. SD Catalog numbers must be quoted; orders must be prepaid and overseas orders must include an additional 25% of the publication price to cover mailing costs.

R. Bock. *Einführung in die Methoden der Analytischen Chemie; Band I: Trennungsmethoden*, Verlag Chemie, Weinheim, 1974, VII + 362 pages; 236 figures et 79 tables, Relié DM 42.

Il est bien spécifié dans le titre général de cette nouvelle série d'ouvrages, qu'il s'agit d'une introduction aux méthodes de la chimie analytique.

On ne trouve donc dans ce premier ouvrage—consacré aux méthodes de séparation—aucun développement théorique important. Ainsi, ce livre n'est pas particulièrement destiné aux étudiants; par contre, il rendra d'éminents services aux praticiens, car il donne tout renseignement utile sur le principe de base des diverses méthodes. Chaque chapitre est suivi d'une bibliographie succinte, mais généralement bien choisie, sur les généralités, applications et techniques spéciales.

L'auteur, dans une courte introduction, traite de la classification des méthodes, de la sélectivité et spécificité, des réactions de masquage, de la dilution isotopique (substoechiométrie incluse).

La seconde partie (env. 370 pages) est consacrée aux méthodes de séparation basées sur le principe du partage entre deux phases non miscibles: solubilité (liquide-liquide, gaz-liquide, précipitation, électrolyse), échange d'ions, adsorption et absorption, changement de phase (distillation, sublimation, cristallisation, condensation).

La dernière partie (env. 50 pages) a trait aux séparations des particules contenues dans une seule phase, basées sur les différences de vitesse de déplacement de celles-ci: spectrométrie de masse, électrophorèse et électrodialyse, diffusion, sédimentation et flottation.

Les nombreuses tables et figures originales sont bien choisies et complètent judicieusement un texte clair et ordonné. Si certaines techniques auraient mérité, de par leur actualité, une plus grande attention (p. ex. chromatographie liquide à haute pression, p. 77), l'ouvrage dans son ensemble est un excellent guide pour les chimistes praticiens qui pourront s'y documenter sans trop grande perte de temps.

W. Haerdi (Genève)

Recent N.B.S. Publications

K. L. Kelly, *Colorimetry and Spectrophotometry, A bibliography of N.B.S. Publications, January 1906–January 1973*, April, 1974, 54 pp., 95 cents (S.D. Cat. No.: C13. 10:393).

J. A. Brennan, R. W. Stokes, C. H. Kneebone and D. B. Mann, *An evaluation of selected angular momentum, vortex shedding and orifice cryogenic flowmeters*, March 1974, 69 pp., 65 cents (S.D. Cat. No.: C13.46:640).

H. Yakowitz, R. L. Myklebust and K. F. J. Heinrich, *FRAME–an on-line correction procedure for quantitative electron probe microanalysis*, October, 1973, 51 pp., 80 cents (S.D. Cat. No.: C13.46:796).

F. Westley, *Vibrationally excited hydrogen halides; a bibliography on chemical kinetics of chemiexcitation and energy transfer processes* (1958–1973), April 1974, 81 pp., $1.30 (S.D. Cat. No.: C13.10:392).

An Index of International Standards, Edited by S. J. Chumas, March 1974, 222 pp., $5.60 (S.D. Cat. No.: C13.10:390). [This index contains over 2700 standards titles from the international organizations, I.S.O., I.E.C., C.E.E., C.I.S.P.R. and O.I.M.L.]

G. R. Freeman, *Radiation chemistry of ethanol–a review of the data on yields, reaction rate parameters, and spectral properties of transients*, February 1974, 43 pp., 80 cents (S.D. Cat. No. C13.48:48).

G. J. Schulz, *Resonances in electron impact on atoms and diatomic molecules*, October 1973, 118 pp., $1.35 (S.D. Cat.No.: C13.48:50).

P. E. Pontius, *Mass and Mass values*, January 1974, 39 pp., 70 cents (S.D. Cat.No.: C13.44:133).

E. Swanson and others, *Standard x-ray diffraction powder patterns–Section 11, Data for 70 substances*, February 1974, 134 pp., $1.55 (S.D. Cat.No.: C13.44:25/sec.11).

L. O. Olsen, *Introduction to liquid flow metering and calibration of liquid flowmeters*, SD Cat. No. C13.46:831, June, 1974, 60 pp., $0.95.

C. N. R. Rao and G. V. Subba Rao, *Transition metal oxides: Crystal chemistry phase transitions and related aspects*, SD Cat. No. C13.48:49, June, 1974, 138 pp., $1.70.

Aerosol measurements: Proceedings of seminar on aerosol measurements, May 7, 1974, edited by W. A. Cassatt and R. S. Maddock, SD Cat. No. C13.10:412, October, 1974, 193 pp., $2.65.

B. Marron, E. Fong and D. Fife, *A mechanized information services catalog*, SD Cat. No. C13.46:814, 56 pp., $0.90.

Copies of the above documents are available from the U.S. Government Printing Office, Washington, D.C. 20402. S.D. Catalogue numbers must be quoted: orders must be prepaid and overseas orders must include an additional 25% of the publication price to cover mailing costs.

Analytica Chimica Acta, 77 (1975) 352

ANNOUNCEMENTS

XVIIth International Conference on Coordination Chemistry September 6–10, 1976, in Hamburg (Federal Republic of Germany)

The XVIIth International Conference on Coordination Chemistry will be organised from 6 to 10 September 1976 in Hamburg (Federal Republic of Germany). The Conference will be concerned with recent developments in the following fields:

(1) Structure and bonding.
(2) Novel synthetic routes.
(3) Kinetics and reaction mechanisms.
(4) Catalytic and technological aspects.
(5) New types and concepts in coordination compounds.

Organisation will be taken over by Gesellschaft Deutscher Chemiker to which all enquiries about this Conference should be sent:

Dr. W. Fritsche
Secretary,
XVIIth I.C.C.C.
c/o Gesellschaft Deutscher Chemiker
P.O. Box 90 04 40
D-6000 Frankfurt/Main 90
Federal Republic of Germany

Journées de Calorimétrie et d'Analyse Thermique, Grenoble, 22–23rd May, 1975

This meeting is sponsored by the Association Française de calorimétrie et d'Analyse Thermique, and Le Groupe de Thermodynamique expérimentale (Société Chimique de France).

The programme with involve three sessions:

(1) Calorimetry and differential scanning calorimetry at low temperature $T < 200$ K.

Specific heats, transitional enthalpies, polymorphism in solid state etc.
Thermodynamic studies.
Experimental techniques.

(2) Studies of the condensed phases at high temperature.

Determination of thermodynamic data.
Phase diagram etc.
Experimental techniques.

(3) Free communications in calorimetry, differential scanning calorimetry, differential thermal analysis.

Further Information can be obtained from:

Secrétariat des Journées de Calorimétrie et Analyse Thermique 1975
Service des Basses Températures–D.T.C.E.–C.E.N. Grenoble
BP 85 Centre de Tri
38041 Grenoble Cedex (France)

ERRATA

E. H. Daughtrey, Jr. and W. W. Harrison, Analysis for Trace Levels of Boron by Ion Exchange–Hollow Cathode Emission, *Anal. Chim. Acta*, 72 (1974) 225–230.
On p. 227, the NBS Standard Orchard Leaves value for boron should read as certified at 33 p.p.m., not 23 p.p.m. non-certified as we reported.

R. Belcher, S. L. Bogdanski, S. A. Ghonaim and A. Townshend, Molecular emission cavity analysis (MECA)—A new flame technique. Part IV. The determination of arsenic and antimony, *Anal. Chim. Acta*, 72 (1974) 183–187.
On p. 186 of this paper, lines 10–12 should read: "anions were tested for interference: 20 μg of Al^{3+}, Ge^{4+}, Ga^{3+}, Cd^{2+}, Mn^{2+}, Co^{2+}, Ni^{2+}, Zn^{2+}, Cl^-, NO_3^-, SO_4^{2-} and PO_4^{3-} did not interfere in the determination of 4 μg of arsenic or antimony; 10 μg of Cu^{2+} and Ag^+ decreased the emission".
On p. 187 of this paper, lines 2–4 should read:
"*Optimal gas flow rates.* Nitrogen: 3.5 l min^{-1} (or helium at the same flow rate). Hydrogen: 1.7 l min^{-1}. Nitrogen carrier gas: 160 ml min^{-1} (or helium at the same flow rate). Oxygen into cavity: 110 ml min^{-1}."

L. Alaerts, J. P. Op de Beeck and J. Hoste, Non-destructive Determination of Silicon in Aluminium–Silicon Alloys by Neutron Activation Analysis with a ^{227}Ac–Be Isotope Neutron Source, *Anal. Chim. Acta*, 73 (1974) 53–59.
On p. 57, line 9, equation (3) should read:

$$SA_{S,2} = SA_{S,1} - SA_{Al}\frac{C_{Al,1}}{100}$$

On p. 57, Table III, the error of the mean for sample A.05 should be -0.29.

On p. 58, the third line from the foot of the page should read:
"Thanks are due to the Nationaal Fonds voor Wetenschappelijk Onderzoek."

On p. 59, Reference 1 should read: "L. Alaerts, J. P. Op de Beeck and J. Hoste, *Anal. Chim. Acta*, 70 (1974) 253."

ANALYTICA CHIMICA ACTA, VOL. 77 (1975)

AUTHOR INDEX

ANALYTICA CHIMICA ACTA, VOL. 77 (1975)

SUBJECT INDEX

(Continued from page 4 of cover)

CONTENTS

(Continued on inside page of cover)